Copyright is owned by the Author of the thesis. Permission is given for a copy to be downloaded by an individual for the purpose of research and private study only. The thesis may not be reproduced elsewhere without the permission of the Author.

Clinical methods for assessment of endothelial glycocalyx integrity in cats

A thesis presented in partial fulfilment of the requirements for the degree of

Doctor of Philosophy

in

Veterinary Science

At Massey University, Manawatū, New Zealand

Ivayla Danielova Yozova, MVM, Dr.med.vet., MBA, FHEA, Dipl.ACVECC, Dipl.ECVECC

2025

Abstract

The endothelial glycocalyx (EG) is critical to vascular homeostasis, regulating permeability, blood flow, and inflammation. Despite its recognized importance in human medicine, clinical tools for EG assessment in veterinary patients remain underdeveloped. This PhD project aimed to explore, validate, and adapt methodologies for EG assessment in cats, with a focus on sidestream dark field videomicroscopy using the GlycoCheck™ system and the evaluation of EG shedding biomarkers.

The project began by establishing tolerance intervals for GlycoCheck™ parameters in a large cohort of healthy cats, confirming the feasibility of sublingual imaging for non-invasive EG thickness estimation. Species-specific features of the feline microvasculature, including variability in vessel counts and perfused vessel densities, were documented, providing essential baseline data.

Attempts to validate a commercial human syndecan-1 ELISA in cats revealed poor assay performance and uncertain specificity, highlighting the challenges of biomarker translation across species and the current lack of reliable EG shedding markers in veterinary medicine.

Two experimental studies investigated the effects of intravenous fluid administration on EG integrity in healthy cats. Neither a standard fluid challenge nor transient volume overload resulted in measurable EG thinning. However, anaesthetic effects and associations with haematological variables such as packed cell volume were identified, underscoring the importance of controlling for confounders. The findings also pointed to limitations of the GlycoCheck™ system, which estimates rather than directly measures EG thickness and may miss subtle microvascular changes.

A subsequent clinical study demonstrated the feasibility of applying GlycoCheck™ in hospitalized cats without disrupting workflow. However, no robust associations with clinical variables, including illness severity, were detected - likely due to small sample size and patient heterogeneity. Minor trends with fluid therapy and packed cell volume were noted but not confirmed.

Overall, this project identifies key methodological constraints in both imaging- and biomarker-based EG assessment. While promising, both approaches remain immature and require further refinement. By highlighting feasibility, limitations, and areas for future development, this work lays a foundation for advancing EG assessment in veterinary medicine and integrating microvascular evaluation into clinical research.

Preface

The start of my small animal emergency and critical care residency in 2013 in Switzerland was marked by "the fall" of hydroxyethyl starches (HES). The fall was set off by a buzz - the UK had suddenly recalled all their HES products from the market, from their hospitals, and from their veterinary clinics (1). People were panicking that they would no longer be able to resuscitate critically ill animals without this magic potion. What led to this recall? There it was - the bang! Joachim Boldt, a prolific human anaesthesiologist and strong proponent for use of HES was implicated in a large-scale scandal of scientific misconduct, leading to retraction of over 200 scientific papers which from the literature, stripping of his professorship titles and subsequent disappearance from the scientific scene (2-4).

Almost as if staged, several large scale well powered randomized controlled trials, accusing HES of being implicated in increased incidence of acute kidney injury and mortality in sick people, appeared in the literature (5-8). Now what happens to the evidence scale when you remove over 90 fraudulent pro-HES papers, and you add a few very powerful anti-HES papers? The scale tips, and here we go, even a conservative meta-analysis engine like Cochrane had to admit that "HES is… not so good!" (9, 10). This all cascaded into an investigation from the European Medicines Agency and the United States Food and Drug Administration to confirm that, yes, HES is not so good and should not be used in people unless really necessary (11-14).

The scientific literature was roaring! There were letters to the editor (15, 16), contra-letters to the editor (17-19), letters to the editor addressing specific points (20-22), studies to disprove the points made in letters to the editor (23), support for the committees investigating the HES debacles(24), or outrage at the committees decisions (25-27), and even public citizen involvement (28). At some point, I could just read the authors' list of a paper (whether a letter, a short communication, a review, or an original study) and already know what the outcome would be – a pro- or contra-HES statement.

Why do I know all this? Well obviously, we were all shaken by this event in the veterinary critical care world. We did not have the option of pouring unlimited amounts of albumin, fresh frozen plasma or other blood products in our patients instead of HES. Our patients had to cost much less to their owners. More importantly our patients were less sick when they were intrusted in our intensive care unit. They did not burden us with unnecessary complications, such as long-term smoking, alcoholism, hypertension, diabetes or frailty. Was HES that bad for small animals? We did not know. So, without further ado, my mentor Katja-Nicole Adamik decided that we should investigate this matter, which marked the start of my first doctoral thesis (not a PhD, but a Dr.med.vet.) looking into safety and efficacy of HES administration in dogs and cats (29-31). In addition, as the story of HES was a thrilling one, we made it our mission to inform and update, which resulted in a few review articles (32-34).

So, I really had to go into the data. And admittedly it was tough. The scandal, the rock starriness, the bias of scientific research groups, the lack of literature with meaningful outcomes to compare, build upon, analyse, appraise, had started to shape me into a very sober, sceptical, dare I say cynical, scientist.

And there in the midst of all this HES-related scientific unpleasantness, there was a word that started popping up in articles – **"the endothelial glycocalyx"**. It was complicated, mystical, novel, uncharted, offering promise of better science and a door into the obscure world of microcirculation, the same microcirculation that feeds and oxygenates our cells. It was like opening Narnia's wardrobe, like looking into another dimension, like falling in love with science again. I caught myself reading late night applied physiology articles (not understanding much, I admit) and lying awake thinking of the endothelial glycocalyx. Ten years later, my relationship with it has transitioned from burning passion to the steady flame of long-term affairs, with all their ups and downs. And improved immensely my overall relationship with science.

Before you dive into it, a few "housekeeping" announcements:

- As much as I tried to avoid it, there is repetition in this work. Most of was inevitable, because the format is "by publication" and as individual articles are published, they will require some of the information to be repeated. Secondly, there is repetition in the citations, mainly because of the scarcity of literature in veterinary medicine. Lastly, sometimes I had to repeat a concept to simply remind the reader about something.
- Abbreviations were listed throughout, once in the non-publication chapters, and then again spelled in each publication. However, when I felt that a term has not been used for a while, I used the abbreviation and added the full spelling in brackets as a reminder.
- To comply with thesis formatting requirements, all figures and tables are included within the body of each experimental chapter, rather than placed at the end as would typically be done for journal publication. To maintain consistency with publication standards, the chapters formatted as manuscripts (Chapters II, IV, V, and VI) do not refer to other thesis chapters by number (e.g., "Chapter II" or "Chapter IV"). Instead, they reference the studies as standalone publications (or abstract publications) and include brief study descriptions where appropriate. References to chapter numbers are used only in prefaces, bridging paragraphs, and the final discussion chapter.
- Lastly, there is the question of referring to *homo sapiens* throughout the work. Should it be "people" or "humans". When I started off as a researcher and my scientific writing needed a lot of work, Judith Howard, a very experienced scientific writer and brilliant editor, told me that it should be "people", and I just kept it as such since. There is probably room for debate, but it is beyond the scope of this work. Likewise, animals are addressed as "animals" and not "non-human animals", mostly because there are already enough words in this text.

With this little story and clarifications, I will leave you to your read.

Enjoy!

Acknowledgements

I'd like to start by acknowledging my former mentor and dear friend Katja-Nicole Adamik for her contagious enthusiasm, sparking my deep interest in research, for being a role model as a methodical, robust, original scientist – while remaining humble and down-to-earth. You were, and still are, my best "partner in crime".

From that same era, my gratitude also goes to Judith Howard - for "breaking me into" scientific writing, for all the constructive critique (which I won't cite here), and for helping me navigate the strange world of scientific jargon and how things should be said. Thank you, too, for the flash introduction to statistical analysis, it looked like magic at the time, and let's not forget all the Monacos and Hoegaardens we drank at the Big Ben.

Tracing back even further, I remember stepping into the Immunology Department of my original Alma Mater, Trakia University, and meeting Evgeni Slavov and Petko Dzhelebov. You introduced me to veterinary science, experimental design, and the art of presenting findings. I'm not sure how helpful the 18-year-old version of me really was, but that early experience left a lasting impression and influenced the path I've taken ever since.

I feel incredibly lucky to have had three exceptional supervisors. John Monday - for your unwavering support and advice, for always being available, for leading with a collaborative spirit, for not letting me take shortcuts, and (crucially) for reading everything I sent at lightning speed. Neroli Thomson - for pulling me out of the muddiest points in the thesis, for your clear explanations and guidance through the trickiest parts of the project, for your brilliance, your fresh insights, and, of course, for all our productive PhD meetings at the climbing wall. Nick Cave - for your sharp scientific thinking and critical eye, for encouraging my first wobbly steps into statistics, and for the many entertaining tangents during meetings.

Rebeca Owen - thank you for being such a steady presence in my professional life. Your energy never fades. You always catch me before I make a faux pas, and your clear, no-nonsense approach to design and implementation has been foundational to this project. Without you, it simply wouldn't have happened.

I'm also grateful to the FNU staff, especially Karin and Rachael - for your help during the thick of data collection, for your advice on subject selection, your deep knowledge and compassion for the research cats, and for all the good humour, life wisdom, and fun.

To my three collaborators - thank you. Hiroki Sano, for your thoughtful contributions on 'all things' anaesthesia, both theoretical and practical. Leonel Londoño, for helping launch the project, for your patience during massive data collection efforts, and for all the fun we shared in New Zealand and beyond. Mitsuhiro Irie, for making the second part of this project possible, for your insights during data interpretation, and for your patience with extended timelines.

A big thank-you goes to the Massey Companion Animal Hospital staff - for helping with data collection, for your understanding during moments when my attention was split, and for your consistent support throughout the tough phases of the project.

Fernando Avendaño - thank you for being by my side, for the encouragement, the space you made for me, and for taking over so many chores (especially in the final stage). And equally, thank you for your input as a scientist - for all the inspiring conversations and the extensive statistical analysis pillow talk (stats look sexier because of you). You made this journey easier, more fun, and full of "bigger picture" questions.

To my unruly, funky, quirky gang of friends - Brian, Mica, Dimitris, Carmen, Tom, Sunny, Flo, Doreen, Sha, Marija, Caroline, Kurt, Dex, and all the others who came and went in NZ - thank you for the deep conversations, the nerdy chats, the joy, the support, and the understanding that can only come from fellow travellers on this kind of path. This experience would have been much lonelier without you.

Megan Jolly - thank you for our honest, supportive, and close friendship. While I've deeply appreciated your brainy input, it's your steady presence that's meant the most.

And lastly, though I'm not sure I'm supposed to do this, I want to thank my PhD project. Thank you for your patience during the weeks (and months) I wasn't there, for catching curveballs, for being flexible. I had a great time. I learned a lot. I became a better scientist through this process - by growing, understanding, and looking forward to what comes next.

Postscript:

It is with sadness that I add this note while making the final revisions to this thesis: Dr. Irie passed away earlier in 2026.

Although he was the collaborator, I knew the least personally, he was perhaps the one who helped me most at a critical stage of this PhD. He generously shared equipment and provided timely, thoughtful expertise that was instrumental to the success of this work. I had hoped that on my next trip to Japan I would have the opportunity to meet him in person and express my sincere gratitude for his confidence in me and his unwavering support of this project.

Dr. Irie, I only wish I had made the time to know you better. It saddens me deeply that we never had the chance to meet. Thank you for your kindness, generosity, and the lasting contribution you made to this work.

Table of contents

Abstract **2**

Preface **3**

Acknowledgements **5**

Table of contents **7**

List of figures **13**

List of tables **17**

List of abbreviations **19**

Chapter I: Literature review **20**

1. Introduction 22
2. History 22
3. Structure and composition 23
   - 3.1. Proteoglycans 24
   - 3.2. Glycosaminoglycans 26
   - 3.3. Glycoproteins 27
   - 3.4. Soluble components 27
   - 3.5. Endothelial glycocalyx thickness 27
   - 3.6. Appraisal of the evidence on composition and structure of the endothelial glycocalyx 28
4. Function 29
   - 4.1. In health 29
   - 4.2. The revised Starling principle 30
   - 4.3. In disease 31
   - 4.4. Appraisal of the evidence on endothelial glycocalyx function 32
5. Strictly experimental methods for assessment of endothelial glycocalyx integrity 34
6. Methods for assessment of endothelial glycocalyx integrity suitable for experimental and clinical settings 34
   - 6.1. Visualization of capillaries and estimation of endothelial glycocalyx thickness 35
     - 6.1.1. Methodology 35
     - 6.1.2. Probe positioning and image acquisition 36
     - 6.1.3. Glycocheck^{TM} analysis quality checks 38
     - 6.1.4. Perfused boundary region – GlycoCheck^{TM} estimation of endothelial glycocalyx thickness 39
     - 6.1.5. Sidestream dark field videomicroscopy and GlycoCheck^{TM} studies in people 41
     - 6.1.6. Sidestream dark field videomicroscopy and GlycoCheck^{TM} studies in animals 44
     - 6.1.7. Associations between different GlycoCheck^{TM} parameters 46

6.1.8. Associations between GlycoCheck™ parameters and packed cell volume 47
6.1.9. Appraisal of Sidestream dark field videomicroscopy and GlycoCheck™ analysis 48
6.2. Measurements of shed endothelial glycocalyx constituents 48
6.2.1. Studies in people 51
6.2.2. Veterinary studies 51
6.2.3. Summary for animal studies 54
6.2.4. Appraisal of measurements of shed EG constituents 54
7. Understanding the endothelial glycocalyx in cats 55
Chapter II: Rapid patient-side evaluation of endothelial glycocalyx thickness in healthy sedated cats using GlycoCheck™ software 58
1. Chapter II preface 59
2. Title page 61
3. Abstract 62
4. Introduction 63
5. Materials and methods 64
5.1. Animals 64
5.2. Sedation and monitoring 65
5.3. Image acquisition 65
5.4. GlycoCheck™ analysis 66
5.5. Statistical analysis 68
6. Results 68
7. Discussion 71
8. Conclusion 74
9. Conflict of Interest 74
10. Funding 74
11. Chapter II Extended implications 75
Chapter III: Validation of a commercial human enzyme-linked immunosorbent assay to measure syndecan-1 (CD138) concentration in feline sera 77
1. Chapter III preface 80
Contribution statement 80
2. Introduction 81
3. Materials and methods 82
3.1. Materials and methods summary 82
3.2. Animals 83
3.3. Sample collection and processing 84

3.4. ELISA assay validation overview 84
3.4.1. Human syndecan-1 (CD138) enzyme-linked immunosorbent assay protocol 84
3.5. Feline recombinant syndecan-1 production 86
3.5.1. Brief overview 86
3.5.2. Technical protocol 90
3.6. Assay-specific validation steps 91
3.6.1. Determining highly reactive and poorly reactive samples 91
3.6.2. Measuring accuracy (or inaccuracy) 91
3.6.3. Measuring precision (or imprecision) 92
3.6.3.2. Between-run variability 93
3.7. Feline syndecan-1 identification steps 93
3.7.1. Immunoprecipitation 93
3.7.2. Sodium Dodecyl Sulfate Polyacrylamide Gel Electrophoresis 95
3.7.3. Mass spectrometry 96
3.8. Statistical analyses 98
4. Results 99
7.1. Feline recombinant syndecan-1 99
7.2. Human syndecan-1 ELISA kit performance 99
7.3. Sodium Dodecyl Sulfate Polyacrylamide Gel Electrophoresis 100
7.4. Mass spectrometry on electrophoresis gel bands 103
7.5. Mass spectrometry on antigen-antibody complexes from ELISA wells 104
5. Discussion 104
5.1. Initial analysis – highly reactive samples, inaccuracy and imprecision 104
5.2. Lack of binding of the ELISA antibody to feline recombinant syndecan-1 105
5.2.1. Type of antibody 105
5.2.2. Syndecan-1 sequence, structure and glycosylation 105
5.3. Identification of the protein binding to the ELISA antibody 106
5.3.1. Immunoprecipitation and mass spectrometry 107
5.4. Appraisal of commercial syndecan-1 ELISA kits for use in cats 107
5.5. Limitations 108
6. Conclusion 109
7. Chapter III extended implications 110
Chapter IV: Immediate effects of an intravenous fluid challenge on the endothelial glycocalyx in healthy anaesthetized cats 111
1. Chapter IV preface 112
2. Title page 114
3. Abstract 115

4. Introduction 116
5. Materials and methods 118
5.1. Study population 118
5.2. Intervention protocol 118
5.3. Image acquisition 118
5.4. GlycoCheck™ analysis 119
5.5. Packed cell volume and total solids 119
5.6. Statistical analysis 120
6. Results 120
7. Discussion 124
8. Conclusion 128
9. Chapter IV extended implications 130
Chapter V: Effects of transient intravascular volume overload on endothelial glycocalyx thickness in healthy anaesthetized cats 131
1. Chapter V preface 132
2. Title page 135
3. Abstract 136
4. Introduction 137
5. Materials and methods 138
5.1. Study population 138
5.2. Intervention protocol 138
5.3. Image acquisition 140
5.4. GlycoCheck™ analysis 140
5.5. Packed cell volume and total solids 141
5.6. Statistical analyses 142
6. Results 142
7. Discussion 147
8. Conclusion 152
9. Conflict of Interest 152
10. Funding 152
11. Chapter V extended implications 153
Chapter VI: Endothelial glycocalyx thickness in cats with naturally occurring trauma or non-traumatic illness – an exploratory study 156
1. Chapter VI preface 157
2. Title page 159
3. Abstract 160

4. Introduction 161
5. Materials and methods 162
5.1. Study population 162
5.2. Data collection 162
5.3. Image acquisition 163
5.4. GlycoCheck™ analysis 163
5.5. Statistical analysis 164
6. Results 165
6.1. Clinical data 165
6.2. GlycoCheck™ data 167
7. Discussion 169
8. Conclusion 174
9. Authors contributions 175
10. Footnotes 175
11. Chapter VI extended implications 176
Chapter VII: General discussion 178
1. Introduction 179
2. Objectives and hypotheses 180
3. Core research findings 181
3.1. Interspecies differences and demographic considerations in GlycoCheck™ analysis 181
3.2. Effects of IV fluids on GlycoCheckTM parameters 182
3.3. Effects of disease on GlycoCheck™ parameters 184
4. Methodological considerations 185
4.1. Lack of validation of a human SDC-1 ELISA assay 185
4.2. Effects of packed cell volume on GlycoCheck™ parameters 186
4.3. Vascular segment count distribution in GlycoCheck™ analysis 187
4.4. Effects of anaesthetics on GlycoCheck™ parameters 187
5. Theoretical and Practical Implications 188
5.1. IV fluids implications 189
5.2. Implications in disease 190
5.3. Methodological implications 191
5.3.1. Endothelial glycocalyx shedding biomarkers 191
5.3.2. Packed cell volume 191
5.3.3. Anaesthetics 191
6. Strengths 192
7. Limitations 192

7.1. Methodological challenges in microvascular research 192
7.2. Project-related limitations 195
7.3 Species-related limitations of the GlycoCheck™ system 196
8. Future Perspectives 197
9. Final Conclusion 199
Annexes 200
Annex I: Chapter II Unformatted statistical report 200
Annex II: Chapter III Unformatted statistical report 279
Annex III: Chapter III Optic density results 283
Annex IV: Chapter IV Unformatted statistical report 295
Annex V: Chapter IV Anaesthetic variable summary statistics 337
Annex VI: Chapter V Unformatted statistical report 339
Annex VII: Chapter VI Unformatted statistical report 384
Annex VIII: Chapter VI Supplementary table 2 452
Annex IX: Statement of Contribution Forms 454
References 458

List of figures

Figure 1.1. The Fåhræus–Lindqvist effect as a first hint to the existence of an endothelial glycocalyx. Larger vessels contain relatively more RBC per volume due to the cell-excluding layer on the surface of the endothelium formed by the endothelial glycocalyx (A); Smaller vessels contain relatively less RBC per volume due to the same layer lining the endothelium. This leads to the observed reduced viscosity in small compared to larger blood vessels (B). 23

Figure 1.2. Schematic diagram of the endothelial surface layer, illustrating the structural relationships between key components. Shown are endothelial cells, membrane-bound proteoglycans and glycoproteins and non-membrane bound elements such as albumin, antithrombin and antioxidants. Proportions are intentionally distorted (e.g. endothelial cells drawn smaller) to emphasize the endothelial glycocalyx components. 24

Figure 1.3. Representative sidestream dark field videomicroscopy images of feline sublingual mucosal capillaries acquired at different sites using the Glycocheck™ recording system. 36

Figure 1.4. Computer interface of the GlycoCheck™ recording system. Video quality checks for motion, light intensity, and focus displayed as horizontal bars to the left of the screen. Images are recorded only when all parameters meet optimal conditions, indicated by the slider falling within the green zone of each bar. Real-time video feed appears in the central area of the screen, while a vertical progress bar on the right indicates the status of image acquisition. Each recording session is technically limited to five minutes. If sufficient images are not acquired within five minutes the recording resumes for additional five minutes. Note: the camera used here had a minor defect, visible as small black lines on the screen, which according to the manufacturer, did not interfere with data processing. 37

Figure 1.5. Sidestream dark field videomicroscopy and GlycoCheck™ images of feline sublingual capillaries without (left) and with (right) overlay of marker lines. Red wavy lines indicate vessel centrelines; green straight lines represent valid vascular segments; yellow straight lines indicate invalid segments excluded from analysis. 38

Figure 1.6. Example of the curve-fitting approach used by GlycoCheck™ software. A sigmoidal regression model is fitted to the normalized intensity profile measured across a vascular segment. The fitted curve is used to determine the median red blood cell column width (Median P50) and the perfused vessel diameter, which are subsequently used to calculate the perfused boundary region (PBR), an inverse estimate of endothelial glycocalyx thickness. 39

Figure 1.7. Schematic representation of the perfused boundary region (PBR) as an inverse estimate of endothelial glycocalyx (EG) thickness. Left: Visualisation of red blood cell (RBC) penetration into the EG layer in vessels with a small (A, healthy thicker EG) versus large (B, damaged thinner EG) PBR.

Right: Corresponding intensity distribution curves of median RBC column widths for small (C) and large (D) PBR. 40

Figure 2.1. Schematic representation of a capillary with endothelium in yellow, endothelial glycocalyx in blue, perfused boundary region in red dashed lines, and erythrocytes in red. Please note that the different components of this cartoon are scaled for emphasis. A. Intact endothelial glycocalyx characterized by a small perfused boundary region. B. Damaged (thinner) endothelial glycocalyx characterized by a large perfused boundary region..... 64

Figure 2.2. Probe positioning of the SDFV camera for GlycoCheck^{TM} analysis. 65

Figure 2.3. Sidestream dark field videomicroscopy image of the sublingual mucosal capillaries in a cat. 66

Figure 3.1. Stepwise diagram of a Sandwich (quantitative) Enzyme-linked Immunosorbent Assay for human Syndecan-1 (CD138) Detection. 85

Figure 3.2. Comparison of feline recombinant, feline native, and human native syndecan-1 proteins. **(A)** Amino acid sequences of the feline recombinant syndecan-1 ectodomain (top), feline native syndecan-1 (UniProt accession M3W3X8; middle), and human native syndecan-1 (UniProt accession P18827; bottom). The recombinant construct comprises the feline ectodomain with a C-terminal His-tag to facilitate purification. **(B)** Schematic comparison of protein domain architecture, demonstrating that the recombinant protein contains only the extracellular domain, whereas the native feline and human proteins also include transmembrane and cytoplasmic domains. **(C)** BLAST sequence alignment between the feline recombinant syndecan-1 (His-tag removed) and the ectodomain of human native syndecan-1. Grey regions indicate conserved amino acid residues, while red regions indicate mismatches. Native feline and human protein sequences were obtained from UniProt. 88

Figure 3.3. Gene sequence used for production of feline recombinant syndencan-1. A – adenine, C – cytosine, G – guanine, T – thymine. 90

Figure 3.4. Purification column using Sodium Dodecyl Sulfate–Polyacrylamide Gel Electrophoresis (SDS-PAGE) with 13% separating gel for feline recombinant syndecan-1 (left, non-reducing (NR) and right, reducing (R) conditions). Purity estimated 94.4%. 91

Figure 3.5. Stepwise diagram of an immunoprecipitation (“pull down”) assay with magnetic beads used to isolate the presumed feline SDC-1 antigen-antibody complex from other antigens..... 94

Figure 3.6. Amino acid sequence alignment of syndecan-1 from Felis catus (Query) and Homo sapiens (Subject). The alignment demonstrates high homology, with 81% identical residues and 87% similarity. Red arrows indicate predicted trypsin cleavage sites with >50% probability. Predicted glycosylation sites are highlighted in green, and phosphorylation sites in cyan. 97

Figure 3.7. Comparison of optical density across presumably feline syndecan-1 concentrations for dilutional linearity (navy), parallelism (red), and the standard curve (grey). Navy squares and red triangles represent each two-fold dilution up to the seventh dilution for dilutional linearity and parallelism, respectively. 100

Figure 3.8. Sodium dodecyl sulfate–polyacrylamide gel electrophoresis (SDS-PAGE) analysis of recombinant syndecan-1 proteins, controls, and selected feline serum samples under reducing conditions. The green arrow indicates the ~30 kilodalton (kDa) protein band excised for mass spectrometry analysis. Lane assignments: 1 and 12, PageRuler Plus Prestained Protein Ladder; 2, human recombinant syndecan-1; 3, feline recombinant syndecan-1 (frSDC-1); 4, beads-only control; 5, empty; 6, Non-biotinylated anti-syndecan-1 antibody (Anti-Syndecan-1 antibody [SP152], ab130405, Abcam Ltd); 7, Serum 2 (highly reactive, two-fold dilution); 8, Serum 4 (poorly reactive, 10-fold dilution); 9, Serum 4 (poorly reactive, two-fold dilution); 10, Serum 1 (highly reactive, two-fold dilution); 11, Serum 1 (highly reactive, 10-fold dilution). Samples were denatured in lithium dodecyl sulfate (LDS) sample buffer containing 50 millimolar (mM) dithiothreitol (DTT), separated on 12% bis(tris) polyacrylamide gels using 2-(N-morpholino) ethanesulfonic acid (MES)-sodium dodecyl sulfate (SDS) running buffer at 100 V for 100 min, stained with SimplyBlue SafeStain, and imaged using a ChemiDoc MP imaging system. Apparent molecular sizes are shown on either side of the gel. 102

Figure 3.9. Chromatographic comparison of sample peaks to the bovine serum albumin (BSA) digestion control. Traces represent results from the ~30 kDa band (black), ~50 kDa band (red), ~75 kDa band (green), and BSA control (blue). Note the sparse and low-intensity peaks in all sample traces compared to the dense peak pattern of the BSA control, suggesting low protein concentration in the samples. 103

Figure 4.1. Perfused Boundary Region (PBR) measurements over time across different vessel diameter classes in cats receiving a fluid challenge with either a synthetic colloid (HES), a balanced isotonic crystalloid (CRYS), or no fluid (Control). Each panel shows mean ± standard error (SE) values for: (A) PBR 5–25 µm, (B) PBR 5–9 µm, (C) PBR 10–19 µm, and (D) PBR 20–25 µm. Dashed horizontal lines represent the upper and lower tolerance interval limits for each parameter. Data points were collected at baseline (0 min), 10 min, and 20 min (end of infusion). 122

Figure 5.1. Intervention protocol timeline for a crossover study involving 20 healthy anaesthetized cats, randomised to receive either 30 mL/kg of Hartmann's solution over 10 minutes (volume overload group) or no fluids (control group), with a 7-day washout period between interventions. 139

Figure 5.2. Sidestream dark field videomicroscopy and GlycoCheck™ images of feline sublingual capillaries without (A) and with (B) marker lines indicating vascular segments. Red wavy lines represent vascular segments, green straight lines indicate valid segments, and yellow straight lines denote invalid segments. 141

Figure 5.3. Changes in perfused boundary regions over time in vessels with diameters of 5–25 µm (A), 5–9 µm (B), 10–19 µm (C), and 20–25 µm (D) in 20 healthy anaesthetized cats with transient volume overload (navy circles) or control (red triangles), measured at four timepoints over 24 hours: T0 (baseline), T1 (10 min), T2 (3 h), and T3 (24 h). 144

Figure 5.4. Distribution of major vascular segment counts by vessel diameter (5–25 µm) in healthy anaesthetized cats. Bars represent the number of valid vascular segments identified per diameter subgroup using GlycoCheck™ analysis. Vertical dashed lines separate the predefined vessel size categories: 5–9 µm, 10–19 µm, and 20–25 µm. 145

Figure 5.5. Pie chart showing the distribution of vascular segment counts across vessel diameter subgroups: 5–9 µm (navy), 10–19 µm (red), and 20–25 µm (yellow). 145

Figure 5.6. Changes in packed cell volume (A) and total solids (B) over time in 20 healthy anaesthetized cats with transient volume overload (navy circles) or control (red triangles), measured at four timepoints over 24 hours: T0 (baseline), T1 (10 min), T2 (3 h), and T3 (24 h). 146

Figure 5.7. Changes in PBR 5 – 25 µm over time per group for individual cats. 155

Figure 6.1. Sidestream dark field videomicroscopy image obtained from the sublingual region of a cat with trauma (A) and with sepsis (B). Capillaries appear dark on a bright background. 163

Figure 6.2. Distribution of major vascular segment counts by vessel diameter (5–25 µm) as measured using GlycoCheck™ analysis in 19 cats with naturally occurring disease (trauma, n = 10; non-traumatic illness, n = 9). Bars represent the number of valid vascular segments identified per diameter subgroup. Vertical dashed lines separate the predefined vessel size categories: 5–9 µm, 10–19 µm, and 20–25 µm. 168

Figure 6.3. Pie chart showing the distribution of vascular segment counts by diameter subgroup: 5–9 µm (navy), 10–19 µm (red), and 20–25 µm (yellow)..... 169

Figure 7.1. Roadmap to future feline endothelial glycocalyx studies. 198

List of tables

Table 1.1. Overview of GlycoCheck™ output parameters and their interpretation. 40

Table 1.2. Summary of endothelial glycocalyx biomarker origin and characteristics. 49

Table 2.1. Description and interpretation of GlycoCheck™ parameters. 67

Table 2.2 Summary statistics for anaesthetic monitoring variables in 101 healthy sedated cats undergoing GlycoCheck™ analysis 68

Table 2.3. GlycoCheck™ parameters in a population of healthy cats (n = 101). 69

Table 2.4. Tolerance Intervals for GlycoCheck™ parameters in a population of healthy cats (n = 101). 70

Table 2.5. Variance Component Estimates for GlycoCheck™ parameters in a population of healthy cats (n = 101) 70

Table 2.6. Comparison of GlycoCheck™ parameters in cats, dogs and people expressed as Mean ± Standard Deviation 71

Table 3.1. Sample Processing Details for Syndecan-1 Mass Spectrometry 98

Table 3.2. Summary statistics for performance variables assessed during the validation of a human syndecan-1 enzyme-linked immunosorbent assay (ELISA) for use in feline serum. Variables include within- and between-run variability, dilutional linearity, and parallelism, expressed in both optical density and calculated presumably feline syndecan-1 concentrations (ng/mL). 99

Table 4.1. Summary statistics for Glycocheck™ parameters, packed cell volume and total tolids in 29 healthy male neutered cats receiving a fluid challenge (Hartman's solution or Hydroxyethyl starch) or not (control). 121

Table 5.1. GlycoCheck™ parameters in 20 healthy anaesthetized cats subjected to transient volume overload (30 mL/kg Hartmann's solution over 10 minutes) or control (no intravenous fluids), measured at four timepoints over 24 hours*. 143

Table 5.2. Correlation between packed cell volume and GlycoCheck™ parameters using Pearson's test (except for perfused boundary region 20 – 25 µm*). 147

Table 5.3. Within-subject baseline variability from random intercepts standard deviation 154

Table 6.1. Individual patient data: diagnoses, outcomes, severity of illness scores, and selected clinical variables. 165

Table 6.2. Demographic and clinical variables for 11 cats with trauma and eight cats with non-traumatic disease enrolled for GlycoCheck™ analysis 166

Table 6.3. GlycoCheck™ parameters for 10 cats with trauma and nine cats with non-traumatic disease compared to previously established tolerance intervals. 167

Table 6.4. Sample size estimates required to detect associations between PBR 5–25 µm and selected clinical variables in linear models with a single predictor. Calculations assume a power of 0.80 and a significance level of 0.05. Effect sizes are expressed as model R^2 and corresponding Cohen's f^2. Total sample size indicates the estimated number of subjects needed; the number of observations reflects the current dataset. 168

List of abbreviations

%RBC filling	Percentage red blood cell filling
ANP	Atrial natriuretic peptide
APPLEfast	Acute Patient Physiologic and Laboratory Evaluation (fast)
ATT	Animal Trauma Triage (score)
COP	Colloid osmotic pressure
CRI	Continuous rate infusion
CS	Chondroitin sulfate
DL	Dilutional linearity
Dperf	Perfused diameter
EG	Endothelial glycocalyx
ELISA	Enzyme-linked immunosorbent assay
ESL	Endothelial surface layer
GAG	Glycosaminoglycans
GP	Glycoproteins
HA	Hyaluronan
HES	Hydroxyethyl starch
HS	Heparan sulfate
IV	Intravenous
Median P50	Median red blood cell column width
MMP	Matrix metalloproteinases
NO	Nitric oxide
NP	Natriuretic peptides
NSAIDs	Non-steroidal anti-inflammatory drugs
PBR	Perfused boundary region
PCV	Packed cell volume
PG	Proteoglycans
PO	Per Os (by mouth)
RBC	Red blood cells
ROS	Reactive oxygen species
SDS-PAGE	Sodium Dodecyl Sulfate Polyacrylamide Gel Electrophoresis
SC	Sub-cutaneous
SD	Standard deviation
SDC-1	Syndecan-1
SDFV	Sidestream dark field videomicroscopy
TBI	Traumatic brain injury
TNF- α	Tumour Necrosis Factor-α
TS	Total solids
VO	Volume overload
VVD	Valid vessel density
VVS	Valid vascular segments

Chapter I: Literature review

Chapter plan

1. Introduction

2. History

3. Structure and Composition

3.1. Proteoglycans

3.2. Glycosaminoglycans

3.3. Glycoproteins

3.4. Soluble components

3.5. Endothelial glycocalyx thickness

3.6. Appraisal of the evidence

4. Function

4.1. In health

4.2. The revised Starling principle

4.3. In disease

4.4. Appraisal of the evidence

5. Strictly experimental methods for assessment of endothelial glycocalyx integrity

6. Methods for assessment of endothelial glycocalyx integrity suitable for the experimental and clinical settings

6.1. Visualization of capillaries and estimation of endothelial glycocalyx thickness

6.1.1. Methodology

6.1.2. Probe positioning and image acquisition

6.1.3. Glycocheck^{TM} analysis quality checks

6.1.4. Perfused boundary region – GlycoCheck^{TM} estimation of endothelial glycocalyx thickness

6.1.5. Sidestream dark field videomicroscopy and GlycoCheck^{TM} studies in people

6.1.5.1. Heathy subjects and repeatability studies
6.1.5.2. Interventions on healthy subjects
6.1.5.3. Sick patients and patients at risk of microcirculatory dysfunction

6.1.6. Sidestream dark field videomicroscopy and GlycoCheck^{TM} studies in animals

6.1.7. Associations between different GlycoCheck^{TM} parameters

6.1.8. Associations between GlycoCheckTM parameters and packed cell volume

6.1.9. Appraisal of Sidestream dark field videomicroscopy and GlycoCheckTM analysis

6.2. Measurement of shed endothelial glycocalyx constituents

6.2.1. Studies in people

6.2.2. Veterinary studies

6.2.2.1. Cats
6.2.2.2. Dogs
6.2.2.3. Horses

6.2.3. Summary for animal studies

6.2.4. Appraisal of measurements of shed EG constituents

7. Understanding the endothelial glycocalyx in cats

1. Introduction

Aerobic cells require a continuous supply of oxygen and nutrients to survive. In single-celled organisms, this exchange occurs directly across the cell membrane, with nutrients readily absorbed and waste products expelled into the surrounding environment. In contrast, the cells of multicellular organisms, such as mammals, depend on complex physiological systems, including respiration and circulation, to achieve the same outcome. In mammals, oxygen delivery begins with pulmonary ventilation and diffusion across alveolar-capillary membranes, where oxygen binds to haemoglobin within red blood cells (RBCs), with a small portion remaining dissolved in plasma. Oxygen is then transported through a hierarchical vascular network, from large vessels to capillaries, to reach individual tissues (35).

Regulation of vascular function occurs at multiple levels: large vessels are primarily controlled by central mechanisms and systemic hormones, while the microcirculation operates under more localised, tissue-specific regulation.

Importantly, while a failure of macrocirculatory supply inevitably disrupts tissue perfusion, we now recognise that adequate macrocirculatory function does not guarantee effective oxygen delivery at the microcirculatory level. The microvasculature, due to its specialised structure and local control mechanisms, can fail independently resulting in impaired oxygen and nutrient exchange, even in the presence of normal systemic haemodynamics.

The microcirculation is the terminal vascular network of the systemic circulation consisting of microvessels with diameters <20 μm (36). It is increasingly recognised as a central player in the disruption of oxygen delivery during critical illness, contributing directly to cellular dysfunction, multi-organ failure, and death (37). The endothelial surface layer, which coats the luminal side of blood vessels, and particularly the endothelial glycocalyx (EG), has emerged as a key functional structure (38). The EG plays an essential role in regulating vascular permeability, facilitating cell-to-cell signalling, modulating local blood flow, and coordinating inflammatory and coagulation responses (39). As a result, the EG has received significant research attention, focusing on understanding its complex dynamic structure, functions, alterations in disease states and systemic consequences.

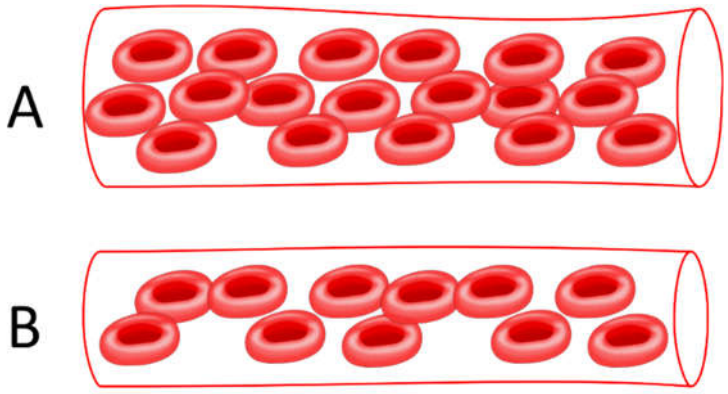
This literature review presents an overview of current knowledge on EG structure and function, with particular emphasis on methods used to assess its integrity in both humans and other animal species. It critically appraises the existing body of evidence and highlights key knowledge gaps that have shaped the rationale for the present PhD project. Before delving further, a brief look at the history of the EG helps frame its scientific journey.

2. History

The existence of the EG has been hypothesized since 1931 when Swedish scientists observed a decrease in blood viscosity in association with a decrease in capillary diameter. This phenomenon, now known as the Fåhræus–Lindqvist effect (40) (Figure 1.1), was attributed to the migration of RBC

towards the centre of the vessel, leaving a cell-free plasma layer near the wall. This cell-free plasma layer remains relatively constant in thickness regardless of vessel diameter, resulting in a reduced ratio of RBC to plasma in small blood vessels. Since blood viscosity is primarily determined by the presence of RBC, this reduced ratio could explain the observed decrease in viscosity within vessels.

Figure 1.1. The Fåhræus–Lindqvist effect as a first hint to the existence of an endothelial glycocalyx. Larger vessels contain relatively more RBC per volume due to the cell-excluding layer on the surface of the endothelium formed by the endothelial glycocalyx (A); Smaller vessels contain relatively less RBC per volume due to the same layer lining the endothelium. This leads to the observed reduced viscosity in small compared to larger blood vessels (B).



In the 1940s, the concept of a non-cellular immobile plasma layer capable of absorbing plasma proteins was introduced (41, 42). At the time, direct visualisation of that layer was not possible. However, in subsequent experiments using frog mesentery stained with Evans blue, a dye with high affinity for albumin - "thin strands and sheets of a faintly coloured blue, translucent material … sloughing off the inner surface of the capillary" were observed (42).

By the 1960s, advances in light and electron microscopy, along with the development of specific stains, finally enabled visualization of the EG. In 1963 it was noted that all cells are covered with an extracellular polysaccharide layer and the term glycocalyx (from Greek "γλυκός" – sweet and "καλύψω" – to cover, husk) was proposed by Bennet et al (43). In 1966, Luft used transmission electron microscopy and a cationic stain with high affinity for acidic mucopolysaccharides (ruthenium red), to study the endothelial surface, demonstrating the presence of the EG (44).

3. Structure and composition

The EG is a carbohydrate-rich layer lining the luminal surface of all mammalian vessels (45). It is a dynamic structure, maintained in a delicate equilibrium between shedding, synthesis and incorporation of various components. The EG is primarily composed of membrane-bound proteoglycans (PGs) which provide structural scaffolding, glycoproteins (GPs), which often act as

docking sites for signalling molecules, and glycosaminoglycans (GAGs) forming the side chains of PGs. In addition to those structural components, the EG contains numerous soluble elements, either bound or flowing freely through its meshwork - such as albumin, antithrombin, additional GAGs and various antioxidants. Viewed this way, the EG may be best understood as a constantly self-assembling three-dimensional mesh of polysaccharides and associated molecules (Figure 1.2) (46, 47). The PGs, GPs, GAGs, soluble constituents and fluid within the EG form what is known as the endothelial surface layer (ESL) (38).

Figure 1.2. Schematic diagram of the endothelial surface layer, illustrating the structural relationships between key components. Shown are endothelial cells, membrane-bound proteoglycans and glycoproteins and non-membrane bound elements such as albumin, antithrombin and antioxidants. Proportions are intentionally distorted (e.g. endothelial cells drawn smaller) to emphasize the endothelial glycocalyx components.

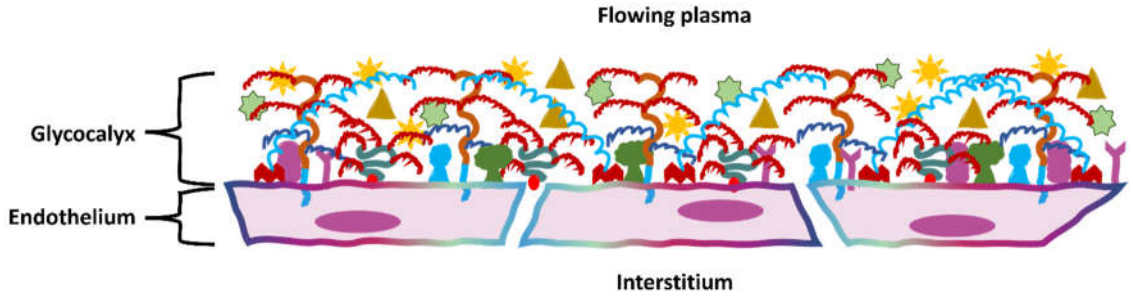
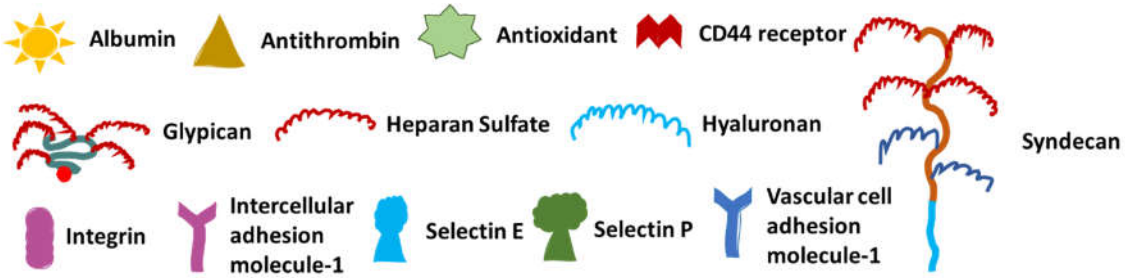


Figure 1.2 Legend



The following sections do not attempt to capture all components of the EG or the full complexity of their interactions. Rather, they provide a focused overview of the main structural and functional players most relevant to the context of this thesis. These elements form a dynamic and responsive network, with each component contributing to the EG's role in vascular integrity, inflammation, coagulation, and signalling. The aim here is not to be exhaustive, but to highlight the building blocks that contribute to the structural and functional shifts of the EG in health and disease.

3.1. Proteoglycans

Membrane-bound proteoglycans (PGs) produced by the endothelial cells form the "backbone" of the EG (38). They consist of a core protein, that binds to GAG side chains , which help maintain the

integrity of the meshwork (46). Proteoglycans typically have a long core protein with short unbranched GAGs attached (38). There are two main families of PGs found within the EG: syndecans and glypicans.

The word "syndecan" comes from the Greek word "συνδέω" (sundéō, "bind together") (48). Syndecans are not unique to the EG – they are found on most vertebrate cell surfaces (49). They are transmembrane molecules, composed of a cytosolic, transmembrane, and extracellular domains (or ectodomains). The transmembrane domain is a signature domain. However, both the cytosolic and transmembrane domains are highly homologous among different syndecans and between species (50). Heparan sulfate is the predominant GAG found in syndecans, though chondroitin sulfate (CS) is also present (51). For this reason, syndecans are also known as heparan sulfate PGs. Heparan sulfate chains attach to the extracellular domain distal to the cell membrane, contributing to structural diversity and glycosylation (52). Furthermore, the extracellular domain contains a dibasic cleavage site at which the molecule can be detached from the cell surface by proteases (53, 54). This is relevant during inflammation, as increased activity of proteases stimulated by cytokines, contributes to increased syndecans shedding (55).

There are four groups of syndecans - 1, 2, 3 and 4 (49). Their expression varies by tissue: syndecan-1 (SDC-1) is found mostly in epithelial cells (including the endothelial cells) and plasma cells; syndecan-2 in endothelial cells and fibroblasts; syndecan-3 in the nervous system; and syndecan-4 is more universally expressed in smaller amounts (49, 51, 55, 56). Notably, syndecans can be synthetized de novo in response to stimuli (such as inflammation), even in tissues where baseline expression is low (47, 49, 55, 56). Syndecan-1 is the most studied PG in relation to the endothelium.

Syndecan-1 (cluster of differentiation 138, CD138) is involved in numerous physiological processes both during foetal development and in adult tissues (49). As mentioned above, SDC-1 serves as a major structural component of the EG (57). In addition, SDC-1 acts as a mechanotransducer, responding to sheer stress from the blood flow (58). One proposed model, the "bumper car" model, suggests that mechanical forces from the bloodstream are transmitted to the core protein of SDC-1, rather than directly to the endothelial cell surface. This activates intracellular signalling pathways, triggering cytoskeletal rearrangement reinforcing cell-to-cell junctions - similar to how a car bumper absorbs impact to protect the rest of the vehicle (59).

Syndecan-1 also appears to regulate leukocyte adhesion, by inhibiting interactions with endothelial cell receptors: P- and E-selectin and adhesion molecules: intercellular adhesion molecule-1 and vascular cell adhesion molecule11 (50, 55). This supports the assumption that as part of the ESL, SDC-1 exerts anti-inflammatory effects. The deliberate removal of SDC-1 from the endothelial surface during inflammation may be a physiological mechanism to facilitate leukocyte adhesion and promote a local inflammatory response and tissue repair. However, during systemic inflammation, widespread EG degradation and shedding of components like SDC-1 can become maladaptive. Soluble SDC-1 levels increase during inflammation (49), likely due to enzymatic cleavage by matrix metalloproteinases (60). Once in the circulation, soluble SDC-1 may further perpetuate inflammation (56). This is primarily

through its HS side chains, which act as damage-associated molecular patterns, stimulating cytokine release and the amplifying the inflammatory cascade (61). Interestingly, expression of SDC-1 also increases during tissue repair following inflammation-induced injury (49, 50, 62).

Glypicans form another family of PGs. They are not transmembrane proteins but are instead anchored to the endothelial membrane via a glycosyl phosphatidylinositol link (53). Glypicans carry only HS GAGs (53). From the six glypicans found in mammalian tissues, glypican-1 is expressed on the endothelium (46, 63). Like SDC-1, glypican-1 is involved in a range of signalling pathways and contributes to mechanotransduction response to shear stress. However, unlike SDC-1, glypican-1 appears to promote nitric oxide production from the endothelial cells, resulting in vasodilation (49, 53, 63).

3.2. Glycosaminoglycans

Glycosaminoglycans are polysaccharides composed of unbranched chains of 20 to 200 repeating disaccharide units (49). As the only side chain extending from the core protein of PG, they are largely responsible for the mesh-like structure of the EG. Five different GAGs can be found in the EG: HS, CS, dermatan sulfate, keratin sulfate and hyaluronan (HA). These molecules are not exclusive to the EG and are present in other tissues – for example, the interstitium, is particularly abundant in HA (64). Glycosaminoglycans are not evenly distributed within the EG (65). Heparan sulphate is considered most abundant, accounting for approximately 50-90% of the GAG side chains (62). The roles of GAGs also differ. Heparan sulfate tends to be located towards the luminal surface of the EG, a positioning reflecting its primary structural function (66). Bound HS appears to protect SDC-1 from excessive cleavage at its extracellular domain and subsequent shedding (66), further supporting the idea of HS playing a key stabilizing role. The loss of HS not only compromises the structural integrity of the EG, but – as discussed earlier, soluble HS contributes to the amplification of inflammation (56, 61).

In contrast, HA and CS are found closer to the endothelial surface and are thought to play a more prominent role in regulating vascular permeability (66). Hyaluronan is a larger GAG and unlike others, is not bound to a PG but instead attaches directly on the cell surface via its receptor CD44 (67, 68). These loose attachments might explain why plasma HA levels peak earlier than other EG components following an insult (58).

The GAG side chains offer numerous protein-binding sites (49). These sites determine the unique functions of PGs in cell signalling and cell-to-cell interactions and structural changes within the EG in response to stimuli such as heparinase and matrix metalloproteases (produced during sepsis) as well as atrial natriuretic peptide (released during volume overload) (45, 46). Due to the abundance of highly sulphated GAGs, the EG carries a strong overall negative charge. This contributes to its barrier function, by forming an exclusion layer that repels negatively charged molecules (45).

3.3. Glycoproteins

Closer to the endothelial surface, "sheltered" by the PGs, GPs can be found. These are relatively smaller, membrane-bound proteins with shorter and more branched GAG side chains than those of PGs (46). Glycoproteins include members of the extensively studied selectin, integrin and immunoglobulin families, all of which are involved with cellular signalling, particularly in coagulation and inflammation (69). Within the EG, P- and E-selectin are the primary selectins and are mainly involved in leukocyte and platelet adhesion (69). Integrins are found on a range of cells, including leukocytes, platelets, and endothelial cells, and are also important in mediating cell attachment to the endothelium (70). Immunoglobulin superfamily members, intercellular adhesion molecule-1 and vascular cell adhesion molecule-1 are expressed on the EG and contribute to regulation of leukocyte adhesion and transmigration between endothelial cells (69). While some GPs are continuously expressed on the endothelial surface, others are upregulated in response to cell activation, adding to the dynamic nature of the EG structure (46, 47).

Many structural components of the EG, including PGs, GPs, and GAGs have been studied as potential biomarkers for EG injury by measuring their concentrations in the plasma. The most commonly used biomarkers for structural EG damage are SDC-1, HS and HA, with SDC-1 being the most studied.

3.4. Soluble components

Non-membrane bound constituents such as albumin, antithrombin, superoxide dismutase (antioxidant) and confined GAGs contribute to its barrier, anticoagulant function and structural stability of the EG (45, 46). Albumin helps establish a colloid osmotic pressure (COP) gradient across the EG and sub-glycocalyx space, thereby minimizing fluid filtration through the vascular wall (71). It also acts as a "binding agent" for GAG chains, stabilizing the EG scaffold (72). The protective role of albumin is believed to be related to the effects of sphingosine-1-phosphate, a signalling molecule it carries (73). These effects have been demonstrated in experimental models and are particularly relevant in critical care settings where hypoalbuminemia is common (57).

Antithrombin is a potent anti-coagulant that enhances the activity of heparin by up to 1000-fold. Its presence within the EG prevents excessive coagulation and therefore potential microthrombus formation. In addition, antithrombin appears to exert a protective effect on the EG, as suggested by experimental models of sepsis and ischemia-reperfusion injury (74, 75).

Superoxide dismutase, an antioxidant, scavenges reactive oxygen species that damage PGs and GPs (76).

3.5. Endothelial glycocalyx thickness

The overall range in reported EG thickness, based various methodologies is approximately 0.5 – 5 μm (45). However, even with current technologies, including advanced imaging techniques such as

transmission and scanning electron microscopy, visualization and accurate assessment of EG thickness remains technically challenging (77). These methods require intravenous fixation of the entire specimen (organ, animal) and the use of specific stains (e.g. lanthanum) to create the electron-dense contrast needed for visualization. As a result, EG thickness is predominantly studied *in vitro* or *ex vivo.*

Nonetheless, studies have shown that EG dimensions differ between *in vitro* and *in vivo* conditions, making extrapolations problematic (78). The wide range of EG thickness reported across the literature likely reflects differences in methodological approaches – including various microscopy techniques, indirect estimations using tracer molecules and mathematical modelling (79-84). Additional variability may result from physiological differences in EG thickness between vessels in different tissues or between individuals (78, 82, 85-87).

Recent advances in intravital microscopy have enabled *in vivo* visualization of the EG (83, 88). Furthermore, Sidestream dark field videomicroscopy (SDFV) combined with proprietary software (GlycoCheck^{TM})(89) allows for evaluation of capillary beds and real-time estimation of EG thickness (90). This method calculates the *perfused boundary region* (PBR), a parameter inversely related to EG thickness, and has been reported in healthy people (90-92), dogs (93-95), rabbits (96-99) and (from this project) cats (100). While this methodology holds promise in clinical settings, a key limitation for any intravital microscopy method is that they are restricted to superficial vessels. Therefore, methodological differences and vascular-specific variation in EG thickness must be carefully considered when interpreting study results.

3.6. Appraisal of the evidence on composition and structure of the endothelial glycocalyx

Numerous studies have investigated the composition and structure of the EG and this literature review does not aim to capture their entirety. Notably, there are some weaknesses and gaps in the current literature, that merit mention.

The experimental approaches have employed a variety of techniques, including specific staining (86, 101-104), effects of enzymatic degradation (66, 105, 106), immunohistochemistry (75, 107, 108), and immunofluorescence, intravital (85, 109) and confocal microscopy (59, 110, 111) among others. These studies have primarily been conducted *in vitro* in cell cultures, *ex vivo* in isolated vessels or organs, and occasionally, in animal models. As a result, little is known about the true composition of the EG *in vivo*. Given the dynamic nature of the EG, including stimulus-dependent changes in expression of components, turnover and variations across vascular beds, extrapolations from *in vitro* or *ex vivo* models to the "living EG" should be made with caution. Nonetheless, such extrapolations are common and may contribute to the persistent discrepancies observed between experimental and clinical findings.

Indeed, results from experimental studies have often been synthetized in a number of review articles, offering a general overview of building blocks and dynamic architecture of the EG (35, 38, 45,

46, 49, 50, 52, 54-58, 61, 62, 67, 68, 77, 112-129). These reviews also frequently explore potential mechanisms by which the EG exerts its diverse physiological functions, drawing on amalgamated experimental findings from multiple species, including people and small animals, and often presenting confident associations between these mechanisms and clinical observations, diagnostic approaches and therapeutic strategies. For example, the evolving understanding of the EG has influenced intravenous fluid administration practices, largely based on theoretical frameworks and experimental data rather than direct clinical evidence (71, 112, 113, 118, 119, 124).

Beyond the limitations of experimental models in guiding clinical applications of EG-related findings, there are also challenges inherent to the EG itself that complicate extrapolations between species. While some components of the EG are conserved across species, others are species-specific (49). For example, the transmembrane and intracellular domains of syndecans are highly conserved across species, while the extracellular is not (49). Moreover, there is growing evidence that the EG structure and potentially function, varies depending on the location on the endothelial surface (luminal vs non-luminal) (49) and between vascular beds of different organs (86). This further complicates the interpretation of localized observations when attempting to draw conclusions about systemic changes.

Since its relatively recent discovery, the scientific interest in the EG has increased exponentially. Nonetheless, substantial knowledge gaps remain regarding species- and even tissue-specific features of the EG, and this continues to limit translation in the clinical setting. This highlights the need to explore the EG in target species of scientific interest with study designs tailored to their specific physiological and pathophysiological features. For example, while the impact IV fluid administration on the EG in people appears limited, the outcome may differ in a species inherently predisposed to intravascular volume overload and fluid overload such as the cat (130, 131).

4. Function

With its structural complexity, the EG plays a critical role in maintaining vascular homeostasis. It serves as a dynamic interface between circulating blood and the endothelium, contributing to a wide range of physiological processes. These include the regulation of vascular permeability, modulation of inflammation and coagulation, mechanotransduction of shear stress, and the facilitation of microvascular perfusion. The EG also influences cell-cell interactions by regulating leukocyte and platelet adhesion. Together, these functions position the EG as a central player in both local and systemic vascular responses, with its dysfunction contributing to the pathophysiology of numerous disease states. This section focuses on the key functions of the EG in health and disease.

4.1. In health

The EG is often regarded as the sentinel of the endothelium and underlying tissues. Its overall negative charge forms an exclusion layer against other negatively charged molecules. In addition, its fine mesh-like structure limits the passage of large molecules across the endothelium, making it a key determinant of vascular permeability (38, 45). The EG also modulates blood cell-vascular wall

interactions: in health it repels RBC, platelets and leucocytes, while in disease states, it stimulates platelet and leucocyte adhesion.

Beyond acting as a passive barrier, the EG functions as a mechanotransducer, converting shear stress from blood flow into signals within the endothelial cells. This stimulates nitric oxide (NO) production and endothelial cytoskeletal reorganization, resulting in vasodilation particularly in small vessels, thereby enhancing tissue-level perfusion (46).

The variety of GAG side chains provides numerous docking sites for plasma-derived molecules influencing the local environment of the EG. Adequate concentrations of molecules such as integrins and selectins enables effective signalling and receptor binding, particularly in relation to inflammation and coagulation pathways. When present in sufficient amounts, other molecules, including anticoagulants and albumin enhance the protective functions of the EG, by stabilizing its structure, generating COP gradients to limit fluid extravasation and preventing thrombosis (46).

4.2. The revised Starling principle

The discovery of the EG and its many roles has prompted a revision of one of the most deeply imbedded concepts in vascular physiology: the Starling principle (46, 71, 119, 132). In 1896, Ernest Henry Starling stipulated that transvascular exchange occurs as a balance between hydrostatic and oncotic pressure gradients. According to his model, fluid is filtered to the interstitial space under a the influence of a dominant hydrostatic pressure gradient at the arteriolar end of capillaries and reabsorbed at the venous end, where COP is assumed to be predominant (132, 133).

However, several physiological observations contradict the classical Starling principle. More recent studies have demonstrated that, in most tissues under steady-state conditions, reabsorption does not occur in the venous capillary bed (71). Instead, fluid is continuously filtered throughout the capillary bed and excess is returned to the circulation via the lymphatic system. Reabsorption appears to occur only transiently, in response to acute hypovolemia when capillary pressure is abruptly lowered. Moreover, the present of significant amounts of protein in the interstitial space challenges the assumptions underlying the original equation. Namely that reabsorption is drive by the relatively higher COP in the vessel compared to the interstitium (71, 124, 132).

The so called “COP paradox” further challenges the classical Starling principle. While “physiological” levels of intravascular COP are theoretically necessary to prevent fluid extravasation, both experimental and clinical studies have shown that even sub-physiological concentrations of albumin (which contributes to 80% of COP) can effectively limit fluid loss, regardless of their COP effect (132). This has been attributed to the interaction between albumin and the intact EG, which helps maintain vascular barrier integrity (71).

These insights led to the development of the *revised Starling principle*, which largely dismisses the role of interstitial COP in fluid exchange. Instead, it proposes that the effective oncotic gradient opposing fluid filtration is created between the intravascular space and a virtually protein-free sub-

glycocalyx space (119). Because proteins, especially albumin, are retained within the EG, the sub-glycocalyx space has a virtually non-existent COP. In addition, the tight endothelial junctions syphon proteins away from this area (71, 124). Some authors suggest that the critical oncotic gradient is actually between the COP within the EG and that of the sub-glycocalyx area, with plasma albumin serving primarily as a reservoir (46). In this model, actual fluid filtration is determined almost entirely by the capillary hydrostatic pressure (119).

This paradigm shift has important clinical applications, particularly for IV fluid administration (119). In hypovolemia, where capillary hydrostatic pressure is reduced, any intravenous fluid (whether crystalloid or colloid) can contribute to volume expansion (71). However, in disease states that involve EG disruption, patients are more susceptible to fluid extravasation, interstitial oedema, decreased oxygen delivery to tissues and resulting multi-organ disfunction, complications that could be exacerbated by excessive IV fluid administration (35). As a result of the revised Starling principle among other insights in peri-operative critical care, IV fluid administration has shifted from liberal to rational and in some settings restrictive in the past three decades (124, 134, 135). Intravascular fluids are now recognised as drugs with indications, contraindications and side effects (136). Concepts such as resuscitation, optimization, stabilisation, elimination, aimed to minimize unnecessary IV fluid administration, are currently applied in human medicine and to some extend in veterinary practice (137, 138).

4.3. In disease

Systemic inflammatory states such as sepsis, severe trauma, and ischemia reperfusion injury cause damage to the EG. The underlying mechanisms are multifactorial. One of the major cytokines triggering the inflammatory response is Tumour Necrosis Factor-α (TNF- α). Tumour Necrosis Factor-α induces upregulation of heparinase, which cleaves heparan sulphate GAGs from the PGs. It also stimulates reactive oxygen species formation, leading to protein oxidation. Notably, TNF- α activates matrix metalloproteinases (MMPs) released from leukocytes, which are the main mechanism for cleaving of PGs (such as syndecans) from their ectodomains (57). Direct EG injury due to adrenergic hyperactivation is also proposed as a contributing factor (139).

Cleavage of PGs exposes the “underlying” GPs, promoting activation and adhesion of leucocytes and platelets, thereby amplifying inflammation and coagulation (46). Furthermore, shed EG constituents, especially heparan sulphate act as damage-associated molecular patterns (or alarmins). Once released systemically, these molecules trigger cytokine production and perpetuate the inflammation cascade (140). Additionally, the released heparan sulphate can interfere with coagulation, increasing the risk of bleeding (141).

Intravascular volume overload, whether naturally occurring or (more commonly) iatrogenic, can result in fluid overload, interstitial oedema, impaired oxygen delivery to the tissues and subsequent

multi-organ dysfunction (35). It is proposed that IV volume overload leads to fluid extravasation and interstitial fluid accumulation through directed damage of the EG.

Excess intravascular volume causes mechanical stretching of the heart, which in turn triggers natriuretic peptides (NP) release into the circulation (142, 143). The primary function of NP is to reduce IV volume and counteract hypertension. This is achieved through four mechanisms – natriuresis, vasorelaxation, inhibition of the renin-angiotensin-aldosterone system and increased vascular permeability (144). The latter effect is believed to be through damage to the endothelial glycocalyx (EG) caused by the NPs triggering enzymatic shedding (145). Subsequently, fluid shifts from the IV into the interstitial space.

In healthy individuals, excess fluid can be returned to the circulation via the lymphatic system. However, this process is disrupted in critically ill patients (58), resulting in fluid accumulation in the interstitium. This increases the diffusion distance for oxygen between the microvasculature and cells, leading to impaired cellular energy production, cellular death, multi-organ dysfunction and potentially increased mortality (132). Numerous studies have demonstrated that a positive fluid balance (or fluid overload) is associated with increased morbidity and mortality. Moreover, several critical illnesses have been linked to EG with IV fluids potentially only exacerbating this preexisting injury (113, 146-158). Damage to the EG has been reported in critically ill people with hypervolemia (159, 160).

Regardless of the cause, EG degradation results in increased vascular permeability, interstitial oedema, and impaired oxygen delivery to tissues (35, 60, 129, 161). Local activation of coagulation contributes to microcirculatory disturbances. Alteration of RBC rheology and shape impair oxygen unloading, contributing to reduced oxygen supply to tissues. Binding of the “exposed” selectins and integrins activates the inflammatory cascade. Although, those mechanisms can be protective when activated locally and transiently, their systemic and sustained activation contributes to multi-organ failure and, ultimately, death.

At present, microcirculatory abnormalities, alongside mitochondrial dysfunction, are considered key contributors to multi-organ failure in critical illnesses such as sepsis (162, 163). As such, current research is increasingly focused on elucidating the pathophysiology of microcirculatory dysfunction and developing appropriate diagnostic and therapeutic strategies. With the EG at the core of microcirculatory regulation, this naturally prompts a need for deeper investigation, not only into its structure and function, but also into clinically applicable assessment tools.

4.4. Appraisal of the evidence on endothelial glycocalyx function

The revised Starling principle has received a substantial amount of research attention and has been the topic of discussion at numerous human and veterinary medical conferences. However, the principle remains largely theoretical. A recent review from a research group specializing in volume kinetics (the pharmacokinetics of IV fluids) called into question the validity of the revised principle

(118). The authors argue that the model is based primarily on experimental data and that predictions often fail to align with clinical observations.

For example, fluid reabsorption has been shown to occur in skeletal muscle, particularly following a decrease in capillary filtration pressure. Additionally, hypertonic fluids such as hypertonic saline, or hyperoncotic albumin are known to exert volume effect three- to four -fold greater than the volume infused. The fluid they "draw" into the intravascular space must, by necessity, originate from the interstitial compartment. Finally, the revised Starling principle frequently describes a "steady state", whereas in physiological conditions, vessels, especially smaller ones, exist in a constantly dynamic state.

Despite these limitations, the revised Starling principle has served as a pivotal conceptual shift, supporting more rational approaches to IV fluid administration. This has been an important step in reducing morbidity and mortality associated with fluid overload. However, much remains to be learned about its applicability in clinical practice.

While current research has focused predominantly on assessing EG damage in both experimental and naturally occurring conditions, little is known about the relationship between EG structural integrity and its functional role. Indeed, a recent review article has challenged the prevailing of the EG serves as a primary barrier to vascular permeability (112). The authors argue that many permeability studies are flawed, as they rely on enzymatic degradation of PGs and GPs, interventions that may themselves increase vascular permeability. Furthermore, reported EG thicknesses (typically of 500 nm – 2 μm) do not correspond well with known dimensions of its scaffolding components. For example, SDC-1 is estimated to be approximately 100 in length. To account for the accepted EG thickness, additional proteins would need to be "stacked" multiple times atop the scaffold, which raises questions about the spatial organization of the layer.

Importantly, vascular permeability does not occur across the general endothelial surface per se, where most of the PGs and GPs are located. Instead, it is believed to take place at the endothelial junctional clefts where adjacent endothelial cells are tightly joined by structural proteins such as occludins, cadherins and catenins (112, 132, 164). The surface composition of this junctional region differs from that of the rest of the endothelial surface. Various stimuli and substances can affect specifically this area, increasing permeability (112). This could explain why, studies that assess EG shedding and markers of increased vascular permeability do not often report a correlation between the two (112).

The EG thinning observed with SDFV and GlycoCheck^{TM} analysis, as well as increased EG shedding, may in fact be epiphenomena that accompany injury to the highly functional endothelial junctional zone. While the composition and physiology of endothelial junctions are relatively well studies, they comprise only a very small area (~ 1%) of the endothelial surface (164). As a result, damage to this area may be diluted or obscured when assessing bulk concentrations of PGs and GPs from non-junctional regions. Future studies, specifically targeting the EG within endothelial junctions

are needed to further explore this hypothesis. All of these discrepancies highlight the need for deeper investigation, not only into the structural composition of the EG, but also into the intricate relationships between its structure and function. Such efforts should consider physiological differences across distinct regions of the endothelial surface and prioritise translational research that bridges theoretical models with clinical observations.

5. Strictly experimental methods for assessment of endothelial glycocalyx integrity

The thickness of the EG was previously estimated using indirect methods, such as the disparity between the measured and theoretical haematocrit within blood vessels, mathematical simulations, flow resistance differences or tracer dilution techniques (77). While these approaches demonstrate the existence of an endocapillary layer, they provide no information about its composition or functional roles. With recent advances in electron microscopy, specific stains and fixation techniques, direct visualization of the EG became possible (45).

Transmission and scanning electron microscopy have been widely used to study the structure of the intact or damaged EG in isolated organs or animal models. A series of studies on isolated perfused guinea pig hearts have compared baseline images of the EG with those obtained following application of substances known to damage it, such as heparinase, TNF-α and lipopolysaccharide or following ischemia-reperfusion injury (81, 165, 166). These studies have also investigated the potential protective effects of molecules such as albumin, antithrombin, and hydrocortisone (72, 75, 167). While the published images clearly illustrate differences in EG integrity before and after injury, few, if any, quantitative measures of EG have been reported using such techniques.

Another promising technique for direct visualization is fluorescence microscopy, which uses antibodies targeting specific EG carbohydrates or proteins. This method enables high-resolution imaging of the luminal EG, especially when paired with confocal or two-photon scanning microscopy techniques (77).

However, due to the rapid degradation of the EG, accurate visualization requires rapid fixation immediately after death for any electron microscopy technique. This necessitates perfusion-fixation, typically achieved by administering the fixative intravenously to the whole organ or study animal prior to death and tissue harvesting (45). As a result, this methodology remains impossible to apply in the clinical setting (77). Furthermore, these techniques offer only a "snapshot" of the EG at a single point in time, without accounting for its dynamic changes or allowing accurate evaluation of its functionality.

6. Methods for assessment of endothelial glycocalyx integrity suitable for experimental and clinical settings

Clinical or bedside methods for assessment of EG integrity have been developed over recent decades. These approaches involve either direct visualization of the microcirculation and estimation of

EG thickness or measurement of EG constituents shed into the plasma following EG degradation (109, 168).

Determining whether either of these techniques is applicable for use in cats is the central research question of this thesis. Accordingly, this section will provide a detailed description of both methods and summarise relevant findings from the human and veterinary literature.

6.1. Visualization of capillaries and estimation of endothelial glycocalyx thickness

Sidestream dark field videomicroscopy (SDFV) is a non-invasive optical imaging technique used to visualise the microcirculation in people and other animal species (169-174). It is based on the principles of dark field illumination, where light is emitted from a ring-shaped source and directed sideways into the tissue - hence the term sidestream (175). Red blood cells within capillaries appear as dark silhouettes against a bright background due to their strong light absorption properties. Sidestream dark field videomicroscopy also incorporates orthogonal polarization spectral imaging, a technique that uses polarised light to reduce surface glare and enhance contrast, allowing clearer visualisation of microvasculature just beneath the tissue surface. This method is typically applied to easily accessible mucosal surfaces, such as the sublingual region, to evaluate capillary density, flow characteristics, and overall microvascular perfusion. When combined with GlycoCheck™ software, SDFV can also be used to estimate EG thickness.

This technique provides a direct, real-time, and dynamic assessment of the microvasculature in live subjects, along with simultaneous characterisation of EG integrity. It has been widely adopted in clinical research and critical care settings, where microvascular function is often compromised by severe illness. The methodology and relevant studies supporting the use of this technique are detailed in the sections below.

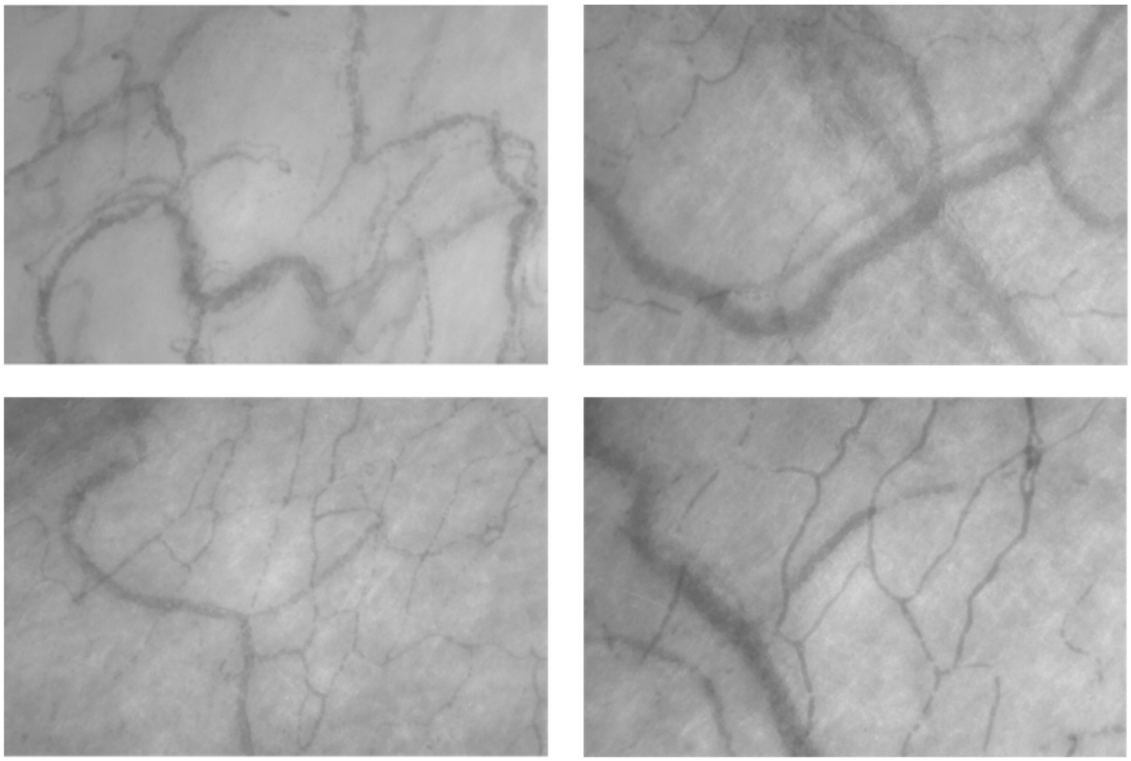
6.1.1. Methodology

Sidestream dark field videomicroscopy is performed by placing a handheld videomicroscope on an accessible mucosal capillary bed: sublingual reported in people, dogs and cats, gingival – reported in dogs and auricular pina reported in human neonates (169-174). Light is emitted at the haemoglobin absorption wavelength (540 nm), causing capillaries and the RBC within them to appear dark against a bright background, due to the haemoglobin's light absorption properties (173) (Figure 1.3).

From the acquired images, microcirculatory parameters such as total vessel density, perfused vessel density and microcirculatory flow index are calculated. In earlier applications, image analysis was performed manually, which limited the techniques applicability in clinical settings (171). Newer devices now offer automated processing, streamlining the procedure and enabling real-time analysis. In that regard, the Glycocheck™ is a more recent software to SDFV (176). In addition to automated microcirculatory assessment, this proprietary software also provides a real-time estimation of EG

thickness from acquired SDFV images. A detailed explanation of the GlycoCheck™ system and its underlying methodology is provided in the following section.

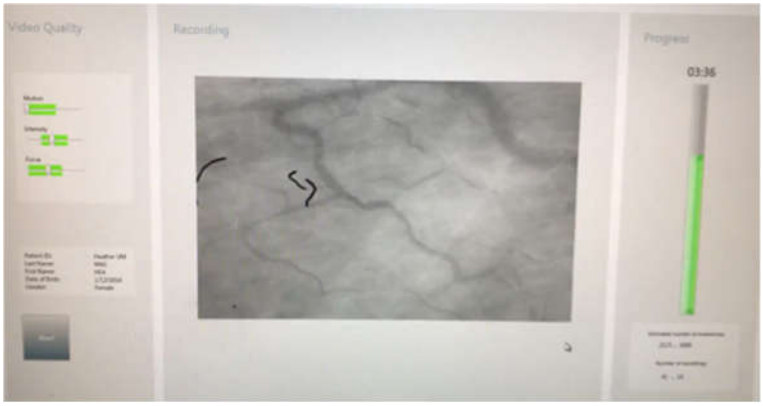
Figure 1.3. Representative sidestream dark field videomicroscopy images of feline sublingual mucosal capillaries acquired at different sites using the Glycocheck™ recording system.



6.1.2. Probe positioning and image acquisition

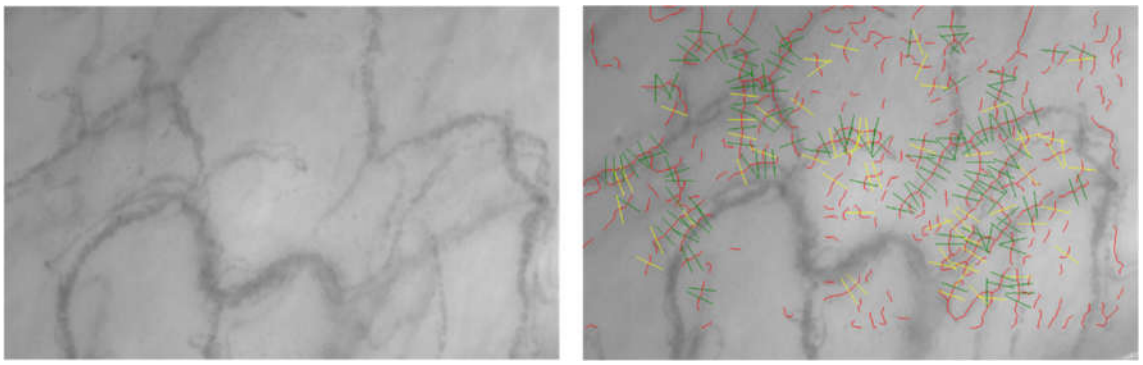
The device is positioned on the mucosal surface by the operator and a real-time recording appears on the computer interface (Figure 1.4). The video recording is displayed on the screen, and the operator can perform real-time quality checks including focus, pressure and motion artifacts (177). Images are captured using an 5X objective with a 0.2 numerical aperture, providing a 325-fold magnification in 720 X 576 pixels (tissue dimension: 950/670 mm; tissue area: 0.665 mm^2) at 23 frames per second. The system makes up to 840 measurements of the width of the RBC column at a specific site. These individual width measurements are obtained after 8-fold pixel size interpolations of the corresponding radial intensity profiles, allowing detection of small changes in width between individual width measurements as small as 0.1 mm, which translates in accuracy of estimates of boundary layer of approximately 0.05 mm (94). The software includes built-in quality checks for motion, light intensity and focus, with a progress bar visible during image acquisition. Images are recorded only if optimal conditions are met. This semi-automated process helps reduce operator-dependent variability and other pre-analytical errors (90).

Figure 1.4. Computer interface of the GlycoCheck™ recording system. Video quality checks for motion, light intensity, and focus displayed as horizontal bars to the left of the screen. Images are recorded only when all parameters meet optimal conditions, indicated by the slider falling within the green zone of each bar. Real-time video feed appears in the central area of the screen, while a vertical progress bar on the right indicates the status of image acquisition. Each recording session is technically limited to five minutes. If sufficient images are not acquired within five minutes the recording resumes for additional five minutes. Note: the camera used here had a minor defect, visible as small black lines on the screen, which according to the manufacturer, did not interfere with data processing.



The GlycoCheck™ system records a series of short video clips – typically 10 recordings of 2 seconds each per site (93). From these, approximately 40 frames are extracted, and the software automatically identifies vessels smaller than 30 µm by analysing the contrast between the RBC and the background. These vessels are the subdivided into 10 µm major vascular segments using marker lines, resulting in approximately 3000 vascular segments assessed per site (Figure 1.5).

Figure 1.5. Sidestream dark field videomicroscopy and GlycoCheck™ images of feline sublingual capillaries without (left) and with (right) overlay of marker lines. Red wavy lines indicate vessel centrelines; green straight lines represent valid vascular segments; yellow straight lines indicate invalid segments excluded from analysis.



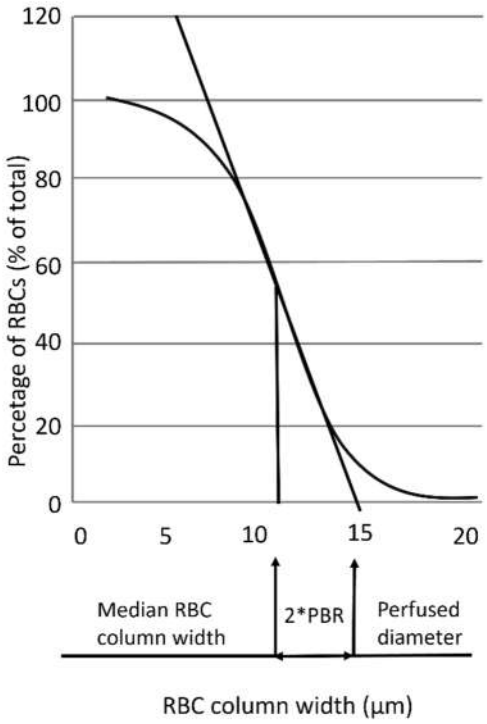
6.1.3. Glycocheck™ analysis quality checks

Subsequently, the software ensures that measurements are performed only on vascular segments of sufficient quality by applying a series of automated quality checks. First, vascular segments are further divided by 0.5 μm markers into minor segments and each segment analysed for sufficient contrast. Major segments in which more than 60% of minor segments meet the contrast threshold are classified as valid vascular segments (VVS). Valid vessel density (VVD) per site is then calculate by multiplying 10 μm by the number of VVS identified.

A second quality check involves analysing RBC column width across all 40 frames for each recording. Parameters assessed include minimal column width, column position and signal-to-noise ratio. The software also calculates RBC filling percentage (%RBC filling) based on the proportion of time a particular VVS contains RBC throughout the 40-frame recording. Both VVD and %RBC filling are used to estimate microvascular perfusion. Segments with insufficient perfusion are excluded from analysis.

A final quality check involves assessing the curve fit used to calculate the median RBC column penetration depth (Median P50), a central value required for estimation of EG thickness (90). While the previous checks assess raw signal quality, this step ensures that the RBC intensity profile across vessel width can be accurately modelled. The software uses a fitting algorithm to determine the boundary at which RBC penetrate into the ESL (Figure 1.6). If the curve is irregular, or fails to meet internal consistence thresholds, the segment is excluded for further analysis. Only segments that pass all quality control steps are used for estimation of EG thickness.

Figure 1.6. Example of the curve-fitting approach used by GlycoCheck™ software. A sigmoidal regression model is fitted to the normalized intensity profile measured across a vascular segment. The fitted curve is used to determine the median red blood cell column width (Median P50) and the perfused vessel diameter, which are subsequently used to calculate the perfused boundary region (PBR), an inverse estimate of endothelial glycocalyx thickness.



6.1.4. Perfused boundary region – GlycoCheck™ estimation of endothelial glycocalyx thickness

The dynamic lateral position of RBC within each VVS is tracked to determine the distribution of RBC column widths. From this, a cumulative distribution is generated, and the median RBC column width is calculated. To estimate the perfused diameter, linear regression is applied to the central portion of this distribution, specifically the range between the 25th to the 75th percentile.

The perfused boundary region (PBR), an *inverse* surrogate marker of EG thickness is then calculated using the formula:

([Perfused diameter – median RBC column width]/2) (Figure 1.7).

The software reports overall PBR value for vessels ranging from 5 to 25 µm, along with separate values for three vessel size subgroups: PBR 5-9 µm, PBR 10-19 µm, PBR 20-25 µm. For simplicity, the term PBR in this text refers to the overall 5-25 µm measurement. As it is an inverse

parameter for estimated EG thickness, a larger PBR indicates deeper RBC penetration and thus a thinner or damaged EG, while a smaller PBR reflects a thicker, healthier EG (176).

Parameters reported in the GlycoCheck™ patient record are summarized in Table 1.1. Additional data, available for research purposes, include full distribution of vessel diameters (0-30 µm, in 1 µm increments), and the corresponding values for VVD, %RBC filling, total diameter, perfused diameter and PBR. Marker line analysis also provides segment-level data on the validity of each vessel, allowing distinction between valid and total vessel density.

Figure 1.7. Schematic representation of the perfused boundary region (PBR) as an inverse estimate of endothelial glycocalyx (EG) thickness. Left: Visualisation of red blood cell (RBC) penetration into the EG layer in vessels with a small (A, healthy thicker EG) versus large (B, damaged thinner EG) PBR. Right: Corresponding intensity distribution curves of median RBC column widths for small (C) and large (D) PBR.

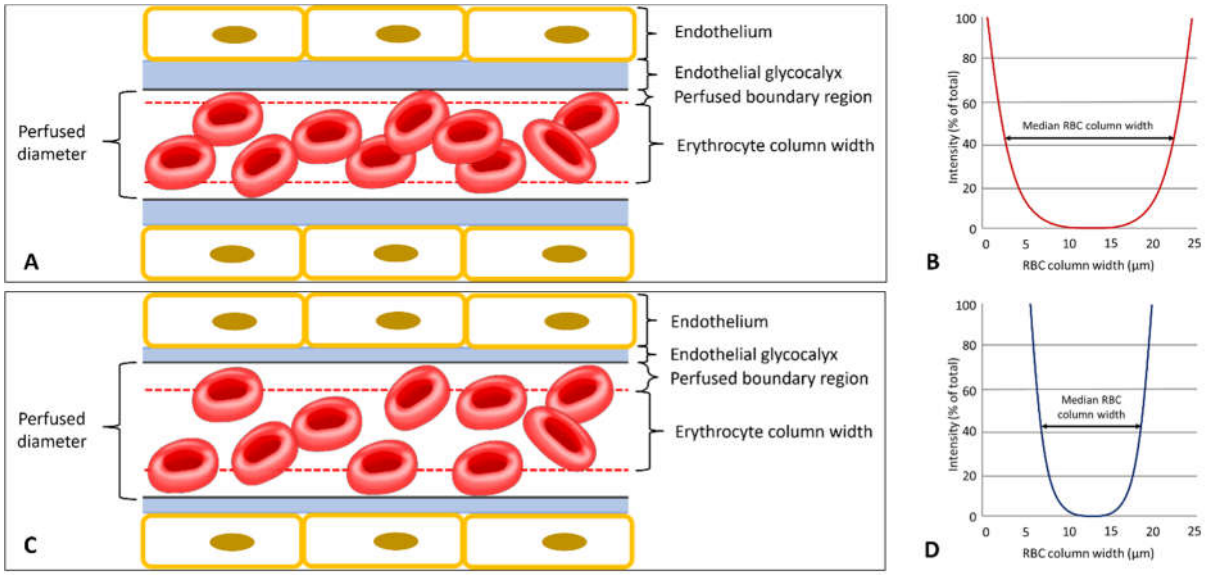


Table 1.1. Overview of GlycoCheck™ output parameters and their interpretation.

Parameter	Description	Interpretation
Valid Vessel Segment (VVS)	A 10 µm major vascular segment in which at least 60% of 0.5 µm minor segments show sufficient background contrast.	Identifies adequately perfused vessel segments.
Valid Vessel Density (VVD)	Calculated by multiplying the number of valid vessel segments by 10 µm.	Estimates the density of perfused microvessels in the examined region.
Percentage of RBC Filling (% RBC filling)	Proportion of valid vascular segments containing RBC across all 40 frames per recording.	Reflects the consistency of RBC presence over time; used to assess microvascular perfusion.

Median RBC Column Width (P50)	Median (50 percentile) value derived from the distribution of RBC column widths, based on dynamic lateral RBC positions across the vessel segment (from all recorded frames).	Represents the average width of the RBC column; used in the calculation of EG thickness.
Perfused Vessel Diameter (D-perf)	Derived by applying linear regression to the segment of the RBC column width distribution curve between the 25th and 75th percentiles and identifying the x-intercept of this line as the outermost RBC penetration point, representing the D-perf.	Represents the outer limit of RBC lateral movement; used to calculate EG thickness.
Perfused Boundary Region (PBR)	Calculated as: (Perfused diameter – Median RBC column width) / 2.	Inverse estimate of EG thickness. Reported for vessel subgroups (5–9 µm, 10–19 µm, 20–25 µm) and overall (5–25 µm).

EG: Endothelial glycocalyx; RBC: Red blood cells

6.1.5. Sidestream dark field videomicroscopy and GlycoCheck™ studies in people

6.1.5.1. Healthy subjects and repeatability studies

Several studies have focused on feasibility and performance of SDFV with the GlycoCheck™ software. Multiple investigations have assessed the PBR on the sublingual mucosa in healthy subjects, reporting values ranging from mean ± standard deviation (SD) of 1.88 ± SD 0.2 to 2.08 ± SD 0.24 µm (92, 178-181). One study reported a higher PBR 5 – 25 µm of 2.46 (Interquartile range (IQR), 2.37–2.59) µm (182). The reason for this outlier remains unclear, though it may be due to methodological differences, such as the number of measurements acquired, operator variability, or differences in technique. However, the study in question did not provide sufficient methodological detail to confirm this.

Several studies have evaluated reliability and repeatability of the GlycoCheck™ with varying results. A 2018 study compared measurements obtained by nurses and physicians in 70 patients admitted to the emergency room and intensive care unit (91). Intraclass correlation coefficient showed excellent reproducibility: between the two measurements acquired by the physician 0.77 [CI 95%: 0.52-0.89] for repeated physician-acquired measurements and 0.75 (95% CI: 0.52–0.87) between physician and nurse-acquired measurements for PBR (91). In neonates, another study found a good level of agreement between three consecutive measurements obtained by two investigators. Interobserver variability was low, with a coefficient of variation of 7.6% (183).

However, several subsequent studies failed to produce these levels of agreement. One study in 169 individuals reported poor reproducibility for PBR, VVD and %RBC filling between two operators (184). Another study investigated three and five consecutive measurements obtained by two operators

on two separate days within a seven-day period (185). Small, but statistically significant day-to-day variations were found for PBR and %RBC filling, with improved reproducibility when averaging three to five measurements.

A more recent study evaluated intra- and interobserver agreement for three consecutive measurements obtained from healthy volunteers by two experienced operators (181). Intraobserver agreement for single PBR, %RBC filling and VVD measurements was poor (<0.4), but increased to good when three consecutive measurements were averaged (>0.6). Similar repeatability results were previously found by the same research group for critically ill patients (186).

Differences in PBR were found across ethnic groups (187). Additionally, one study reported sex-specific association between higher PBR and procoagulant profile in women compared to men (188). Two studies have demonstrated feasibility in obtaining SDFV images and GlycoCheck™ measurements intra-operatively on cerebral (189, 190) and jejunal (191) microcirculation.

Collectively, these studies suggest that GlycoCheck™ analysis might be influenced by operator technique. While differences between individual operators do not consistently increase variability, subtle variations in handling may still affect data quality. Importantly, averaging at least three consecutive measurements substantially improves reliability, and enhances both intra- and inter-observer agreements across studies. This highlights the need for standardised acquisition protocols and appropriate training to ensure consistency across research and clinical settings. In addition to technical factors, biological variables such as ethnicity and sex may also influence PBR measurements. This highlights the need to account for both technical and biological factors when interpreting GlycoCheck™ data.

6.1.5.2. Interventions on healthy subjects

To date few studies have evaluated effects of physiological stimuli on GlycoCheck™ measurements in healthy individuals. One study evaluated immediate impact of a 500 ml of blood donation and found no significant changes in PBR (192). Another study investigated EG thickness after administration of a single 5000 U dose of heparin, also reporting no measurable effect (193). Interestingly, in people, more subtle physiological factors, such as smoking or consuming a meal within 180 min prior to image acquisition, have been shown to affect GlycoCheck™ measurements (184).

The limited number of studies in this area may reflect a shift in research focus. After initial feasibility studies in healthy subjects demonstrated that the technique was usable and generally reliable, most subsequent research has concentrated on sick or hospitalised populations. Interventional studies in healthy subjects have likely been reserved for animal models, where physiological manipulation can be performed more freely under controlled conditions.

6.1.5.3. Sick patients and patients at risk of microcirculatory dysfunction

Over the past decade, increasing attention has been directed toward the role of the EG in critical illness, as visualisation technologies such as GlycoCheck™ have made bedside assessment of the

microcirculation possible. Damage to the endothelium and the resulting microcirculatory disturbances are now understood to be central features of conditions such as sepsis (135) and severe trauma (139). With recent technological developments, numerous studies have used GlycoCheck™ to evaluate microvascular alterations in a variety of pathological conditions.

Most of these studies are observational in nature, with some including comparisons to healthy cohorts. The majority include studies in sepsis and septic shock patients (149, 156-158, 194) including paediatric populations (154, 155, 195), patients with dengue infection (196), patients with kidney disease (197-200), patients undergoing cardio-pulmonary bypass (201, 202), including infants (203) and more recently patients with COVID19 (204-206).

A growing body of GlycoCheck™ research has also examined microvascular changes in surgical patients, particularly in the context of general anaesthesia. A recent meta-analysis including 13 studies reported changes in PBR in the immediate and early post-operative period in a heterogenous group of surgical patients (116). However, the available data were insufficient to determine whether these changes were associated with surgical complications or were related to the effect of general anesthesia itself. One study in patients undergoing joint surgery (which typically involves less tissue trauma than abdominal or thoracic procedures), showed that general anesthesia significantly increased PBR compared to only neuraxial (regional) anesthesia (207). Similarly, a study in women undergoing gynecologic surgery found a significant increase in PBR (6.4%) at the end of surgery (after two hours) compared to baseline (208). Although these procedures involved abdominal surgery, the timing suggests that the observed effects may be attributable to anaesthesia rather than surgical inflammation.

These studies suggest that anaesthesia itself can induce changes in PBR, highlighting the need for caution when interpreting, and especially when comparing, measurements obtained from anaesthetised versus awake patients. More importantly, while GlycoCheck™ measurements can be reliably performed in awake humans, this is not feasible in animals. Image acquisition requires either deep sedation or general anaesthesia to allow for proper probe placement on the sublingual mucosa. As a result, the effects of sedative or anaesthetic agents will always introduce a degree of bias in the interpretation of data from animal studies.

Few studies have investigated the effects of intravenous fluid administration on GlycoCheck™ measurements in human patients. This relative scarcity may be due to the later development of the GlycoCheck™ methodology compared to assays measuring shed EG constituents, as well as ongoing uncertainty surrounding the impact of IV fluids on the EG. A recent study demonstrated that administering a fluid bolus of unbalanced vs balanced crystalloid in septic children resulted in increases in PBR 6h after the intervention (odds ratio of 84.5% vs 60.4%; adjusted odds ratio, 3.78; 95% CI, 1.49-9.58; $p < 0.01$) (155). Furthermore, the patients receiving an unbalanced crystalloid had greater odds for metabolic acidosis associated with increases in SDC-1 (odds ratio [OR], 4.88; 95% CI, 1.23-28.08) and acute kidney injury, associated with EG damage. To the author's knowledge this is the only study investigating specifically IV fluid effects on EG thickness in the clinical setting.

Outside of the critical care setting, GlycoCheck™ parameters have been evaluated in chronically ill patients, including those with diabetes (209-211), hypertension (212), psoriasis (213). Alterations have also been observed in patients at risk of development of microvascular disfunction, such as obese patients (90, 214) and pregnant women with preeclampsia (215).

In summary, while changes in PBR have been observed across a range of clinical contexts, only a few studies have demonstrated clear, stimulus-specific effects. Notably, the study in septic children showed increased PBR following unbalanced crystalloid administration, alongside biochemical markers of endothelial damage (155), and another study reported higher PBR under general anaesthesia compared to regional anaesthesia (207). These findings highlight the potential of PBR as a marker of acute EG dysfunction in response to specific interventions.

However, other studies have produced more variable results. This may reflect limitations in reproducibility of the SDFV system, sensitivity to operator technique, or the challenges of studying microvascular responses in heterogeneous clinical populations with multiple confounders. Still, the ability of GlycoCheck™ to detect subtle microvascular changes in both acute and chronic conditions suggest strong potential. As methodology improves and protocols are standardised, its role in clinical research, and possibly in bedside decision-making, will likely continue to grow.

6.1.6. Sidestream dark field videomicroscopy and GlycoCheck™ studies in animals

At the time of designing this research project, no published studies had evaluated the use of GlycoCheck™ in non-human species. Since then, several small animal studies have emerged, providing important insights into the feasibility and application of the technique in veterinary research.

A series of experimental studies in anaesthetized rabbits, conducted by a group of human neuro-anaesthetists evaluated the effects of different IV fluids on both the sublingual and cerebral microcirculation using GlycoCheck™. In one study rabbits received 30 ml/kg/h of 0.9% saline for one hour (high-volume) or <2 ml/kg/h of saline (control) (96). Cerebral PBR increased in the high-volume group, while sublingual PBR remained unchanged. In a separate experiment, a single bolus of 5 ml/kg of 10% hypertonic saline resulted in increased sublingual, but not cerebral PBR (99). In contrast, 3.2% hypertonic saline did not produce significant changes (97). The authors attributed the observed effects to the compression of the EG from transient hypervolaemia as measured SDC-1 levels remained unchanged. Together, these studies suggest that not only fluid volume, but also the degree of hypertonicity, may influence the impact of intravenous fluids on PBR.

GlycoCheck™ has also been studied in dogs, beginning with a feasibility study on 60 healthy anaesthetised dogs has been published in an abstract form (95). Image acquisition was found to be feasible and PBR values were comparable to those reported in people. Neither demographic variables and nor anaesthetic protocols had a significant effect on GlycoCheck™ parameters.

Two canine haemorrhagic shock models evaluated the impact of haemorrhage and resuscitation on GlycoCheck™ parameters (93, 94). In the first, eight dogs were subjected to a short (10 min)

haemorrhagic shock phase followed by staged autotransfusion of the removed blood (94). No significant changes in PBR or other microcirculatory parameters were observed, leading the authors to conclude that the brief shock duration may have been insufficient to cause measurable EG damage.

In another study six dogs underwent a longer (45 min) shock phase, followed by a randomized resuscitation with five different fluid regimens including crystalloids, synthetic colloids, natural and synthetic blood products in a crossover design (93). The PBR increased significantly after resuscitation when dogs receive a combination of crystalloids and synthetic colloids (not containing RBC), but not with natural blood products (containing RBC). Interestingly, no statistical difference was found between the synthetic blood product groups and either crystalloid/synthetic colloids or natural blood product groups. PBR values following resuscitation with synthetic products appeared intermediate between the other groups. However, in the absence of statistically significant between-group differences, this may reflect random variation rather than a true protective effect. While the authors concluded that synthetic blood products preserve the EG to a similar extent as natural transfusion products, further studies with larger sample sizes are needed to confirm this interpretation. One prospective clinical study evaluated 12 dogs undergoing cardiopulmonary bypass for surgery of naturally occurring cardiac diseases (216). Measurements were obtained at baseline, during cardiopulmonary bypass, after removal of the aortic cross clamp, and at surgical closure. The PBR was found to increase significantly after each timepoint. These findings were corroborated by previous studies in people underdoing cardiopulmonary bypass (201, 202). To date, this remains the only animal study evaluating effects of interventions on GlycoCheck™ parameters in patients with naturally occurring disease.

Sites other than the sublingual mucosa have also been studied in dogs. One observational study evaluated the jejunal microcirculation in 30 healthy shelter dogs undergoing ovariohysterectomy (191). GlycoCheck™ parameter values were found to be similar to those obtained from the sublingual microcirculation in a previous canine study, suggesting normal microcirculatory function of the healthy intestine during elective anaesthesia (95).

Collectively, these studies demonstrate good feasibility of acquiring SDFV images and GlycoCheck™ measurements in veterinary patients, even in smaller animals, such as rabbits. Across studies, parameters were broadly consistent with data in people, supporting transitional value. Moreover, several investigations demonstrated the ability to assess different vascular beds intra-operatively, opening possibilities adapting image acquisition to clinically relevant sites depending on patient population and research question.

However, despite growing feasibility data, clear demonstration of PBR increases in response to EG damage in animals remains limited. In experimental models, this may reflect ethical constraints on inducing significant systemic injury, uncertainty regarding optimal timing for measurement, or technical challenges in capturing early EG alterations. Clinical studies, on the other hand, face their own challenges, including small sample sizes, anaesthesia timing and workflow constraints, and heterogeneous patient populations.

The canine cardiopulmonary bypass study provides some of the strongest evidence to date that disease and clinical interventions can indeed damage the EG. However, the study was conducted under relatively controlled conditions, limiting its comparability to more typical clinical settings. Further research is needed to clarify the relationship between GlycoCheck™ measurements and clinically meaningful EG disruption in animals. Notably, all published animal studies have been performed under general anaesthesia or heavy sedation - a requirement that is unlikely to change, as animals cannot tolerate sublingual probe placement while awake. This represents an important limitation, as anaesthesia may influence vascular tone and microcirculatory dynamics, potentially affecting GlycoCheck™ readings.

6.1.7. Associations between different GlycoCheck™ parameters

Although GlycoCheck™ parameters are interdependent, as they are calculated from overlapping image data and algorithms, several studies have nonetheless examined associations between them, aiming to gain additional insights into microvascular perfusion and EG integrity. While this approach may have analytical limitations, it reflects a growing interest in exploring whether structural changes, such as EG thinning, estimated by PBR, are linked to functional consequences like altered RBC distribution and microvascular perfusion, estimated by %RBC filling and VVD.

A population-based study of 900 participants from the Netherlands Epidemiology of Obesity cohort investigated associations between GlycoCheck™ parameters in middle-aged individuals. A strong negative correlation was found between PBR and %RBC filling ($r^2 = 0.475$, $p < 0.001$) and a weaker correlation between PBR and VVD ($r^2 = 0.030$) (90). The authors interpreted these findings as evidence of impaired microvascular perfusion (reduced %RBC filling) in association with EG damage (increased PBR). However, 42% of the cohort were lean, 42% overweight, and 16% obese, and no subgroup analysis was performed, limiting the interpretation of whether observed associations were more pronounced in at-risk individuals.

A similar negative association between PBR and %RBC filling was demonstrated in a study involving preterm and term neonates (Pearson $r^2 = -0.87$, $p < 0.0001$)(183). Although the investigators did not perform separate analyses by gestational age, preterm neonates did have significantly higher PBR, and lower %RBC filling, and VVD. Interestingly, the authors questioned the validity of interpreting this association as indicative of EG damage, since all three parameters are part of the same analytical algorithm.

This pattern has also been observed in a clinical study of diabetic patients, where PBR correlated strongly and negatively with %RBC filling ($r = -0.754$, $p < .001$) and moderately with VVD ($r^2 = -0.505$, $p = 0.002$) (217). Similar trends were present in the control group, although only the association between PBR and %RBC filling reached significance ($r^2 = -0.701$, $p < .001$).

Additionally, a canine study evaluating the jejunal microcirculation during ovariohysterectomy found a significant negative correlation between PBR and %RBC filling (191). The presence of this

association in healthy populations raises questions about its interpretation as a marker of disease. While VVD and %RBC filling are GlycoCheck™ parameters estimating microvascular perfusion, they are also part of the quality control process used to determine which vascular segments are suitable for PBR calculation (90). It is therefore possible that observed correlations reflect analytical artifacts, rather than true physiological relationships (impaired perfusion and EG damage). Because the software uses logistic PBR calculated from the median width of RBC columns widths, relative to the perfused vessel diameters, reduced RBC presence (lower %RBC filling) in VVS could increase variability and skew results towards higher PBR values.

To clarify the biological significance of these associations, future studies incorporating independent measures of microvascular perfusion, such as near-infrared spectroscopy (218) or laser Doppler flowmetry (219) may be necessary to confirm whether these observed patterns represent physiological dysfunction or methodological bias.

6.1.8. Associations between GlycoCheck™ parameters and packed cell volume

GlycoCheck™ parameters are calculated based on RBC profiles. Therefore, changes in packed cell volume (PCV) or haematocrit could affect GlycoCheck™ measurements and calculations. For instance, a decrease in PCV can alter RBC rheology within microvessels (220), potentially reducing median RBC column width through lateral migration of RBC and thereby increasing PBR. Conversely, higher PCV could reduce PBR by maintaining a broader RBC column.

A study in preterm neonates, found haematocrit to be an independent predictor of PBR, with PBR increasing as haematocrit decreased (183). This suggests that lower PCV could influence GlycoCheck™ measurements and estimated EG thickness. Whether this reflects actual EG damage or is primarily an analytical artifact remains to be determined.

Similarly, a study examining the microcirculation and EG thickness in a healthy cohort across three ethnic groups found that PBR decreased independently with increasing haematocrit (187). In this study mean haematocrit ranged from 41.1 to 43.3% (well within reference intervals for the species), suggesting that the association may persist across haematocrit levels.

Changes in PCV, both decreased (anaemia) and increased (haemoconcentration) are common in critically ill patients, with anaemia being particularly prevalent (221). Therefore, associations between PCV and GlycoCheck™ parameters merit further exploration. To the author's knowledge no other studies to date have directly explored these associations.

In addition, transient anaemia due to haemodilution can also be observed during anaesthesia and has even been used to estimate blood volume changes in response to anaesthetic agents (222). Given that animals must be sedated or anaesthetized for GlycoCheck™ image acquisition, the influence of PCV on parameter interpretation should be considered.

6.1.9. Appraisal of Sidestream dark field videomicroscopy and GlycoCheck™ analysis

Strengths and limitations of the GlycoCheck™ system have been discussed throughout the previous sections. These are briefly summarised below.

The GlycoCheck™ system offers a promising, non-invasive method for assessing microcirculatory function and estimating EG thickness in real time. Its automated software enables objective analysis of thousands of capillary segments with minimal user input, improving reproducibility compared to earlier, manually assessed methods. In addition to the PBR, the system provides multiple perfusion-related parameters such as VVD and %RBC filling, offering a comprehensive insight into microvascular dynamics. Its application has been demonstrated in a range of clinical and experimental settings across human and animal species, and the ability to use accessible mucosal sites makes the methodology relatively versatile.

Nonetheless, the system comes with important limitations. Perfused boundary region remains a surrogate marker and is indirectly derived from RBC movement rather than direct EG visualisation. It is sensitive to changes in packed cell volume and haematocrit, motion artefacts, and technical factors such as lighting and probe positioning. Furthermore, the proprietary nature of the algorithm limits transparency.

The GlycoCheck™ software was developed for human use and has not been specifically adapted for animal physiology. As such, it does not account for potential interspecies anatomical and functional differences, which may influence certain derived parameters. Current veterinary data remain sparse, with limited functional validation. In animals, the need for general anaesthesia introduces a confounding variable, as vascular tone and EG integrity may be affected by anaesthetic agents.

Despite encouraging variability data, the technique is currently better suited for population-based studies rather than guiding clinical decision-making in individual patients. While the technique shows clear potential, careful consideration of its limitations is necessary when interpreting results, especially in clinical or comparative research contexts.

6.2. Measurements of shed endothelial glycocalyx constituents

Endothelial glycocalyx damage results in the enzymatic cleavage of its structural components. Transmembrane proteoglycans such as syndecan-1 (SDC-1) are cleaved by matrix metalloproteinases in response to inflammatory cytokines and their ectodomains shed into the circulation (49, 51, 55, 56, 114, 223-227). Similarly, during volume overload, natriuretic peptides (NP), released by the heart in response to mechanical stretch, also activate MMPs and lead to cleavage of structural components of the EG (114, 143, 228, 229). Heparan sulfate (HS), a glycosaminoglycan side chain, is cleaved from its core protein by heparinases via similar inflammatory mechanisms (62). Depending on the mode of attachment, other constituents may also be released from their binding sites. This shedding process is amplified during disease states, leading to increased plasma concentrations of these constituents. Glycocalyx integrity can therefore be assessed using these circulating fragments as damage biomarkers.

A variety of PGs, GPs, and other molecules have been investigated in relation to EG degradation (Table 1.2). While some of them are structural components of the EG, others are signalling molecules, coagulation and inflammation modulators and molecules affecting vascular tone. Only a few biomarkers are considered relatively specific to the endothelium, namely vascular endothelial cadherin (230), thrombomodulin (231), angiopoietin-2 (232), and endocan (233). Most others originate from multiple tissues. For example, hyaluronan is also found abundantly in the interstitium (67, 68), which can confound its interpretation as an endothelial-specific marker.

Despite this, the most frequently reported EG biomarkers in the literature remain SDC-1, HS, and HA, with SDC-1 being the most studied. These are widely regarded as validated indicators of EG degradation due to their consistent elevation in pathological states such as sepsis, trauma, and ischemia-reperfusion injury (53, 194, 234, 235). While some studies report measuring one of these constituents, most combine at least two, commonly SDC-1 and HA, or measure all three alongside other biomarkers of endothelial activation.

Table 1.2. Summary of endothelial glycocalyx biomarker origin and characteristics.

Biomarker	Origin / Type	Brief Description
Structural components		
Syndecan-1	Transmembrane proteoglycan on endothelial cells	Major core protein of the EG; elevated plasma levels indicate glycocalyx shedding and endothelial damage.
Heparan Sulfate	Glycosaminoglycan attached to core proteins like syndecan-1	Released upon EG degradation; contributes to anticoagulation and permeability.
Hyaluronan	Non-sulfated glycosaminoglycan attaching to the EG through its CD44 receptor	Maintains hydration and structural integrity; elevated levels suggest glycocalyx disruption.
Syndecan-4	Transmembrane proteoglycan with distinct tissue roles	Involved in cell adhesion and signalling; less commonly measured in EG studies.
Glypican-1	Glycosylphosphatidylinositol--anchored proteoglycan on endothelial cells	Plays a role in cell signalling; rarely studied in the context of EG damage.
Chondroitin Sulfate	Sulfated glycosaminoglycan; found on syndecans	Released during EG degradation; associated with various pathological conditions.
Junctional structural components		
Vascular endothelial cadherin	Adherent junction protein between endothelial cells	Maintains endothelial barrier integrity; soluble form in plasma reflects endothelial injury and permeability.

Adhesion and signalling molecules		
Intercellular adhesion molecule-1	Cell adhesion molecule on activated endothelial cells	Facilitates leukocyte adhesion; soluble form indicates endothelial activation and inflammation.
Vascular cell adhesion molecule-1	Endothelial adhesion molecule induced by cytokines	Promotes leukocyte adhesion; elevated levels reflect endothelial activation and cardiovascular inflammation.
P-selectin	Expressed on platelets and endothelial cells	Mediates leukocyte rolling; soluble P-selectin reflects endothelial and platelet activation.
E-selectin	Endothelial-specific adhesion molecule	Induced by inflammatory cytokines; soluble levels indicate inflammatory endothelial activation.
Coagulation and inflammation modulators		
Thrombomodulin	Endothelial surface glycoprotein	Regulates coagulation; elevated soluble thrombomodulin indicates endothelial damage and dysfunction.
Endocan	Soluble dermatan sulfate proteoglycan	Secreted by endothelial cells; elevated levels correlate with endothelial activation and inflammation.
Vascular tone and angiogenesis regulators		
Angiopoietin-2	Endothelial growth factor stored in Weibel-Palade bodies	Antagonizes Tie2-receptor signalling, destabilizing vasculature; elevated in inflammation and poor outcomes.
Vascular endothelial growth factor	Vascular endothelial growth factor	Stimulates angiogenesis; altered levels reflect endothelial activation and vascular remodelling.
Endothelin-1	Vasoconstrictor peptide from endothelium	Regulator of vascular tone; elevated in dysfunction and associated with cardiovascular disease.

Biomarkers of EG damage are almost exclusively measured using Enzyme-Linked Immunosorbent Assays (ELISAs), with sandwich ELISAs employing monoclonal antibodies being the most commonly used format in the literature. Sandwich ELISAs are well-suited for detecting low-abundance analytes in complex biological samples such as plasma or serum, offering both high specificity and sensitivity. This method relies on two antibodies binding to distinct epitopes on the target molecule: a capture antibody immobilized on the plate, and a detection antibody linked to a reporter enzyme. Monoclonal antibodies, derived from a single B-cell clone, bind a single epitope with high specificity, minimizing cross-reactivity and ensuring assay consistency. Polyclonal antibodies, by contrast, recognize multiple epitopes, which can enhance signal but reduce specificity. While useful in exploratory studies, polyclonal antibodies are less suited for standardized assays. Monoclonals remain the preferred choice for reliable, reproducible measurement of EG biomarkers.

Numerous studies have assessed EG damage in people by measuring circulating shed constituents. Recent review articles have identified over 200 original studies investigating EG biomarkers across a range of disease processes, as well as in healthy individuals exposed to various stimuli such as altitude and exercise (113, 142). The following section provides a concise overview of the human literature and a more detailed focus on recent developments in the veterinary field.

6.2.1. Studies in people

A wide range of studies in people have associated EG shedding with systemic inflammatory conditions such as naturally occurring trauma (141, 236, 237), surgical trauma (150, 238), particularly cardiovascular surgery (146-148, 151, 202), sepsis (149, 200, 234) and ischemia-reperfusion injury (239). Earlier investigations typically relied on single timepoint measurements, hardly capturing the dynamic nature of EG turnover (47). While these studies often showed increases in biomarker levels, the association between these elevations and clinically relevant outcomes such as morbidity and mortality remained inconsistent. More recent studies have evaluated temporal changes in EG constituents (234, 240, 241). One such study in septic patients found persistent high concentrations of SDC-1 and HA in non-survivors compared to survivors (234), suggesting that dynamic profiling may offer greater prognostic value.

The effects of IV fluid administration and hypervolaemia on EG shedding has been explored in a variety of clinical and experimental settings. A recent systematic review synthesized data from 20 studies, half of which involved septic or critically ill patients, while the remainder used postoperative and healthy participants (142). While a trend emerged linking higher IV fluid rate and volume with increased EG shedding in non-septic cohorts, this relationship was not consistently observed in septic cohorts.

Together, these findings highlight the complex and context-dependent nature of EG shedding. Although measurable increases in shed constituents are frequently observed across a range of pathological states, their relationship with clinical outcomes remains variable and, at times, contradictory. It is therefore plausible that EG shedding represents an epiphenomenon of critical illness- a marker of disease severity rather than a direct driver of complications. This possibility, combined with variability in study design, timing of measurement, and biomarker specificity, highlights the need for cautious interpretation. This and other methodological limitations are presented at the end of this section.

6.2.2. Veterinary studies

This section focuses on recent experimental and clinical studies in veterinary species, both small and large animals, that are relevant to veterinary practice. It does not include the extensive body of research involving laboratory animals (e.g., mice, rats, and pigs) used primarily as models for human disease and translational medicine.

6.2.2.1. Cats

At the time of initiating this project, no studies had investigated the EG in cats. Since then, two clinical studies evaluating EG biomarkers in small cohorts of sick cats have been published. One study assessed EG biomarkers in 25 cats infected with *Mycoplasma haemofelis* (haemotropic mycoplasmosis) compared to 10 healthy controls (242). Biomarkers measured using feline-specific ELISA kits included SDC-1, endothelin-1, asymmetric dimethylarginine, and vascular endothelial growth factor-A. While both SDC-1 and endothelin-1 increased significantly in the affected cats, SDC-1 levels remained relatively low.

Another study evaluated EG biomarkers in 25 cats with traumatic brain injury measured within 48h of admission compared to 10 healthy controls (243). The measured SDC-1 and thrombomodulin were not significantly different between groups.

While both studies contribute to the emerging body of literature on EG assessment in cats, several methodological limitations should be acknowledged. These include small sample sizes, heterogeneous populations, and limited clinical detail. Additionally, the validation status of some biomarker assays marketed as species-specific remains unclear, potentially affecting the accuracy of reported values. Neither study included longitudinal sampling, and the absence of complementary techniques, limits the strength of their conclusions. Nonetheless, these initial reports highlight the feasibility of EG biomarker measurement in feline patients.

6.2.2.2. Dogs

To date, all but one of the canine studies investigating EG shedding have been experimental, focusing mostly on effects of IV fluid administration. The only clinical study evaluated the effect of IV fluid administration on plasma EG constituents in healthy, euvolemic dogs undergoing elective procedures. The remaining studies used haemorrhagic shock models with or without an IV fluid resuscitation phase and an earlier septic shock model. A summary of these findings is provided below.

A clinical pilot study evaluated intra-operative IV fluid rates in healthy, euvolemic dogs undergoing elective surgeries and demonstrated that both low (5 ml/kg/h) and high (10 ml/kg/h) intra-operative IV fluid rates increase HA concentrations 2-3-fold (244). As HA is abundant in the interstitium (68), and crystalloids are rapidly redistributed from the intravascular into the interstitial space in euvolaemic patients, these increases may represent lymphatic washout from the interstitial space, rather than HA shedding from the EG (64, 245, 246). Therefore, the origin (endothelium or interstitium) of the measured HA is unknown.

A canine haemorrhagic shock model involving a single large volume bolus (80 ml/kg) of IV crystalloid fluids, observed a 10-fold increase in HA (247). This marked elevation may suggest EG damage secondary to fluid overload; however, similar to the previous study, the endothelial versus interstitial origin of HA could not be determined. Interestingly, the authors' attempts to measure SDC-1 with a canine-specific ELISA yielded no detectable results.

In another haemorrhagic shock model with a crossover design, six dogs underwent a 45 min haemorrhagic shock phase, followed by randomly assigned resuscitation with five different fluid regimens including crystalloids, synthetic colloids, natural and synthetic blood (55). Biomarkers including SDC-1, HS, HA, vascular endothelial cadherin, and total GAG and were measured at several timepoints, during and up to two weeks post-resuscitation. Although changes in biomarker concentrations were observed, they did not follow typical temporal patterns described in other species. Notably, SDC-1 concentrations remained low and even decreased following resuscitation. The authors proposed that either the shock was insufficient to cause EG shedding or that typical EG biomarkers may not reflect EG damage in dogs as they do in other species. A canine haemorrhagic shock model, without IV fluid administration phase, evaluated effects haemorrhage and autotransfusion on GlycoCheck™ parameters and SDC-1, HA and HS (94). Dogs underwent controlled hypotension for 20 minutes followed by autotransfusion of shed blood. The same canine-specific SDC-1 ELISA was used, again yielding no detectable SDC-1 at any timepoint. HA and HS concentrations fluctuated-decreasing after blood removal and increasing modestly after autotransfusion.

Finally, a septic shock model explored the effects of unfractionated heparin on EG integrity in dogs (248). This study reported 2–3-fold increases in both SDC-1 and HS concentrations in the shock group within 1 hour, with elevated SDC-1 levels persisting over 12 hours. However, SDC-1 values remained relatively low compared to reports in other species, while HS concentrations continued to rise over the study period.

Collectively, these studies demonstrate that while EG biomarker analysis is technically feasible in dogs, consistent and biologically meaningful changes in response to EG injury remain difficult to demonstrate. Haemorrhagic and septic shock models show variable responses, particularly in SDC-1, which are often undetectable using currently available assays. This raises questions about species-specific differences in biomarker kinetics or assay sensitivity. Moreover, the origin of increased HA remains unclear, as it may reflect interstitial washout rather than EG disruption. These findings highlight the need for more robust, standardised methods to assess EG damage in dogs and suggest caution when interpreting biomarker changes in isolation. Furthermore, clinical studies in sick populations are acutely lacking.

6.2.2.3. Horses

A recent retrospective study compared SDC-1 concentrations in healthy (n = 66), sick non-septic (n = 83) and septic (n = 42) adult horses (200). SDC-1 levels were significantly higher in septic horses (50.73 ± 84.24 ng/mL) compared to both healthy controls (15.69 ± 11.28 ng/mL) and sick non-septic horses (16.88 ± 15.30 ng/mL). A mild correlation was observed between SDC-1 concentrations and systemic inflammatory response syndrome (SIRS) scores, suggesting that SDC-1 may serve as a marker of illness severity. However, due to the retrospective nature of the study, no conclusions could be drawn regarding the prognostic value of SDC-1 in this population.

A more resent prospective, multicentre, longitudinal study evaluated EG and other illness severity biomarkers, including SDC-1, HS, angiopoietin-2, aldosterone, and plasma atrial natriuretic peptide in 90 neonatal foals (55 septic; 19 sick non-septic and 16 healthy controls) measured over a 72-hour period (201). Serum SDC-1, HS and angiopoietin-2 concentrations were significantly elevated in septic foals compared to healthy controls. Furthermore, higher admission concentrations of HS and angiopoietin-2 were associated with increased odds of non-survival.

To the author's knowledge, these are the only animal studies to date demonstrating biologically meaningful increases in SDC-1 concentrations consistent with patterns reported in human medicine. This may reflect the inclusion of more severely ill (namely septic) populations or possibly the use of more analytically robust ELISA assays for biomarker measurement.

6.2.3. Summary for animal studies

In summary, the available animal studies represent important early steps in advancing our understanding of EG injury in veterinary species. Some have demonstrated changes in EG biomarkers and GlycoCheck™ parameters that mirror findings reported in human medicine, particularly in critically ill cohorts. However, most studies to date have been experimental in nature, often with small sample sizes and variable methodologies. Discrepancies between results, limited longitudinal data, and a lack of standardised, species-validated assays complicate interpretation. Substantial gaps remain, particularly in characterising EG changes in clinically ill dogs and cats, highlighting the need for robust, prospective studies that not only gather data from sick patients but also validate assessment methodologies to ensure that findings can be confidently applied for clinical decision making.

6.2.4. Appraisal of measurements of shed EG constituents

Measuring shed EG constituents is a relatively quick and technically straightforward method to assess EG integrity. However, this approach has several limitations that merit discussion.

Firstly, the synthesis and turnover of EG components are dynamic and context-dependent (47). For instance cellular production of SDC-1 increases during inflammatory states (49), raising the possibility that elevated SDC-1 concentrations may reflect increased availability, rather than enhanced shedding. Furthermore, the biomarkers commonly used, SDC-1, HS, and HA, are not exclusive to the EG. Many are also present in other tissues, particularly HA in the interstitium. Consequently, elevated circulating concentrations may reflect tissue injury and systemic uptake rather than EG-specific shedding. Despite the growing body of literature, there remains a lack of clarity around origin of the shed constituents, shedding kinetics, the persistence of biomarker elevation, and the time to recovery with different disease processes. Some authors have argued that this variability, combined with other methodological constraints, limits the utility of EG constituents as reliable biomarkers (168). This is supported by the wide range of discriminatory performance reported across studies.

Renal clearance represents another important confounder. Shed EG constituents are primarily excreted via the kidneys, meaning that serum concentrations are influenced not only by production and

shedding, but also renal function (249). Given the high prevalence of acute kidney injury in critically ill human patients, elevated EG biomarker concentrations may reflect impaired clearance rather than increased degradation (249). Unfortunately, most studies have not accounted for this variable, nor reported associations between EG biomarkers and renal function indicators.

Assay-related factors further complicate interpretation and cross-study comparisons. To the author's knowledge, currently there are no commercially available ELISA kits for clinical use in measuring SDC-1, HS, or HA. Most are labelled for research use only, and there are currently no established reference intervals for these markers in any species. Reported values in healthy human subjects vary substantially, for example, published SDC-1 concentrations range from ~1 to ~20 ng/mL. This discrepancy may result from differences in assay design, such as the detection ranges of various kits (e.g., from 0.156–10 ng/mL to 4.7–300 ng/mL). In dogs and cats specifically, SDC-1 concentrations are often undetectable or reported at very low levels. While most studies claim to use species-specific assays, closer examination of the assay documentation reveals that suitability is often inferred from sequence homology, rather than from species-specific assay development and validation. Without standardisation, comparing results across studies, or even interpreting the magnitude of biomarker elevation within the same species, remains problematic. Finally, few studies to date have examined the relationship between EG shedding with actual changes in EG function. When explored, this has primarily been limited to the experimental setting using tracer extravasation to assess barrier integrity. As such, the connection between structural EG disruption and functional consequences remains largely uncharacterised.

Circulating biomarkers offer a promising, accessible means of assessing EG injury. However, their clinical utility remains limited by inconsistent methodology, lack of assay validation, and biological complexity. While encouraging findings have emerged, many markers are non-specific and influenced by confounding factors such as synthesis, turnover and renal clearance. To advance the field, standardised protocols, validated assays, and studies linking biomarkers to functional outcomes are urgently needed.

7. Understanding the endothelial glycocalyx in cats

Cats have unique circulatory physiology with respect to volume status, responses to volume depletion, tolerance of fluid administration and circulatory shock phenotypes, which can possibly be traced back to their origins.

While they have a remarkable water-conservation capacity (250), they are considered fluid-intolerant species, with a tendency of fluid accumulation and slower fluid elimination rates (130, 131, 251). Descended from the African wildcat (*Felis lybica*), cats evolved in arid environments where selection likely favoured mechanisms for conserving water rather than eliminating excess fluid. Consequently, physiological adaptations that are advantageous during dehydration may become maladaptive when large volumes of intravenous fluids are administered.

Compared with dogs and humans, cats possess a smaller circulating blood volume, (49.0± SD 9.6 ml/kg) (252) compared to dogs (84-97 ml/kg) (253) . This feature could potentially be explained by the feline habitus. As ambush predators, cats spend prolonged periods resting interspersed with short bursts of intense activity. This lifestyle may have favoured a relatively smaller circulating blood volume, thus reducing cardiac workload at rest. Conversely, their relatively large and highly contractile spleen provides a reserve of RBCs that can be rapidly mobilised during stress or exercise (254, 255).

Studies suggest that cats have a relatively low capillary density (170). This could also be considered an adaptation to their behavioural ecology. Cats are predominantly solitary hunters, for whom injury may have substantial consequences by impairing hunting ability and increasing vulnerability to predation. In this context, a comparatively sparse vascular network, together with an enhanced haemostatic response (256), may represent adaptations that limit blood loss following injury and facilitate recovery. Furthermore, lower capillary density may limit transvascular fluid fluxes and subcutaneous oedema formation. While this remains a speculation, it could potentially explain why cats tend to accumulate preferentially cavitary effusions (fluid accumulates in their chest and sometimes abdomen) as a result of disease processes and fluid overload, as opposed to more pronounced sub-cutaneous oedema common in other species.

The unique feline circulatory physiology is equally reflected in their response to circulatory shock, typically characterised by a "shock triad" of hypothermia, bradycardia, and hypotension, rather than the hyperdynamic shock state seen in people and dogs (257, 258). Clinically, this is reflected by markedly lower fluid responsiveness, with only 37-40% of hemodynamically unstable cats responding to IV fluid resuscitation (259, 260), in contrast to 66-80% of dogs (261, 262).

Despite these observations, the feline vascular system and especially their microcirculation remains poorly characterized. Indeed, much of the available literature consists of small clusters of experimental studies using feline mesenteric capillaries, predominantly employing direct pressure measurements. These investigations have focused on establishing fundamental principles of microvascular flow regulation (263), the role of local autoregulatory mechanisms in buffering systemic arterial pressure changes (264), the biological regulation of microvascular density (265) and the effects of vasoactive agents such as fenoldopam (266). More recently, contrast-enhanced ultrasonography and scintigraphy have been used to evaluate changes in feline renal perfusion (267, 268) while flow cytometry has been shown to be a feasible technique for assessing microvascular reactivity following haemorrhage and fluid resuscitation (269). Notably, only one study has established the feasibility of sidestream dark-field videomicroscopy (SDFV) for assessment of the feline sublingual microcirculation (170). Collectively, these studies provide valuable but fragmented insights into feline microvascular physiology, making it difficult to develop a cohesive understanding of the feline microcirculation. Furthermore, they provide little to no information regarding the structure, function, or pathophysiology of the feline endothelial glycocalyx (EG).

Given the unique characteristics of the feline circulation and physiological responses to changes in intravascular volume, a better understanding of the feline microcirculation is warranted. This is particularly relevant in light of the growing recognition of the central role of the microcirculation, and especially the EG, in fluid homeostasis, vascular permeability, and the development of fluid overload. Understanding how the feline EG behaves in health and disease is therefore critical. This knowledge could support more tailored, species-specific management strategies, especially in the context of critical illness. For example, intravenous fluid plans could be more appropriately adjusted in critically ill cats with confirmed EG damage, helping to avoid complications such as fluid overload and respiratory compromise. Furthermore, fundamentally understanding how IV fluids and other drugs affect the feline EG can support more evidence-based fluid practices in both healthy and sick patients. The experimental work in this thesis lays the groundwork for addressing this knowledge gap. Building on the methodologies and evidence critically appraised in this review, it explores the feasibility of assessing EG integrity in cats using established human techniques and provides tolerance intervals in healthy subjects to support future research. It investigates the effects of intravenous fluid administration on the EG and microcirculatory parameters, examining dose regimens, physiological associations, and potential confounders such as anaesthetic influences. Furthermore, it generates unique initial data on EG integrity in clinically ill cats. In doing so, this work contributes the first foundational insights into feline EG structure and behaviour, helping to bridge the translational gap between theory, species, and clinical application.

Chapter II: Rapid patient-side evaluation of endothelial glycocalyx thickness in healthy sedated cats using GlycoCheck™ software

Chapter plan

1. Chapter II preface

2. Title page

3. Abstract

4. Introduction

5. Materials and methods

5.1. Animals

5. 2. Sedation and monitoring

5.3. Image acquisition

5.4. GlycoCheck™ analysis

5.5. Statistical analyses

6. Results

7. Discussion

8. Conclusion

9. Conflict of interest

10. Funding

11. Chapter II extended implications

1. Chapter II preface

The first experimental chapter of this thesis aimed to validate the use of sidestream dark field videomicroscopy with the novel GlycoCheck™ software in cats. This project was an international collaboration between the School of Veterinary Science – Tāwharau Ora, Massey University, and the University of Florida College of Veterinary Medicine.
To achieve this, a large cohort of healthy cats from the Massey University Feline Nutrition Unit was enrolled, representing a wide range of ages, sexes, and neuter statuses. While the initial target was to collect data from 120 cats - the recommended number for reference interval validation (270), data from 108 cats were successfully obtained.

The overarching aim of this study was to generate robust, reproducible data on the performance of this technique in cats, including reference intervals to lay groundwork for the remainder of the experimental chapters in this thesis and support future research. Additional objectives included assessing demographic influences and comparing feline data to those reported in other species, to inform cross-species translation and interpretation of results.

Statement of Contribution – Doctorate with Publications/Manuscripts:

The author of this thesis led the establishment of the collaboration, secured funding, designed the project, and was responsible for data collection, interpretation, reporting, and manuscript preparation.

Initial data from this study was presented as an oral abstract at the International Veterinary Emergency and Critical Care Symposium in 2019 by one of the co-authors (KK Millar) and the abstract published in the Journal of Veterinary Emergency and Critical Care in 2019:

Millar KK, Yozova. ID, Londoño LA, Monday JS, Thomson N, Sano H. (2019). Evaluation of the Endothelial Glycocalyx in Healthy Anesthetized Cats Using Rapid, Patient-Side Glycocheck Analysis Software. In: Abstracts from the International Veterinary Emergency and Critical Care Symposium, the European Veterinary Emergency and Critical Care Annual Congress, and the ACVECC VetCOT Veterinary Trauma and Critical Care Conference 2019. Journal of Veterinary Emergency and Critical Care, 29(S1), S11 doi: https://doi.org/10.1111/vec.12877

This manuscript has been fully published in Frontiers in Veterinary Science in 2021:

Yozova, I. D., Londono, L. A., Millar, K. K., Sano, H., Weidgraaf, K., Thomson, N. A., & Munday, J. S. (2021). Rapid Patient-Side Evaluation of Endothelial Glycocalyx Thickness in Healthy Sedated Cats Using GlycoCheck(R) Software. Front Vet Sci, 8, 727063. doi:10.3389/fvets.2021.727063

The format of the manuscript has been altered from the original to conform with Massey University thesis formatting guidelines.

Copyright note from publication:

Copyright © 2022 Yozova, Londoño, Millar, Sano, Weidgraaf, Thomson and Munday. This is an open-access article distributed under the terms of the Creative Commons Attribution License (CC BY). The use, distribution or reproduction in other forums is permitted, provided the original author(s) and the copyright owner(s) are credited and that the original publication in this journal is cited, in accordance with accepted academic practice. No use, distribution or reproduction is permitted which does not comply with these terms.

2. Title page

Rapid patient-side evaluation of endothelial glycocalyx thickness in healthy sedated cats using GlycoCheck™ software

Ivayla D. Yozova1,*, Leonel A. Londoño2, Kristina K. Millar3, Hiroki Sano1, Karin Weidgraaf4, Neroli Thomson1, John S. Munday1

[1]School of Veterinary Science, Massey University, New Zealand

[2]Department of Small Animal Clinical Sciences, College of Veterinary Medicine, University of Florida, Unites States

[3] Veterinary Teaching Hospital, College of Veterinary Medicine, University of Georgia, United States

[4]Centre for Feline Nutrition, Massey University, New Zealand

* Correspondence:

Ivayla D. Yozova: i.yozova@massey.ac.nz

Keywords: microcirculation, feline, capillaries, perfused boundary region, sidestream dark field videomicroscopy

3. Abstract

The endothelial glycocalyx (EG) determines transvascular fluid fluxes, and influences inflammation, coagulation, and capillary blood flow. The GlycoCheck™ software calculates EG thickness using sidestream dark field videomicroscopy recordings. This method has not been evaluated for use in cats. The aim of the present study was to evaluate the use of GlycoCheck™ for estimating EG thickness in healthy cats, and to investigate the variability of EG thickness in this population.

One hundred and one healthy research-purposed cats were included in the study. The cats were sedated, and a handheld videomicroscope, connected to GlycoCheck™ software, was used to evaluate the sublingual microvasculature. The parameters measured included perfused boundary region (PBR, an indirect measurement of EG thickness) in vessels between 5 and 25 µm in diameter, valid vessel density, percentage red blood cell filling, and median red blood cell column. Heart rate, respiratory rate, pulse oximetry and oscillometric blood pressure readings were also recorded.

There were 35 neutered male cats, 11 intact males, 38 neutered females, and 17 intact females. The average age was 63 months (range, 11–160 months). Tolerance intervals for PBR were 1.89 – 3.00 µm (95% CI, lower limit 1.76 – 2.04, upper limit 2.83 – 3.13 µm); for valid vessel density were 73.33 – 333.33 µm/mm^2 (95% CI, lower limit 77.00 – 99.33, upper limit 312.67 – 350.33 µm/mm^2); for red blood cell filling percentage were 59.85 – 85.07% (95% CI, lower limit 58.97 – 63.33, upper limit 83.07 – 88.20 %); and for median red blood cell column width were 5.63 - 8.59 µm (95% CI, lower limit 5.28 – 6.07, upper limit 8.14 – 9.51 µm). There was a negative association between median red blood cell column width and body weight ($p = 0.007$). The median red blood cell column was significantly wider in intact females when compared to spayed females ($p = 0.033$).

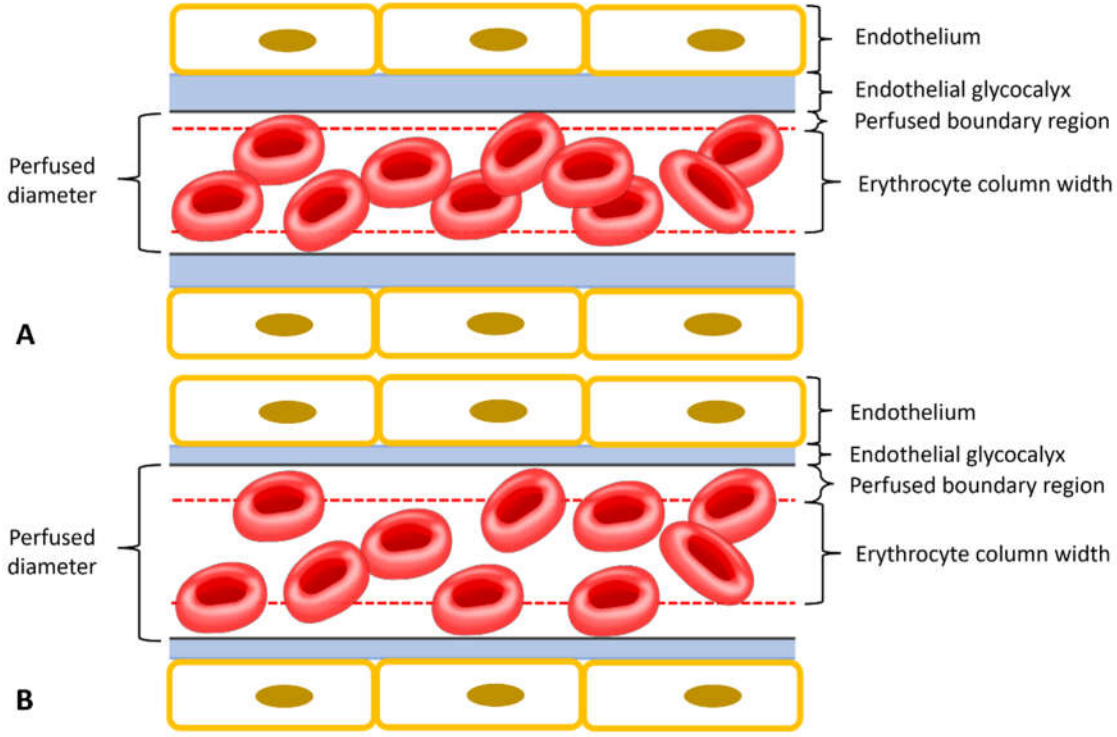
The GlycoCheck™ analysis was easily performed in healthy sedated cats. Clinical variables did not have an effect on the EG thickness. These results suggest that this technique could be valuable for evaluation of the EG and microvascular parameters in cats.

4. Introduction

The endothelial glycocalyx (EG) lines the endothelial surface of mammalian blood vessels, and consists of complex sugars bound directly to the endothelial membrane, and to each other. Furthermore, it incorporates a variety of smaller molecules (e.g. albumin, antithrombin) relevant to maintenance of blood vessel structure and function (45). The EG is a major determinant of transvascular fluid fluxes, it participates in local regulation of capillary blood flow, and influences inflammation and coagulation (71, 132). Systemic inflammatory states such as sepsis, trauma, ischemia-reperfusion injury, hypervolemia, and chronic illnesses can damage the EG. This can allow more fluid to leak from compromised blood vessels, exacerbating interstitial oedema. Damage to the EG can also alter capillary blood flow, promote inflammation, and trigger intravascular coagulation (60, 128, 139, 271). The significance of EG integrity and functionality in disease has been increasingly recognized in recent years, and altered EG has been associated with increased morbidity and mortality risk in critical illness in people (60, 141, 146, 272, 273).

One method for assessment of EG integrity includes measurement of the plasma concentration of shed EG constituents (236). Membrane-bound glycoproteins such as syndecan-1 are cleaved from the endothelial surface when the EG is damaged. The resultant increase of these glycoproteins can be measured in the plasma (146, 236, 271). Elevated plasma EG glycoprotein concentrations have been associated with increased morbidity and mortality in people with conditions leading to systemic inflammation (125, 274). However, while some evidence suggests syndecan-1 may be a useful prognostic indicator in people (141, 236), a relationship between syndecan-1 concentration and disease severity has not been seen in all studies (57). Alternatively, EG thickness can be estimated using sidestream dark field videomicroscopy (SDFV) and proprietary software (GlycoCheck™) (91). The software allows EG thickness to be determined by analysing multiple SDFV images and calculating the parameter perfused boundary region (PBR). Larger PBR represents thinner EG and vice versa (Figure 2.1). This tool has recently been validated for use in dogs (95). Although SDFV has been previously used to assess microcirculaton in cats, dogs and people, using GlycoCheck™ software to estimate EG thickness has not been done in this species (169-171, 173, 174).

Figure 2.1. Schematic representation of a capillary with endothelium in yellow, endothelial glycocalyx in blue, perfused boundary region in red dashed lines, and erythrocytes in red. Please note that the different components of this cartoon are scaled for emphasis. A. Intact endothelial glycocalyx characterized by a small perfused boundary region. B. Damaged (thinner) endothelial glycocalyx characterized by a large perfused boundary region.



The aim of the present study was to investigate whether the EG thickness of cats can be evaluated using SDFV and the GlycoCheck™ software. A secondary aim was to determine the tolerance intervals for GlycoCheck™ parameters. The hypothesis was that estimation of EG thickness using the GlycoCheck™ software would be feasible in cats.

5. Materials and methods

5.1. Animals

This project was approved by Massey University's Animal Ethics Committee (MUAEC Protocol 18/126) and was conducted in compliance with ARRIVE guidelines (275). One hundred and eight cats from the Centre for Feline Nutrition, Massey University, New Zealand were enrolled in the study. Cats met inclusion criteria if they were considered healthy based on no history of ongoing disease, physical examination findings, and blood work (complete blood count and serum biochemistry, T4) results. Predefined exclusion criteria were signs of illness shown after enrolment and prior to

intervention. Predefined humane endpoints and stopping criteria included clinically relevant anaesthetic complications (e.g. cardiovascular instability, respiratory compromise), procedural limitations (e.g. IV catheter dislodgement, resistance to low-stress handling) or any adverse event deemed to compromise animal welfare. In such cases, animals were recovered as appropriate, and no further data were collected. Feasibility had been investigated on a small number of cats (n = 3) prior to initiation of the project.

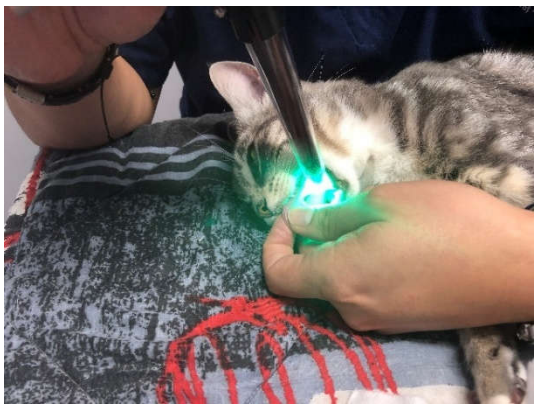
5.2. Sedation and monitoring

All animals were sedated with butorphanol 0.3 mg/kg SC for intravenous catheter placement in the left or right cephalic vein. Twelve cats were additionally sedated with medetomidine 10 µg/kg SC, based on previous handling challenges. Propofol was then administered intravenously to achieve heavy sedation (relaxation of jaw tone) to effect. The sedation was maintained using a continuous rate infusion of propofol (0.05-0.2 mg/kg/min) for the duration of the procedure. Sedation was overseen by a board-certified anaesthesiologist and clinical variables such as heart rate (HR), respiratory rate (RR), mucous membrane colour, capillary refill time, temperature, pulse oximetry (SpO_2), and oscillometric blood pressure (oBP) readings were monitored.

5.3. Image acquisition

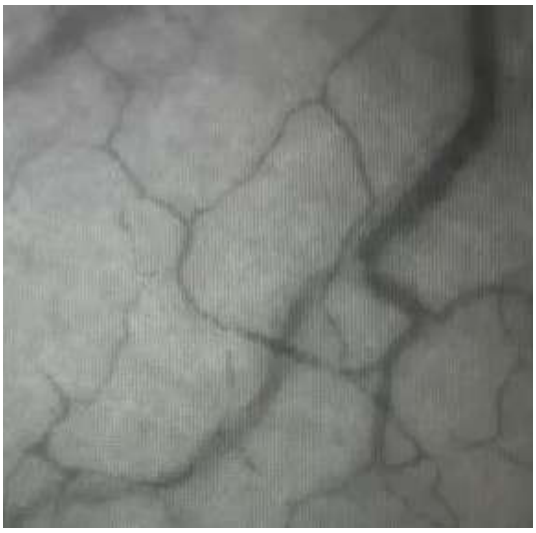
Cats were placed in lateral recumbency, and the tongue was positioned such that the sublingual mucosa was exposed at the base of the tongue (Figure 2.2).

Figure 2.2. Probe positioning of the SDFV camera for GlycoCheck™ analysis.



A hand-held SDFV camera connected to a laptop with GlycoCheck™ software (MicroVascular Health Solutions, USA) was placed in contact with the sublingual mucosa by the operator (LL). Three video recordings were taken from different sublingual mucosal sites (Figure 2.3).

Figure 2.3. Sidestream dark field videomicroscopy image of the sublingual mucosal capillaries in a cat.



The software automatically determines whether a sufficient number of suitable images has been acquired prior to moving to an additional site. This is signalled through a progress bar on the monitor display. Additionally, the software corrects for operator-induced errors such as movement and focus artifacts.

5.4. GlycoCheck™ analysis

The method for measuring and calculating GlycoCheck™ parameters has been described elsewhere (90). Briefly, the SDFV camera emits green light at 540 nm wavelength which is absorbed by haemoglobin in circulating red blood cells (RBC). Therefore, vessels appear dark on a bright background. The software automatically identifies vessels that are less than 30 µm in diameter by analysing the contrast between the RBC and the background. The software then subdivides vessels into 10 µm major vascular segments and subsequently records 40 frames containing on average 300 segments. The software ensures measurements are performed on vascular segments of good quality. Firstly, the vascular segments from the first frame of each recording are further divided by 0.5 µm markers into minor segments and each segment is analysed for sufficient contrast. Major segments with > 60% of minor segments with sufficient contrast are considered valid vascular segments. Valid vessel density per site is then expressed by multiplying 10 µm by the number of valid vascular segments identified. Secondly, RBC column widths are measured for all 40 frames of each recording including minimal column width, column position, and signal-to-noise ratio. The software then calculates the percentage of major vascular segments with RBC present during all 40 frames recorded to determine

the percentage of RBC filling. After those quality checks, the dynamic lateral position of RBC per column width is determined. A cumulative distribution is calculated using the intensity profiles of the distribution of RBC column widths. A median column width is then calculated for this distribution. Linear regression analysis on the median column width is performed to derive the perfused diameter. Finally, the PBR, an estimate of EG thickness, is calculated as the distance between the median RBC column width and the perfused diameter ([Perfused diameter – median RBC column width]/2). Reported GlycoCheck^{TM} parameters, therefore, include valid vessel density (VVD), percentage of RBC filling (RBC filling %), median RBC column width (Median P50), perfused vessel diameter (D_{perf}) and PBR for vessels with diameter from 5 to 25 µm. The PBR is further established for vessels with diameters from 5 – 9 µm, 10 – 19 µm and 20 – 25 µm. All GlycoCheck^{TM} parameters are described in Table 2.1.

Table 2.1. Description and interpretation of GlycoCheck^{TM} parameters.

Parameter	Description	Interpretation
Valid Vessel Segment (VVS) *Not automatically reported*	Determined by the amount of minor vascular segments (0.5 µm) within a major vascular segment (10 µm) with sufficient background contrast	Identifies adequately perfused vessel segments.
Valid Vessel Density (VVD)	Determined by multiplying the number of valid vessel segments by 10 µm	Identifies adequate microvascular perfusion in the examined regions
Percentage of RBC filling (% RBC filling)	Percentage of vascular segments with RBC in them in all 40 frames per recording	Identifies adequate microvascular perfusion in the examined regions
Median RBC column width (P50)	Calculated using the intensity profiles of distribution of RBC column widths in segments based on the dynamic lateral position of RBC in the column	Represents the portion of RBC column without RBC lateralization. Used to calculate endothelial glycocalyx thickness
Perfused vessel diameter (D_{perf})	Derived from the median RBC column width using linear regression	Represents the outer limit of lateral movement of RBC. Used to calculate endothelial glycocalyx thickness
Perfused boundary region (PBR)	Calculated using the formula (Perfused diameter – median RBC column width)/2	Estimation of endothelial glycocalyx thickness. Reported for vessel diameters 5-9 µm, 10-

		19 µm and 20-25 µm vessels separately and as an average 5-25 µm

5.5. Statistical analysis

Statistical analyses were performed by an independent statistical consultant using the commercially available software program JMP (Version 16, SAS Institute, Cary, NC, USA). All variables were analysed for normality using the Kolmogorov- Smirnov method and reported as mean ± standard deviation. Covariate analysis for continuous and non-continuous variables using a simple linear regression and one way ANOVA were performed respectively to assess relationships between microvascular measurements, and independent clinical variables monitored during sedation (HR, RR, SpO_2, oBP), or macrovascular monitored parameters. If the ANOVA was significant, then Tukey's multiple comparison procedure was used to determine differences in levels for categorical variables. Restricted maximum likelihood estimation was used for intra-individual and inter-individual variance component estimates. Non-parametric tolerance estimates and point estimates confidence intervals were estimated using 2500 bootstrap samples from the average of three measurements. For all analyses a P-value <0.05 was considered significant. A post hoc sample size calculation was performed for clinical variables monitored during sedation with a power set to 80% and $\alpha = 0.05$.

6. Results

Complete data acquisition was possible from 101 cats. Seven cats were excluded from the study due to recording malfunction (n = 3), development of post-sedation heart murmur (n = 1), lethargy (n = 1) and elevated T4 (n = 2). Of those included, 46 were male (11 intact and 35 neutered) and 55 were female (38 intact and 17 spayed). Mean age ± standard deviation was 67 ± 46 months. Mean body weight was 3.58 ± 0.79 kg.

Average image acquisition time per site was 167 seconds (range, 45-269 seconds) and per cat was 490 seconds (range, 118-808 seconds). The average number of valid recordings obtained per subject were 50 (range, 25-64). Success rate for image acquisition and analysis was 93.5%.

Heart rate, RR, SpO_2, oBP of all the cats remained within normal limits throughout the short period of sedation required for image acquisition (Table 2.2).

Table 2.2 Summary statistics for anaesthetic monitoring variables in 101 healthy sedated cats undergoing GlycoCheck™ analysis

Variable	Mean +/- SD
HR (beats per minute)	120 ± 19.4
RR (breaths per minute)	18 ± 4.9
SpO2 (%)	95.4 ± 1.66

SAP (mmHg)	115.9 ± 15.3
DAP (mmHg)	62.7 ± 14.5
MAP (mmHg)	80.7 ± 13.7

HR, Heart Rate; RR, Respiratory Rate; SpO2, pulse oximetry; SAP, Systolic Arterial Pressure, DAP, Diastolic Arterial Pressure, MAP, Mean Arterial Pressure

Mean ± SD values for GlycoCheckTM parameters are included in Table 2.3.

Table 2.3. GlycoCheck^{TM} parameters in a population of healthy cats (n = 101).

Parameter	Mean ± SD	SE	Min	Max
VVD (µm/mm^2)	173.00 ± 64.80	6.50	77.00	350.00
% RBC Filling	72.70 ± 6.16	0.61	60.00	88.20
PBR 5-25 (µm)	2.39 ± 0.26	0.03	1.76	3.13
PBR 5-9 (µm)	1.34 ± 0.15	0.02	0.91	1.94
PBR 10-19 (µm)	2.70 ± 0.30	0.03	2.05	3.51
PBR 20-25 (µm)	2.92 ± 0.57	0.06	1.51	5.22
Median P50 (µm)	7.00 ± 0.68	0.07	5.28	9.51
D_{perf}, 2PBR + P50 (µm)	11.80 ± 0.88	0.09	9.51	15.20

D_{perf}, Perfused Vessel Diameter; Median P50, Median Red Blood Cell Column Width; PRB, Perfused boundary region; % RBC Filling, Percentage Red Blood Cell Filling; VVD, Valid Vessel Density; SD, Standard Deviation; SE, Standard Error

There was no significant association between clinical variables monitored during sedation (HR, RR, SpO_2, oBP) and VVD, RBC filling %, median P50, Dperf, and PBR. Furthermore, there was no significant association between GlycoCheck^{TM} parameters of the cats that received medetomidine (n = 12) compared to the GlycoCheck^{TM} parameters of those that did not receive medetomidine (n = 89). There was no significant association between age and GlycoCheck^{TM} parameters. However, there was a negative association between median P50 and body weight (R^2 = 0.029; *p = 0.007*). Additionally,

median P50 was significantly wider ($R^2 = 0.087$; $p = 0.033$) in intact females than in spayed females. Tolerance intervals for GlycoCheck™ parameters are presented in Table 2.4.

Table 2.4. Tolerance Intervals for GlycoCheck™ parameters in a population of healthy cats (n = 101).

Parameter	Lower Limit	95% CI	Upper Limit	95% CI
VVD (µm/mm2)	73.33	70.00 – 99.33	333.33	312.67 – 350.33
RBC Filling %	59.85	58.97 – 63.33	85.07	83.07 – 88.20
PBR 5-25 (µm)	1.89	1.76 – 2.04	3.00	2.83 – 3.13
PBR 5-9 (µm)	0.97	0.91 – 1.08	1.58	1.55 – 1.64
PBR 10-19 (µm)	2.11	2.05-2.25	3.48	3.25 – 3.51
PBR 20-25 (µm)	1.87	1.51 – 2.26	4.02	3.94 – 5.23
Median P50 (µm)	5.63	5.28 – 6.07	8.59	8.14 – 9.51

CI, Confidence Intervals; Median P50, Median Red Blood Cell Column Width; PBR, Perfused boundary region; % RBC Filling, Percentage Red Blood Cell Filling; VVD, Valid Vessel Density;

Variance component estimates are presented in Table 2.5. A comparison of GlycoCheck™ parameters in healthy cats, dogs, and people is presented in Table 2.6. All statistical analyses are presented in the supplementary material.

Table 2.5. Variance Component Estimates for GlycoCheck™ parameters in a population of healthy cats (n = 101).

Parameter	Inter-individual Variance Components				Intra-individual Variance Components			
	Component	**SE**	**95% CI**	**% of Total Variance**	**Component**	**SE**	**95% CI**	**% of Total Variance**
VVD	3170.18	611.86	1970.96 – 4369.40	50.13	3153.78	322.75	2605.76 – 3895.88	49.87
% RBC Filling	21.82	5.59	10.87 – 32.77	32.22	45.91	4.70	37.93 – 56.73	67.78

PBR 5-25	0.03	0.01	0.01 – 0.05	26.48	0.09	0.01	0.08 – 0.12	73.52
PBR 5-9	0.01	< 0.01	0.01 – 0.02	29.52	0.03	< 0.01	0.02 – 0.04	70.48
PBR 10-19	0.05	0.01	0.02 – 0.08	28.43	0.12	< 0.01	0.10 – 0.15	71.57
PBR 20-25	0.05	0.05	- 0.05 – 0.15	6.98	0.69	0.07	0.56 – 0.85	93.02
Median P50	0.29	0.07	0.16 – 0.43	35.41	0.53	0.05	0.44 – 0.66	64.59

CI, Confidence Intervals; Median P50, Median Red Blood Cell Column Width; PBR, Perfused boundary region; % RBC Filling, Percentage Red Blood Cell Filling; VVD, Valid Vessel Density; SE, Standard Error

Table 2.6. Comparison of GlycoCheck™ parameters in cats, dogs and people expressed as Mean ± Standard Deviation.

Parameter	Cats (n = 101)	Dogs (n = 54) (17)	People (n = 915) (23)
VVD (µm/mm2)	173.00 ± 64.80	2030.68 ± 733.41	3213.00 ± 691.00
% RBC Filling	72.70 ± 6.16	77.4 ± 6.22	73.20 ± 5.00
PBR 5-25 (µm)	2.39 ± 0.26	2.04 ± 0.31	2.14 ± 0.25
Median P50 (µm)	7.00 ± 0.68	7.90 ± 0.85	10.56 ± 1.12
D_{perf} (µm)	11.80 ± 0.88	11.97 ± 1.05	14.84 ± 1.18

D_{perf}, Perfused Vessel Diameter; Median P50, Median Red Blood Cell Column Width; PBR, Perfused boundary region; % RBC Filling, Percentage Red Blood Cell Filling; VVD, Valid Vessel Density

7. Discussion

This study demonstrated that measuring microcirculatory parameters such as VVD, % RBC filling, median P50, and D_{perf} using SDFV and the GlycoCheck™ software is feasible and easily performed in healthy sedated cats. Furthermore, PBR can be calculated using these measured parameters in an acceptable period of time under heavy sedation with a high success rate. Effects of body weight and neuter status on median RBC column width were found. However, those did not alter the PBR and therefore the estimated EG thickness.

The importance of microcirculatory derangements, including EG damage in the context of the pathophysiology of circulatory shock has been brought forward in recent years (35, 121). Domestic cats present a challenge for circulatory assessment with tools designed for people and dogs, due to their small size. Furthermore, they typically present in a hypodynamic shock state, manifested as

bradycardia, hypothermia, and hypotension, making it difficult to rely on conventional monitoring tools (257). There is increasing evidence that microcirculatory abnormalities can be present beyond macrohaemodynamic stabilisation. Therefore, a tool that robustly evaluates the microcirculation and EG thickness specifically in a species where macrocirculatory evaluation is already challenging might prove particularly useful. GlycoCheck™ parameters were evaluated in a large population of cats - not only to account for potential age and gender differences, but to also establish tolerance intervals. Tolerance intervals are a crucial step in generating expected values of a given parameter in healthy individuals. As such, they allow for identifying abnormalities in sick patients in the clinical setting and facilitate comparison and reproducibility in further research.

In this study, all cats were heavily sedated for GlycoCheck™ evaluation because they were considered unlikely to tolerate having the SDFV camera in the oral cavity. Twelve cats required additional sedation using medetomidine as they were difficult to handle despite using Low Stress Handling®. However, the addition of this drug did not significantly alter any of the GlycoCheck™ parameters. These results suggest that the method of sedation may not be a confounding factor for using GlycoCheck™ in clinical practice, although additional studies using a greater range of sedation protocols are required to confirm this. Our results are consistent with a previous study in healthy dogs where the different sedation protocols also did not seem to alter GlycoCheck™ parameters (95). Additionally, the need to sedate or anaesthetize a cat for image acquisition might preclude the use of the device in debilitated critically ill patients, because of the anaesthetic risk. However, evaluation of EG integrity would be most valuable in such patients. Therefore, evaluation of alternative image acquisition sites may prove helpful. Overall, changes in HR, RR, SpO_2, oBP were not associated with significant changes in the GlycoCheck™ parameters measured during this investigation. The cats were sedated for a brief period of time, and the clinical variables monitored during sedation remained close to normal. This might explain the lack of effects of those on GlycoCheck™ parameters. Noteworthily, only a post hoc sample size calculation was made. It determined that the study was underpowered for some clinical variables monitored during sedation (see supplementary material). However, the sample size was sufficient to detect differences in mean arterial pressure, which is a measured parameter potentially affecting the microcirculation.

In people, PBR has been reported to increase with age (187). Such an association with PBR and age was not observed in this population of cats, despite the cats having an age range of 11 – 160 months. Whether this is a species-specific reflection of good vascular health, or rather the absence of age-related vascular comorbidities often seen in people is unknown. Furthermore, the study might have been underpowered to detect such differences.

Women have been found to have thinner EGs than men and their EG structure varies somewhat with their menstual cycle (90, 276, 277). Typically, pet cats are neutered or spayed, therefore hormone-related gender dimorphism might not be a significant factor for their EG integrity. Nonetheless, the lack of sex hormones might result in changes in EG structure and functionality. While no significant effects

were found for the estimated EG thickness in females compared to male cats, P50 was significantly wider in entire compared to spayed females. This signifies less RBC lateralization in the intact females. Increased RBC lateralisation could be interpreted as an early marker of EG damage according to a recent study in people (90).

In previous studies in people, an increase in body mass index was associated with evidence of potential capillary damage, manifested as increased perfused-to-total capillary density (187). In the present study, P50 decreased as body weight increased. It should be noted that although body mass and gender status were associated with changes in P50, these were not associated with any detectible differences in the estimated EG thickness. Whether the neuter status and body weight differences in domestic cats are related to a milder form of EG damage not affecting its actual thickness is currently uncertain.

Although direct comparison between different studies is not possible, the results of the present study suggest that vessel density is higher in the oral submucosa in dogs and people than in cats (90, 95). Anatomical differences in capillary density between species have been previously reported for several vascular beds (278, 279). Furthermore, previous studies measuring perfused vessel density have also reported differences between species (170, 173, 174, 280). This signifies that caution is warranted when extrapolating results from one species to another, including experimental to clinical data.

Sidestream dark field videomicroscopy uses polarized light emitted in the absorption wavelength of haemoglobin giving RBC their dark appearance on a contrasting light background. Therefore, peculiarities of feline haemoglobin, such as three pH-dependent forms of haemoglobin and eight sulfhydryl groups, might have affected the results (281). Furthermore, feline RBC contain haemoglobin that has a lower oxygen affinity compared to human and canine haemoglobin. However, while the oxygen affinity is lower, the oxygen content in RBC appears to be similar between cats and people (282). Additionally, absorbance spectra seem to be similar between cats, dogs, horses, pigs, and people; suggesting that peculiarities of feline haemoglobin would not affect measurements (283).

In the present study, sublingual microcirculation was evaluated in healthy sedated cats. While perfusion of this area is expected to be adequate in such subjects, this might not be the case in patients with circulatory impairment. Indeed, using the sublingual microcirculation as a surrogate for all capillaries represents a major limitation of the technique as damage to the EG might not be equally represented during disease processes. Furthermore, hypoxia or severe anaemia might also affect results in sick patients (122). Image acquisition was performed by a single operator in this study, which represents another major limitation. In a previous study in people, intra and inter-rater reproducibility was found to be poor (272). The GlycoCheck™ is a novel software estimating EG thickness. A comparison with a gold standard would have increased the validity of the obtained measurements. However currently there is no gold standard methodology to evaluate EG dimensions, integrity, or functionality.

8. Conclusion

Based on this study, estimating EG thickness in healthy sedated cats was feasible using SDFV and the GlycoCheck™ software. This is the first study evaluating the EG in the feline species and will serve as a stepping stone for investigating the feline EG in health and disease. Tolerance intervals were established as a critical step for future studies in domestic cats.

9. Conflict of Interest

This project was funded by the Massey University Research Fund, which played no role in the study design; nor in the collection, analysis, and interpretation of data; nor in the decision to submit the manuscript for publication. None of the authors has any other financial or personal relationships that could inappropriately influence or bias the content of the paper.

10. Funding

This project was funded by the Massey University Research Fund - RM 21500.

11. Chapter II Extended implications

This study was the first to evaluate the feline microcirculation and EG, providing valuable insights into normal findings, demographic variability, and refinement of the data collection technique used in this and future investigations. Most notably, it established species-specific reference intervals (tolerance intervals in this case) for SDFV-acquired GlycoCheck™ parameters, an advancement that, to the author's knowledge, has not been robustly reported in any other species to date.

When interpreting biological data, it is essential to distinguish between statistical descriptors, such as means or medians, and clinically defined reference intervals. While both summarize data, they serve distinct purposes - means and medians are used to compare groups and assess statistical significance through hypothesis testing, but they do not define clinical normality. Reference intervals, by contrast, describe the expected range of values in a healthy population, typically the central 95%, and are used to determine whether an individual result is physiologically typical.

Taking into consideration the characteristics of the SDFV device and GlycoCheck™ software, tolerance intervals rather than classical reference intervals were established. GlycoCheck™ parameters differ from many traditional clinical pathology variables in that they represent mathematically derived estimates based on image analysis rather than direct measurements of biological constituents. As a result, tolerance intervals were considered more appropriate for describing the expected range of values.

Although both reference intervals and tolerance intervals describe the distribution of values within a population, they serve different purposes. Reference intervals estimate the range encompassing a specified proportion of observations in a reference population, whereas tolerance intervals estimate bounds that are expected, with a defined level of confidence, to contain a specified proportion of the population. This additional confidence component makes tolerance intervals particularly useful when characterising variability and establishing expected ranges for device-derived parameters.

Given the use of a measurement device, the mathematical derivation of GlycoCheck™ parameters, and the objective of defining expected ranges for future observations, tolerance intervals were selected. Their principal advantage is that they provide a statistically rigorous estimate of the range within which a specified proportion of values is expected to fall. However, tolerance intervals are less commonly reported than reference intervals in veterinary medicine and therefore often require additional explanation during scientific communication. In veterinary medicine, establishing tolerance intervals for emerging diagnostics like the GlycoCheck™ system enables clinicians to interpret glycocalyx metrics, such as the Perfused Boundary Region (PBR), at the level of individual patients. This represents a key step toward integrating the methodology into clinical practice, rather than restricting its use to population-based research.

In support of clinical translation, this study also assessed the relative contributions of inter-individual and intra-individual variance for each GlycoCheck™-derived parameter (Table 2.4). The findings revealed that most parameters, particularly PBR and % RBC filling, exhibited a predominance

of intra-individual variance, indicating considerable within-subject variability over time or across replicates. For example, over 70% of the total variance for PBR across different vessel size categories was attributable to intra-individual sources, reaching 93% in the largest capillaries (20–25 μm). Only VVD demonstrated a near-equal split between inter- and intra-individual variability, suggesting it may be a more stable and reliable parameter. Similar patterns of variability have been reported in previous studies involving both healthy and critically ill human patients (181, 185, 186). To mitigate the effects of intra-individual variation, the current recommendation is obtaining a minimum of three consecutive measurements, an approach adopted in this study. These results highlight the importance of accounting for within-subject variability when interpreting GlycoCheck™ parameters, particularly in longitudinal or individual-patient monitoring contexts.

Another salient finding of this study was the confirmation that cats, and likely other animal species, require deep sedation or general anaesthesia to successfully perform GlycoCheck™ analysis. During the initial training phase, several pilot attempts were made using minimal sedation to simply maintain mouth opening; however, it became evident that cats are highly sensitive to intraoral manipulation, and reliable imaging was only achievable when the patient was rendered nearly unconscious. This necessity introduces an important consideration: the inevitable impact of anaesthetic agents on the microcirculation, particularly during longer data collection sessions. At the same time, it presents valuable research opportunities, such as identifying anaesthetic protocols that minimise microvascular interference, or establishing optimal equilibration periods to mitigate anaesthesia-induced volume shifts prior to measurement. Although these aspects were not directly investigated in the present study, the findings lay a foundation for future work in this area.

Notably, small animals are frequently anaesthetized for procedures that would not typically require anaesthesia in human medicine, including diagnostic imaging and therapeutic interventions such as wound care. As such, the need for anaesthesia during GlycoCheck™ analysis is unlikely to limit clinical application but rather necessitates thoughtful adjustments to study design.

Chapter III: Validation of a commercial human enzyme-linked immunosorbent assay to measure syndecan-1 (CD138) concentration in feline sera

Chapter plan

1. Chapter III preface
2. Introduction
3. Materials and methods
   - 3.1. Materials and methods summary
   - 3.2. Animals
   - 3.3. Sample collection and processing
   - 3.4. ELISA assay validation overview
     - 3.4.1. Human syndecan-1 (CD138) enzyme-linked immunosorbent assay protocol
       - 3.4.1.1. Brief overview
       - 3.4.1.2. Technical protocol
   - 3.5. Feline recombinant syndecan-1 production
     - 3.5.1. Brief overview
     - 3.5.2. Technical protocol
   - 3.6. Assay-specific validation steps
     - 3.6.1. Determining positive and negative samples
     - 3.6.2. Measuring accuracy
       - 3.6.2.1. Parallelism
       - 3.6.2.2. Matrix effects
         - Dilutional linearity
         - Recovery
     - 3.6.3. Measuring precision
       - 3.6.3.1. Within-run variability
       - 3.6.3.2. Between run variability
       - 3.6.3.3. Determining limits of quantification
   - 3.7. Feline syndecan-1 identification steps
     - 3.7.1. Immunoprecipitation

3.7.1.1. Brief overview
3.7.1.2. Technical protocol
3.7.2. Gel electrophoresis
3.7.2.1. Brief overview
3.7.2.2. Technical protocol
3.7.3. Mass spectrometry
3.7.3.1. Brief overview
3.7.3.2. Technical report for mass spectrometry on electrophoresis bands
3.7.3.3. Technical report for mass spectrometry on samples from ELISA wells
3.8. Statistical analyses
4. Results
4.1. Feline recombinant syndecan-1
4.2. Human ELISA kit performance
4.3. Gel electrophoresis
4.4. Mass spectrometry on gel electrophoresis bands
4.5. Mass spectrometry on antigen-antibody complexes from ELISA wells
5. Discussion
5.1. Initial analysis – highly positive samples, inaccuracy and imprecision
5.2. Lack of binding of the ELISA antibody to feline recombinant syndecan-1
5.2.1. Type of antibody
5.2.2. Syndecan-1 sequence, structure and glycosylation
5.3. Identification of the protein binding to the ELISA antibody
5.3.1. Immunoprecipitation and mass spectrometry
5.4. Appraisal of commercial syndecan-1 ELISA kits for use in cats
5.5. Limitations
6. Conclusion

7. Chapter III extended implications

1. Chapter III preface

Following the establishment of tolerance intervals for the GlycoCheck™ system, the next step was to investigate biomarkers of endothelial glycocalyx (EG) shedding in feline serum. The rationale was that these two approaches would offer complementary insights: the GlycoCheck™ system evaluates structural changes in the EG (e.g., thinning), while measurements of shed constituents provide information on the biochemical footprint of glycocalyx damage. Moreover, one method may be more suitable than the other in specific clinical scenarios. For example, measuring shed EG constituents requires only a routine blood sample and does not necessitate anaesthesia, making it more feasible in critically ill patients.

At the time of study design, only a limited number of EG constituents had been evaluated as biomarkers of EG injury, with SDC-1 being the most extensively studied. Syndecan-1 was selected for this project based on the presumed conservation of EG composition across vertebrates, and due to the complete lack of published data on feline EG constituents. Developing a feline-specific ELISA for SDC-1 was beyond the project's scope and budget, so an existing human SDC-1 ELISA was selected for validation, following homology research using databases such as UniProt.com. Due to financial constraints and limited blood volume in cats (~25 mL total blood volume, restricting the safe volume per sampling point), only a single biomarker could be investigated.

This chapter is not formatted for publication and intentionally presents a detailed account of the steps taken to validate the ELISA assay. The study was conducted in parallel with data collection for Chapters IV, V, and VI, with the ultimate aim of comparing GlycoCheck™ parameters with serum SDC-1 concentrations.

Contribution statement

The author of this thesis secured funding and designed the project with support from supervisors. The author was responsible for data collection, interpretation, reporting, and manuscript preparation. While the author was responsible for critical parts of the laboratory work, the supervisors led delicate parts of the validation process, namely immunoprecipitation and gel electrophoresis. Synthesis of feline recombinant SDC-1 and mass spectrometry were entirely outsourced.

2. Introduction

The endothelial glycocalyx (EG) has been a burgeoning field of research over the past decade (38, 45, 46, 57, 58, 77, 86, 112, 113, 115, 117-119, 122, 123, 125, 126, 128, 129, 132, 139, 142, 271, 284, 285). Since its discovery in the mid-20th century, researchers have focused on defining its physiology and the consequences of EG damage in disease (38). In response to the need for reliable assessment tools, several methods have been developed to evaluate EG integrity. Most of these can be grouped in three general categories. The first involves estimating or directly measuring EG thickness, as "thinning" is associated with structural damage and potentially loss of function. The second focuses on detecting increased levels of "shed" EG constituents in the bloodstream, released from the endothelial surface following injury. The third, used less frequently, involves assessing changes in vascular permeability, resulting from EG damage, often in combination with one of the other two methods (38).

Some methodologies assessing the EG remain confined to experimental settings, such as electron microscopy and mathematical modelling, while others are suitable for use in clinical settings as well (38). Clinically applicable approaches include direct observation of the microvasculature using sidestream dark field videomicroscopy and estimation of EG thickness (or "thinning") using proprietary software (the GlycoCheck^{TM}) (90), and measurement of shed EG constituents found unbound in the serum (60). Both techniques are widely used in human medicine (90, 146-149, 151-153, 156, 158, 185, 190, 192, 193, 196, 206, 234, 286, 287) and are gradually being adopted in veterinary medicine (93-95, 100, 216, 242, 243, 288).

Commonly measured shed EG constituents in people include proteoglycans, such as syndecan-1 (SDC-1), heparan sulfate and hyaluronan. However, less commonly measured glycoproteins, such as intercellular adhesion molecule-1 and vascular adhesion molecule-1, have also been reported in the literature (271). Syndecan-1 has been by far the most commonly measured molecule to investigate EG shedding. It is considered a biomarker of EG damage in people (234).

Syndecan-1 (cluster of differentiation designation – CD138) is a highly glycosylated transmembrane proteoglycan of approx. 30 – 70 kDa molecular weight. The molecular weight varies depending on the degree of glycosylation. The glycosaminoglycan responsible for glycosylation is heparan sulfate. This is why SDC-1 is defined as heparan sulfate proteoglycan (38, 49, 51, 55). It consists of cytoplasmic, transmembrane and extracellular domains (49). The cytoplasmic and transmembrane domains of SDC-1 show strong homology across vertebrate species, while the extracellular domain exhibits greater variation in composition (49, 50). The extracellular domain (or ectodomain) is cleaved after EG damage and it is this part of the proteoglycan that can be measured in serum (49, 56).

The most common methodology for measuring SDC-1 concentrations is enzyme-linked immunosorbent assay (ELISA) and multiple species-specific and cross-species commercial kits exist

on the market. Several previous studies have reported measuring SDC-1 in dogs; however, all showed low or undetectable concentrations of SDC-1 (93, 94, 216, 247, 248).

At the time of undertaking this project, there were no commercial feline-specific SDC-1 ELISA kits available to the authors' knowledge. Considering the reported homology between human and feline SDC-1 and therefore potential cross-reactivity, we attempted to validate a human SDC-1 commercial ELISA (Human Syndecan-1 ELISA Kit (CD138), ab46506, Abcam Ltd.) for use on feline sera. The aim was to then investigate the potential of SDC-1 as a biomarker of EG damage in cats.

3. Materials and methods

3.1. Materials and methods summary

Sera from sick cats (expected to have high concentrations of feline SDC-1) and healthy cats (expected to have low concentrations of feline SDC-1) were collected for the validation process. A human SDC-1 sandwich ELISA kit (ab46506; Syndecan-1 (CD138) Human ELISA Kit; Abcam Ltd) was chosen for validation to use in feline sera. After detection of highly and poorly reactive serum samples, an initial validation focused on characterising the antibody (AB) binding by assessing dilutional linearity, parallelism, and assay precision. The premise of these tests is that high-affinity binding and low assay variability suggest the AB is binding to a specific target antigen (such as feline SDC-1) without interference from other serum components and therefore the assay may be suitable for use in cats. In contrast, low-affinity binding and high assay variability would suggest non-specific binding to various components of feline sera, and/or inhibition of the ELISA reactions, suggesting the kit would not be suitable for use in cats. Since the human positive control from the kit was not ideal to use as a positive control for feline sera, a species-specific SDC-1 was required. This served as an additional verification that the AB in the kit binds to the correct protein. No feline-specific SDC-1 was readily available. Therefore, in an additional step, feline recombinant SDC-1 (frSDC-1) was synthetized in HEK293 cell cultures.

For further validation, namely identification of the protein bound to the ELISA kit AB (presumably feline SDC-1), immunoprecipitation was used. For this, highly reactive serum samples were mixed with the biotinylated detection AB from the ELISA kit and streptavidin-coated magnetic beads. These beads were then "pulled down" on the bottom of the test tube by a magnetic stand, wwith the attached antigen-antibody complex (AG-AB). The supernatant containing all the unbound proteins was removed, leaving only the AG-AB complex (presumably feline SDC-1 and ELISA kit detection AB) and magnetic beads in the sample. The bonds between the AG and AB and the AB and beads were then chemically severed. Immunoprecipitation ensured that a minimal number of unbound proteins is contained in the samples and reduced potential interference in the next steps of the analysis.

Sodium Dodecyl Sulfate Polyacrylamide gel electrophoresis (SDS-PAGE) was used to further separate the immunoprecipitated proteins contained in the samples by their molecular weight. Since proteins can have similar molecular weights and therefore can overlap on the gel, minimization of types

of proteins contained in the sample was required (through immunoprecipitation, see above). However, SDS-PAGE does not actually identify the measured protein as feline SDC-1. For this, finer identification was required. Therefore, gel bands with molecular weights similar to human (and presumably feline) SDC-1 were extracted from the gel and sent for mass spectrometry analysis.

Mass spectrometry was used to determine whether the protein bound to the ELISA kit AB was indeed feline SCD-1 by analysing molecular weight to charge ratio and comparing to known database of mass spectra. It was performed on selected electrophoresis gel bands (see above) and additionally, on samples containing only AG-AB complexes (presumably feline SDC-1 and ELISA kit capture AB) collected from the ELISA wells directly (without immunoprecipitation and electrophoresis steps).

A detailed report of the validation process including each of the above-mentioned steps in analysis is provided below.

3.2. Animals

The project received approval from the Massey University Animal Ethics Committee (MUAEC protocol 19/133). Serum samples from healthy and systemically ill cats were collected over a period of six months. The healthy population, serving as potential negative controls, consisted of cats from the Massey University Centre for Feline Nutrition. They were deemed healthy based on no history of weight loss, normal physical exam findings and no abnormalities on annual clinicopathologic health check (complete blood count and serum biochemistry). The diseased population, serving as potential positive controls, consisted of sick client-owned cats admitted to the Massey University Companion Animal Hospital. Cats presented with severe conditions such as circulatory shock, sepsis, trauma, congestive heart failure among others, were enrolled. Demographic and clinical characteristics of the cats from which serum samples were obtained are presented in Table 3.1.

Table 3.1. Signalment, health status, and diagnoses of cats from which serum samples were obtained for validation of the feline syndecan-1 ELISA. Highly reactive samples – in bold.

ID	Age (years)	Sex	Neuter status	Breed	Health status	Diagnosis
S1	11	M	N	Norwegian Forest	Diseased	Open - inappetence
S2	10	M	N	Domestic Short Hair	Diseased	Open - abdominal effusion
S3	15	M	N	Domestic Short Hair	Diseased	Feline Aortic Thromboembolism
S4	8	F	S	Domestic Short Hair	Diseased	Open - Status epilepticus
S5	3	F	Unknown	Ragdoll	Diseased	Crush injury, ischemia reperfusion injury
S6	**3**	**F**	**E**	**Ragdoll**	**Diseased**	**Road traffic accident and sepsis due to post-partum metritis**
S7	10	F	S	Domestic Short Hair	Diseased	Sepsis due to penetrating trauma
S8	12	F	S	Siamese	Diseased	Sepsis due to pyothorax
S9	8	M	N	Domestic Long Hair	Diseased	Traumatic cardiac tamponade
S10	12	M	N	Domestic Short Hair	Diseased	Suspected lymphoma

S11	1	M	N	Domestic Short Hair	Diseased	Head trauma, suspected traumatic brain injury
S12	10	F	S	Domestic Short Hair	Diseased	Open - suspected Feline Aortic Thromboembolism
S13	**Unknown**	**M**	**E**	**Domestic Short Hair**	**Diseased**	**Road traffic accident, severe traumatic injuries (stray cat)**
S14	10	F	S	Domestic Short Hair	Diseased	Open - haemorrhagic vomiting, collapse
S15	10	F	S	Domestic Short Hair	Diseased	Open - suspected Feline Aortic Thromboembolism
S16	**3**	**M**	**N**	**Domestic Short Hair**	**Diseased**	**Feline Infectious Peritonitis**
H1	2	M	N	Domestic Short Hair	Healthy	NA
H2	2	F	S	Domestic Short Hair	Healthy	NA
H3	7	M	N	Domestic Short Hair	Healthy	NA
H4	7	F	S	Domestic Short Hair	Healthy	NA
H5	12	F	E	Domestic Short Hair	Healthy	NA
H6	3	F	E	Domestic Short Hair	Healthy	NA
H7	3	F	S	Domestic Short Hair	Healthy	NA
H8	5	F	S	Domestic Short Hair	Healthy	NA
H9	3	M	N	Domestic Short Hair	Healthy	NA
H10	3	F	E	Domestic Short Hair	Healthy	NA

3.3. Sample collection and processing

Blood samples of 2 ml or less were collected from the jugular vein, preferably during venepuncture for other scheduled blood sampling. The samples were stored in serum tubes containing a clot activator (red top tubes) and left to clot at 4°C for 1-2h. After this, the samples were spun at 3000 G for 15 min and stored in 0.5 ml aliquots at -80°C for further analysis.

3.4. ELISA assay validation overview

The aim of assay validation was to confirm that the ELISA kit for measuring human SDC-1 concentrations will detect and measure accurately feline SDC-1 and to establish whether there are significant non-specific binding and/or matrix effects - interferences from biological components that may alter analyte detection. This validation process was performed following the practical guide to immunoassay method validation published in 2015 by Andreasson et al (289) and several documented validation protocols including one used to validate a human hyaluronan assay in cats (290-292). The validation involved several steps performed using the assay itself and additional steps aiming to identify the protein captured by the ELISA assay.

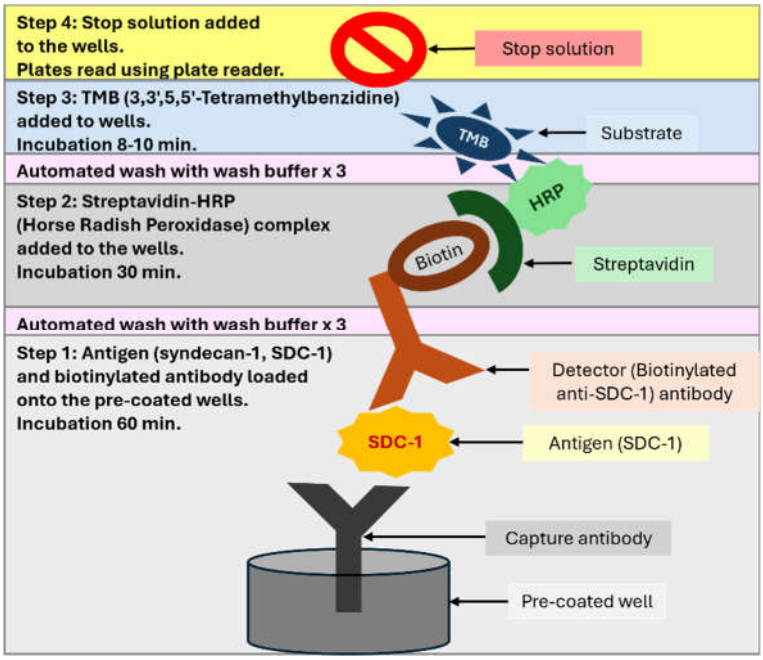
3.4.1. Human syndecan-1 (CD138) enzyme-linked immunosorbent assay protocol

3.4.1.1. Brief overview

The following section describes the protocol used for all ELISA analyses performed during the validation process as per manufacturer guidelines.

The human sandwich ELISA assay (ab46506; Syndecan-1 (CD138) Human ELISA Kit; Abcam Ltd) used in this chapter was manufactured to measure human SDC-1 levels in serum samples using specific monoclonal anti-SDC-1 AB and a colour-based detection system (Figure 3.1). First, the human SDC-1 AG bound to a capture AB that was already attached to the wells of a plate. A biotin-labelled detection AB was then added, which also bound to the AG, forming a sandwich-like complex. This sandwich method improves sensitivity and specificity in detecting the correct AG (human SDC-1). After washing away any unbound material, a streptavidin-conjugated enzyme was introduced, which attached to the biotin-labelled AB, before a substrate was added, causing a colour reaction proportional to the amount of human SDC-1 in the sample. The reaction was then "stopped" using sulfuric acid (Stop solution) and the intensity of the colour (optical density, OD_{450nm}) was measured and transformed into human SDC-1 concentrations. This was performed by plotting OD_{450nm} against a standard curve of OD_{450nm} from samples with previously known SDC-1 concentrations (a.k.a. standards) provided by the manufacturer as part of the kit. A detailed technical protocol is described below. For validation purposes feline serum, and therefore, feline SDC-1 was presumed to be detected.

Figure 3.1. Stepwise diagram of a Sandwich (quantitative) Enzyme-linked Immunosorbent Assay for human Syndecan-1 (CD138) Detection.



3.4.1.2. Technical protocol

A human Syndecan-1 (CD138) sandwich (quantitative) ELISA for human serum, plasma, buffered solutions, and cell culture media with monoclonal AB was used (ab46506; Syndecan-1 (CD138) Human ELISA Kit; Abcam Ltd). All analyses were completed following manufacturer instructions (Figure 3.1).

Reagents were left for equilibration at room temperature (18-22°C) for 30 min before analysis. The concentrated standard diluent and wash buffer were diluted 10-fold and 200-fold, respectively. The 256 ng/mL standard was reconstituted and five 1:2 dilutions were prepared using the standard diluent. The positive control (human recombinant SDC-1) was also reconstituted using standard diluent. The samples were thawed to room temperature (18-22°C). The microplate contained wells pre-coated with the capture AB. The six standards, positive control and samples were loaded onto the plate with 100 µl into each well in duplicate. Additionally, two wells were always left blank (only standard diluent). The biotinylated anti-Syndecan-1 AB was reconstituted in the biotinylated AB diluent, as required per well strips used, and 50 µl were added into each well. The microplate was incubated at 20°C for 60 min.

After the incubation, the plates were washed using an automated plate wash (BioTek 50 TS Microplate Washer, BioTek Instruments, Inc.) by aspirating the fluid from each well, adding 300 µl of wash buffer to each well and repeating the procedure for three washes. The Streptavidin-Horseradish peroxidase (HRP) was reconstituted using HRP diluent and 100 µl were added to each well. The microplate was then once more incubated at room temperature for 30 min. The wash procedure was then repeated as previously described. Hundred µl of Chromogen 3,3',5,5'-Tetramethylbenzidine (TMB) were then added to each well and incubated in the dark for 10-15 min. Once the colour changes were sufficient, 100 µl of the Stop Reagent were added to each well. The microplate was then read with a spectrophotometer (BioTek Epoch 2 Microplate Spectrophotometer, BioTek Instruments, Inc) using 450 nm as a primary wavelength and 620 nm as a reference wavelength. A spectrophotometer software was used to display the generated optic density (OD450nm) and calculate standard curves (BioTek Gen5 Microplate Reader and Imager Software Version 3.12, Agilent Technologies, Inc). The generated standard curves were then used to calculate feline SDC-1 concentrations using the linear regression equation $y=mx+b$, where m is the slope and b the y-intercept. The background (noise) OD450nm, determined by averaging the OD450nm of the blank samples was subtracted from the final human recombinant (standard and control) and feline SDC-1 concentration results.

3.5. Feline recombinant syndecan-1 production

3.5.1. Brief overview

This section describes the process of producing feline recombinant syndecan-1 (frSDC-1) to use during specific ELISA validation steps. This process was outsourced to SinoBiological Ltd, Beijing, China.

A commercial frSDC-1 was produced to serve as a species-specific positive control for the validation of this assay and comparison with the protein captured by the ELISA for further identification (see below). To produce frSDC-1, the feline SDC-1 gene was synthesized and inserted into a plasmid, which was then transformed into immortalized human embryotic kidney cells (HEK293) to produce the frSDC-1 protein. After six days of growth, the protein was collected from the cell culture, purified and then analysed for size and structure.

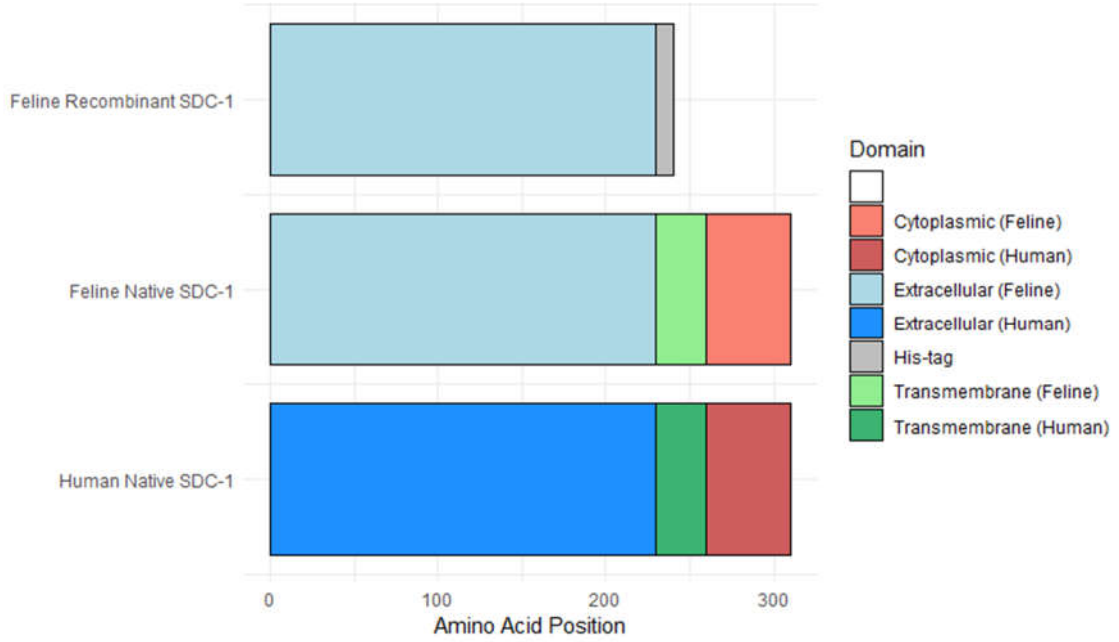
The protein sequences used to produce the frSDC-1, and the known sequences for native feline and human SDC-1 (source UniProt.com) are displayed in Figure 3.2 A and visually compared in Figure 3.2 B. The latter two showed 81% homology using a Basic Local Alignment Search Tool (293). Since only the ectodomain of human and presumably feline SDC-1 is shed during EG damage and remains available for AB binding, only that domain was reproduced in the frSDC-1. The protein sequence used for feline recombinant SDC-1 showed 77% homology with the ectodomain of the human SDC-1 (Figure 3.2 C). The gene sequence used to produce the frSDC-1 is presented in Figure 3.3. A detailed technical protocol is described below.

Figure 3.2. Comparison of feline recombinant, feline native, and human native syndecan-1 proteins. **(A)** Amino acid sequences of the feline recombinant syndecan-1 ectodomain (top), feline native syndecan-1 (UniProt accession M3W3X8; middle), and human native syndecan-1 (UniProt accession P18827; bottom). The recombinant construct comprises the feline ectodomain with a C-terminal His-tag to facilitate purification. **(B)** Schematic comparison of protein domain architecture, demonstrating that the recombinant protein contains only the extracellular domain, whereas the native feline and human proteins also include transmembrane and cytoplasmic domains. **(C)** BLAST sequence alignment between the feline recombinant syndecan-1 (His-tag removed) and the ectodomain of human native syndecan-1. Grey regions indicate conserved amino acid residues, while red regions indicate mismatches. Native feline and human protein sequences were obtained from UniProt.

A.

Feline recombinant SDC-1	MRRAALWLCLCALALRLQPALPQIVATNVPPEDQDGSGDDSDNFSGSGAGALQDLTLSQQPSSTWKGTELLT AVPTAPEPSGTDNTATSTSVLPAGERPEDREAVLPAEVEPGFTAREKETTHPPGETTPQPTTHQASTARATTAQ GPVTSHPHRDMKPDHHETSAPAGPSQLDSHAPSVEDRGPSATEKAAEDGVSTQLPAGEGSGEQDFTFDISGE NTAVAAVEPDQRNQPPVDRGATGASQGLLDRKEAHHHHHHHHHH
Feline native SDC-1	MRRAALWLCLCALALRLQPALPQIVATNVPPEDQDGSGDDSDNFSGSGAGALQDLTLSQQPSSTWKGTELTA VPTAPEPSGTDNTATSTSVLPAGERPEDREAVLPAEVEPGFTAREKETTHPPGETTPQPTTHQASTARATTQGP VTSHPHRDMKPDHHETSAPAGPSQLDSHAPSVEDRGPSATEKAAEDGVSTQLPAGEGSGEQDFTFDISENTA VAAVEPDQRNQPPVDRGATGASQGLLDRKEVLGGVIAGGLVGLIFAVCLVGFMLYRMKKKDEGSYSLEPKQA NGGAYQKPSKQEEFYA
Human native SDC-1	MRRAALWLWLCALALSLQPALPQIVATNLPPEDQDGSGDDSDNFSGSGAGALQDITLSQQTPSTWKDTQLT AIPTSPEPTGLEATAASTSTLPAGEGPKEGEAVVLPEVEPGLTAREQEATPRPRETTQLPTTHLASTTTATTAQPAT SHPHRDMQPGHHETSTPAGPSQADLHTPHTEDGGPSATERAAEDGASSQLPAAEGSGEQDFTFETSGNTAV VAVEPDRRNQSPVDQGATGASQGLLDRKEVLGGVIAGGLVGLIFAVCLVGFMLYRMKKKDEGSYSLEEKQAN GGAYQKPTKQEEFYA

B.


Feline Recombinant SDC-1
Feline Native SDC-1
Human Native SDC-1
0
100
200
300
Amino Acid Position
Domain
Cytoplasmic (Feline)
Cytoplasmic (Human)
Extracellular (Feline)
Extracellular (Human)
His-tag
Transmembrane (Feline)
Transmembrane (Human)

C.


Query_3691155
Find:
Tools
Tracks
Download
Sequence
(U) BLAST Results for: UNNAMED PROTEIN PRODUCT
Query_3691157
Query_3691155: 1..252 (252 aa)
Tracks shown: 2/3

Figure 3.3. Gene sequence used for production of feline recombinant syndecan-1. A – adenine, C – cytosine, G – guanine, T – thymine.



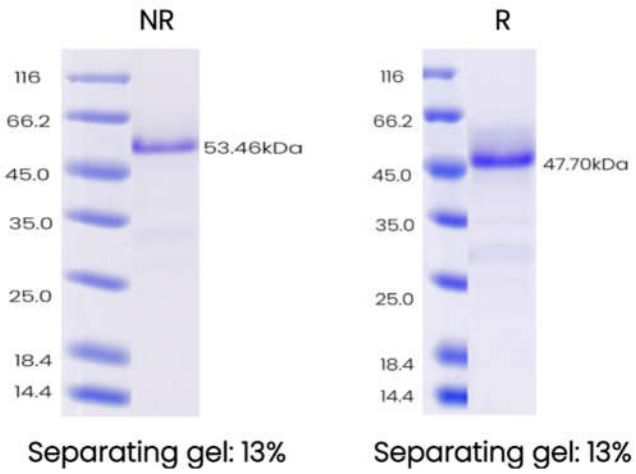
3.5.2. Technical protocol

Production of recombinant feline syndecan-1 (frDC-1) was outsourced to SanoBiological Ltd. and the following description was reproduced from their protocol with some edits for clarity. The plasmid (the circular dsDNA to be inserted into the HEK293 cells for expressing feline recombinant SDC-1) preparation was performed by target gene amplification by polymerase chain reaction and insertion into the corresponding expression vector (the plasmid). The sequence of the constructed vector was validated by sequencing.

The plasmid was amplified and prepared for transfection (introduction of the plasmid DNA into the HEK293 cell line). The plasmids were mixed with transfection reagents at an optimal ratio and then added into the flask containing HEK293 cells. The cells were cultured in a serum-free medium and maintained in Erlenmeyer Flasks on an orbital shaker by a suitable stirring speed at 37°C for 6 days to ensure optimal production of frSDC-1.

For purification and analysis, the cell culture broth was centrifuged, and the supernatant loaded onto affinity purification column (with an affinity resin binding to the tag of the produced protein) at an appropriate flow rate to separate SDC-1 from other molecules. The purified protein was analysed by Sodium Dodecyl Sulfate–Polyacrylamide Gel Electrophoresis (SDS-PAGE) under reducing (breaking covalent disulfide molecular bonds to unfold the protein) and non-reducing (maintaining molecular bonds and protein folding) conditions (Figure 3.4).

Figure 3.4. Purification column using Sodium Dodecyl Sulfate–Polyacrylamide Gel Electrophoresis (SDS-PAGE) with 13% separating gel for feline recombinant syndecan-1 (left, non-reducing (NR) and right, reducing (R) conditions). Purity estimated 94.4%.



3.6. Assay-specific validation steps

This section contains information regarding the specific steps used to evaluate the overall performance of the assay, including detection of highly reactive vs poorly reactive samples and measuring accuracy and precision (or more specifically, inaccuracy or imprecision).

3.6.1. Determining highly reactive and poorly reactive samples

An initial run of all collected samples was performed to establish potential highly and poorly reactive samples. Furthermore, selected samples were heat treated at 56 °C for 60 min and compared to non-heat-treated samples to establish potential interference of complement (294). Highly reactive and poorly reactive samples were then pooled separately and used for the initial validation procedure.

3.6.2. Measuring accuracy (or inaccuracy)

To ensure the reliability of ELISA assay results, it is crucial to evaluate inaccuracy, as deviations between measured and true values can affect the interpretation of biomarker concentrations. Inaccuracy refers to the degree of variation between measured values and true or expected values. This was assessed indirectly through parallelism, dilutional linearity and recovery.

3.6.2.1. Parallelism

Parallelism assesses the strength of antibody AG-AB binding. If the intensity of the signal reduces proportionally to the sample dilution this indicates high-affinity AG-AB binding. For instance, diluting the sample with a series of 2-fold dilutions should result in a linear reduction in signal intensity within the assay limits of quantification, and the shape of this curve should be similar (parallel) to the standard curve generated by the kit standards/diluent. In contrast, non-specific binding of various serum

components to the kit antibodies is generally low-affinity binding, where the signal reduces markedly when the sample is diluted, resulting in a non-linear curve that is a different shape to the standard curve. To assess parallelism, a highly reactive sample was diluted 2-fold for 11 dilutions. The mean concentrations of each dilution within the linear part of the curve were then calculated, and percentage recovery was determined to assess the assay's performance across dilutions.

3.6.2.2. Matrix effects

- Dilutional linearity

Similar to parallelism, dilutional linearity assesses the shape of the signal intensity versus sample dilution curve, with the expectation that this curve should be linear. However, whereas parallelism tests for falsely elevated values in undiluted or minimally diluted samples due to non-specific binding, dilutional linearity tests for matrix effects whereby serum components interfere with ELISA reactions leading to suppression of the expected signal intensity in undiluted or minimally diluted samples.

To assess dilutional linearity, poorly reactive samples were spiked with the assay's positive control human recombinant SDC-1 to a concentration at the Upper end of the human recombinant SDC-1 standard curve. A serial 2-fold dilution was then performed extending across 11 dilutions. Measured concentrations were adjusted for the dilution factor and mean concentrations were calculated alongside the percentage recovery to determine accuracy.

- Recovery

Another way to assess the impact of matrix effects is to compare the recovery of a known amount of analyte (target protein) from a biological matrix (in this case serum) compared to recovery of the same amount of analyte (target protein) from diluent. This determines whether the signal-to-concentration correlation is consistent between the calibration curve (standard curve) and test samples.

To assess this, poorly reactive serum samples were divided in four aliquots. Three of the aliquots were spiked with the ELISA kit's positive control to an expected concentration of 512 ng/ml. Dilutions were performed over the linear range of the standard curve, i by adding 40 µl of the spiked serum to 280 µl of diluent to make a 64 ng/ml dilution, then 40 µl of the diluted spiked serum to 280 µl of diluent to make an 8 ng/ml dilution. The fourth aliquot was spiked with measurand-free diluent as a control. Both pure and spiked samples were analysed in the same run to determine essay performance.

Recovery was calculated using the following equation:

% Recovery = [(Measured concentration (spiked) - Measured concentration (neat sample)/ Theoretical concentration (spiked)] x 100

3.6.3. Measuring precision (or imprecision)

To ensure the reliability and consistency of ELISA assay results, it is essential to assess precision, as variability in measurements can impact the accuracy and reproducibility of biomarker quantification. Precision refers to the closeness of agreement between independent test results obtained

under specific conditions. It can be evaluated in different ways depending on the conditions under which measurements are performed, including repeatability, intermediate precision, and reproducibility. Repeatability assesses precision under highly controlled conditions, where variables such as microplate and reagent lot, technician, laboratory etc. are kept constant and time between measurements is minimized. In contrast, reproducibility evaluated precision under various conditions, where measurements are performed across different laboratories, technicians, and equipment over multiple days. Intermediate precision represents an intermediate level of variability, where only the laboratory remains constant. Repeatability is often referred to as within-run variability and intermediate precision – between-run variability. Practically, though precision is difficult to measure, therefore the inverse variable imprecision is reported.

3.6.3.1. Within-run variability

Within-run variability was tested by analysing the pooled highly and poorly reactive samples each 10 times in random order within one run. Intra-assay standard deviations (SD) and coefficients of variation (CV) were determined.

3.6.3.2. Between-run variability

Between-run variability was tested by analysing the pooled highly and poorly reactive samples each 10 times in random order using two different kits split in halves in two non-consecutive days. Intra-assay SD and CV were determined.

3.7. Feline syndecan-1 identification steps

The initial ELISA validation results were promising but inconclusive, prompting further investigation. The assay demonstrated strong binding to a protein in serum from sick cats with acceptable precision and accuracy (see Results section for details). However, the ELISA antibody failed to bind the frSDC-1, leaving the identity of the bound protein uncertain. This section outlines the steps used to identify the protein (presumably feline SDC-1) that was binding to the ELISA kit AB.

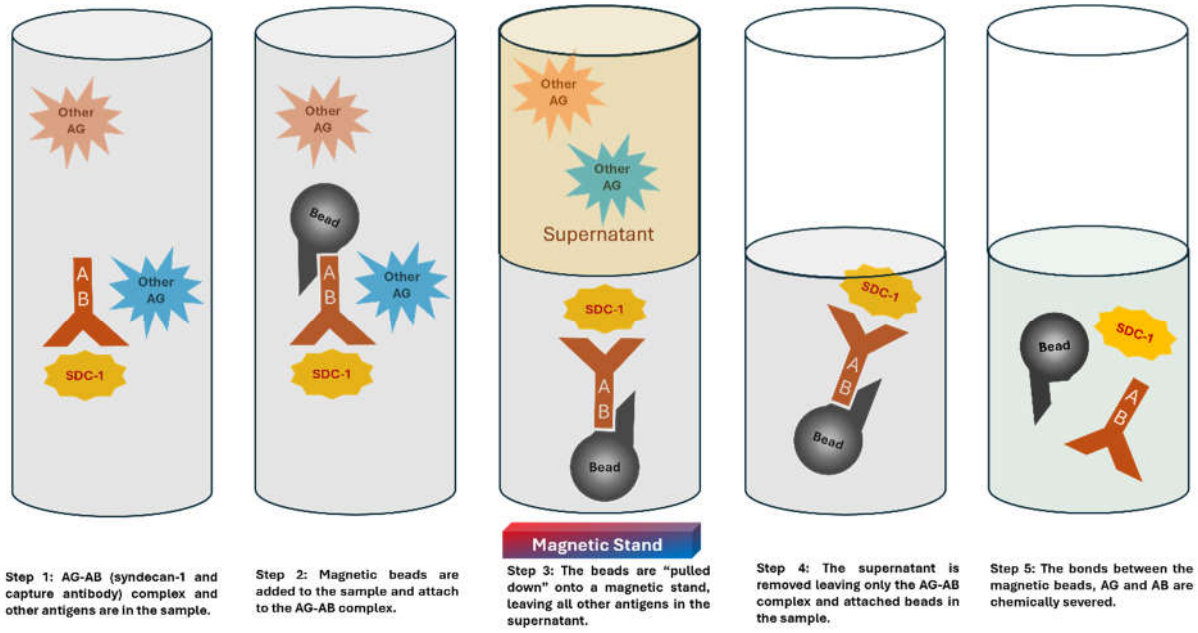
3.7.1. Immunoprecipitation

3.7.1.1. Brief overview

In order to isolate the protein (presumably feline SDC-1) bound to the detection AB from the ELISA kit and prepare for further identification, an immunoprecipitation assay was performed (Figure 3.5). The goal of this procedure was to minimize the presence of other AG in the samples undergoing analysis and therefore interference with result interpretation. For this, the biotinylated detection AB from the ELISA kit was added to highly and poorly reactive samples. This AG-AB complex was then mixed with streptavidin-coated magnetic beads. The beads were then “pulled down” at the side of the test tube using a magnetic stand. The supernatant was removed, leaving only the AG-AB complex and attached beads in the test tube. The bond between the AG, AB and the beads is then disrupted, the beads

collected, and the AG and AB stored for further analysis. A detailed technical protocol from the immunoprecipitation assay is described below.

Figure 3.5. Stepwise diagram of an immunoprecipitation ("pull down") assay with magnetic beads used to isolate the presumed feline SDC-1 antigen-antibody complex from other antigens.



3.7.1.2. Technical protocol

Highly (serum 1) and moderately reactive (serum 2 and 3) reactive samples, and poorly (serum 4) reactive samples and wash buffer were used. The latter two acted as negative controls. An aliquot of 50 µL (0.5 mg) of Sera-Mag™ SpeedBeads Streptavidin-Blocked Magnetic Particles (Cytiva, Global Life Sciences Solutions USA LLC) were placed into a 1.5 mL microcentrifuge tube for the pre-wash procedure. The tubes were placed on a magnetic stand to collect the particles at the side of the tube. The storage buffer was discarded, and 1 ml of wash buffer was added into the tube. The tube was gently vortexed to mix. Then the tube was placed on the magnetic stand and the buffer removed. The serum samples were then washed to remove any non-specific binging to the beads and endogenous biotinylated molecules. The serum samples were diluted with 200 µL of wash buffer where volume was not sufficient. The samples were then mixed with 50 µL (0.5 mg) of Sera-Mag™ SpeedBeads Streptavidin Blocked Magnetic Particles, with no additional of capture antibody, and incubated on orbital shaker at room temperature for 45 mins. The tubes were then placed on the magnetic stand to collect the particles against the side of the tube. The supernatant (serum samples) was then collected into 1.5 ml microcentrifuge tubes and these pre-washed serum samples were used for further analysis.

To capture the ELSIA kit antigen (presumably feline SDC-1), the biotinylated anti-SDC-1 AB from ELISA kit and diluent from the kit were combined into a 1.5 mL microcentrifuge tubes, using 75-

150 µL of AB, 300-1000 µL of diluent along with 400 µL of serum sample. The combined samples were then incubated on an orbital shaker at room temperature (18-22°C) for two hours. Each combined sample then received 50 µL (0.5 mg) of Sera-Mag™ SpeedBeads Streptavidin Blocked Magnetic Particles, including a bead only control. The samples were again incubated at room temperature (18-22°C) for one hour. The beads were then washed three times by first collecting the particles on a magnetic stand, removing the supernatant, and storing for later analysis and washing the beads three times with wash buffer. The AG, AB and streptavidin was then denaturated from the magnetic beads. The beads were resuspended in 26 µL of wash buffer with 10 µL of lithiumdodecylsulfate (LDS) and 4 µL of reducing agent dithiothreitol (DTT). This was incubated at 70°C for 10 mins on a heat block. The particles were collected with the magnetic stand and the supernatant removed and stored for electrophoresis.

3.7.2. Sodium Dodecyl Sulfate Polyacrylamide Gel Electrophoresis

3.7.2.1. Brief overview

Sodium Dodecyl Sulfate Polyacrylamide Gel Electrophoresis (SDS-PAGE) was used to separate the proteins bound to the ELISA AB contained in the samples based on their size and charge and compare to the size and charge of known proteins (such as human recombinant SDC-1 and frSDC-1) in order to isolate proteins and perform further identification analysis. The sample was loaded into a gel matrix and subjected to an electric field, which drove the molecules through the gel. Proteins have generally a negative charge and will migrate toward the positive electrode on the gel but require an additional step (such as LDS treatment) to achieve a more uniform negative charge and accurately separate on the gel based on molecular weight.

Once electrophoresis was complete, the gel was stained with a specific technique and the protein "bands" formed during the separation visualized and further analysed. For this procedure, samples (Table 3.1) collected during the previous immunoprecipitation step containing the AG, the AB detached (denaturated) from the AG were compared to various control samples. A detailed technical protocol of the gel electrophoresis is described below.

3.7.2.2. Technical protocol

A NuPAGE Bis-Tris 12% gel (Thermo Scientific Inc.) with serum samples that were highly reactive (presumably SDC-1 detected) and poorly reactive (presumably SDC-1 not detected) on ELISA, along with various control samples were used with a total volume of 15 µL for each sample loaded onto the gels (see Figure 3.11 in results section). Control samples included the human recombinant SDC-1 control from ELISA kit, feline recombinant SDC-1, magnetic beads only in buffer and anti-SDC-1 AB only in buffer. A poorly reactive negative (with no ELISA signal) and a highly reactive (high ELISA signal) sample were included with at two- and 10-fold dilution each. Electrophoresis was performed for 42 minutes at 200V. The gels were stained using methylene blue. The molecular weights were identified using a standard ladder on each end of the electrophoresis gel. After the procedure, specific

electrophoresis gel bands differing between the highly and poorly reactive samples and matching expected feline SDC-1 molecular weight (MW) were incised and stored at -80°C for mass spectrometry analysis (295).

3.7.3. Mass spectrometry

3.7.3.1. Brief overview

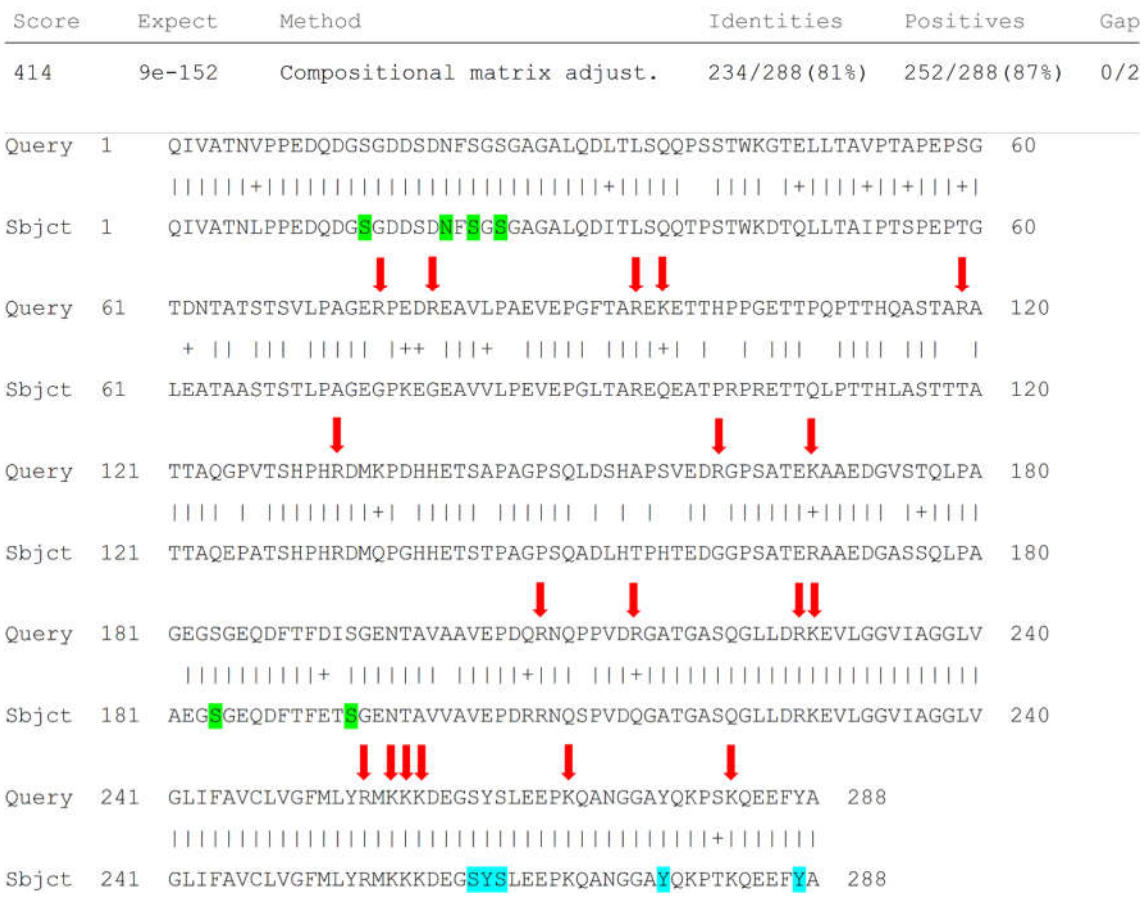
Following the gel electrophoresis, mass spectrometry was used to identify the protein in selected gel bands presumed to contain feline SDC-1. Mass spectrometry is a technique used to identify and measure molecules by determining their mass. The process started with ionization, where the sample was converted into charged particles. These charged particles, or ions, were then guided through an instrument where they were separated based on their mass-to-charge ratio. A detector then measured the ions, creating a mass spectrum, which is like a molecular fingerprint that helps identify the components in the sample. For identification of unknown compounds, their mass spectrum was compared to existing databases with known molecules. In the present case, the electrophoresis bands matching the potential molecular weight of feline SDC-1 were analysed using mass spectrometry and compared to existing databases. Furthermore, samples obtained directly from the ELISA wells containing only the AG and capture AB (without the immunoprecipitation and electrophoresis step) and negative controls were sent for an additional mass spectrometry analysis at a different facility. Detailed technical reports from both mass spectrometry analyses are described below.

3.7.3.2. Technical report for mass spectrometry on electrophoresis bands

This mass spectrometry analysis was performed at the Massey University Mass Spectrometry Laboratory. The electrophoresis gel bands were chemically treated with dithiothreitol (DTT) and iodoacetamide to modify disulphide-bridge forming cysteine residues to facilitate trypsin access and to reduce complexity during data analysis. The resulting peptides were separated by their affinity for water on a reverse-phase C18 column and analysed by mass spectrometry using a Top 10 method. For this, a survey scan was performed and the top 10 most intense peptide ions within a specified scan range were fragmented to obtain their sequence information. The process was repeated every scan cycle in the chromatographic run, and additional settings enabled the mass spectrometry to ignore repeating ions within a specified time window. This allowed for more low abundance ions to be targeted and improve overall coverage.

Mass spectrometry data obtained were analysed by Proteome Discoverer search engine (Ver. 2.4.1.15, ThermoFisher Inc) against a non-redundant National Center for Biotechnology Information database under taxonomy: *Felis* (296) with 57,316 protein sequences and a custom database for common contaminants from sample handling. Human SDC-1 is predicted to have multiple O-linked heparan sulfate and chondroitin sulfate on serine residues, one N-linked glycosylation on asparagine and multiple phosphorylated serine/tyrosine residues (Figure 3.6).

Figure 3.6. Amino acid sequence alignment of syndecan-1 from Felis catus (Query) and Homo sapiens (Subject). The alignment demonstrates high homology, with 81% identical residues and 87% similarity. Red arrows indicate predicted trypsin cleavage sites with >50% probability. Predicted glycosylation sites are highlighted in green, and phosphorylation sites in cyan.



The length and branching of the glycosylation cannot be predicted by sequence alone and were ignored by the Proteome Discoverer software. The search parameters used accounts for chemical treatment and predicted natural modifications (phosphorylation on Serine/Threonine). The search results were filtered by a false discovery rate (FDR) of 1% and each hit must contain a minimum of 2 unique peptides to ensure high confidence.

A gel slice of bovine serum albumin (BSA) was digested under the same conditions as the samples and serve as a digestion control. Peptides from 1 µl of tryptic digestion of BSA are routinely used as quality control to check the performance of the liquid chromatogram system (gradient accuracy and peptide separation) and mass spec (resolution and sensitivity).

Due to the low sample concentration, a maximum of 4 µl was injected and separated on a 50 cm long C18 column with a diameter of 75 µm over a gradient from 3-30% acetonitrile over 60 min at a flow rate of 300 nl/min at 50°C.

3.7.3.3. Technical report for mass spectrometry on samples from ELISA wells

Samples for mass spectrometry analysis without immunoprecipitation or gel electrophoresis were prepared. Highly reactive and a poorly reactive serum samples were incubated in ELISA wells for 1 hour. The wells were washed three times with phosphate-buffered saline (to avoid proprietary wash buffers containing bovine serum albumin). The protein was eluted (separated from the AB) using Glycine-HCl (pH 2.5) with two consecutive procedures. Another aliquot of the highly reactive serum sample was eluted using Lithium Dodecyl Sulfate at 90°C for 10 minutes offering a stronger elution. The samples were neutralized to adjust the pH. Details on sample preparation including negative and positive control samples are presented in Table 5. Samples were frozen and stored at -20°C until further analysis.

Mass spectrometry analysis was performed at the Otago University Centre for Protein Research on selected samples (Table 3.1). Samples were run on an Orbitrap Exploris 240 LC-MS system after trypsin digestion. The resulting mass spectra were compared against feline Syndecan-1 (Uniprot M3W3X8). Specific peptides from the ectodomain of human SDC-1 were targeted for identification, avoiding predicted glycosylation sites.

Table 3.1. Sample Processing Details for Syndecan-1 Mass Spectrometry.

Sample ID	Source	Preparation	Purpose
N1	Feline serum (highly reactive SDC-1 on ELISA)	Incubated in ELISA wells for 1 hour, washed 3× with PBS, eluted with 2× 200 µL 0.1M Glycine-HCl (pH 2.5), neutralized with 40 µL 1M Tris Base, stored at -20°C.	Test for SDC-1 detection in highly reactive SDC-1 on ELISA.
N2	Feline serum (poorly reactive SDC-1 on ELISA)	Same as N1 but using negative serum instead of positive.	Negative control to check for non-specific ELISA binding.
N4	Feline serum (highly reactive SDC-1 on ELISA)	Incubated in ELISA wells for 1 hour, washed 3× with PBS, eluted with 200 µL LDS buffer (pH 6.5), heated at 90°C for 10 min, stored at -20°C.	Test stronger elution method (LDS + heat) for better protein release.

ELISA: Enzyme-linked immunosorbent assay; LDS: Lithium dodecyl sulfate; PBS: Phosphate-buffered saline; MS: Mass spectrometry; SDC-1: Syndecan-1

3.8. Statistical analyses

Measurands related to imprecision, limits of quantification and inaccuracy were tested for normality using Shapiro-Wilk test and Q-Q plots. Mean and SD and CV were generated for all measurands. All statistical analyses were conducted in R (Team, 2023) (297).

4. Results

7.1. Feline recombinant syndecan-1

Concentrations of frSDC-1 were not detectable by the human SDC-1 ELISA kit, therefore the positive control from the kit was used for spiking when assessing recovery. The frSDC-1 was included as a control for expected molecular weight and detected by gel electrophoresis.

7.2. Human syndecan-1 ELISA kit performance

Three highly reactive samples (out of 16 sampled subjects) including two with very high OD from the diseased cat cohort were identified by the kit. The subjects from which these samples were taken had disease processes expected to damage the vasculature and increase concentrations of feline SDC-1 in the serum (sepsis, trauma and feline infectious peritonitis, respectively). Heat inactivation did not result in differences in OD in both highly reactive and poorly reactive samples. Therefore, heat treatment was not used for the remainder of the analysis.

Data was normally distributed. The assay showed overall good precision and accuracy, or rather a low degree of imprecision and inaccuracy (Table 3.2). Within and between run variability showed low CV (4.95% and 4.80% respectively). Dilutional linearity and parallelism were comparable to the standard curve (Figure 3.7). However, both were no longer precise after the 7th (1:64) dilution. Within run and between run variability and recovery for serum samples from low reactors were below detection limit and were not statistically analysed.

Table 3.2. Summary statistics for performance variables assessed during the validation of a human syndecan-1 enzyme-linked immunosorbent assay (ELISA) for use in feline serum. Variables include within- and between-run variability, dilutional linearity, and parallelism, expressed in both optical density and calculated presumably feline syndecan-1 concentrations (ng/mL).

Variable	Mean	SD	Median	1st Quartile	3rd Quartile	Min	Max	%CV
Within run variability OD¶	0.61	0.03	0.61	0.60	0.62	0.58	0.69	4.95
Within run variability SDC-1 (ng/mL)	61.90	2.97	61.34	60.24	62.27	58.35	69.14	4.80
Between run variability OD¶	0.72	0.05	0.71	0.68	0.77	0.66	0.78	7.22
Between run variability SDC-1 (ng/mL)	46.65	5.58	45.67	43.12	48.46	40.56	55.04	11.96
Dilutional linearity OD¶	0.63	0.76	0.28	0.09	0.98	0.03	2.00	NA
Dilutional linearity OD¶ compensated*	2.09	0.38	2.02	1.83	2.31	1.66	2.69	18.10
Dilutional linearity SDC-1 (ng/L)	63.84	74.38	28.79	10.59	97.50	4.43	197.47	NA

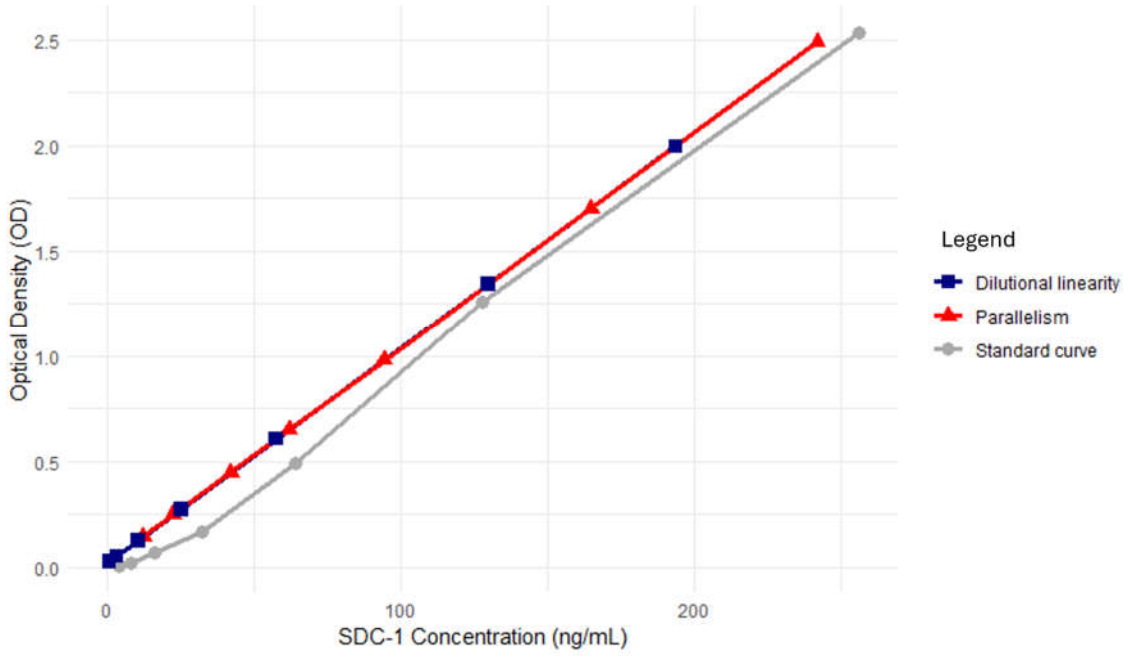
Dilutional linearity SDC-1 (ng/mL) compensated*	239.09	29.02	230.35	224.78	256.33	197.47	283.61	12.14
Parallelism OD¶	0.68	0.88	0.25	0.07	0.98	0.03	2.49	NA
Parallelism OD¶ compensated*	4.42	1.61	3.94	3.58	4.59	2.49	8.19	36.44
Parallelism SDC-1 (ng/mL)	65.08	85.81	22.24	5.03	94.15	1.25	242.04	NA
Parallelism SDC-1 (ng/mL) compensated*	326.03	48.69	329.47	321.25	355.76	242.04	389.96	14.93

%CV: Percentage coefficient of variation; OD: Optical density at 450 nm; SDC-1: syndecan-1

¶OD read at 450 nm wavelength

*Compensated values accounting for dilution factors were obtained by multiplying the result with the dilution factor to assess coefficient of variation

Figure 3.7. Comparison of optical density across presumably feline syndecan-1 concentrations for dilutional linearity (navy), parallelism (red), and the standard curve (grey). Navy squares and red triangles represent each two-fold dilution up to the seventh dilution for dilutional linearity and parallelism, respectively.

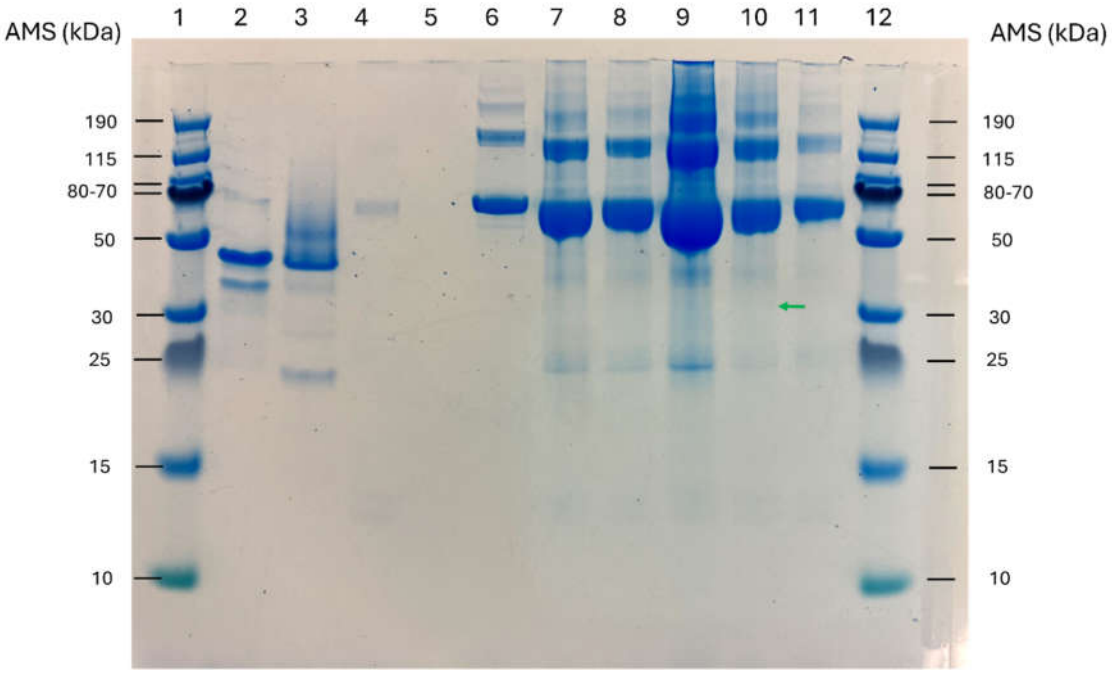


7.3. Sodium Dodecyl Sulfate Polyacrylamide Gel Electrophoresis

Sodium Dodecyl Sulfate Polyacrylamide Gel Electrophoresis (SDS-PAGE) of proteins from the immunoprecipitated magnetic beads resulted in many bands that were consistent with denatured antibody fragments, being present in the antibody only sample as well as the serum samples. There were several faint bands ≤100 kDa present only in the serum samples, however these were present in both

highly and poorly reactive serum samples. The purified human recombinant SDC-1 showed a strong band at around 46 kDa and a weaker band at ~38 kDa, while the feline recombinant SDC-1 showed a main band at ~45 kDa, consistent with the information from the manufacturer. There were no distinct bands at these apparent molecular weights in the serum samples. One very weak band at around 30 kDa was present in one of the highly reactive serum samples, but not in the poorly reactive serum or control samples (Figure 3.8). This was excised from the gel for further analysis, along with two larger bands (50 and 75 kDa) that appeared slightly stronger in positive serum samples and were not present in the antibody only control in a replicate gel (not shown). These larger bands were selected based on the assumption that they could potentially contain feline SDC-1 and parts of the ELISA kit AB.

Figure 3.8. Sodium dodecyl sulfate–polyacrylamide gel electrophoresis (SDS-PAGE) analysis of recombinant syndecan-1 proteins, controls, and selected feline serum samples under reducing conditions. The green arrow indicates the ~30 kilodalton (kDa) protein band excised for mass spectrometry analysis. Lane assignments: 1 and 12, PageRuler Plus Prestained Protein Ladder; 2, human recombinant syndecan-1; 3, feline recombinant syndecan-1 (frSDC-1); 4, beads-only control; 5, empty; 6, Non-biotinylated anti-syndecan-1 antibody (Anti-Syndecan-1 antibody [SP152], ab130405, Abcam Ltd); 7, Serum 2 (highly reactive, two-fold dilution); 8, Serum 4 (poorly reactive, 10-fold dilution); 9, Serum 4 (poorly reactive, two-fold dilution); 10, Serum 1 (highly reactive, two-fold dilution); 11, Serum 1 (highly reactive, 10-fold dilution). Samples were denatured in lithium dodecyl sulfate (LDS) sample buffer containing 50 millimolar (mM) dithiothreitol (DTT), separated on 12% bis(tris) polyacrylamide gels using 2-(N-morpholino) ethanesulfonic acid (MES)-sodium dodecyl sulfate (SDS) running buffer at 100 V for 100 min, stained with SimplyBlue SafeStain, and imaged using a ChemiDoc MP imaging system. Apparent molecular sizes are shown on either side of the gel.



AMS: Apparent Molecular Sizes; kDA: kilodaltons;

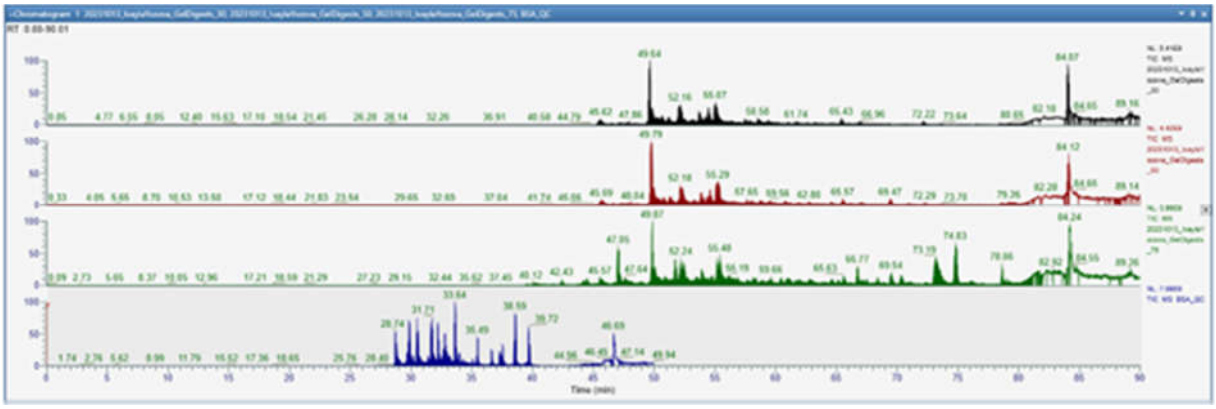
7.4. Mass spectrometry on electrophoresis gel bands

Three bands were sent for mass spectrometry analysis, the above mentioned ~30 kDa band, a ~50 kDa band and a ~75 kDa band. Selection of those bands was based on comparison between highly and poorly reactive samples and the assumption that they either contain only feline SDC-1 (~30 kDa band), or feline SDC-1 and fragments of the capture AB (~ 50 and ~75 kDa bands).

The mass spectrometry analysis revealed very low sample concentration, as indicated by weak chromatogram signals (Figure 3.10). Specifically, the ~30 kDa gel band, which was analyzed for feline SDC-1, did not yield any detectable feline SDC-1 peptides. The search was conducted using both the SwissProt sequence (M3W3X8) and the NCBI sequence (XP_0039845), which are identical in amino acid composition (Figure 3.9). Even when broadening the database to include human, feline, and mouse proteins, no evidence of SDC-1 was found. These findings suggest that the protein concentration was too low for reliable detection.

The ~50 kDa band contained a wide range of peptides, with most frequent matches corresponding to complement components and IgGFc-binding protein. The ~75 kDa band predominantly contained peptides consistent with fragments of IgM, albumin, serotransferrin and complement components. No peptide matches for feline SDC-1 were identified in either of these higher molecular weight bands.

Figure 3.9. Chromatographic comparison of sample peaks to the bovine serum albumin (BSA) digestion control. Traces represent results from the ~30 kDa band (black), ~50 kDa band (red), ~75 kDa band (green), and BSA control (blue). Note the sparse and low-intensity peaks in all sample traces compared to the dense peak pattern of the BSA control, suggesting low protein concentration in the samples.



7.5. Mass spectrometry on antigen-antibody complexes from ELISA wells

This mass spectrometry analysis aimed to identify feline SDC-1 in samples obtained from ELISA-based extractions of feline serum. Despite targeted efforts, feline SDC-1 was not detected in any of the analysed samples. Instead, the identified proteins were primarily plasma proteins, including albumin, complement components, and immunoglobulins, which were expected due to the nature of the serum samples.

For sample N4, which underwent a stronger elution process using LDS buffer, the results were similarly negative for feline SDC-1, despite the sample not being excessively overloaded with BSA or immunoglobulins. To ensure a thorough search, peptide sequences from the extracellular region of feline SDC-1 were targeted, avoiding glycosylation sites that could interfere with detection.

5. Discussion

This attempt to validate a commercial human SDC-1 ELISA kit for detection of feline SDC-1 yielded inconclusive results. Several cats with appropriate disease type and severity had highly reactive samples, suggesting that the anti-SDC-1 AB in the kit may bind to feline SDC-1. Initial quality assessments, including parallelism and dilutional linearity, indicated good assay performance. Additionally, heat treatment of samples with varying levels of reactivity did not alter binding intensity, supporting the absence non-specific complement binding (294). However, the kit failed to detect the frSDC-1. Furthermore, mass spectrometry following immunoprecipitation, failed to identify any protein matching feline SDC-1 in known databases. These findings suggest that while a protein did bind to the ELISA AB, it could not be identified and therefore, we cannot conclusively confirm it was feline SDC-1. Several possible explanations for these outcomes are discussed below.

5.1. Initial analysis – highly reactive samples, inaccuracy and imprecision

All enrolled cats were affected by illnesses that, based on extrapolation from human data, would be expected to increase SDC-1 concentrations. However, only three cats showed markedly elevated levels, and these individuals appeared to have subjectively more severe disease than the sick cats with poorly reactive serum samples. Given the limited understanding of SDC-1 shedding patterns in cats, factors such as disease type, severity, and timing of sampling may have contributed to the lower-than-expected number of high reactors. Nonetheless, the detection of clearly high reactors in appropriately ill cats suggests that the assay was capable of detecting feline SDC-1. This was further supported by low inaccuracy, as demonstrated by multiple validation metrics.

Parallelism was acceptable, with signal intensity from highly reactive samples decreasing linearly with serial dilution, indicating high-affinity, specific antigen binding rather than non-specific interactions. Similarly, dilutional linearity was demonstrated by the consistent linear reduction in signal after spiking purified human recombinant SDC-1 into feline serum, supporting the assay's responsiveness across a range of concentrations. Recovery testing also showed accurate detection of

expected SDC-1 levels over the assay's working range, suggesting minimal interference from matrix effects. Finally, the assay demonstrated good precision, with low variability within and between runs. Taken together, these findings supported the assay's reliable performance and justified progression to further validation steps.

5.2. Lack of binding of the ELISA antibody to feline recombinant syndecan-1

Surprisingly, though, the assay did not bind to the frSDC-1. Possible explanations include the type of AB used in the kit, the degree of homology between the native and recombinant protein among other structural differences. All of these are outlined below.

5.2.1. Type of antibody

The ELISA kit used in this study contained monoclonal mouse human SDC-1 specific AB. Monoclonal antibodies are a highly specific, meaning all antibody molecules recognize and bind to one specific epitope on an AG. In contrast, polyclonal antibodies are a mixture of antibodies that recognize multiple epitopes on the same AG. While monoclonal antibodies provide high specificity and batch-to-batch consistency, polyclonal antibodies offer higher sensitivity and broader target recognition, making them useful in applications where AG variability is expected. When compared to polyclonal, monoclonal antibodies are less likely to produce cross-reactions. They are in return highly specific to their binding site (298). This high specificity might have been a disadvantage in this study.

Indeed, syndecans have multiple AB binding sites (49) making it potentially challenging for a monoclonal AB to recognise a specific site, which would need to be identical in sequence and/or conformation between human and feline syndecan-1. While it seemed unlikely from the outset that a monoclonal antibody against human SDC-1 would detect feline SDC-1, the initial test of samples looked very promising and warranted further investigation. Another consideration may be differences in SDC-1 from different locations. A research group developing an ELISA for canine SDC-1 identified 11 domains for AB binding. Additionally, the 11 antibodies produced as part of the development process were binding with varying intensity to endothelial SDC-1 found in different tissues (107).

The composition and binding affinity of antibodies used in commercial ELISA kits targeting endothelial SDC-1 are unknown. Given the potential structural differences (as outlined below), this mismatch between the AG and AB may have reduced binding affinity of the monoclonal AB, specifically to the frSDC-1 as compared to the native feline SDC-1 presumably detected during the initial checks.

5.2.2. Syndecan-1 sequence, structure and glycosylation

Syndecans are structurally conserved proteoglycans across vertebrates, with high interspecies homology primarily in their cytosolic and transmembrane domains (49, 50). However, the ectodomain, the portion cleaved and released into circulation is less conserved. The Basic Local Alignment Search Tool (source: https://blast.ncbi.nlm.nih.gov/Blast.cgi) demonstrated 81% homology between the human

and feline SDC-1 and 77% between the ectodomain of human SDC-1 and frSDC-1, suggesting a generally acceptable level of similarity to support cross-reactivity. However, the evidence for the existence of feline SDC-1 is based on inference, meaning that the native protein has not yet been studied or confirmed at the protein level, and its exact structure remains uncharacterized.

Given that syndecans are structurally and functionally conserved across vertebrates, it is likely that human and feline SDC-1 share a similar glycoprotein structure (49). Nonetheless, the frSDC-1 produced for this study may differ significantly from the native feline protein, introducing further heterogeneity. This is supported by the observation that the ELISA AB did not bind to the frSDC-1, while it did yield strong positive signals in sick cats, suggesting that the AB may recognize the native feline SDC-1, but not the recombinant form. This could further be explained by differences in protein folding and glycosylation.

The ability of an AB to bind to its target AG is highly dependent on the AG three-dimensional structure or "shape" and accessibility to specific binding sites (epitopes), both of which are heavily influenced by glycosylation. Syndecan-1, with its extensive glycosaminoglycan side chains (especially heparan sulfate), presents a variable and complex "shape" that complicates immunochemical detection (49, 107, 299). Furthermore, highly glycosylated proteoglycans are challenging to produce on immortalized cell lines, especially if non-mammal cell lines are used.

To mitigate potential discrepancies in protein folding and glycosylation, the frSDC-1 used in this study was produced in HEK293, a mammalian expression system. Despite this, the precise degree of glycosylation and resulting shape of the frSDC-1 remains unknown. We believe this to be one of the main reasons for failure of the frSDC-1 to bind to the ELISA AB.

In disease states, SDC-1 is shed from the endothelial surface via cleavage of its ectodomain, primary by matrix metalloproteinases (50, 227). Simultaneously, heparan sulfate chains may also be cleaved from the core protein, further altering the SDC-1 structure (61). Because of the extent and pattern of cleavage are poorly understood across species, it is possible that SDC-1 present in the feline serum differs structurally from the frSDC-1.

Nonetheless, highly reactive serum samples were observed in some cats with appropriate disease severity, indicating that the ELISA AB could be capable of detecting native feline SDC-1. These findings support the idea that while the ELISA may recognize the native, shed form of SDC-1, the recombinant protein lacked the necessary structural features, most likely due to glycosylation discrepancies, to permit AB binding.

5.3. Identification of the protein binding to the ELISA antibody

Given the shortcomings of the frSDC-1 detection and the potential of the ELISA in detecting native feline SDC-1 based on the highly positive ELISA results, a further analysis was undertaken to attempt to identify the protein that did bind strongly to the ELISA AB. This was performed through

immunoprecipitation and SDS-PAGE to prepare samples concentrated with the target protein and finally mass spectrometry to identify the protein. Analysis of these results is outlined below.

5.3.1. Immunoprecipitation and mass spectrometry

We performed an immunoprecipitation assay to isolate the protein (presumably feline SDC-1) bound to the ELISA kit AB, with the goal of facilitating downstream SDS-PAGE and mass spectrometry. Given the high protein content of feline serum, in this step we aimed to reduce background interference from proteins with similar size and charge, thereby decreasing the risk of "masking" of the bound feline SDC-1. However, the effectiveness of this approach may have been limited or introduced additional discrepancies. Immunoprecipitation was chosen over western blot in this study because our rabbit anti-mouse secondary antibodies did not bind to the biotinylated detection antibody in the ELISA kit. We presume that biotinylating interfered with secondary antibody binding.

The immunoprecipitation was performed using the detection AB from the ELISA kit. While we used a highly reactive serum sample. It is possible that this procedure reduced the concentration of target protein. Notably, SDS-PAGE revealed only a faint band in one highly reactive sample that was suspected to correspond to feline SDC-1.

Identifying appropriate bands was further complicated by the unknown actual molecular weight of the target protein, influenced by the variable glycosylation, size of the ectodomain, and the potential presence of AB or magnetic bead fragments bound to the AG. Indeed, the process of immunoprecipitation involves enzymatic degradation of the presumably feline SDC-1-AB-magnetic beads complexes, but the resulting fragment sizes are not always predictable. As a result, the gel electrophoresis step may have been inadequate for distinguishing the correct band by comparison with controls. As shown on the images above, the selected bands were faint, potentially representing proteins other than SDC-1, or they might have contained SDC-1 at concentrations too low for detection.

To overcome these challenges, we also tested an alternative approach, by namely analysing eluted AG-AB complexes directly from the ELISA plate wells and submitting them for mass spectrometry without the immunoprecipitation and SDS-PAGE. However, this method also failed to identify feline SDC-1. Several explanations are possible, including: the ELISA AB may bind to a different protein (false positives), the AG was "lost" during the processing or its concentration in the samples remained below the detection limits of the mass spectrometer. Further studies using larger sample volumes from sick cats with high AG-AB binding are warranted to definitively identify the protein interacting with the ELISA AB.

5.4. Appraisal of commercial syndecan-1 ELISA kits for use in cats

At the time of undertaking of this project no feline-specific ELISA kits for SDC-1 were commercially available, prompting this attempt to validate a human assay to use in cats. Ideally, a feline-specific ELISA should be developed *de novo* and fully validated for quantification of feline SDC-1.

However, such development is costly and carries ethical implications, that might outweigh the breadth of feline EG research.

Since then, two studies have reported using commercial kits labelled as feline, to evaluate EG damage in small groups of diseased cats. One study investigated cats with haemotropic mycoplasma infection, using a kit from Bioassay Technology Laboratory, China (Lot: E0068Cat) (242), while another assessed cats with head trauma, using a kit from MyBioSource, Inc., USA (ID: MBS1603385) (243). Both studies reported very low concentrations of SDC-1. Notably, these kits were marketed as feline based on protein homology rather than *de novo* development and validation (personal communication). Thus, the reported low concentrations may reflect insufficient AB binding to feline SDC-1 for the reasons previously discussed.

Interestingly, several studies using canine-specific SDC-1 ELISA kits have been reported in the literature. These include two canine haemorrhagic shock models (94, 247), a canine septic shock model (248), a study in dogs undergoing cardiac surgery with cardio-pulmonary bypass (216) and a pilot study in dogs with gastric-dilation volvulus (unpublished data). Most of these studies used a kit from MyBioSource, Inc., USA (ID: MBS2611112), which the manufacturer stated as specifically developed for dogs (personal communication). Despite this, all reported very low concentrations or undetectable concentrations of SDC-1 in diseased dogs or experimental models. The underlying reasons for these findings remain unclear.

Other possibility, unrelated to kit performance, is that cats and dogs may exhibit species- or order-specific SDC-1 expression, or turnover patterns in both health and disease (47). The density of SDC-1 on the endothelial surface in these species and it is possible that they inherently express less SDC-1 compared to other species. Additionally, the extent of SDC-1 cleavage for a given disease severity may be lower in cats and dogs than in people. Although SDC-1 expression is known to increase during disease, sampling timepoints in these studies may not have captured peak shedding(49). Further research, into the structure, composition and shedding patterns of the feline EG is needed to identify reliable biomarkers of EG damage in this species.

5.5. Limitations

This study has several limitations related to the sampled cohorts, sample volume, the use of unmatched highly reactive samples across validation steps, and protein identification methods used.

Obtaining highly reactive samples proved challenging, despite opportunistic sampling of a relatively large feline cohort. We selected patients with subjectively comparable illness severity to human cases where high SDC-1 concentrations would be observed. However, only a small number of very severely ill cats demonstrated elevated concentrations of SDC-1. It is possible that sicker cats were either not presented for treatment or were euthanasized early during admission, prior to sample collection. Furthermore, it remains unknown which disease processes in cats contribute to EG damage

and to what extent. These findings highlight the need for broader investigation into feline disease types and severity associated with EG disruption.

Due to limited sample volumes, and need to repeat certain steps to confirm findings, not all the validation procedures were performed on the same highly reactive samples. This may have introduced additional variability into the validation results.

We used immunoprecipitations and mass spectrometry for protein identification as we considered Western Blotting unsuitable for the conditions of this experiment due to failure of our secondary anti-mouse antibody to bind to the biotinylated detection antibody from the ELISA kit. However, a more sensitive method, such as nuclear magnetic resonance, might have been more effective for detecting SDC-1. Unfortunately, this was not feasible due to the relatively low concentration of SDC-1 in serum compared to the abundance of other proteins.

Lastly, a major limitation of this study was the lack of a suitable positive control for comparison. The recombinant feline SDC-1 produced specifically for this project did not bind to the ELISA AB, making it unusable as a reference material. Without a validated positive control, it was not possible to confidently assess the assay performance. This limited our ability to distinguish between true negative results and technical failures and constrained the overall robustness of the validation.

6. Conclusion

Our experiment could not determine whether this commercial human ELISA is suitable for quantifying SDC-1 in feline serum, despite the initially promising detection of high concentrations of SDC-1 in sick cats. Several factors may explain these results. The use of a monoclonal antibody, which targets a single epitope, may have limited the assay's ability to detect a structurally heterogeneous protein like feline SDC-1, particularly given the limited information on its exact structure, degree of glycosylation, and three-dimensional conformation. Additional factors may include species-specific differences in antibody binding sites and a low abundance of the target protein in the samples.

Future directions include developing an alternative form of rfSDC-1, potentially derived from endothelial cell lines, to serve as a positive control, as well as evaluating other ELISA platforms, particularly those with polyclonal AB or targeting endothelial SDC-1 binding sites. Optimising detection methodologies, or exploring alternative methods such as nuclear magnetic resonance, may also improve protein identification. Finally ensuring sufficient sample volumes from severely ill cats will be essential for robust assay validation. If SDC-1 proves unsuitable as feline biomarker, EG components with validated ELISA assays, such as hyaluronan (291), may offer a viable alternative for future studies.

7. Chapter III extended implications

The failure to validate this ELISA for detecting feline SDC-1 highlights a broader, often underestimated challenge in clinical biomarker research: the complexity and variability of biological shedding processes. Biomarker studies frequently rely on the apparent simplicity of blood sampling and statistical comparison, but this work demonstrates that the interpretative cracks lie beneath the surface. What initially seemed like a straightforward task, validating a commercial ELISA, evolved into a technically demanding process, influenced by protein structure, antibody specificity, assay design, and sample variability.

This experience was eye-opening, revealing the layers of complexity that underpin biochemical methods applied in both clinical research and clinical decision-making facing individual patients. Hence, the critical importance of rigorous validation. It has reshaped how the author interprets published studies; where once was accepted results at face value, are now approached with greater scrutiny, especially when methodological details are limited.

Ultimately, this chapter raises important questions about the reliability of shedding markers in clinical research and whether their measurement and interpretation are oversimplified. While homology across vertebrate species and the availability of species-labelled commercial assays may suggest feasibility, the reality may be that many of these tools remain insufficiently validated. The process of designing, conducting, and interpreting this study, and reflecting on the results, has led to a broader and more critical question: is there a true role for shed EG constituents in clinical practice? Given the biological variability and the often weak or inconsistent associations with clinically meaningful outcomes, the utility of these biomarkers in guiding care may need to be re-evaluated.

In this study, only three out of 16 sampled sick cats showed high ELISA signals, suggesting that SDC-1 may only be elevated in the most severely ill individuals. This limits its potential utility in detecting EG damage in the broader hospital population, where the majority of patients present with moderate illness. Importantly, this observation holds even if the assay were to be fully validated, if only the most critically ill cats produce measurable increases in SDC-1, the biomarker may have limited clinical relevance in less severe cases. The ELISA used may simply lack the sensitivity to detect anything but the most substantial changes, which in turn diminishes its clinical value and the incentive for commercial assay development.

Furthermore, SDC-1 shedding patterns in cats remain undefined, and peak increases may be easily missed depending on the timing of presentation and disease progression, further complicating interpretation and clinical applicability. Nevertheless, once validated, serum biomarkers like SDC-1 offer a promising, less technically demanding, and potentially more affordable alternative to tools like the GlycoCheck™, which are costly and likely to remain restricted to high-volume, well-resourced veterinary settings. This underscores the need for accessible, reliable biomarkers of EG damage that can be implemented across a range of clinical environments, without sacrificing diagnostic utility.

Chapter IV: Immediate effects of an intravenous fluid challenge on the endothelial glycocalyx in healthy anaesthetized cats

Chapter plan

1. Chapter IV preface
2. Title page
3. Abstract
4. Introduction
5. Materials and methods
    - 5.1. Study population
    - 5.2. Intervention protocol
    - 5.3. Image acquisition
    - 5.4. GlycoCheck™ analysis
    - 5.5. Packed cell volume and total solids
    - 5.6. Statistical analyses
6. Results
7. Discussion
8. Conclusion
9. Authors contributions
10. Footnotes
11. Chapter IV extended implications

1. Chapter IV preface

After first establishing tolerance intervals for GlycoCheck™ parameters in cats, the next step was to evaluate the system's ability to detect changes in the EG in a controlled setting. To do this, I chose a stimulus commonly encountered in clinical practice: administration of an IV fluid challenge using two different, but widely used, resuscitation fluids. This approach aimed to generate data that could inform the design of future clinical studies in sick cats.

The experimental setup was intended to mimic a clinical scenario in which IV fluids are administered to a patient with suspected intravascular volume depletion and circulatory shock. In such cases, a fluid challenge is often used both diagnostically and therapeutically, to assess fluid responsiveness when the underlying cause of shock is not yet confirmed. A positive response typically supports further fluid administration, while a lack of response suggests fluids may not be beneficial. As a result, even cats who ultimately do not require ongoing IV fluids are likely to receive at least one fluid challenge during cardiovascular assessment if shock is suspected.

Admittedly, healthy euvolemic cats (with normal blood volume and hydration) such as those in this study would not typically receive IV fluids. However, because cats are considered particularly sensitive to IV fluid administration, it was appropriate to begin investigating the microcirculatory effects of fluids in a healthy population. Fluid dynamics are likely to differ in sick cats, and the safety of IV fluid dosing in this group remains uncertain. Volume kinetics, the pharmacokinetics of IV fluids, are only just beginning to be studied in feline medicine, and current dosing practices are largely empirical, often extrapolated from data in dogs or people. Moreover, the impact of these empirical rates on the feline microcirculation has not been investigated.

Together, the desire to assess GlycoCheck™'s ability to detect EG changes following a stimulus, and the need to establish baseline effects of IV fluids in healthy cats, provided the rationale for the study design reported in this chapter.

Statement of Contribution – Doctorate with Publications/Manuscripts:

The author of this thesis led the establishment of the collaboration, secured funding, designed the project, and was responsible for data collection, interpretation, reporting, and manuscript preparation.

Initial data from this study was presented as an oral abstract at the European Emergency and Critical Care Congress 2020 (Online due to COVID 19) by the author of this thesis and published in an abstract form in the Journal of Veterinary Emergency and Critical Care in 2020.

Yozova ID, Londoño L, Sano H, Thomson N, Munday J, Cave N. (2020). Assessment of the Endothelial Glycocalyx after a Fluid Bolus in Healthy Anesthetized Cats Using Rapid, Patient-Side Glycocheck Analysis Software. In: Abstracts from the International Veterinary Emergency and Critical

Care Symposium, and the European Veterinary Emergency and Critical Care Annual Congress 2020. Journal of Veterinary Emergency and Critical Care, 30(S1), S27. doi:https://doi.org/10.1111/vec.12988

This manuscript has been fully published in the Veterinary Journal in 2025:

Yozova ID, Londoño LL, Sano H, Thomson N, Munday JS. Immediate effects of an intravenous fluid challenge on the endothelial glycocalyx in healthy anaesthetized cats. Vet J. 2025 Dec;314:106487. doi: 10.1016/j.tvjl.2025.106487. Epub 2025 Nov 8. PMID: 41213396.

2. Title page

Immediate effects of an intravenous fluid challenge on the endothelial glycocalyx in healthy anaesthetized cats

Ivayla D Yozova[1*], Leonel L Londoño[2], Hiroki Sano[1] Kristina K Millar[2], Neroli Thomson[1], John J Munday[1], J Nicholas J Cave[1]

[1]School of Veterinary Science, Massey University, New Zealand

[2]Department of Small Animal Clinical Sciences, College of Veterinary Medicine, University of Florida, Unites States

*Correspondence:

Ivayla D Yozova

School of Veterinary Science - Tāwharau Ora, Massey University, Private Bag 11222, Palmerston North 4222, New Zealand,

email: i.yozova@massey.ac.nz

This study received funding from the Massey University Research Fund 2019.

The authors declare no conflict of interest.

Preliminary results from this study were presented as an oral abstract at the 17th European Veterinary Emergency and Critical Care Congress in 2020 (online due to COVID-19)

Keywords: capillaries, crystalloids, GlycoCheck™, feline, IV fluids, hydroxyethyl starch, microcirculation, perfused boundary region, sidestream dark field videomicroscopy

3. Abstract

Introduction: The endothelial glycocalyx (EG) is meshwork of membrane-bound and soluble constituents lining the endothelial surface of vessels, influencing vascular permeability and blood flow. Overzealous IV fluid administration can negatively affect the EG in dogs and people. EG thickness can be estimated using sidestream dark field videomicroscopy and Glycocheck™ software. This study evaluated whether administration of a fluid challenge results in changes in EG thickness measured using the Glycocheck™ system.

Methods: This was a prospective, randomized, blind, parallel-group single centre experimental study. Thirty male neutered cats were randomized to receive either 10 ml/kg of Hartman's solution (CRYS group) or 10 ml/kg of 6% 130/0.4 hydroxyethyl starch (HES group), or no fluids (control group) over 20 min. Operators in charge of image acquisition were blinded to the treatment allocations. After sedation (butorphanol 0.3 mg/kg SC) for IV catheter placement, anaesthesia was induced with propofol IV CRI to effect (relaxed jaw tone). A video microscope connected to GlycoCheck™ software was placed under the tongue to evaluate the sublingual microvasculature. Images were acquired at baseline (T0), 10 min into IV fluid administration or control (T1) and at the end of infusion – 20 min (T2). The perfused boundary region (PBR), an inverse estimate of EG thickness, was determined by the GlycoCheck™ software along with valid vessel density (VVD), % red blood cell (RBC) filling and median RBC column width (Median P50). The effect of group and treatment over time was tested using linear mixed effects regression modelling, with cat as a random effect.

Results: Twenty-nine cats with a median age of 8.2 years (IQR; 4.04 – 9.46 years) were included for analysis. One cat was excluded due to an elevated T4. Baseline PBR 10-19 µm was significantly higher in the HES group compared to the control group ($p = 0.023$). The PBR 10-19 µm increased significantly over time in the control group ($p = 0.029$) and was significantly lower in the HES group compared to the control group ($p = 0.013$). Decreases in PCV were significantly associated with increases in PBR 5-9 µm ($p = 0.003$) and decreases in PBR 20-25 µm ($p = 0.047$), VVD ($p < 0.001$) and %RBC filling ($p = 0.006$). All changes were within previously established tolerance intervals for cats.

Conclusion: A single fluid challenge of Hartman's solution or hydroxyethyl starch did not result in immediate EG damage in healthy anesthetized cats. However, an increase in PBR 10-19 µm was observed in the control group, suggesting potential anaesthetic effects on EG thickness. In addition, changes in PCV were associated with GlycoCheck™ parameter changes. This study provides initial evidence characterizing the feline EG's response to stimuli and offers a foundation for future research in critically ill cats.

4. Introduction

Few interventions in medicine are as universally applied, and as deceptively simple, as the administration of intravenous (IV) fluids. Popularized during the 19th century cholera pandemic (300), IV fluids were long considered benign, but are now increasingly regarded as pharmacologic agents with defined indications, contraindications, and adverse effects (137, 301). Key indications include fluid resuscitation for shock, rehydration, and maintenance of daily fluid requirements. Excessive or inappropriate administration result in key side effects - intravascular volume overload, subsequent fluid overload and oedema formation (302).

The relationship between circulatory shock and fluid responsiveness is complex, influenced by both patient factors (e.g. cause and severity of shock, comorbidities) and fluid variables (type, dose, rate, duration). Because not all patients in shock respond to IV fluids, their administration should not be automatic. Nevertheless, veterinary practice has traditionally relied on large volume "shock rates" (90 mL/kg/h for dogs and 60 mL/kg/h for cats) to reverse circulatory shock (303, 304). However, with growing recognition of the potential harms of overzealous IV fluids, the fluid challenge approach has gained traction in both human and veterinary critical care (138, 305).

A fluid challenge is both a diagnostic and therapeutic manoeuvre. It involves administering a relatively large volume of IV fluid over a short time period and monitoring for improvement in cardiovascular parameters such as perfusion, blood pressure, or point-of-care ultrasound findings, a.k.a. a "fluid response" (305). A positive response confirms fluid-responsive circulatory shock and justifies ongoing IV fluid resuscitation. Conversely, a lack of response signals the need to pursue alternative interventions (e.g. vasopressors or transfusion). In non-responders, the fluid challenge may result in transient volume overload, which may be inconsequential in healthy individuals but problematic in critically ill or fluid-sensitive patients.

Cats are less tolerant to IV fluid administration, compared to dogs. While this is mostly an empirical notion, there is evidence to contributing factors. Cats have a smaller blood volume (49.0 ± SD 9.6 mL/kg (252) vs. 84–97 mL/kg in dogs (253)). This makes commonly used "dog" fluid resuscitation rates excessive, potentially resulting in fluid overload. Recent volume kinetic studies have demonstrated that even healthy cats have slower IV fluid elimination rates slower elimination rates of IV fluids (130, 131), making them susceptible to fluid accumulation. . In addition, clinical studies have demonstrated that only 37-40% of hemodynamically unstable cats respond to IV fluid administration (259, 260), compared to 66-80% of dogs (261, 262). Fluid overload has not been extensively investigated in cats. A study in 11 cats with urethral obstruction showed an association between fluid overload increased length of hospitalization and cost, suggesting detrimental effects (160). While the fluid challenge approach is considered safer than "shock rates", safe dose rates in cats are largely unknown and merit investigation.

In recent years specific consideration in regard to IV fluid safety has been given to the microcirculation. Indeed, excessive IV fluid administration can lead to microvascular injury, particularly degradation of the endothelial glycocalyx (EG), a gel-like layer lining the luminal surface of blood vessels, acting as a barrier for vascular permeability (132). Intravascular volume overload triggers cardiac stretch and the release of natriuretic peptides (NPs) (142, 143), which promote natriuresis, vasodilation, renin angiotensin aldosterone system inhibition, and increased vascular permeability (144). The latter is thought to result from NP-mediated stimulation of matrix metalloproteinases, which cleave structural components of the EG (145). This facilitates movement of fluid from the vasculature into the interstitial space. While healthy animals can compensate via lymphatic return, this mechanism is often impaired in critical illness, leading to fluid accumulation, tissue oedema, impaired oxygen diffusion, and downstream organ dysfunction (58, 132). Numerous studies have associated fluid overload with increase mortality in the human intensive care setting (159, 307, 308).

While IV fluids are often associated with fluid overload and EG damage, they are rarely the sole cause for either. In critically ill patients, these complications are typically multifactorial, driven by underlying disease, vascular permeability, inflammation, and comorbidities (113, 146-158). Although studies have shown increases in shed EG biomarkers following IV fluid administration, the relationship is complex, and the current evidence is inconclusive, not supporting a causal link (113, 142). Rather, it reflects the interplay between patient condition, fluid characteristics, and baseline vascular integrity.

Fewer studies have investigated fluid effects on the EG via direct microvascular imaging, such as sidestream dark field videomicroscopy (SDFV) and GlycoCheck^{TM} software analysis (176). This software estimates EG thickness indirectly by calculating the perfused boundary region (PBR) in capillaries, with higher PBR values indicating a thinner damaged EG (90). In recent human studies, PBR increased transiently in stable surgical patients following a fluid challenge and more persistently in septic patients (155, 309). Conversely, animal studies have shown mixed results: one series in anaesthetised rabbits found no PBR change with fluid loading except after hypertonic saline infusion (96, 97), while a recent canine haemorrhagic shock model demonstrated increased PBR following crystalloid and colloid resuscitation compared to blood products (93). To date, the impact of IV fluids on EG integrity has not been studied in cats. Despite mixed results in other species, the issue remains relevant in cats given their fluid sensitivity and low rates of fluid responsiveness.

This study aims to evaluate the immediate effects on GlycoCheck^{TM} parameters of two commonly used resuscitation fluids in equal volumes - 10 ml/kg IV of either a buffered balanced isotonic crystalloid (Hartman's Solution) or synthetic colloid (hydroxyethyl starch 130/0.4, tetrastarch) administered as a fluid challenge over 20 min. The hypothesis is that PBR of all analysed vascular diameters will increase within 20 min of administration in the cats receiving isotonic crystalloids and synthetic colloids compared to a no fluid control group. A secondary aim was to investigate potential associations between packed cell volume (PCV) and GlycoCheckTM parameters.

5. Materials and methods

5.1. Study population

This was a prospective, randomized, blind, parallel-group, single centre, experimental study, approved by Massey University's Animal Ethics Committee (MUAEC Protocol 18/126), complying with the Animal Research Reporting for In Vivo Experiments guidelines for experimental studies with animals (275). Thirty healthy male neutered research-purposed cats were initially enrolled. They were considered healthy based on no history of weight loss, physical examination findings, complete blood count, serum biochemistry and thyroxine 4 concentrations. One cat was excluded for a low-grade heart murmur observed at the start of sedation, not present during initial physical exam. Therefore, 29 cats were included for analysis. The median age of the cats was 8.2 years (IQR: 4.04–9.46 years), the mean body weight was 4.24 ± 0.72 kg, and body condition score was 4 to 5 out of 9.

5.2. Intervention protocol

Cats were placed in single cages the night before intervention and food withheld with ad libitum access of water. At the start of intervention, all cats were sedated with butorphanol 0.3 mg/kg SC for intravenous catheter placement in the left or right cephalic vein. Propofol was then administered intravenously to achieve relaxation of jaw tone to effect and maintained in medium to deep plane of sedation. No endotracheal intubation was performed, and the cats were spontaneously breathing. Anaesthesia was maintained using a continuous rate infusion of propofol (0.05-0.2 mg/kg/min) for the duration of the intervention. Anaesthesia was overseen by a board-certified anaesthesiologist and variables such as heart rate (HR), respiratory rate (RR), mucous membrane colour, capillary refill time, temperature, pulse oximetry (SpO2), and oscillometric blood pressure (oBP) readings were monitored. The pulse oximetry probe was placed on the ear or interdigital skin fold to leave the tongue available for image acquisition.

The cats were then randomized using an online tool (randomizer.org) to either receive 10 ml/kg of a buffered balanced isotonic crystalloid solution[c] (CRYS group); or 6% 130/0.4 hydroxyethyl starch[d] (HES group) over 20 min; or no fluid challenge (anaesthesia only, control group). All cats remained under propofol anaesthesia for the duration of the intervention (image acquisition and fluid challenge). At the end of intervention, the cats were recovered, fed, monitored in the single cages throughout the day and then moved to their habitual housing.

5.3. Image acquisition

Cats were placed in lateral recumbency, and the base of the tongue exposed such as the sublingual mucosa was accessible for the videomicroscope. A hand-held SDFV camera connected to a laptop with GlycoCheck™ software[e] was placed in contact with the sublingual mucosa. Three video

recordings were taken from different sublingual mucosal sites at three different timepoints; T0 (baseline), T1 (intermediate, 10 min into fluid challenge administration or anaesthesia only for the control group), and T2 (end of fluid challenge or 20 min after baseline for the control group), resulting in three recordings per timepoint for each cat. The operator was blinded to group allocation by covering the fluid bag and pump with opaque material and having the control group subjects attached to a giving set without receiving IV fluids.

.

5.4. GlycoCheck™ analysis

The method for measuring and calculating GlycoCheck™ parameters has been previously described (90, 91, 100). Briefly, the SDFV camera emits green light at 540 nm wavelength which is absorbed by haemoglobin in circulating red blood cells (RBC). Therefore, vessels appear dark on a bright background. The system records approximately 10 2 second videos of the sublingual vascular network. The software automatically identifies vessels that are less than 30 µm in diameter by analysing the contrast between the RBC and the background. The software then subdivides vessels into major (10 µm in length) vascular segments. To ensure that each vascular segment image is of sufficient quality for analysis, the software further subdivides major segments into minor vascular segments (0.5 µm in length) and determines the percentage of minor segments with sufficient contrast for analysis. Major segments with > 60% of minor segments with sufficient contrast are considered valid vascular segments. Further analysis is performed on valid vascular segments (VVS) only. Valid vessel density (VVD) per site is then expressed by multiplying 10 µm by the number of valid vascular segments (VVS) identified.

Secondly, RBC column widths are assessed for minimal column width, column position, and signal-to-noise ratio. From the measured column widths, the software then calculates the percentage of RBC filling (%RBC filling) based on the proportion of time a particular VVS contains RBC throughout all recordings per site. The median RBC column width (Median P50) is calculated using the intensity profiles of the dynamic lateral positions of RBCs in all measured column widths.

Finally, linear regression analysis on the Median P50 is performed to derive the perfused diameter of VVS. From that, the PBR (perfused boundary region), an inverse estimate of EG thickness, is calculated as the distance between the Median P50 and the perfused diameter ([Perfused diameter – median RBC column width]/2). Reported GlycoCheck™ parameters, therefore, include VVD, %RBC filling, Median P50, D_{perf} and PBR for vessels with diameter from 5 to 25 µm and for subgroups of vessels with diameters from 5 – 9 µm, 10 – 19 µm and 20 – 25 µm. The PBR is therefore an inverse estimation of EG thickness, the higher the PBR the thinner the EG and vice versa.

5.5. Packed cell volume and total solids

Packed cell volume (PCV) and total solids (TS) were measured at T0 and T2 for each cat. For PCV measurements, whole blood was placed in capillary microhematocrit tubes, and the tubes then

centrifuged in a bench-top centrifuge[f] at 3000G for 5 min. The measurements were then read manually by the same operator using a sliding microhematocrit tube reader. Total solids were measured using a hand-held refractometer[g]. After reading PCV, the microhematocrit tube was snapped to allow for the serum component to be placed onto the measuring prism of the refractometer and spread by placing the illuminator flap over it. The refractometer was then pointed towards a light source by the operator and the shadow boundary in relation to the graduation for TS observed through the eyepiece.

5.6. Statistical analysis

A sample size calculation was based on data from 60 healthy dogs, where the mean ± SD of PBR 5–25 µm was 2.04 ± 0.31 (95). A standardized effect size corresponding to 25% of the mean was empirically chosen, in line with guidelines for statistical analysis in experiments with laboratory animals (Festing & Altman, 2002). To achieve 80% power with an alpha of 0.05 the required number was calculated to be ~9 per group. The final sample size was rounded up to 10 cats per group allowing for a conservative margin, giving a total of 30 cats for the study.

Triplicates from measured GlycoCheck™ parameters were averaged for further analysis as recommended in previous reports in healthy and critically ill people (181, 186). Data normality was tested using Shapiro-Wilk test and visually inspected using histograms or Q-Q plots. Normally distributed data is presented as mean ± standard deviation (SD), not normally distributed data is presented as median (Interquartile Range). Interactions between GlycoCheck™ parameters (PBR, VVD, %RBC filling, and Median P50) and (1) group, timepoint, and their interaction; (2) PCV as a continuous variable; and (3) PCV and TS as dependent variables against group, timepoint, and their interaction were analysed using separate linear mixed-effects regression models, with cat as a random effect. For investigating interactions between PBR and other GlycoCheck™ parameters (VVD, RBC filling, and MedianP50), a stepwise model reduction was performed starting from a full model including VVD, RBC filling, and Median P50 retaining variables based on significance and model fit. This analysis included all data points, irrespective of group or timepoint. All statistical analyses were conducted in R (Team, 2023) (297).

6. Results

Descriptive statistics for anaesthetic monitoring parameters per group and timepoint are presented in Table 1 and comparisons between group and timepoint in supplementary material. No adverse effects occurred. Results for GlycoCheck™ parameters are presented in Table 4.1. Temporal changes in PBR across vessel size categories (5–9 µm, 10–19 µm, 20–25 µm, and 5–25 µm) are illustrated in Figure 4.1. No significant effects of group, timepoint, or group–timepoint interaction were observed for PBR 5–25 µm, PBR 5–9 µm, PBR 20–25 µm, %RBC filling, or Median P50. However, PBR for vessels measuring 10–19 µm increased significantly from baseline (T0) to 20 minutes (T2) in the control group ($p = 0.029$) and decreased significantly in the HES group compared to the control group at T2 ($p = 0.013$). Additionally, baseline PBR in the 10–19 µm range was significantly higher in

the HES group than in the control group (p = 0.023). Valid vessel density was significantly lower at T2 in the CRYS group compared to the control group (p = 0.048). All GlycoCheck™ parameter values remained within previously established tolerance intervals across all intervention groups and timepoints (100).

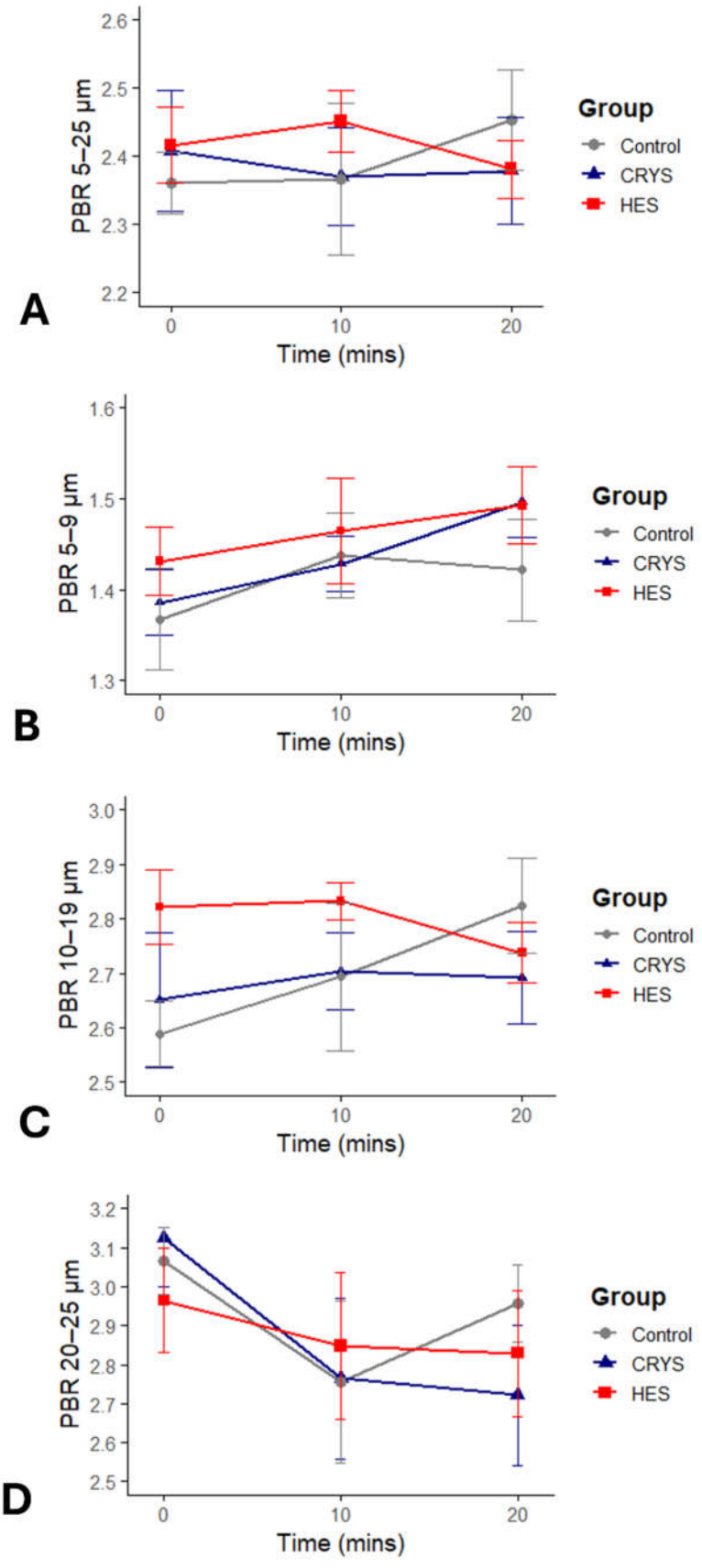
Table 4.1. Summary statistics for Glycocheck™ parameters, packed cell volume and total tolids in 29 healthy male neutered cats receiving a fluid challenge (Hartman's solution or Hydroxyethyl starch) or not (control).

	Baseline		**Intermediate (10 min)**		**End of fluid challenge (20 min)**	
Hartman's solution group						
Variable	**Mean ± SD**	**Min - Max**	**Mean ± SD**	**Min - Max**	**Mean ± SD**	**Min - Max**
PBR 5-25 (µm)	2.39±0.30	2.04-3.00	2.36±0.21	2.07-2.64	2.40±0.26	1.96-2.73
PBR 5-9 (µm)	1.37±0.10	1.23-1.51	1.43±0.09	1.34-1.62	1.49±0.13	1.35-1.68
PBR 10-19 (µm)	2.63±0.41	2.05-3.50	2.70±0.22	2.37-2.96	2.71±0.28	2.23-3.10
PBR 20-25 (µm)	3.10±0.42	2.35-3.59	2.61±0.43	2.08-3.06	2.77±0.58	1.73-3.85
VVD	206.81±101.75	77.00-350.33	145.14±75.38	53.00-264.00	**129.74±43.71***	77.00-224.33
%RBC filling	74.93±6.18	64.03-83.07	72.43±5.39	65.43-78.53	69.94±5.01	59.93-77.10
Median P50	7.09±0.66	5.63-7.86	7.76±0.91	6.48-9.21	7.75±1.27	5.34-9.08
PCV	36.27±4.54	30.50-43.00	No measurement		25.00±2.72	21.50-29.00
TS	76.22±9.60	64.00-95.00	No measurement		59.78±3.77	54.00-64.00
Hydroxyethyl starch group						
Variable	**Mean ± SD**	**Min - Max**	**Mean ± SD**	**Min - Max**	**Mean ± SD**	**Min - Max**
PBR 5-25 (µm)	2.47±0.14	2.24-2.63	2.45±0.13	2.19-2.62	2.37±0.14	2.15-2.55
PBR 5-9 (µm)	1.44±0.12	1.23-1.64	1.46±0.17	1.13-1.72	1.51±0.14	1.35-1.78
PBR 10-19 (µm)	**2.86±0.18***	2.48-3.04	2.82±0.11	2.67-3.00	**2.70±0.18¶**	2.49-2.97
PBR 20-25 (µm)	3.01±0.44	2.29-3.47	2.95±0.62	2.09-3.83	2.72±0.49	1.91-3.43

VVD (µm/mm)	182.90±63.53	79.00-301.33	134.05±32.59	96.50-202.33	116.12±29.80	60.00-150.00
%RBC filling (%)	70.87±5.50	60.63-79.63	69.02±5.91	61.87-77.07	68.95±4.07	62.77-75.67
Median P50 (µm)	6.61±0.61	5.28-7.58	6.73±0.67	5.50-8.16	6.62±0.51	6.00-7.48
PCV (%)	36.20±4.98	30.00-47.00	No measurement		**23.90±4.18**¶	19.50-33.00
TS (g/L)	77.50±5.28	70.00-88.00	No measurement		61.60±6.50	55.00-78.00
Control group						
Variable	**Mean ± SD**	**Min - Max**	**Mean ± SD**	**Min - Max**	**Mean ± SD**	**Min - Max**
PBR 5-25 (µm)	2.33±0.16	2.08-2.58	2.37±0.33	1.91-2.84	2.44±0.22	2.19-2.91
PBR 5-9 (µm)	1.38±0.16	1.06-1.60	1.44±0.14	1.30-1.66	1.42±0.16	1.19-1.73
PBR 10-19 (µm)	2.58±0.17	2.18-2.81	2.69±0.41	2.09-3.21	**2.83±0.25***	2.53-3.34
PBR 20-25 (µm)	3.05±0.25	2.65-3.45	2.76±0.62	2.00-3.73	3.00±0.31	2.57-3.57
VVD (µm/mm)	153.13±62.83	86.00-292.00	146.41±54.54	68.50-262.00	148.83±36.74	105.67-219.33
%RBC filling (%)	72.27±5.23	64.00-78.80	70.49±4.67	62.75-79.40	71.91±5.65	62.17-79.07
Median P50 (µm)	7.09±0.78	6.22-8.59	7.02±0.84	6.11-8.37	7.08±0.52	6.16-7.70
PCV (%)	34.85±4.26	28.50-43.00	No measurement		**26.90±3.28***	22.00-34.00
TS (g/L)	75.00±8.55	66.00-92.00	No measurement		67.20±7.79	54.00-78.00

PBR – perfused boundary region; PCV – packed cell volume; SD – standard deviation; TS – total solids; VVD – valid vessel density
*Significantly different compared to baseline within group
¶Significantly different compared to the control group

Figure 4.1. Perfused Boundary Region (PBR) measurements over time across different vessel diameter classes in cats receiving a fluid challenge with either a synthetic colloid (HES), a balanced isotonic crystalloid (CRYS), or no fluid (Control). Each panel shows mean ± standard error (SE) values for: (A) PBR 5–25 µm, (B) PBR 5–9 µm, (C) PBR 10–19 µm, and (D) PBR 20–25 µm. Dashed horizontal lines represent the upper and lower tolerance interval limits for each parameter. Data points were collected at baseline (0 min), 10 min, and 20 min (end of infusion).


A
PBR 5–25 µm
2.6
2.5
2.4
2.3
2.2
0
10
20
Time (mins)
Group
Control
CRYS
HES
B
PBR 5–9 µm
1.6
1.5
1.4
1.3
0
10
20
Time (mins)
Group
Control
CRYS
HES
C
PBR 10–19 µm
3.0
2.9
2.8
2.7
2.6
2.5
0
10
20
Time (mins)
Group
Control
CRYS
HES
D
PBR 20–25 µm
3.2
3.1
3.0
2.9
2.8
2.7
2.6
2.5
0
10
20
Time (mins)
Group
Control
CRYS
HES

Decreases in both %RBC filling and Median P50 were associated with significant increases in PBR across multiple vessel size ranges: 5–25 µm ($p = 0.025$ and $p = 0.005$, respectively), 5–9 µm ($p < 0.001$ and $p = 0.038$), and 10–19 µm ($p = 0.005$ and $p = 0.021$). For vessels 20–25 µm, only increases in Median P50 were associated with a decrease in PBR ($p < 0.001$).

Summary statistics for PCV and TS are presented in Table 4.1. Packed cell volume (PCV) decreased significantly from baseline over time in the control group ($p < 0.001$), and this reduction was significantly greater in the HES group compared to the control group ($p = 0.049$). Total solids (TS) also declined significantly over time in the control group ($p < 0.001$), with additional significant decreases observed in both the CRYS and HES groups relative to the control group ($p = 0.001$ and $p = 0.002$, respectively). Decreases in PCV were significantly associated with increases in PBR 5-9 µm ($p = 0.003$). In addition, lower PCV was significantly associated with decreases in lower PBR 20-25 µm ($p = 0.047$), VVD ($p < 0.001$) and %RBC filling ($p = 0.006$).

7. Discussion

In this study, administration of 10 ml/kg of Hartman's solution or HES over 20 min did not result in a significant increase PBR during the 20 minutes intervention interval, suggesting that the fluid challenge did not acutely damage the EG in the study population. This contrasts with some findings in other species, where IV fluid administration has been associated with transient increases in PBR indicating EG thinning. For example, a study in people reported a temporary increase in PBR following Lactated Ringer's Solution infusion during spinal surgery (309). Experimental studies in rabbits have shown inconsistent results, with most fluid types having no measurable effect on PBR, except for a marked increase after administration of 10% hypertonic saline (96, 99). A recent canine haemorrhagic shock model found increased PBR in the group receiving resuscitation with crystalloids and synthetic colloids, compared to the group receiving blood products (93). These discrepancies likely reflect multiple factors, including species-specific physiology, the clinical versus experimental context, and importantly, differences in fluid type, dose, and infusion duration. Therefore, comparisons between this and the above-mentioned studies cannot be made. The question of whether and in which circumstances is the feline endothelial glycocalyx affected by IV fluids is to be answered in future studies focusing on longer term outcomes and diseased populations.

Intravenous fluids vary considerably in their indications and physiological effects (136). While buffered balanced isotonic crystalloids can be used for resuscitation, rehydration, or maintenance, fluids such as hypertonic saline and synthetic colloids are typically restricted to resuscitation due to their concentrated volume-expanding properties. Moreover, mammals differ widely in their ability to tolerate and respond to volume changes. Species adapted to arid environments possess enhanced water conservation mechanisms compared to those from temperate regions, further complicating cross-species extrapolation (310, 311). Crucially, the effects of IV fluids on GlycoCheck™ parameters remain sparsely studied, particularly when compared to broader investigations of IV fluid administration. In addition to physiological and methodological variability, clinical studies introduce numerous uncontrolled variables that limit direct comparison with experimental research. Taken together, robust comparisons or extrapolations between studies where species, types of fluids, and administration protocols varied cannot be directly made. Therefore, these results are to be compared to results in the same species and similar settings.

Two commonly used resuscitation fluids in small animal practice were evaluated in this study: a buffered balanced isotonic crystalloid (Hartman's solution) and an isotonic synthetic colloid (6% HES 130/0.42) with the same experimental setting. Both remain in clinical use for IV fluid resuscitation, despite ongoing debate regarding the efficacy and safety of synthetic colloids (32-34, 312, 313). Equal volumes (10 ml/kg) were administered to facilitate direct comparison. Although HES is generally considered to exert greater and more sustained IV volume expansion than crystalloids, particularly in euvolaemic patients with intact EG and adequate vascular permeability (34), these effects tend to manifest over time rather than immediately following administration (32). This supported the use of equivalent volumes in the current experimental design, as both were expected to exert similar volume effects in the short term. A relatively high, yet clinically appropriate, dose was selected to maximise the likelihood of detecting microvascular effects without exceeding safe physiological limits. The aim was to deliver a meaningful fluid challenge capable of influencing the EG, if susceptible. We expected that both types of fluids will negatively impact the EG. Contrary to this expectation, no significant increase in PBR was observed following administration of either fluid. The lack of a significant PBR increase may reflect insufficient time for a physiological response to occur. A 20-minute window may be too short for atrial stretch-induced natriuretic peptides to trigger measurable EG disruption (114, 143, 227). Additionally, the EG in healthy individuals may be more resilient, and findings from other species suggest that IV fluid alone do not consistently induce shedding of EG constituents.

Hydroxyethyl starch administration was associated with a subtle decrease in PBR 10 – 19 µm. This finding is corroborated by several experimental rodent models, suggesting a potential protective effect of HES on the EG (314-318). Proposed mechanisms include modulation of inflammation and inhibition of enzymatic "sheddases" such as heparinase, hyaluronidase, and neuraminidase (318) as well as volume-sparing effects relative to crystalloids (312). However, given the substantial evidence of adverse effects associated with HES in human medicine (9), and similar though less pronounced

concerns in veterinary patients (34), the clinical relevance of this finding remains limited. Any potential benefit is likely outweighed by the known risks, precluding broad clinical application. Further investigation may be warranted in carefully selected veterinary patient subpopulations where HES could offer targeted benefit.

Interestingly, PBR 10–19 µm increased significantly in the control group that did not receive IV fluids. The cause of this finding remains unclear. One possibility is that anaesthetic-related effects, such as changes in circulating volume, increased vascular permeability, or direct drug-related EG damage, may have contributed, and were potentially mitigated by IV fluid administration. In this study propofol was used for anaesthesia due to its short duration of action and relatively good safety profile (319). Interestingly, in vitro and in vivo experimental studies have shown that propofol can damage the EG (320-322). Propofol is known to induce oxidative stress, particularly at high doses or with prolonged use, which may compromise the integrity of the endothelial surface layer (323, 324). However, clinical studies in people have not consistently demonstrated greater EG disruption with propofol compared to other anaesthetic agents (320, 325-327). The present study was not specifically designed to investigate the effects of propofol on the endothelial glycocalyx. Therefore, parallels with other studies cannot be drawn.

The effects of propofol on the feline EG remain unknown. Nonetheless, cats are particularly sensitive to propofol and may develop oxidative lesions such as Heinz bodies and anaemia following repeated administration (328-331), raising the possibility that similar oxidative effects could impact the EG. These considerations highlight the potential for anaesthetic agents to confound microcirculatory research and support the need for further investigation into anaesthetic protocols optimized for experimental studies.

Although a decrease in PCV is expected following IV fluid administration due to haemodilution, a significant drop was also observed in the control group, which did not receive fluids. The drop in PCV can likely be attributed to anaesthesia-related fluid shifts, where fluid moves from the interstitial to the IV space, resulting in haemodilution (119). Additionally, anaesthesia is known to cause splenorelaxation in cats (254, 255), allowing the spleen to act as a reservoir for RBC, potentially contributing further to the reduction in PCV. Notably, propofol infusions have been specifically associated with transient decreased PCV in cats (328), making these observations unsurprising. What is more noteworthy, however, are the associations between PCV and GlycoCheck™ parameters, specifically an increase in PBR 5 – 9 µm and decreases in VVD and %RBC filling with decreasing PCV. GlycoCheck™ measurements are based on contrast from RBC and their lateralization, which may be influenced by changes in blood viscosity and RBC rheology associated with altered PCV. Despite this plausible link, such associations have not been widely described in the existing literature. Nonetheless, two human studies that did examine this relationship found similar trends: decreased PCV was associated with increased PBR (183, 187).

Interestingly, in the present study, PBR 20–25 µm showed a decrease with decreasing PCV, an opposite association compared to PBR 5–9 µm. This discrepancy might be explained by differences in EG thickness across vessel calibres, PBR 5–9 µm averaging 1.34 ± 0.15 µm in cats, versus 2.92 ± 0.57 µm for PBR 20–25 µm, suggesting potential distinct responses of the EG to changes in blood viscosity and flow dynamics (100). More likely, the observed inverse relationship for PBR 20 – 25 µm, though statistically significant ($p = 0.047$), may reflect a type I error, given the smaller sample size within this subgroup of vascular sizes (215). Since anaemia is common in sick veterinary patients, these findings warrant further investigation in specifically designed studies to determine their significance in in both the experimental and clinical settings.

Overall, our findings demonstrated that vessels of different diameters were not equally affected by the interventions. The cause for this observation remains unclear. Most studies in both animals and people do not report PBR values stratified by vessel size; with most presenting a single aggregate PBR measurement across the 5–25 µm range (90, 91, 93, 94, 154, 216). However, the microvascular segments captured by the GlycoCheck™ system may differ in both structure and function and may dynamically adapt their diameter in response to physiological demand (332, 333). It is therefore plausible that external stimuli affect vessels of different calibres in distinct ways, as suggested by the current findings. While this study was not designed to determine the mechanisms underlying these diameter-specific differences in PBR, the results underscore the importance of analysing and reporting vessel size–specific PBR values in future research.

In this study, several associations between GlycoCheck™ parameters were identified, including increases in PBR across most vascular size groups in conjunction with decreases in Median P50 and %RBC filling. Similar findings have been reported in human studies, particularly the association between %RBC filling and PBR (90, 215, 217). These changes have often been interpreted as indicative of deeper RBC penetration into the EG, with reduced %RBC filling reflecting a thinner or less healthy EG. However, similar associations have also been observed in healthy human cohorts, where such pathological interpretations are less convincing (90, 191, 217). In this context, it is important to highlight that the present study also involved healthy cats. The association between Median P50 and PBR is expected, given that PBR is mathematically derived from the perfused vessel diameter and the median RBC column width (Median P50) (90, 100). Percentage RBC filling reflects the proportion of valid vessel segments in which RBCs are present across all recorded frames (90, 100). Because %RBC filling is based on how often RBCs are seen in the same vessel segments used to calculate PBR, it is not a fully independent measure. Changes in %RBC filling are, therefore, likely to occur alongside changes in other parameters that describe RBC distribution, and any correlations should be interpreted with caution.

This study has several limitations. The cohort examined was relatively small, which may have limited the statistical power to detect significant differences and type I errors. At the time of study design, however, the lack of prior research in cats and the overall paucity of relevant literature made a

meaningful sample size calculation unfeasible. Only the immediate, short-term effects of IV fluids were evaluated, and as discussed above, this limited timeframe might not have captured the full magnitude of effects. Additionally, the 20-minute duration was arbitrary, based on IV fluid rates empirically used in clinical practice, rather than previous evidence. Baseline differences were detected in the PBR 10 – 19 µm subgroup, suggesting that between individual variability may be of significance in cats, despite averaging three measurements as recommended by variability studies (181, 185, 186). Therefore, a parallel-group design might not be appropriate for the experimental setting. The requirement to anaesthetise animals for GlycoCheck™ measurements represents a persistent confounder, as anaesthesia-related fluid shifts (from the interstitial to the intravascular space) may transiently alter EG thickness or interfere with measurements by inducing haemodilution and decreasing PCV. For clinical applications, the authors recommend (where possible) performing measurements in the beginning of anaesthesia, before these volume effects occur. Finally, because only healthy cats were included, the findings should not be extrapolated to sick cats.

8. Conclusion

Administering an IV fluid challenge using two types of fluids (Hartman's and HES) to a small group of healthy anaesthetized cats did not decrease EG thickness. Changes in endothelial glycocalyx thickness were observed in only one vessel subgroup (10 – 19 µm diameter), with an increase in the HES group compared to the control group, and an unexpected decrease in the control group. Decreases in PCV were associated with increased PBR of the smallest analysed vessels (5 – 9 µm). Changes in PCV should be taken into consideration when interpreting GlycoCheckTM results and images should preferably be acquired at the beginning of anaesthesia to avoid anaesthesia-related volume effects. Future studies should focus on evaluating the longer-term effects of IV fluids on the EG in cats to better assess the full magnitude of the response.

Authors contributions

IY secured funding, designed the study, collected and interpreted data and wrote the original draft and edited the manuscript; LL designed the study; collected and interpreted data and edited the manuscript; HS helped with study design, collected and interpreted data and edited the manuscript; KM collected and interpreted data and edited the manuscript; NT helped secure funding, interpreted data and edited the manuscript; NC interpreted data and edited the manuscript; JM secured funding, interpreted data and edited the manuscript.

Footnotes

a Torbugesic-SA®, Zoetis New Zealand Limited

b Provive 1%, Baxter Healthcare Ltd

c Hartman's solution, Baxter, New Zealand

d Voluven®, Fresenius Kabi, New Zealand

e MicroVascular Health Solutions, USA

f IFuge HCT NXT, Neuation, Accumax Group, Gujarat, India
g RHC-200 Clinical ATC, Shoof International Ltd

9. Chapter IV extended implications

Results from this study provide initial insight into how the healthy feline EG responds to administration of a relatively large dose of two types of IV fluids. In addition to the reported findings, the study design was successfully implemented, with no adverse effects observed from either the anaesthesia or the IV fluid administration. This suggests that similar experimental models could be safely used to investigate the effects of IV fluids on the microcirculation or other physiological parameters.

While the results did not support the alternative hypothesis, that large volumes of IV fluids would cause EG damage, this hypothesis was based on somewhat inconclusive human data, particularly in light of the limited use of sidestream dark field videomicroscopy (SDFV) and GlycoCheck™ analysis in evaluating fluid effects. Moreover, the notion that cats are "not tolerant to IV fluids" remains largely empirical, with new evidence (specifically feline volume kinetics) only beginning to emerge to support and better define this observation (130, 131). Conducting research with limited prior data, especially in an understudied species, inevitably involves an exploratory element. Therefore, while the outcomes were not entirely as expected, they are not altogether surprising.

The association between GlycoCheck™ parameters and PCV was somewhat unexpected and has been scarcely reported in the literature, yet it may represent a key insight. Given that haemodilution, whether from anaesthetic effects or IV fluid administration, or disease-related anaemia, is common in clinical settings, these associations warrant further investigation and should be considered in the interpretation of clinical data.

An attempt was made to measure syndecan-1 with the ELISA assay used in chapter III. However, given the partially successful validation, no conclusions could be drawn.

Lastly, a key limitation of this study, one that could not be overcome given the lack of prior data on the effects of IV fluids on the feline EG, was the short duration of evaluation. This may not have allowed sufficient time for any EG damage to develop or be detected. Although the fluid doses used were relatively high, they may still have been insufficient to induce the degree of transient intravascular volume overload needed to stretch the heart and affect the EG. In addition, we observed differences in parameters at baseline, suggesting that a parallel group design may not be the most suitable approach for GlycoCheck™ studies. These limitations ultimately informed the design and rationale for the next chapter of this thesis.

Chapter V: Effects of transient intravascular volume overload on endothelial glycocalyx thickness in healthy anaesthetized cats

Chapter plan

1. Chapter V preface
2. Title page
3. Abstract
4. Introduction
5. Materials and methods
    - 5.1. Study population
    - 5.2. Intervention protocol
    - 5.3. Image acquisition
    - 5.4. GlycoCheck™ analysis
    - 5.5. Packed cell volume and total solids
    - 5.6. Statistical analyses
6. Results
7. Discussion
8. Conclusion
9. Conflict of interest
10. Funding
11. Chapter V extended implications

1. Chapter V preface

The previous fluid challenge study (Chapter IV) provided a strong foundation for evaluating the effects of IV fluids on the EG. While a single fluid challenge using either buffered balanced isotonic crystalloids or synthetic colloids did not appear to cause EG damage, the study revealed several important findings, namely potential negative anaesthetic effects on GlycoCheck™ parameters, possible protective effects of IV fluid administration, and key associations between these parameters and packed cell volume (PCV).

Building on those observations and recognising that the fluid doses used may have been insufficient to cause EG injury, this chapter focuses more specifically on volume overload and longer-term effects, with the aim of assessing whether any changes in EG thickness persist over time. A crossover design was used to minimise between-subject variability and strengthen the reliability of our findings.

To maintain consistency with the previous study (Chapter IV), the anaesthetic protocol was deliberately left unchanged. This decision allowed for direct comparison of findings between chapters and avoided introducing new confounders, such as alternative anaesthetic agents. It also enabled exploration of whether the observed changes in GlycoCheck™ parameters persisted over time under similar anaesthetic conditions.

In this chapter, a different but identical GlycoCheck™ device was used. For the first time, additional parameters such as vascular segment counts were available for analysis, allowing for a more comprehensive evaluation of microvascular dynamics beyond those measured in the previous study.

Statement of Contribution – Doctorate with Publications/Manuscripts:

The author of this thesis led the establishment of the collaboration, secured funding, designed the project, and was responsible for data collection, interpretation, reporting, and manuscript preparation.

Initial data from this study was presented as an oral abstract at the European Emergency and Critical Care Congress 2024 by the author of this thesis and published in an abstract form in the Journal of Veterinary Emergency and Critical Care in 2024.

Yozova ID, Munday JS, Avendaño Veas FA, Irie M, Thomson N (2024). Effects of acute intravascular volume overload on endothelial glycocalyx thickness in healthy cats – preliminary results. In: Abstracts from the International Veterinary Emergency and Critical Care Symposium and the European Veterinary Emergency and Critical Care Annual Congress 2024. Journal of Veterinary Emergency and Critical Care, 34(S2), S36. doi:https://doi.org/10.1111/vec.13420

A full manuscript is currently in review in Frontiers in Veterinary Science, as part of the research topic: Innovations in Hemodynamic Monitoring in Veterinary Medicine: From Macrohemodynamics to Microcirculation.

2. Title page

Effects of transient intravascular volume overload on endothelial glycocalyx thickness in healthy anaesthetized cats

Ivayla D. Yozova[1,*], Neroli Thomson[1], Mitsuhiro Irie[2], Rebecca Owen[1], John S. Munday[1]

[1]School of Veterinary Science, Massey University, New Zealand

[2]Shikoku Veterinary Medical Center, Miki 761-0701, Japan

* Correspondence:

Ivayla D. Yozova i.yozova@massey.ac.nz

Keywords: capillaries, GlycoCheck™, feline, fluid overload, intravenous fluids, microcirculation, perfused boundary region, sidestream dark field videomicroscopy

3. Abstract

Introduction: Previous studies suggest that the endothelial glycocalyx is damaged by volume overload. This study assessed the effects of transient intravascular volume overload on endothelial glycocalyx thickness in healthy cats, using sidestream dark field videomicroscopy and the Glycocheck™ software.

Methods: This was a prospective blinded cross-over single-centre experimental study on twenty healthy cats. Cats were sedated with gabapentin PO and butorphanol SC and maintained anaesthetized with propofol CRI for each image acquisition. They were randomized to either receive 30 ml/kg/10 min of Hartman's solution (volume overload group) or no fluids (control) with a washout of 7 days. Sublingual mucosa videomicroscopy images were acquired at T0 (baseline), T1 (immediately after intervention), T2 (3h after end of intervention) and T3 (24h after end of intervention) with three measurements performed per timepoint. The perfused boundary region (PBR), an inverse estimate for endothelial glycocalyx thickness, for vessels with diameter of 5-25, 5-9, 10-19 and 20-25 µm, respectively, was then automatically calculated with the Glycocheck™ software. Other microcirculatory parameters included vascular segment counts, valid vessel density (VVD), % red blood cell filling (RBC), and median RBC column width (Median P50). Packed cell volume (PCV) and total solids were measured at each timepoint. Data normality was assessed using the Shapiro-Wilk test and visual inspection. Linear mixed-effects regression modelling, with cat as a random effect, analysed interactions between GlycoCheck™ and other parameters.

Results: PBR 5 – 25 µm, 5 – 9 µm and 10 – 19 µm increased over time, reaching significance at T2 ($p=0.001$, $p=0.017$ and $p=0.008$, respectively). A significant group x timepoint interaction was identified for PBR 5 – 9 with decreased values at T2 ($p=0.028$) and T3 ($p=0.010$) in the volume overload group. Decreases in PCV were significantly associated with increases in PBR 5 – 25 µm ($p=0.003$) and PBR 10 – 19 µm ($p=0.013$). Vascular segment counts were unevenly distributed across the 5–25 µm range ($p<0.001$), with smaller diameter vessels (5–9 µm) being overrepresented.

Conclusion: This study did not demonstrate damage to the endothelial glycocalyx after transient volume overload in healthy cats. The PBR did increase over time in the control group, suggesting potential anaesthetic effects. These might have been mitigated by the administration of IV fluid administration for vessels 5 – 9 µm, as their PBR decreased overtime. Changes in PCV affected GlycoCheck™ parameters and this finding should be further explored. Further studies designed with understanding of feline volume kinetics are required to investigate the effects of IV fluids on the feline endothelial glycocalyx.

4. Introduction

Intravascular volume overload (VO) and the resulting fluid overload are harmful, as they contribute to interstitial oedema, impair oxygen delivery to cells, and ultimately promote multi-organ dysfunction and mortality (159). Volume overload and fluid overload are commonly iatrogenic, resulting from overzealous intravenous (IV) fluid administration, particularly in critically ill patients with reduced adaptive capacity (58, 142). Volume overload is counteracted by a group of molecules called natriuretic peptides (NP), secreted primarily by cardiac muscle (143, 144). Mechanical stretch of the heart, due to excessive intravascular volume, triggers NP release. Natriuretic peptides mitigate VO through four mechanisms – natriuresis, inhibition of the renin-angiotensin-aldosterone system, vasorelaxation and increased vascular permeability (144). It is believed that NP increase vascular permeability by damaging the endothelial glycocalyx (EG) and allowing fluid to shift from the intravascular into the interstitial space (143). While these mechanisms are protective and even benign in healthy individuals, they can become maladaptive, especially in critically ill patients, potentially exacerbating pre-existing EG damage (58, 113).

Numerous experimental and clinical studies have investigated the effects of VO on the EG with conflicting results, primarily by measuring shed EG damage biomarkers. While some report NP release and EG damage with VO states and aggressive IV fluid administration (93, 148, 244, 247, 286, 334, 335), others (typically more recent) fail to demonstrate such effects (96, 238, 336-338). Whether these findings are seen mostly in stable patients or critically ill patients with pre-existing EG damage remains controversial (113, 142). Additionally, most studies have focused on the immediate effects of VO, and information on medium- and long-term consequences is lacking.

Cats may be particularly predisposed to VO due to their relatively smaller blood volume compared to dogs and people (252, 254, 255), a high incidence of asymptomatic heart disease (306, 339) and lower fluid elimination rates (130, 131). For these reasons, cats offer a compelling model to explore effects of IV fluid-induced VO on the EG.

While shed EG biomarkers are widely used, their interpretation remains challenging - particularly in the context of IV fluid administration, as elevations are often inconsistent, of low magnitude, and influenced by study design (113, 142, 249). Considering these limitations, real-time sidestream dark field videomicroscopy (SDFV) of mucosal capillaries (113) combined with the proprietary GlycoCheckTM software, offers a clinically applicable measure for estimating EG thickness. The software analyses SDFV-acquired images and calculates the perfused boundary region (PBR) an inverse estimate of EG thickness in capillaries ranging from 5 to 25 μm in diameter. Higher PBR values indicate thinner (damaged) EG while lower value, indicate a thicker (healthy) layer. Tolerance intervals for GlycoCheckTM parameters have been established in cats (100). Moreover, our group has previously evaluated the immediate effects of a fluid challenge on the EG in heathy anaesthetized cats using the GlycoCheck^{TM}, though findings have been inconclusive (340).

The aim of this study was to investigate the effects of a transient IV fluid-induced VO on the EG thickness in healthy anaesthetized cats using SDFV and the GlycoCheckTM software (90). We hypothesized that VO induced by rapid administration of 30 ml/kg of buffered balanced isotonic crystalloid solution given over 10 min will lead to transient increase in perfused boundary region (PBR), indicating decreased EG thickness, compared to a control group. Additionally, decreases in PCV (due to haemodilution and/or anaesthetic effects) may affect RBC lateralization in assessed vessels which would impact above-mentioned PBR.

5. Materials and methods

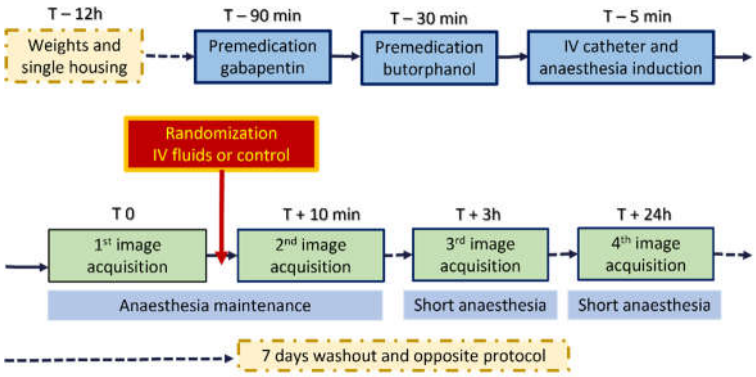
5.1. Study population

This was a prospective, randomized, blinded, cross-over experimental study, approved by Massey University's Animal Ethics Committee (MUAEC Protocol 22/81), and adhering to the Animal Research Reporting of In Vivo Experiments guidelines (275). Twenty healthy research-purposed cats were enrolled. Cats met inclusion criteria if they were healthy based on history, no weight loss, physical examination findings, complete blood count, serum biochemistry and T4 concentrations (performed during the first week of the study prior to intervention) and the two-minute focused echocardiography exam to screen for occult heart disease (341), performed up to two weeks prior start of study. No animals met predefined exclusion criteria for enrolment. Predefined humane endpoints and stopping criteria included clinically relevant anesthetic complications (e.g. cardiovascular instability, respiratory compromise), procedural limitations (e.g. IV catheter dislodgement, resistance to low-stress handling) or any adverse event deemed to compromise animal welfare. In such cases, animals were recovered as appropriate, and no further data were collected at subsequent timepoints.

5.2. Intervention protocol

The cats were placed in individual cages and food withheld 12h prior to beginning of each intervention with *ad libitum* access to water. All cats were sedated with gabapentin (Neurontin™, Viatris Specialty LLC) 100 mg PO 90 min prior and butorphanol (Torbugesic, Zoetis Inc.) 0.3 mg/kg SC 30 min prior to intravenous catheter placement in the left or right cephalic vein. Propofol (Provive 1%, Baxter Healthcare Ltd.) was then administered IV to effect (relaxation of jaw tone). Anaesthesia was maintained using a continuous rate infusion of propofol (0.05-0.2 mg/kg/min) for the duration of image acquisitions. Anaesthesia was overseen by an experienced veterinary technician and anaesthetic variables - heart rate (HR), pulse quality, mucous membrane colour, capillary refill time, temperature, respiratory rate (RR), pulse oximetry (SpO_2), and oscillometric blood pressure (oBP) were frequently monitored (every 5 min for clinical parameters, 10 min for blood pressure and continuous for pulse oximetry). The timeline of the intervention is presented in Figure 5.1.

Figure 5.1. Intervention protocol timeline for a crossover study involving 20 healthy anaesthetized cats, randomised to receive either 30 mL/kg of Hartmann's solution over 10 minutes (volume overload group) or no fluids (control group), with a 7-day washout period between interventions.



Each cat was randomized using an online randomization tool (https://www.randomizer.org/) to either receive 30 ml/kg over 10 min of a buffered balanced isotonic crystalloid solution (Hartman's solution, Baxter Healthcare Ltd.) via a fluid infusion pump (Niki V4 Volumetric Infusion Pump, Caesarea Medical Electronics Ltd., Israel) at room temperature – volume overload (VO) group; or no fluids - control group. All cats remained under propofol anaesthesia for the initial image acquisition (T0), IV fluid administration (or control) and second image acquisition (T1) after which they were allowed to recover and placed in their individual cages to be re-anaesthetized briefly with propofol IV for image acquisitions at T2 (3h) and T3 (24h) timepoints (see below). After the T2 image acquisition, cats were placed in their individual cages with the IV catheters maintained in place, fed *ad libitum* and food removed 12h prior to the T3 image acquisition the following day with *at libitum* access to water. At the end of the 24h period, the IV catheters were removed and the cats returned to their usual group housing. Blood for packed cell volume (PCV) and total solids (TS) measurements was collected under

anaesthesia via jugular venepuncture at each timepoint. Each cat then underwent a washout period of 7 days after which it received the opposite intervention.

5.3. Image acquisition

All image acquisitions were performed by the same operator (IY), blinded to subject allocation. Cats were placed in lateral recumbency, and the base of the tongue exposed such as the sublingual mucosa was accessible for the videomicroscope as previously described (100). A hand-held SDFV camera connected to a laptop with GlycoCheck™ software (MicroVascular Health Solutions, USA) was placed in contact with the sublingual mucosa by the operator. Three video recordings were taken from different sublingual mucosal sites at each of four different time points – T0 (baseline), T1 (end of volume overload or 10 min after baseline for the control group), T2 (3h after end of intervention) and T3 (24h after end of intervention).

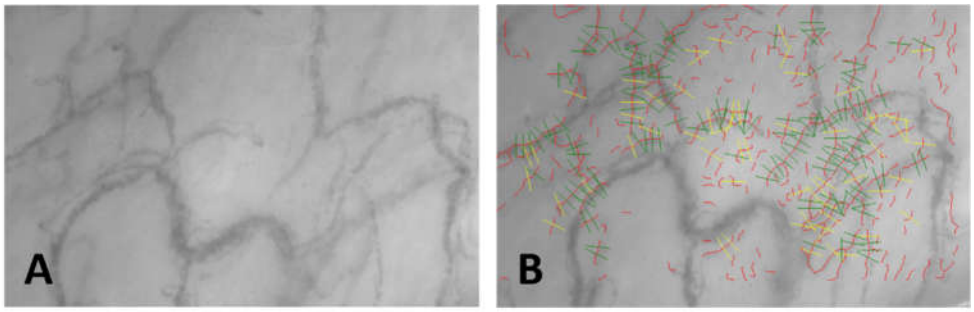
5.4. GlycoCheck™ analysis

The method for measuring and calculating GlycoCheck™ parameters has been previously described (100). Briefly, the SDFV camera emits green light at 540 nm wavelength which is absorbed by haemoglobin in circulating red blood cells (RBC). Therefore, vessels appear dark on a bright background.

Video recordings are displayed in real-time to allow the operator to assess image quality, including focus, pressure and motion artifacts (177). The software additionally provides linear quality indicator bars for motion, intensity and focus with green segments denoting acceptable ranges and records images only when predefined quality criteria are met. Automatic adjustments for motion, focus and intensity are applied to optimize image acquisition.

Each measurement is performed from approximately 10 video recordings containing 40 frames each (90). The software automatically identifies vessels that are less than 30 μm in diameter by analysing the contrast between the RBC and the background. The software then subdivides vessels into major (10 μm) and subsequently minor (0.5 μm) vascular segments in length and further determines the percentage of minor segments within a major segment with sufficient contrast for analysis (Figure 5.2).

Figure 5.2. Sidestream dark field videomicroscopy and GlycoCheck™ images of feline sublingual capillaries without (A) and with (B) marker lines indicating vascular segments. Red wavy lines represent vascular segments, green straight lines indicate valid segments, and yellow straight lines denote invalid segments.



A total of approximately 3000 major vascular segments including vessels ranging from ~ 3 – 30 µm diameter is recorded for analysis during each measurement. The counts for major vascular segments of each analysed diameter are additionally recorded. Major segments with > 60% of minor segments with sufficient contrast are considered valid vascular segments (VVS). Valid vessel density (VVD) per mm^2 is then expressed by multiplying 10 µm by the number of VVS identified.

Secondly, RBC column widths are assessed for minimal column width, column position, and signal-to-noise ratio. From the measured column widths, the software then calculates the percentage of RBC filling (%RBC filling) based on the proportion of time a particular VVS contains RBC throughout all recordings per site. The median RBC column width (Median P50) is calculated using the intensity profiles of the dynamic lateral positions of RBCs in all measured column widths.

Finally, linear regression analysis on the Median P50 is performed to derive the perfused diameter of vascular segments. From that, the PBR (perfused boundary region), an inverse estimate of EG thickness, is calculated as the distance between the Median P50 and the perfused diameter ([Perfused diameter – median RBC column width]/2). Reported GlycoCheck™ parameters, therefore, include VVD, RBC filling %, Median P50 and PBR for vessels with diameter from 5 to 25 µm and for subgroups of vessels with diameters from 5 – 9 µm, 10 – 19 µm and 20 – 25 µm. Higher PBR is, therefore, an indication for a thinner EG and a lower PBR indicates a thicker EG.

5.5. Packed cell volume and total solids

Packed cell volume and total solids (TS) were measured at each timepoint for each cat using centrifuged capillary microhematocrit tubes and a hand-held refractometer, respectively, by the same operator.

5.6. Statistical analyses

Sample size calculation was based on a study in anesthetized rabbits receiving volume expansion with hypertonic saline (99). The reported mean difference for PBR 5 – 25 µm was 0.19 µm and reported baseline and post-intervention standard deviation (SD) of 0.30 and 0.18, respectively. As paired-difference data were not available from that study, the SD of the within-subject differences for the present crossover design was estimated using these reported SDs and an assumed within-subject correlation. Using a two-sided α of 0.05 and 80% power, this yielded an estimated sample size of approximately 20 cats.

Triplicates from measured GlycoCheck™ parameters were averaged for further analysis as recommended in previous reports in healthy and critically ill people (181, 186). Data normality was tested using Shapiro-Wilk test and visually inspected using histograms and Q-Q plots (342, 343). Normally distributed data is presented as mean ± standard deviation (SD), not normally distributed data is presented as median (Interquartile Range, IQR) (344). Interaction between various GlycoCheck™ parameters (dependent variables) and group, timepoint (model 1) and PCV (model 2) as independent variables were analysed using linear mixed effects regression modelling with cat as a random effect (345). Interaction between PCV and TS (dependent variables) and group and timepoint were analysed similarly (model 3). Model assumptions were assessed by evaluating normality and heteroscedasticity using the Shapiro–Wilk test and visual inspection of residual histograms. Fixed-effect estimates from the linear mixed-effects models are presented with approximate 95% confidence intervals derived using the Wald method, based on the estimated coefficient ± 1.96 × standard error (345). No formal adjustment for multiple comparisons was applied; model-derived estimates are reported and interpreted in an exploratory context. Outliers were investigated using the interquartile range method, with lower boundary set as Quartile 1 minus 1.5 times IQR and upper boundary – Quartile 3 plus 1.5 times IQR. Modelling was performed with both outliers included and excluded to compare model accuracy and fit.

Vascular segment count distribution within subgroups of vessels with diameters from 5 – 9 µm, 10 – 19 µm and 20 – 25 µm was compared using Friedman's test and Wilcoxon-signed ranking test. Correlation between PCV and GlycoCheck™ parameters was calculated using Pearson's test for normally distributed data and Kendall's tau for not normally distributed data. All statistical analyses were conducted in R (Team, 2023) (297).

6. Results

Twenty cats were included in the analysis: nine male neutered, seven female entire, and four female spayed. The median age was 3.21 years (IQR: 1.68), and the mean body weight was 3.77 ± 0.76 kg. Images from a total of 156 timepoints were analysed. Four image acquisitions in three cats were not completed during the second week due to short-term complications. One cat developed a transient oxygen desaturation during anaesthesia at the end of T1 image acquisition. The anaesthesia was discontinued and the cat recovered uneventfully, showing no further clinical signs. Two cats

experienced IV catheter dislodgment prior to final datapoint collection, and IV catheters could not be replaced. This resulted in an overall success rate of 97%. Anaesthetic monitoring parameters remained within normal limits throughout the procedures, except for the above-mentioned cat. Both sets of models (with and without outliers) yielded similar findings and exhibited consistent overall trends. Models with outliers included. were used for reporting results.

Summary statistics for other GlycoCheckTM parameters are presented in Table 5.1. None of the analysed parameters were significantly different at baseline.

Table 5.1. GlycoCheck™ parameters in 20 healthy anaesthetized cats subjected to transient volume overload (30 mL/kg Hartmann's solution over 10 minutes) or control (no intravenous fluids), measured at four timepoints over 24 hours*.

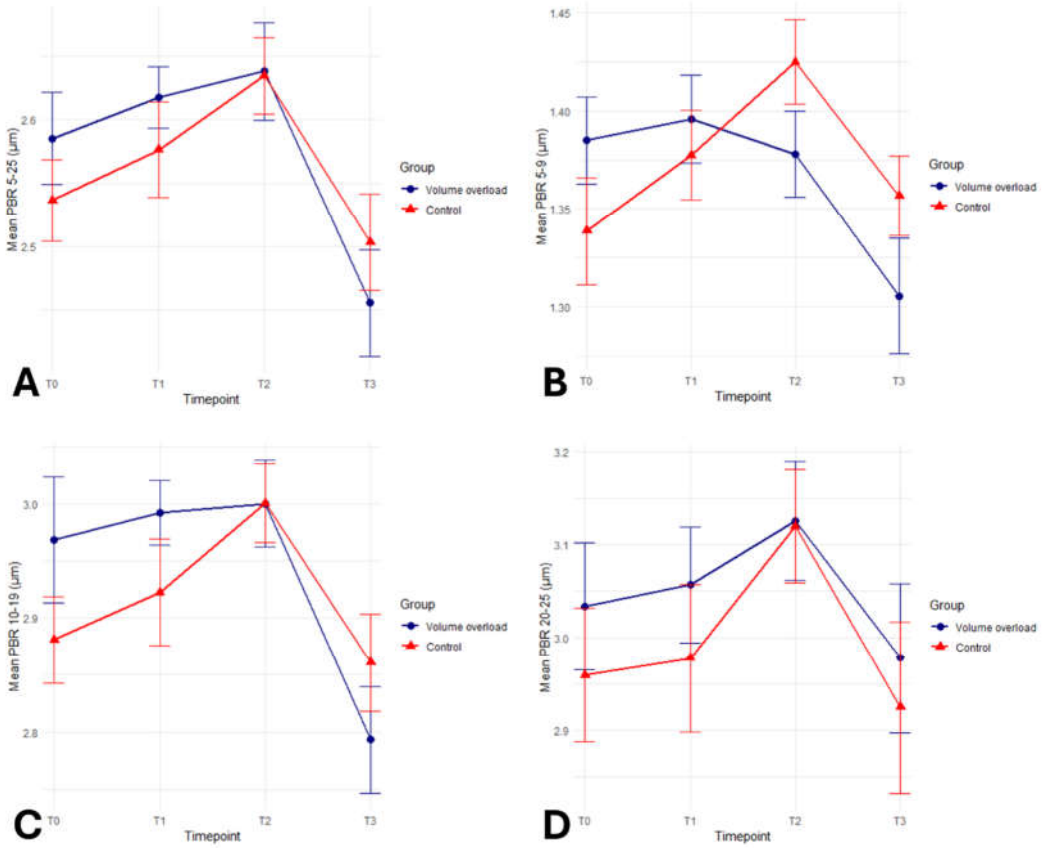
	Volume overload group							
	Baseline		10 min		3h		24h	
	Mean	SD	Mean	SD	Mean	SD	Mean	SD
VVD (mm^2/mm^2)	452.96	98.08	405.98	106.42	429.56	100.86	444.63	109.12
%RBC filling (%)	0.60	0.07	0.59	0.05	0.59	0.06	0.62	0.06
Median P50 (µm)	9.11	1.52	8.95	1.28	8.49	1.07	8.41	1.06
PBR 5-25 (µm)	2.59	0.25	2.62	0.11	2.64	0.17	2.44	0.18
PBR 5-9 (µm)	1.40	0.13	1.38	0.12	1.38	0.09	1.29	0.14
PBR 10-19 (µm)	2.95	0.28	2.99	0.13	3.00	0.17	2.79	0.20
	Median	IQR	Median	IQR	Median	IQR	Median	IQR
PBR 20-25 (µm)	3.08	0.26	3.03	0.28	3.22	0.41	2.92	0.32
	Control group							
	Baseline		10 min		3h		24h	
	Mean	SD	Mean	SD	Mean	SD	Mean	SD
VVD (mm^2/mm^2)	466.93	134.28	448.82	87.40	442.03	81.30	463.09	88.81
%RBC filling (%)	0.62	0.06	0.59	0.04	0.57	0.06	0.62	0.04
Median P50 (µm)	8.69	1.53	8.91	1.38	8.73	1.39	8.24	1.33
PBR 5-25 (µm)	2.49	0.21	2.56	0.19	2.63	0.14	2.46	0.18
PBR 5-9 (µm)	1.34	0.15	1.38	0.10	1.42	0.10	1.36	0.09
PBR 10-19 (µm)	2.83	0.24	2.93	0.21	3.00	0.16	2.80	0.22
	Median	IQR	Median	IQR	Median	IQR	Median	IQR
PBR 20-25 (µm)	2.96	0.40	2.93	0.41	3.17	0.26	2.74	0.60

IQR – interquartile range; PBR – perfused boundary region; RBC – red blood cells; SD – standard deviation; VVD – valid vessel density
*Outliers were removed

Perfused boundary region trended upward over time with apparent peak values at T2 (3 hours post-intervention). Mixed-effects modeling identified a significant effect of time on PBR 5 – 25 µm, PBR 5 – 9 µm and PBR 10 – 19 µm. For PBR 5 – 25 µm and PBR 10 – 19 µm model estimate values at T2 were higher relative to baseline (estimate 0.150, 95% CI 0.037 to 0.264, p = 0.001 and estimate 0.175, 95% CI 0.047 to 0.303, p = 0.008, respectively).

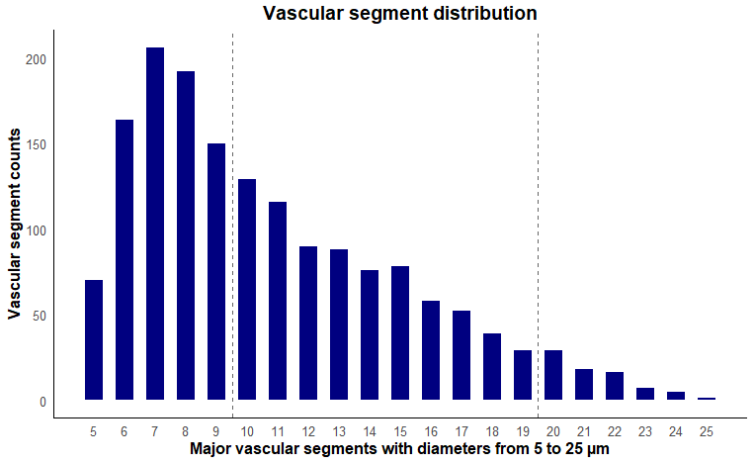
For PBR 5–9 µm, a significant effect of time was also observed, with increased values at T2 relative to baseline (estimate 0.887, 95% CI 0.016 to 0.161, p = 0.017). However, significant group x timepoint interactions were identified at T2 (estimate -0.116, 95% CI -0.219 to -0.013, p = 0.028) and T3 (estimate -0.138, 95% CI -.0242 to -0.033, p = 0.010), indicating that this time-dependent increase was attenuated in the VO group, resulting in lower PBR 5 – 9 µm compared to the control group at these timepoints. Group and timepoint interactions for PBR are illustrated in Figure 5.3.

Figure 5.3. Changes in perfused boundary regions over time in vessels with diameters of 5–25 µm (A), 5–9 µm (B), 10–19 µm (C), and 20–25 µm (D) in 20 healthy anaesthetized cats with transient volume overload (navy circles) or control (red triangles), measured at four timepoints over 24 hours: T0 (baseline), T1 (10 min), T2 (3 h), and T3 (24 h).



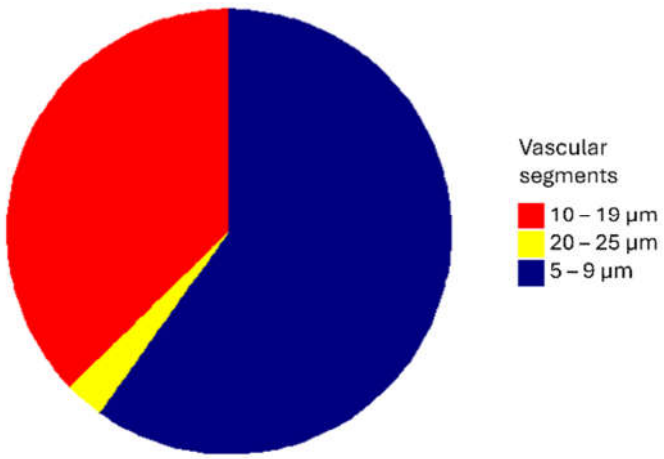
The median (IQR) count for major (10 µm) vascular segments with diameters 5 – 25 µm was 1520.05 (356.50). Within this range, median counts for the 5–9 µm, 10–19 µm, and 20–25 µm subgroups were 910.32 (348.75), 566.91 (172.83), and 42.82 (33.83), respectively (Figure 5.4).

Figure 5.4. Distribution of major vascular segment counts by vessel diameter (5–25 µm) in healthy anaesthetized cats. Bars represent the number of valid vascular segments identified per diameter subgroup using GlycoCheck™ analysis. Vertical dashed lines separate the predefined vessel size categories: 5–9 µm, 10–19 µm, and 20–25 µm.



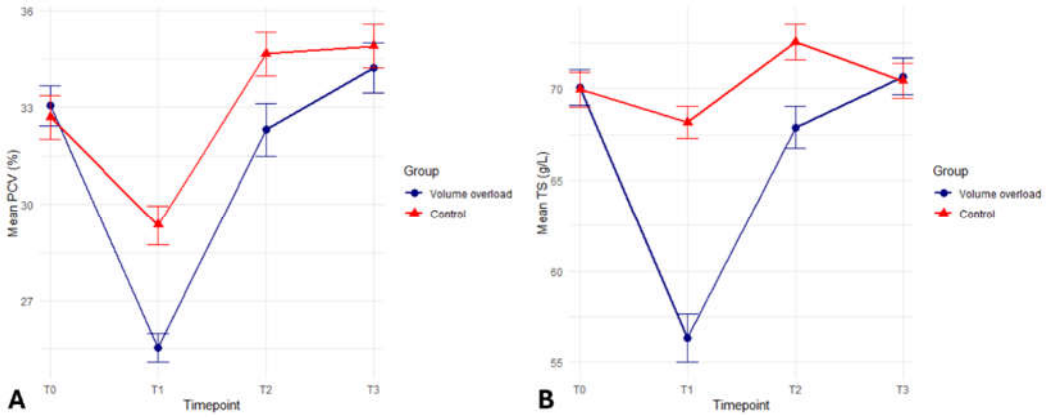
There was a statistically significant difference in vascular segment counts across all diameter subgroups ($p < 0.001$). The distribution of vascular segment counts by size category is illustrated in Figure 5.5.

Figure 5.5. Pie chart showing the distribution of vascular segment counts across vessel diameter subgroups: 5–9 µm (navy), 10–19 µm (red), and 20–25 µm (yellow).



Group and timepoint interactions for PCV and TS are presented in Figure 5.6.

Figure 5.6. Changes in packed cell volume (A) and total solids (B) over time in 20 healthy anaesthetized cats with transient volume overload (navy circles) or control (red triangles), measured at four timepoints over 24 hours: T0 (baseline), T1 (10 min), T2 (3 h), and T3 (24 h).



Packed cell volume fluctuated significantly over time, with mixed effects modeling identifying a significant effect of timepoint (Figure 5.3). Relative to baseline, model-estimated PCV was lower at T1 (estimate -3.350, 95% CI -4.863 to -1.837, $p < 0.001$), and higher at T2 (estimate 1.950, 95% CI 0.437 to 3.463, $p = 0.012$) and T3 (estimate 2.234, 95% CI 0.699 to 3.767, $p = 0.005$). Significant group x timepoint interactions were identified at T1 (estimate -4.200, 95% CI -6.339 to -2.061, $p < 0.001$) and T2 (estimate -2.554, 95% CI -4.709 to -0.399, $p = 0.021$), indicating lower PCV in the VO group compared to the control group at these timepoints.

Similarly, TS varied over time, with mixed-effects modelling identifying a significant effect of timepoint. Relative to baseline, model-estimated TS was lower at T1 (estimate -2.200, 95% CI -4.292 to -0.108, $p = 0.04$) and higher at T2 (estimate 2.600, 95% CI 0.508 to 4.692, $p = 0.016$). Significant group x timepoint interactions were identified at (estimate -12.450 95% CI -15.409 to -9.491, $p < 0.001$) and T2 (estimate -5.812, 95% CI -8.793 to -2.831, $p < 0.001$), indicating lower TS values in the VO group compared to the control group at these timepoints.

Packed cell volume showed positive associations with VVD (estimate 5.747, 95% CI 1.956 to 9.537, $p = 0.003$) and %RBC filling (estimate 0.004, 95% CI 0.002 to 0.006, $p < 0.001$), and negative associations with PBR 5–25 µm (estimate -0.011, 95% CI -0.018 to -0.004, $p = 0.003$) and PBR 10–19 µm (estimate -0.013, 95% CI 0.021 to -0.005, $p = 0.013$). Correlation coefficients for PCV and GlycoCheckTM parameters are presented in Table 2 and, although statistically significant, were overall weak.

Correlation coefficients for PCV and GlycoCheckTM parameters are presented in Table 5.2 and, although statistically significant, were overall weak.

Table 5.2. Correlation between packed cell volume and GlycoCheck™ parameters using Pearson's test (except for perfused boundary region 20 – 25 µm*).

Parameter	**r**	**95% CI**	***p – value***
VVD	0.235	0.081 – 0.378	**0.003**
%RBC filling	0.277	0.126 – 0.416	**< 0.001**
Median P50	-0.071	-0225 – 0.088	0.382
PBR 5 – 25 µm	-0.238	-0.381 – -0.0841	**0.003**
PBR 5 – 9 µm	-0.102	-0.255 – 0.056	0.203
PBR 10 – 19 µm	-0.255	-0.396 – -0.102	**0.001**
PBR 20 -25 µm	τ = -0.111	-	**0.048**

CI – confidence interval; Median P50 – median red blood cell column diameter; PBR – perfused boundary region; RBC – red blood cells; VVD – valid vessel density
*Correlation calculated using Kendall's tau method for non-parametric data

7. Discussion

Results from this study suggest that rapid IV administration of 30 ml/kg of buffered balanced isotonic crystalloid solution does not damage the EG in healthy cats as IV fluid administration did not result in a decrease in EG thickness over 24h. However, the PBR 5-25 µm, 5 – 9 µm, and 10 – 19 µm, increased (suggesting a decreased EG thickness) 3h after intervention in the control group, suggesting transient decrease in EG thickness potentially secondary to anaesthetic effects. Interestingly, the PBR of small vessels (5 – 9 µm) was lower over time in the VO group at later timepoints, suggesting these negative effects might have been mitigated by the administration of IV fluids.

Transient volume overload did not result in increases in PBR in this group of healthy cats. This aligns with findings from a previous study in healthy cats from our group, which showed no increase in PBR following a fluid challenge (10 mL/kg over 20 min) using either Hartmann's solution or 6% hydroxyethyl starch 130/0.4 (340). Similar results have been reported in anaesthetized rabbits, where only a hypertonic saline bolus (5 mL/kg of 10% NaCl) increased PBR, while volume loading with Lactated Ringer's solution (30 mL/kg/h) had no effect (96, 99).

In canine haemorrhagic shock models, PBR generally remained unchanged during haemorrhage and autotransfusion in the absence of IV fluids (94). However, one study showed increased PBR following resuscitation with 30 mL/kg of LRS or 7.5 mL/kg of hydroxyethyl starch compared to natural or synthetic blood products (93). Likewise, in septic children, fluid boluses with unbalanced versus balanced crystalloids led to PBR increases 6 hours post-intervention (155). Taken together, these studies suggest that IV fluids alone may not alter PBR in healthy animals, while more

severe interventions (e.g., haemorrhage, sepsis) or underlying disease states may predispose to detectable EG alterations. Nevertheless, differences in study design, species, and methodology limit direct comparison or translational conclusions.

Most published studies assessing EG damage after IV fluid administration rely on measuring shed EG constituents rather than using GlycoCheck™ analysis. A recent review of 20 clinical studies in people suggested a dose-dependent increase in EG biomarkers in stable surgical patients (142), whereas another review emphasized this trend in critically ill populations (113), highlighting the inconsistent findings between types of patient cohorts in the current literature. Animal studies similarly show mixed results. In dogs, hyaluronan increased after an extreme crystalloid bolus (80 mL/kg over 10 min) after haemorrhage (247), and also following anaesthetic fluid rates of 5–10 mL/kg/h (244). However, in both studies, the source of hyaluronan (endothelial vs interstitial) was unclear; it may have been mobilized from the interstitium due to fluid shifts (64). Other canine haemorrhagic shock models reported variable or paradoxical changes in EG biomarkers following fluid or blood product administration (94, 346). Overall, findings from EG shedding studies reveal high variability and mostly modest, inconsistent increases after fluid administration. Differences in species, disease states, experimental protocols, and assay performance limit their interpretability. Moreover, results from GlycoCheck™ and EG shedding studies cannot be directly compared due to fundamental differences in methodology, a point supported by the few studies that have applied both techniques without identifying consistent trends. Given these considerations, it is plausible that the fluid doses used in this study were insufficient to induce EG damage, particularly in healthy cats. It is equally possible that the negative findings reflect the literature challenging earlier reports of EG vulnerability to VO.

The PBR 5 – 25 µm, 5 – 9 µm and 10 – 19 µm increased over time and returned to baseline by 24h in this study. These changes cannot be attributed to IV fluid-associated VO. Therefore, alternative explanations should be considered. Anaesthesia-related changes in blood volume are well documented in the literature and primarily attributed to fluid shifts from the interstitial into the IV space in response to anaesthesia-induced hypotension (222, 338, 347). In addition, most anaesthetics, including propofol, cause splenic relaxation in dogs and cats, leading to sequestration of RBC and transient reductions in PCV (254, 328, 348-352). In the present study both PCV and TS decreased transiently across both groups, supporting anaesthesia-related changes in blood volume, particularly during the initial longer anaesthetic period (T0 and T1 combined).

Whether such changes in blood volume would be associated with EG damage remains uncertain. While some studies report increased NP production following peri-anaesthetic plasma volume expansion (148, 286), others fail to reproduce these findings (238, 335, 338). A recent study examining plasma volume changes in hypotensive versus normotensive human surgery patients demonstrated a tenfold increase in plasma volume in the hypotensive group. However, this was not associated with increased NP production or EG shedding (338). As this physiological response is thought to compensate for anaesthesia-induced hypotension, it is unlikely to trigger the degree of

cardiac stretch required for NP release and subsequent EG damage. In this light, anaesthesia-related volume effects are unlikely to account for the observed increase PBR in the control group, especially given haemodynamic stability of the subjects and the absence of hypotension across groups and timepoints. In previous studies investigating GlycoCheck™ parameters in a large cohort of healthy cats (Chapter II) and the immediate effects of a fluid challenge on healthy cats (Chapter IV) using similar anaesthetic protocols, anaesthetic variables had no significant effects on GlycoCheck™ parameters. Nonetheless, neither study was designed to investigate anaesthesia-related volume effects, including hypotension. Non-invasive blood pressure monitoring was used as part of standard anaesthetic monitoring to prevent complications during data collection. Proper exploration of anaesthesia-induced volume effects on the EG would require a more targeted setup, including direct blood pressure measurement, cardiovascular point-of-care ultrasound, and collection of additional haemodynamic parameters.

Another anaesthesia-related factor worth considering is the choice of anaesthetic agent itself, particularly propofol, which may have direct effects on the endothelium and its glycocalyx. Propofol is an anaesthetic widely used in human and veterinary critical care, due to its favourable pharmacokinetics and relatively good safety profile (319). However, repeated or prolonged administration in cats has been associated with oxidative stress, Heinz body formation, anaemia, facial oedema, anorexia and diarrhoea (329-331). In people, prolonged infusions of propofol (doses exceeding 4-5 mg/kg/h administered for more than 48h) have been associated with a life-threatening complication known as propofol-related infusion syndrome (323, 324). This syndrome is thought to arise from the disruption of the mitochondrial electron transport chain, resulting in mitochondrial dysfunction, multiorgan damage and potentially death (323).

More recently, both *in vitro* and *in vivo* experimental studies have demonstrated endothelial cell and EG damage after propofol overdose (321, 322, 353).In contrast, clinical studies comparing the effects of propofol and volatile anaesthetics in people have not consistently demonstrated increased EG damage following propofol administration (320, 325-327). These effects appear to be dose-dependent and time-related, and confounding factors such as underlying EG-damaging illnesses limit the conclusions that can be drawn from clinical data.

Propofol has been successfully used in previous studies evaluating the EG in cats (100, 340), though these studies did not include repeated propofol administration within 3h. In a previous study from our group evaluating effects of an IV fluid challenge on GlycoCheck™ parameters in healthy cats, increases in PBR 10 – 19 µm were found at the end of infusion in the control group, compared to baseline (340). Considering the relative feline "sensitivity" to propofol-related oxidative stress (329-331), longer half-life and slower metabolism of phenolic compounds in cats (328), it is possible that the dose used in the current study was sufficient to sustain a transient reduction in EG thickness, especially considering the repeated administrations between T0 and T2. Further studies comparing effects of repeated administrations and use of different anaesthetics are necessary to investigate this possibility.

Surprisingly, the PBR 5 – 9 µm was lower at later timepoints (T2 and T3) in the VO group when compared to the control group. While administration of 30 ml/kg of Hartman's solution over 10 min did not lead to increase in PBR, it is possible that this intervention mitigated some of the overall negative effects observed across both groups, specifically in the smallest analysed vessels. This may have resulted from dilution of anaesthetic agents and counteraction of propofol effects on blood viscosity (354, 355) and potentially from "rehydrating" the EG. A previous study from our group, investigating the immediate effects of an IV fluid challenge using Hartman's solution or hydroxyethyl starch in healthy cats similarly reported decreases in PBR in the hydroxyethyl starch group, compared to no IV fluid controls, though in larger vessels (10 – 19 µm) (340). These findings suggest that IV fluid rates used in this study, while not sufficient to damage a healthy EG, might have exerted mild protective effects. Further studies specifically designed to investigate anaesthetic influences on the EG are warranted to support this hypothesis.

It is not surprising that both PBR 5 – 25 µm, PBR 5 – 9 µm and PBR 10 – 19 µm were mostly affected in this study, as these results are likely interdependent. The proportions of vascular segments of different diameters making up the totality of analysed vascular segments is not equal and vascular segments of 5 – 9 µm diameters are overrepresented (~ 60%), followed by 10 – 19 µm (~ 37%). Similar findings have been reported in people (215), suggesting that PBR 5 – 9 µm may carry more weight in the overall PRB 5 – 25 µm analysis. Additionally, PBR values for 5 – 9 µm vessels are approximately twofold lower than those in the 10 – 19 µm and 20 -25 µm ranges, indicating a relatively thicker EG in smaller vessels (100, 340). Based on findings from this study, it is possible that the PBR 5 – 9 µm respond differently to various physiological stimuli. Unfortunately, few studies report data stratified by vessel size, and most present only the overall BPR 5 – 25 µm, limiting comparisons. Given their higher prevalence and distinct characteristics, the authors recommend that PBR measurements for 5–9 µm vessels be analysed and reported separately in future studies.

This study demonstrated weak associations between PCV and GlycoCheck™ parameters, suggesting that the drop in PCV, whether due to haemodilution (from either IV fluids or anaesthesia-related fluid shifts) or clinical anaemia in sick patients may influence PBR measurements. Associations between PCV and PBR have been previously found in adult and neonate human patients (183, 187). These findings are broadly consistent with a previous study from our group, which evaluated the effects of a fluid challenge on GlycoCheck™ parameters in cats and found that VVD and %RBC filling decreased and PRB increased with decreasing PCV (340).

However, some differences between the two studies were observed. Notably, in the present study PCV was not associated with PBR 5 – 9 µm whereas a significant association was found in the earlier fluid challenge study. Conversely, PBR 10 –19 µm was significantly affected by PCV in the present study, but not the previous one. These discrepancies may be explained differences in study design (parallel groups vs crossover groups), the larger fluid volume in the present study potentially introducing more variability or masking certain effects or differing effect sizes between the two

experiments. These observations highlight the importance of considering haematological variables, particularly PCV, when interpreting GlycoCheck™ results, as their influence may vary across vessel sizes and study conditions.

Ultimately, all GlycoCheck™ parameters rely on identification of RBCs against a contrasting background, with PBR calculations dependent on the presence of vessels meeting criteria for "valid" density and adequate % RBC filling (90). The influence of PCV on these measurements warrants further investigation in specifically designed studies to determine whether such effects are clinically meaningful. In the present study, correlations between PCV and the GlycoCheck™ parameters were generally weak to moderate. However, if consistent associations are established, this could justify applying statistical adjustments when interpreting PBR values in relation to PCV, particularly in clinical research. Given that anaemia is relatively common in critically ill cats, increases in PBR attributed to EG damage should not be confounded by concurrent reductions in PCV.

Interestingly, most GlycoCheck™ parameters returned to baseline by 24 hours, suggesting that any EG disturbance was either transient or rapidly resolved. However, this contrasts with current understanding of EG shedding, turnover, and repair (47). While EG shedding can occur rapidly (within minutes to hours) following a significant stimulus, the biosynthesis of new components typically requires several hours to days, depending on the molecule and mechanism involved (47, 106). Therefore, the return to baseline at 24 hours may represent dimensional recuperation or functional rehydration, rather than full structural restoration. It is conceivable that, rather than true loss of glycocalyx components, IV fluids and anaesthetic stimuli caused a form of EG "desiccation" or "contraction," leading to temporarily reduced thickness without substantial structural damage. In this context, the adequacy of the 7-day washout period warrants consideration, as incomplete structural recovery between study periods could theoretically influence subsequent responses. However, the return of measurements to baseline within 24 hours supports the interpretation that any such carryover effects were unlikely to be clinically meaningful. Unfortunately, EG shedding biomarkers were not assessed in this study. Given their limitations in detecting fluid-induced changes to the EG, the reliability of such additional analyses remains uncertain. Importantly, the relationship between dimensional or structural changes of the EG and its functional integrity has not been well studied and warrants further investigation.

In considering the potential stimulus for EG change, the selected IV fluid dose warrants further reflection. Beyond representing empirically "high" IV fluid rate, the dose chosen for this VO model was based on a previous study evaluating cardiac ultrasound and caudal vena cava parameters in healthy cats with induced VO (356). In the referenced study, rapid infusion of 30 ml/kg of Hartman's solution resulted in a mild but statistically significant increase in cardiac chamber and caudal vena cava size (356), suggesting cardiac stretch on imaging. However, whether this stretch was sufficient to trigger NP production remains unclear. By comparison, a canine study using much higher overall dose over a longer time (90 ml/kg of isotonic crystalloids over 1h) demonstrated marked increases in NP (357),

confirming that IV fluids can stimulate NP release under certain conditions. Considering the feline predisposition to volume overload, the present study employed a more conservative dosing strategy, delivering the highest fluid rate considered ethically and physiologically acceptable to potentially affect the EG without causing harm. However, NP concentrations were not measured in this study, so any involvement of NP in the EG modulation could not be confirmed. Further investigations should incorporate species-specific volume kinetic data to guide fluid dosing strategies in cats, where related to microcirculatory or other IV fluid research (130, 358).

Additional limitations in this study include the relatively small sample size and somewhat arbitrary timepoints. Notably, T0 and T1 measurements were obtained under the same longer anaesthesia, whereas shorter anaesthesias were used for T2 and T3, which may have introduced variability affecting the results. Although not statistically significant, there was notable baseline variability, despite the cross over design, suggesting that evaluating individual longitudinal changes in PBR might be limited in feline patients with this version of the software. Nonetheless, the GlycoCheckTM may be useful for investigating changes in estimated EG thickness on a populational level. Finally, the GlycoCheck™ software was developed for human use and has not been specifically adapted for feline physiology. As such, it does not account for potential interspecies anatomical and functional differences, which may influence certain derived parameters, although the overall methodology remains consistent with established SDFV principles.

8. Conclusion

This study did not demonstrate decreases in EG thickness after transient, mild VO. However, changes in PBR increased over time may suggest potential anaesthesia-related effects. As short anaesthesia is inevitably required for SDFV imaging in small animals, further studies specifically designed to optimize anaesthetic protocols are essential. Changes in PCV were associated with alterations in GlycoCheck™ parameters, and the clinical significance of these associations warrants further investigation. Given the known predisposition of cats to VO, the effects of IV fluids on the feline microcirculation should continue to be explored, ideally through study designs informed by a more detailed understanding of volume kinetics in this species.

9. Conflict of Interest

This project was funded by the Massey University Wenzel fund and REaDI fund, which played no role in the study design; nor in the collection, analysis, and interpretation of data; nor in the decision to submit the manuscript for publication. None of the authors has any other financial or personal relationships that could inappropriately influence or bias the content of the paper.

10. Funding

This project was funded by the Massey University Wenzel fund (RM25666) and REaDI Fund (RM252481222SVS04).

11. Chapter V extended implications

This chapter builds upon the findings of Chapter IV and reinforces several trends and associations that are important for future GlycoCheck™ research. As in the previous IV fluid challenge study, no evidence of EG damage was found in healthy cats, even after inducing transient volume overload. This aligns with other studies suggesting that in healthy individuals, IV fluids alone - unless administered at extremely high doses, may not be sufficient to cause structural EG damage. Possible reasons for this outcome are discussed in detail in the chapter.

More importantly, this study confirmed earlier trends suggesting that anaesthesia itself may negatively impact EG thickness, and that IV fluid administration might mitigate these effects. These observations support the need for focused research into optimal anaesthetic protocols specifically for microcirculatory studies. In addition, they highlight potential interactions between anaesthetic agents and IV fluids, which are often co-administered in clinical practice and may influence the interpretation of research findings. Although propofol is widely regarded as pharmacokinetically favourable and generally safe, it may not be the most suitable anaesthetic for studies assessing EG integrity in cats. These questions are particularly relevant in small animal research, where anaesthesia is always required for data acquisition and thus represents an unavoidable confounding factor. Given that most anaesthesia-related fluid shifts occur within the first 10–30 minutes of induction, it may also be beneficial to include a stabilisation period prior to data collection (222, 328, 338).

The associations between GlycoCheck™ parameters and PCV observed in Chapter IV were again identified here. This consistency raises important considerations for the interpretation of EG data, particularly in settings involving anaemia (decreased PCV), a common condition in critically ill patients. While haemodilution was significant in relative terms in both chapter IV and V, absolute PCV levels remained within ranges commonly tolerated in clinical settings. Nonetheless, the possibility that PCV influences EG measurements to a clinically relevant degree supports the need for further studies, ideally focused on adjusting GlycoCheck™ outputs to account for concurrent PCV changes.

Another contribution of this chapter is the inclusion of longer-term follow-up. While Chapter IV only assessed immediate effects, Chapter V demonstrated that GlycoCheck™ parameters largely returned to baseline by 24 hours, regardless of the changes observed earlier. This finding raises the question of whether true structural damage occurred or whether observed changes reflected transient dimensional shifts, such as EG “desiccation” or “contraction”, rather than loss of constituents. While EG shedding can occur within minutes to hours, full structural regeneration typically requires several days (47). Therefore, the rapid return to baseline values in this study is more likely attributable to temporary volume-related effects than to true injury and repair. Distinguishing between functional, dimensional, and structural EG changes remains a critical research need, particularly in clinical studies of critically ill animals. For this GlycoCheck™ analysis may need to be integrated with validated EG biomarkers and evaluated over time.

This study also benefited from access to additional data not available in the previous chapter. Analysis of vascular segment counts revealed that vessels with diameters of 5–9 µm were overrepresented (~60%) in the image dataset, while those in the 20–25 µm range were underrepresented (~3%). These imbalances raise concerns about the interpretation of the overall PBR 5–25 µm metric, particularly when vessel subgroups respond differently to stimuli. Notably, PBR changes varied by vascular diameter in both Chapters IV and V, and the underrepresentation of larger vessels may reduce analytical power or introduce error. Since vessel distribution reflects anatomical reality and cannot be adjusted during analysis, future studies should report subgroup breakdowns and interpret results from underrepresented segments with caution.

Using a crossover design in this chapter also enabled exploration of within-subject variability. Baseline variability was low for most GlycoCheck™ parameters, moderate for Median P50 and PBR 20–25 µm, and high for VVD (Table 5.3).

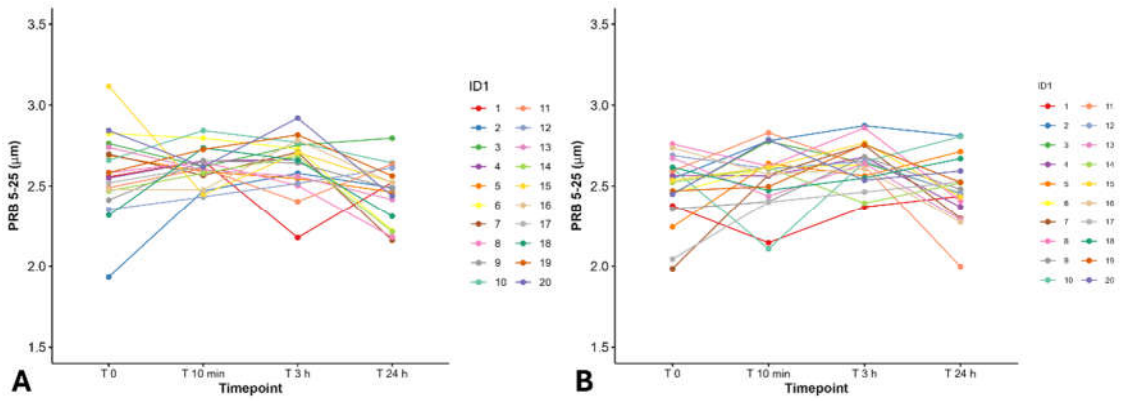
Table 5.3. Within-subject baseline variability from random intercepts standard deviation.

Parameter	Intercept SD	Variability
PBR 5–25 µm	0.0443	Low
PBR 5–9 µm	0.0197	Low
PBR 10–19 µm	0.0319	Low
PBR 20–25 µm	0.0624	Moderate
VVD	23.58	High
%RBC filling	0.0074	Low
Median P50	0.55	Moderate

These differences were not associated with statistically significant baseline imbalances between groups, unlike the finding for PBR 10–19 µm in Chapter IV. For this reason, they were not reported in the manuscript. Still, such variability may obscure subtle intervention effects, particularly in studies with limited sample sizes or in clinical settings where additional noise is expected. As illustrated in Figure 7, individual PBR 5–25 µm trajectories varied considerably over time, despite no group-level significance, emphasising the need for cautious interpretation of individual measurements.

Such findings raise the question of overall within-subject variability for GlycoCheck™ parameters, especially when temporal changes are explored in the experimental and especially clinical settings as it may obscure intervention effects across subjects. Figure 5.7 represents all individual PBR 5 – 25 µm values across timepoints to illustrate how this variability while not statistically significant could potentially affect results.

Figure 5.7. Changes in PBR 5 – 25 µm over time per group for individual cats.



Prior studies in people have shown that reproducibility improves with averaging multiple GlycoCheck™ measurements, but residual variability persists even under controlled conditions (91, 181, 185, 186). As such, the tool may be best suited for population-level research or for monitoring trends within individuals, rather than for one-off diagnostic assessments in individual patients.

Lastly, as in chapter IV, SDC-1 ELISA measurements were performed for all cats at all timepoints, as the assay validation process was conducted in parallel with data collection for this chapter. Consistent with the previous findings from chapter IV, SDC-1 concentrations remained below the detectable limit across the entire cohort. Potential explanations for this outcome are provided in chapter IV and will not be reiterated here, as they remain unchanged.

In summary, this chapter confirmed key trends observed in the previous experimental study, while expanding the understanding of GlycoCheck™ parameter variability and recovery over time. The findings underscore the importance of accounting for anaesthetic effects, fluid interactions, and changes in PCV when interpreting EG measurements in small animals. With these considerations in mind, the next chapter presents an exploratory clinical study in a small cohort of critically ill cats, offering a first look at how these experimental insights translate into a real-world setting.

Chapter VI: Endothelial glycocalyx thickness in cats with naturally occurring trauma or non-traumatic illness – an exploratory study

Chapter plan

1. Chapter VI preface
2. Title page
3. Abstract
4. Introduction
5. Materials and methods
    - 5.1. Study population
    - 5.2. Data collection
    - 5.3. Image acquisition
    - 5.4. GlycoCheck^{TM} analyses
    - 5.5. Statistical analyses
6. Results
7. Clinical data
8. GlycoCheckTM data
9. Discussion
10. Conclusion
11. Authors contribution
12. Footnotes
13. Chapter VI extended implications

1. Chapter VI preface

The overarching aim of this PhD project was to explore and validate clinical methodologies for assessing EG integrity. As such, a final chapter applying the previously evaluated methodologies to a clinical setting offered a logical and meaningful conclusion. This study, while small and exploratory in design, provides an initial perspective on the feasibility of implementing SDFV and GlycoCheck™ analysis in a clinical context where numerous variables are less controlled. We also aimed to determine whether the methodology would be sufficiently sensitive to detect changes in a general cohort of critically ill cats, presenting with potentially varying degrees of illness severity.

In clinical environments, logistical and patient-related factors introduce substantial variability. Scheduling changes, patient instability, inconsistent imaging environments (e.g., different rooms or tables), and operator variability all challenge the consistency of data acquisition. Additionally, critically ill feline patients present with a multitude of confounding factors that cannot be fully accounted for, such as variable disease progression, diverse therapeutic interventions, and differing anaesthetic protocols. Given these limitations, an exploratory approach was warranted to evaluate practical feasibility, identify major barriers to implementation, and inform refinement of future study design and workflow.

This chapter also aimed to assess whether key methodological considerations, such as vascular segment distribution, associations with packed cell volume (PCV), and potential anaesthetic effects, identified in previous experimental work translate meaningfully into the clinical setting. Evaluating the relevance and applicability of these findings in a real-world context helps determine whether methodological adjustments or further investigations are needed.

Finally, the study examined potential trends between markers of illness severity and GlycoCheck™ parameters, as well as possible effects of IV fluid administration, consistent with the objectives of Chapters IV and V. While the study was not powered to detect robust statistical effects, these preliminary insights may inform hypothesis generation and cohort selection in future multi-centre investigations.

Statement of Contribution – Doctorate with Publications/Manuscripts:

The author of this thesis led the establishment of the collaboration, secured funding, designed the project, and was responsible for data collection, interpretation, reporting, and manuscript preparation.

Initial data from this study was presented as an oral abstract at the International Emergency and Critical Care Symposium 2024 by the author of this thesis and published in an abstract form in the Journal of Veterinary Emergency and Critical Care in 2024.

Yozova ID, Cave NJ, Thomson N, Irie M, Munday JS. (2024). Endothelial glycocalyx thickness in cats with naturally occurring trauma and nontraumatic disease - an exploratory study. In: Abstracts from the International Veterinary Emergency and Critical Care Symposium and the European Veterinary Emergency and Critical Care Annual Congress 2024. Journal of Veterinary Emergency and Critical Care, 34(S2), S12. doi:https://doi.org/10.1111/vec.13420

This manuscript has been fully published in Frontiers in Veterinary Science in 2026 as part of the research topic: Innovations in Hemodynamic Monitoring in Veterinary Medicine: From Macrohemodynamics to Microcirculation

Yozova ID, Thomson N, Irie M, Owen R, Munday JS. Endothelial glycocalyx thickness in cats with naturally occurring trauma or non-traumatic illness: an exploratory study. Front Vet Sci. 2026 Feb 23;13:1751034. doi: 10.3389/fvets.2026.1751034.

2. Title page

Endothelial glycocalyx thickness in cats with naturally occurring trauma or non-traumatic illness – an exploratory study

Ivayla D. Yozova[1,*], Neroli Thomson[1], Mitsuhiro Irie[2], Rebecca Owen[1], John S. Munday[1]

[1]School of Veterinary Science, Massey University, New Zealand
[2]Shikoku Veterinary Medical Center, Miki 761-0701, Japan

*Correspondence:
Ivayla D Yozova
School of Veterinary Science - Tāwharau Ora, Massey University, Private Bag 11222, Palmerston North 4222, New Zealand,
email: i.yozova@massey.ac.nz

This study received funding from the Massey University Research Fund 2019.

The authors declare no conflict of interest.

Preliminary results from this study were presented as an oral abstract at the 30th International Veterinary Emergency and Critical Care Symposium in 2024

Keywords: $APPLE_{fast}$, ATT, capillaries, Glycocheck™, feline, length of hospitalisation, microcirculation, perfused boundary region, sidestream dark field videomicroscopy

3. Abstract

Introduction: Endothelial glycocalyx damage contributes to morbidity and mortality in critical illness. In this exploratory study in cats with trauma and non-traumatic illness, the endothelial glycocalyx thickness was estimated using sidestream dark field videomicroscopy and the Glycocheck™ software, with the primary aims of assessing feasibility, describing of Glycocheck™ microcirculatory parameters and exploring potential effects of illness severity and IV fluid administration.

Methods: This was a prospective, single centre, observational study. Recorded variables included age, weight, diagnosis, length of hospitalization (LOH), packed cell volume (PCV) and IV fluid administration. Each patient was assigned a fast Acute Patient Physiologic and Laboratory Evaluation score ($APPLE_{fast}$). In addition, cats with traumatic injuries were also assigned an Animal Trauma Triage score (ATT). Within 24h from admission, cats were anaesthetised, and images from the sublingual mucosal vessels obtained for Glycocheck™ analysis. The perfused boundary region (PBR), an inverse estimate for endothelial glycocalyx thickness, was calculated for vessels with diameter of 5-25, 5-9, 10-19 and 20-25 µm, respectively. Other microcirculatory parameters included vascular segment counts, valid vessel density (VVD), % red blood cell filling (RBC) and median RBC column width (Median P50). Normality was assessed using Shapiro-Wilk test and histograms. The effects of $APPLE_{fast}$, LOH, ATT, PCV, IV fluid administration, and illness group on PBR were analysed using generalised linear models. Distribution of vascular segment counts was assessed using Friedman's test and Wilcoxon rank-signed test.

Results: Nineteen cats were included, 11 with trauma. Success rate for measurements was 95%. Survival to discharge was 95%. Mean ± standard deviation for PBR 5-25 was 2.60±0.22 µm, PBR 5-9: 1.38±0.15 µm, PBR 10-19: 3.02±0.22 µm and PBR 20-25: 3.03±0.38 µm, within previously established tolerance intervals. There were no statistically significant effects of group, LOH, ATT, $APPLE_{fast}$, PCV and IV fluids on any PBR measurements. There were significant effects of IV fluid rate on VVD ($p=0.038$) and Median P50 ($p=0.031$). PCV had a significant effect on VVD ($p=0.044$). Vascular segment counts across the 5 – 25 µm range were not equally distributed ($p<0.001$).

Conclusion: This exploratory study demonstrates the feasibility of assessing endothelial glycocalyx thickness in hospitalized sick cats. While only minor associations with clinical variables were identified, the study highlights important methodological considerations and provides valuable insights to guide future, larger-scale investigations.

4. Introduction

Microcirculatory abnormalities are a recognised contributor to increased morbidity and mortality in critically ill people (163, 359, 360). More recently, damage to the endothelial glycocalyx (EG) has been proposed as a key factor to these disturbances (46, 58, 60, 113) and found to correlate illness severity in people with trauma (141, 237), sepsis (360, 361) and kidney disease (197, 198).
Endothelial glycocalyx degradation contributes to microvascular dysfunction and the progression to multi-organ failure. The underlying mechanisms are multifactorial. Systemic inflammatory states (such as sepsis, severe trauma and ischemia reperfusion injury) lead to cytokine release (362), which in turn stimulates matrix metalloproteinases (MMPs) and reactive oxygen species (ROS) synthesis. These enzymatic and oxidative mediators cleave major structural EG components, such as syndecans and heparan sulfate, from the endothelial surface (57). The resulting fragments enter the circulation, where they act as alarmins, amplifying inflammation through further cytokine release (50, 61). Concurrently, EG degradation exposes proteoglycans on the endothelial surface layer, activating coagulation (46). Excessive coagulation leads to microthrombosis, impairing oxygen and nutrient delivery to the tissues (60). Catecholamine surges in shock states further exacerbates EG damage by stimulating MMP and ROS production, a phenomenon known as shock-induced endotheliopathy (139). Similarly in kidney disease, circulating uremic toxins similarly contribute to EG damage, although the exact mechanism is not fully understood (153, 198, 363).

Beyond propagating inflammation and coagulation, EG damage increases vascular permeability, leading to interstitial oedema, and impaired oxygen delivery at a cellular level, key contributors to multi-organ dysfunction (35). These effects can be further compounded by intravenous (IV) fluid administration, which is a cornerstone of supportive care in both human and veterinary critical care (134, 364), despite the risk for iatrogenic fluid overload (58, 113). Numerous experimental and clinical studies have investigated the impact various regimens of IV fluid administration on the EG with conflicting results (93, 148, 238, 244, 247, 286, 334-336, 338). Whether IV fluids independently cause EG damage to the EG or exacerbate pre-existing injury remains debated (58, 113, 142).

In veterinary medicine, clinical studies investigating EG injury are limited. Some studies have reported increased circulating EG constituents in septic adult horses (288) and foals (365), while marginal increases have been observed in cats with haemotropic mycoplasma (242). Other studies have found no changes in cats with head trauma (243) or dogs undergoing cardio-pulmonary bypass (216). However, reliance on shed EG constituents as biomarkers has inherent limitations: their concentrations are influenced by variable synthesis rates, turnover, and renal clearance (47, 113, 118, 168, 249), making them challenging to interpret in the clinical setting.

An alternative method for *in vivo* assessment of the microcirculation is sidestream dark field videomicroscopy (SDFV), which can be combined with the proprietary software GlycoCheck™ to estimate EG thickness (90). This technique has been applied in numerous human studies, primarily in

sepsis, to explore the effects of critical illness on the microvasculature (90, 156, 158, 194, 196, 198, 204-206). In veterinary research, GlycoCheck™ has been thus far used predominantly in the experimental setting (93, 94, 96, 99, 100, 340, 366), except for one clinical study in dogs undergoing cardio-pulmonary bypass (216). The technique has been used to establish tolerance intervals (prediction-based intervals suited for repeated measurements or devices rather than population-derived biomarkers) in a healthy population (100) and evaluate the effects of IV fluid administration in healthy cats under experimental conditions (340, 366). To date, however, no studies have assessed GlycoCheck™ parameters in cats with naturally occurring disease.

Considering the challenges of translating experimental protocols to the clinical setting, the aims of this exploratory study were to assess feasibility of obtaining GlycoCheck™ measurements in hospitalized cats, identify potentially suitable clinical cohorts and determine optimal data collection timepoints for future multi-centre studies. In addition, this study sought to examine potential associations of GlycoCheck™ parameters, markers of disease severity and IV fluid administration, with results intended to inform power calculations and guide design of future research.

5. Materials and methods

5.1. Study population

This was a prospective, single centre, observational exploratory study, approved by Massey University's Animal Ethics Committee (MUAEC Protocol 21/77). Cats admitted to the Massey University Companion Animal Hospital with trauma or non-traumatic illness were enrolled between March 2023 and March 2024 after obtaining written owner consent. Cats were eligible if they were admitted for trauma or had signs of non-traumatic systemic illness on initial diagnostic work up and had sedation or general anaesthesia planned within 24h of admission (after stabilization, if required) for diagnostic or therapeutic procedures. Cats were excluded if they were deemed too unstable to undergo sedation or general anaesthesia at the primary clinician's discretion or were < 3 months of age.

5.2. Data collection

Recorded variables included age, weight, diagnosis (or suspected diagnosis if definitive diagnosis not available), length of hospitalization (LOH) and outcome (survival to discharge). Variables related to IV fluids administration included whether the cats received IV fluids prior to data collection, IV fluid type, IV fluid challenge (IV fluid bolus administered to assess fluid responsiveness by evaluating changes in haemodynamic variables before and after infusion) volume (ml) during resuscitation, IV fluid hourly rate (ml/h), total volume (ml) and duration (h). Each cat was assigned a feline Acute Patient Physiologic and Laboratory Evaluation fast score ($APPLE_{fast}$; score range 0 - 50) with data obtained within 24h of admission (367). In addition, cats with trauma were assigned an Animal Trauma Triage score (ATT; score range 0 - 18) (368). Wherever multiple entries were available, the most adverse value was used for scoring as performed during the original development of the

APPLE score (367) and the closest to admission for the ATT score (368). Packed cell volume (PCV) was measured as part of the $APPLE_{fast}$ score. Serum Amyloid A was also measured as a marker for systemic inflammation.

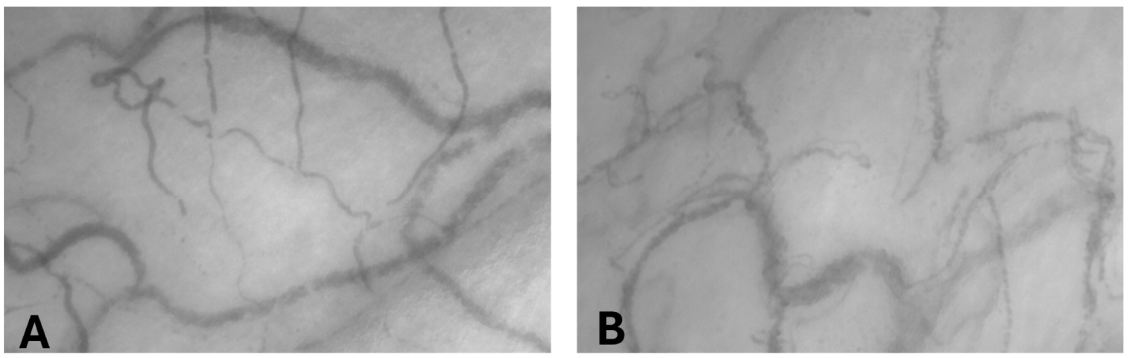
5.3. Image acquisition

All image acquisitions were performed by one of two experienced operators with the animals sedated enough to obtain jaw relaxation or under general anaesthesia (if scheduled). Cats were placed in lateral recumbency, and the base of the tongue exposed such as the sublingual mucosa was accessible for the videomicroscope as previously described (100). A hand-held SDFV camera connected to a laptop with GlycoCheck™ software[a] was placed in contact with the sublingual mucosa by the operator. Three measurements per datapoint were obtained in accordance with current recommendations (181, 186).

5.4. GlycoCheck™ analysis

The method for measuring and calculating GlycoCheck™ parameters has been previously described (100). Briefly, the SDFV camera emits green light at 540 nm wavelength which is absorbed by haemoglobin in circulating red blood cells (RBC). Therefore, vessels appear dark on a bright background (Figure 6.1).

Figure 6.1. Sidestream dark field videomicroscopy image obtained from the sublingual region of a cat with trauma (A) and with sepsis (B). Capillaries appear dark on a bright background.



A video recording is displayed on the screen, and the operator can perform a real-time quality check including focus, pressure and motion artifacts. Furthermore, the software assesses and adjusts for motion and focus and records images only if optimal conditions are present. Each measurement is performed from approximately 10 video recordings containing 40 frames each. The software automatically identifies vessels that are less than 30 μm in diameter by analysing the contrast between the RBC and the background. The software then subdivides vessels into major (10 μm) and

subsequently minor (0.5 µm) vascular segments in length and further determines the percentage of minor segments within a major segment with sufficient contrast for analysis.

A total of approximately 3000 major vascular segments including vessels ranging from ~ 3 – 30 µm diameter is recorded for analysis during each measurement. The counts for major vascular segments of each analysed diameter are additionally recorded. Major segments with > 60% of minor segments with sufficient contrast are considered valid vascular segments (VVS). Valid vessel density (VVD) per mm^2 is then expressed by multiplying 10 µm by the number of valid vascular segments identified.

Secondly, RBC column widths are assessed for minimal column width, column position, and signal-to-noise ratio. From the measured column widths, the software then calculates the percentage of RBC filling (%RBC filling) based on the proportion of time a particular VVS contains RBC throughout all recordings per site. The median RBC column width (Median P50) is calculated using the intensity profiles of the dynamic lateral positions of RBCs in all measured column widths. Finally, linear regression analysis on the Median P50 is performed to derive the perfused diameter of vascular segments.

From that, the perfused boundary region (PBR), an inverse estimate of EG thickness, is calculated as the distance between the Median P50 and the perfused diameter ([Perfused diameter – median RBC column width]/2). Reported GlycoCheck™ parameters, therefore, include VVD, RBC filling %, Median P50 and PBR for vessels with diameter from 5 to 25 µm and for subgroups of vessels with diameters from 5 – 9 µm, 10 – 19 µm and 20 – 25 µm. Higher PBR is, therefore, an indication for a thinner EG and lower PBR indicates a thicker EG.

5.5. Statistical analysis

This study was exploratory, and no formal power-driven sample size calculation was required. Nonetheless, an approximate sample-size estimate was conducted to satisfy ethical requirements and to demonstrate feasibility. Based on similar studies in critically ill people, the difference in PBR 5 – 25 µm between live and dead cats was estimated to be least 0.4 µm (158). The standard deviation in a previous study of healthy cats was 0.26 µm (100). Thus, with an effect size of $d = 0.4/0.26 = 1.54$, this study would require at least 8 cats per group (alive vs. dead) to detect that difference, with a power of 80% and $\alpha = 0.05$. Based on an approximate mortality rate of 20% for critically ill cats, 40 cats would need to be enrolled to ensure sufficient cats that die from their disease (20% of 40 ≈ 8). This estimate remains speculative in the absence of appropriate species-specific prior data to inform the calculations. Therefore, it should be interpreted as illustrative rather than inferential.

Triplicates from measured GlycoCheck™ parameters were averaged for further analysis as recommended in previous reports in healthy and critically ill people (181, 186). Normality was analysed using Shapiro-Wilk test and direct visualization with histograms (342, 343). Normally distributed data was presented as mean ± standard deviation and not normally distributed data as median (interquartile

range) (344). Equivalent linear models were initially fitted as sensitivity analyses and yielded comparable effect directions (297). However, generalized linear models with a Gamma distribution and log link were retained for inference due to the strictly positive nature of GlycoCheck™ parameters and improved residual behaviour (297). These were used to evaluate associations between clinical variables and PBR, as well as other GlycoCheck^{TM} parameters. One model included $APPLE_{fast}$, LOH, and clinical group (trauma or non-traumatic) as predictors. A second model was restricted to cats that received IV fluids and included total IV fluid volume, rate and duration as predictors. A third model assessed the effect of ATT within the trauma subgroup. Model estimates are reported with corresponding 95% confidence intervals. Statistical significance was defined as $p < 0.05$. Linear models with single predictors were used for post hoc power and sample-size calculations, as reliable analytical power calculations for Gamma-distributed GLMs are not readily available. These provide approximate estimates for illustrative quantification. Vascular segment count distributions were compared across diameter categories using Friedman's test and Wilcoxon-signed ranking tests. All statistical analyses were conducted in R (Team, 2023) (297).

6. Results

6.1. Clinical data

Nineteen cats were included for analysis, 11 with trauma and 8 with non-traumatic illness. The cats with non-traumatic illness included two with sepsis (pyothorax diagnosed based on history, physical exam findings and clinic-pathological abnormalities consistent with systemic inflammation and a pleural effusion cytology and culture), two with mucometra progressing toward pyometra with mild systemic signs, three with severe azotemia (two with complicated urethral obstruction and one with acute kidney injury of unknown origin), and one with mediastinal lymphoma. Individual patient data is presented in Table 6.1.

Table 6.1. Individual patient data: diagnoses, outcomes, severity of illness scores, and selected clinical variables.

ID	Diagnosis	Detail	LOH	Outcome	$APPLE_{fast}$	ATT	PCV	SAA
1	Trauma	SC emphysema, Pneumothorax, Pneumomediastinum, Pneumoretroperitoneum	4	Discharged	17	4	45	-
2	Azotaemia	Urethral obstruction	9	Discharged	17	-	39	128
3	Pyothorax	Pyothorax	10	Discharged	24	-	48	-
4	Pyothorax	Pyothorax	7	Discharged	15	-	28	77
5	Trauma	HBC, tail pull injury	7	Discharged	19	4	33	-
6	Trauma	HBC, stifle instability, open wounds	2	Discharged	13	5	39	102
7	Trauma	Dog attack, extensive degloving injuries	0	Euthanized (financial)	15	6	-	60

8	Trauma	Caught under garage door	1	Discharged	17	4	39	10
9	Trauma	HBC, Bilateral femoral Fx	4	Discharged	13	4	18	196
10	GI haemorrhage, AKI	Severe anaemia, melena, azotaemia following NSAIDs	7	Discharged	8	-	13	61
11	Trauma	Fibula Fx	2	Discharged	13	1	28	75
12	Trauma	HBC, ileum Fx, open wounds	6	Discharged	21	6	37	85
13	FeLV Lymphoma	Mediastinal mass, pleural effusion	1	Discharged	24	-	34	1
14	Mucometra	Progressing to pyometra	1	Discharged	16	-	24	10
15	Trauma	Dog attack, wounds, urethral tear	5	Discharged	23	4	21	90
16	Trauma	HBC; TBI, mandibular symphyseal Fx, lung contusions	3	Discharged	22	5	46	-
17	Azotaemia	Urethral obstruction	4	Discharged	14	-	40	54
18	Trauma	Multiple cat bites	0	Discharged	15	2	36	76
19	Mucometra	Progressing to pyometra	1	Discharged	18	-	23	11

$APPLE_{fast}$ - Feline Acute Patient Physiologic and Laboratory Analysis Score (fast) (score range 0 – 50); ATT - Animal Trauma Triage score (score range 0 – 18); Fx – fracture; HBC – hit by car; LOH – length of hospitalization (days); NSAIDs – non-steroidal anti-inflammatory drugs; PCV – Packed cell volume (%); SAA – serum amyloid A (mg/L); TBA – traumatic brain injury

One cat was excluded for incomplete GlycoCheck™ analysis and another for missing clinical data. Success rate for obtaining measurements was 95%. Survival to discharge was 95%. One cat was euthanised due to financial constraints after trauma. Two cats had measurements obtained after >24h from admission (36 and 40h respectively, due to delays in anaesthesia planning). Six cats were considered anaemic (PCV < 28%). Summary statistics for recorded demographic and clinical variables are presented in Table 6.2.

Table 6.2. Demographic and clinical variables for 11 cats with trauma and eight cats with non-traumatic disease enrolled for GlycoCheck™ analysis.

Variable	Value
Age (years)	2.00 (0.83 - 8.84)
Weight (kg)	4.26 (2.90 - 5.31)
LOH (days)	3.89 ± 3.07
$APPLE_{fast}$	17.05 ± 4.29
ATT	2.00 (0 - 4.00)
SAA (mg/L)ǂ	69.10 ± 51.30
PCV (%)¶	32.8 ± 10.1
IV fluid challenge (ml)*	50 (40.75 - 57.5)
IV fluid rate (ml/h)*	11.65 ± 7.38
IV fluids duration (h)*	18.7 ± 11.90
IV fluids total (ml)*	126 (115 - 333.25)

$APPLE_{fast}$ - Feline Acute Patient Physiologic and Laboratory Analysis Score (fast) (score range 0 – 50); ATT - Animal Trauma Triage score (score range 0 – 18); LOH – length of hospitalization; PCV – Packed cell volume; SAA – serum amyloid A
ǂn = 15; ¶n = 18; *Values obtained only from cats that received IV fluids (n = 10);

Ten cats received IV fluids with four of these cats receiving IV fluid challenges, as part of their initial stabilization plan. The IV fluid type consisted almost exclusively of Lactated Ringer's solution (LRS). One cat received a blood transfusion. No synthetic colloids were used. All anaesthetised cats received total intravenous anaesthesia. No vasoactive agents were used during image acquisition.

Normally distributed data included PCV, LOH, $APPLE_{fast}$, IV fluid rate and duration, and not normally distributed data – age, weight, ATT, IV fluid challenge and IV fluid total volume.

6.2. GlycoCheck™ data

GlycoCheck™ parameters VVD, %RBC filling, Median P50, and PBR were normally distributed. Summary statistics for GlycoCheck™ parameters are presented in Table 6.3 and per group in supplementary table (Annex VI).

Table 6.3. GlycoCheck™ parameters for 10 cats with trauma and nine cats with non-traumatic disease compared to previously established tolerance intervals.

Parameter	Mean	SD	95% CI	TI[43]
VVD µm/mm^2	385.75	112.18	331.69 – 439.82	73.33 – 333.33
RBC filling %	59.00	8.00	55.00 – 62.00	59.85 – 85.07
Median P50 µm	8.26	1.12	7.71 – 8.79	5.63 – 8.59
PBR 5-25 µm	2.60	0.22	2.50 – 2.71	1.89 – 3.00
PBR 5-9 µm	1.38	0.15	1.31 – 1.45	0.97 – 1.58
PBR 10-19 µm	3.02	0.22	2.91 – 3.12	2.11 – 3.48
PBR 20-25 µm	3.03	0.38	2.85 – 3.22	1.87 – 4.02

PBR – perfused boundary region; RBC – red blood cells; TI – tolerance intervals; SD – standard deviation; VVD – valid vessel density

The PBR in all cats were within previously established tolerance intervals for the species (100). There were no statistically significant effects of group (trauma or non-traumatic disease), LOH, ATT (for trauma group) and $APPLE_{fast}$ on GlycoCheck™ parameters. For the 10 patients receiving IV fluids, none of the IV fluid variables had a statistically significant effect on PBR. IV fluid rate had a statistically significant positive effect on VVD (mean ratio = 1.07, 95% CI 1.02–1.14, $p = 0.038$) and a negative effect on Median P50 (mean ratio = 0.98, 95% CI 0.97–0.99, $p = 0.031$). IV fluid duration showed a negative effect on Median P50 (mean ratio = 0.98, 95% CI 0.97–0.99, $p = 0.018$), while the total volume had a positive effect on Median P50 (mean ratio = 1.001, 95% CI 1.000–1.002, $p = 0.027$). PCV had a significant effect on VVD (mean ratio = 1.02, 95% CI 1.00–1.03, $p = 0.044$), but not on other GlycoCheck™ parameters. Sample size estimates for effects on selected clinical variables on PBR 5 – 25 µm are presented in Table 6.4.

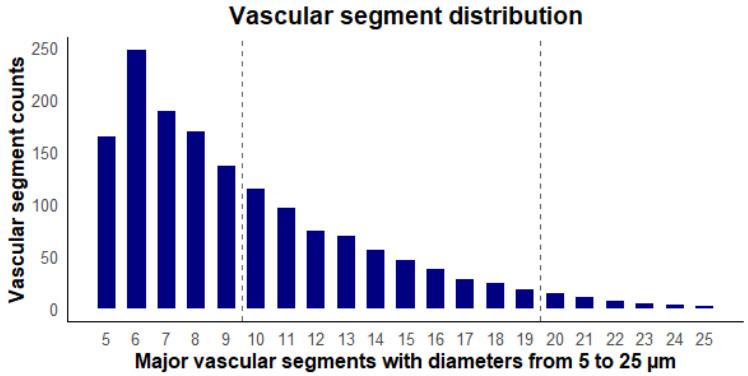
Table 6.4. Sample size estimates required to detect associations between PBR 5–25 µm and selected clinical variables in linear models with a single predictor. Calculations assume a power of 0.80 and a significance level of 0.05. Effect sizes are expressed as model R^2 and corresponding Cohen's f^2. Total sample size indicates the estimated number of subjects needed; the number of observations reflects the current dataset.

Variable	Model R^2	Cohen f^2	Total sample size	Number of observations
PCV	0.011	0.011	729	19
LOH	0.005	0.005	1564	19
APPLE$_{fast}$	0.029	0.030	256	19
ATT¶	0.029	0.030	256	11
IV fluids rate*	0.153	0.181	46	10

APPLE$_{fast}$ - Feline Acute Patient Physiologic and Laboratory Analysis Score (fast) (score range 0 – 50); ATT - Animal Trauma Triage score (score range 0 – 18); IV fluids rate – intravenous fluid rate (ml/kg/h); LOH – length of hospitalization (days); PCV – packed cell volume (%);
¶From subset of cats with trauma (n = 10)
*From subset of cats that received IV fluids (n = 10)

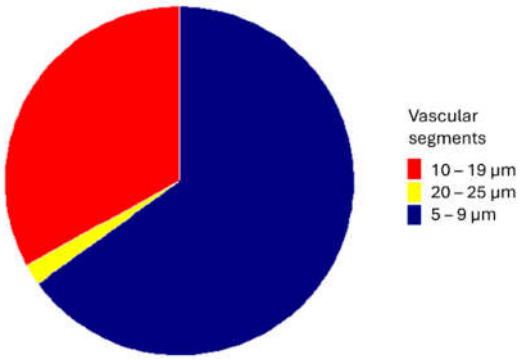
The count for vascular segments with diameters 5 – 25 µm was 1529.42 (±356.04), and for the subgroups with diameter 5 – 9 µm, 910 (515); 10 – 19 µm, 505 (285.5) and 20 – 25 µm 28 (29), respectively. The distribution of vascular segment counts from 5 to 25 µm is presented in Figure 6.2.

Figure 6.2. Distribution of major vascular segment counts by vessel diameter (5–25 µm) as measured using GlycoCheck™ analysis in 19 cats with naturally occurring disease (trauma, n = 10; non-traumatic illness, n = 9). Bars represent the number of valid vascular segments identified per diameter subgroup. Vertical dashed lines separate the predefined vessel size categories: 5–9 µm, 10–19 µm, and 20–25 µm.



There was a statistically significant difference between all the vascular count subgroups ($p < 0.001$ for all comparisons. The distribution of vascular segment counts per diameter subgroup is presented in Figure 6.3.

Figure 6.3. Pie chart showing the distribution of vascular segment counts by diameter subgroup: 5–9 µm (navy), 10–19 µm (red), and 20–25 µm (yellow).



7. Discussion

This exploratory study demonstrates that SDFV image acquisition and EG thickness estimation using GlycoCheck™ can be reliably performed in critically ill cats. All measured GlycoCheck™ parameters remained within previously established tolerance intervals for healthy cats (100). Clinical variables reflecting illness severity, $APPLE_{fast}$ and ATT scores, LOH and type of illness (trauma vs non-traumatic had no effects on GlycoCheck™ parameters. Minor and inconsistent effects of IV fluid variables on selected GlycoCheck™ parameters were observed. Additionally, a significant difference was found in the distribution of vascular segment subgroups contributing the overall PBR 5 – 25 µm measurement, highlighting the importance of examining vessel size breakdown.

The study cohort comprised 19 critically ill cats, including a relatively homogeneous trauma group and a more heterogeneous non-traumatic group. Trauma cases predominantly involved blunt or penetrating injury of varying severity, whereas non-traumatic cases encompassed a broad range of systemic illnesses with differing pathophysiology and illness severity, including sepsis, reproductive disease, renal dysfunction, and neoplasia. This heterogeneity reflects the case mix of a tertiary referral hospital and was an inherent feature of this exploratory feasibility study. While this diversity enhances generalisability, it may also have contributed to variability in microcirculatory measurements and limited the detection of condition-specific effects.

No associations were found between GlycoCheck™ parameters and selected clinical outcome variables. This lack of detectable effects is likely multifactorial. First, the small sample size limited the

statistical power to identify significant associations. Post hoc sample size calculations confirmed that this study was underpowered to detect meaningful effects of selected clinical variables, such as $APPLE_{fast}$ and ATT scores, LOH, PCV, IV fluids rates on PBR 5 – 25 µm, - the summary parameter for EG thickness across vascular diameters. These calculations provide useful guidance for future study design but should be interpreted with caution, as patient characteristics, disease severity, hospitalization practices, and outcomes may differ across institutions and regions.

Another possible explanation is that the enrolled cats, either affected by trauma or non-traumatic illness, did not experience sufficient severity of illness to cause significant damage to the EG. The mean $APPLE_{fast}$ score of 17 in this cohort corresponds to an estimated mortality rate of 6.35% (367), and the mean ATT score of 2 in the trauma subgroup aligns with a predicted mortality rate of approximately 7% (368), based on the original score validation studies. It is plausible that more severely ill cats were either too unstable to undergo general anaesthesia or were euthanized shortly after admission due to poor prognosis and financial constraints. This selection bias is supported by previous feline trauma studies reporting early euthanasia decisions driven by financial limitations (369-371). Moreover, global data consistently show that owners spend less on cats than dogs in veterinary care, which may further explain the inclusion of less severely ill cats (with potentially better prognosis for a given expenditure) in this cohort (372-374). The centre where the study was performed is in a region facing socio-economic challenges at the time of data collection, potentially exacerbating a financial bias. Therefore, the relatively low severity of illness among enrolled patients in this study likely reflects both medical and financial considerations.

Finally, the lack of effects of severity of illness (or injury) on GlycoCheck™ parameters, may reflect limitations inherent to the severity of illness scores themselves. Severity of illness scores require extensive external validation to ensure performance outside their original development setting. While the ATT score has undergone such validation (368), the APPLE score has not, and its use in other populations should be interpreted with caution. Together, these factors highlight the complexity of applying standardized illness metrics to GlycoCheck™ data and the need for larger, multicentre studies with robust case diversity or focusing on specific cohorts with higher illness severity (such as for example septic cases).

In contrast with the absence of associations between severity of illness variables and GlycoCheck™ parameters, this study demonstrated some minor and varying effects of IV fluid administration source GlycoCheck parameters VVD and median P50, without a consistent directional pattern. The significance of these remains unknown. They may represent type I errors arising from model instability associated with small sample size (only 10 cats received intravenous fluids) and the inclusion of multiple covariates.

In this study IV fluid administration variables had no effect of PBR. This contrasts human medicine studies where IV fluid-related increases in PBR have been observed in both stable surgical patients (142) and critically ill patients (113). However, results are largely inconsistent and changes

often marginal. In addition, most studies in people, have focused on EG shedding biomarkers, (such as syndecan-1), rather than GlycoCheck™ analysis, complicating comparisons.

In veterinary medicine, published studies evaluating the impact of IV fluids on GlycoCheck™ parameters are limited to the experimental setting with reports from rabbits (96, 99), dogs (93, 94) and cats (340, 366). These generally demonstrate changes in PBR only when large volumes are administered, typically following a prior insult, such as haemorrhage. In a series of studies in heathy anaesthetized cats conducted by this group, IV fluid administration was associated with a marginal protective effect on estimated EG thickness, with lower PBR values observed in the intervention groups, compared to controls (340, 366). The absence of a detectable effect of intravenous fluids on PBR in the present study should be interpreted with caution, as limited statistical power may have masked subtle associations. In addition, measurements were obtained at a single timepoint, which constrains interpretability compared with more robust before-and-after designs. Taken together, these findings underscore the complexity of the relationship between intravenous fluid administration and endothelial glycocalyx injury, for which no single explanatory model is likely to apply. Observed effects may be species-specific and dependent on patient population, study design, and research setting. Therefore, direct extrapolation should be avoided. To specifically investigate the effects of intravenous fluids in sick cats, future prospective, adequately powered studies incorporating species-specific volume kinetics principles are required.

Building on the interpretation of GlycoCheck™ data, this study also highlighted important methodological considerations related to vascular segment distribution within the analysis. The GlycoCheck™ software detects vessels up to 30 µm in diameter, subdividing them into major vascular segments of 10 µm length based on sufficient image contrast. Up to 3000 segments may be analysed per scan, with only those passing internal quality checks contributing to the calculation of PBR. In the current study, these 10 µm vascular segments (vascular segment counts) were unevenly distributed across diameter ranges with a marked overrepresentation (~60%) of vessels measuring 5 – 9 µm in diameter. This disproportion was statistically significant compared to segments from 10–19 µm and 20–25 µm vessels, a finding consistent with previous reports in both feline studies (366) and human cohorts, including patients with pre-eclampsia (215) and type 2 diabetes (375).

This uneven representation is noteworthy for two key reasons. First, the PBR values for 5 – 9 µm vessels are approximately twofold smaller than the other PBRs in cats, dogs and people (100). When this subgroup dominates the overall PBR 5 – 25 µm calculation, the resulting average may underrepresent actual EG thinning, potentially skewing interpretation. Second, different vessel sizes may respond differently to physiological and pathological stimuli. For instance, in a previous feline study from this research group, PBR 5 – 9 µm decreased following transient volume overload in cats, while other PBRs did not (366). These variations suggest that interpreting only the average across all vessel sizes may obscure meaningful subgroup-specific changes.

Despite this, most veterinary studies continue to report only the overall PBR 5 – 25 µm, potentially overlooking important microvascular dynamics (93, 94, 96, 99, 216). Since the distribution of vascular diameters reflects the inherent anatomy of the sublingual mucosa, this discrepancy is an unavoidable feature of the analysis. As such, methodological approaches should account for it. Future studies are encouraged to report PBR values stratified by vessel diameter to provide a more detailed understanding of EG responses and enhance clinical interpretation.

Another potential methodological consideration is the effects of PCV on GlycoCheck™ parameters. In this study lower PCV was associated with decrease in VVD. This finding aligns with previous experimental work from this group, which demonstrated associations between decreasing PCV and changes in a number of GlycoCheck™ parameters, including increases in PBR values (340, 366). Similar trends have been observed in human studies; one in healthy individuals with different ethnicities reported lower PBR with higher PCV (187), while a study in neonates, found increased PBR in the pre-term cohort with lower PCV (183).

All GlycoCheck™ parameters are derived based on identification of RBCs on a contrasting background. Therefore, haemodilution from anaemia may reduce contrast and affect measurement reliability. In the present study, only VVD was significantly affected by PCV. This may reflect the limited number of anaemic cats (n = 6), reducing power to detect changes in other parameters. In contrast, the anaesthetic protocol and IV fluid administration in the above-mentioned feline experimental studies induced more pronounced haemodilution. Notably, VVD appeared to be the most consistently PCV-sensitive parameter across studies (340, 366). Additionally, PCV and GlycoCheck™ measurements were precisely paired in the experimental work, whereas timing differed in the clinical setting. These factors may explain the discrepancy in findings between the experimental and clinical studies. Further clinical studies are needed to define the magnitude and clinical relevance of PCV effects on GlycoCheck™ parameters and to guide appropriate interpretation.

This study assessed the feasibility of prospectively collecting GlycoCheck™ data in critically ill cats. Image acquisition and analysis proved practical and safe, and data collection could be integrated into the clinical workflow. However, several adaptations to the study design (from an “ideal” such) were necessary to ensure successful data collection. A relatively broad time window for image acquisition was permitted, which may have introduced variability in the degree of microcirculatory alteration and PBR measurements. Measurements obtained closer to admission might have better captured EG injury in sick cats. However, this was not feasible due to the need for initial patient stabilisation, multidisciplinary planning, obtaining owner consent among other.

Only cats requiring sedation or general anaesthesia were eligible for inclusion, resulting in the exclusion of a substantial proportion of admitted patients, potentially more severely ill. This resulted in a relatively homogeneous trauma cohort and a more heterogenous non-traumatic cohort, reflecting the facility’s case load. In addition, longitudinal data collection was not feasible, largely due to owner reluctance to consent to sedation or general anaesthesia solely for image acquisition when no additional

interventions were planned. Although efforts were made to acquire images at the onset of sedation whenever possible, this could not always be achieved, as urgent clinical procedures (often emergency department–led imaging or wound care) necessarily took priority. In contrast, image acquisition proved more practical at the start of general anaesthesia, while the patient was being prepared and instrumented.

Based on these observations, future studies should aim to streamline image acquisition by targeting timepoints that are both clinically relevant to disease progression and as close to admission as feasible, standardising timing in relation to sedation and anaesthesia, and exploring approaches that allow enrolment of patients irrespective of whether sedation or general anaesthesia is planned, while including longitudinal data collection.

As a result of this adaptive exploratory design, this study has several limitations. The small sample size limited statistical power, and furthermore, the target of 40 subjects could not be reached for the duration of the study. This could have resulted in type II errors. Therefore, results from this study should be interpreted with caution and direct extrapolations to other populations of sick cats – avoided. Generalised linear modelling was selected based on the characteristics of the outcome variables, with predictors grouped into smaller, biologically and clinically plausible models rather than a single data-driven model. While this approach reduces model complexity, it may still carry a risk of overfitting in a small exploratory dataset. In larger datasets with longitudinal sampling, alternative analytical approaches such as generalized linear mixed-effects models, linear mixed models, and principal component analysis or trajectory-based modelling could be applied to better capture group differences and temporal patterns in microcirculatory parameters.

While the aim was to include patients within 24 hours of admission, this timepoint was somewhat arbitrarily selected and not reflective of disease progression. Moreover, critically ill patients are often subject to multiple interventions during the initial 24 hours, which may have influenced the measurements. Inclusion was restricted to cats requiring anaesthesia, excluding all critically ill patients who were too unstable or did not undergo procedures under anaesthesia, which may have introduced selection bias. This resulted in a relatively homogeneous trauma cohort and a more heterogenous non-traumatic cohort, reflecting the facility's case load. Trauma patients are more likely to undergo anaesthesia for imaging or surgery, further skewing representation. The true composition of the broader clinical cohort is unknown, as only cats admitted for diagnostics and treatment requiring anaesthesia were enrolled. This potentially introduces a survival bias and affects results. Records were not kept for non-enrolled cases, including those euthanised early, too unstable for anaesthesia, or not pursued due to financial constraints. As a result, the representativeness of the study cohort could not be fully assessed. The study cohort, particularly the non-traumatic group, was heterogeneous with respect to illness severity. In combination with the arbitrary timing of sample collection, this heterogeneity may have increased variability and obscured potential effects. Lastly, only single measurements were obtained, not allowing for exploration of longitudinal effects.

Anaesthetic effects represent a potential confounder in small animal microcirculatory imaging studies, as deep sedation or general anaesthesia is required for image acquisition. Future research should therefore aim to establish protocols that minimise these effects. Anaesthetic influences were deliberately not included within the aims of the present study, as the dataset was not suited to reliably address hypotheses related to anaesthetic effects. Consequently, some degree of variability may have arisen from differences in anaesthetic protocols and the timing of image acquisition relative to anaesthesia. Previous studies have demonstrated no effect of alpha-2 agonists when added to a to a butorphanol and propofol containing protocol (100), propofol alone has been associated with changes in PBR over time in cats (340, 366). The effects of other anaesthetic agents remain unknown, and the sample size was insufficient to compare protocols.

Although images were ideally collected at the start of anaesthesia, clinical flow occasionally required deviation from this protocol. The timing of image acquisition relative to anaesthetic induction represents an additional potential source of bias. Measurements were obtained at variable timepoints during anaesthesia, depending on clinical stabilisation and procedural priorities, and could not be standardised. Early measurements may have coincided with haemodynamic transitions and intravascular volume shifts, whereas later measurements may have reflected more stable but pharmacologically altered conditions. This variability in timing may have introduced additional noise and masked subtle microcirculatory changes, and its direction and magnitude could not be assessed within the current study design.

The GlycoCheck™ software was developed in human subjects and does not explicitly account for inter-species differences. Such differences may influence the analytical performance of the system and the interpretation of parameters related to capillary function. Accordingly, until comparative validation data across species become available, results should be interpreted with caution and direct inter-species comparisons avoided.

Finally, two operators performed GlycoCheck™ measurements. Although inter-operator variability for GlycoCheck™ measurements appears minimal in human studies (91), this has not been validated in cats. It is also important to acknowledge that microvascular beds vary in composition and response to stimuli (376) and sublingual measurements may not fully represent systemic microcirculatory changes. Therefore, assessments from the sublingual capillary bed should not be extrapolated to the remainder of the microcirculation with caution.

8. Conclusion

This exploratory study demonstrated that obtaining GlycoCheck™ measurements is feasible in a diverse cohort of critically ill cats. While no strong associations were identified between severity of illness scores and EG thickness, minor effects of IV fluid variables and PCV were observed. Despite the study's limited statistical power, these findings add to the growing body of literature on feline microcirculation and support the potential utility of GlycoCheck™ in veterinary critical care settings.

However, results should be interpreted with caution, as cohort characteristics may differ between institutions, influencing both clinical variables and disease outcomes. Nonetheless, the study provides a valuable foundation for future work in this area of research and highlights important considerations for the interpretation and application of microcirculatory data in feline patients.

9. Authors contributions

IY secured funding, designed the study, collected and interpreted data and wrote the original draft and edited the manuscript; NT helped secure funding, interpreted data and edited the manuscript; NC interpreted data and edited the manuscript; MI interpreted data and edited manuscript; RO helped collected data and edited manuscript; JM secured funding, interpreted data and edited the manuscript.

10. Footnotes

[a]MicroVascular Health Solutions, USA

11. Chapter VI extended implications

With this chapter, the project transitions from a controlled experimental setting into the clinical environment, where ultimately, methodologies for assessing EG integrity should be applied. Although no strong associations were found between GlycoCheck™ parameters and clinical variables, this study highlights important considerations for implementing the methodology in real-world veterinary practice and designing future investigations.

A key limitation was the relatively small and heterogeneous cohort, with the exception of trauma patients who were sufficiently represented to form a distinct subgroup. This distribution reflects the natural caseload of the facility: trauma is among the most common small animal presentations in New Zealand (unpublished survey data). Moreover, cats with trauma frequently require diagnostic imaging or surgical intervention under general anaesthesia, making them readily eligible for inclusion. In contrast, critically ill patients not requiring anaesthesia (due to instability or lack of intervention) were excluded, as inducing anaesthesia purely for research purposes was deemed ethically unjustifiable in an exploratory study. This approach may have skewed the cohort further toward less severely ill trauma patients.

Additionally, illness severity was generally low in the enrolled cats, reflected in low APPLEfast and ATT scores and a 5% mortality rate (the one cat that did not survive was euthanized due to financial concerns). Financial constraints may have influenced early euthanasia decisions, particularly for cats with non-traumatic illness, contributing to underrepresentation of sicker animals. Combined with socio-economic challenges in the region, low population density, and limited project duration, these factors contributed to a smaller-than-anticipated sample size and limited generalisability. Future studies should aim for multi-centre recruitment over longer timeframes, enrolling larger and more severely ill cohorts to better evaluate clinical relevance and EG damage.

As in Chapters IV and V, SDC-1 concentrations were measured using the ELISA kit evaluated in Chapter III. All samples yielded results below the detection limit, consistent with previous findings. However, as the assay was not fully validated for feline samples, these findings should not be interpreted as definitive evidence of absent SDC-1 elevation. Nonetheless, unlike the healthy experimental cats, in which IV fluids or anaesthetics were potentially not a sufficient stimulus for SDC-1 elevations, the clinical cohort in this study included sick cats, who were expected to exhibit at least some elevation in SDC-1, similar to the cats recruited for assay validation. The absence of detectable concentrations in this context may further support the notion that the enrolled cats were not sufficiently ill for structural EG damage to be detected.

Despite its limitations, this study reaffirmed several methodological considerations identified in the experimental chapters. For instance, associations between PCV and GlycoCheck™ parameters were less robust than previously reported - likely due to the lower frequency of anaemia in this cohort compared to the significant haemodilution observed under experimental conditions. Nevertheless, the

association between PCV and VVD persisted, reinforcing the need for further study into PCV or haematocrit's impact on microcirculatory metrics.

Similar to Chapters IV and V, some trends suggesting effects of IV fluid administration on GlycoCheck™ parameters were noted in this study, although their significance is likely limited by the small number of cats that received IV fluids (n = 10). At the facility where this study was conducted, IV fluids are administered very cautiously in feline patients, which may differ from practices at other institutions worldwide and helps explain the small subgroup. Nevertheless, as IV fluid administration is a cornerstone of feline critical care and given the lack of evidence-based dosing guidelines, and the recognized sensitivity of cats to fluid administration, future studies should investigate associations between IV fluids and GlycoCheck™ parameters. At a minimum, IV fluid variables should be considered as potential confounders in microvascular research.

Additionally, anaesthetic protocols varied considerably among patients in this study, precluding even preliminary evaluation of their effects on GlycoCheck™ parameters. Since anaesthesia is an inherent component of SDFV data acquisition in small animals, its influence should be further explored in both experimental and clinical contexts to better understand its potential confounding effects on EG assessment.

Lastly, vascular segment count distribution remained uneven, as in chapter V, with vessels of 5–9 µm again comprising the majority (~60%) of segments analysed. While this mirrors the sublingual microvascular anatomy and cannot be altered, it has implications for interpretation. Specifically, PBR 20–25 µm - derived from only ~3% of vascular segments - may be prone to high variability and underpowered analyses. In addition, vessel diameters can dynamically adapt to physiological stimuli, further complicating analysis. Although the current GlycoCheck™ software groups vessel diameters into somewhat arbitrary categories, future versions are already moving toward diameter-specific analyses and new microcirculatory markers with a focus on functional differentiation of smaller capillaries (93, 94, 156, 216). These advancements should enhance accuracy and clinical interpretability in future research.

This study could not determine whether GlycoCheck™ has a definitive role in individual patient monitoring or in guiding diagnostic and therapeutic decisions in clinical feline practice. However, it was neither designed nor powered to answer this question. Based on current veterinary literature and the findings of this exploratory investigation, GlycoCheck™ remains best suited as a population-level research tool. Nonetheless, it holds promising potential for future translation into individual patient monitoring, paralleling its current trajectory in human medicine.

Chapter VII: General discussion

Chapter plan

1. Introduction
2. Objectives and hypotheses
3. Core research findings
   - 3.1. Interspecies differences and demographic considerations in GlycoCheck™ analysis
   - 3.2. Effects of IV fluids on GlycoCheck™ parameters
   - 3.3. Effects of disease on GlycoCheck™ parameters
4. Methodological considerations
   - 4.1. Lack of validation of a human SDC-1 ELISA assay
   - 4.2. Effects of packed cell volume on GlycoCheck™ parameters
   - 4.3. Vascular segment count distribution in GlycoCheck™ analysis
   - 4.4. Effects of anaesthetics on GlycoCheck™ parameters
5. Theoretical and Practical Implications
   - 5.1. IV fluids implications
   - 5.2. Implications in disease
   - 5.3. Methodological implications
     - 5.3.1. Endothelial glycocalyx shedding biomarkers
     - 5.3.2. Packed cell volume
     - 5.3.3. Anaesthetics
6. Strengths
7. Limitations
   - 7.1. Methodological challenges in microvascular research
   - 7.2. Project-related limitations
8. Future perspectives
9. Final conclusion

1. Introduction

The microcirculation serves as a gateway to delivering oxygen and nutrients to cells, playing a crucial role in maintaining homeostasis. Microcirculatory impairment is considered a hallmark of critical illness, particularly in conditions associated with systemic inflammation (e.g. sepsis, severe trauma, ischemia-reperfusion injury) and contributes to morbidity and mortality associated with multiorgan dysfunction (37). The endothelial surface layer, including its endothelial glycocalyx (EG) is central to microcirculatory function, and its damage results in altered vascular permeability, impaired capillary blood flow, and sustained inflammation, potentially further contributing to multiorgan dysfunction (38, 200, 206).

The relatively recent discovery and ongoing study of the EG have significantly enhanced our understanding of microcirculatory involvement in critical illness in human medicine and are improving diagnostic and therapeutic strategies (60, 124). Despite these advances, veterinary EG research remains in its early stages, with very little known about its structure and function in cats. Cats, however, display a unique - albeit understudied - vascular physiology, which may predispose them to volume and fluid overload, compared to other mammalian species (e.g. dogs). These complications contribute to increased morbidity and mortality, particularly when compounded by higher costs of care. A deeper understanding of the feline microcirculation and its EG will therefore help improve feline patient care in the context of increases in feline pet ownership and demands for advanced veterinary care.

This thesis offers a detailed investigation into the feline EG. It addressed multiple knowledge gaps within the field. First, it successfully adapted EG assessment tools developed for human medicine for use in cats. Second, it provided initial insights into how intravenous (IV) fluids and disease processes may affect the feline EG. Third, it identified species-specific differences in microcirculatory parameters, contributing to our understanding of interspecies variability. Finally, it highlighted several key methodological challenges that influence EG assessment, including the effects of haematological variables, anaesthetic protocols, and limitations in biomarker validation. While this study provides important first steps, it does not offer definitive conclusions but rather a foundation for further investigation.

This chapter synthetizes the key findings from this project, placing the results within a broader scientific and clinical context. By drawing connections across different aspects of the study, theoretical and clinical applications are outlined, strengths and limitations are evaluated, and future research directions are proposed.

2. Objectives and hypotheses

The following section will revisit the original objectives and hypotheses of this study, outlining how they were addressed by the experimental chapters. This will provide an overview for interpreting the broader significance of the results and placing them into a wider research context.

This thesis aimed to investigate the application of methods for assessment of EG integrity in cats, focusing on techniques suitable for clinical research (as opposed to exclusively experimental research). The first method involves direct visualization of capillary beds using sidestream dark field videomicroscopy (SDFV), combined with proprietary GlycoCheck™ software, which calculates the perfused boundary region (PBR) - an inverse estimate of EG thickness. The second method involves measuring biomarkers for EG damage, specifically unbound EG constituents in serum or plasma, using Enzyme-Linked Immunosorbent Assays (ELISA). Syndecan-1 (SDC-1) was selected as the biomarker of interest, based on research in human medicine and its expected structural and physiological similarities between people and cats.

The primary objectives of this study were: first, to establish feasibility and tolerance intervals for these two methods in healthy cats; second, to investigate the effects of different IV fluid regimens on the feline EG in a controlled setting; and third, to explore potential EG alterations associated with naturally occurring critical illness in a cohort of hospitalized sick cats. An additional objective was to compare efficacy of both assessment methods and determine whether either, or a combination of both, might provide a reliable means of evaluating EG integrity in cats.

The hypothesis was that both the SDFV with GlycoCheck™ and ELISA-based biomarker detection would be adaptable for use in cats; that IV fluid administration will negatively impact the EG; and the EG will be damaged in sick cats as compared to healthy cats. The specific objectives of each chapter were:

- To use a large cohort of healthy heavily sedated cats and investigate feasibility of performing GlycoCheck™ analyses, including positioning and time for image acquisition, establishment of tolerance intervals for GlycoCheck™ parameters and exploring for potential effects of demographic variables (age, weight, sex) on those parameters (Chapter II).
- To validate a human SDC-1 sandwich (quantitative) ELISA for detection of SDC-1 in feline sera, using a comprehensive validation process including assay quality checks, such as precision and accuracy, as well as identification of the captured protein (Chapter III).
- To evaluate the immediate effects of a fluid challenge on the EG, comparing two types of IV fluids - buffered balanced isotonic crystalloid and hydroxyethyl starch - to a no-fluid control group. The EG was assessed using SDFV and GlycoCheck™ software, with serum collected simultaneously for SDC-1 measurements (Chapter IV).

- To evaluate 24h effects of transient IV volume overload on the EG through administration of a relatively large volume of buffered balanced isotonic crystalloid compared to a no-fluid crossed-over control group. The EG was assessed using SDFV and GlycoCheck™ software, with serum collected simultaneously for SDC-1 measurements (Chapter V).
- To broadly explore the effect of critical illness on the EG using SDFV and GlycoCheck™ and SDC-1 measurements in a group of cats with naturally occurring disease and compare to established tolerance intervals (Chapter VI).

3. Core research findings

The following section presents the core research findings of this thesis, addressing the original objectives and hypotheses by synthesizing results from both experimental and clinical studies. It describes inter-species and demographic considerations, the effects of IV fluid administration and disease processes on the feline EG assess using SDFV and GlycoCheck™ analysis.

3.1. Interspecies differences and demographic considerations in GlycoCheck™ analysis

Acquiring SDFV images for GlycoCheck™ analysis in cats was feasible at the same anatomical sites as in dogs and people (sublingual mucosa) and within comparable time frames (91, 95). Overall, the measured GlycoCheck™ parameters in cats were similar values to those reported in other species.

One exception was VVD (valid vessel density), which was approximately 10-fold lower in cats than studies in healthy dogs and people (90, 95). These observed differences may be due to inherent anatomical and physiological variation; for example, cats have about 70% of the blood volume per kilogram of body weight, of dogs and people (252, 253, 377), which may translate into less dense capillary networks. Noteworthily, VVD serves as a baseline parameter for identifying vascular segments suitable for PBR analysis. Therefore, markedly lower VVD in cats could reduce "sample size" of usable segments, potentially increasing intra- and inter-subject variability. This limitation was mitigated in this study by including a relatively large cohort of healthy cats (n = 102) to establish tolerance intervals. Lastly, as VVD is not systematically reported in other species, this comparison is based on limited data, and it remains unclear whether this represents a true species variation.

Cats also had a 10-15% higher mean PBR than dogs and people (90, 93, 95, 181), suggesting that cats have a thinner EG. However, direct comparisons are complicated by differences in study design and cohort characteristics. Importantly, similarly to VVD, PBR values also show certain variability in the human and canine literature, so species comparisons should be interpreted with caution.

Another possible contributor to species differences is feline haemoglobin, which differs in structure, oxygen affinity, and light absorbance compared to canine and human haemoglobin (281-283). GlycoCheck™ relies on haemoglobin's light absorption at 540 nm. If feline RBCs absorb less light at

this wavelength - as some reports suggest (283) - this could reduce RBC contrast, increase light scatter, and affect background noise and image processing, potentially altering PBR calculations. While these effects are likely minor and would not compromise the application of GlycoCheck™ in cats - particularly with proper validation - they may still limit the validity of direct interspecies comparisons.

In human studies, demographic factors such as age, sex, weight, and ethnicity have been associated with differences in PBR values (90, 187, 188, 214, 375). This does not seem to be the case in healthy cats, based on results from chapter II of this study. A range of ages, sexes, and neuter statuses were included, but the population primarily consisted of adult to mature, spayed and neutered cats (3–10 years old). Additionally, as these were research-purposed cats maintained on regular diets with close weight monitoring, few were likely to be overweight.

Obesity and diabetes are well-established contributors to microcirculatory dysfunction in humans, even before the discovery of the EG (378, 379). More recent studies have shown that these conditions are associated with EG thinning as part of broader microvascular derangements (90, 188, 214, 375). This suggests a need to further explore these effects in client-owned cats, where conditions such as obesity and diabetes are more common. Gaining insight into EG changes in these populations may help refine the clinical management of feline metabolic disorders, including IV fluid protocols and anaesthesia planning, prognostication and therapeutic targeting.

3.2. Effects of IV fluids on GlycoCheckTM parameters

Administering IV fluids to healthy cats, even in large amounts resulted in only minor changes to the EG as assessed using SDFV and the GlycoCheck™ (chapter IV and chapter V). These effects were confounded with potential anaesthetic influences, particularly repeated propofol administration (chapter V). These inconclusive findings align with recent research, suggesting that IV fluids alone may not be sufficient to induce significant EG shedding (113, 249). Currently, the effects of IV fluids on GlycoCheck™ parameters specifically remain poorly studied in human medicine, most studies focusing on biomarkers of EG shedding. Therefore, direct comparisons are challenging. Earlier studies reported statistically significant but minor increases in SDC-1 following IV fluid administration in healthy or stable surgical human patients, often requiring multiple statistical adjustments to detect differences (142, 286, 335). More recent studies failed to corroborate these results, demonstrating no EG damage after IV fluid administration in similar cohorts of human patients (238, 337). The ongoing debate of whether IV fluids alone, or in combination with critical illness, contribute to EG damage (113, 142) partially supports the inconclusive findings observed in the experimental studies in cats. This topic has been discussed in detail in previous chapters, highlighting the complexity and variability of reported effects across species and study designs.

Given that cats are particularly sensitive to IV fluid administration and prone to volume overload (130, 131, 251), the hypothesis that IV fluids might damage the EG even in healthy subjects warranted investigation, despite previous inconclusive findings in human research. Indeed,

experimental volume kinetics (the pharmacokinetics of IV fluids) evidence suggests that cats eliminate IV fluids more slowly than other species (130) and tend to retain IV fluids under anaesthesia (251) and during hypothermia (131). Additionally, clinical observations highlight frequent complications from excessive IV fluid administration in cats (such as pleural effusions and pulmonary oedema) (138, 257, 380, 381), reinforcing the above-mentioned experimental volume kinetics findings.

The proposed mechanism by which IV fluids might induce EG damage involves release of NP (natriuretic peptides) by the cardiac muscle in response to volume expansion from IV fluids (143). Natriuretic peptides act to reduce excessive intravascular volume via four primary mechanisms: natriuresis, vasodilation, inhibition of the renin-angiotensin-aldosterone system, and increased vascular permeability (143, 144). The latter is believed to occur through EG disruption, as NPs stimulate the production of matrix metalloproteinases, which cleave structural components of the EG from the endothelial surface. This degradation impairs the barrier function of the EG, allowing fluid to shift from the intravascular to the interstitial space. However, this mechanism is not yet fully validated in clinical research. For instance, infusion of atrial NP did not induce EG damage in a porcine model (336), and the effects of NPs may differ between healthy and critically ill subjects (144).

In cats, it remains unknown how much IV fluid is required to sufficiently stretch cardiomyocytes to trigger NP release. Overall, studies on feline volume kinetics are limited (130, 131, 251). Currently, there is little evidence to support specific dosing rates, nor is there a clear definition of what constitutes an IV fluid "overdose" in cats (138). The volume overload protocol used in Chapter V was empirically derived, aiming to avoid long-term harm while inducing a degree of cardiac stretch, as suggested by previous feline cardiac point-of-care ultrasound data (356). However, it is possible that the fluid volumes used were insufficient in magnitude or duration to elicit a meaningful physiological response. Future research incorporating advances in feline volume kinetics will help refine IV fluid dosing strategies and better clarify their impact on the EG.

The effects of IV fluids are expected to differ between healthy and diseased subjects, because of differences in physiological and pathophysiological responses to stimuli. Unsurprisingly, the exploratory clinical study (chapter VI) yielded mixed findings, showing both "positive" and "negative" changes in GlycoCheck™ parameters following IV fluid administration in sick cats. These inconsistencies likely reflect the diverse clinical presentations of the study population, where disease type and progression, may influence whether IV fluids damage or protect the EG. Additionally, fluid volume and duration were not standardized, as they were left to clinician discretion, introducing variability and potential bias. The small sample size and exploratory nature of the study further limited its power to detect significant effects.

Examining the microcirculation and EG under IV fluid stimuli is only one aspect of a broader and largely understudied topic of IV fluid administration in veterinary medicine (382). While IV fluids are a mainstay of small animal practice, the scientific evidence supporting their use remains sparse, and clinical decision-making is often empirical (29, 138, 382-384). This study represents the first

investigation of IV fluid effects on the feline microcirculation and EG, using the GlycoCheck™ system, contributing to this understudied yet widely implemented intervention. While no robust effects of IV fluids were identified, these results reinforce the need for further investigation, including feline-specific volume kinetics studies, refined dosing regiments, and more standardized assessment protocols. Within the context of this thesis, these findings help define knowledge gaps and support the rationale for well-designed, adequately powered clinical trials to establish evidence based IV fluid practices in cats.

3.3. Effects of disease on GlycoCheck™ parameters

Effects of disease type and severity on GlycoCheck™ parameters were explored in the final part (chapter VI) of this project. In human medicine, multiple studies have demonstrated EG thinning in critical illnesses such as sepsis (149, 156-158, 194, 196), and more recently COVID-19 (204-206). However, this small-scale explorative study in cats did not find a clear association between type and severity of illness and GlycoCheck™ parameters.

The lack of detectable differences was likely due to the study being underpowered to detect significant associations. However, the illness severity of the hospitalized cats included in this study may have been insufficient to induce substantial EG thinning, particularly when compared to the severity of illness in similar human cohorts. In human medicine, most EG studies are conducted in developed countries, where advanced healthcare systems allow for the treatment of critically ill, highly dependent patients (385). As a result, these studies may be inherently skewed toward more severe disease states.

By contrast, veterinary care, even in well-developed regions, typically operates within greater resource limitations, with financial constraints and welfare considerations often influencing treatment decisions. Consequently, veterinary patients tend to be less severely ill at the time of hospitalization, potentially explaining the absence of significant EG alterations in this study. This highlights the importance of aligning clinical study designs with the true distribution of illness severity in veterinary patients, ensuring that research objectives and expected outcomes are clinically relevant.

Despite these limitations, this study serves as an important first step in clinical GlycoCheck™ research. It provides a foundation to establish suitable patient cohorts optimizing data acquisition points, and constructing larger prospective studies aimed at better understanding the role of the EG in feline critical illness.

One notably absent cohort in this study - but one that merits further exploration – is cats diagnosed with feline infectious peritonitis (FIP), a disease caused by a mutated enteric coronavirus (386). Feline infectious peritonitis causes “vasculitis”, vascular and perivascular pyogranuloma formation, with effusive forms often presenting with severe systemic involvement (386, 387). Until 2020, FIP was a fatal disease with no effective treatment (386, 388-390). However, following the COVID-19 pandemic, antiviral drugs originally developed for COVID-19, were made available for use in cats, leading to successful treatment outcomes (387, 391-393). In the present study, the absence of FIP cases likely reflects the inclusion criteria: diagnosis of FIP does not often require procedures under

general anaesthesia, excluding these patients from enrolment. With FIP being a treatable condition, efforts to optimize treatment regiments (394, 395) are ongoing, creating research opportunities. These can justify incorporating a short anaesthesia specifically for data collection to assess the microcirculatory responses to treatment, refine antiviral protocols, and identify responders versus non-responders early in the disease process.

Given the pathophysiological parallels between the feline coronavirus causing FIP and the SARS-CoV-2 (396, 397), as well as the association between microvascular dysfunction and prolonged COVID-19 in people (204, 206), cats may serve as valuable models for translational microvascular research.

4. Methodological considerations

This section outlines key methodological considerations that emerged as important findings throughout the project. Some of these support the validity of the core research results, while others highlight limitations in current EG assessment methods, emphasizing the need for cautious interpretation and further methodological refinement. Specifically, it addresses the incomplete validation of the ELISA assay, the influence of packed cell volume (PCV) on GlycoCheck™ parameters, the distribution of vascular counts, and the effects of anaesthetic protocols on microcirculatory measurements.

4.1. Lack of validation of a human SDC-1 ELISA assay

The validation of a human SDC-1 ELISA kit for use on feline sera, was less successful than the adaption of SDFV and GlycoCheck™ for use in cats. Initial steps were promising, with the assay detecting strong binding and high optical densities in serum from a small number of critically ill cats, suggesting it could measure feline SDC-1. However, the assay failed to detect the recombinant feline SDC-1 (frSDC-1) that was produced for use as a positive control. This may have been due to the capture antibody binding a different protein, or more likely, insufficient antigenicity of the frSDC-1 due to differences in glycosylation or conformation. Had this step succeeded, validation could have proceeded with mass spectrometry as a confirmatory method.

Mass spectrometry, despite additional steps such as immunoprecipitation and gel electrophoresis, also failed to detect SDC-1 in samples with high optical densities. As discussed in chapter III, possible explanations include low abundance of the protein in the analysed samples, or its molecular structure differing from expected targets.

The validation process ran in parallel with the sampling for the experimental (Chapter IV and V) and clinical (Chapter VI) studies, instead of stepwise as originally planned, due to logistical delays and staffing constraints, extending timelines. Therefore, samples collected from Chapters IV, V and VI were batch-analysed while validation steps were taking place. As the ELISA validation was incomplete, the measurements were not reported or discussed in the chapters.

Despite the incomplete validation, this step is important to discuss for another reason. Recently several studies have reported the use of species-specific feline SDC-1 ELISA assays, reporting very low or undetectable concentrations. However, these assays were not developed *de novo* for the species, nor thoroughly validated, but rather assumed specificity based on SDC-1 protein sequence homology (personal communication). This raises concerns about the validity of published findings using unvalidated tools. In general, any test adapted for another species should undergo at least partial validation, particularly if used in clinical research where results may influence diagnosis or treatment. Unfortunately, this is still not standard practice in veterinary biomarker studies.

Syndecan-1 was selected for this thesis due to its relative specificity to the EG and wide use in human studies. However, it is not the only marker of EG damage. Hyaluronan, although not exclusive to the EG, is commonly measured alongside SDC-1 in both humans and dogs (94, 234, 247, 277, 325, 398) and validated assays exist for dogs and cats (291, 399). One limitation is that hyaluronan is abundant in interstitial tissue and may enter circulation due to fluid overload or inflammation, potentially being misinterpreted as EG-derived (64, 247).

Heparan sulfate, another biomarker widely used in EG research, is a glycosaminoglycan found on syndecans and other proteoglycans, responsible for their glycosylation (49, 56, 94, 193, 248, 273). It is cleaved from the proteoglycan structure in disease and can be measured unbound in serum or plasma (61). In human studies, it is often measured in combination with SDC-1 and other biomarkers. Future feline research should consider using multiple validated biomarkers of EG shedding to improve detection and interpretation.

4.2. Effects of packed cell volume on GlycoCheck™ parameters

Another notable finding from this project was the association between PCV and GlycoCheck™ parameters, namely valid vessel density (VVD), percentage red blood cell filling and (%RBC filling) and PBR. As PCV decreased, VVD and %RBC filling also decreased, while PBR increased, suggesting thinning of the EG. This relationship has been rarely documented in human literature, with only a single study in neonates (183) and one in adults (187) discussing it.

Since GlycoCheck™ parameters rely on sufficient RBC contrast for accurate calculation, this association suggests causality rather than mere correlation, as rarefication of the RBC during anaemia would potentially influence RBC contrast, potentially reducing number of vascular segments available for analysis (lower VVD), thus increasing signal variability and analytical errors calculating parameters deriving PBR, such as median P50 (median RBC column width) and perfused vascular diameter. The study protocol in Chapters IV and V induced transient but substantial PCV decreases following IV fluid administration and anaesthetic-induced fluid shifts in the control groups. These controlled conditions facilitated the identification of these associations in an experimental setting.

In contrast, the clinical study (Chapter VI) identified an effect of PCV on VVD but not PBR. This discrepancy may be due to the relatively small dataset and the low number of clinically anaemic

cats in the study population. Anaemia is common in sick animals, particularly in hospitalized cats, either as a presenting condition or as a secondary complication (400, 401). If PCV consistently influences GlycoCheck™ parameters, this warrants further investigation through specifically designed studies to account for haematological variability when interpreting microcirculatory data.

4.3. Vascular segment count distribution in GlycoCheck™ analysis

The GlycoCheck™ software initially detects vascular segments with 1 – 50 µm diameter, but only analyses and reports parameters from those with 5 – 25 µm. The GlycoCheck™ parameter estimating EG thickness – PBR, is further subdivided and reported as PBR 5 – 9 µm, 10 – 19 µm and 20 – 25 µm, all of which contribute to an average PBR 5 – 25 µm.

The number of 10 µm-long vascular segments contributing to each PBR subgroup - referred to here as vascular counts - is not included in the standard GlycoCheck™ report but is accessible through deeper exploration of the software. Perhaps for this reason, the distribution of vascular counts is rarely reported in the literature, with only two studies in people providing such data (215, 375). Notably, both studies reported a distribution similar to that observed in the current project.

In this study, vascular counts were analysed in Chapters V and VI, based on data availability. The distribution across PBR subsets was found to be significantly skewed, with segments in the 5–9 µm range accounting for approximately 60% of the total count. This finding is important for two reasons.

First, the PBR 5–9 µm is roughly half the size of the other PBR subsets in cats, dogs, and people. Its overrepresentation in the averaged PBR 5–25 µm may artificially lower the overall value and mislead interpretation. Second, vascular segments of different sizes may not respond to stimuli in a similar way. For example, in the study from chapter V, PBR 5–9 µm remained unchanged following volume overload, whereas larger PBRs increased over time in the control group. Such discrepancies suggest that overrepresentation of smaller segments could mask meaningful changes in the overall PBR, especially in studies that do not analyse subgroups separately. Unfortunately, most studies not only omit vascular counts, but also fail to report PBR subgroup breakdowns, which may lead to missed insights or misinterpretation of results (93, 94, 96, 99, 216). Since the vascular diameter distribution is inherently related to sublingual mucosal anatomy and cannot be altered, future studies should report PBR values stratified by vascular size. Notably, newer versions of the GlycoCheck™ system appear to have adopted this approach, alongside further functional distinction between smaller (5 – 7 µm) and larger capillaries, thereby enhancing interpretability in subsequent studies (93, 94, 156, 216).

4.4. Effects of anaesthetics on GlycoCheck™ parameters

Unlike adult people, all GlycoCheck™ image acquisition in small animals (dogs and cats) requires heavy sedation or general anaesthesia to sufficiently relax the jaw and allow safe insertion of the SDFV probe under the tongue. This procedural difference contributes to the discrepancies in GlycoCheck™ research between human and veterinary studies.

Furthermore, anaesthetic agents can have differing effects on the cardiovascular system, and by extension, on the microcirculation. In Chapter II, the use of an α2-agonist (medetomidine) - known to cause peripheral vasoconstriction - was compared with a non-α2-agonist sedation protocol, and no significant differences were found. However, the study was not powered to detect such effects, and subtle changes may have been missed.

In chapter IV, PBR 10 – 19 µm increased over time (20 min) in the control group, compared to baseline. A similar trend was observed in Chapter V, with increases in both PBR 5 – 25 µm and PBR 5 – 9 µm were documented in the control group. These changes extended beyond the initial anaesthesia period, peaking at 3 hours and returning to baseline by 24 hours. Notably, in the same chapters, PBR 10 – 19 µm decreased over time in the hydroxyethyl starch group (chapter IV) and PBR 5–9 µm diameter decreased at 3 hours in the IV fluid group (chapter V), suggesting a potential protective effect of IV fluids at the administered dose.

The mechanism behind the increase in PBR observed in the control groups remains unclear. However, as propofol was the primary anaesthetic agent used in both studies, its role in these changes warrants consideration.

Cats are known to be particularly sensitive to excessive propofol administration, which has been associated with oxidative damage and related complications (329-331). In people, high doses of propofol have been linked to the life-threatening "propofol-related infusion syndrome," suspected to result from mitochondrial dysfunction (323, 324). More recently, *in vitro* and *in vivo* studies have demonstrated EG damage following propofol overdose (321, 322). While a direct causative link between propofol and PBR changes remains unconfirmed, these findings raise the question of whether alternative anaesthetic agents may be more appropriate for microcirculatory research.

Since sedation or anaesthesia is a prerequisite for GlycoCheck™ imaging in veterinary patients, future research should aim to identify optimal anaesthetic regimens that minimise microcirculatory interference. This is particularly important for studies acquiring multiple datapoints over short timeframes (e.g. within 24 hours). In a clinical context - where anaesthetic protocols are often tailored to individual patient needs, rather than research needs - understanding how different agents affect the EG is essential for result interpretation. Determining which anaesthetics are most suitable for research purposes will improve data quality and reduce confounding variables in both experimental and clinical studies.

5. Theoretical and Practical Implications

Building on the key findings and methodological considerations outlined earlier, this section explores the broader theoretical and clinical implications of the study, including its relevance to current IV fluid practices, biomarker validation, and future directions in both veterinary and translational microvascular research.

5.1. IV fluids implications

This study did not identify measurable damage to the EG following IV fluid administration in healthy cats, as assessed by GlycoCheck™ parameters. These findings challenge the assumption that IV fluids necessarily cause EG injury in stable subjects and align with emerging data in human medicine. However, the absence of detectable harm should not be interpreted as confirmation that IV fluids, at the administered doses, are universally safe in cats. Rather, it highlights a critical gap in our understanding of feline-specific responses to IV fluids, and whether current assessment methods are sensitive enough to detect early or subtle EG changes.

Emerging data on feline volume kinetics reinforces long-held clinical observations: even healthy cats eliminate IV fluids slowly (130), especially when hypothermic (a common presentation in critical care) (131) and under general anaesthesia (251). These physiological characteristics may predispose cats to cumulative fluid overload, even if markers of EG disruption such as PBR remain unchanged. Furthermore, the dose used in the volume overload model (chapter V), although empirically considered "excessive", may not have been sufficient to induce detectable cardiac stretch or metabolic disturbance to provoke measurable EG alterations. Alternatively, current methodologies may simply lack the sensitivity required to detect minor or early-stage EG damage.

The lack of a validated "gold standard" for EG assessment in veterinary medicine further complicates interpretation. Negative findings, particularly in a methodological context, may reflect limitations of the tools used rather than true absence of pathology. Nonetheless, these are the best tools currently available, and their limitations must be addressed through thoughtful study design and cautious interpretation.

Importantly, the absence of overt EG disruption does not preclude the possibility of subclinical damage. In stable animals, such changes may be inconsequential; however, in critically ill cats, where compensatory mechanisms are often already strained, such subtle perturbations could carry significant clinical implications, especially potential for exacerbation. The fact that no EG injury was observed in the experimental studies does not confirm the absence of harm, particularly when extrapolating to sick patients. The exploratory clinical study was not able to address this question, primarily due to the limited number of cats receiving IV fluids. Thus, while the administered doses appeared safe in healthy animals, their impact on the EG in unwell cats remains unknown.

Ultimately, determining the true safety and appropriateness of IV fluid regimens in cats, whether in relation to microcirculatory disturbances or other potential complications, will require moving beyond empirical norms. Well-designed, adequately powered studies are needed to investigate feline-specific physiology, incorporate refined volume kinetics, and assess potential microcirculatory effects, including cumulative or delayed responses. IV fluid research, particularly in feline medicine, is still in its early stages. Similarly, these experimental chapters of this thesis were largely exploratory, lacking foundation on prior feline research. As such, they were not equipped to answer whether IV

fluids are harmful to the feline EG. Rather, they offer foundational step toward understanding the feline microcirculation in response to IV fluids and open the door to future lines of inquiry.

5.2. Implications in disease

While the clinical part of this project did not establish a definitive link between disease type or severity and GlycoCheck™ parameters in cats, it represents the first step in clinical feline microcirculatory research. The study findings highlight the challenges in evaluating EG changes in naturally occurring disease in veterinary cohorts, where illness severity in patients that reach access to diagnostics and treatments might be milder compared to human critical care settings, with more compromised veterinary patients potentially being euthanized because of severity, associated costs and welfare. The results emphasize the need for larger well-powered studies to determine how the GlycoCheck™ can be useful to monitor the microcirculation in sick veterinary patients. From a translational perspective, FIP, a viral disease with microvascular involvement could prove to be a valuable model for future research, as there are similarities between FIP and other viral diseases such as COVID-19 to be explored.

At this stage, the GlycoCheck™ system is not suitable for individual patient monitoring, particularly in veterinary medicine, and is therefore not a tool for routine inclusion in clinical practice. However, it represents a promising step toward addressing a critical gap in patient care: the lack of clinically applicable tools for assessing microcirculatory health. This need is especially relevant given the growing body of evidence linking microcirculatory dysfunction to multi-organ failure and poor outcomes in critically ill patients (46, 58, 60, 113, 163, 359, 360). While some limitations of the system are methodological, many reflect a lack of foundational research to guide patient selection, timing of assessments, and appropriate clinical responses. These challenges are further compounded by global disparities in socio-economic conditions. In wealthier regions, severely ill patients may undergo advanced diagnostics and treatments, facilitating research and clinical implementation. In contrast, financial constraints in less affluent settings often lead to earlier euthanasia, limiting opportunities for data collection and translational progress.

To determine the real-world utility of this tool, multi-centre studies across diverse cohorts and clinical settings are essential. For instance, the GlycoCheck™ system may never be practical for general practice, yet it could become invaluable in high-dependency critical care environments - provided ongoing research renders it suitable for individual patient monitoring.

Addressing these gaps through targeted investigation is therefore critical, not only to refine the technology itself, but to ensure we are developing tools capable of meeting clinical needs. In this context, GlycoCheck™ may represent the most feasible path forward, and improving its clinical utility remains a worthwhile goal. Encouragingly, ongoing advances in technology, including automated analysis, machine learning, and artificial intelligence, may help accelerate this refinement, improving the system's reliability, usability, and adaptability across a range of clinical environments.

5.3. Methodological implications

5.3.1. Endothelial glycocalyx shedding biomarkers

The methodological considerations that emerged from this project underscore key factors that may influence the theoretical and clinical applications in microcirculatory research. The challenges with the SDC-1 ELISA assay validation highlight the need for species-specific biomarker development and robust validation of assays with provenances from other species. Unvalidated biomarker uses risks result misinterpretation and negatively impacts advancements of not only EG-related research, but veterinary research in general. Currently, interpretation of SDC-1 studies in veterinary medicine remains unreliable and clinicians using biomarkers should be cautious in translating this into therapeutic decision-making. This is further complicated by the broader debate surrounding the clinical utility of EG shedding assessment, even in human medicine, which raises questions about the justification for adopting this methodology (47, 113, 168, 249). However, EG shedding biomarkers such as SDC-1 do address a key limitation of GlycoCheck™ analysis in small animals, namely, the requirement for general anaesthesia, by relying solely on a blood sample. As such, they may offer a feasible alternative for patients unsuitable for anaesthesia, provided that robust validation and further research establish their reliability and clinical relevance in veterinary medicine.

5.3.2. Packed cell volume

This study found that PCV might be a confounding factor in GlycoCheck™ microcirculatory analysis, suggesting that EG thickness estimations might not solely reflects endothelial health, but be influenced by haematological changes. Since anaemia is commonly associated with critical illness in dogs and cats, establishing and applying PCV adjustments for GlycoCheck™ parameters in clinical practice might be the topic of future research and subsequent clinical practices. Until then, PCV should be measured alongside GlycoCheck™ analysis in both research and clinical settings, and results in anaemic patients should be interpreted with appropriate caution.

5.3.3. Anaesthetics

Finally, the influence of anaesthetic agents on EG measurements suggests that microvascular studies should carefully standardize anaesthetic protocols to minimize confounding effects. Although propofol is widely considered safe, it may not be the optimal agent for EG studies based on the findings from chapter IV and V, suggesting potential negative effects on the EG. That said, these effects are at least partially characterized and can be accounted for in data interpretation. In contrast, the use of other anaesthetic agents, particularly in clinical research, should be approached cautiously unless their impact on the EG has been validated, at minimum, in healthy subjects.

Overall, this project has advanced both theoretical and clinical aspects of the largely uncharted field of feline microcirculatory research. While the findings are not groundbreaking, they serve as important stepping stones for future experimental and clinical studies, including translational research.

6. Strengths

Having outlined the core findings and their broader implications, this section reflects on the study's strengths and limitations - highlighting both the methodological rigor that supports its contributions and the challenges that should guide future feline microvascular research.

This project serves as initiator in feline microvascular research, with its strengths lying in the systematic adaptation and validation of EG assessment tools before investigating EG changes in response to stimuli (IV fluids and disease) - a crucial step often overlooked in veterinary studies. By establishing species-specific tolerance intervals through GlycoCheck™ analysis in a large, demographically varied cohort, the study sets a strong foundation for assessing pathological changes. Additionally, an attempted validation of a human ELISA assay for detecting SDC-1 in feline sera, while inconclusive, highlights the challenges of biomarker adaptation and the need for species-specific validation.

Each chapter was conducted in a logical sequence, building upon prior results - from feasibility and tolerance intervals (Chapter II) to the effects of clinically relevant IV fluid doses (Chapter IV), fluid overload (Chapter V), and finally, an exploration of methodologies in a clinical setting (Chapter VI). The experimental studies were rigorously controlled, with randomized groups, blinded operators, and predefined sample sizes, ensuring data reliability. Chapter IV compared two clinically used IV fluids - crystalloids and synthetic colloids - against a no fluid control, contributing to the long-standing debate on their relative effects. Chapter V improved upon this design by implementing a crossover model, allowing each subject to serve as its own control, thereby reducing inter-subject variability.

Although the clinical study was small-scale, it demonstrated the feasibility of collecting microcirculatory data in a clinical workflow, an essential consideration for future large-scale investigations. Collectively, these findings lay the groundwork for future studies in both experimental and clinical settings.

7. Limitations

Several limitations of this thesis merit consideration. Some relate to broader methodological challenges in microvascular research, while others are specific to this project's design and execution.

7.1. Methodological challenges in microvascular research

One of the fundamental challenges in endothelial glycocalyx (EG) research is the lack of a universally accepted "gold standard" for its assessment in any species, including cats. This limitation makes it difficult to establish definitive reference values and to confidently interpret deviations from normal. However, the concept of a "gold standard", especially in clinical monitoring, is itself somewhat arbitrary, often relying on invasive methods that are impractical or even unethical in many settings. For example, the use of a pulmonary artery catheter (placed in the heart) is considered the gold standard for measuring cardiac output, yet its invasiveness renders it unsuitable for routine or even experimental use

in many veterinary contexts. Instead, modern approaches increasingly favour less invasive alternatives such as ultrasound or bioimpedance, which are becoming mainstream.

Rather than relying on comparison with outdated or impractical gold standards, many clinical monitoring tools are now developed as standalone methodologies, validated through the establishment of reference intervals and their ability to detect clinically relevant abnormalities. In this context, the current project offered important initial steps in validating GlycoCheck™ in cats. However, interpretation was hindered by the lack of existing data defining which deviations from normal are clinically meaningful. For example, while we assumed that administering 30 ml/kg of Hartmann's solution would induce volume overload, robust evidence supporting this assumption in cats is lacking, limiting our ability to interpret changes as pathological. Similarly, we hypothesized that critically ill cats would have a thinner EG compared to healthy controls, but data establishing how "sick" a cat must be to exhibit EG thinning are currently unavailable.

Thus, the primary limitation may not be the absence of a gold standard per se, but rather the lack of prior research defining what constitutes pathophysiological deviation. To assess the clinical reliability of tools like GlycoCheck™, future studies must be conducted within the context of known physiological extremes or disease states and in sufficiently powered, well-designed cohorts.

Another key limitation lies in the current focus on structural assessment of the EG, without well-established guidelines to correlate EG changes to functional impairment (e.g., at what point a thinner EG begins to compromise vascular function) (113, 118, 249). Although EG thinning and shedding are associated with disease processes in studies, direct causal links to clinically meaningful outcomes, such as oedema formation, impaired oxygen delivery, or increased morbidity and mortality, remain poorly defined (113). For example, EG shedding increases during sepsis and may correlate with illness severity (156, 158, 200, 234, 271, 274). However, because EG constituent synthesis (e.g., SDC-1) also increases during sepsis, it is unclear whether observed elevations truly reflect pathological shedding (47, 55, 56).

Moreover, while EG covers the entire endothelial surface, most vascular permeability is regulated at intercellular tight junctions, which represent only a small fraction of the endothelial surface area (113). Shedding of junctional components (e.g., VE-cadherin) is rarely measured, and most EG shedding biomarkers reflect loss from the broader glycocalyx, not the tight junctions critical to barrier function. This raises the question of whether EG shedding is merely an epiphenomenon of endothelial injury or a direct contributor to the downstream consequences observed in disease states.

Further complicating the interpretation of shedding studies is the question of assay validity. Currently available ELISA kits, often developed for human medicine, may not reliably quantify EG biomarkers in veterinary patients. For instance, syndecan-1 has yielded consistently detectable results in horses and foals (288, 365) but produced low or undetectable concentrations in cats and dogs (94, 242, 243, 247, 346), raising doubts about its applicability. The attempt to validate a human SDC-1

assays for cats in this project, was unsuccessful. Hyaluronan, another commonly measured EG component, may have better sensitivity but its abundance in the interstitium complicates interpretation.

Beyond methodological concerns, the clinical relevance of EG shedding biomarkers remains unclear. Should elevations be correlated with outcomes such as weight gain from fluid overload, inflammatory biomarkers, hospital duration, or mortality? Until these associations are better defined, the clinical utility of EG shedding measurements will remain limited.

Similar considerations apply to GlycoCheck™ analysis. Importantly, GlycoCheck™ does not directly measure EG thickness, but estimates it based on the lateral movement of red blood cells (RBCs) into the vessel wall (90). The assumption is that a thinner EG allows RBCs to move closer to the endothelium. However, this has not been conclusively validated. Other factors such as changes in blood viscosity (e.g., from anaemia or haemoconcentration) or vascular tone could also potentially influence RBC behaviour, confounding interpretations (220).

In the present studies, propofol administration may have influenced EG measurements not only through potential EG damage but also via osmotic effects leading to dehydration of the glycocalyx. Similarly, IV fluids might either damage the EG or overhydrate it, affecting RBC lateralization. Sequential PBR measurements across time in chapter V of this thesis, demonstrated relatively rapid returns to baseline, which may not align with current understanding of EG repair timelines (typically hours to days) (47). This raises further questions about what exactly GlycoCheck™ measurements reflect.

The inability of this project to establish a definitive link between EG changes and clinical outcomes likely reflects both the inherent complexities of EG research and the exploratory nature of the study. It is also influenced by the relatively minor insults delivered to the EG in healthy subjects and the limited severity of illness among the enrolled clinical cohort. Future research should move beyond simply documenting EG injury, whether through GlycoCheck™ analysis or EG shedding biomarkers, and focus on demonstrating whether such injury translates into clinically meaningful consequences. These include whether EG disruption affects critical outcomes such as survival, hospitalization duration, financial aspects of care, or long-term recovery. Moreover, it is important to recognize that EG damage undoubtedly existed long before we could measure it. The value of EG research now lies in clarifying what these measurable changes mean for patient care. Currently, both sublingual SDFV and biomarkers of EG shedding are restricted to research applications, with limited utility in real-time clinical decision-making for individual patients. While these tools provide valuable insights into microvascular health at a population level, their role in guiding bedside diagnostics or treatment strategies remains uncertain. This limitation reflects not only the methodological challenges outlined above but also the relative novelty of EG research itself. Nonetheless, this uncertainty should serve as a driver for future research. Establishing clear causal links between EG measurements and clinical outcomes, identifying appropriate patient cohorts, determining optimal timing for assessments, and evaluating therapeutic interventions represent critical next steps toward transforming these promising

clinically applicable tools into ***clinical necessities***, guiding individual clinical decision making, whether in selecting IV fluid regimens, monitoring progress of disease or specific therapeutic interventions targeting the EG.

Another important methodological constraint specific to GlycoCheck™ analysis in small animals is the requirement for heavy sedation or general anaesthesia. Anaesthetic agents can influence microcirculatory function, introducing an additional layer of variability, This was demonstrated by the results in chapter IV and V, where propofol administration alone (without IV fluids) resulted in increases in PBR over time. Furthermore, anaesthesia-related microcirculatory changes have been reported in human studies, although these findings may be confounded by surgery-induced inflammation in surgical patients (116). This makes distinguishing true biological changes from drug-induced alterations challenging. Standardizing anaesthesia protocols, or at minimum understanding their impact, will be essential for minimizing this confounding factor in future studies. Addressing such technical challenges is particularly important as research progresses from controlled experimental settings into more heterogeneous clinical environments, as reflected in the limitations of the present project.

7.2. Project-related limitations

Due to time constraints and the necessity of limiting anaesthetic duration, inter-operator variability could not be formally assessed. While studies in humans suggest minimal variation, the degree to which this holds true in feline research remains unknown. In the clinical study, two operators were separately responsible for data collection, potentially introducing bias in image acquisition and analysis. Additionally, logistical constraints, including COVID-19-related delays, required the use of two different, though identical, GlycoCheck™ devices across different study phases. While no major discrepancies were expected, this factor necessitates caution when comparing results across chapters.

Regarding study power, sample size calculations were performed where necessary, but initial estimates were extrapolated from other species, primarily humans and rabbits. While adjustments were made based on preliminary feline data, the interventions used for these calculations were not perfectly aligned with this next study design. For example, in Chapter V, sample size was based on data from Chapter IV, but the study designs differed in scope - one assessed an IV fluid challenge, while the other focused on IV volume overload. This may have resulted in the experimental studies being underpowered to detect subtle effects. Additionally, interventions were intentionally mild to avoid harm to research cats, meaning that only transient effects were assessed.

The validation of the SDC-1 ELISA assay also presented challenges. A limited volume of positive samples restricted the ability to repeat tests, particularly for mass spectrometry detection of SDC-1. The requirement for batch analysis led to delayed identification of positive samples, preventing additional sample collection. Furthermore, unexpected technical setbacks - including lab relocations, supply chain disruptions, and prolonged validation timelines - may have contributed to inconsistencies.

Notably, the recombinant feline SDC-1 failed to appear in any analysis, raising questions about whether the synthesized protein was structurally or functionally comparable to true feline SDC-1. Future research should prioritize identifying and synthesizing a validated feline-specific SDC-1 control, whether by using a different cell line for expression (e.g. endothelial cells) or modifying glycosylation. This should be accompanied by sample volumes for other detection techniques and potentially combining mass spectrometry with nuclear magnetic resonance.

The clinical study component, while designed to integrate smoothly into hospital workflow, was ultimately limited in scale. The final sample size was lower than anticipated due to a significant decline in clinical caseload, reducing statistical power. Additionally, the cohort was biased toward trauma cases, which, while reflective of typical hospital admissions, may not be fully representative of broader feline patient populations. The lower-than-expected severity of illness among enrolled cats may have also contributed to negative findings, as the degree of EG damage in these patients may not have been sufficient to detect measurable changes. However, this reflects the true patient distribution in clinical practice, and future studies should account for "real-world" variability in severity of illness when designing inclusion criteria. Future clinical studies should focus on multi-centre enrolment to ensure sufficient sample size and the identification of cohorts with a severity of illness high enough to detect EG changes and link them to clinical outcomes.

Despite these limitations, this project provides foundational insights into feline microvascular research. The study highlights key areas for methodological refinement, including the need for validated feline-specific biomarkers, standardized sedation protocols, and improved clinical integration of microcirculatory assessment tools. While some limitations were inherent to the research field itself, others offer opportunities for future investigation, helping to shape more robust and clinically applicable studies in veterinary microvascular health.

7.3 Species-related limitations of the GlycoCheck™ system

The GlycoCheck™ software was developed for use in human subjects. The analysed range of vascular diameters (5–25 μm) broadly corresponds to what is defined by experts as "microvessels" (<20 μm), encompassing arterioles, capillaries, and venules, with capillaries measuring <10 μm in diameter (177, 402, 403). However, this classification is based on human microvascular anatomy, and does not explicitly account for anatomic or functional inter-species differences. Such inter-species differences may influence both the analytical performance of the system and the interpretation of parameters related to capillary function. One example is valid vessel density (VVD), which appears to be substantially lower in cats compared with dogs and people (90, 95, 100). Whether this reflects true anatomical and physiological differences or limitations in software performance when applied to feline microcirculatory images remains unclear. In support of genuine inter-species differences, cats have a lower blood volume than dogs and people (approximately 55 ml/kg lean body weight) (252) and subjectively appear to have a less dense sublingual capillary network under a videomicroscope

(personal observation). Differences in capillary bed density have been reported across mammalian species (279) including studies using SDFV to assess perfused vessel density in cats, dogs, and horses (170, 173, 174, 280). Conversely, analytical performance may also contribute. Feline haemoglobin exhibits lower oxygen affinity (282), while maintaining similar oxygen content compared with other species (283). Although subtle, these differences may influence image-based software analysis. In addition, lower capillary density would result in fewer detectable vessel segments and datapoints, potentially increasing measurement noise and variability. Consistent with this, moderate intra- and inter-subject variability has been reported in a large cohort of healthy cats (n = 101) (100). However, since human studies have also demonstrated variability, this could not be a species-specific difference, but rather an analytical limitation (181, 185, 186). Accordingly, until comparative validation data across species become available, results should be interpreted with caution and direct inter-species comparisons avoided. Large samples sizes and robust study designs, allowing replicability would improve within-species result interpretation and therefore, integration of knowledge into practice.

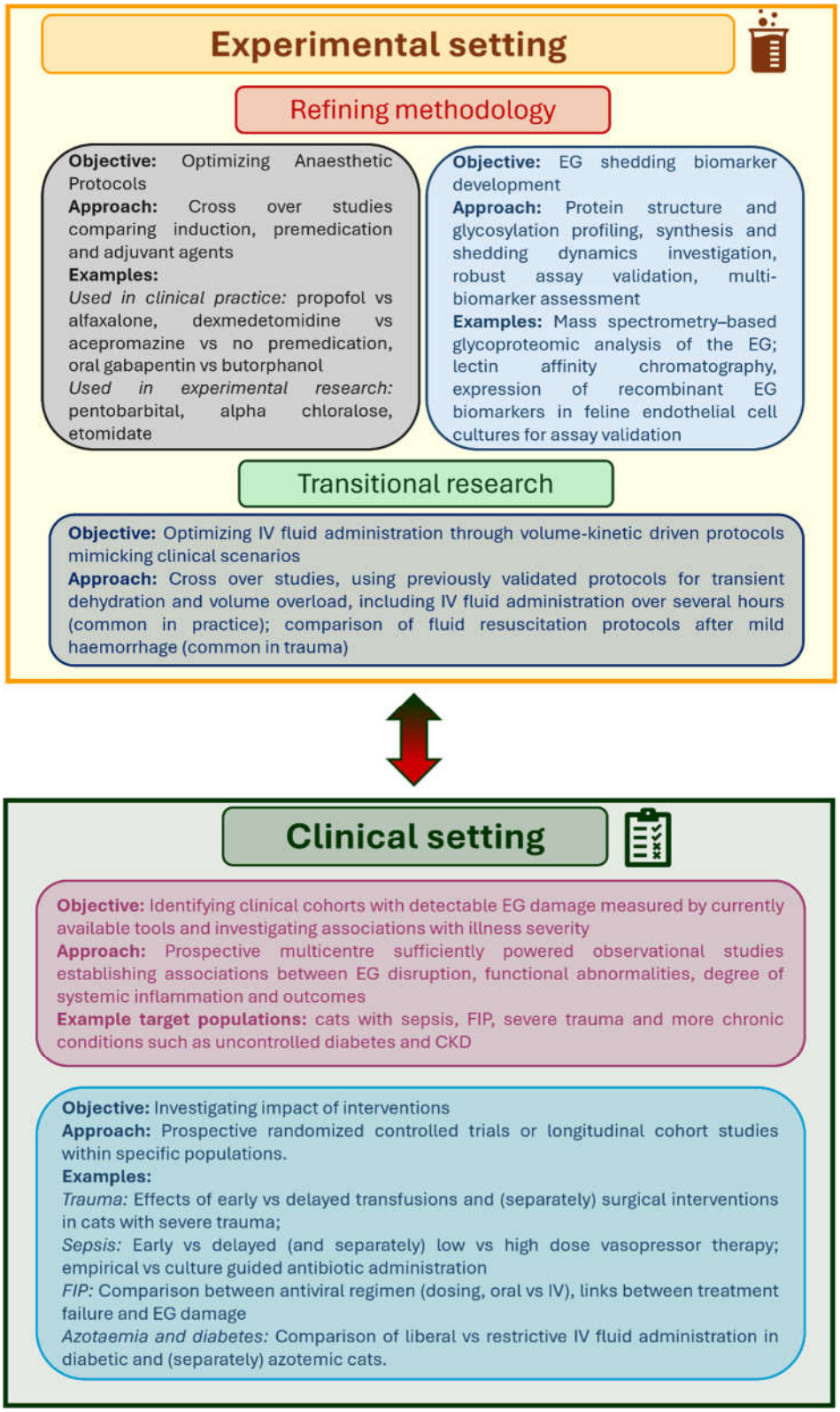
8. Future Perspectives

This project lays the groundwork for a focused research agenda aimed at translating microcirculatory assessment into feline clinical practice. Building on its findings and identified gaps, a clear progression from methodological refinement to clinical validation is now possible. The proposed roadmap (Figure 7.1) outlines key next steps, from optimizing anaesthetic protocols and fluid regimens in controlled experimental settings, to identifying disease cohorts and conducting multicentre observational and interventional studies. While current tools such as GlycoCheck™ are not yet suitable for individual patient monitoring, they hold considerable promise if refined through targeted research.

Microcirculatory dysfunction plays a central role in the pathophysiology of critical illness yet remains inaccessible to routine assessment. Existing surrogate markers lack the sensitivity and specificity to detect early microvascular derangements. Direct evaluation of the endothelium and capillary networks could offer a transformative dimension in managing feline critical illness. Development of feline-specific biomarkers for EG shedding, although currently having substantial limitations, would further expand accessibility by reducing reliance on imaging tools, and could facilitate microvascular monitoring in general practice settings.

As interest in feline medicine grows, there is an urgent need to address the species-specific physiological nuances that shape disease expression and therapeutic response. Advancing our understanding of the feline microcirculation will be key to developing evidence-based guidelines for care, and ultimately, improving outcomes in this unique and often understudied patient population.

Figure 7.1. Roadmap to future feline endothelial glycocalyx studies.



9. Final Conclusion

This study achieved several key milestones in feline microvascular research, including the first comprehensive evaluation of the feline EG and the validation and adaptation of a human microcirculatory assessment tool for veterinary use. It also provided the first investigation into the effects of IV fluids on the feline EG, contributing to the broader and understudied field of IV fluid administration in cats. Additionally, it identified PCV as a potential confounding factor in GlycoCheck™ analysis, reinforcing the need to account for haematological variables in microcirculatory research.

Beyond these findings, this study offers novel insights into inter-species differences in microvascular structure, highlighting the limitations of direct species comparisons due to anatomical and physiological variations. It also raises concerns about the use of unvalidated biomarker assays in feline research, emphasizing the importance of species-specific validation before clinical application. Furthermore, it demonstrates that anaesthetic protocols may influence GlycoCheck™ parameters, underscoring the need for refined sedation or anaesthesia protocols in microcirculatory studies.

Collectively, these findings lay the groundwork for future experimental and clinical studies in feline microvascular health. By addressing methodological challenges, refining assessment tools, and expanding clinical applications, this work provides a strong foundation for advancing evidence-based veterinary practices in feline critical care and IV fluid administration.

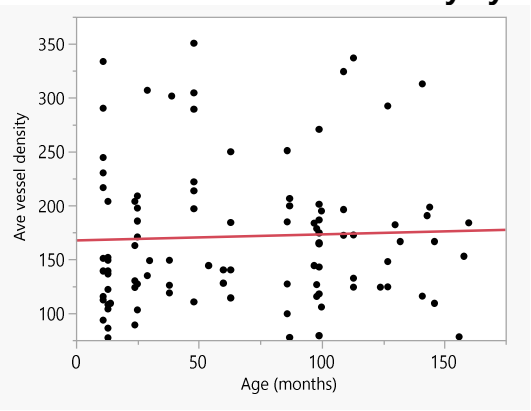
Annexes

Annex I: Chapter II Unformatted statistical report

Rapid patient-side evaluation of endothelial glycocalyx thickness in healthy sedated cats using GlycoCheck™ software

Fit Group

Bivariate Fit of Ave vessel density By Age (months)



Linear Fit

Ave vessel density = 167.33719 + 0.0565904*Age (months)

Summary of Fit

RSquare	0.0016
RSquare Adj	-0.00869
Root Mean Square Error	65.82423
Mean of Response	171.1699
Observations (or Sum Wgts)	99

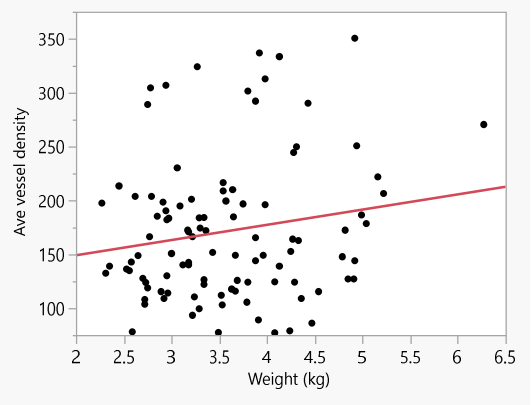
Analysis of Variance

Source	DF	Sum of Squares	Mean Square	F Ratio
Model	1	673.65	673.65	0.1555
Error	97	420284.47	4332.83	**Prob > F**
C. Total	98	420958.12		0.6942

Parameter Estimates

Term	Estimate	Std Error	t Ratio	Prob>|t|
Intercept	167.33719	11.75789	14.23	<.0001*
Age (months)	0.0565904	0.143519	0.39	0.6942

Bivariate Fit of Ave vessel density By Weight (kg)



Linear Fit

Linear Fit

Ave vessel density = 120.85621 + 14.087966*Weight (kg)

Summary of Fit

RSquare	0.029314
RSquare Adj	0.019509
Root Mean Square Error	64.42348
Mean of Response	171.2688
Observations (or Sum Wgts)	101

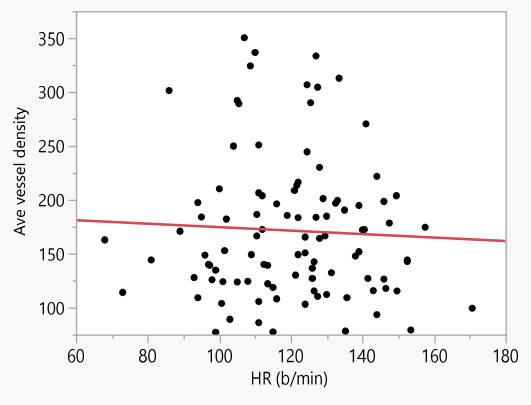
Analysis of Variance

Source	DF	Sum of Squares	Mean Square	F Ratio
Model	1	12408.62	12408.6	2.9898
Error	99	410888.03	4150.4	**Prob > F**
C. Total	100	423296.65		0.0869

Parameter Estimates

Term	Estimate	Std Error	t Ratio	Prob>|t|
Intercept	120.85621	29.85197	4.05	0.0001*
Weight (kg)	14.087966	8.147618	1.73	0.0869

Bivariate Fit of Ave vessel density By HR (b/min)



Linear Fit

Linear Fit

Ave vessel density = 190.47295 - 0.1599388*HR (b/min)

Summary of Fit

RSquare	0.002269
RSquare Adj	-0.00781
Root Mean Square Error	65.31478
Mean of Response	171.2688
Observations (or Sum Wgts)	101

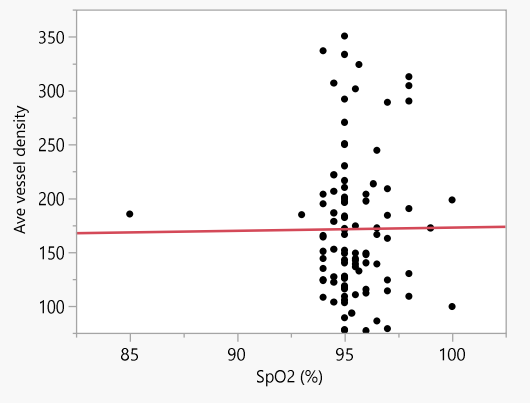
Analysis of Variance

Source	DF	Sum of Squares	Mean Square	F Ratio
Model	1	960.60	960.60	0.2252
Error	99	422336.05	4266.02	**Prob > F**
C. Total	100	423296.65		0.6362

Parameter Estimates

Term	Estimate	Std Error	t Ratio	Prob>|t|
Intercept	190.47295	40.98866	4.65	<.0001*
HR (b/min)	-0.159939	0.33705	-0.47	0.6362

Bivariate Fit of Ave vessel density By SpO2 (%)



Linear Fit

Linear Fit

Ave vessel density = 142.05379 + 0.3061228*SpO2 (%)

Summary of Fit

RSquare	0.000061
RSquare Adj	-0.01004
Root Mean Square Error	65.38703
Mean of Response	171.2688
Observations (or Sum Wgts)	101

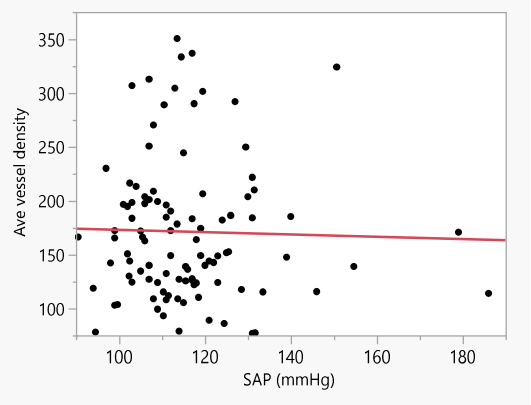
Analysis of Variance

Source	DF	Sum of Squares	Mean Square	F Ratio
Model	1	25.78	25.78	0.0060
Error	99	423270.87	4275.46	**Prob > F**
C. Total	100	423296.65		0.9383

Parameter Estimates

Term	Estimate	Std Error	t Ratio	Prob>|t|
Intercept	142.05379	376.2828	0.38	0.7066
SpO2 (%)	0.3061228	3.942202	0.08	0.9383

Bivariate Fit of Ave vessel density By SAP (mmHg)



Linear Fit

Ave vessel density = 183.61534 - 0.1065462*SAP (mmHg)

Summary of Fit

RSquare	0.000629
RSquare Adj	-0.00947
Root Mean Square Error	65.36844
Mean of Response	171.2688
Observations (or Sum Wgts)	101

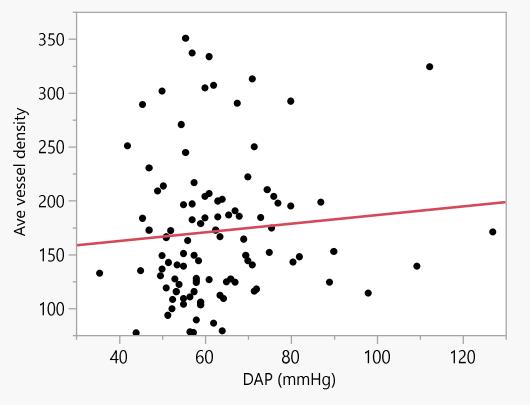
Analysis of Variance

Source	DF	Sum of Squares	Mean Square	F Ratio
Model	1	266.40	266.40	0.0623
Error	99	423030.25	4273.03	**Prob > F**
C. Total	100	423296.65		0.8033

Parameter Estimates

Term	Estimate	Std Error	t Ratio	Prob>|t|
Intercept	183.61534	49.87383	3.68	0.0004*
SAP (mmHg)	-0.106546	0.426718	-0.25	0.8033

Bivariate Fit of Ave vessel density By DAP (mmHg)



Linear Fit

Linear Fit

Ave vessel density = 145.99516 + 0.4027939*DAP (mmHg)

Summary of Fit

RSquare	0.00812
RSquare Adj	-0.0019
Root Mean Square Error	65.12299
Mean of Response	171.2688
Observations (or Sum Wgts)	101

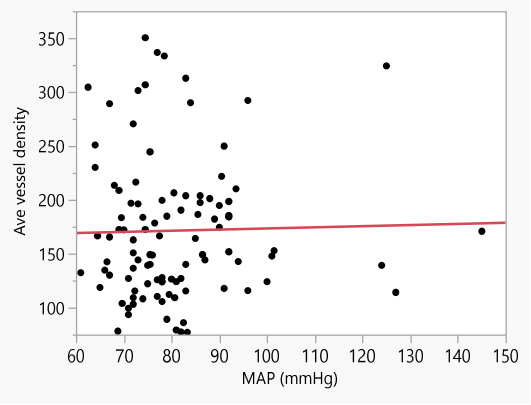
Analysis of Variance

Source	DF	Sum of Squares	Mean Square	F Ratio
Model	1	3437.28	3437.28	0.8105
Error	99	419859.38	4241.00	**Prob > F**
C. Total	100	423296.65		0.3702

Parameter Estimates

Term	Estimate	Std Error	t Ratio	Prob>|t|
Intercept	145.99516	28.81157	5.07	<.0001*
DAP (mmHg)	0.4027939	0.447415	0.90	0.3702

Bivariate Fit of Ave vessel density By MAP (mmHg)



Linear Fit

Linear Fit

Ave vessel density = 162.88007 + 0.1040704*MAP (mmHg)

Summary of Fit

RSquare	0.000481
RSquare Adj	-0.00961
Root Mean Square Error	65.37328
Mean of Response	171.2688
Observations (or Sum Wgts)	101

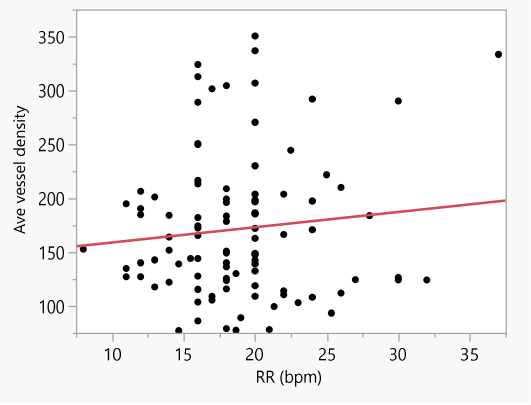
Analysis of Variance

Source	DF	Sum of Squares	Mean Square	F Ratio
Model	1	203.69	203.69	0.0477
Error	99	423092.96	4273.67	**Prob > F**
C. Total	100	423296.65		0.8276

Parameter Estimates

Term	Estimate	Std Error	t Ratio	Prob>|t|
Intercept	162.88007	38.97111	4.18	<.0001*
MAP (mmHg)	0.1040704	0.476691	0.22	0.8276

Bivariate Fit of Ave vessel density By RR (bpm)



Linear Fit

Linear Fit

Ave vessel density = 144.52109 + 1.4201085*RR (bpm)

Summary of Fit

RSquare	0.011297
RSquare Adj	0.00131
Root Mean Square Error	65.01864
Mean of Response	171.2688
Observations (or Sum Wgts)	101

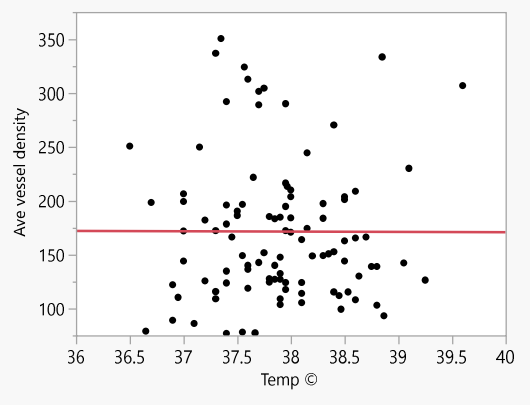
Analysis of Variance

Source	DF	Sum of Squares	Mean Square	F Ratio
Model	1	4781.78	4781.78	1.1311
Error	99	418514.87	4227.42	**Prob > F**
C. Total	100	423296.65		0.2901

Parameter Estimates

Term	Estimate	Std Error	t Ratio	Prob>|t|
Intercept	144.52109	25.96833	5.57	<.0001*
RR (bpm)	1.4201085	1.335256	1.06	0.2901

Bivariate Fit of Ave vessel density By Temp ©



Linear Fit

Ave vessel density = 182.91444 - 0.3074091*Temp ©

Summary of Fit

RSquare	8.219e-6
RSquare Adj	-0.01009
Root Mean Square Error	65.38875
Mean of Response	171.2688
Observations (or Sum Wgts)	101

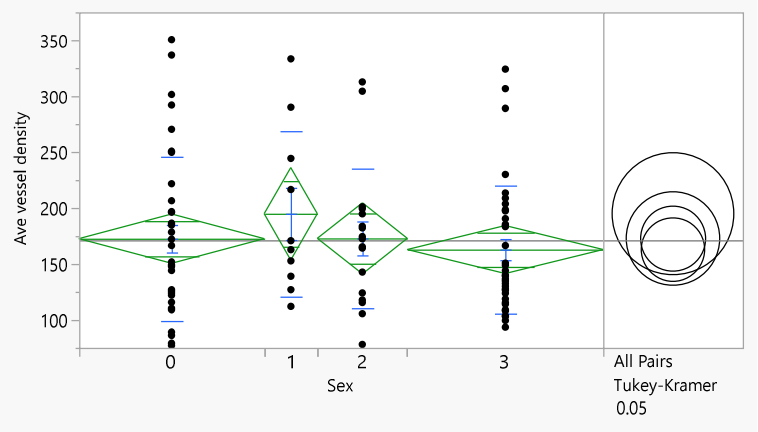
Analysis of Variance

Source	DF	Sum of Squares	Mean Square	F Ratio
Model	1	3.48	3.48	0.0008
Error	99	423293.17	4275.69	**Prob > F**
C. Total	100	423296.65		0.9773

Parameter Estimates

Term	Estimate	Std Error	t Ratio	Prob>|t|
Intercept	182.91444	408.3073	0.45	0.6551
Temp ©	-0.307409	10.7767	-0.03	0.9773

Oneway Analysis of Ave vessel density By Sex



Oneway Anova
Summary of Fit

Rsquare	0.01976
Adj Rsquare	-0.0112
Root Mean Square Error	65.90584
Mean of Response	171.1699
Observations (or Sum Wgts)	99

Analysis of Variance

Source	DF	Sum of Squares	Mean Square	F Ratio	Prob > F
Sex	3	8318.02	2772.67	0.6383	0.5922
Error	95	412640.11	4343.58		
C. Total	98	420958.12			

Means and Std Deviations

Level	Number	Mean	Std Dev	Std Err Mean	Lower 95%	Upper 95%
0	35	172.55229	73.395394	12.406086	147.34009	197.76449
1	10	194.8	73.881447	23.363365	141.9484	247.6516
2	17	172.75471	62.413643	15.137532	140.66457	204.84484
3	37	162.74757	57.259748	9.4134446	143.65622	181.83892

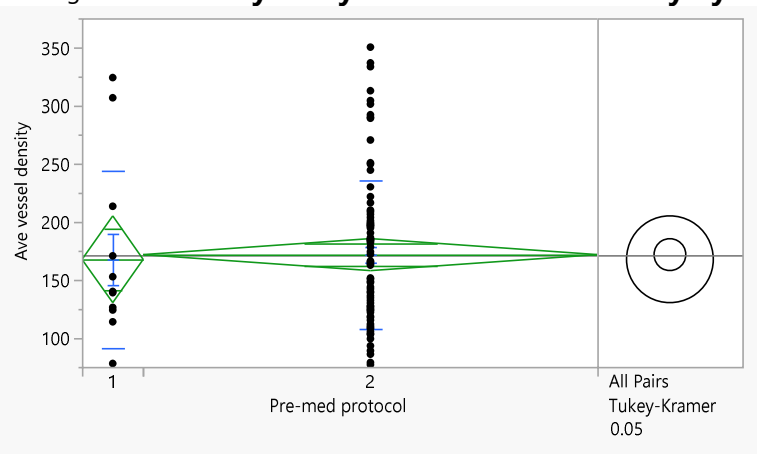
Means Comparisons
Comparisons for all pairs using Tukey-Kramer HSD

Connecting Letters Report

Level		Mean
1	A	194.80000
2	A	172.75471
0	A	172.55229
3	A	162.74757

Levels not connected by same letter are significantly different.

Missing Rows2**Oneway Analysis of Ave vessel density By Pre-med protocol**



Oneway Anova
Summary of Fit

Rsquare	0.000405
Adj Rsquare	-0.00969
Root Mean Square Error	65.37579
Mean of Response	171.2688
Observations (or Sum Wgts)	101

Analysis of Variance

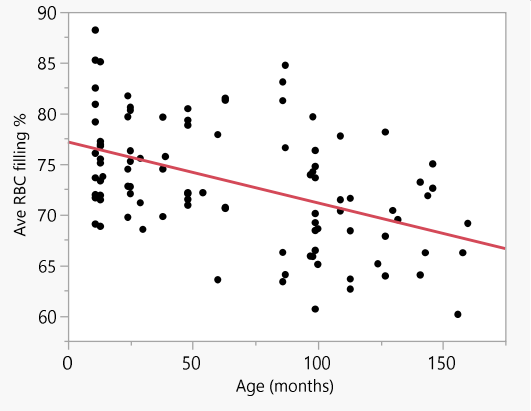
Source	DF	Sum of Squares	Mean Square	F Ratio	Prob > F
Pre-med protocol	1	171.26	171.26	0.0401	0.8418
Error	99	423125.39	4273.99		
C. Total	100	423296.65			

Means and Std Deviations

Level	Number	Mean	Std Dev	Std Err Mean	Lower 95%	Upper 95%
1	12	167.7225	76.342994	22.038324	119.21648	216.22852
2	89	171.74697	63.872619	6.7704841	158.29205	185.20188

Means Comparisons
Comparisons for all pairs using Tukey-Kramer HSD

Bivariate Fit of Ave RBC filling % By Age (months)



Linear Fit

Linear Fit

Ave RBC filling % = 77.139487 - 0.0602504*Age (months)

Summary of Fit

RSquare	0.222053
RSquare Adj	0.214033
Root Mean Square Error	5.251652
Mean of Response	73.05889
Observations (or Sum Wgts)	99

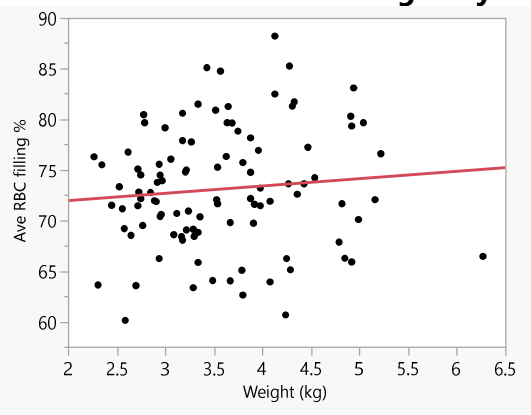
Analysis of Variance

Source	DF	Sum of Squares	Mean Square	F Ratio
Model	1	763.6081	763.608	27.6872
Error	97	2675.2453	27.580	**Prob > F**
C. Total	98	3438.8534		<.0001*

Parameter Estimates

Term	Estimate	Std Error	t Ratio	Prob>|t|
Intercept	77.139487	0.938079	82.23	<.0001*
Age (months)	-0.06025	0.01145	-5.26	<.0001*

Bivariate Fit of Ave RBC filling % By Weight (kg)



Linear Fit

Linear Fit

Ave RBC filling % = 70.467774 + 0.7283626*Weight (kg)

Summary of Fit

RSquare	0.009457
RSquare Adj	-0.00055
Root Mean Square Error	5.92387
Mean of Response	73.07416
Observations (or Sum Wgts)	101

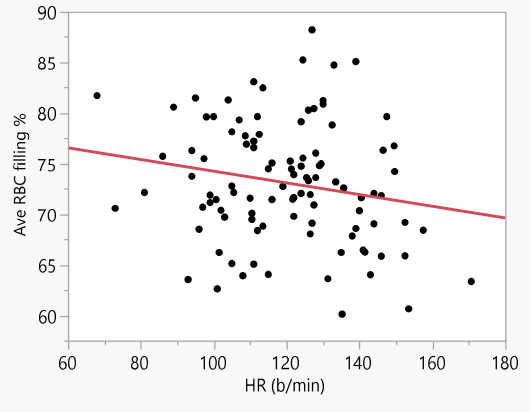
Analysis of Variance

Source	DF	Sum of Squares	Mean Square	F Ratio
Model	1	33.1682	33.1682	0.9452
Error	99	3474.1308	35.0922	**Prob > F**
C. Total	100	3507.2991		0.3333

Parameter Estimates

Term	Estimate	Std Error	t Ratio	Prob>|t|
Intercept	70.467774	2.744949	25.67	<.0001*
Weight (kg)	0.7283626	0.74919	0.97	0.3333

Bivariate Fit of Ave RBC filling % By HR (b/min)



Linear Fit

Linear Fit

Ave RBC filling % = 80.005461 - 0.0577263*HR (b/min)

Summary of Fit

RSquare	0.035679
RSquare Adj	0.025938
Root Mean Square Error	5.844935
Mean of Response	73.07416
Observations (or Sum Wgts)	101

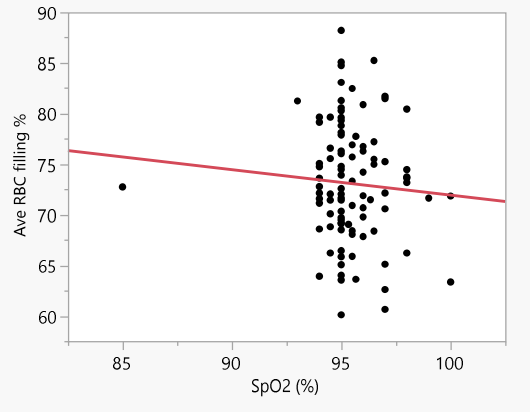
Analysis of Variance

Source	DF	Sum of Squares	Mean Square	F Ratio
Model	1	125.1363	125.136	3.6629
Error	99	3382.1628	34.163	**Prob > F**
C. Total	100	3507.2991		0.0585

Parameter Estimates

Term	Estimate	Std Error	t Ratio	Prob>|t|
Intercept	80.005461	3.668021	21.81	<.0001*
HR (b/min)	-0.057726	0.030162	-1.91	0.0585

Bivariate Fit of Ave RBC filling % By SpO2 (%)



Linear Fit

Linear Fit

Ave RBC filling % = 97.096901 - 0.2517167*SpO2 (%)

Summary of Fit

RSquare	0.00497
RSquare Adj	-0.00508
Root Mean Square Error	5.937271
Mean of Response	73.07416
Observations (or Sum Wgts)	101

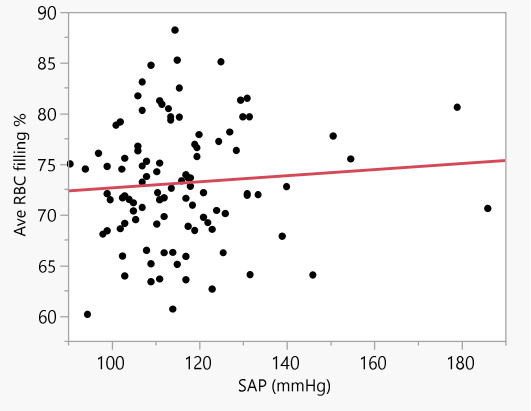
Analysis of Variance

Source	DF	Sum of Squares	Mean Square	F Ratio
Model	1	17.4313	17.4313	0.4945
Error	99	3489.8678	35.2512	**Prob > F**
C. Total	100	3507.2991		0.4836

Parameter Estimates

Term	Estimate	Std Error	t Ratio	Prob>|t|
Intercept	97.096901	34.16722	2.84	0.0054*
SpO2 (%)	-0.251717	0.35796	-0.70	0.4836

Bivariate Fit of Ave RBC filling % By SAP (mmHg)



Linear Fit

Linear Fit

Ave RBC filling % = 69.571582 + 0.030226*SAP (mmHg)

Summary of Fit

RSquare	0.006113
RSquare Adj	-0.00393
Root Mean Square Error	5.933861
Mean of Response	73.07416
Observations (or Sum Wgts)	101

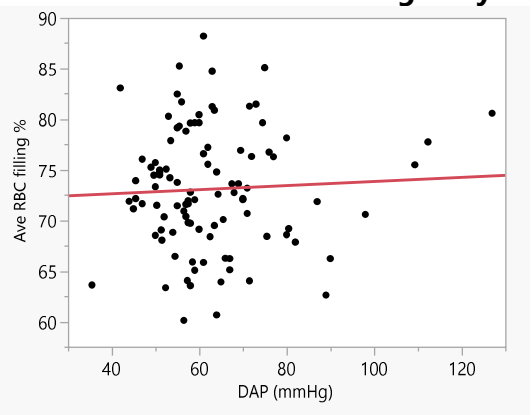
Analysis of Variance

Source	DF	Sum of Squares	Mean Square	F Ratio
Model	1	21.4396	21.4396	0.6089
Error	99	3485.8595	35.2107	**Prob > F**
C. Total	100	3507.2991		0.4371

Parameter Estimates

Term	Estimate	Std Error	t Ratio	Prob>|t|
Intercept	69.571582	4.527328	15.37	<.0001*
SAP (mmHg)	0.030226	0.038736	0.78	0.4371

Bivariate Fit of Ave RBC filling % By DAP (mmHg)



Linear Fit

Linear Fit

Ave RBC filling % = 71.818484 + 0.0200121*DAP (mmHg)

Summary of Fit

RSquare	0.002419
RSquare Adj	-0.00766
Root Mean Square Error	5.944877
Mean of Response	73.07416
Observations (or Sum Wgts)	101

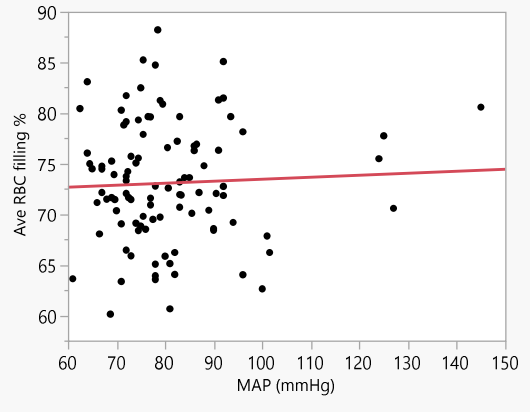
Analysis of Variance

Source	DF	Sum of Squares	Mean Square	F Ratio
Model	1	8.4846	8.4846	0.2401
Error	99	3498.8144	35.3416	**Prob > F**
C. Total	100	3507.2991		0.6252

Parameter Estimates

Term	Estimate	Std Error	t Ratio	Prob>|t|
Intercept	71.818484	2.63012	27.31	<.0001*
DAP (mmHg)	0.0200121	0.040843	0.49	0.6252

Bivariate Fit of Ave RBC filling % By MAP (mmHg)



Linear Fit

Linear Fit

Ave RBC filling % = 71.489129 + 0.0196638*MAP (mmHg)

Summary of Fit

RSquare	0.002073
RSquare Adj	-0.00801
Root Mean Square Error	5.945907
Mean of Response	73.07416
Observations (or Sum Wgts)	101

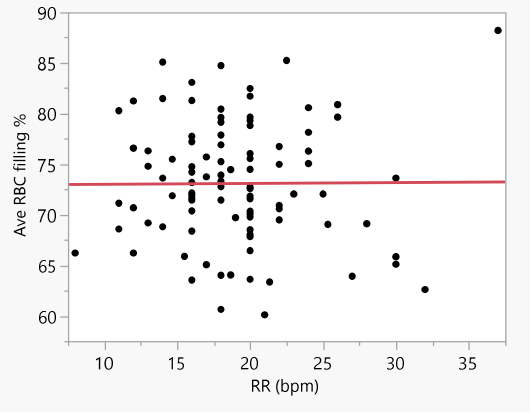
Analysis of Variance

Source	DF	Sum of Squares	Mean Square	F Ratio
Model	1	7.2721	7.2721	0.2057
Error	99	3500.0269	35.3538	**Prob > F**
C. Total	100	3507.2991		0.6512

Parameter Estimates

Term	Estimate	Std Error	t Ratio	Prob>|t|
Intercept	71.489129	3.544546	20.17	<.0001*
MAP (mmHg)	0.0196638	0.043357	0.45	0.6512

Bivariate Fit of Ave RBC filling % By RR (bpm)



Linear Fit

Ave RBC filling % = 72.931417 + 0.0075785*RR (bpm)

Summary of Fit

RSquare	3.883e-5
RSquare Adj	-0.01006
Root Mean Square Error	5.951965
Mean of Response	73.07416
Observations (or Sum Wgts)	101

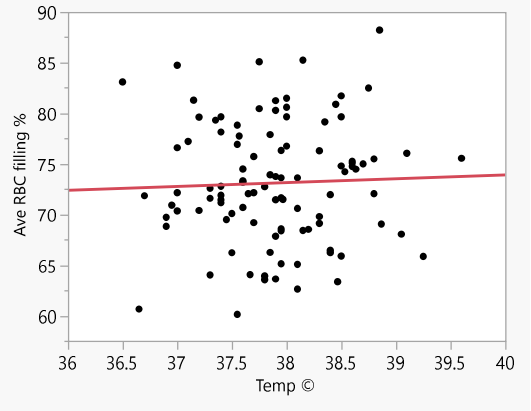
Analysis of Variance

Source	DF	Sum of Squares	Mean Square	F Ratio
Model	1	0.1362	0.1362	0.0038
Error	99	3507.1629	35.4259	**Prob > F**
C. Total	100	3507.2991		0.9507

Parameter Estimates

Term	Estimate	Std Error	t Ratio	Prob>|t|
Intercept	72.931417	2.377204	30.68	<.0001*
RR (bpm)	0.0075785	0.122233	0.06	0.9507

Bivariate Fit of Ave RBC filling % By Temp ©



Linear Fit

Linear Fit

Ave RBC filling % = 58.610757 + 0.3817896*Temp ©

Summary of Fit

RSquare	0.00153
RSquare Adj	-0.00856
Root Mean Square Error	5.947525
Mean of Response	73.07416
Observations (or Sum Wgts)	101

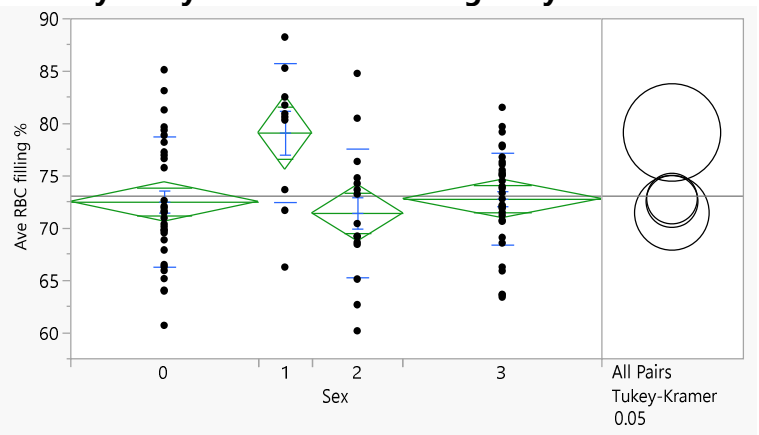
Analysis of Variance

Source	DF	Sum of Squares	Mean Square	F Ratio
Model	1	5.3664	5.3664	0.1517
Error	99	3501.9327	35.3731	**Prob > F**
C. Total	100	3507.2991		0.6977

Parameter Estimates

Term	Estimate	Std Error	t Ratio	Prob>|t|
Intercept	58.610757	37.13816	1.58	0.1177
Temp ©	0.3817896	0.98021	0.39	0.6977

Oneway Analysis of Ave RBC filling % By Sex



Oneway Anova
Summary of Fit

Rsquare	0.123439
Adj Rsquare	0.095758
Root Mean Square Error	5.632952
Mean of Response	73.05889
Observations (or Sum Wgts)	99

Analysis of Variance

Source	DF	Sum of Squares	Mean Square	F Ratio	Prob > F
Sex	3	424.4898	141.497	4.4594	0.0056*
Error	95	3014.3636	31.730		
C. Total	98	3438.8534			

Means and Std Deviations

Level	Number	Mean	Std Dev	Std Err Mean	Lower 95%	Upper 95%
0	35	72.475143	6.2313748	1.0532946	70.334591	74.615695
1	10	79.074	6.6468091	2.1019056	74.319159	83.828841
2	17	71.391765	6.1464596	1.4907354	68.231547	74.551983
3	37	72.751351	4.3845006	0.7208075	71.289486	74.213217

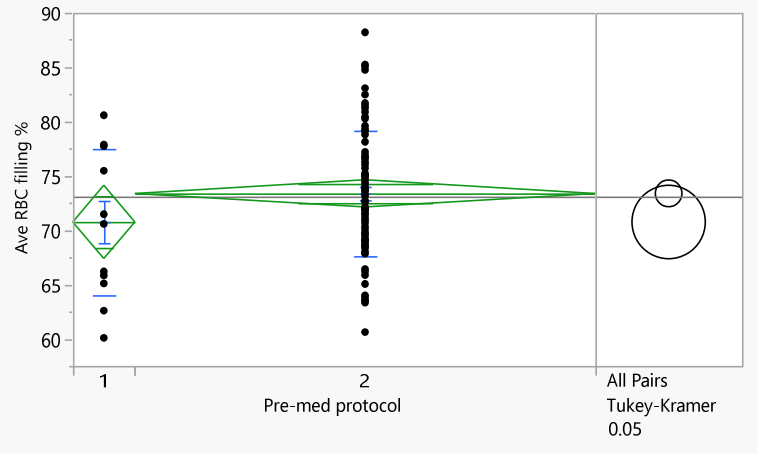
Means Comparisons
Comparisons for all pairs using Tukey-Kramer HSD

Connecting Letters Report

Level		Mean
1	A	79.074000
3	B	72.751351
0	B	72.475143
2	B	71.391765

Levels not connected by same letter are significantly different.

Missing Rows2**Oneway Analysis of Ave RBC filling % By Pre-med protocol**



Oneway Anova
Summary of Fit

Rsquare	0.020913
Adj Rsquare	0.011024
Root Mean Square Error	5.889513
Mean of Response	73.07416
Observations (or Sum Wgts)	101

Analysis of Variance

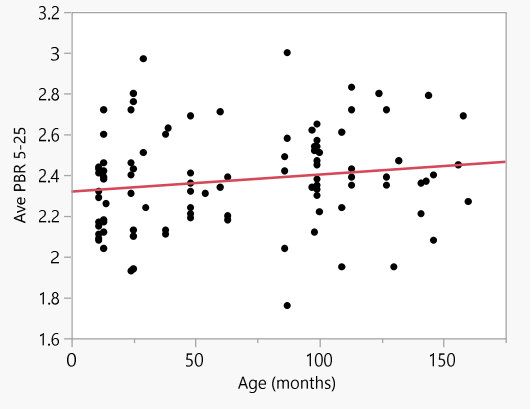
Source	DF	Sum of Squares	Mean Square	F Ratio	Prob > F
Pre-med protocol	1	73.3495	73.3495	2.1147	0.1491
Error	99	3433.9495	34.6864		
C. Total	100	3507.2991			

Means and Std Deviations

Level	Number	Mean	Std Dev	Std Err Mean	Lower 95%	Upper 95%
1	12	70.753333	6.7298593	1.942743	66.477385	75.029282
2	89	73.387079	5.775879	0.6122419	72.170376	74.603781

Means Comparisons
Comparisons for all pairs using Tukey-Kramer HSD

Bivariate Fit of Ave PBR 5-25 By Age (months)



Linear Fit

Linear Fit

Ave PBR 5-25 = 2.3192371 + 0.000833*Age (months)

Summary of Fit

RSquare	0.025439
RSquare Adj	0.015392
Root Mean Square Error	0.240109
Mean of Response	2.375657
Observations (or Sum Wgts)	99

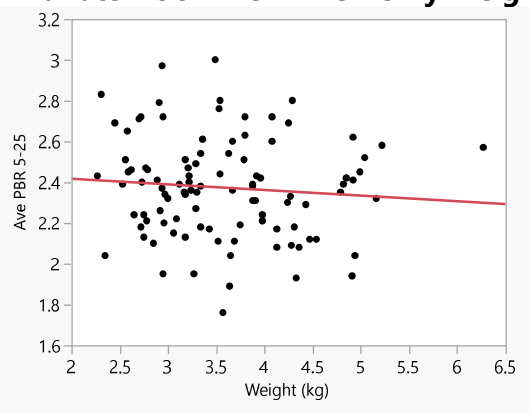
Analysis of Variance

Source	DF	Sum of Squares	Mean Square	F Ratio
Model	1	0.1459756	0.145976	2.5320
Error	97	5.5922567	0.057652	**Prob > F**
C. Total	98	5.7382323		0.1148

Parameter Estimates

Term	Estimate	Std Error	t Ratio	Prob>|t|
Intercept	2.3192371	0.04289	54.07	<.0001*
Age (months)	0.000833	0.000524	1.59	0.1148

Bivariate Fit of Ave PBR 5-25 By Weight (kg)



Linear Fit

Linear Fit

Ave PBR 5-25 = 2.4704427 - 0.0274603*Weight (kg)

Summary of Fit

RSquare	0.007869
RSquare Adj	-0.00215
Root Mean Square Error	0.245027
Mean of Response	2.372178
Observations (or Sum Wgts)	101

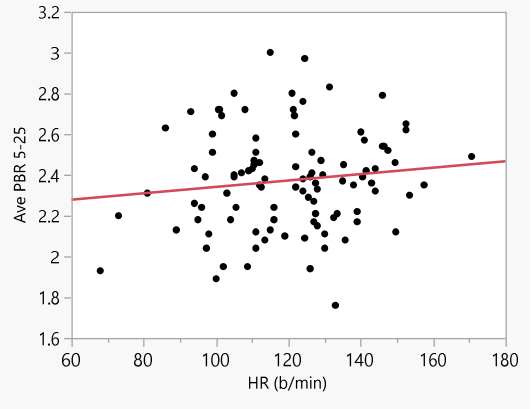
Analysis of Variance

Source	DF	Sum of Squares	Mean Square	F Ratio
Model	1	0.0471453	0.047145	0.7853
Error	99	5.9437755	0.060038	**Prob > F**
C. Total	100	5.9909208		0.3777

Parameter Estimates

Term	Estimate	Std Error	t Ratio	Prob>|t|
Intercept	2.4704427	0.113538	21.76	<.0001*
Weight (kg)	-0.02746	0.030988	-0.89	0.3777

Bivariate Fit of Ave PBR 5-25 By HR (b/min)



Linear Fit

Linear Fit

Ave PBR 5-25 = 2.1834612 + 0.0015717*HR (b/min)

Summary of Fit

RSquare	0.015484
RSquare Adj	0.005539
Root Mean Square Error	0.244085
Mean of Response	2.372178
Observations (or Sum Wgts)	101

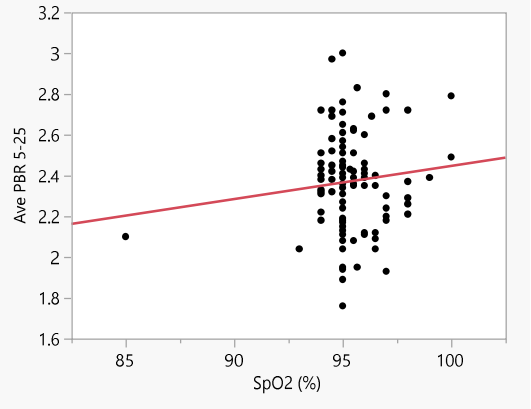
Analysis of Variance

Source	DF	Sum of Squares	Mean Square	F Ratio
Model	1	0.0927632	0.092763	1.5570
Error	99	5.8981576	0.059577	**Prob > F**
C. Total	100	5.9909208		0.2150

Parameter Estimates

Term	Estimate	Std Error	t Ratio	Prob>|t|
Intercept	2.1834612	0.153177	14.25	<.0001*
HR (b/min)	0.0015717	0.00126	1.25	0.2150

Bivariate Fit of Ave PBR 5-25 By SpO2 (%)



Linear Fit

Linear Fit

Ave PBR 5-25 = 0.820668 + 0.0162571*SpO2 (%)

Summary of Fit

RSquare	0.012137
RSquare Adj	0.002158
Root Mean Square Error	0.244499
Mean of Response	2.372178
Observations (or Sum Wgts)	101

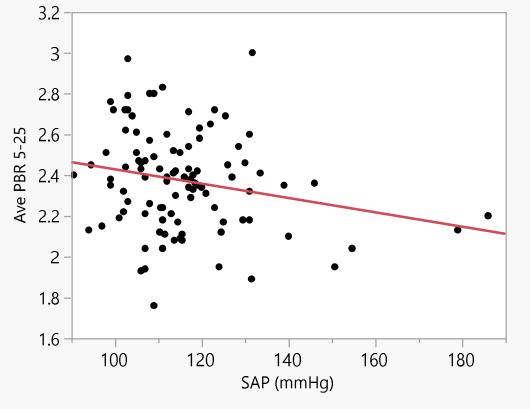
Analysis of Variance

Source	DF	Sum of Squares	Mean Square	F Ratio
Model	1	0.0727099	0.072710	1.2163
Error	99	5.9182109	0.059780	**Prob > F**
C. Total	100	5.9909208		0.2728

Parameter Estimates

Term	Estimate	Std Error	t Ratio	Prob>|t|
Intercept	0.820668	1.40702	0.58	0.5610
SpO2 (%)	0.0162571	0.014741	1.10	0.2728

Bivariate Fit of Ave PBR 5-25 By SAP (mmHg)



Linear Fit

Linear Fit

Ave PBR 5-25 = 2.7798119 - 0.0035177*SAP (mmHg)

Summary of Fit

RSquare	0.048472
RSquare Adj	0.03886
Root Mean Square Error	0.239961
Mean of Response	2.372178
Observations (or Sum Wgts)	101

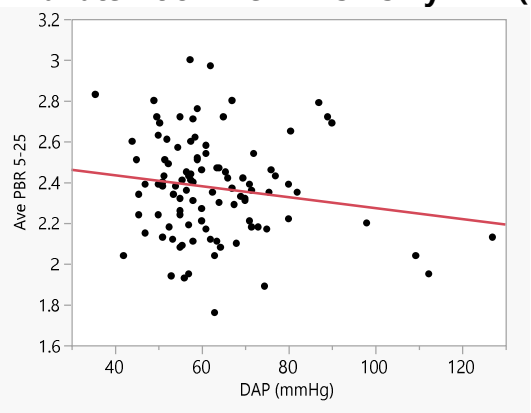
Analysis of Variance

Source	DF	Sum of Squares	Mean Square	F Ratio
Model	1	0.2903897	0.290390	5.0431
Error	99	5.7005310	0.057581	**Prob > F**
C. Total	100	5.9909208		0.0269*

Parameter Estimates

Term	Estimate	Std Error	t Ratio	Prob>|t|
Intercept	2.7798119	0.183082	15.18	<.0001*
SAP (mmHg)	-0.003518	0.001566	-2.25	0.0269*

Bivariate Fit of Ave PBR 5-25 By DAP (mmHg)



Linear Fit

Linear Fit

Ave PBR 5-25 = 2.5400726 - 0.0026758*DAP (mmHg)

Summary of Fit

RSquare	0.02532
RSquare Adj	0.015474
Root Mean Square Error	0.242862
Mean of Response	2.372178
Observations (or Sum Wgts)	101

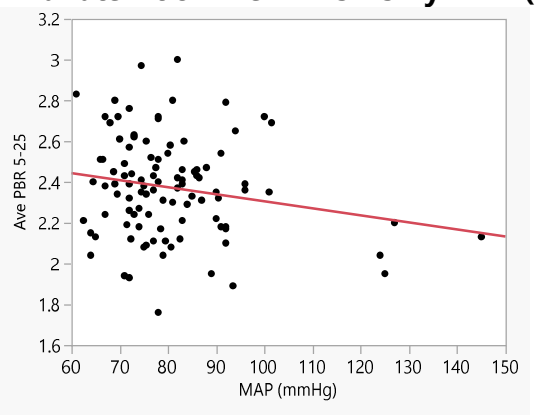
Analysis of Variance

Source	DF	Sum of Squares	Mean Square	F Ratio
Model	1	0.1516877	0.151688	2.5718
Error	99	5.8392330	0.058982	**Prob > F**
C. Total	100	5.9909208		0.1120

Parameter Estimates

Term	Estimate	Std Error	t Ratio	Prob>|t|
Intercept	2.5400726	0.107447	23.64	<.0001*
DAP (mmHg)	-0.002676	0.001669	-1.60	0.1120

Bivariate Fit of Ave PBR 5-25 By MAP (mmHg)



Linear Fit

Linear Fit

Ave PBR 5-25 = 2.650506 - 0.0034529*MAP (mmHg)

Summary of Fit

RSquare	0.037429
RSquare Adj	0.027706
Root Mean Square Error	0.241349
Mean of Response	2.372178
Observations (or Sum Wgts)	101

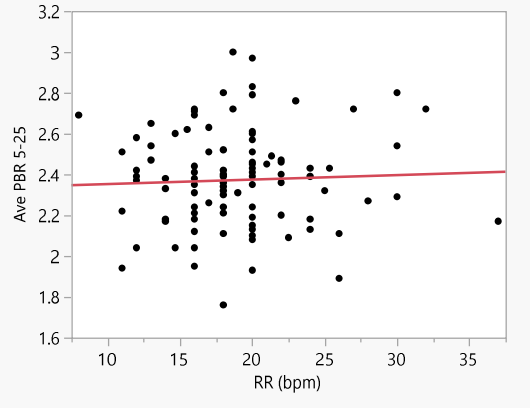
Analysis of Variance

Source	DF	Sum of Squares	Mean Square	F Ratio
Model	1	0.2242331	0.224233	3.8495
Error	99	5.7666877	0.058249	**Prob > F**
C. Total	100	5.9909208		0.0526

Parameter Estimates

Term	Estimate	Std Error	t Ratio	Prob>|t|
Intercept	2.650506	0.143876	18.42	<.0001*
MAP (mmHg)	-0.003453	0.00176	-1.96	0.0526

Bivariate Fit of Ave PBR 5-25 By RR (bpm)



Linear Fit

Linear Fit

Ave PBR 5-25 = 2.3306492 + 0.0022049*RR (bpm)

Summary of Fit

RSquare	0.001924
RSquare Adj	-0.00816
Root Mean Square Error	0.24576
Mean of Response	2.372178
Observations (or Sum Wgts)	101

Analysis of Variance

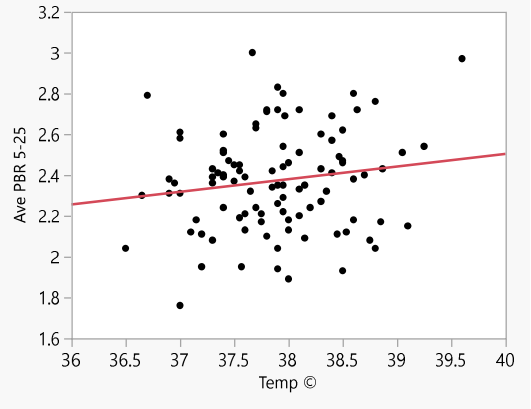
Source	DF	Sum of Squares	Mean Square	F Ratio
Model	1	0.0115271	0.011527	0.1909
Error	99	5.9793937	0.060398	**Prob > F**
C. Total	100	5.9909208		0.6632

Parameter Estimates

Term	Estimate	Std Error	t Ratio	Prob>|t|
Intercept	2.3306492	0.098156	23.74	<.0001*

Term	Estimate	Std Error	t Ratio	Prob>|t|
RR (bpm)	0.0022049	0.005047	0.44	0.6632

Bivariate Fit of Ave PBR 5-25 By Temp ©



Linear Fit

Linear Fit

Ave PBR 5-25 = 0.0262123 + 0.0619263*Temp ©

Summary of Fit

RSquare	0.023566
RSquare Adj	0.013703
Root Mean Square Error	0.243081
Mean of Response	2.372178
Observations (or Sum Wgts)	101

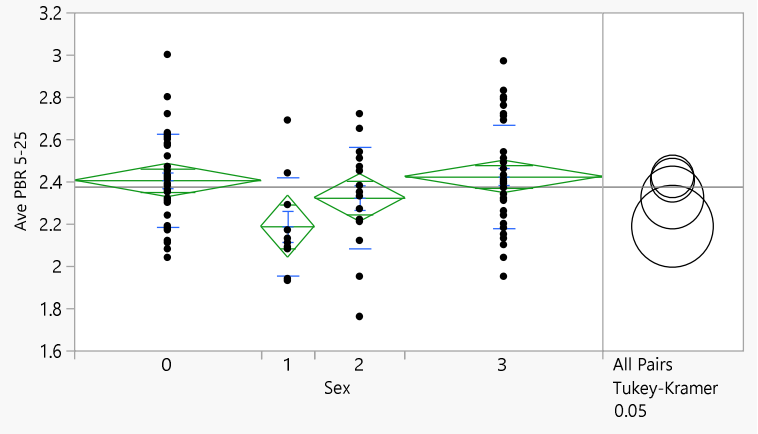
Analysis of Variance

Source	DF	Sum of Squares	Mean Square	F Ratio
Model	1	0.1411840	0.141184	2.3894
Error	99	5.8497368	0.059088	**Prob > F**
C. Total	100	5.9909208		0.1254

Parameter Estimates

Term	Estimate	Std Error	t Ratio	Prob>|t|
Intercept	0.0262123	1.51787	0.02	0.9863
Temp ©	0.0619263	0.040062	1.55	0.1254

Oneway Analysis of Ave PBR 5-25 By Sex



Oneway Anova
Summary of Fit

Rsquare	0.089997
Adj Rsquare	0.06126
Root Mean Square Error	0.234449
Mean of Response	2.375657
Observations (or Sum Wgts)	99

Analysis of Variance

Source	DF	Sum of Squares	Mean Square	F Ratio	Prob > F
Sex	3	0.5164221	0.172141	3.1317	0.0292*
Error	95	5.2218102	0.054966		
C. Total	98	5.7382323			

Means and Std Deviations

Level	Number	Mean	Std Dev	Std Err Mean	Lower 95%	Upper 95%
0	35	2.4051429	0.2208056	0.037323	2.3292935	2.4809922
1	10	2.187	0.2321422	0.0734098	2.0209355	2.3530645
2	17	2.3229412	0.2404882	0.0583269	2.1992936	2.4465888
3	37	2.422973	0.2445956	0.0402113	2.3414207	2.5045252

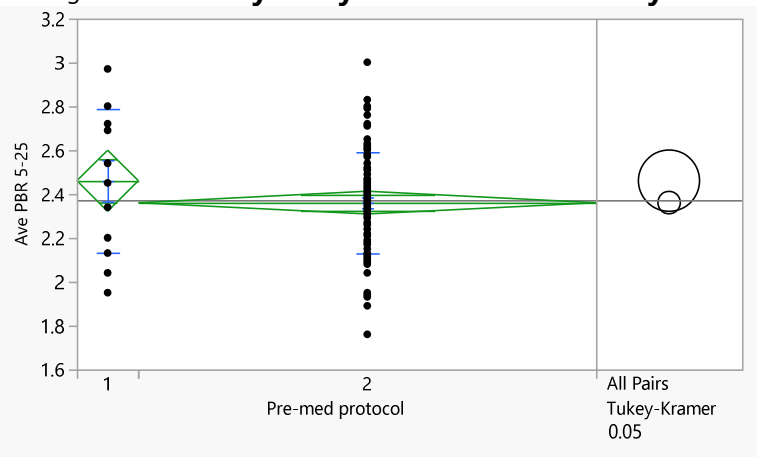
Means Comparisons
Comparisons for all pairs using Tukey-Kramer HSD

Connecting Letters Report

Level			Mean
3	A		2.4229730
0	A	B	2.4051429
2	A	B	2.3229412
1		B	2.1870000

Levels not connected by same letter are significantly different.

Missing Rows2**Oneway Analysis of Ave PBR 5-25 By Pre-med protocol**



Oneway Anova
Summary of Fit

Rsquare	0.017532
Adj Rsquare	0.007608
Root Mean Square Error	0.243831
Mean of Response	2.372178
Observations (or Sum Wgts)	101

Analysis of Variance

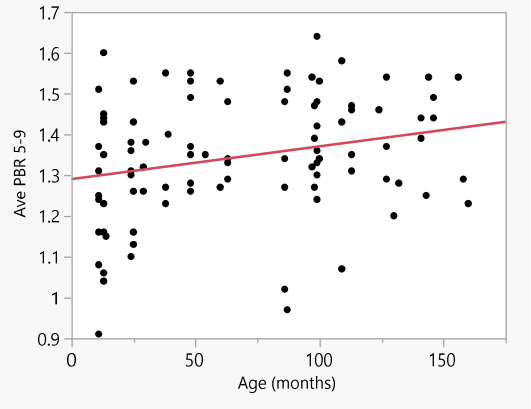
Source	DF	Sum of Squares	Mean Square	F Ratio	Prob > F
Pre-med protocol	1	0.1050309	0.105031	1.7666	0.1869
Error	99	5.8858899	0.059453		
C. Total	100	5.9909208			

Means and Std Deviations

Level	Number	Mean	Std Dev	Std Err Mean	Lower 95%	Upper 95%
1	12	2.46	0.3279412	0.0946685	2.2516361	2.6683639
2	89	2.3603371	0.2311751	0.0245045	2.3116395	2.4090346

Means Comparisons
Comparisons for all pairs using Tukey-Kramer HSD

Bivariate Fit of Ave PBR 5-9 By Age (months)



Linear Fit

Linear Fit

Ave PBR 5-9 = 1.2901444 + 0.0008017*Age (months)

Summary of Fit

RSquare	0.063725
RSquare Adj	0.054073
Root Mean Square Error	0.143111
Mean of Response	1.344444
Observations (or Sum Wgts)	99

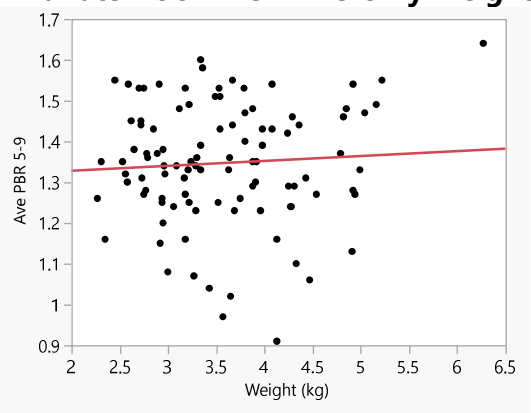
Analysis of Variance

Source	DF	Sum of Squares	Mean Square	F Ratio
Model	1	0.1352143	0.135214	6.6020
Error	97	1.9866301	0.020481	**Prob > F**
C. Total	98	2.1218444		0.0117*

Parameter Estimates

Term	Estimate	Std Error	t Ratio	Prob>|t|
Intercept	1.2901444	0.025563	50.47	<.0001*
Age (months)	0.0008017	0.000312	2.57	0.0117*

Bivariate Fit of Ave PBR 5-9 By Weight (kg)



Linear Fit

Linear Fit

Ave PBR 5-9 = 1.3034502 + 0.0120124*Weight (kg)

Summary of Fit

RSquare	0.004184
RSquare Adj	-0.00587
Root Mean Square Error	0.147268
Mean of Response	1.346436
Observations (or Sum Wgts)	101

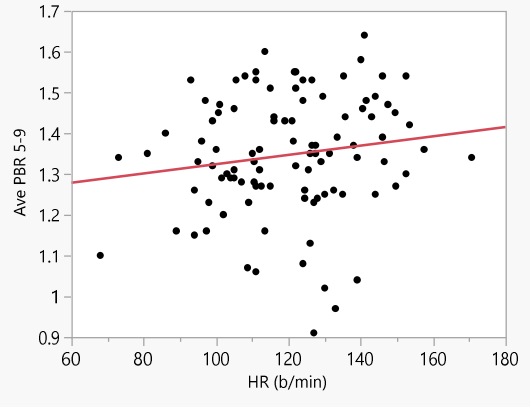
Analysis of Variance

Source	DF	Sum of Squares	Mean Square	F Ratio
Model	1	0.0090217	0.009022	0.4160
Error	99	2.1470952	0.021688	**Prob > F**
C. Total	100	2.1561168		0.5204

Parameter Estimates

Term	Estimate	Std Error	t Ratio	Prob>|t|
Intercept	1.3034502	0.06824	19.10	<.0001*
Weight (kg)	0.0120124	0.018625	0.64	0.5204

Bivariate Fit of Ave PBR 5-9 By HR (b/min)



Linear Fit

Linear Fit

Ave PBR 5-9 = 1.2103729 + 0.0011332*HR (b/min)

Summary of Fit

RSquare	0.022365
RSquare Adj	0.012489
Root Mean Square Error	0.145917
Mean of Response	1.346436
Observations (or Sum Wgts)	101

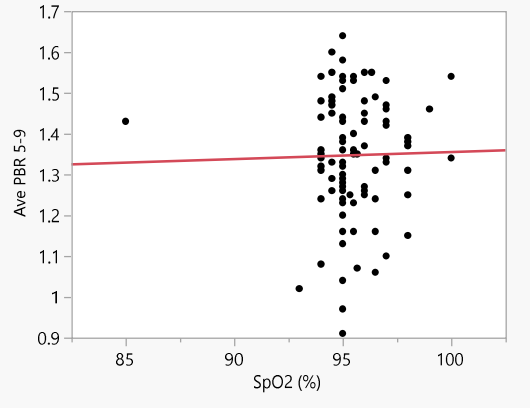
Analysis of Variance

Source	DF	Sum of Squares	Mean Square	F Ratio
Model	1	0.0482205	0.048221	2.2647
Error	99	2.1078963	0.021292	**Prob > F**
C. Total	100	2.1561168		0.1355

Parameter Estimates

Term	Estimate	Std Error	t Ratio	Prob>|t|
Intercept	1.2103729	0.091571	13.22	<.0001*
HR (b/min)	0.0011332	0.000753	1.50	0.1355

Bivariate Fit of Ave PBR 5-9 By SpO2 (%)



Linear Fit

Linear Fit

Ave PBR 5-9 = 1.1821788 + 0.0017211*SpO2 (%)

Summary of Fit

RSquare	0.000378
RSquare Adj	-0.00972
Root Mean Square Error	0.147549
Mean of Response	1.346436
Observations (or Sum Wgts)	101

Analysis of Variance

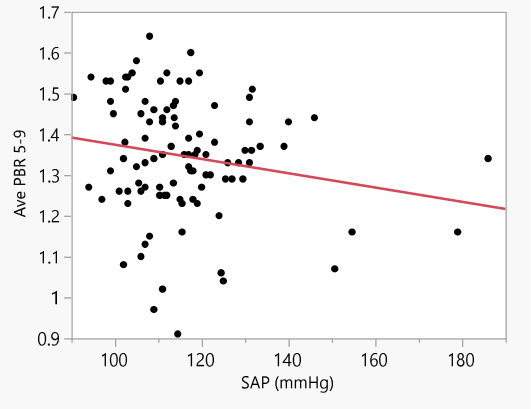
Source	DF	Sum of Squares	Mean Square	F Ratio
Model	1	0.0008150	0.000815	0.0374
Error	99	2.1553019	0.021771	**Prob > F**
C. Total	100	2.1561168		0.8470

Parameter Estimates

Term	Estimate	Std Error	t Ratio	Prob>|t|
Intercept	1.1821788	0.849101	1.39	0.1670

Term	Estimate	Std Error	t Ratio	Prob>|t|
SpO2 (%)	0.0017211	0.008896	0.19	0.8470

Bivariate Fit of Ave PBR 5-9 By SAP (mmHg)



Linear Fit

Linear Fit

Ave PBR 5-9 = 1.5489848 - 0.0017479*SAP (mmHg)

Summary of Fit

RSquare	0.033253
RSquare Adj	0.023488
Root Mean Square Error	0.145103
Mean of Response	1.346436
Observations (or Sum Wgts)	101

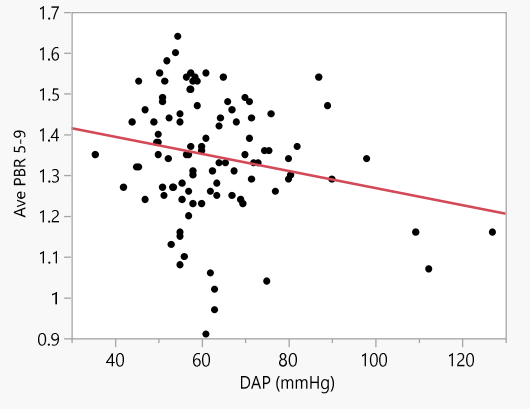
Analysis of Variance

Source	DF	Sum of Squares	Mean Square	F Ratio
Model	1	0.0716972	0.071697	3.4053
Error	99	2.0844196	0.021055	**Prob > F**
C. Total	100	2.1561168		0.0680

Parameter Estimates

Term	Estimate	Std Error	t Ratio	Prob>|t|
Intercept	1.5489848	0.110708	13.99	<.0001*
SAP (mmHg)	-0.001748	0.000947	-1.85	0.0680

Bivariate Fit of Ave PBR 5-9 By DAP (mmHg)



Linear Fit

Linear Fit

Ave PBR 5-9 = 1.4779382 - 0.0020958*DAP (mmHg)

Summary of Fit

RSquare	0.043159
RSquare Adj	0.033494
Root Mean Square Error	0.144357
Mean of Response	1.346436
Observations (or Sum Wgts)	101

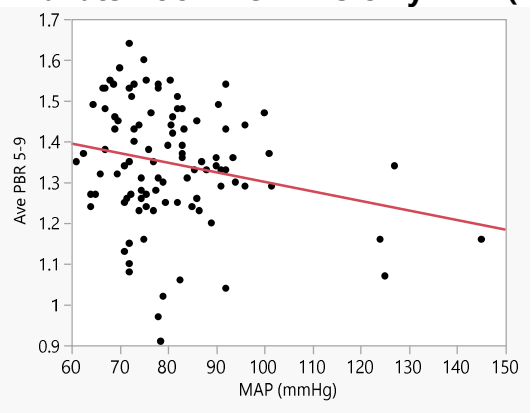
Analysis of Variance

Source	DF	Sum of Squares	Mean Square	F Ratio
Model	1	0.0930565	0.093056	4.4655
Error	99	2.0630604	0.020839	**Prob > F**
C. Total	100	2.1561168		0.0371*

Parameter Estimates

Term	Estimate	Std Error	t Ratio	Prob>|t|
Intercept	1.4779382	0.063866	23.14	<.0001*
DAP (mmHg)	-0.002096	0.000992	-2.11	0.0371*

Bivariate Fit of Ave PBR 5-9 By MAP (mmHg)



Linear Fit

Linear Fit

Ave PBR 5-9 = 1.5355411 - 0.002346*MAP (mmHg)

Summary of Fit

RSquare	0.048009
RSquare Adj	0.038393
Root Mean Square Error	0.143991
Mean of Response	1.346436
Observations (or Sum Wgts)	101

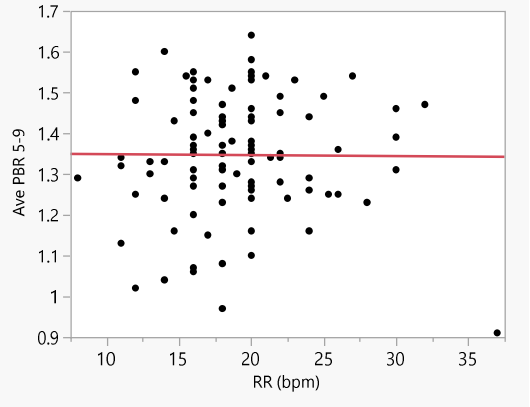
Analysis of Variance

Source	DF	Sum of Squares	Mean Square	F Ratio
Model	1	0.1035129	0.103513	4.9926
Error	99	2.0526039	0.020733	**Prob > F**
C. Total	100	2.1561168		0.0277*

Parameter Estimates

Term	Estimate	Std Error	t Ratio	Prob>|t|
Intercept	1.5355411	0.085838	17.89	<.0001*
MAP (mmHg)	-0.002346	0.00105	-2.23	0.0277*

Bivariate Fit of Ave PBR 5-9 By RR (bpm)



Linear Fit

Linear Fit

Ave PBR 5-9 = 1.3509853 - 0.0002416*RR (bpm)

Summary of Fit

RSquare	6.416e-5
RSquare Adj	-0.01004
Root Mean Square Error	0.147572
Mean of Response	1.346436
Observations (or Sum Wgts)	101

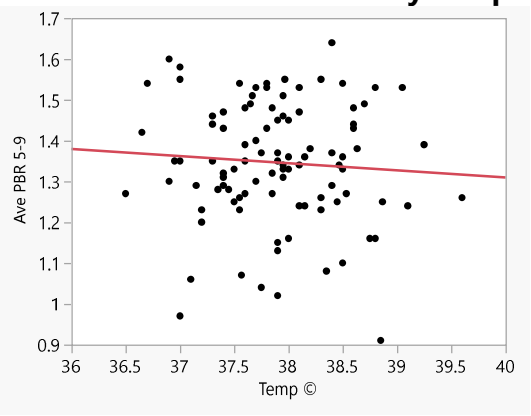
Analysis of Variance

Source	DF	Sum of Squares	Mean Square	F Ratio
Model	1	0.0001383	0.000138	0.0064
Error	99	2.1559785	0.021778	**Prob > F**
C. Total	100	2.1561168		0.9366

Parameter Estimates

Term	Estimate	Std Error	t Ratio	Prob>|t|
Intercept	1.3509853	0.05894	22.92	<.0001*
RR (bpm)	-0.000242	0.003031	-0.08	0.9366

Bivariate Fit of Ave PBR 5-9 By Temp ©



Linear Fit

Linear Fit

Ave PBR 5-9 = 2.0098531 - 0.0175122*Temp ©

Summary of Fit

RSquare	0.005237
RSquare Adj	-0.00481
Root Mean Square Error	0.14719
Mean of Response	1.346436
Observations (or Sum Wgts)	101

Analysis of Variance

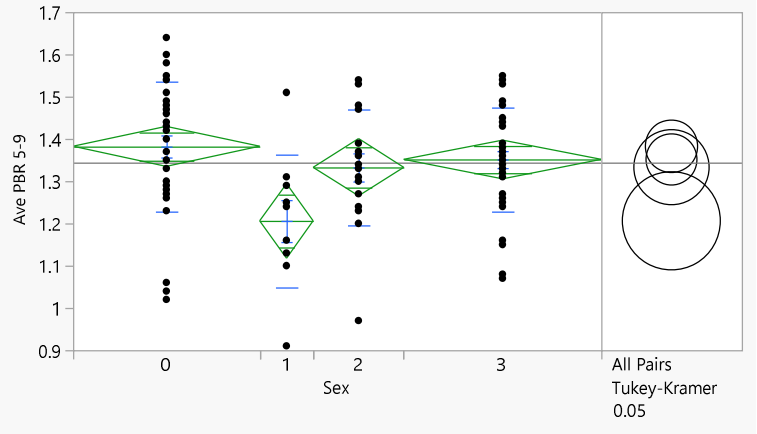
Source	DF	Sum of Squares	Mean Square	F Ratio
Model	1	0.0112906	0.011291	0.5211
Error	99	2.1448263	0.021665	**Prob > F**
C. Total	100	2.1561168		0.4721

Parameter Estimates

Term	Estimate	Std Error	t Ratio	Prob>|t|
Intercept	2.0098531	0.9191	2.19	0.0311*

Term	Estimate	Std Error	t Ratio	Prob>|t|
Temp ©	-0.017512	0.024258	-0.72	0.4721

Oneway Analysis of Ave PBR 5-9 By Sex



Oneway Anova
Summary of Fit

Rsquare	0.115844
Adj Rsquare	0.087923
Root Mean Square Error	0.140527
Mean of Response	1.344444
Observations (or Sum Wgts)	99

Analysis of Variance

Source	DF	Sum of Squares	Mean Square	F Ratio	Prob > F
Sex	3	0.2458019	0.081934	4.1490	0.0083*
Error	95	1.8760425	0.019748		
C. Total	98	2.1218444			

Means and Std Deviations

Level	Number	Mean	Std Dev	Std Err Mean	Lower 95%	Upper 95%
0	35	1.3822857	0.1538732	0.0260093	1.3294284	1.435143
1	10	1.206	0.1571411	0.0496924	1.093588	1.318412
2	17	1.3329412	0.1373301	0.0333074	1.2623325	1.4035498
3	37	1.3513514	0.1232694	0.0202654	1.3102513	1.3924514

Means Comparisons
Comparisons for all pairs using Tukey-Kramer HSD

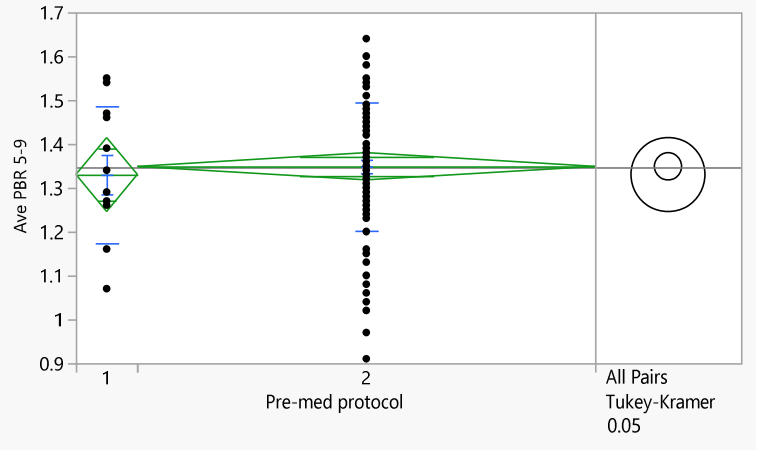
Connecting Letters Report

Level		Mean
0	A	1.3822857

Level			Mean
3	A		1.3513514
2	A	B	1.3329412
1		B	1.2060000

Levels not connected by same letter are significantly different.

Missing Rows2**Oneway Analysis of Ave PBR 5-9 By Pre-med protocol**



Oneway Anova
Summary of Fit

Rsquare	0.001706
Adj Rsquare	-0.00838
Root Mean Square Error	0.147451
Mean of Response	1.346436
Observations (or Sum Wgts)	101

Analysis of Variance

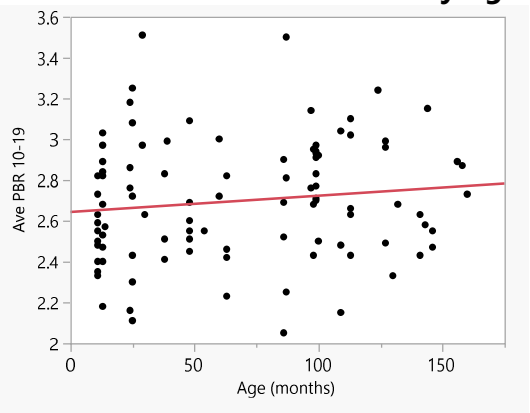
Source	DF	Sum of Squares	Mean Square	F Ratio	Prob > F
Pre-med protocol	1	0.0036786	0.003679	0.1692	0.6817
Error	99	2.1524382	0.021742		
C. Total	100	2.1561168			

Means and Std Deviations

Level	Number	Mean	Std Dev	Std Err Mean	Lower 95%	Upper 95%
1	12	1.33	0.1561468	0.0450757	1.2307891	1.4292109
2	89	1.3486517	0.1463277	0.0155107	1.3178274	1.379476

Means Comparisons
Comparisons for all pairs using Tukey-Kramer HSD

Bivariate Fit of Ave PBR 10-19 By Age (months)



Linear Fit

Linear Fit

Ave PBR 10-19 = 2.6428889 + 0.000797*Age (months)

Summary of Fit

RSquare	0.015859
RSquare Adj	0.005714
Root Mean Square Error	0.292376
Mean of Response	2.696869
Observations (or Sum Wgts)	99

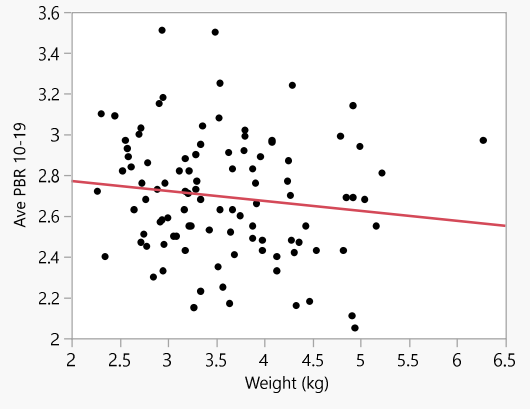
Analysis of Variance

Source	DF	Sum of Squares	Mean Square	F Ratio
Model	1	0.1336243	0.133624	1.5632
Error	97	8.2919050	0.085484	**Prob > F**
C. Total	98	8.4255293		0.2142

Parameter Estimates

Term	Estimate	Std Error	t Ratio	Prob>|t|
Intercept	2.6428889	0.052226	50.61	<.0001*
Age (months)	0.000797	0.000637	1.25	0.2142

Bivariate Fit of Ave PBR 10-19 By Weight (kg)



Linear Fit

Linear Fit

Ave PBR 10-19 = 2.8678925 - 0.0487442*Weight (kg)

Summary of Fit

RSquare	0.017005
RSquare Adj	0.007076
Root Mean Square Error	0.294511
Mean of Response	2.693465
Observations (or Sum Wgts)	101

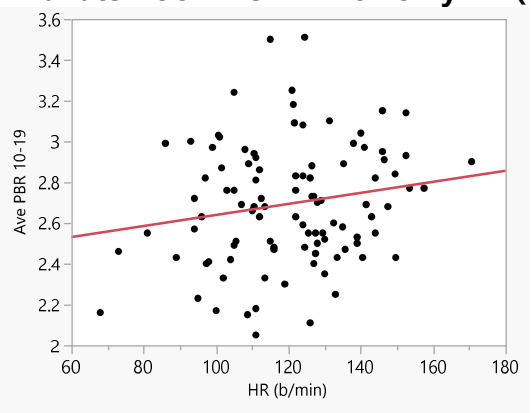
Analysis of Variance

Source	DF	Sum of Squares	Mean Square	F Ratio
Model	1	0.1485503	0.148550	1.7127
Error	99	8.5869368	0.086737	**Prob > F**
C. Total	100	8.7354871		0.1937

Parameter Estimates

Term	Estimate	Std Error	t Ratio	Prob>|t|
Intercept	2.8678925	0.136468	21.02	<.0001*
Weight (kg)	-0.048744	0.037247	-1.31	0.1937

Bivariate Fit of Ave PBR 10-19 By HR (b/min)



Linear Fit

Linear Fit

Ave PBR 10-19 = 2.367639 + 0.0027136*HR (b/min)

Summary of Fit

RSquare	0.031655
RSquare Adj	0.021873
Root Mean Square Error	0.292308
Mean of Response	2.693465
Observations (or Sum Wgts)	101

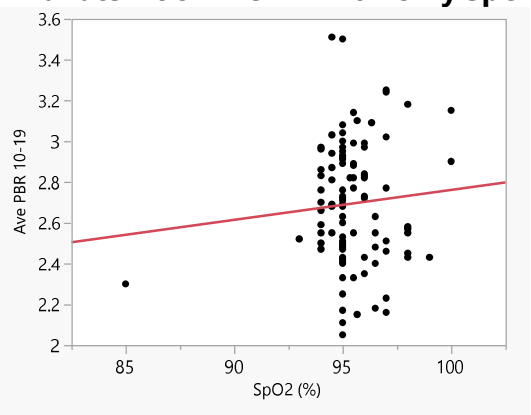
Analysis of Variance

Source	DF	Sum of Squares	Mean Square	F Ratio
Model	1	0.2765197	0.276520	3.2363
Error	99	8.4589675	0.085444	**Prob > F**
C. Total	100	8.7354871		0.0751

Parameter Estimates

Term	Estimate	Std Error	t Ratio	Prob>|t|
Intercept	2.367639	0.18344	12.91	<.0001*
HR (b/min)	0.0027136	0.001508	1.80	0.0751

Bivariate Fit of Ave PBR 10-19 By SpO2 (%)



Linear Fit

Linear Fit

Ave PBR 10-19 = 1.29458 + 0.0146579*SpO2 (%)

Summary of Fit

RSquare	0.006766
RSquare Adj	-0.00327
Root Mean Square Error	0.296041
Mean of Response	2.693465
Observations (or Sum Wgts)	101

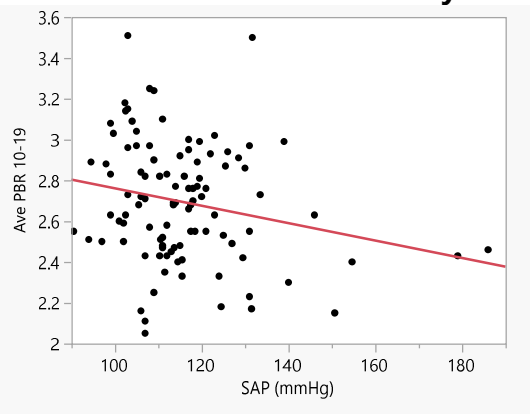
Analysis of Variance

Source	DF	Sum of Squares	Mean Square	F Ratio
Model	1	0.0591083	0.059108	0.6744
Error	99	8.6763788	0.087640	**Prob > F**
C. Total	100	8.7354871		0.4135

Parameter Estimates

Term	Estimate	Std Error	t Ratio	Prob>|t|
Intercept	1.29458	1.703627	0.76	0.4491
SpO2 (%)	0.0146579	0.017848	0.82	0.4135

Bivariate Fit of Ave PBR 10-19 By SAP (mmHg)



Linear Fit

Ave PBR 10-19 = 3.1882352 - 0.0042697*SAP (mmHg)

Summary of Fit

RSquare	0.048973
RSquare Adj	0.039367
Root Mean Square Error	0.289683
Mean of Response	2.693465
Observations (or Sum Wgts)	101

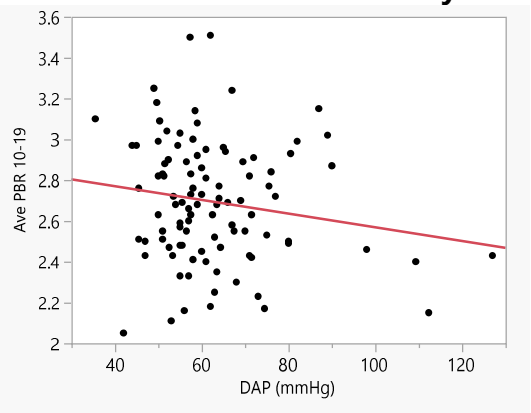
Analysis of Variance

Source	DF	Sum of Squares	Mean Square	F Ratio
Model	1	0.4278068	0.427807	5.0980
Error	99	8.3076804	0.083916	**Prob > F**
C. Total	100	8.7354871		0.0261*

Parameter Estimates

Term	Estimate	Std Error	t Ratio	Prob>|t|
Intercept	3.1882352	0.221018	14.43	<.0001*
SAP (mmHg)	-0.00427	0.001891	-2.26	0.0261*

Bivariate Fit of Ave PBR 10-19 By DAP (mmHg)



Linear Fit

Linear Fit

Ave PBR 10-19 = 2.9037717 - 0.0033517*DAP (mmHg)

Summary of Fit

RSquare	0.027246
RSquare Adj	0.01742
Root Mean Square Error	0.292973
Mean of Response	2.693465
Observations (or Sum Wgts)	101

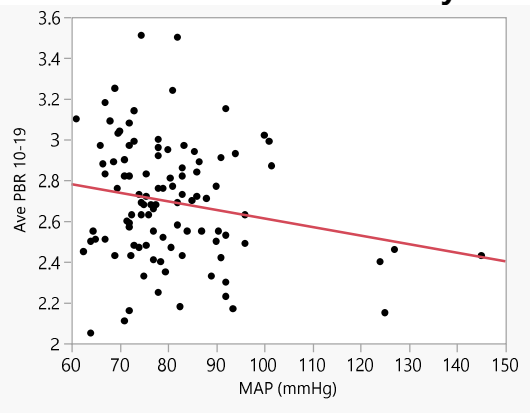
Analysis of Variance

Source	DF	Sum of Squares	Mean Square	F Ratio
Model	1	0.2380033	0.238003	2.7729
Error	99	8.4974838	0.085833	**Prob > F**
C. Total	100	8.7354871		0.0990

Parameter Estimates

Term	Estimate	Std Error	t Ratio	Prob>|t|
Intercept	2.9037717	0.129616	22.40	<.0001*
DAP (mmHg)	-0.003352	0.002013	-1.67	0.0990

Bivariate Fit of Ave PBR 10-19 By MAP (mmHg)



Linear Fit

Linear Fit

Ave PBR 10-19 = 3.0320767 - 0.0042008*MAP (mmHg)

Summary of Fit

RSquare	0.037993
RSquare Adj	0.028276
Root Mean Square Error	0.29135
Mean of Response	2.693465
Observations (or Sum Wgts)	101

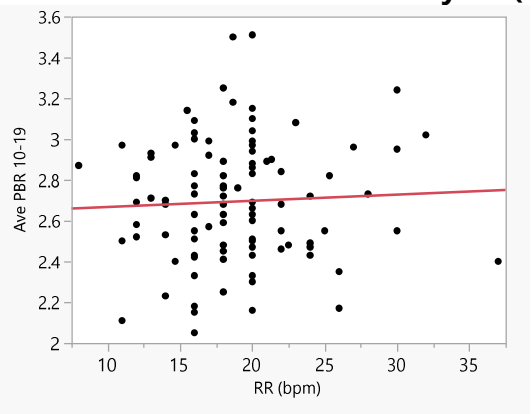
Analysis of Variance

Source	DF	Sum of Squares	Mean Square	F Ratio
Model	1	0.3318865	0.331887	3.9098
Error	99	8.4036006	0.084885	**Prob > F**
C. Total	100	8.7354871		0.0508

Parameter Estimates

Term	Estimate	Std Error	t Ratio	Prob>|t|
Intercept	3.0320767	0.173683	17.46	<.0001*
MAP (mmHg)	-0.004201	0.002124	-1.98	0.0508

Bivariate Fit of Ave PBR 10-19 By RR (bpm)



Linear Fit

Linear Fit

Ave PBR 10-19 = 2.6371364 + 0.0029907*RR (bpm)

Summary of Fit

RSquare	0.002428
RSquare Adj	-0.00765
Root Mean Square Error	0.296687
Mean of Response	2.693465
Observations (or Sum Wgts)	101

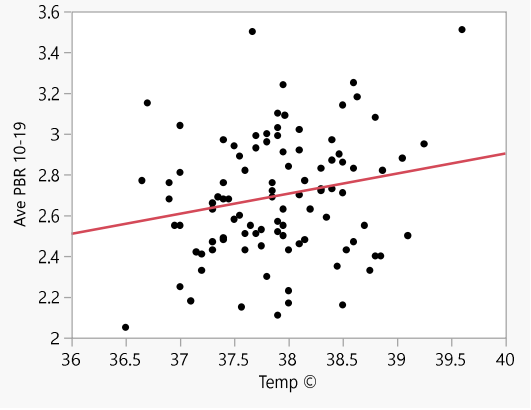
Analysis of Variance

Source	DF	Sum of Squares	Mean Square	F Ratio
Model	1	0.0212070	0.021207	0.2409
Error	99	8.7142801	0.088023	**Prob > F**
C. Total	100	8.7354871		0.6246

Parameter Estimates

Term	Estimate	Std Error	t Ratio	Prob>|t|
Intercept	2.6371364	0.118496	22.26	<.0001*
RR (bpm)	0.0029907	0.006093	0.49	0.6246

Bivariate Fit of Ave PBR 10-19 By Temp ©



Linear Fit

Ave PBR 10-19 = -1.039603 + 0.0985416*Temp ©

Summary of Fit

RSquare	0.040925
RSquare Adj	0.031237
Root Mean Square Error	0.290906
Mean of Response	2.693465
Observations (or Sum Wgts)	101

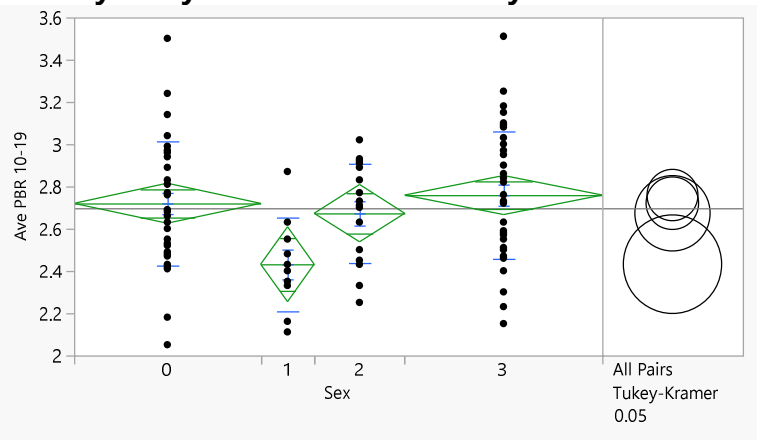
Analysis of Variance

Source	DF	Sum of Squares	Mean Square	F Ratio
Model	1	0.3574982	0.357498	4.2244
Error	99	8.3779889	0.084626	**Prob > F**
C. Total	100	8.7354871		0.0425*

Parameter Estimates

Term	Estimate	Std Error	t Ratio	Prob>|t|
Intercept	-1.039603	1.816504	-0.57	0.5684
Temp ©	0.0985416	0.047944	2.06	0.0425*

Oneway Analysis of Ave PBR 10-19 By Sex



Oneway Anova
Summary of Fit

Rsquare	0.103891
Adj Rsquare	0.075592
Root Mean Square Error	0.281914
Mean of Response	2.696869
Observations (or Sum Wgts)	99

Analysis of Variance

Source	DF	Sum of Squares	Mean Square	F Ratio	Prob > F
Sex	3	0.8753336	0.291778	3.6713	0.0149*
Error	95	7.5501957	0.079476		
C. Total	98	8.4255293			

Means and Std Deviations

Level	Number	Mean	Std Dev	Std Err Mean	Lower 95%	Upper 95%
0	35	2.7197143	0.2939536	0.0496872	2.6187377	2.8206909
1	10	2.431	0.2218834	0.0701657	2.2722742	2.5897258
2	17	2.6723529	0.2353595	0.0570831	2.5513422	2.7933637
3	37	2.7583784	0.3019797	0.0496452	2.6576933	2.8590634

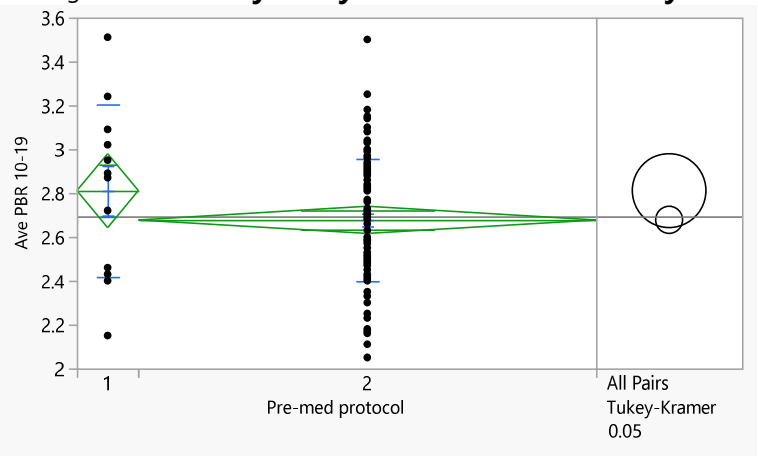
Means Comparisons
Comparisons for all pairs using Tukey-Kramer HSD

Connecting Letters Report

Level			Mean
3	A		2.7583784
0	A		2.7197143
2	A	B	2.6723529
1		B	2.4310000

Levels not connected by same letter are significantly different.

Missing Rows2**Oneway Analysis of Ave PBR 10-19 By Pre-med protocol**



Oneway Anova
Summary of Fit

Rsquare	0.021475
Adj Rsquare	0.01159
Root Mean Square Error	0.293841
Mean of Response	2.693465
Observations (or Sum Wgts)	101

Analysis of Variance

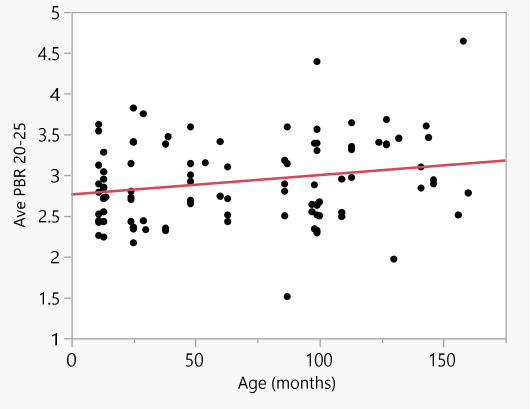
Source	DF	Sum of Squares	Mean Square	F Ratio	Prob > F
Pre-med protocol	1	0.1875910	0.187591	2.1726	0.1437
Error	99	8.5478962	0.086342		
C. Total	100	8.7354871			

Means and Std Deviations

Level	Number	Mean	Std Dev	Std Err Mean	Lower 95%	Upper 95%
1	12	2.8108333	0.3937802	0.1136746	2.5606373	3.0610294
2	89	2.6776404	0.278841	0.0295571	2.6189019	2.736379

Means Comparisons
Comparisons for all pairs using Tukey-Kramer HSD

Bivariate Fit of Ave PBR 20-25 By Age (months)



Linear Fit

Linear Fit

Ave PBR 20-25 = 2.7628391 + 0.0023578*Age (months)

Summary of Fit

RSquare	0.045861
RSquare Adj	0.036024
Root Mean Square Error	0.500817
Mean of Response	2.922525
Observations (or Sum Wgts)	99

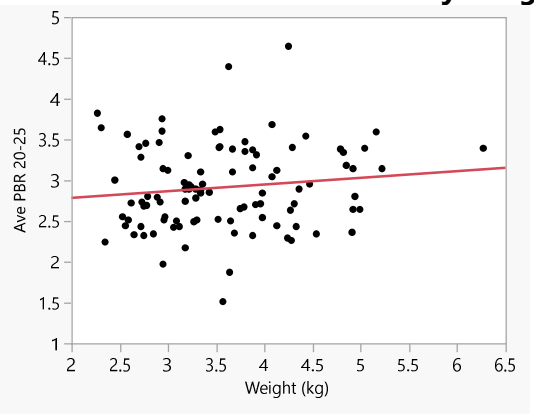
Analysis of Variance

Source	DF	Sum of Squares	Mean Square	F Ratio
Model	1	1.169385	1.16939	4.6623
Error	97	24.329283	0.25082	**Prob > F**
C. Total	98	25.498669		0.0333*

Parameter Estimates

Term	Estimate	Std Error	t Ratio	Prob>|t|
Intercept	2.7628391	0.089459	30.88	<.0001*
Age (months)	0.0023578	0.001092	2.16	0.0333*

Bivariate Fit of Ave PBR 20-25 By Weight (kg)



Linear Fit

Linear Fit

Ave PBR 20-25 = 2.6180859 + 0.0820744*Weight (kg)

Summary of Fit

RSquare	0.015835
RSquare Adj	0.005894
Root Mean Square Error	0.51419
Mean of Response	2.911782
Observations (or Sum Wgts)	101

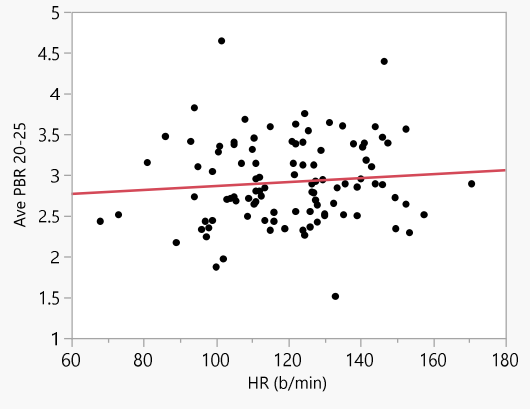
Analysis of Variance

Source	DF	Sum of Squares	Mean Square	F Ratio
Model	1	0.421155	0.421155	1.5929
Error	99	26.174724	0.264391	**Prob > F**
C. Total	100	26.595879		0.2099

Parameter Estimates

Term	Estimate	Std Error	t Ratio	Prob>|t|
Intercept	2.6180859	0.238261	10.99	<.0001*
Weight (kg)	0.0820744	0.065029	1.26	0.2099

Bivariate Fit of Ave PBR 20-25 By HR (b/min)



Linear Fit

Linear Fit

Ave PBR 20-25 = 2.6218882 + 0.0024143*HR (b/min)

Summary of Fit

RSquare	0.00823
RSquare Adj	-0.00179
Root Mean Square Error	0.516173
Mean of Response	2.911782
Observations (or Sum Wgts)	101

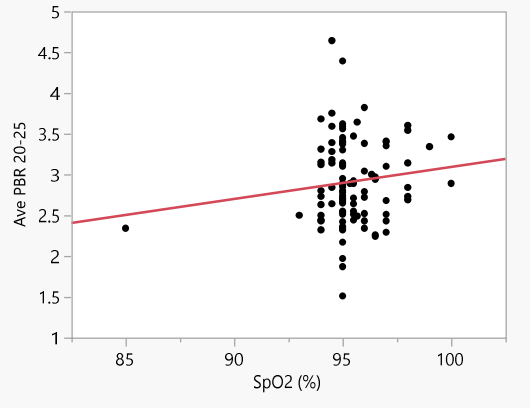
Analysis of Variance

Source	DF	Sum of Squares	Mean Square	F Ratio
Model	1	0.218893	0.218893	0.8216
Error	99	26.376986	0.266434	**Prob > F**
C. Total	100	26.595879		0.3669

Parameter Estimates

Term	Estimate	Std Error	t Ratio	Prob>|t|
Intercept	2.6218882	0.323927	8.09	<.0001*
HR (b/min)	0.0024143	0.002664	0.91	0.3669

Bivariate Fit of Ave PBR 20-25 By SpO2 (%)



Linear Fit

Ave PBR 20-25 = -0.831825 + 0.0392265*SpO2 (%)

Summary of Fit

RSquare	0.015917
RSquare Adj	0.005976
Root Mean Square Error	0.514169
Mean of Response	2.911782
Observations (or Sum Wgts)	101

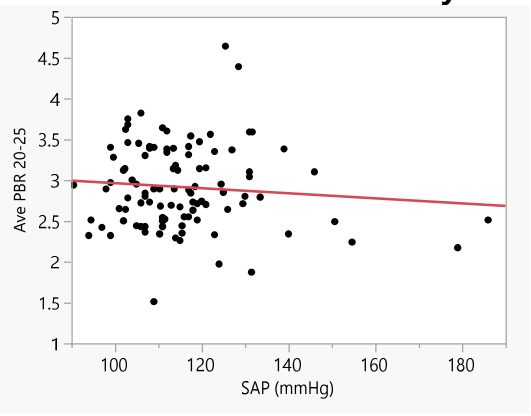
Analysis of Variance

Source	DF	Sum of Squares	Mean Square	F Ratio
Model	1	0.423316	0.423316	1.6012
Error	99	26.172563	0.264369	**Prob > F**
C. Total	100	26.595879		0.2087

Parameter Estimates

Term	Estimate	Std Error	t Ratio	Prob>|t|
Intercept	-0.831825	2.958886	-0.28	0.7792
SpO2 (%)	0.0392265	0.030999	1.27	0.2087

Bivariate Fit of Ave PBR 20-25 By SAP (mmHg)



Linear Fit

Linear Fit

Ave PBR 20-25 = 3.2715821 - 0.0031049*SAP (mmHg)

Summary of Fit

RSquare	0.008506
RSquare Adj	-0.00151
Root Mean Square Error	0.516101
Mean of Response	2.911782
Observations (or Sum Wgts)	101

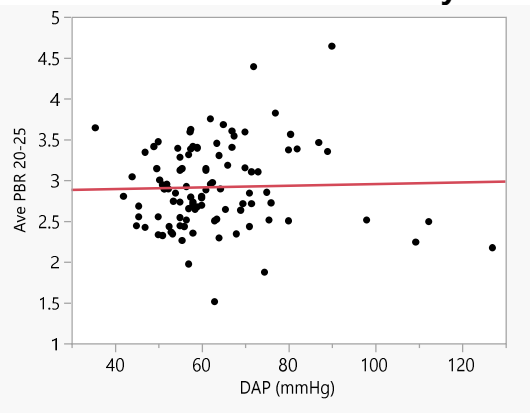
Analysis of Variance

Source	DF	Sum of Squares	Mean Square	F Ratio
Model	1	0.226237	0.226237	0.8494
Error	99	26.369642	0.266360	**Prob > F**
C. Total	100	26.595879		0.3590

Parameter Estimates

Term	Estimate	Std Error	t Ratio	Prob>|t|
Intercept	3.2715821	0.393767	8.31	<.0001*
SAP (mmHg)	-0.003105	0.003369	-0.92	0.3590

Bivariate Fit of Ave PBR 20-25 By DAP (mmHg)



Linear Fit

Linear Fit

Ave PBR 20-25 = 2.8472699 + 0.0010282*DAP (mmHg)

Summary of Fit

RSquare	0.000842
RSquare Adj	-0.00925
Root Mean Square Error	0.518092
Mean of Response	2.911782
Observations (or Sum Wgts)	101

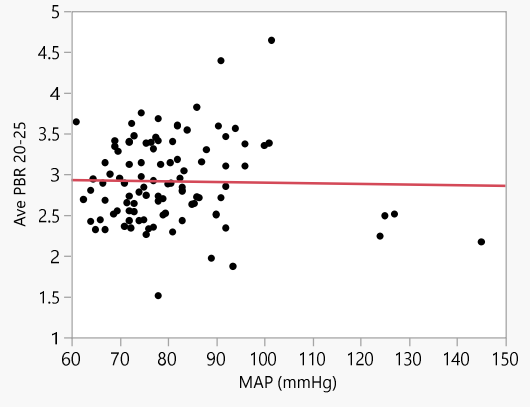
Analysis of Variance

Source	DF	Sum of Squares	Mean Square	F Ratio
Model	1	0.022396	0.022396	0.0834
Error	99	26.573484	0.268419	**Prob > F**
C. Total	100	26.595879		0.7733

Parameter Estimates

Term	Estimate	Std Error	t Ratio	Prob>|t|
Intercept	2.8472699	0.229213	12.42	<.0001*
DAP (mmHg)	0.0010282	0.003559	0.29	0.7733

Bivariate Fit of Ave PBR 20-25 By MAP (mmHg)



Linear Fit

Linear Fit

Ave PBR 20-25 = 2.9762745 - 0.0008001*MAP (mmHg)

Summary of Fit

RSquare	0.000453
RSquare Adj	-0.00964
Root Mean Square Error	0.518193
Mean of Response	2.911782
Observations (or Sum Wgts)	101

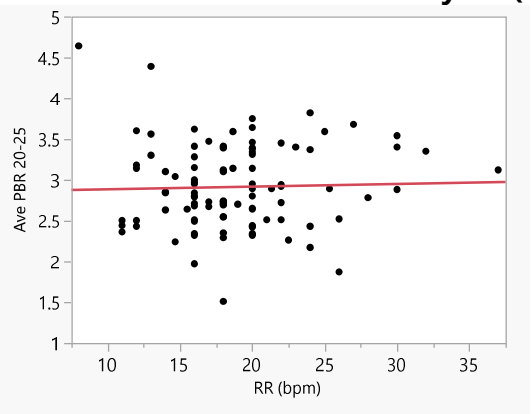
Analysis of Variance

Source	DF	Sum of Squares	Mean Square	F Ratio
Model	1	0.012039	0.012039	0.0448
Error	99	26.583840	0.268524	**Prob > F**
C. Total	100	26.595879		0.8327

Parameter Estimates

Term	Estimate	Std Error	t Ratio	Prob>|t|
Intercept	2.9762745	0.308911	9.63	<.0001*
MAP (mmHg)	-0.0008	0.003779	-0.21	0.8327

Bivariate Fit of Ave PBR 20-25 By RR (bpm)



Linear Fit

Linear Fit

Ave PBR 20-25 = 2.8501156 + 0.003274*RR (bpm)

Summary of Fit

RSquare	0.000956
RSquare Adj	-0.00914
Root Mean Square Error	0.518062
Mean of Response	2.911782
Observations (or Sum Wgts)	101

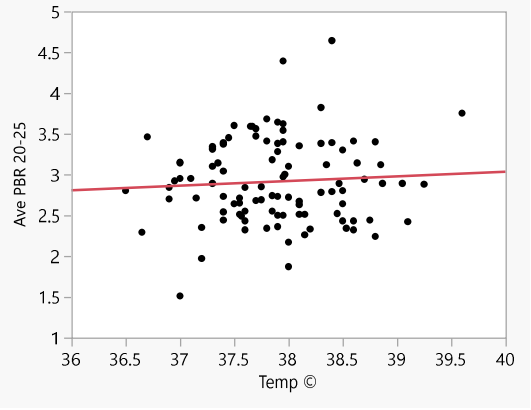
Analysis of Variance

Source	DF	Sum of Squares	Mean Square	F Ratio
Model	1	0.025417	0.025417	0.0947
Error	99	26.570463	0.268389	**Prob > F**
C. Total	100	26.595879		0.7589

Parameter Estimates

Term	Estimate	Std Error	t Ratio	Prob>|t|
Intercept	2.8501156	0.206913	13.77	<.0001*
RR (bpm)	0.003274	0.010639	0.31	0.7589

Bivariate Fit of Ave PBR 20-25 By Temp ©



Linear Fit

Ave PBR 20-25 = 0.74744 + 0.057132*Temp ©

Summary of Fit

RSquare	0.004518
RSquare Adj	-0.00554
Root Mean Square Error	0.517138
Mean of Response	2.911782
Observations (or Sum Wgts)	101

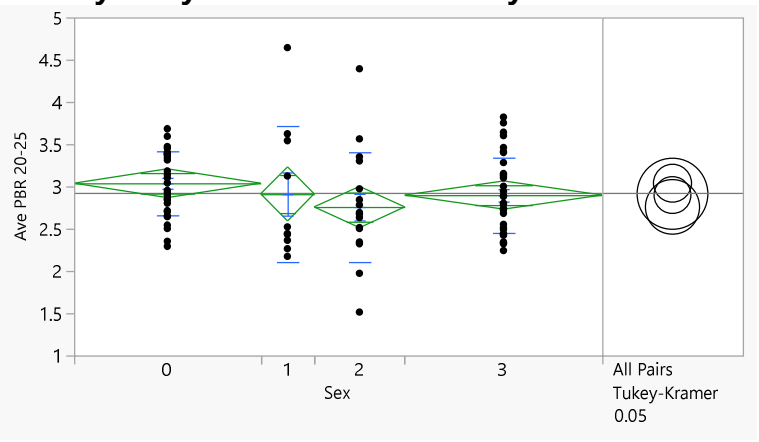
Analysis of Variance

Source	DF	Sum of Squares	Mean Square	F Ratio
Model	1	0.120169	0.120169	0.4493
Error	99	26.475710	0.267431	**Prob > F**
C. Total	100	26.595879		0.5042

Parameter Estimates

Term	Estimate	Std Error	t Ratio	Prob>|t|
Intercept	0.74744	3.229166	0.23	0.8174
Temp ©	0.057132	0.085229	0.67	0.5042

Oneway Analysis of Ave PBR 20-25 By Sex



Oneway Anova
Summary of Fit

Rsquare	0.037559
Adj Rsquare	0.007166
Root Mean Square Error	0.508258
Mean of Response	2.922525
Observations (or Sum Wgts)	99

Analysis of Variance

Source	DF	Sum of Squares	Mean Square	F Ratio	Prob > F
Sex	3	0.957704	0.319235	1.2358	0.3011
Error	95	24.540965	0.258326		
C. Total	98	25.498669			

Means and Std Deviations

Level	Number	Mean	Std Dev	Std Err Mean	Lower 95%	Upper 95%
0	35	3.0362857	0.3780918	0.0639092	2.9064066	3.1661648
1	10	2.91	0.8037413	0.2541653	2.3350381	3.4849619
2	17	2.7552941	0.6502991	0.1577207	2.4209412	3.0896471
3	37	2.8951351	0.4441072	0.0730108	2.7470624	3.0432079

Means Comparisons
Comparisons for all pairs using Tukey-Kramer HSD

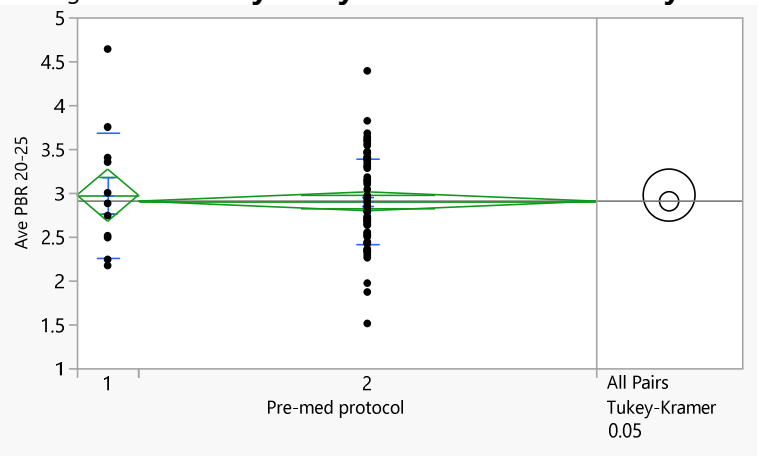
Connecting Letters Report

Level		Mean
0	A	3.0362857
1	A	2.9100000
3	A	2.8951351

Level		Mean
2	A	2.7552941

Levels not connected by same letter are significantly different.

Missing Rows2**Oneway Analysis of Ave PBR 20-25 By Pre-med protocol**



Oneway Anova
Summary of Fit

Rsquare	0.00194
Adj Rsquare	-0.00814
Root Mean Square Error	0.517807
Mean of Response	2.911782
Observations (or Sum Wgts)	101

Analysis of Variance

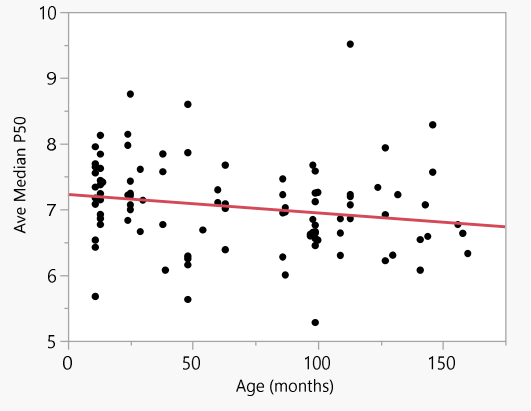
Source	DF	Sum of Squares	Mean Square	F Ratio	Prob > F
Pre-med protocol	1	0.051592	0.051592	0.1924	0.6619
Error	99	26.544287	0.268124		
C. Total	100	26.595879			

Means and Std Deviations

Level	Number	Mean	Std Dev	Std Err Mean	Lower 95%	Upper 95%
1	12	2.9733333	0.7144525	0.2062447	2.5193918	3.4272748
2	89	2.9034831	0.4876826	0.0516943	2.8007517	3.0062146

Means Comparisons
Comparisons for all pairs using Tukey-Kramer HSD

Bivariate Fit of Ave Median P50 By Age (months)



Linear Fit

Linear Fit

Ave Median P50 = 7.2260562 - 0.0028307*Age (months)

Summary of Fit

RSquare	0.036911
RSquare Adj	0.026982
Root Mean Square Error	0.673336
Mean of Response	7.034343
Observations (or Sum Wgts)	99

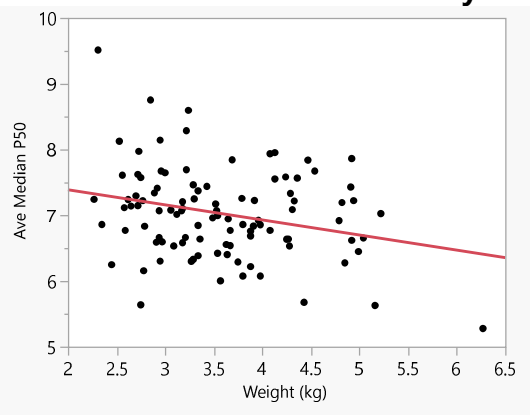
Analysis of Variance

Source	DF	Sum of Squares	Mean Square	F Ratio
Model	1	1.685486	1.68549	3.7176
Error	97	43.978052	0.45338	**Prob > F**
C. Total	98	45.663538		0.0568

Parameter Estimates

Term	Estimate	Std Error	t Ratio	Prob>|t|
Intercept	7.2260562	0.120275	60.08	<.0001*
Age (months)	-0.002831	0.001468	-1.93	0.0568

Bivariate Fit of Ave Median P50 By Weight (kg)



Linear Fit

Linear Fit

Ave Median P50 = 7.8423016 - 0.2287988*Weight (kg)

Summary of Fit

RSquare	0.070749
RSquare Adj	0.061363
Root Mean Square Error	0.658953
Mean of Response	7.023564
Observations (or Sum Wgts)	101

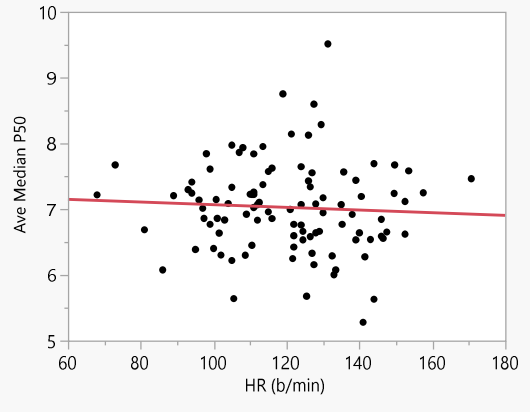
Analysis of Variance

Source	DF	Sum of Squares	Mean Square	F Ratio
Model	1	3.272913	3.27291	7.5375
Error	99	42.987710	0.43422	**Prob > F**
C. Total	100	46.260622		0.0072*

Parameter Estimates

Term	Estimate	Std Error	t Ratio	Prob>|t|
Intercept	7.8423016	0.30534	25.68	<.0001*
Weight (kg)	-0.228799	0.083338	-2.75	0.0072*

Bivariate Fit of Ave Median P50 By HR (b/min)



Linear Fit

Linear Fit

Ave Median P50 = 7.2662474 - 0.0020211*HR (b/min)

Summary of Fit

RSquare	0.003316
RSquare Adj	-0.00675
Root Mean Square Error	0.682444
Mean of Response	7.023564
Observations (or Sum Wgts)	101

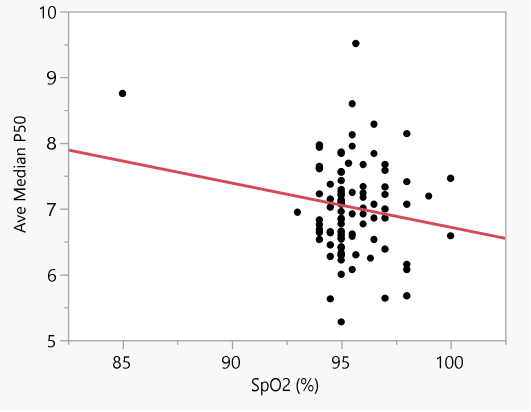
Analysis of Variance

Source	DF	Sum of Squares	Mean Square	F Ratio
Model	1	0.153402	0.153402	0.3294
Error	99	46.107220	0.465729	**Prob > F**
C. Total	100	46.260622		0.5673

Parameter Estimates

Term	Estimate	Std Error	t Ratio	Prob>|t|
Intercept	7.2662474	0.428271	16.97	<.0001*
HR (b/min)	-0.002021	0.003522	-0.57	0.5673

Bivariate Fit of Ave Median P50 By SpO2 (%)



Linear Fit

Linear Fit

Ave Median P50 = 13.421047 - 0.0670345*SpO2 (%)

Summary of Fit

RSquare	0.026723
RSquare Adj	0.016892
Root Mean Square Error	0.674382
Mean of Response	7.023564
Observations (or Sum Wgts)	101

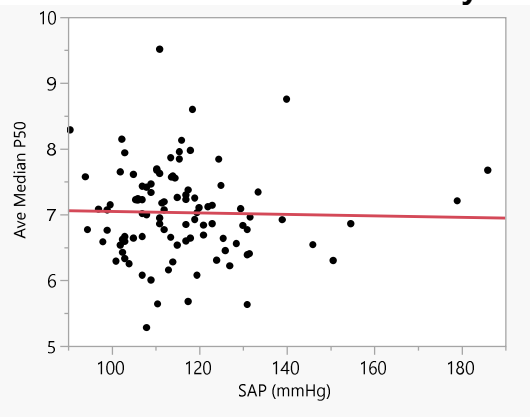
Analysis of Variance

Source	DF	Sum of Squares	Mean Square	F Ratio
Model	1	1.236239	1.23624	2.7183
Error	99	45.024383	0.45479	**Prob > F**
C. Total	100	46.260622		0.1024

Parameter Estimates

Term	Estimate	Std Error	t Ratio	Prob>|t|
Intercept	13.421047	3.88087	3.46	0.0008*
SpO2 (%)	-0.067035	0.040659	-1.65	0.1024

Bivariate Fit of Ave Median P50 By SAP (mmHg)



Linear Fit

Ave Median P50 = 7.1487455 - 0.0010803*SAP (mmHg)

Summary of Fit

RSquare	0.000592
RSquare Adj	-0.0095
Root Mean Square Error	0.683376
Mean of Response	7.023564
Observations (or Sum Wgts)	101

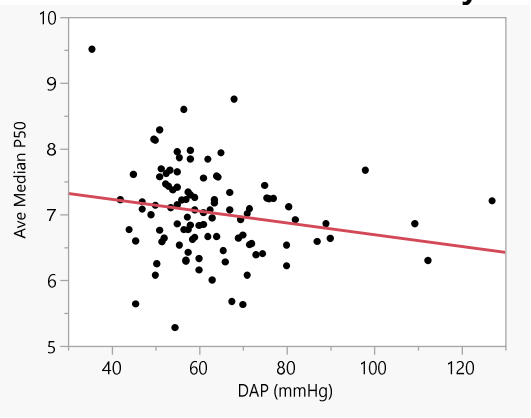
Analysis of Variance

Source	DF	Sum of Squares	Mean Square	F Ratio
Model	1	0.027385	0.027385	0.0586
Error	99	46.233237	0.467002	**Prob > F**
C. Total	100	46.260622		0.8092

Parameter Estimates

Term	Estimate	Std Error	t Ratio	Prob>|t|
Intercept	7.1487455	0.521392	13.71	<.0001*
SAP (mmHg)	-0.00108	0.004461	-0.24	0.8092

Bivariate Fit of Ave Median P50 By DAP (mmHg)



Linear Fit

Linear Fit

Ave Median P50 = 7.5843423 - 0.0089373*DAP (mmHg)

Summary of Fit

RSquare	0.03658
RSquare Adj	0.026849
Root Mean Square Error	0.670959
Mean of Response	7.023564
Observations (or Sum Wgts)	101

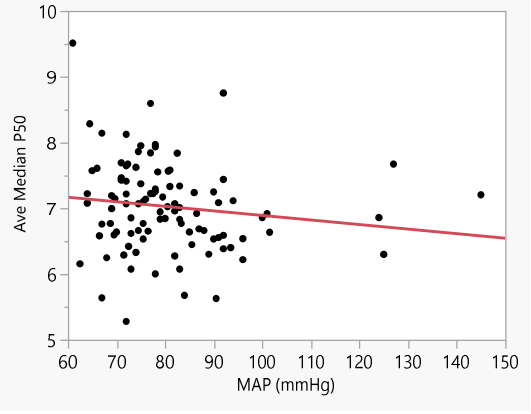
Analysis of Variance

Source	DF	Sum of Squares	Mean Square	F Ratio
Model	1	1.692232	1.69223	3.7590
Error	99	44.568390	0.45019	**Prob > F**
C. Total	100	46.260622		0.0554

Parameter Estimates

Term	Estimate	Std Error	t Ratio	Prob>|t|
Intercept	7.5843423	0.296844	25.55	<.0001*
DAP (mmHg)	-0.008937	0.00461	-1.94	0.0554

Bivariate Fit of Ave Median P50 By MAP (mmHg)



Linear Fit

Linear Fit

Ave Median P50 = 7.5811621 - 0.0069175*MAP (mmHg)

Summary of Fit

RSquare	0.019454
RSquare Adj	0.00955
Root Mean Square Error	0.676896
Mean of Response	7.023564
Observations (or Sum Wgts)	101

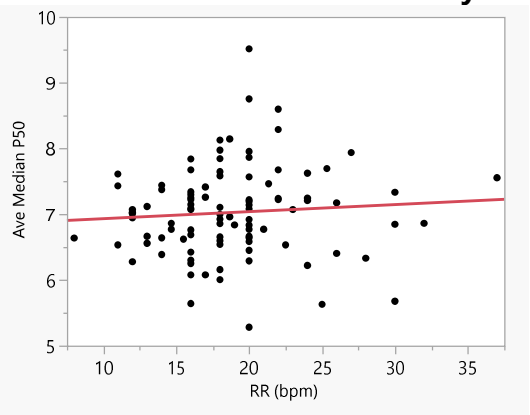
Analysis of Variance

Source	DF	Sum of Squares	Mean Square	F Ratio
Model	1	0.899971	0.899971	1.9642
Error	99	45.360651	0.458188	**Prob > F**
C. Total	100	46.260622		0.1642

Parameter Estimates

Term	Estimate	Std Error	t Ratio	Prob>|t|
Intercept	7.5811621	0.40352	18.79	<.0001*
MAP (mmHg)	-0.006918	0.004936	-1.40	0.1642

Bivariate Fit of Ave Median P50 By RR (bpm)



Linear Fit

Linear Fit

Ave Median P50 = 6.8217879 + 0.0107129*RR (bpm)

Summary of Fit

RSquare	0.005882
RSquare Adj	-0.00416
Root Mean Square Error	0.681565
Mean of Response	7.023564
Observations (or Sum Wgts)	101

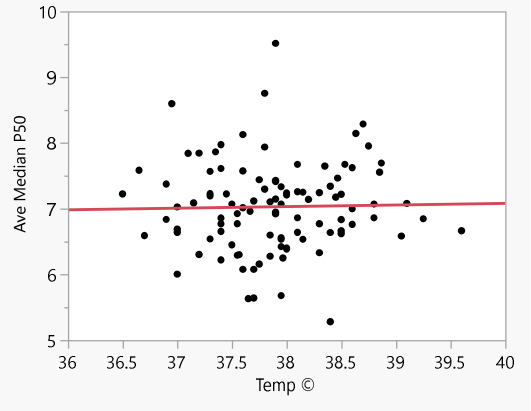
Analysis of Variance

Source	DF	Sum of Squares	Mean Square	F Ratio
Model	1	0.272118	0.272118	0.5858
Error	99	45.988504	0.464530	**Prob > F**
C. Total	100	46.260622		0.4459

Parameter Estimates

Term	Estimate	Std Error	t Ratio	Prob>|t|
Intercept	6.8217879	0.272216	25.06	<.0001*
RR (bpm)	0.0107129	0.013997	0.77	0.4459

Bivariate Fit of Ave Median P50 By Temp ©



Linear Fit

Linear Fit

Ave Median P50 = 6.0956961 + 0.0244929*Temp ©

Summary of Fit

RSquare	0.000477
RSquare Adj	-0.00962
Root Mean Square Error	0.683415
Mean of Response	7.023564
Observations (or Sum Wgts)	101

Analysis of Variance

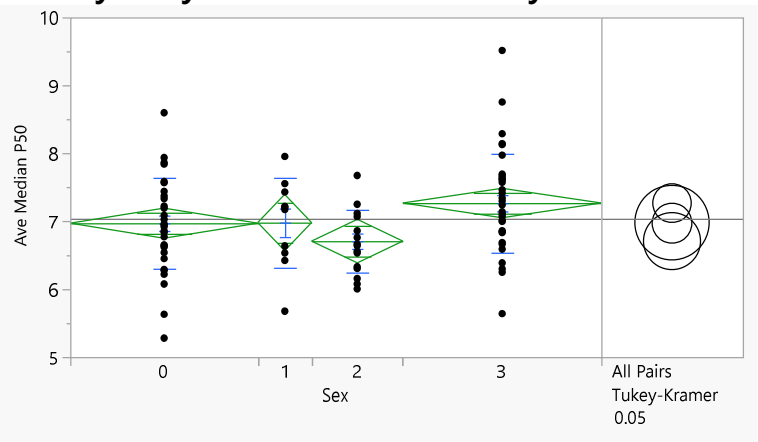
Source	DF	Sum of Squares	Mean Square	F Ratio
Model	1	0.022086	0.022086	0.0473
Error	99	46.238537	0.467056	**Prob > F**
C. Total	100	46.260622		0.8283

Parameter Estimates

Term	Estimate	Std Error	t Ratio	Prob>|t|
Intercept	6.0956961	4.267451	1.43	0.1563

Term	Estimate	Std Error	t Ratio	Prob>|t|
Temp ©	0.0244929	0.112633	0.22	0.8283

Oneway Analysis of Ave Median P50 By Sex



Oneway Anova

Summary of Fit

Rsquare	0.08739
Adj Rsquare	0.058571
Root Mean Square Error	0.662316
Mean of Response	7.034343
Observations (or Sum Wgts)	99

Analysis of Variance

Source	DF	Sum of Squares	Mean Square	F Ratio	Prob > F
Sex	3	3.990554	1.33018	3.0324	0.0331*
Error	95	41.672983	0.43866		
C. Total	98	45.663538			

Means and Std Deviations

Level	Number	Mean	Std Dev	Std Err Mean	Lower 95%	Upper 95%
0	35	6.9685714	0.6700528	0.1132596	6.7384002	7.1987426
1	10	6.9771667	0.6624944	0.2094991	6.5032467	7.4510866
2	17	6.7038235	0.4624639	0.112164	6.4660465	6.9416005
3	37	7.2638739	0.7271696	0.1195459	7.0214235	7.5063243

Means Comparisons

Comparisons for all pairs using Tukey-Kramer HSD

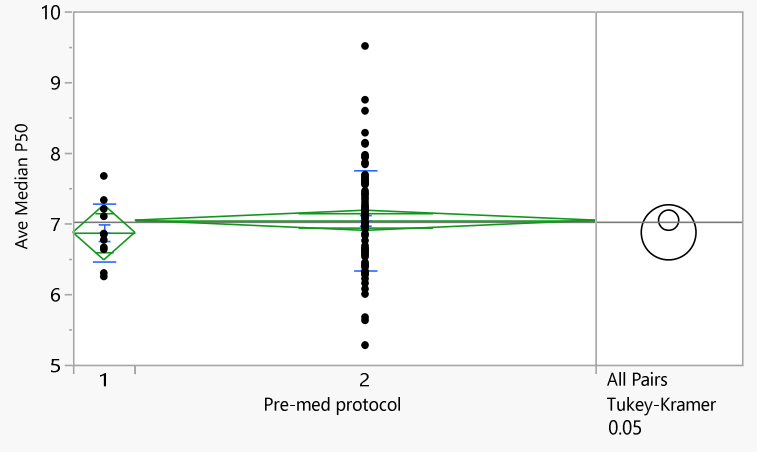
Connecting Letters Report

Level			Mean
3	A		7.2638739
1	A	B	6.9771667

Level			Mean
0	A	B	6.9685714
2		B	6.7038235

Levels not connected by same letter are significantly different.

Missing Rows2**Oneway Analysis of Ave Median P50 By Pre-med protocol**



Oneway Anova
Summary of Fit

Rsquare	0.006767
Adj Rsquare	-0.00327
Root Mean Square Error	0.681261
Mean of Response	7.023564
Observations (or Sum Wgts)	101

Analysis of Variance

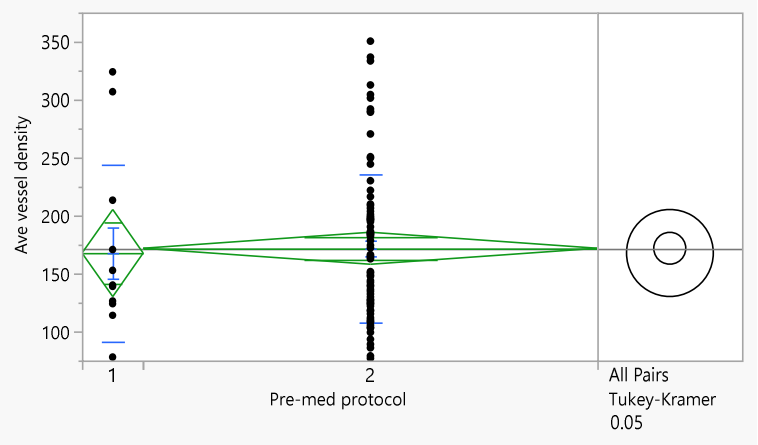
Source	DF	Sum of Squares	Mean Square	F Ratio	Prob > F
Pre-med protocol	1	0.313058	0.313058	0.6745	0.4135
Error	99	45.947564	0.464117		
C. Total	100	46.260622			

Means and Std Deviations

Level	Number	Mean	Std Dev	Std Err Mean	Lower 95%	Upper 95%
1	12	6.8719444	0.4095093	0.1182152	6.6117546	7.1321343
2	89	7.0440075	0.707933	0.0750408	6.8948798	7.1931352

Means Comparisons
Comparisons for all pairs using Tukey-Kramer HSD

Oneway Analysis of Ave vessel density By Pre-med protocol



Oneway Anova
Summary of Fit

Rsquare	0.000405
Adj Rsquare	-0.00969
Root Mean Square Error	65.37579
Mean of Response	171.2688
Observations (or Sum Wgts)	101

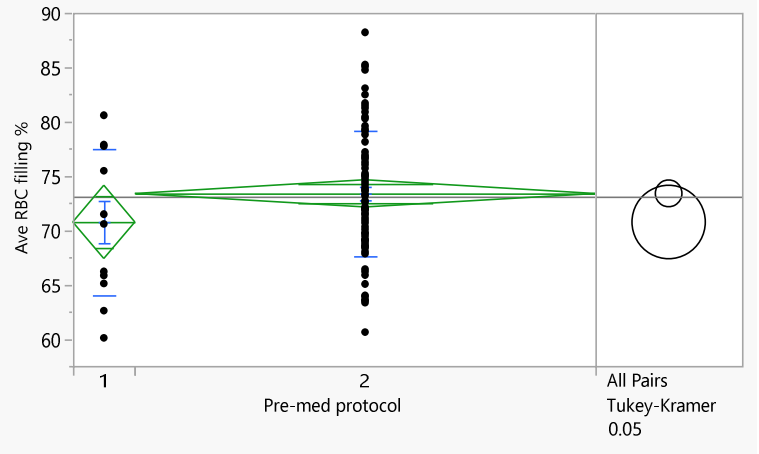
Analysis of Variance

Source	DF	Sum of Squares	Mean Square	F Ratio	Prob > F
Pre-med protocol	1	171.26	171.26	0.0401	0.8418
Error	99	423125.39	4273.99		
C. Total	100	423296.65			

Means and Std Deviations

Level	Number	Mean	Std Dev	Std Err Mean	Lower 95%	Upper 95%
1	12	167.7225	76.342994	22.038324	119.21648	216.22852
2	89	171.74697	63.872619	6.7704841	158.29205	185.20188

Oneway Analysis of Ave RBC filling % By Pre-med protocol



Oneway Anova
Summary of Fit

Rsquare	0.020913
Adj Rsquare	0.011024
Root Mean Square Error	5.889513
Mean of Response	73.07416
Observations (or Sum Wgts)	101

Analysis of Variance

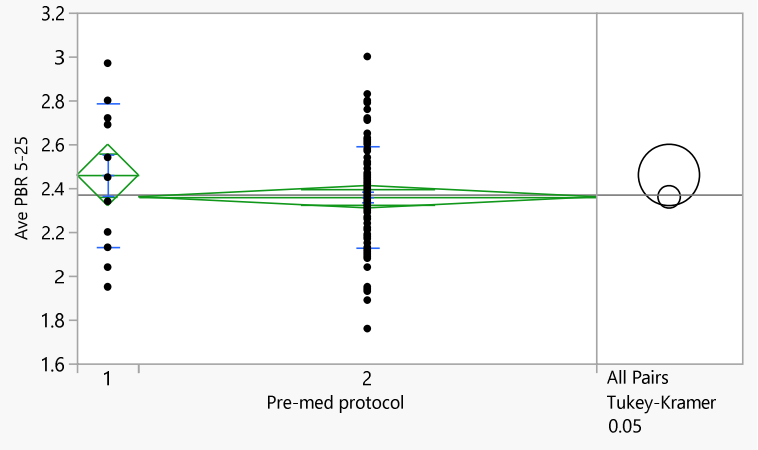
Source	DF	Sum of Squares	Mean Square	F Ratio	Prob > F
Pre-med protocol	1	73.3495	73.3495	2.1147	0.1491
Error	99	3433.9495	34.6864		
C. Total	100	3507.2991			

Means and Std Deviations

Level	Number	Mean	Std Dev	Std Err Mean	Lower 95%	Upper 95%
1	12	70.753333	6.7298593	1.942743	66.477385	75.029282
2	89	73.387079	5.775879	0.6122419	72.170376	74.603781

Means Comparisons
Comparisons for all pairs using Tukey-Kramer HSD

Oneway Analysis of Ave PBR 5-25 By Pre-med protocol



Oneway Anova
Summary of Fit

Rsquare	0.017532
Adj Rsquare	0.007608
Root Mean Square Error	0.243831
Mean of Response	2.372178
Observations (or Sum Wgts)	101

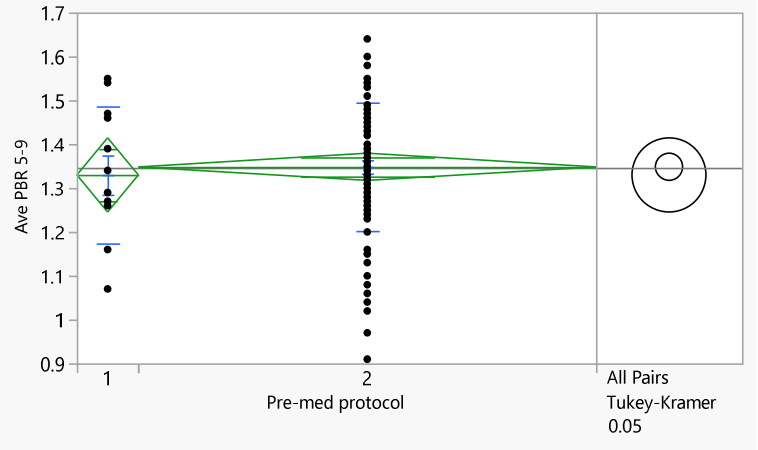
Analysis of Variance

Source	DF	Sum of Squares	Mean Square	F Ratio	Prob > F
Pre-med protocol	1	0.1050309	0.105031	1.7666	0.1869
Error	99	5.8858899	0.059453		
C. Total	100	5.9909208			

Means and Std Deviations

Level	Number	Mean	Std Dev	Std Err Mean	Lower 95%	Upper 95%
1	12	2.46	0.3279412	0.0946685	2.2516361	2.6683639
2	89	2.3603371	0.2311751	0.0245045	2.3116395	2.4090346

Oneway Analysis of Ave PBR 5-9 By Pre-med protocol



Oneway Anova
Summary of Fit

Rsquare	0.001706
Adj Rsquare	-0.00838
Root Mean Square Error	0.147451
Mean of Response	1.346436
Observations (or Sum Wgts)	101

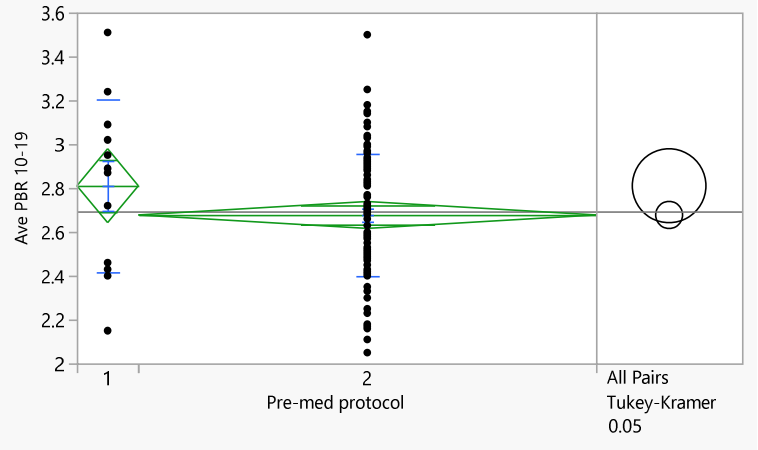
Analysis of Variance

Source	DF	Sum of Squares	Mean Square	F Ratio	Prob > F
Pre-med protocol	1	0.0036786	0.003679	0.1692	0.6817
Error	99	2.1524382	0.021742		
C. Total	100	2.1561168			

Means and Std Deviations

Level	Number	Mean	Std Dev	Std Err Mean	Lower 95%	Upper 95%
1	12	1.33	0.1561468	0.0450757	1.2307891	1.4292109
2	89	1.3486517	0.1463277	0.0155107	1.3178274	1.379476

Oneway Analysis of Ave PBR 10-19 By Pre-med protocol



Oneway Anova
Summary of Fit

Rsquare	0.021475
Adj Rsquare	0.01159
Root Mean Square Error	0.293841
Mean of Response	2.693465
Observations (or Sum Wgts)	101

Analysis of Variance

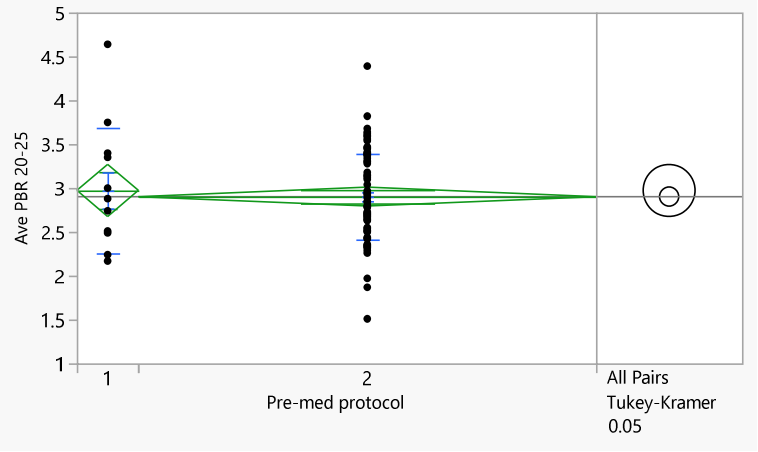
Source	DF	Sum of Squares	Mean Square	F Ratio	Prob > F
Pre-med protocol	1	0.1875910	0.187591	2.1726	0.1437
Error	99	8.5478962	0.086342		
C. Total	100	8.7354871			

Means and Std Deviations

Level	Number	Mean	Std Dev	Std Err Mean	Lower 95%	Upper 95%
1	12	2.8108333	0.3937802	0.1136746	2.5606373	3.0610294
2	89	2.6776404	0.278841	0.0295571	2.6189019	2.736379

Means Comparisons
Comparisons for all pairs using Tukey-Kramer HSD

Oneway Analysis of Ave PBR 20-25 By Pre-med protocol



Oneway Anova
Summary of Fit

Rsquare	0.00194
Adj Rsquare	-0.00814
Root Mean Square Error	0.517807
Mean of Response	2.911782
Observations (or Sum Wgts)	101

Analysis of Variance

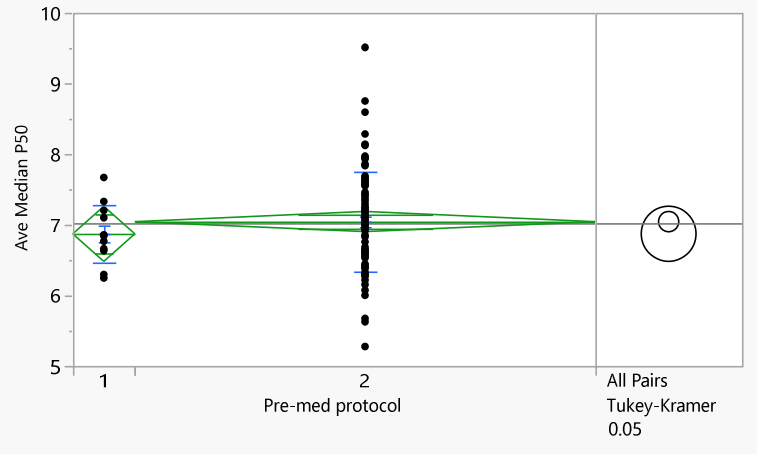
Source	DF	Sum of Squares	Mean Square	F Ratio	Prob > F
Pre-med protocol	1	0.051592	0.051592	0.1924	0.6619
Error	99	26.544287	0.268124		
C. Total	100	26.595879			

Means and Std Deviations

Level	Number	Mean	Std Dev	Std Err Mean	Lower 95%	Upper 95%
1	12	2.9733333	0.7144525	0.2062447	2.5193918	3.4272748
2	89	2.9034831	0.4876826	0.0516943	2.8007517	3.0062146

Means Comparisons
Comparisons for all pairs using Tukey-Kramer HSD

Oneway Analysis of Ave Median P50 By Pre-med protocol



Oneway Anova
Summary of Fit

Rsquare	0.006767
Adj Rsquare	-0.00327
Root Mean Square Error	0.681261
Mean of Response	7.023564
Observations (or Sum Wgts)	101

Analysis of Variance

Source	DF	Sum of Squares	Mean Square	F Ratio	Prob > F
Pre-med protocol	1	0.313058	0.313058	0.6745	0.4135
Error	99	45.947564	0.464117		
C. Total	100	46.260622			

Means and Std Deviations

Level	Number	Mean	Std Dev	Std Err Mean	Lower 95%	Upper 95%
1	12	6.8719444	0.4095093	0.1182152	6.6117546	7.1321343
2	89	7.0440075	0.707933	0.0750408	6.8948798	7.1931352

Means Comparisons
Comparisons for all pairs using Tukey-Kramer HSD

Ave vessel density

Coverage	BC Lower	BC Upper
0.95	265.186	320.451
0.90	269.558	316.643
0.80	275.313	311.63
0.50	284.028	303.344

Original Estimate 293.1572

Coverage	BC Lower	BC Upper
0.95	34.5801	62.6777
0.90	37.1746	60.1317
0.80	39.2955	57.6029
0.50	43.6767	53.1583

Original Estimate 49.38046

Ave RBC filling %

Coverage	BC Lower	BC Upper
0.95	82.4026	86.1986
0.90	82.7221	85.9011
0.80	83.0693	85.5375
0.50	83.6271	84.9661

Original Estimate 84.16913

Coverage	BC Lower	BC Upper
0.95	60.253	63.6012
0.90	60.4959	63.3162
0.80	60.8051	63.006
0.50	61.3281	62.476

Original Estimate 61.97919

Ave PBR 5-25

Coverage	BC Lower	BC Upper
0.95	2.75697	2.91732
0.90	2.76971	2.90263
0.80	2.78379	2.88877
0.50	2.80776	2.86477

Original Estimate 2.830728

Coverage	BC Lower	BC Upper
0.95	1.83824	1.98003
0.90	1.84795	1.96941
0.80	1.86178	1.95579
0.50	1.88435	1.93356

Original Estimate 1.913628

Ave PBR 5-9

Coverage	BC Lower	BC Upper
0.95	1.58452	1.66533

Coverage	BC Lower	BC Upper
0.90	1.59105	1.65883
0.80	1.59884	1.65068
0.50	1.6111	1.63813

Original Estimate 1.621526

Coverage	BC Lower	BC Upper
0.95	1.01555	1.12398
0.90	1.02311	1.11592
0.80	1.03424	1.10583
0.50	1.05096	1.08863

Original Estimate 1.071345

Ave PBR 10-19

Coverage	BC Lower	BC Upper
0.95	3.15235	3.35943
0.90	3.17003	3.3421
0.80	3.18813	3.32257
0.50	3.21894	3.29043

Original Estimate 3.247177

Coverage	BC Lower	BC Upper
0.95	2.04789	2.22387
0.90	2.06181	2.20787
0.80	2.07814	2.19378
0.50	2.10492	2.16644

Original Estimate 2.139754

Ave PBR 20-25

Coverage	BC Lower	BC Upper
0.95	3.69093	4.09097
0.90	3.7173	4.05819
0.80	3.75057	4.01788
0.50	3.80983	3.95166

Original Estimate 3.877938

Coverage	BC Lower	BC Upper
0.95	1.76567	2.09066
0.90	1.79313	2.0685
0.80	1.82936	2.04328
0.50	1.88081	1.99289

Original Estimate 1.945627

Median P50

Coverage	BC Lower	BC Upper
0.95	8.04696	8.63283
0.90	8.08684	8.57636
0.80	8.13531	8.508
0.50	8.21837	8.42093

Original Estimate 8.297788

Coverage	BC Lower	BC Upper
0.95	5.5126	5.967
0.90	5.54766	5.92902
0.80	5.58554	5.88946
0.50	5.65911	5.81793

Original Estimate 5.749341

Response Ave PBR 5-25 Label=Age (months)
Whole Model

Lack Of Fit

Source	DF	Sum of Squares	Mean Square	F Ratio
Lack Of Fit	30	1.6221397	0.054071	0.9125
Pure Error	67	3.9701170	0.059255	**Prob > F**
Total Error	97	5.5922567		0.5994
				Max RSq
				0.3081

Power Details
Test Data
Power

α	σ	δ	Number	Power	AdjPower	LowerCL	UpperCL
0.0500	0.240109	0.038399	99	0.3505	0.2257	0.0500	0.9430

Least Significant Number

α	σ	δ	Number(LSN)
0.0500	0.240109	0.038399	152.6414

Least Significant Value

α	σ	Number	LSV
0.0500	0.240109	99	0.001039

Response Ave PBR 5-25 Label=HR (b/min)
Whole Model

Lack Of Fit

Source	DF	Sum of Squares	Mean Square	F Ratio
Lack Of Fit	72	4.4012659	0.061129	1.1026
Pure Error	27	1.4968917	0.055440	**Prob > F**
Total Error	99	5.8981576		0.3999
				Max RSq
				0.7501

Data

Power Details
Test Data
Power

α	σ	δ	Number	Power	AdjPower	LowerCL	UpperCL
0.0500	0.244085	0.030306	101	0.2352	0.1108	0.0500	0.8926

Least Significant Number

α	σ	δ	Number(LSN)
0.0500	0.244085	0.030306	251.6196

Least Significant Value

α	σ	Number	LSV
0.0500	0.244085	101	0.002499

Response Ave PBR 5-25 Label=RR (bpm)
Whole Model

Lack Of Fit

Source	DF	Sum of Squares	Mean Square	F Ratio
Lack Of Fit	25	1.9447293	0.077789	1.4267
Pure Error	74	4.0346644	0.054522	**Prob > F**
Total Error	99	5.9793937		0.1221
				Max RSq
				0.3265

Data

Power Details
Test Data
Power

α	σ	δ	Number	Power	AdjPower	LowerCL	UpperCL
0.0500	0.24576	0.010683	101	0.0717	0.0500	0.0500	0.6692

Least Significant Number

α	σ	δ	Number(LSN)
0.0500	0.24576	0.010683	2035.341

Least Significant Value

α	σ	Number	LSV
0.0500	0.24576	101	0.010014

Response Ave PBR 5-25 Label=SpO2 (%)
Whole Model

Lack Of Fit

Source	DF	Sum of Squares	Mean Square	F Ratio
Lack Of Fit	13	0.9610635	0.073928	1.2826
Pure Error	86	4.9571473	0.057641	**Prob > F**
Total Error	99	5.9182109		0.2392
				Max RSq
				0.1726

Data

Power Details
Test Data
Power

α	σ	δ	Number	Power	AdjPower	LowerCL	UpperCL
0.0500	0.244499	0.026831	101	0.1939	0.0718	0.0500	0.8637

Least Significant Number

α	σ	δ	Number(LSN)
0.0500	0.244499	0.026831	321.4227

Least Significant Value

α	σ	Number	LSV
0.0500	0.244499	101	0.029249

Response Ave PBR 5-25 Label=Temp ©
Whole Model

Lack Of Fit

Source	DF	Sum of Squares	Mean Square	F Ratio
Lack Of Fit	46	2.7163201	0.059050	0.9988
Pure Error	53	3.1334167	0.059121	**Prob > F**
Total Error	99	5.8497368		0.4990
				Max RSq

Source	DF	Sum of Squares	Mean Square	F Ratio
				0.4770

Data

Power Details
Test Data
Power

α	σ	δ	Number	Power	AdjPower	LowerCL	UpperCL
0.0500	0.243081	0.037388	101	0.3341	0.2090	0.0500	0.9377

Least Significant Number

α	σ	δ	Number(LSN)
0.0500	0.243081	0.037388	164.8213

Least Significant Value

α	σ	Number	LSV
0.0500	0.243081	101	0.079492

Response Ave PBR 5-25 Label=Weight (kg)
Whole Model

Lack Of Fit

Source	DF	Sum of Squares	Mean Square	F Ratio
Lack Of Fit	95	5.8101053	0.061159	1.8297
Pure Error	4	0.1337000	0.033425	**Prob > F**
Total Error	99	5.9438053		0.2980
				Max RSq
				0.9777

Data

Power Details
Test Data
Power

α	σ	δ	Number	Power	AdjPower	LowerCL	UpperCL
0.0500	0.245027	0.021598	101	0.1418	0.0500	0.0500	0.8112

Least Significant Number

α	σ	δ	Number(LSN)
0.0500	0.245027	0.021598	496.8333

Least Significant Value

α	σ	Number	LSV
0.0500	0.245027	101	0.061491

Response Ave PBR 5-25 Label=Sex
Whole Model

α	σ	δ	Number	Power	AdjPower	LowerCL	UpperCL
0.05	0.234449	0.072225	99	0.7121	0.5142	0.0527	0.9994
α	σ	δ	Number(LSN)				
0.05	0.234449	0.072225	85.86412				

Power details for MAP

α	σ	δ	Number (LSN)
0.05	13.52265	2.640009	103.2413

α	σ	δ	Number	Power	Adj Power	Lower CL	Upper CL
0.05	13.52265	2.640009	101	0.4933	0.378	0.05	0.9743

Response Data Label=Median P50
Whole Model

REML Variance Component Estimates

Random Effect	Var Ratio	Var Component	Std Error	95% Lower	95% Upper	Wald p-Value	Pct of Total
ID	0.5482353	0.2917241	0.069278	0.1559417	0.4275064	<.0001*	35.410
Label 4[ID]		0.5321147	0.0542929	0.4398913	0.6568865	<.0001*	64.590
Total		0.8238387	0.0761163	0.6928661	0.9960206		100.000

-2 LogLikelihood = 740.18743196
Note: Total is the sum of the positive variance components.
Total including negative estimates = 0.8238387

Residual is confounded with Label 4[ID] and has been removed.

Response Data Label=PBR 10-19
Whole Model

REML Variance Component Estimates

Random Effect	Var Ratio	Var Component	Std Error	95% Lower	95% Upper	Wald p-Value	Pct of Total
ID	0.397329	0.0481092	0.0135221	0.0216065	0.074612	0.0004*	28.435
Label 4[ID]		0.1210816	0.0124261	0.099991	0.1496663	<.0001*	71.565
Total		0.1691909	0.015132	0.1430496	0.2032565		100.000

-2 LogLikelihood = 292.48248725
Note: Total is the sum of the positive variance components.
Total including negative estimates = 0.1691909

Residual is confounded with Label 4[ID] and has been removed.

Response Data Label=PBR 20-25
Whole Model

REML Variance Component Estimates

Random Effect	Var Ratio	Var Component	Std Error	95% Lower	95% Upper	Wald p-Value	Pct of Total
ID	0.075078	0.0515914	0.0506327	-0.047647	0.1508297	0.3082	6.983
Label 4[ID]		0.6871702	0.0722173	0.5649986	0.8539758	<.0001*	93.017
Total		0.7387616	0.0620204	0.6308201	0.8771484		100.000

-2 LogLikelihood = 731.83042032
Note: Total is the sum of the positive variance components.
Total including negative estimates = 0.7387616

Residual is confounded with Label 4[ID] and has been removed.

Response Data Label=PBR 5-9
Whole Model

REML Variance Component Estimates

Random Effect	Var Ratio	Var Component	Std Error	95% Lower	95% Upper	Wald p-Value	Pct of Total
ID	0.4189157	0.0121683	0.0032685	0.0057622	0.0185745	0.0002*	29.524
Label 4[ID]		0.0290472	0.0029607	0.0240174	0.0358501	<.0001*	70.476
Total		0.0412156	0.0036949	0.0348343	0.0495365		100.000

-2 LogLikelihood = -118.6566111
Note: Total is the sum of the positive variance components.
Total including negative estimates = 0.0412156

Residual is confounded with Label 4[ID] and has been removed.

Response Data Label=PBR 5-25
Whole Model

REML Variance Component Estimates

Random Effect	Var Ratio	Var Component	Std Error	95% Lower	95% Upper	Wald p-Value	Pct of Total
ID	0.3601122	0.0333543	0.0099677	0.013818	0.0528907	0.0008*	26.477
Label 4[ID]		0.092622	0.0095368	0.0764427	0.1145725	<.0001*	73.523
Total		0.1259764	0.0111781	0.1066472	0.1511121		100.000

-2 LogLikelihood = 209.67071446

Note: Total is the sum of the positive variance components.
Total including negative estimates = 0.1259764

Residual is confounded with Label 4[ID] and has been removed.

Response Data Label=RBC filling %
Whole Model

REML Variance Component Estimates

Random Effect	Var Ratio	Var Component	Std Error	95% Lower	95% Upper	Wald p-Value	Pct of Total
ID	0.4753324	21.823407	5.5865779	10.873916	32.772899	<.0001*	32.219
Label 4[ID]		45.91189	4.703672	37.926549	56.728967	<.0001*	67.781
Total		67.735297	6.1678561	57.103247	81.657246		100.000

-2 LogLikelihood = 2024.434958
Note: Total is the sum of the positive variance components.
Total including negative estimates = 67.735297

Residual is confounded with Label 4[ID] and has been removed.

Response Data Label=Valid vessel density
Whole Model

REML Variance Component Estimates

Random Effect	Var Ratio	Var Component	Std Error	95% Lower	95% Upper	Wald p-Value	Pct of Total
ID	1.0052017	3170.1821	611.85919	1970.9601	4369.4041	<.0001*	50.130
Label 4[ID]		3153.7772	322.75363	2605.7628	3895.8805	<.0001*	49.870
Total		6323.9593	638.82361	5237.3655	7789.6015		100.000

-2 LogLikelihood = 3300.589548
Note: Total is the sum of the positive variance components.
Total including negative estimates = 6323.9593

Residual is confounded with Label 4[ID] and has been removed.

Annex II: Chapter III Unformatted statistical report

Validation of a commercial human enzyme-linked immunosorbent assay to measure syndecan-1 (CD138) concentration in feline sera

```
> file_path <- file.choose()  # This will allow you to select the file int
eractively
> data <- read_excel(file_path)
>
> # Function to perform Shapiro-Wilk test and Q-Q plot for one variable
> test_normality_one_var <- function(x, variable_name) {
+     # Remove NA values
+     x <- na.omit(x)
+
+     # Shapiro-Wilk test
+     shapiro_test <- shapiro.test(x)
+
+     # Print the Shapiro-Wilk test result
+     cat("\nShapiro-Wilk Test for", variable_name, "\n")
+     print(shapiro_test)
+
+     # Q-Q plot
+     qqplot <- ggplot(data.frame(x), aes(sample = x)) +
+         stat_qq() +
+         stat_qq_line() +
+         ggtitle(paste("Q-Q Plot for", variable_name)) +
+         theme_minimal() # Add a theme for better visualization
+
+     print(qqplot)
+ }
>
> # Loop through each numeric column and perform the normality test
> for (var_name in names(data)) {
+     if (is.numeric(data[[var_name]])) {
+         test_normality_one_var(data[[var_name]], var_name)
+     }
+ }

Shapiro-Wilk Test for WRVH_OD

        Shapiro-Wilk normality test

data:  x
W = 0.85152, p-value = 0.06056


Shapiro-Wilk Test for WRVH_SDC-1

        Shapiro-Wilk normality test

data:  x
W = 0.85142, p-value = 0.06039


Shapiro-Wilk Test for BRVH_OD

        Shapiro-Wilk normality test

data:  x
W = 0.85716, p-value = 0.1125


Shapiro-Wilk Test for BRVH_SDC-1

        Shapiro-Wilk normality test

data:  x
```

```
W = 0.84749, p-value = 0.08985


Shapiro-Wilk Test for DL_OD

        Shapiro-Wilk normality test

data:  x
W = 0.82363, p-value = 0.06958


Shapiro-Wilk Test for DL_SDC-1

        Shapiro-Wilk normality test

data:  x
W = 0.82348, p-value = 0.06935


Shapiro-Wilk Test for DL_SDC-1_corr

        Shapiro-Wilk normality test

data:  x
W = 0.96824, p-value = 0.8855


Shapiro-Wilk Test for P_OD

        Shapiro-Wilk normality test

data:  x
W = 0.78469, p-value = 0.01364


Shapiro-Wilk Test for P_SDC-1

        Shapiro-Wilk normality test

data:  x
W = 0.78469, p-value = 0.01364


Shapiro-Wilk Test for P_SDC-1_corr

        Shapiro-Wilk normality test

data:  x
W = 0.92938, p-value = 0.4754


Shapiro-Wilk Test for SRH_OD

        Shapiro-Wilk normality test

data:  x
W = 0.71098, p-value = 0.01547


Shapiro-Wilk Test for SRH_SDC-1

        Shapiro-Wilk normality test

data:  x
W = 0.71112, p-value = 0.01552


> cv <- function(x) {
```

```
+     return (sd(x, na.rm = TRUE) / mean(x, na.rm = TRUE))
+ }
> cv_values <- sapply(data, cv)
>
> print("Coefficient of Variation:")
[1] "Coefficient of Variation:"
> print(cv_values)
      WRVH_OD     WRVH_SDC-1        BRVH_OD     BRVH_SDC-1          DL_OD
   0.04952593     0.04803848     0.07224239     0.11960669     1.19997831
     DL_SDC-1 DL_SDC-1_corr           P_OD       P_SDC-1  P_SDC-1_corr
   1.16516645     0.12137149     1.28151740     1.31858448     0.14934127
       SRH_OD      SRH_SDC-1         SRL_OD      SRL_SDC-1
   1.17771228     1.23292111     1.14257818     1.19092386


library(readxl)

file_path<-file.choose()
data<-read_excel(file_path)
summary(data)
summary_stats <- summary(data)
summary_stats_df <- as.data.frame(t(as.matrix(summary_stats)))
write_xlsx(summary_stats_df, "Summary_Statistics.xlsx")
View(summary_stats_df)
cat("Summary_Statistics.xlsx has been saved to:", getwd(), "\n")
summary_stats_df$Statistic <- rownames(summary_stats_df)

# Reorder the columns to have 'Statistic' as the first column
summary_stats_df <- summary_stats_df[, c(ncol(summary_stats_df), 1:(ncol(su
mmary_stats_df) - 1))]
 # Write the tidied summary statistics to an Excel file
write_xlsx(summary_stats_df, "Summary_Statistics_Tidied.xlsx")
# Confirm the location
cat("Summary_Statistics_Tidied.xlsx has been saved to:", getwd(), "\n")
Summary_Statistics_Tidied.xlsx has been saved to: C:/Users/ivayl/Documents
compute_summary <- function(df) {
  +     summary_stats <- data.frame(
    +         Statistic = c("Min", "1st Qu.", "Median", "Mean", "3rd Qu.",
"Max"),
    +         row.names = NULL
    +     )
  +
    +     for (col in names(df)) {
      +         if (is.numeric(df[[col]])) {
        +             col_stats <- summary(df[[col]])
        +             summary_stats[[col]] <- col_stats[c("Min.", "1st Qu."
, "Median", "Mean", "3rd Qu.", "Max.")]
        +         }
      +     }
  +
    +     return(summary_stats)
  + }

# Compute summary statistics
summary_stats_df <- compute_summary(data)
# Write the tidied summary statistics to an Excel file
write_xlsx(summary_stats_df, "Summary_Statistics_Tidied.xlsx")

# Confirm the location
cat("Summary_Statistics_Tidied.xlsx has been saved to:", getwd(), "\n")
Summary_Statistics_Tidied.xlsx has been saved to: C:/Users/ivayl/Documents
compute_summary_with_sd <- function(df) {
  +     summary_stats <- data.frame(
```

```
    +         Statistic = c("Min", "1st Qu.", "Median", "Mean", "3rd Qu.",
"Max", "SD"),
    +         row.names = NULL
    +     )
  +
    +     for (col in names(df)) {
      +         if (is.numeric(df[[col]])) {
        +             col_stats <- summary(df[[col]])
        +             col_sd <- sd(df[[col]], na.rm = TRUE)
        +             summary_stats[[col]] <- c(
          +                 col_stats[c("Min.", "1st Qu.", "Median", "Mean"
, "3rd Qu.", "Max.")],
          +                 col_sd
          +             )
        +         }
      +     }
  +
    +     return(summary_stats)
  + }

# Compute summary statistics including standard deviation
summary_stats_df <- compute_summary_with_sd(data)

# Write the tidied summary statistics to an Excel file
write_xlsx(summary_stats_df, "Summary_Statistics_with_SD.xlsx")
```

Annex III: Chapter III Optic density results

Validation of a commercial human enzyme-linked immunosorbent assay to measure syndecan-1 (CD138) concentration in feline sera

1. Undiluted and diluted (1:10) samples from healthy and diseased cats and feline recombinant SDC-1 standard dilutions

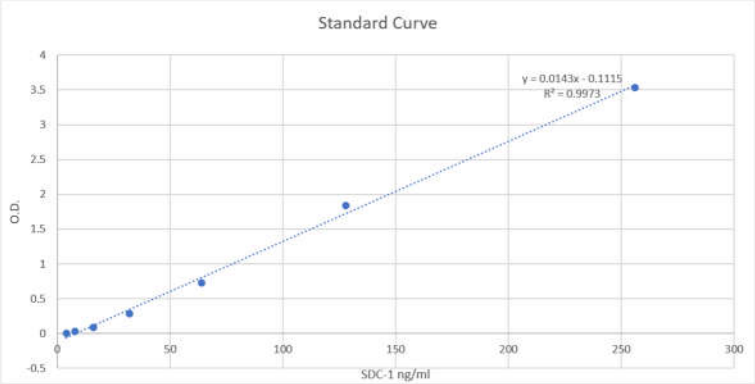
1.1 Plate layout

	1	2	3	4	5	6	7	8	9	10	11	12
A	Standard 256	256	frSDC 256	frSDC 256	S1	S1	S1 1:10	S1 1:10	S15	S15	S15 1:10	S15 1:10
B	Standard 128	128	frSDC 128	frSDC 128	S2	S2	S2 1:10	S2 1:10	S14	S14	S14 1:10	S14 1:10
C	Standard 64	64	frSDC 64	frSDC 64	S4	S4	S4 1:10	S4 1:10	S9	S9	S9 1:10	S9 1:10
D	Standard 32	32	frSDC 65	frSDC 65	S5	S5	S5 1:10	S5 1:10	S8	S8	S8 1:10	S8 1:10
E	Standard 16	16	frSDC 16	frSDC 16	S6	S6	S6 1:10	S6 1:10	S7	S7	S7 1:10	S7 1:10
F	Standard 8	8	frSDC 8	frSDC 8	S10	S10	S10 1:10	S10 1:10	H1	H1	H1 1:10	H1 1:10
G	Standard 4	4	frSDC 4	frSDC 4	S11	S11	S11 1:10	S11 1:10	H2	H1	H1 1:10	H1 1:10
H	Blank	0	frSDC 2	frSDC 2	S3	S13	S13 1:10	S13 1:10	Control	Control	Empty	Empty

Optic densities at 450 nm

	1	2	3	4	5	6	7	8	9	10	11	12
A	3.512	3.731	0.096	0.089	0.107	0.108	0.074	0.077	0.066	0.065	0.069	0.071
B	2.02	1.834	0.087	0.09	0.064	0.071	0.069	0.072	0.087	0.071	0.094	0.101
C	0.828	0.812	0.082	0.076	0.063	0.063	0.068	0.075	0.062	0.097	0.072	0.068
D	0.361	0.385	0.08	0.09	0.068	0.065	0.066	0.064	0.069	0.072	0.075	0.063
E	0.169	0.183	0.081	0.084	3.764	3.907	4.276	4.309	0.141	0.135	0.111	0.101
F	0.122	0.123	0.085	0.086	0.074	0.063	0.065	0.069	0.111	0.12	0.087	0.088
G	0.086	0.098	0.082	0.081	0.067	0.066	0.067	0.066	0.095	0.142	0.071	0.064
H	0.091	0.087	0.085	0.087	2.906	2.604	0.531	0.539	0.995	1.118	0.097	0.048

2.2 Standard curve



1. Samples from healthy and diseased cats analysed with and without heat treatment.

2.1 Plate layout

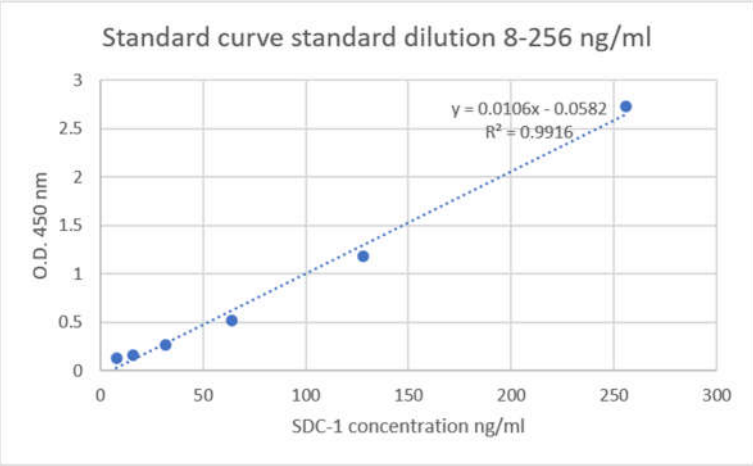
	1	2	3	4	5	6	7	8	9	10	11	12	
A	Standard 1	Standard 1	Standard 9	Standard 9	H1	H1	H5	H5	H9	H9	S3	S3	A
B	Standard 2	Standard 2	Standard 10	Standard 10	H1T	H1T	H5T	H5T	H9T	H9T	S3T	S3T	B
C	Standard 3	Standard 3	Standard 11	Standard 11	H2	H2	H6	H6	H10	H10	S4	S4	C
D	Standard 4	Standard 4	Standard 12	Standard 12	H2T	H2T	H6T	H6T	H10T	H10T	S4T	S4T	D
E	Standard 5	Standard 5	Pos ctrl	Pos ctrl	H3	H3	H7	H7	S1	11	S5	S5	E
F	Standard 6	Standard 6	Neg Ctrl	Neg Ctrl	H3T	H3T	H7T	H7T	S1T	S1T	S5T	S5T	F
G	Standard 7	Standard 7			H4	H4	H8	H8	S1	S1			G
H	Standard 8	Standard 8			H4T	H4T	H8T	H8T	S2T	S2T			H
	1	2	3	4	5	6	7	8	9	10	11	12	

T – Temperature treatment

2.2 Optic densities at 450 nm.

	1	2	3	4	5	6	7	8	9	10	11	12	
A	2.855	2.605	0.082	0.09	0.144	0.158	0.121	0.083	0.057	0.106	0.084	0.098	450 [Test]
B	1.26	1.11	0.138	0.1	0.15	0.155	0.105	0.079	0.058	0.105	0.117	0.201	450 [Test]
C	0.533	0.495	0.079	0.114	0.077	0.073	0.075	0.071	0.096	0.121	0.095	0.105	450 [Test]
D	0.281	0.256	0.073	0.075	0.106	0.097	0.095	0.087	0.129	0.099	0.099	0.154	450 [Test]
E	0.182	0.144	0.763	0.893	0.067	0.059	0.088	0.076	0.049	0.089	3.574	4.091	450 [Test]
F	0.137	0.117	0.08	0.072	0.082	0.068	0.089	0.144	0.071	0.107	OVRFLW	0.09	450 [Test]
G	0.109	0.085	0.088	0.087	0.075	0.067	0.075	0.068	0.068	0.085	0.149	0.085	450 [Test]
H	0.13	0.093	0.083	0.093	0.084	0.085	0.086	0.062	0.071	0.094	0.082	0.087	450 [Test]

2.4 Standard curve



3 Inter-run variability performed from highly reactive and poorly reactive pooled samples

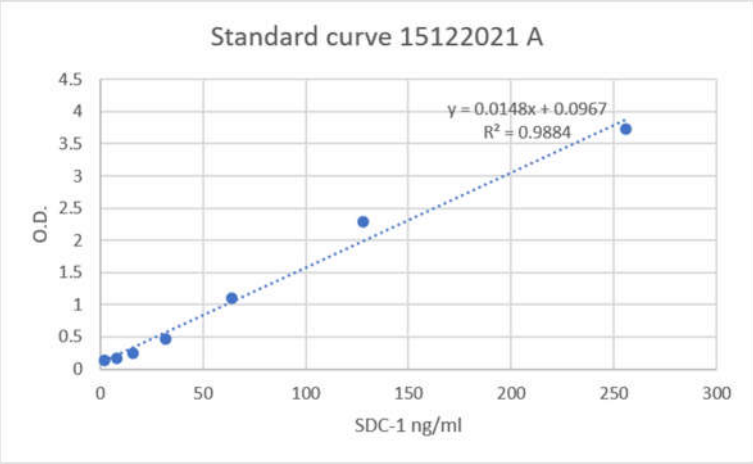
3.1 Plate layout

	1	2	3	4	5	6	7	8	9	10	11	12
A	St 256	256	Control	Control	IRV-H9	empty	no wells	no wells	no wells	no wells	no wells	no wells
B	St 128	128	FT-H1	FT-H1	FT-L1	FT-L1	no wells	no wells	no wells	no wells	no wells	no wells
C	St 64	64	FT-H2	FT-H2	FT-L2	FT-L2	no wells	no wells	no wells	no wells	no wells	no wells
D	St 32	32	FT-H3	FT-H3	FT-L3	FT-L3	no wells	no wells	no wells	no wells	no wells	no wells
E	St 16	16	FT-H4	FT-H4	FT-L4	FT-L4	no wells	no wells	no wells	no wells	no wells	no wells
F	St 8	8	IRV-H6	IRV-H7	frSDC-1 ND	frSDC-1 ND	no wells	no wells	no wells	no wells	no wells	no wells
G	St 2	2	IRV-H8	IRV-L7	frSDC-1 ND	frSDC-1 ND	no wells	no wells	no wells	no wells	no wells	no wells
H	Blank	Blank	LRV-L8	IRV-L9	Empty	Empty	no wells	no wells	no wells	no wells	no wells	no wells

3.2 Optic densities at 450 nm

	1	2	3	4	5	6	7	8	9	10	11	12
A	3.862	3.606	1.625	1.519	0.885	0.129	0	0	0	0	0	0
B	2.304	2.258	0.174	0.14	0.101	0.123	0	0	0	0	0	0
C	1.096	1.116	0.195	0.161	0.14	0.142	0	0	0	0	0	0
D	0.477	0.472	0.171	0.199	0.128	0.148	0	0.001	0	0	0	0
E	0.234	0.252	0.151	0.183	0.132	0.147	0	0	0	0	0	0
F	0.171	0.176	0.829	0.878	0.194	0.143	0	0.001	0	0.001	0	0
G	0.131	0.147	0.36	0.874	0.166	0.144	0	0	0	0	0	0
H	0.112	0.095	0.08	0.072	0.139	0.124	0.001	0.001	0	0.001	0.001	0

3.3 Standard curve


Standard curve 15122021 A
y = 0.0148x + 0.0967
R² = 0.9884
O.D.
SDC-1 ng/ml
4.5
4
3.5
3
2.5
2
1.5
1
0.5
0
0
50
100
150
200
250
300

4 Spike and recovery and inter-run variability from highly reactive and poorly reactive pooled samples

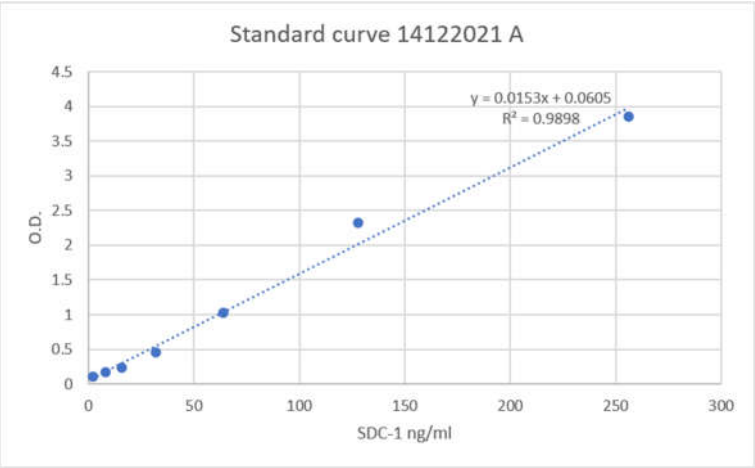
4.1 Plate layout

	1	2	3	4	5	6	7	8	9	10	11	12
A	St 256	256	Control	Control	SR-L4	SR-L4	No wells	No wells	No wells	No wells	No wells	No wells
B	St 128	128	SR-H1	SR-H1	IRV-H1	IRV-L1	No wells	No wells	No wells	No wells	No wells	No wells
C	St 64	64	SR-H2	SR-H2	IRV-L2	IRV-H2	No wells	No wells	No wells	No wells	No wells	No wells
D	St 32	32	SR-H3	SR-H3	IRV-H3	IRV-L3	No wells	No wells	No wells	No wells	No wells	No wells
E	St 16	16	SR-H4	SR-H4			No wells	No wells	No wells	No wells	No wells	No wells
F	St 8	8	SR-L1	SR-L1			No wells	No wells	No wells	No wells	No wells	No wells
G	St 2	2	SR-L2	SR-L2			No wells	No wells	No wells	No wells	No wells	No wells
H	Blank	Blank	SR-L3	SR-L3			No wells	No wells	No wells	No wells	No wells	No wells

4.2 Optic densities at 450 nm

	1	2	3	4	5	6	7	8	9	10	11	12
A	3.812	3.889	1.499	1.531	0.118	0.123	0	0	0	0	0	0
B	2.241	2.407	3.801	3.89	0.843	0.12	0	0	0	0	0	0
C	1.029	1.029	0.896	0.918	0.088	0.794	0	0	0	0	0	-0.001
D	0.456	0.454	0.588	0.568	0.804	0.143	0	0.001	0	0.001	0.001	0.001
E	0.251	0.227	0.535	0.538	0.11	0.119	0	0	0	0	0	0
F	0.183	0.161	2.782	2.827	0.151	0.111	0	0	0	0.001	0.001	0.001
G	0.103	0.109	0.387	0.411	0.091	0.101	0	0	0	0	0	0
H	0.134	0.092	0.096	0.112	0.118	0.118	0	0	0	0.001	0.001	0.001

4.3 Standard curve



5 Dilutional linearity, parallelism and within run variability from highly reactive and poorly reactive pooled samples and undiluted and diluted feline recombinant syndecan-1

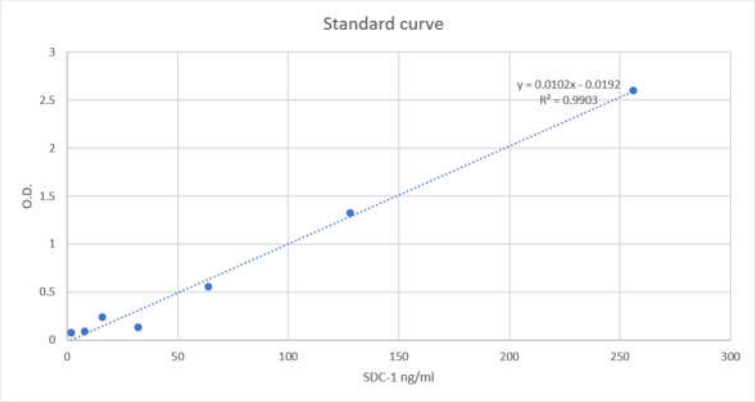
	1	2	3	4	5	6	7	8	9	10	11	12
A	St 256	256	frSDC-1 151000	frSDC-1 151000	P3	P3	P11	P11	DL7	DL7	WRV-L2	WRV-H4
B	St 128	128	frSDC-1 75500	frSDC-1 75500	P4	P4	P12	P12	DL8	DL8	WRV-L3	WRV-H5
C	St 64	64	frSDC-1 37750	frSDC-1 37750	P5	P5	DL1	DL1	DL9	DL9	WRV-H6	WRV-L4
D	St 32	32	frSDC-1 18875	frSDC-1 18875	P6	P6	DL2	DL2	DL10	DL10	WRV-H7	WRV-H8
E	St 16	16	frSDC-1 9437.5	frSDC-1 9437.5	P7	P7	DL3	DL3	DL11	DL11	WRV-L5	WRV-H9
F	St 8	8	Control	Control	P8	P8	DL4	DL4	DL12	DL12	WRV-L6	WRV-L7
G	St 2	2	P1	P1	P9	P9	DL5	DL5	WRV-H1	WRV-H2	WRV-L8	WRV-L9
H	Blank	Blank	P2	P2	P10	P10	DL6	DL6	WRV-L1	WRV-H3	WRV-H10	WRV-L10

5.2 Optic densities at 450 nm

	1	2	3	4	5	6	7	8	9	10	11	12
A	2.567	2.63	0.068	0.069	1.031	1.064	0.08	0.081	0.093	0.095	0.062	0.644
B	1.253	1.401	0.074	0.079	0.483	0.549	0.075	0.081	0.089	0.081	0.076	0.701
C	0.509	0.606	0.066	0.062	0.698	0.74	2.05	2.076	0.071	0.068	0.67	0.061
D	0.127	0.143	0.069	0.067	0.307	0.321	1.392	1.432	0.07	0.07	0.662	0.667
E	0.224	0.248	0.061	0.059	0.206	0.217	0.674	0.675	0.078	0.069	0.069	0.659
F	0.088	0.089	0.936	0.86	0.143	0.134	0.347	0.338	0.072	0.07	0.065	0.064

G	0.072	0.077	2.725	2.387	0.1	0.116	0.191	0.197	0.681	0.754	0.072	0.061
H	0.069	0.067	1.887	1.648	0.106	0.094	0.121	0.118	0.058	0.679	0.685	0.062

5.3 Standard curve



6 Inter-run variability. Note OST was a rerun of an old standard solution for verification purposes. Results not reported in chapter.

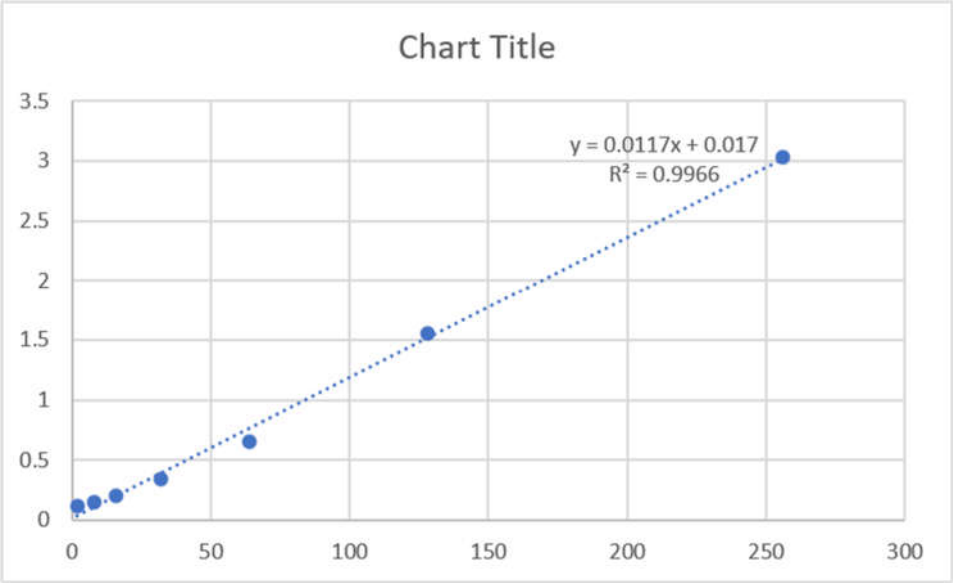
6.1 Plate layout

	1	2	3	4	5	6	7	8	9	10	11	12
A	St 256	256	Control	Control	OST 256	OST 256	no wells	no wells	no wells	no wells	no wells	no wells
B	St 128	128	IRV-L4	IRV-L5	OST 128	OST 128	no wells	no wells	no wells	no wells	no wells	no wells
C	St 64	64	IRV-H4	IRV-H5	OST 64	OST 64	no wells	no wells	no wells	no wells	no wells	no wells
D	St 32	32	empty	IRV-L6	OST 32	OST 32	no wells	no wells	no wells	no wells	no wells	no wells
E	St 16	16	empty	empty	OST 16	OST 16	no wells	no wells	no wells	no wells	no wells	no wells
F	St 8	8	empty	empty	OST 8	OST 8	no wells	no wells	no wells	no wells	no wells	no wells
G	St 2	2	empty	empty	OST 4	OST 4	no wells	no wells	no wells	no wells	no wells	no wells
H	Blank	Blank	empty	empty	Blank	Blank	no wells	no wells	no wells	no wells	no wells	no wells

6.2 Optic densities at 450 nm

	1	2	3	4	5	6	7	8	9	10	11	12
A	3.166	2.907	1.054	1.088	3.046	2.906	0	0	0	0	0	0
B	1.517	1.579	0.141	0.104	1.51	1.564	0	0	0	0	0	0
C	0.635	0.672	0.944	0.767	0.639	0.596	0	0	0	0	0	0
D	0.348	0.339	0.118	0.137	0.313	0.327	0	0.001	0	0	0	0
E	0.189	0.22	0.101	0.152	0.181	0.195	0	0	0	0	0	0
F	0.143	0.156	0.113	0.125	0.164	0.16	0	0.001	0	0	0	0
G	0.094	0.139	0.109	0.134	0.128	0.162	0	0	0	0	0	0
H	0.117	0.095	0.137	0.116	0.123	0.1	0	0.001	0	0	0	0.001

6.3 Standard curve



Annex IV: Chapter IV Unformatted statistical report

Immediate effects of an intravenous fluid challenge on the endothelial glycocalyx in healthy anaesthetized cats

Linear mixed effects model for Glycocheck variables

Time categorical E 10 min F 20 min

A – control (reference group)

B – HES

C - CRYS

```
> modelPBR525<-lme(PBR525~Group*Time, random=~1|Patient, data = Fluid_chal
lenge_dataset_noNAs_noPCV_TS)
> summary(modelPBR525)
Linear mixed-effects model fit by REML
  Data: Fluid_challenge_dataset_noNAs_noPCV_TS
       AIC      BIC    logLik
  25.06921 50.56158 -1.534606

Random effects:
 Formula: ~1 | Patient
         (Intercept)  Residual
StdDev: 1.499962e-05 0.2160712

Fixed effects:  PBR525 ~ Group * Time
                 Value  Std.Error DF  t-value p-value
(Intercept)   2.3330000 0.06832772 49 34.14427  0.0000
GroupB        0.1360000 0.09662999 26  1.40743  0.1711
GroupC        0.0536667 0.09927788 26  0.54057  0.5934
TimeE         0.0340370 0.09927788 49  0.34285  0.7332
TimeF         0.1040000 0.09662999 49  1.07627  0.2871
GroupB:TimeE -0.0490370 0.13854043 49 -0.35395  0.7249
GroupC:TimeE -0.0654656 0.14735350 49 -0.44428  0.6588
GroupB:TimeF -0.1988333 0.13665544 49 -1.45500  0.1520
GroupC:TimeF -0.0940000 0.14040012 49 -0.66952  0.5063
 Correlation:
             (Intr) GroupB GroupC TimeE  TimeF  GrB:TE GrC:TE
GroupB       -0.707
GroupC       -0.688  0.487
TimeE        -0.688  0.487  0.474
TimeF        -0.707  0.500  0.487  0.487
GroupB:TimeE  0.493 -0.697 -0.339 -0.717 -0.349
GroupC:TimeE  0.464 -0.328 -0.674 -0.674 -0.328  0.483
GroupB:TimeF  0.500 -0.707 -0.344 -0.344 -0.707  0.493  0.232
GroupC:TimeF  0.487 -0.344 -0.707 -0.335 -0.688  0.240  0.476
             GrB:TF
GroupB
GroupC
TimeE
TimeF
GroupB:TimeE
GroupC:TimeE
GroupB:TimeF
GroupC:TimeF  0.487

Standardized Within-Group Residuals:
        Min          Q1         Med          Q3         Max
-2.11521473 -0.65487665  0.06663612  0.61746614  2.85399716

Number of Observations: 84
Number of Groups: 29
> shapiro.test(residuals(modelPBR525))
```

```
        Shapiro-Wilk normality test

data:  residuals(modelPBR525)
W = 0.98455, p-value = 0.4142

>
> modelPBR59<-lme(PBR59~Group*Time, random=~1|Patient, data = Fluid_challe
nge_dataset_noNAs_noPCV_TS)
> summary(modelPBR59)
Linear mixed-effects model fit by REML
  Data: Fluid_challenge_dataset_noNAs_noPCV_TS
        AIC       BIC   logLik
  -42.51728 -17.02491 32.25864

Random effects:
 Formula: ~1 | Patient
        (Intercept)  Residual
StdDev:  0.03666786 0.1330505

Fixed effects:  PBR59 ~ Group * Time
                 Value  Std.Error DF   t-value p-value
(Intercept)   1.3746667 0.04364282 49 31.498116  0.0000
GroupB        0.0673333 0.06172027 26  1.090944  0.2853
GroupC       -0.0068889 0.06341155 26 -0.108638  0.9143
TimeE         0.0642430 0.06123846 49  1.049063  0.2993
TimeF         0.0486667 0.05950198 49  0.817900  0.4174
GroupB:TimeE -0.0489097 0.08538521 49 -0.572812  0.5694
GroupC:TimeE  0.0048387 0.09101131 49  0.053166  0.9578
GroupB:TimeF  0.0166667 0.08414851 49  0.198063  0.8438
GroupC:TimeF  0.0698519 0.08645437 49  0.807962  0.4230
 Correlation:
             (Intr) GroupB GroupC TimeE  TimeF  GrB:TE GrC:TE
GroupB       -0.707
GroupC       -0.688  0.487
TimeE        -0.662  0.468  0.456
TimeF        -0.682  0.482  0.469  0.486
GroupB:TimeE  0.475 -0.672 -0.327 -0.717 -0.348
GroupC:TimeE  0.446 -0.315 -0.648 -0.673 -0.327  0.483
GroupB:TimeF  0.482 -0.682 -0.332 -0.344 -0.707  0.493  0.231
GroupC:TimeF  0.469 -0.332 -0.682 -0.334 -0.688  0.240  0.475
             GrB:TF
GroupB
GroupC
TimeE
TimeF
GroupB:TimeE
GroupC:TimeE
GroupB:TimeF
GroupC:TimeF  0.487

Standardized Within-Group Residuals:
       Min         Q1        Med         Q3        Max
-2.1580238 -0.6053022 -0.1635619  0.6150044  2.1515804

Number of Observations: 84
Number of Groups: 29
> shapiro.test(residuals(modelPBR59))

        Shapiro-Wilk normality test

data:  residuals(modelPBR59)
W = 0.97584, p-value = 0.1152

>
> modelPBR1019<-lme(PBR1019~Group*Time, random=~1|Patient, data = Fluid_ch
allenge_dataset_noNAs_noPCV_TS)
> summary(modelPBR1019)
Linear mixed-effects model fit by REML
```

```
  Data: Fluid_challenge_dataset_noNAs_noPCV_TS
       AIC      BIC    logLik
  52.31015 77.80251 -15.15507

Random effects:
 Formula: ~1 | Patient
        (Intercept)  Residual
StdDev:  0.05293527 0.2538503

Fixed effects:  PBR1019 ~ Group * Time
                  Value Std.Error DF   t-value p-value
(Intercept)   2.5770000 0.0820013 49 31.426330  0.0000
GroupB        0.2803333 0.1159674 26  2.417347  0.0229
GroupC        0.0544815 0.1191451 26  0.457270  0.6513
TimeE         0.1165022 0.1167589 49  0.997801  0.3233
TimeF         0.2546667 0.1135253 49  2.243259  0.0294
GroupB:TimeE -0.1540022 0.1628516 49 -0.945660  0.3490
GroupC:TimeE -0.0409313 0.1734364 49 -0.236002  0.8144
GroupB:TimeF -0.4128333 0.1605490 49 -2.571384  0.0132
GroupC:TimeF -0.1746667 0.1649485 49 -1.058917  0.2948
 Correlation:
             (Intr) GroupB GroupC TimeE  TimeF  GrB:TE GrC:TE
GroupB       -0.707
GroupC       -0.688  0.487
TimeE        -0.673  0.476  0.463
TimeF        -0.692  0.489  0.476  0.486
GroupB:TimeE  0.483 -0.682 -0.332 -0.717 -0.349
GroupC:TimeE  0.453 -0.320 -0.658 -0.673 -0.327  0.483
GroupB:TimeF  0.489 -0.692 -0.337 -0.344 -0.707  0.493  0.231
GroupC:TimeF  0.476 -0.337 -0.692 -0.335 -0.688  0.240  0.476
             GrB:TF
GroupB
GroupC
TimeE
TimeF
GroupB:TimeE
GroupC:TimeE
GroupB:TimeF
GroupC:TimeF  0.487

Standardized Within-Group Residuals:
        Min          Q1         Med          Q3         Max
-2.37100375 -0.64389340  0.03930914  0.46879585  3.26227558

Number of Observations: 84
Number of Groups: 29
> shapiro.test(residuals(modelPBR1019))

        Shapiro-Wilk normality test

data:  residuals(modelPBR1019)
W = 0.97537, p-value = 0.1071
```

Change in reference point to compare B to C for PBR 10-19

```
> Fluid_challenge_complete_dataset$Group <- as.factor(Fluid_challenge_complete_dataset
oup)
> Fluid_challenge_complete_dataset$Group <- relevel(
+   Fluid_challenge_complete_dataset$Group, ref = "B"
+ )
> modelPBR1019_Bref <- lme(
+   PBR1019 ~ Group * Time,
+   random = ~1 | Patient,
+   data = Fluid_challenge_complete_dataset
+ )
> summary(modelPBR1019_Bref)
Linear mixed-effects model fit by REML
```

```
  Data: Fluid_challenge_complete_dataset
       AIC      BIC    logLik
  52.31015 77.80251 -15.15507

Random effects:
 Formula: ~1 | Patient
        (Intercept)  Residual
StdDev:  0.05293527 0.2538503

Fixed effects:  PBR1019 ~ Group * Time
                  Value Std.Error DF  t-value p-value
(Intercept)   2.8573333 0.0820013 49 34.84497  0.0000
GroupA       -0.2803333 0.1159674 26 -2.41735  0.0229
GroupC       -0.2258519 0.1191451 26 -1.89560  0.0692
TimeE        -0.0375000 0.1135253 49 -0.33032  0.7426
TimeF        -0.1581667 0.1135253 49 -1.39323  0.1698
GroupA:TimeE  0.1540022 0.1628516 49  0.94566  0.3490
GroupC:TimeE  0.1130709 0.1712762 49  0.66017  0.5122
GroupA:TimeF  0.4128333 0.1605490 49  2.57138  0.0132
GroupC:TimeF  0.2381667 0.1649485 49  1.44389  0.1551
 Correlation:
             (Intr) GroupA GroupC TimeE  TimeF  GrA:TE GrC:TE GrA:TF
GroupA       -0.707
GroupC       -0.688  0.487
TimeE        -0.692  0.489  0.476
TimeF        -0.692  0.489  0.476  0.500
GroupA:TimeE  0.483 -0.682 -0.332 -0.697 -0.349
GroupC:TimeE  0.459 -0.324 -0.667 -0.663 -0.331  0.462
GroupA:TimeF  0.489 -0.692 -0.337 -0.354 -0.707  0.493  0.234
GroupC:TimeF  0.476 -0.337 -0.692 -0.344 -0.688  0.240  0.482  0.487

Standardized Within-Group Residuals:
        Min          Q1         Med          Q3         Max
-2.37100375 -0.64389340  0.03930914  0.46879585  3.26227558

Number of Observations: 84
Number of Groups: 29


>
> modelPBR2025<-lme(PBR2025~Group*Time, random=~1|Patient, data = Fluid_ch
allenge_dataset_noNAs_noPCV_TS)
> summary(modelPBR2025)
Linear mixed-effects model fit by REML
  Data: Fluid_challenge_dataset_noNAs_noPCV_TS
       AIC      BIC    logLik
  143.6648 169.1572 -60.83241

Random effects:
 Formula: ~1 | Patient
         (Intercept)  Residual
StdDev: 1.375174e-05 0.4763941

Fixed effects:  PBR2025 ~ Group * Time
                  Value Std.Error DF   t-value p-value
(Intercept)   3.0480000 0.1506490 49 20.232456  0.0000
GroupB       -0.0340000 0.2130499 26 -0.159587  0.8744
GroupC        0.0494074 0.2188880 26  0.225720  0.8232
TimeE        -0.2924444 0.2188880 49 -1.336046  0.1877
TimeF        -0.0456667 0.2130499 49 -0.214347  0.8312
GroupB:TimeE  0.2247778 0.3054541 49  0.735881  0.4653
GroupC:TimeE -0.1925820 0.3248852 49 -0.592769  0.5561
GroupB:TimeF -0.2490000 0.3012981 49 -0.826424  0.4126
GroupC:TimeF -0.2854444 0.3095543 49 -0.922114  0.3610
 Correlation:
             (Intr) GroupB GroupC TimeE  TimeF  GrB:TE GrC:TE
GroupB       -0.707
GroupC       -0.688  0.487
TimeE        -0.688  0.487  0.474
```

```
TimeF         -0.707  0.500  0.487  0.487
GroupB:TimeE   0.493 -0.697 -0.339 -0.717 -0.349
GroupC:TimeE   0.464 -0.328 -0.674 -0.674 -0.328  0.483
GroupB:TimeF   0.500 -0.707 -0.344 -0.344 -0.707  0.493  0.232
GroupC:TimeF   0.487 -0.344 -0.707 -0.335 -0.688  0.240  0.476
              GrB:TF
GroupB
GroupC
TimeE
TimeF
GroupB:TimeE
GroupC:TimeE
GroupB:TimeF
GroupC:TimeF  0.487

Standardized Within-Group Residuals:
        Min          Q1         Med          Q3         Max
-2.16829508 -0.67860983  0.00155489  0.71789304  2.28180210

Number of Observations: 84
Number of Groups: 29
> shapiro.test(residuals(modelPBR2025))

        Shapiro-Wilk normality test

data:  residuals(modelPBR2025)
W = 0.9902, p-value = 0.7831

>
> modelSegements<-lme(Segements~Group*Time, random=~1|Patient, data = Flui
d_challenge_dataset_noNAs_noPCV_TS)
> summary(modelSegements)
Linear mixed-effects model fit by REML
  Data: Fluid_challenge_dataset_noNAs_noPCV_TS
       AIC     BIC    logLik
  1155.817 1181.31 -566.9087

Random effects:
 Formula: ~1 | Patient
        (Intercept) Residual
StdDev:    230.3264  353.524

Fixed effects:  Segements ~ Group * Time
                 Value Std.Error DF   t-value p-value
(Intercept)  2121.3333  133.4277 49 15.898750  0.0000
GroupB        200.5000  188.6952 26  1.062560  0.2978
GroupC        138.2963  193.8659 26  0.713361  0.4820
TimeE         -50.4373  163.4114 49 -0.308652  0.7589
TimeF         -39.4000  158.1007 49 -0.249208  0.8042
GroupB:TimeE  -86.5960  227.3744 49 -0.380852  0.7050
GroupC:TimeE -225.6946  243.6286 49 -0.926388  0.3588
GroupB:TimeF -308.2333  223.5882 49 -1.378576  0.1743
GroupC:TimeF -236.2296  229.7150 49 -1.028360  0.3088
 Correlation:
              (Intr) GroupB GroupC TimeE  TimeF  GrB:TE GrC:TE
GroupB        -0.707
GroupC        -0.688  0.487
TimeE         -0.573  0.405  0.395
TimeF         -0.592  0.419  0.408  0.484
GroupB:TimeE   0.412 -0.583 -0.284 -0.719 -0.348
GroupC:TimeE   0.384 -0.272 -0.559 -0.671 -0.324  0.482
GroupB:TimeF   0.419 -0.592 -0.288 -0.342 -0.707  0.492  0.229
GroupC:TimeF   0.408 -0.288 -0.592 -0.333 -0.688  0.239  0.471
              GrB:TF
GroupB
GroupC
TimeE
TimeF
GroupB:TimeE
```

```
GroupC:TimeE
GroupB:TimeF
GroupC:TimeF  0.487

Standardized Within-Group Residuals:
        Min          Q1         Med          Q3         Max
-2.40781850 -0.55112249  0.08718744  0.68590594  1.50660159

Number of Observations: 84
Number of Groups: 29
> shapiro.test(residuals(modelSegements))

        Shapiro-Wilk normality test

data:  residuals(modelSegements)
W = 0.96226, p-value = 0.01465

>
> modelVVD<-lme(VVD~Group*Time, random=~1|Patient, data = Fluid_challenge_
dataset_noNAs_noPCV_TS)
> summary(modelVVD)
Linear mixed-effects model fit by REML
  Data: Fluid_challenge_dataset_noNAs_noPCV_TS
       AIC      BIC    logLik
  864.6359 890.1282 -421.3179

Random effects:
 Formula: ~1 | Patient
        (Intercept) Residual
StdDev:    19.95606 55.11665

Fixed effects:  VVD ~ Group * Time
                 Value Std.Error DF   t-value p-value
(Intercept)  153.13333  18.53669 49  8.261092  0.0000
GroupB        29.76667  26.21484 26  1.135489  0.2665
GroupC        53.68148  26.93319 26  1.993135  0.0568
TimeE         -7.09098  25.39348 49 -0.279244  0.7812
TimeF         -4.30000  24.64892 49 -0.174450  0.8622
GroupB:TimeE -41.75902  35.38923 49 -1.179992  0.2437
GroupC:TimeE -54.85959  37.76720 49 -1.452572  0.1527
GroupB:TimeF -62.48333  34.85883 49 -1.792468  0.0792
GroupC:TimeF -72.77407  35.81405 49 -2.031998  0.0476
 Correlation:
             (Intr) GroupB GroupC TimeE  TimeF  GrB:TE GrC:TE
GroupB       -0.707
GroupC       -0.688  0.487
TimeE        -0.645  0.456  0.444
TimeF        -0.665  0.470  0.458  0.485
GroupB:TimeE  0.463 -0.655 -0.319 -0.718 -0.348
GroupC:TimeE  0.434 -0.307 -0.630 -0.672 -0.326  0.482
GroupB:TimeF  0.470 -0.665 -0.324 -0.343 -0.707  0.493  0.231
GroupC:TimeF  0.458 -0.324 -0.665 -0.334 -0.688  0.240  0.474
             GrB:TF
GroupB
GroupC
TimeE
TimeF
GroupB:TimeE
GroupC:TimeE
GroupB:TimeF
GroupC:TimeF  0.487

Standardized Within-Group Residuals:
       Min         Q1        Med         Q3        Max
-2.0872681 -0.5449012 -0.1286190  0.4011693  2.3957849

Number of Observations: 84
Number of Groups: 29
> shapiro.test(residuals(modelVVD))
```

```
        Shapiro-Wilk normality test

data:  residuals(modelVVD)
W = 0.95984, p-value = 0.01028

>
> modelMedianP50<-lme(MedianP50~Group*Time, random=~1|Patient, data = Flui
d_challenge_dataset_noNAs_noPCV_TS)
> summary(modelMedianP50)
Linear mixed-effects model fit by REML
  Data: Fluid_challenge_dataset_noNAs_noPCV_TS
       AIC      BIC    logLik
  206.2191 231.7115 -92.10956

Random effects:
 Formula: ~1 | Patient
        (Intercept)  Residual
StdDev:   0.4785335 0.6048351

Fixed effects:  MedianP50 ~ Group * Time
                 Value Std.Error DF   t-value p-value
(Intercept)   7.092000 0.2438893 49 29.078769  0.0000
GroupB       -0.480000 0.3449115 26 -1.391661  0.1758
GroupC       -0.006815 0.3543629 26 -0.019231  0.9848
TimeE        -0.058680 0.2799280 49 -0.209627  0.8348
TimeF        -0.014000 0.2704905 49 -0.051758  0.9589
GroupB:TimeE  0.181347 0.3892618 49  0.465874  0.6434
GroupC:TimeE  0.706537 0.4177271 49  1.691385  0.0971
GroupB:TimeF  0.017333 0.3825313 49  0.045312  0.9640
GroupC:TimeF  0.681407 0.3930135 49  1.733801  0.0892
 Correlation:
             (Intr) GroupB GroupC TimeE  TimeF  GrB:TE GrC:TE
GroupB       -0.707
GroupC       -0.688  0.487
TimeE        -0.536  0.379  0.369
TimeF        -0.555  0.392  0.382  0.483
GroupB:TimeE  0.385 -0.545 -0.265 -0.719 -0.347
GroupC:TimeE  0.359 -0.254 -0.522 -0.670 -0.324  0.482
GroupB:TimeF  0.392 -0.555 -0.270 -0.342 -0.707  0.491  0.229
GroupC:TimeF  0.382 -0.270 -0.555 -0.333 -0.688  0.239  0.470
             GrB:TF
GroupB
GroupC
TimeE
TimeF
GroupB:TimeE
GroupC:TimeE
GroupB:TimeF
GroupC:TimeF  0.487

Standardized Within-Group Residuals:
        Min          Q1         Med          Q3         Max
-2.66444750 -0.52223242  0.01249714  0.51307543  1.72148874

Number of Observations: 84
Number of Groups: 29
> shapiro.test(residuals(modelMedianP50))

        Shapiro-Wilk normality test

data:  residuals(modelMedianP50)
W = 0.97607, p-value = 0.1193

>
> modelRBC_filling<-lme(RBC_filling~Group*Time, random=~1|Patient, data =
Fluid_challenge_dataset_noNAs_noPCV_TS)
> summary(modelRBC_filling)
Linear mixed-effects model fit by REML
```

```
  Data: Fluid_challenge_dataset_noNAs_noPCV_TS
      AIC      BIC    logLik
  499.422 524.9143 -238.711

Random effects:
 Formula: ~1 | Patient
        (Intercept) Residual
StdDev:    2.963427 4.421772

Fixed effects:  RBC_filling ~ Group * Time
                Value Std.Error DF  t-value p-value
(Intercept)  72.26667  1.683270 49 42.93232  0.0000
GroupB       -1.39333  2.380503 26 -0.58531  0.5634
GroupC        2.66296  2.445734 26  1.08882  0.2862
TimeE        -1.68057  2.044275 49 -0.82209  0.4150
TimeF        -0.35667  1.977477 49 -0.18036  0.8576
GroupB:TimeE -0.17276  2.844200 49 -0.06074  0.9518
GroupC:TimeE -1.25602  3.048201 49 -0.41205  0.6821
GroupB:TimeF -1.56667  2.796574 49 -0.56021  0.5779
GroupC:TimeF -4.62852  2.873207 49 -1.61092  0.1136
 Correlation:
             (Intr) GroupB GroupC TimeE  TimeF  GrB:TE GrC:TE
GroupB       -0.707
GroupC       -0.688  0.487
TimeE        -0.568  0.402  0.391
TimeF        -0.587  0.415  0.404  0.484
GroupB:TimeE  0.408 -0.578 -0.281 -0.719 -0.348
GroupC:TimeE  0.381 -0.269 -0.554 -0.671 -0.324  0.482
GroupB:TimeF  0.415 -0.587 -0.286 -0.342 -0.707  0.492  0.229
GroupC:TimeF  0.404 -0.286 -0.587 -0.333 -0.688  0.239  0.471
             GrB:TF
GroupB
GroupC
TimeE
TimeF
GroupB:TimeE
GroupC:TimeE
GroupB:TimeF
GroupC:TimeF  0.487

Standardized Within-Group Residuals:
        Min          Q1         Med          Q3         Max
-1.90096942 -0.70202912 -0.04756628  0.59786724  1.96711522

Number of Observations: 84
Number of Groups: 29
> shapiro.test(residuals(modelRBC_filling))

        Shapiro-Wilk normality test

data:  residuals(modelRBC_filling)
W = 0.98871, p-value = 0.6813
```

PBR vs other GlycoCheck Variables

```
> modelPBR525_auxilliary<-lme(PBR525~VVD+RBC_filling+MedianP50, random =~1
|Patient, data = Fluid_challenge_complete_dataset)
> summary(modelPBR525_auxilliary)
Linear mixed-effects model fit by REML
  Data: Fluid_challenge_complete_dataset
       AIC      BIC    logLik
  4.399768 18.69193 3.800116

Random effects:
 Formula: ~1 | Patient
        (Intercept)  Residual
StdDev:  0.05632566 0.1858631

Fixed effects:  PBR525 ~ VVD + RBC_filling + MedianP50
                Value  Std.Error DF   t-value p-value
(Intercept)  3.654862 0.31101111 52 11.751549  0.0000
VVD          0.000246 0.00044118 52  0.556968  0.5799
RBC_filling -0.011226 0.00504929 52 -2.223244  0.0306
MedianP50   -0.070108 0.03169165 52 -2.212184  0.0314
 Correlation:
            (Intr) VVD    RBC_fl
VVD          0.069
RBC_filling -0.697 -0.562
MedianP50   -0.285  0.508 -0.470

Standardized Within-Group Residuals:
          Min            Q1           Med
-3.0607298830 -0.7643817598  0.0001148626
           Q3           Max
 0.5975111077  2.6422711948

Number of Observations: 84
Number of Groups: 29
>
> modelPBR525_auxilliary<-lme(PBR525~RBC_filling+MedianP50, random =~1|Pat
ient, data = Fluid_challenge_complete_dataset)
> summary(modelPBR525_auxilliary)
Linear mixed-effects model fit by REML
  Data: Fluid_challenge_complete_dataset
       AIC      BIC  logLik
  -10.9082 1.064046 10.4541

Random effects:
 Formula: ~1 | Patient
        (Intercept)  Residual
StdDev:  0.05464618 0.1854219

Fixed effects:  PBR525 ~ RBC_filling + MedianP50
                Value  Std.Error DF   t-value p-value
(Intercept)  3.638910 0.30848665 53 11.796004  0.0000
RBC_filling -0.009615 0.00415703 53 -2.312994  0.0246
MedianP50   -0.078818 0.02715648 53 -2.902347  0.0054
 Correlation:
            (Intr) RBC_fl
RBC_filling -0.797
MedianP50   -0.371 -0.260

Standardized Within-Group Residuals:
        Min          Q1         Med          Q3
-3.11883071 -0.75027460  0.02817787  0.63363942
        Max
 2.62080230

Number of Observations: 84
Number of Groups: 29
>
```

```
> modelPBR525_auxilliary<-lme(PBR525~MedianP50, random =~1|Patient, data =
 Fluid_challenge_complete_dataset)
> summary(modelPBR525_auxilliary)
Linear mixed-effects model fit by REML
  Data: Fluid_challenge_complete_dataset
        AIC       BIC   logLik
  -16.98504 -7.358161 12.49252

Random effects:
 Formula: ~1 | Patient
        (Intercept) Residual
StdDev:  0.03160099 0.194904

Fixed effects:  PBR525 ~ MedianP50
                 Value  Std.Error DF   t-value p-value
(Intercept)  3.0493085 0.18680574 54 16.323420   0e+00
MedianP50   -0.0922133 0.02630231 54 -3.505903   9e-04
 Correlation:
          (Intr)
MedianP50 -0.993

Standardized Within-Group Residuals:
        Min          Q1         Med          Q3
-2.92469973 -0.72690759  0.05545407  0.52068646
        Max
 2.96177545

Number of Observations: 84
Number of Groups: 29
>
> modelPBR525_auxilliary<-lme(PBR525~RBC_filling, random =~1|Patient, data
 = Fluid_challenge_complete_dataset)
> summary(modelPBR525_auxilliary)
Linear mixed-effects model fit by REML
  Data: Fluid_challenge_complete_dataset
        AIC        BIC   logLik
  -10.42204 -0.7951666 9.211022

Random effects:
 Formula: ~1 | Patient
        (Intercept)  Residual
StdDev:  0.02852085 0.1988069

Fixed effects:  PBR525 ~ RBC_filling
                Value  Std.Error DF   t-value p-value
(Intercept)  3.283208 0.29434790 54 11.154174  0.0000
RBC_filling -0.012430 0.00412588 54 -3.012752  0.0039
 Correlation:
             (Intr)
RBC_filling -0.997

Standardized Within-Group Residuals:
        Min          Q1         Med          Q3
-2.71172755 -0.72184008  0.04578883  0.60000703
        Max
 2.56180917

Number of Observations: 84
Number of Groups: 29
>
> modelPBR59_auxilliary<-lme(PBR59~VVD+RBC_filling+MedianP50, random =~1|P
atient, data = Fluid_challenge_complete_dataset)
> summary(modelPBR59_auxilliary)
Linear mixed-effects model fit by REML
  Data: Fluid_challenge_complete_dataset
        AIC       BIC   logLik
  -76.11329 -61.82113 44.05665

Random effects:
```

```
 Formula: ~1 | Patient
        (Intercept)  Residual
StdDev:  0.03749138 0.1114894

Fixed effects:  PBR59 ~ VVD + RBC_filling + MedianP50
                 Value  Std.Error DF   t-value p-value
(Intercept)  2.5634023 0.18916798 52 13.550931  0.0000
VVD          0.0001182 0.00026708 52  0.442661  0.6598
RBC_filling -0.0130377 0.00306315 52 -4.256294  0.0001
MedianP50   -0.0306919 0.01925178 52 -1.594239  0.1169
 Correlation:
            (Intr) VVD    RBC_fl
VVD          0.071
RBC_filling -0.696 -0.564
MedianP50   -0.289  0.508 -0.467

Standardized Within-Group Residuals:
        Min          Q1         Med          Q3
-2.18582131 -0.60609281 -0.09716052  0.58555176
        Max
 2.83901317

Number of Observations: 84
Number of Groups: 29
>
> modelPBR59_auxilliary<-lme(PBR59~RBC_filling+MedianP50, random =~1|Patie
nt, data = Fluid_challenge_complete_dataset)
> summary(modelPBR59_auxilliary)
Linear mixed-effects model fit by REML
  Data: Fluid_challenge_complete_dataset
        AIC      BIC    logLik
  -92.54055 -80.5683 51.27027

Random effects:
 Formula: ~1 | Patient
        (Intercept)  Residual
StdDev:  0.03808471 0.1107249

Fixed effects:  PBR59 ~ RBC_filling + MedianP50
                 Value  Std.Error DF   t-value p-value
(Intercept)  2.5592775 0.18800581 53 13.612758  0.0000
RBC_filling -0.0122935 0.00251844 53 -4.881383  0.0000
MedianP50   -0.0350735 0.01651886 53 -2.123241  0.0384
 Correlation:
            (Intr) RBC_fl
RBC_filling -0.797
MedianP50   -0.380 -0.252

Standardized Within-Group Residuals:
        Min          Q1         Med          Q3
-2.27056930 -0.61874214 -0.07656262  0.57366171
        Max
 2.92575896

Number of Observations: 84
Number of Groups: 29
>
> modelPBR59_auxilliary<-lme(PBR59~RBC_filling, random =~1|Patient, data =
 Fluid_challenge_complete_dataset)
> summary(modelPBR59_auxilliary)
Linear mixed-effects model fit by REML
  Data: Fluid_challenge_complete_dataset
        AIC       BIC    logLik
  -96.48216 -86.85528 52.24108

Random effects:
 Formula: ~1 | Patient
        (Intercept)  Residual
StdDev:  0.03679611 0.1136209
```

```
Fixed effects:  PBR59 ~ RBC_filling
                 Value  Std.Error DF   t-value p-value
(Intercept)  2.4050807 0.17724465 54 13.569271       0
RBC_filling -0.0136039 0.00248371 54 -5.477275       0
 Correlation:
             (Intr)
RBC_filling -0.997

Standardized Within-Group Residuals:
       Min         Q1        Med         Q3        Max
-2.3592038 -0.7497149 -0.1131342  0.6392850  2.8975978

Number of Observations: 84
Number of Groups: 29
>
> modelPBR59_auxilliary<-lme(PBR59~MedianP50, random =~1|Patient, data = F
luid_challenge_complete_dataset)
> summary(modelPBR59_auxilliary)
Linear mixed-effects model fit by REML
  Data: Fluid_challenge_complete_dataset
       AIC       BIC  logLik
  -84.0122 -74.38533 46.0061

Random effects:
 Formula: ~1 | Patient
        (Intercept)  Residual
StdDev:  0.02024365 0.1296267

Fixed effects:  PBR59 ~ MedianP50
                 Value  Std.Error DF   t-value p-value
(Intercept)  1.8289598 0.12403512 54 14.745499  0.0000
MedianP50   -0.0555526 0.01746448 54 -3.180892  0.0024
 Correlation:
           (Intr)
MedianP50 -0.993

Standardized Within-Group Residuals:
        Min          Q1         Med          Q3
-2.50385274 -0.58026521 -0.05102312  0.60824790
        Max
 2.21269347

Number of Observations: 84
Number of Groups: 29
>
> modelPBR1019_auxilliary<-lme(PBR1019~VVD+RBC_filling+MedianP50, random =
~1|Patient, data = Fluid_challenge_complete_dataset)
> summary(modelPBR1019_auxilliary)
Linear mixed-effects model fit by REML
  Data: Fluid_challenge_complete_dataset
       AIC      BIC    logLik
  40.26673 54.55889 -14.13336

Random effects:
 Formula: ~1 | Patient
        (Intercept)  Residual
StdDev:  0.08379981 0.2290508

Fixed effects:  PBR1019 ~ VVD + RBC_filling + MedianP50
                Value Std.Error DF   t-value p-value
(Intercept)  4.366397 0.3936206 52 11.092909  0.0000
VVD         -0.000102 0.0005533 52 -0.184315  0.8545
RBC_filling -0.014392 0.0063583 52 -2.263569  0.0278
MedianP50   -0.084958 0.0400111 52 -2.123351  0.0385
 Correlation:
            (Intr) VVD    RBC_fl
VVD          0.073
RBC_filling -0.696 -0.565
```

```
MedianP50   -0.292  0.508 -0.464

Standardized Within-Group Residuals:
        Min          Q1         Med          Q3
-3.16785369 -0.63403071 -0.05457331  0.73316400
        Max
 2.45318763

Number of Observations: 84
Number of Groups: 29
>
> modelPBR1019_auxilliary<-lme(PBR1019~RBC_filling+MedianP50, random =~1|P
atient, data = Fluid_challenge_complete_dataset)
> summary(modelPBR1019_auxilliary)
Linear mixed-effects model fit by REML
  Data: Fluid_challenge_complete_dataset
       AIC      BIC    logLik
  25.13267 37.10491 -7.566334

Random effects:
 Formula: ~1 | Patient
        (Intercept)  Residual
StdDev:   0.0847565 0.2272686

Fixed effects:  PBR1019 ~ RBC_filling + MedianP50
                Value Std.Error DF   t-value p-value
(Intercept)  4.376421 0.3907168 53 11.201006  0.0000
RBC_filling -0.015107 0.0052145 53 -2.897072  0.0055
MedianP50   -0.081362 0.0342889 53 -2.372835  0.0213
 Correlation:
            (Intr) RBC_fl
RBC_filling -0.797
MedianP50   -0.385 -0.247

Standardized Within-Group Residuals:
        Min          Q1         Med          Q3
-3.17147867 -0.62867855 -0.05906301  0.72757386
        Max
 2.47286633

Number of Observations: 84
Number of Groups: 29
>
> modelPBR1019_auxilliary<-lme(PBR1019~RBC_filling, random =~1|Patient, da
ta = Fluid_challenge_complete_dataset)
> summary(modelPBR1019_auxilliary)
Linear mixed-effects model fit by REML
  Data: Fluid_challenge_complete_dataset
       AIC      BIC    logLik
  23.69637 33.32325 -7.848186

Random effects:
 Formula: ~1 | Patient
        (Intercept)  Residual
StdDev:  0.07847586 0.2359299

Fixed effects:  PBR1019 ~ RBC_filling
                Value Std.Error DF   t-value p-value
(Intercept)  4.003997 0.3691554 54 10.846372   0.000
RBC_filling -0.017940 0.0051728 54 -3.468168   0.001
 Correlation:
            (Intr)
RBC_filling -0.997

Standardized Within-Group Residuals:
       Min         Q1        Med         Q3        Max
-2.8697935 -0.5906041 -0.1454312  0.6328229  2.4869500

Number of Observations: 84
```

```
Number of Groups: 29
>
> modelPBR1019_auxilliary<-lme(PBR1019~MedianP50, random =~1|Patient, data
 = Fluid_challenge_complete_dataset)
> summary(modelPBR1019_auxilliary)
Linear mixed-effects model fit by REML
  Data: Fluid_challenge_complete_dataset
       AIC      BIC    logLik
  21.96308 31.58996 -6.981542

Random effects:
 Formula: ~1 | Patient
        (Intercept) Residual
StdDev:  0.04312669 0.246679

Fixed effects:  PBR1019 ~ MedianP50
                Value  Std.Error DF   t-value p-value
(Intercept)  3.454961 0.23730282 54 14.559291  0.0000
MedianP50   -0.103145 0.03341107 54 -3.087145  0.0032
 Correlation:
          (Intr)
MedianP50 -0.993

Standardized Within-Group Residuals:
       Min         Q1        Med         Q3        Max
-2.9371546 -0.7275261 -0.0117969  0.6155121  2.9478813

Number of Observations: 84
Number of Groups: 29
>
> modelPBR2025_auxilliary<-lme(PBR2025~VVD+RBC_filling+MedianP50, random =
~1|Patient, data = Fluid_challenge_complete_dataset)
> summary(modelPBR2025_auxilliary)
Linear mixed-effects model fit by REML
  Data: Fluid_challenge_complete_dataset
       AIC      BIC    logLik
  136.1066 150.3988 -62.05332

Random effects:
 Formula: ~1 | Patient
         (Intercept)  Residual
StdDev: 1.582165e-05 0.4401902

Fixed effects:  PBR2025 ~ VVD + RBC_filling + MedianP50
                Value Std.Error DF   t-value p-value
(Intercept)  4.245617 0.6848630 52  6.199220  0.0000
VVD          0.001317 0.0009950 52  1.323347  0.1915
RBC_filling -0.002044 0.0112646 52 -0.181430  0.8567
MedianP50   -0.199195 0.0701932 52 -2.837807  0.0065
 Correlation:
            (Intr) VVD    RBC_fl
VVD          0.061
RBC_filling -0.698 -0.553
MedianP50   -0.266  0.506 -0.485

Standardized Within-Group Residuals:
        Min          Q1         Med          Q3
-2.42491189 -0.67618307  0.09609449  0.71579835
        Max
 2.13869270

Number of Observations: 84
Number of Groups: 29
>
> modelPBR2025_auxilliary<-lme(PBR2025~RBC_filling+MedianP50, random =~1|P
atient, data = Fluid_challenge_complete_dataset)
> summary(modelPBR2025_auxilliary)
Linear mixed-effects model fit by REML
  Data: Fluid_challenge_complete_dataset
```

```
       AIC      BIC    logLik
  123.8668 135.839 -56.93339

Random effects:
 Formula: ~1 | Patient
         (Intercept)  Residual
StdDev: 1.595937e-05 0.4422268

Fixed effects:  PBR2025 ~ RBC_filling + MedianP50
                Value Std.Error DF   t-value p-value
(Intercept)  4.190301 0.6867489 53  6.101649  0.0000
RBC_filling  0.006196 0.0094309 53  0.656961  0.5140
MedianP50   -0.246206 0.0608203 53 -4.048082  0.0002
 Correlation:
             (Intr) RBC_fl
RBC_filling -0.798
MedianP50   -0.345 -0.286

Standardized Within-Group Residuals:
       Min         Q1        Med         Q3        Max
-2.4701485 -0.5702745  0.1239337  0.7686855  1.9112163

Number of Observations: 84
Number of Groups: 29
>
> modelPBR2025_auxilliary<-lme(PBR2025~RBC_filling+MedianP50, random =~1|P
atient, data = Fluid_challenge_complete_dataset)
> summary(modelPBR2025_auxilliary)
Linear mixed-effects model fit by REML
  Data: Fluid_challenge_complete_dataset
       AIC      BIC    logLik
  123.8668 135.839 -56.93339

Random effects:
 Formula: ~1 | Patient
         (Intercept)  Residual
StdDev: 1.595937e-05 0.4422268

Fixed effects:  PBR2025 ~ RBC_filling + MedianP50
                Value Std.Error DF   t-value p-value
(Intercept)  4.190301 0.6867489 53  6.101649  0.0000
RBC_filling  0.006196 0.0094309 53  0.656961  0.5140
MedianP50   -0.246206 0.0608203 53 -4.048082  0.0002
 Correlation:
             (Intr) RBC_fl
RBC_filling -0.798
MedianP50   -0.345 -0.286

Standardized Within-Group Residuals:
       Min         Q1        Med         Q3        Max
-2.4701485 -0.5702745  0.1239337  0.7686855  1.9112163

Number of Observations: 84
Number of Groups: 29
>
> modelPBR2025_auxilliary<-lme(PBR2025~MedianP50, random =~1|Patient, data
 = Fluid_challenge_complete_dataset)
> summary(modelPBR2025_auxilliary)
Linear mixed-effects model fit by REML
  Data: Fluid_challenge_complete_dataset
       AIC      BIC    logLik
  114.8068 124.4336 -53.40338

Random effects:
 Formula: ~1 | Patient
         (Intercept)  Residual
StdDev: 1.544454e-05 0.4406915

Fixed effects:  PBR2025 ~ MedianP50
```

```
                Value Std.Error DF   t-value p-value
(Intercept)  4.550376 0.4123493 54 11.035248   0e+00
MedianP50   -0.234767 0.0580724 54 -4.042657   2e-04
 Correlation:
          (Intr)
MedianP50 -0.993

Standardized Within-Group Residuals:
       Min         Q1        Med         Q3        Max
-2.5171441 -0.6567911  0.1293634  0.8213155  1.9878730

Number of Observations: 84
Number of Groups: 29
>
> modelPBR2025_auxilliary<-lme(PBR2025~RBC_filling, random =~1|Patient, da
ta = Fluid_challenge_complete_dataset)
> summary(modelPBR2025_auxilliary)
Linear mixed-effects model fit by REML
  Data: Fluid_challenge_complete_dataset
       AIC      BIC   logLik
  133.2068 142.8337 -62.6034

Random effects:
 Formula: ~1 | Patient
         (Intercept)  Residual
StdDev: 1.285204e-05 0.4819351

Fixed effects:  PBR2025 ~ RBC_filling
                Value Std.Error DF   t-value p-value
(Intercept)  3.231494 0.7024923 54  4.600042  0.0000
RBC_filling -0.004734 0.0098475 54 -0.480688  0.6327
 Correlation:
            (Intr)
RBC_filling -0.997

Standardized Within-Group Residuals:
        Min          Q1         Med          Q3
-2.35135544 -0.46493400  0.06995312  0.65633525
        Max
 1.98491902

Number of Observations: 84
Number of Groups: 29
```

Associations per timepoint T0 and T2 only

```
> modelRPBR525<-lme(PBR525~RBC_filling, random =~1|Patient, data = T0_data
set)
> summary(modelPBR525)
Error: object 'modelPBR525' not found
> modelPBR525<-lme(PBR525~RBC_filling, random =~1|Patient, data = T0_datas
et)
> summary(modelPBR525)
Linear mixed-effects model fit by REML
  Data: T0_dataset
       AIC      BIC   logLik
  4.686034 9.869381 1.656983

Random effects:
 Formula: ~1 | Patient
        (Intercept)   Residual
StdDev:   0.1764842 0.06618159

Fixed effects:  PBR525 ~ RBC_filling
                Value Std.Error DF   t-value p-value
(Intercept)  3.484665 0.4563327 27  7.636239   0.000
RBC_filling -0.014985 0.0062660 27 -2.391519   0.024
 Correlation:
```

```
            (Intr)
RBC_filling -0.997

Standardized Within-Group Residuals:
        Min          Q1         Med          Q3
-0.59718760 -0.22013630 -0.03333331  0.21794239
        Max
 0.89085982

Number of Observations: 29
Number of Groups: 29
> modelPBR59<-lme(PBR59~RBC_filling, random =~1|Patient, data = TO_dataset
)
> summary(modelPBR59)
Linear mixed-effects model fit by REML
  Data: TO_dataset
        AIC       BIC   logLik
  -22.99576 -17.81242 15.49788

Random effects:
 Formula: ~1 | Patient
        (Intercept)   Residual
StdDev:   0.1057001 0.03963738

Fixed effects:  PBR59 ~ RBC_filling
                 Value  Std.Error DF   t-value p-value
(Intercept)  2.3024856 0.27330713 27  8.424535  0.0000
RBC_filling -0.0124873 0.00375282 27 -3.327456  0.0025
 Correlation:
            (Intr)
RBC_filling -0.997

Standardized Within-Group Residuals:
         Min           Q1          Med           Q3
-0.866122494 -0.207241862  0.007211568  0.151445441
         Max
 0.622989845

Number of Observations: 29
Number of Groups: 29
> modelPBR2025<-lme(PBR2025~RBC_filling, random =~1|Patient, data = TO_dat
aset)
> summary(modelPBR2025)
Linear mixed-effects model fit by REML
  Data: TO_dataset
      AIC      BIC    logLik
  40.44957 45.63292 -16.22479

Random effects:
 Formula: ~1 | Patient
        (Intercept) Residual
StdDev:   0.3422424 0.128341

Fixed effects:  PBR2025 ~ RBC_filling
                Value Std.Error DF   t-value p-value
(Intercept)  3.772185 0.8849311 27  4.262687  0.0002
RBC_filling -0.009924 0.0121511 27 -0.816679  0.4213
 Correlation:
            (Intr)
RBC_filling -0.997

Standardized Within-Group Residuals:
        Min          Q1         Med          Q3
-0.84261704 -0.24245959 -0.01506129  0.26990072
        Max
 0.51167029

Number of Observations: 29
Number of Groups: 29
```

```
> modelPBR1019<-lme(PBR1019~RBC_filling, random =~1|Patient, data = T0_dat
aset)
> summary(modelPBR1019)
Linear mixed-effects model fit by REML
  Data: T0_dataset
       AIC      BIC    logLik
  19.79727 24.98062 -5.898635

Random effects:
 Formula: ~1 | Patient
        (Intercept)   Residual
StdDev:   0.2334736 0.08755291

Fixed effects:  PBR1019 ~ RBC_filling
                Value Std.Error DF   t-value p-value
(Intercept)  4.639198 0.6036894 27  7.684743  0.0000
RBC_filling -0.026836 0.0082893 27 -3.237394  0.0032
 Correlation:
            (Intr)
RBC_filling -0.997

Standardized Within-Group Residuals:
        Min          Q1         Med          Q3
-0.55031212 -0.26267102 -0.07381889  0.25041520
        Max
 0.81090103

Number of Observations: 29
Number of Groups: 29
> modelPBR525<-lme(PBR525~RBC_filling, random =~1|Patient, data = T2_datas
et)
> summary(modelPBR525)
Linear mixed-effects model fit by REML
  Data: T2_dataset
       AIC      BIC   logLik
  2.241163 7.424511 2.879418

Random effects:
 Formula: ~1 | Patient
        (Intercept)   Residual
StdDev:   0.1695521 0.06358212

Fixed effects:  PBR525 ~ RBC_filling
                Value Std.Error DF   t-value p-value
(Intercept)  3.749337 0.4880599 27  7.682124  0.0000
RBC_filling -0.019160 0.0069281 27 -2.765497  0.0101
 Correlation:
            (Intr)
RBC_filling -0.998

Standardized Within-Group Residuals:
        Min          Q1         Med          Q3
-0.66795013 -0.31393826 -0.02476593  0.26031889
        Max
 0.67559027

Number of Observations: 29
Number of Groups: 29
> modelPBR59<-lme(PBR59~RBC_filling, random =~1|Patient, data = T2_dataset
)
> summary(modelPBR59)
Linear mixed-effects model fit by REML
  Data: T2_dataset
      AIC       BIC logLik
  -21.236 -16.05266 14.618

Random effects:
 Formula: ~1 | Patient
        (Intercept)  Residual
```

```
StdDev:   0.1097712 0.0411642

Fixed effects:  PBR59 ~ RBC_filling
                 Value  Std.Error DF   t-value p-value
(Intercept)  2.6272672 0.31597899 27  8.314689  0.0000
RBC_filling -0.0164405 0.00448536 27 -3.665371  0.0011
 Correlation:
             (Intr)
RBC_filling -0.998

Standardized Within-Group Residuals:
        Min          Q1         Med          Q3
-0.56655598 -0.28607238  0.04312477  0.23225187
        Max
 0.77145971

Number of Observations: 29
Number of Groups: 29
>
> modelPBR1019<-lme(PBR1019~RBC_filling, random =~1|Patient, data = T2_dat
aset)
> summary(modelPBR1019)
Linear mixed-effects model fit by REML
  Data: T2_dataset
       AIC     BIC    logLik
  14.62945 19.8128 -3.314726

Random effects:
 Formula: ~1 | Patient
        (Intercept)   Residual
StdDev:   0.2132731 0.07997741

Fixed effects:  PBR1019 ~ RBC_filling
                Value Std.Error DF   t-value p-value
(Intercept)  3.806666 0.6139116 27  6.200675  0.0000
RBC_filling -0.015054 0.0087146 27 -1.727460  0.0955
 Correlation:
             (Intr)
RBC_filling -0.998

Standardized Within-Group Residuals:
        Min          Q1         Med          Q3
-0.79239294 -0.26285618  0.01781933  0.18020909
        Max
 0.72841526

Number of Observations: 29
Number of Groups: 29
>
> modelPBR2025<-lme(PBR2025~RBC_filling, random =~1|Patient, data = T2_dat
aset)
> summary(modelPBR2025)
Linear mixed-effects model fit by REML
  Data: T2_dataset
       AIC      BIC    logLik
  52.28492 57.46827 -22.14246

Random effects:
 Formula: ~1 | Patient
        (Intercept)  Residual
StdDev:   0.4283313 0.1606243

Fixed effects:  PBR2025 ~ RBC_filling
                Value Std.Error DF   t-value p-value
(Intercept)  4.848559  1.232962 27  3.932449  0.0005
RBC_filling -0.028701  0.017502 27 -1.639848  0.1126
 Correlation:
             (Intr)
RBC_filling -0.998
```

```
Standardized Within-Group Residuals:
        Min          Q1         Med          Q3
-0.69264228 -0.24952986 -0.01685339  0.13218112
        Max
 0.70399794

Number of Observations: 29
Number of Groups: 29
```

Linear mixed effects model for PCV and TS

Group and time effects on PCV and TS

```
> modelPCV<-lme(PCV~Group*Time, random =~1|Patient, data = Fluid_challenge
_baseline_end_dataset_categorical_groups_time )
> summary(modelPCV)
Linear mixed-effects model fit by REML
  Data: Fluid_challenge_baseline_end_dataset_categorical_groups_time
       AIC      BIC    logLik
  318.8588 334.4688 -151.4294

Random effects:
 Formula: ~1 | Patient
        (Intercept) Residual
StdDev:    2.576148 3.161745

Fixed effects:  PCV ~ Group * Time
                Value Std.Error DF   t-value p-value
(Intercept)  34.85000  1.289697 26 27.021859  0.0000
GroupB        1.35000  1.823907 26  0.740170  0.4658
GroupC        1.31667  1.873886 26  0.702640  0.4885
TimeF        -7.95000  1.413976 26 -5.622445  0.0000
GroupB:TimeF -4.35000  1.999663 26 -2.175366  0.0389
GroupC:TimeF -3.21667  2.054459 26 -1.565700  0.1295
 Correlation:
             (Intr) GroupB GroupC TimeF  GrB:TF
GroupB       -0.707
GroupC       -0.688  0.487
TimeF        -0.548  0.388  0.377
GroupB:TimeF  0.388 -0.548 -0.267 -0.707
GroupC:TimeF  0.377 -0.267 -0.548 -0.688  0.487

Standardized Within-Group Residuals:
       Min         Q1        Med         Q3        Max
-1.4446120 -0.6329702 -0.1625938  0.5466854  2.0139178

Number of Observations: 58
Number of Groups: 29
> shapiro.test(residuals(modelPCV))

        Shapiro-Wilk normality test

data:  residuals(modelPCV)
W = 0.97028, p-value = 0.1651

> modelTS<-lme(TS~Group*Time, random =~1|Patient, data = Fluid_challenge_b
aseline_end_dataset_categorical_groups_time)
> summary(modelTS)
Linear mixed-effects model fit by REML
  Data: Fluid_challenge_baseline_end_dataset_categorical_groups_time
       AIC      BIC    logLik
  362.8998 378.5098 -173.4499

Random effects:
 Formula: ~1 | Patient
        (Intercept) Residual
StdDev:     6.11887 3.769096

Fixed effects:  TS ~ Group * Time
                Value Std.Error DF  t-value p-value
(Intercept)  75.00000  2.272590 26 33.00199  0.0000
GroupB        2.50000  3.213928 26  0.77786  0.4437
GroupC        1.22222  3.301997 26  0.37015  0.7143
TimeF        -7.80000  1.685591 26 -4.62746  0.0001
GroupB:TimeF -8.10000  2.383786 26 -3.39796  0.0022
GroupC:TimeF -8.64444  2.449107 26 -3.52963  0.0016
```

```
 Correlation:
            (Intr) GroupB GroupC TimeF  GrB:TF
GroupB      -0.707
GroupC      -0.688  0.487
TimeF       -0.371  0.262  0.255
GroupB:TimeF  0.262 -0.371 -0.180 -0.707
GroupC:TimeF  0.255 -0.180 -0.371 -0.688  0.487

Standardized Within-Group Residuals:
        Min          Q1         Med          Q3
-1.47279609 -0.48362757  0.02447772  0.33458904
        Max
 2.41744913

Number of Observations: 58
Number of Groups: 29
> shapiro.test(residuals(modelTS))

        Shapiro-Wilk normality test

data:  residuals(modelTS)
W = 0.9658, p-value = 0.101
```

Effects of PCV on Glycocheck variables

```
modelPBR525<-lme(PBR525~PCV, random =~1|Patient, data = Fluid_challenge_ba
seline_end_dataset_categorical_groups_time)
> summary(modelPBR525)
Linear mixed-effects model fit by REML
  Data: Fluid_challenge_baseline_end_dataset_categorical_groups_time
        AIC      BIC    logLik
  -0.344845 7.756562 4.172423

Random effects:
 Formula: ~1 | Patient
        (Intercept) Residual
StdDev:  0.06664753 0.191393

Fixed effects:  PBR525 ~ PCV
                Value Std.Error DF   t-value p-value
(Intercept)  2.4216725 0.1227445 28 19.729381  0.0000
PCV         -0.0007209 0.0039182 28 -0.183998  0.8553
 Correlation:
    (Intr)
PCV -0.974

Standardized Within-Group Residuals:
        Min          Q1         Med          Q3
-1.94237256 -0.50290242  0.03409174  0.52670738
        Max
 2.86971913

Number of Observations: 58
Number of Groups: 29
> shapiro.test(residuals(modelPBR525))

        Shapiro-Wilk normality test

data:  residuals(modelPBR525)
W = 0.97346, p-value = 0.2327

> modelSegements<-lme(Segements~PCV, random =~1|Patient, data = Fluid_chal
lenge_baseline_end_dataset_categorical_groups_time)
> summary(modelSegements)
Linear mixed-effects model fit by REML
  Data: Fluid_challenge_baseline_end_dataset_categorical_groups_time
```

```
       AIC     BIC    logLik
  849.2376 857.339 -420.6188

Random effects:
 Formula: ~1 | Patient
        (Intercept) Residual
StdDev:   0.1522561 397.8124

Fixed effects:  Segements ~ PCV
                Value Std.Error DF  t-value p-value
(Intercept) 1612.0242 247.96338 28 6.501057  0.0000
PCV           16.7825   7.94751 28 2.111669  0.0438
 Correlation:
    (Intr)
PCV -0.978

Standardized Within-Group Residuals:
        Min          Q1         Med          Q3
-2.38729542 -0.44026109  0.05319081  0.65257548
        Max
 1.65788886

Number of Observations: 58
Number of Groups: 29
> shapiro.test(residuals(modelSegements))

        Shapiro-Wilk normality test

data:  residuals(modelSegements)
W = 0.95101, p-value = 0.02024

> modelVVD<-lme(VVD~PCV, random =~1|Patient, data = Fluid_challenge_baseli
ne_end_dataset_categorical_groups_time)
> summary(modelVVD)
Linear mixed-effects model fit by REML
  Data: Fluid_challenge_baseline_end_dataset_categorical_groups_time
       AIC      BIC logLik
  632.5999 640.7013 -312.3

Random effects:
 Formula: ~1 | Patient
        (Intercept) Residual
StdDev:  0.01126861 57.49599

Fixed effects:  VVD ~ PCV
               Value Std.Error DF  t-value p-value
(Intercept) 8.883811  35.83825 28 0.247886  0.8060
PCV         4.818300   1.14866 28 4.194725  0.0002
 Correlation:
    (Intr)
PCV -0.978

Standardized Within-Group Residuals:
       Min         Q1        Med         Q3        Max
-1.6645682 -0.5685669 -0.1087112  0.4900007  2.5865721

Number of Observations: 58
Number of Groups: 29
> shapiro.test(residuals(modelVVD))

        Shapiro-Wilk normality test

data:  residuals(modelVVD)
W = 0.97116, p-value = 0.1817

> modelPBR59<-lme(PBR59~PCV, random =~1|Patient, data = Fluid_challenge_ba
seline_end_dataset_categorical_groups_time)
> summary(modelPBR59)
Linear mixed-effects model fit by REML
```

```
  Data: Fluid_challenge_baseline_end_dataset_categorical_groups_time
      AIC       BIC logLik
  -50.042 -41.94059 29.021

Random effects:
 Formula: ~1 | Patient
        (Intercept)  Residual
StdDev:  0.07482224 0.1101897

Fixed effects:  PBR59 ~ PCV
                 Value  Std.Error DF   t-value p-value
(Intercept)  1.6625249 0.07422143 28 22.399526  0.0000
PCV         -0.0074994 0.00234293 28 -3.200868  0.0034
 Correlation:
    (Intr)
PCV -0.963

Standardized Within-Group Residuals:
       Min         Q1        Med         Q3        Max
-2.3021727 -0.6572330 -0.0387926  0.7112238  1.7117257

Number of Observations: 58
Number of Groups: 29
> shapiro.test(residuals(modelPBR59))

        Shapiro-Wilk normality test

data:  residuals(modelPBR59)
W = 0.98044, p-value = 0.4709

> modelPBR1019<-lme(PBR1019~PCV, random =~1|Patient, data = Fluid_challeng
e_baseline_end_dataset_categorical_groups_time)
> summary(modelPBR1019)
Linear mixed-effects model fit by REML
  Data: Fluid_challenge_baseline_end_dataset_categorical_groups_time
       AIC      BIC    logLik
  29.32816 37.42957 -10.66408

Random effects:
 Formula: ~1 | Patient
        (Intercept)  Residual
StdDev:  0.05212171 0.2581892

Fixed effects:  PBR1019 ~ PCV
                 Value  Std.Error DF   t-value p-value
(Intercept)  2.8576977 0.16265774 28 17.568778   0.000
PCV         -0.0045269 0.00520626 28 -0.869517   0.392
 Correlation:
    (Intr)
PCV -0.976

Standardized Within-Group Residuals:
        Min          Q1         Med          Q3
-2.45796215 -0.66518784 -0.04160715  0.54809668
        Max
 2.94472987

Number of Observations: 58
Number of Groups: 29
> shapiro.test(residuals(modelPBR1019))

        Shapiro-Wilk normality test

data:  residuals(modelPBR1019)
W = 0.98266, p-value = 0.5735

> modelPBR2025<-lme(PBR2025~PCV, random =~1|Patient, data = Fluid_challeng
e_baseline_end_dataset_categorical_groups_time)
> summary(modelPBR2025)
```

```
Linear mixed-effects model fit by REML
  Data: Fluid_challenge_baseline_end_dataset_categorical_groups_time
       AIC     BIC    logLik
  81.51289 89.6143 -36.75645

Random effects:
 Formula: ~1 | Patient
         (Intercept)  Residual
StdDev: 1.564161e-05 0.4194946

Fixed effects:  PBR2025 ~ PCV
                Value  Std.Error DF  t-value p-value
(Intercept) 2.4113269 0.26147830 28 9.221901  0.0000
PCV         0.0173844 0.00838068 28 2.074345  0.0474
 Correlation:
    (Intr)
PCV -0.978

Standardized Within-Group Residuals:
        Min          Q1         Med          Q3
-2.65224865 -0.53160876  0.06665563  0.57927838
        Max
 2.44289263

Number of Observations: 58
Number of Groups: 29
> shapiro.test(residuals(modelPBR2025))

        Shapiro-Wilk normality test

data:  residuals(modelPBR2025)
W = 0.98589, p-value = 0.7353

> modelRBC_filling<-lme(RBC_filling~PCV, random =~1|Patient, data = Fluid_
challenge_baseline_end_dataset_categorical_groups_time)
> summary(modelRBC_filling)
Linear mixed-effects model fit by REML
  Data: Fluid_challenge_baseline_end_dataset_categorical_groups_time
       AIC      BIC    logLik
  361.1378 369.2392 -176.5689

Random effects:
 Formula: ~1 | Patient
        (Intercept) Residual
StdDev:    2.409239 4.563019

Fixed effects:  RBC_filling ~ PCV
                Value Std.Error DF   t-value p-value
(Intercept) 62.82359 3.0050601 28 20.905935  0.0000
PCV          0.28270 0.0954276 28  2.962468  0.0062
 Correlation:
    (Intr)
PCV -0.969

Standardized Within-Group Residuals:
        Min          Q1         Med          Q3
-1.84581534 -0.55214977  0.02473456  0.81224367
        Max
 1.96640735

Number of Observations: 58
Number of Groups: 29
> shapiro.test(residuals(modelRBC_filling))

        Shapiro-Wilk normality test

data:  residuals(modelRBC_filling)
W = 0.97879, p-value = 0.402
```

```
> modelMedianP50<-lme(MedianP50~PCV, random =~1|Patient, data = Fluid_chal
lenge_baseline_end_dataset_categorical_groups_time)
> summary(modelMedianP50)
Linear mixed-effects model fit by REML
  Data: Fluid_challenge_baseline_end_dataset_categorical_groups_time
       AIC      BIC    logLik
  156.2894 164.3909 -74.14472

Random effects:
 Formula: ~1 | Patient
        (Intercept)  Residual
StdDev:   0.3777742 0.7363933

Fixed effects:  MedianP50 ~ PCV
                Value Std.Error DF   t-value p-value
(Intercept)  7.187067 0.4838670 28 14.853393  0.0000
PCV         -0.005278 0.0153734 28 -0.343312  0.7339
 Correlation:
    (Intr)
PCV -0.969

Standardized Within-Group Residuals:
        Min          Q1         Med          Q3
-1.95482668 -0.66580517 -0.02791911  0.51561340
        Max
 2.24110613

Number of Observations: 58
Number of Groups: 29
> shapiro.test(residuals(modelMedianP50))

        Shapiro-Wilk normality test

data:  residuals(modelMedianP50)
W = 0.97977, p-value = 0.4419
```

Linear mixed effect models - Anaesthetic variables

```
> modelHR<-lme(HR~Time*Group, random=~1|Patient, data = Fluid_challenge_co
mplete_dataset_categorical_groups_time)
> summary(modelHR)
Linear mixed-effects model fit by REML
  Data: Fluid_challenge_complete_dataset_categorical_groups_time
       AIC     BIC    logLik
  636.2202 662.144 -307.1101

Random effects:
 Formula: ~1 | Patient
        (Intercept) Residual
StdDev:    12.14754 7.595031

Fixed effects:  HR ~ Time * Group
                 Value Std.Error DF   t-value p-value
(Intercept)  123.11667  4.530421 52 27.175544  0.0000
TimeE         -5.55667  3.396601 52 -1.635949  0.1079
TimeF         -5.51667  3.396601 52 -1.624173  0.1104
GroupB         3.23333  6.406983 26  0.504658  0.6180
GroupC        -8.83889  6.582550 26 -1.342776  0.1910
TimeE:GroupB   4.13667  4.803519 52  0.861174  0.3931
TimeF:GroupB   3.59167  4.803519 52  0.747716  0.4580
TimeE:GroupC   4.40111  4.935147 52  0.891789  0.3766
TimeF:GroupC   0.68333  4.935147 52  0.138463  0.8904
 Correlation:
             (Intr) TimeE  TimeF  GroupB GroupC TmE:GB
TimeE        -0.375
TimeF        -0.375  0.500
GroupB       -0.707  0.265  0.265
GroupC       -0.688  0.258  0.258  0.487
TimeE:GroupB  0.265 -0.707 -0.354 -0.375 -0.182
TimeF:GroupB  0.265 -0.354 -0.707 -0.375 -0.182  0.500
TimeE:GroupC  0.258 -0.688 -0.344 -0.182 -0.375  0.487
TimeF:GroupC  0.258 -0.344 -0.688 -0.182 -0.375  0.243
             TmF:GB TmE:GC
TimeE
TimeF
GroupB
GroupC
TimeE:GroupB
TimeF:GroupB
TimeE:GroupC  0.243
TimeF:GroupC  0.487  0.500

Standardized Within-Group Residuals:
        Min          Q1         Med          Q3
-1.93956496 -0.46306864  0.01894022  0.44004827
        Max
 2.06825223

Number of Observations: 87
Number of Groups: 29
> shapiro.test(residuals(modelHR))

        Shapiro-Wilk normality test

data:  residuals(modelHR)
W = 0.98373, p-value = 0.3465

> modelSAP<-lme(SAP~Time*Group, random=~1|Patient, data = Fluid_challenge_
complete_dataset_categorical_groups_time)
> summary(modelSAP)
Linear mixed-effects model fit by REML
  Data: Fluid_challenge_complete_dataset_categorical_groups_time
      AIC      BIC    logLik
  615.075 640.9988 -296.5375
```

```
Random effects:
 Formula: ~1 | Patient
        (Intercept) Residual
StdDev:    10.33361  6.70484

Fixed effects:  SAP ~ Time * Group
                 Value Std.Error DF   t-value p-value
(Intercept)  118.71667  3.895362 52 30.476417  0.0000
TimeE         -3.54667  2.998496 52 -1.182815  0.2423
TimeF         -1.81667  2.998496 52 -0.605859  0.5472
GroupB        -2.01667  5.508873 26 -0.366076  0.7173
GroupC         2.19074  5.659829 26  0.387068  0.7019
TimeE:GroupB   0.04167  4.240513 52  0.009826  0.9922
TimeF:GroupB  -0.25833  4.240513 52 -0.060920  0.9517
TimeE:GroupC  -5.39963  4.356713 52 -1.239381  0.2208
TimeF:GroupC -14.70185  4.356713 52 -3.374528  0.0014
 Correlation:
             (Intr) TimeE  TimeF  GroupB GroupC TmE:GB
TimeE        -0.385
TimeF        -0.385  0.500
GroupB       -0.707  0.272  0.272
GroupC       -0.688  0.265  0.265  0.487
TimeE:GroupB  0.272 -0.707 -0.354 -0.385 -0.187
TimeF:GroupB  0.272 -0.354 -0.707 -0.385 -0.187  0.500
TimeE:GroupC  0.265 -0.688 -0.344 -0.187 -0.385  0.487
TimeF:GroupC  0.265 -0.344 -0.688 -0.187 -0.385  0.243
             TmF:GB TmE:GC
TimeE
TimeF
GroupB
GroupC
TimeE:GroupB
TimeF:GroupB
TimeE:GroupC  0.243
TimeF:GroupC  0.487  0.500

Standardized Within-Group Residuals:
       Min         Q1        Med         Q3        Max
-2.7061671 -0.4519547 -0.0919837  0.4634134  2.4865990

Number of Observations: 87
Number of Groups: 29
> shapiro.test(residuals(modelSAP))

        Shapiro-Wilk normality test

data:  residuals(modelSAP)
W = 0.96265, p-value = 0.01305

> residualsHR <- residuals(modelHR)
> qqnorm(residualsHR)
> qqline(residualsHR)
> modelDAP<-lme(DAP~Time*Group, random=~1|Patient, data = Fluid_challenge_
complete_dataset_categorical_groups_time)
> summary(modelDAP)
Linear mixed-effects model fit by REML
  Data: Fluid_challenge_complete_dataset_categorical_groups_time
       AIC      BIC    logLik
  568.9236 594.8474 -273.4618

Random effects:
 Formula: ~1 | Patient
        (Intercept) Residual
StdDev:    8.431485 4.797019

Fixed effects:  DAP ~ Time * Group
                 Value Std.Error DF   t-value p-value
(Intercept)   63.58333  3.067594 52 20.727427  0.0000
```

```
TimeE          -6.41833  2.145292 52 -2.991822  0.0042
TimeF         -11.00000  2.145292 52 -5.127506  0.0000
GroupB         -2.68333  4.338233 26 -0.618531  0.5416
GroupC         -7.76852  4.457111 26 -1.742949  0.0932
TimeE:GroupB    3.50833  3.033902 52  1.156377  0.2528
TimeF:GroupB    8.90000  3.033902 52  2.933516  0.0050
TimeE:GroupC    3.30352  3.117037 52  1.059826  0.2941
TimeF:GroupC    9.25926  3.117037 52  2.970532  0.0045
 Correlation:
              (Intr) TimeE  TimeF  GroupB GroupC TmE:GB
TimeE         -0.350
TimeF         -0.350  0.500
GroupB        -0.707  0.247  0.247
GroupC        -0.688  0.241  0.241  0.487
TimeE:GroupB   0.247 -0.707 -0.354 -0.350 -0.170
TimeF:GroupB   0.247 -0.354 -0.707 -0.350 -0.170  0.500
TimeE:GroupC   0.241 -0.688 -0.344 -0.170 -0.350  0.487
TimeF:GroupC   0.241 -0.344 -0.688 -0.170 -0.350  0.243
              TmF:GB TmE:GC
TimeE
TimeF
GroupB
GroupC
TimeE:GroupB
TimeF:GroupB
TimeE:GroupC   0.243
TimeF:GroupC   0.487  0.500

Standardized Within-Group Residuals:
       Min         Q1        Med         Q3        Max
-1.8219793 -0.5367468 -0.1010147  0.6420120  2.0202906

Number of Observations: 87
Number of Groups: 29
> shapiro.test(residuals(modelDAP))

        Shapiro-Wilk normality test

data:  residuals(modelDAP)
W = 0.99169, p-value = 0.8608

> modelMAP<-lme(MAP~Time*Group, random=~1|Patient, data = Fluid_challenge_
complete_dataset_categorical_groups_time)
> summary(modelMAP)
Linear mixed-effects model fit by REML
  Data: Fluid_challenge_complete_dataset_categorical_groups_time
      AIC      BIC    logLik
  548.541 574.4648 -263.2705

Random effects:
 Formula: ~1 | Patient
        (Intercept) Residual
StdDev:    8.694939 3.919086

Fixed effects:  MAP ~ Time * Group
                Value Std.Error DF   t-value p-value
(Intercept)  81.86667  3.015977 52 27.144323  0.0000
TimeE        -5.43167  1.752668 52 -3.099084  0.0031
TimeF        -8.01667  1.752668 52 -4.573978  0.0000
GroupB       -2.46667  4.265236 26 -0.578319  0.5680
GroupC       -3.16296  4.382114 26 -0.721789  0.4769
TimeE:GroupB  3.01667  2.478647 52  1.217062  0.2291
TimeF:GroupB  6.10833  2.478647 52  2.464382  0.0171
TimeE:GroupC -0.04981  2.546568 52 -0.019562  0.9845
TimeF:GroupC -0.03889  2.546568 52 -0.015271  0.9879
 Correlation:
              (Intr) TimeE  TimeF  GroupB GroupC TmE:GB
TimeE         -0.291
TimeF         -0.291  0.500
```

```
GroupB       -0.707  0.205  0.205
GroupC       -0.688  0.200  0.200  0.487
TimeE:GroupB  0.205 -0.707 -0.354 -0.291 -0.141
TimeF:GroupB  0.205 -0.354 -0.707 -0.291 -0.141  0.500
TimeE:GroupC  0.200 -0.688 -0.344 -0.141 -0.291  0.487
TimeF:GroupC  0.200 -0.344 -0.688 -0.141 -0.291  0.243
              TmF:GB TmE:GC
TimeE
TimeF
GroupB
GroupC
TimeE:GroupB
TimeF:GroupB
TimeE:GroupC  0.243
TimeF:GroupC  0.487  0.500

Standardized Within-Group Residuals:
        Min          Q1         Med          Q3
-3.07121957 -0.53590365 -0.01977772  0.47076204
        Max
 2.54658744

Number of Observations: 87
Number of Groups: 29
> shapiro.test(residuals(modelMAP))

        Shapiro-Wilk normality test

data:  residuals(modelMAP)
W = 0.96552, p-value = 0.02026

> residualsMAP <- residuals(modelMAP)
> qqnorm(residualsMAP)
> qqline(residualsMAP)
> residualsHR <- residuals(modelHR)
> qqnorm(residualsHR)
> qqline(residualsHR)
> modelTemp<-lme(Temp~Time*Group, random=~1|Patient, data = Fluid_challeng
e_complete_dataset_categorical_groups_time)
> summary(modelTemp)
Linear mixed-effects model fit by REML
  Data: Fluid_challenge_complete_dataset_categorical_groups_time
       AIC     BIC    logLik
  25.37651 51.3003 -1.688253

Random effects:
 Formula: ~1 | Patient
        (Intercept)  Residual
StdDev:   0.3724816 0.1246561

Fixed effects:  Temp ~ Time * Group
                Value  Std.Error DF   t-value p-value
(Intercept)  37.28000 0.12421016 52 300.13647  0.0000
TimeE        -0.08650 0.05574789 52  -1.55163  0.1268
TimeF        -0.19667 0.05574789 52  -3.52779  0.0009
GroupB        0.30000 0.17565970 26   1.70785  0.0996
GroupC       -0.00037 0.18047318 26  -0.00205  0.9984
TimeE:GroupB -0.08300 0.07883942 52  -1.05277  0.2973
TimeF:GroupB -0.12500 0.07883942 52  -1.58550  0.1189
TimeE:GroupC -0.06091 0.08099980 52  -0.75195  0.4555
TimeF:GroupC  0.01704 0.08099980 52   0.21033  0.8342
 Correlation:
              (Intr) TimeE  TimeF  GroupB GroupC TmE:GB
TimeE        -0.224
TimeF        -0.224  0.500
GroupB       -0.707  0.159  0.159
GroupC       -0.688  0.154  0.154  0.487
TimeE:GroupB  0.159 -0.707 -0.354 -0.224 -0.109
TimeF:GroupB  0.159 -0.354 -0.707 -0.224 -0.109  0.500
```

```
TimeE:GroupC  0.154 -0.688 -0.344 -0.109 -0.224  0.487
TimeF:GroupC  0.154 -0.344 -0.688 -0.109 -0.224  0.243
              TmF:GB TmE:GC
TimeE
TimeF
GroupB
GroupC
TimeE:GroupB
TimeF:GroupB
TimeE:GroupC  0.243
TimeF:GroupC  0.487  0.500

Standardized Within-Group Residuals:
       Min         Q1        Med         Q3        Max
-2.1904888 -0.3905158  0.0141091  0.3607567  4.0637567

Number of Observations: 87
Number of Groups: 29
> shapiro.test(residuals(modelTemp))

        Shapiro-Wilk normality test

data:  residuals(modelTemp)
W = 0.88771, p-value = 1.679e-06

>
> residualsTemp <- residuals(modelTemp)
> qqnorm(residualsTemp)
> qqline(residualsTemp)
```

Effects of MAP on Glycocheck variables

```
> model_PBR525_MAP<-lme(PBR525~MAP, random=~1|Patient, dat
a = Fluid_challenge_dataset_noNAs_noPCV_TS)
> summary(model_PBR525_MAP)
Linear mixed-effects model fit by REML
  Data: Fluid_challenge_dataset_noNAs_noPCV_TS
        AIC      BIC    logLik
  -1.265488 8.361389 4.632744

Random effects:
 Formula: ~1 | Patient
        (Intercept)  Residual
StdDev:  2.3951e-05 0.2107439

Fixed effects:  PBR525 ~ MAP
                Value  Std.Error DF   t-value p-value
(Intercept) 2.2559709 0.18455289 54 12.223980  0.0000
MAP         0.0018611 0.00238361 54  0.780808  0.4383
 Correlation:
    (Intr)
MAP -0.992

Standardized Within-Group Residuals:
        Min          Q1         Med          Q3
-2.44177859 -0.59124642  0.02661119  0.64189395
        Max
 2.82214105

Number of Observations: 84
Number of Groups: 29
> shapiro.test(residuals(model_PBR525_MAP))

        Shapiro-Wilk normality test

data:  residuals(model_PBR525_MAP)
W = 0.99219, p-value = 0.9001
```

```
> model_PBR59_MAP<-lme(PBR59~MAP, random=~1|Patient, data
= Fluid_challenge_dataset_noNAs_noPCV_TS)
> summary(model_PBR59_MAP)
Linear mixed-effects model fit by REML
  Data: Fluid_challenge_dataset_noNAs_noPCV_TS
        AIC       BIC   logLik
  -70.51345 -60.88657 39.25673

Random effects:
 Formula: ~1 | Patient
        (Intercept)  Residual
StdDev:  0.04283395 0.1322209

Fixed effects:  PBR59 ~ MAP
                 Value  Std.Error DF   t-value p-value
(Intercept)  1.5446161 0.12907940 54 11.966403  0.0000
MAP         -0.0013963 0.00166678 54 -0.837713  0.4059
 Correlation:
    (Intr)
MAP -0.992

Standardized Within-Group Residuals:
       Min         Q1        Med         Q3        Max
-2.4819069 -0.6590372 -0.1022987  0.7649146  2.2196501

Number of Observations: 84
Number of Groups: 29
> shapiro.test(residuals(model_PBR59_MAP))

        Shapiro-Wilk normality test

data:  residuals(model_PBR59_MAP)
W = 0.98607, p-value = 0.5042

> model_PBR1019_MAP<-lme(PBR1019~MAP, random=~1|Patient, d
ata = Fluid_challenge_dataset_noNAs_noPCV_TS)
> summary(model_PBR1019_MAP)
Linear mixed-effects model fit by REML
  Data: Fluid_challenge_dataset_noNAs_noPCV_TS
       AIC      BIC    logLik
  35.53908 45.16596 -13.76954

Random effects:
 Formula: ~1 | Patient
        (Intercept)  Residual
StdDev:  0.04601574 0.2600018

Fixed effects:  PBR1019 ~ MAP
                Value  Std.Error DF   t-value p-value
(Intercept) 2.5922632 0.23610272 54 10.979387   0.000
MAP         0.0017609 0.00304924 54  0.577474   0.566
 Correlation:
    (Intr)
MAP -0.992

Standardized Within-Group Residuals:
        Min          Q1         Med          Q3
-2.52329363 -0.66432597 -0.01634929  0.66686960
        Max
 2.83342625

Number of Observations: 84
Number of Groups: 29
> shapiro.test(residuals(model_PBR1019_MAP))

        Shapiro-Wilk normality test

data:  residuals(model_PBR1019_MAP)
```

```
W = 0.9889, p-value = 0.6949

> model_PBR2025_MAP<-lme(PBR2025~MAP, random=~1|Patient, d
ata = Fluid_challenge_dataset_noNAs_noPCV_TS)
> summary(model_PBR2025_MAP)
Linear mixed-effects model fit by REML
  Data: Fluid_challenge_dataset_noNAs_noPCV_TS
       AIC      BIC    logLik
  131.2436 140.8705 -61.62179

Random effects:
 Formula: ~1 | Patient
        (Intercept) Residual
StdDev: 1.24019e-05 0.472778

Fixed effects:  PBR2025 ~ MAP
                Value Std.Error DF t-value p-value
(Intercept) 2.1320377 0.4140216 54 5.14958  0.0000
MAP         0.0099284 0.0053473 54 1.85670  0.0688
 Correlation:
    (Intr)
MAP -0.992

Standardized Within-Group Residuals:
        Min          Q1         Med          Q3
-2.29932884 -0.67823348  0.06539028  0.60298962
        Max
 1.96080439

Number of Observations: 84
Number of Groups: 29
> shapiro.test(residuals(model_PBR2025_MAP))

        Shapiro-Wilk normality test

data:  residuals(model_PBR2025_MAP)
W = 0.97995, p-value = 0.2148

> model_Segements_MAP<-lme(Segements~MAP, random=~1|Patien
t, data = Fluid_challenge_dataset_noNAs_noPCV_TS)
> summary(model_Segements_MAP)
Linear mixed-effects model fit by REML
  Data: Fluid_challenge_dataset_noNAs_noPCV_TS
       AIC     BIC    logLik
  1239.763 1249.39 -615.8813

Random effects:
 Formula: ~1 | Patient
        (Intercept) Residual
StdDev:    219.8023 361.1987

Fixed effects:  Segements ~ MAP
                Value Std.Error DF  t-value p-value
(Intercept) 1927.339  419.0650 54 4.599141  0.0000
MAP            2.429    5.4071 54 0.449231  0.6551
 Correlation:
    (Intr)
MAP -0.991

Standardized Within-Group Residuals:
        Min          Q1         Med          Q3
-2.81347249 -0.42689633  0.03718351  0.65836124
        Max
 1.96007562

Number of Observations: 84
Number of Groups: 29
> shapiro.test(residuals(model_Segements_MAP))
```

```
        Shapiro-Wilk normality test

data:  residuals(model_Segements_MAP)
W = 0.9767, p-value = 0.1313

> qqnorm(residuals(model_Segements_MAP))
> qqline(residuals(model_Segements_MAP))
> model_VVD_MAP<-lme(VVD~MAP, random=~1|Patient, data = Fl
uid_challenge_dataset_noNAs_noPCV_TS)
> summary(model_VVD_MAP)
Linear mixed-effects model fit by REML
  Data: Fluid_challenge_dataset_noNAs_noPCV_TS
       AIC      BIC    logLik
  930.7363 940.3632 -461.3682

Random effects:
 Formula: ~1 | Patient
        (Intercept) Residual
StdDev:    8.889678 61.31622

Fixed effects:  VVD ~ MAP
                Value Std.Error DF   t-value p-value
(Intercept) 174.62025  55.04257 54  3.172458  0.0025
MAP          -0.30293   0.71088 54 -0.426137  0.6717
 Correlation:
    (Intr)
MAP -0.992

Standardized Within-Group Residuals:
       Min         Q1        Med         Q3        Max
-1.5207307 -0.5674475 -0.3279795  0.3589486  3.1868310

Number of Observations: 84
Number of Groups: 29
> shapiro.test(residuals(model_VVD_MAP))

        Shapiro-Wilk normality test

data:  residuals(model_VVD_MAP)
W = 0.9037, p-value = 1.131e-05

> qqnorm(residuals(model_VVD_MAP))
> qqline(residuals(model_VVD_MAP))
> model_MedianP50_MAP<-lme(MedianP50~MAP, random=~1|Patien
t, data = Fluid_challenge_dataset_noNAs_noPCV_TS)
> summary(model_MedianP50_MAP)
Linear mixed-effects model fit by REML
  Data: Fluid_challenge_dataset_noNAs_noPCV_TS
       AIC      BIC   logLik
  206.3116 215.9385 -99.1558

Random effects:
 Formula: ~1 | Patient
        (Intercept)  Residual
StdDev:   0.5500088 0.6116681

Fixed effects:  MedianP50 ~ MAP
                Value Std.Error DF   t-value p-value
(Intercept)  8.240496 0.8266912 54  9.968046  0.0000
MAP         -0.015422 0.0106501 54 -1.448106  0.1534
 Correlation:
    (Intr)
MAP -0.989

Standardized Within-Group Residuals:
        Min          Q1         Med          Q3
-2.19714001 -0.47424841 -0.03858948  0.35717360
        Max
 2.08375339
```

```
 Number of Observations: 84
 Number of Groups: 29
 > shapiro.test(residuals(model_MedianP50_MAP))

         Shapiro-Wilk normality test

 data:  residuals(model_MedianP50_MAP)
 W = 0.9693, p-value = 0.04218



> model_MedianP50_Temp_TG<-lme(MedianP50~MAP*Group*Time,  random=~1|Patien
t, data = Fluid_challenge_dataset_noNAs_noPCV_TS)
> summary(model_MedianP50_MAP_TG)
Linear mixed-effects model fit by REML
  Data: Fluid_challenge_dataset_noNAs_noPCV_TS
       AIC      BIC    logLik
  267.0506 310.8437 -113.5253

Random effects:
 Formula: ~1 | Patient
        (Intercept)  Residual
StdDev:   0.4112228 0.6468085

Fixed effects:  MedianP50 ~ MAP * Group * Time
                     Value Std.Error DF   t-value
(Intercept)       9.519914  2.444045 40  3.895146
MAP              -0.029657  0.029707 40 -0.998321
GroupB           -4.767064  3.245470 26 -1.468836
GroupC           -0.211502  3.383992 26 -0.062501
TimeE             1.390964  2.985824 40  0.465856
TimeF            -0.809180  2.884188 40 -0.280557
MAP:GroupB        0.053072  0.039955 40  1.328276
MAP:GroupC        0.001409  0.041909 40  0.033618
MAP:TimeE        -0.020382  0.037144 40 -0.548730
MAP:TimeF         0.007548  0.036433 40  0.207181
GroupB:TimeE      0.053775  3.807112 40  0.014125
GroupC:TimeE     -3.617962  4.105343 40 -0.881281
GroupB:TimeF      1.410422  3.744108 40  0.376704
GroupC:TimeF     -0.946722  4.227393 40 -0.223949
MAP:GroupB:TimeE  0.003944  0.047659 40  0.082747
MAP:GroupC:TimeE  0.057606  0.052308 40  1.101294
MAP:GroupB:TimeF -0.014687  0.047272 40 -0.310695
MAP:GroupC:TimeF  0.023532  0.055486 40  0.424108
                  p-value
(Intercept)        0.0004
MAP                0.3241
GroupB             0.1539
GroupC             0.9506
TimeE              0.6438
TimeF              0.7805
MAP:GroupB         0.1916
MAP:GroupC         0.9733
MAP:TimeE          0.5862
MAP:TimeF          0.8369
GroupB:TimeE       0.9888
GroupC:TimeE       0.3834
GroupB:TimeF       0.7084
GroupC:TimeF       0.8239
MAP:GroupB:TimeE   0.9345
MAP:GroupC:TimeE   0.2774
MAP:GroupB:TimeF   0.7576
MAP:GroupC:TimeF   0.6738
 Correlation:
                  (Intr) MAP    GroupB GroupC TimeE
MAP               -0.995
GroupB            -0.753  0.749
GroupC            -0.722  0.719  0.544
```

```
TimeE             -0.700  0.698  0.527  0.506
TimeF             -0.768  0.766  0.579  0.555  0.629
MAP:GroupB         0.740 -0.743 -0.994 -0.534 -0.519
MAP:GroupC         0.705 -0.709 -0.531 -0.994 -0.495
MAP:TimeE          0.675 -0.679 -0.508 -0.488 -0.994
MAP:TimeF          0.729 -0.733 -0.549 -0.527 -0.607
GroupB:TimeE       0.549 -0.547 -0.703 -0.397 -0.784
GroupC:TimeE       0.509 -0.508 -0.384 -0.664 -0.727
GroupB:TimeF       0.592 -0.590 -0.741 -0.427 -0.485
GroupC:TimeF       0.524 -0.523 -0.395 -0.646 -0.429
MAP:GroupB:TimeE -0.526  0.529  0.681  0.380  0.775
MAP:GroupC:TimeE -0.479  0.482  0.361  0.632  0.706
MAP:GroupB:TimeF -0.562  0.565  0.712  0.406  0.468
MAP:GroupC:TimeF -0.479  0.481  0.361  0.589  0.399
                  TimeF  MAP:GrB MAP:GrC MAP:TE MAP:TF
MAP
GroupB
GroupC
TimeE
TimeF
MAP:GroupB        -0.570
MAP:GroupC        -0.543  0.527
MAP:TimeE         -0.614  0.504   0.481
MAP:TimeF         -0.993  0.545   0.519   0.598
GroupB:TimeE      -0.493  0.699   0.388   0.780  0.476
GroupC:TimeE      -0.458  0.377   0.660   0.723  0.442
GroupB:TimeF      -0.770  0.737   0.418   0.473  0.765
GroupC:TimeF      -0.682  0.389   0.642   0.419  0.678
MAP:GroupB:TimeE  0.478 -0.685  -0.375  -0.779 -0.466
MAP:GroupC:TimeE  0.436 -0.358  -0.635  -0.710 -0.425
MAP:GroupB:TimeF  0.766 -0.715  -0.400  -0.461 -0.771
MAP:GroupC:TimeF  0.652 -0.358  -0.591  -0.393 -0.657
                  GrB:TE GrC:TE GrB:TF GrC:TF MAP:GB:TE
MAP
GroupB
GroupC
TimeE
TimeF
MAP:GroupB
MAP:GroupC
MAP:TimeE
MAP:TimeF
GroupB:TimeE
GroupC:TimeE       0.570
GroupB:TimeF       0.619  0.352
GroupC:TimeF       0.337  0.542  0.526
MAP:GroupB:TimeE -0.994 -0.564 -0.605 -0.326
MAP:GroupC:TimeE -0.554 -0.993 -0.336 -0.525  0.553
MAP:GroupB:TimeF -0.602 -0.341 -0.993 -0.522  0.595
MAP:GroupC:TimeF -0.313 -0.509 -0.502 -0.992  0.306
                  MAP:GC:TE MAP:GB:TF
MAP
GroupB
GroupC
TimeE
TimeF
MAP:GroupB
MAP:GroupC
MAP:TimeE
MAP:TimeF
GroupB:TimeE
GroupC:TimeE
GroupB:TimeF
GroupC:TimeF
MAP:GroupB:TimeE
MAP:GroupC:TimeE
MAP:GroupB:TimeF  0.327
MAP:GroupC:TimeF  0.499     0.506
```

```
Standardized Within-Group Residuals:
        Min          Q1         Med          Q3
-2.78722953 -0.51831987 -0.04368427  0.44356577
        Max
 1.69590882

Number of Observations: 84
Number of Groups: 29
> shapiro.test(residuals(model_MedianP50_MAP_TG))

        Shapiro-Wilk normality test

data:  residuals(model_MedianP50_MAP_TG)
W = 0.97326, p-value = 0.0775
```

Effects of temperature on Glycocheck variables

```
> model_PBR525_Temp<-lme(PBR525~Temp, random=~1|Patient, data = Fluid_chal
lenge_dataset_noNAs_noPCV_TS)
> summary(model_PBR525_Temp)
Linear mixed-effects model fit by REML
  Data: Fluid_challenge_dataset_noNAs_noPCV_TS
       AIC      BIC    logLik
  -8.41275 1.214127 8.206375

Random effects:
 Formula: ~1 | Patient
         (Intercept)  Residual
StdDev: 2.226071e-05 0.2097016

Fixed effects:  PBR525 ~ Temp
                 Value Std.Error DF    t-value
(Intercept) -0.11253978 2.0981645 54 -0.0536373
Temp         0.06739486 0.0563001 54  1.1970641
            p-value
(Intercept)  0.9574
Temp         0.2365
 Correlation:
     (Intr)
Temp -1

Standardized Within-Group Residuals:
        Min          Q1         Med          Q3
-2.36208164 -0.66093647  0.01709122  0.60277394
        Max
 2.75311909

Number of Observations: 84
Number of Groups: 29
> shapiro.test(residuals(model_PBR525_Temp))

        Shapiro-Wilk normality test

data:  residuals(model_PBR525_Temp)
W = 0.98779, p-value = 0.6179

> model_PBR59_Temp<-lme(PBR59~Temp, random=~1|Patient, data = Fluid_challe
nge_dataset_noNAs_noPCV_TS)
> summary(model_PBR59_Temp)
Linear mixed-effects model fit by REML
  Data: Fluid_challenge_dataset_noNAs_noPCV_TS
       AIC       BIC    logLik
  -76.24781 -66.62093 42.12391

Random effects:
 Formula: ~1 | Patient
```

```
        (Intercept)  Residual
StdDev:  0.03902007 0.1337097

Fixed effects:  PBR59 ~ Temp
                Value Std.Error DF   t-value p-value
(Intercept) 1.0469155 1.4769454 54 0.7088383  0.4815
Temp        0.0104765 0.0396306 54 0.2643538  0.7925
 Correlation:
     (Intr)
Temp -1

Standardized Within-Group Residuals:
       Min         Q1        Med         Q3        Max
-2.5459629 -0.6055903 -0.1284347  0.6646699  2.3756583

Number of Observations: 84
Number of Groups: 29
> shapiro.test(residuals(model_PBR59_Temp))

        Shapiro-Wilk normality test

data:  residuals(model_PBR59_Temp)
W = 0.98332, p-value = 0.35

> model_PBR1019_Temp<-lme(PBR1019~Temp, random=~1|Patient, data = Fluid_ch
allenge_dataset_noNAs_noPCV_TS)
> summary(model_PBR1019_Temp)
Linear mixed-effects model fit by REML
  Data: Fluid_challenge_dataset_noNAs_noPCV_TS
       AIC      BIC    logLik
  27.64648 37.27336 -9.823239

Random effects:
 Formula: ~1 | Patient
        (Intercept)  Residual
StdDev:  0.04119009 0.2582221

Fixed effects:  PBR1019 ~ Temp
                 Value Std.Error DF    t-value p-value
(Intercept) -0.9770568 2.6683891 54 -0.3661598  0.7157
Temp         0.0994103 0.0716008 54  1.3883958  0.1707
 Correlation:
     (Intr)
Temp -1

Standardized Within-Group Residuals:
         Min           Q1          Med           Q3
-2.493450819 -0.645219247 -0.007675765  0.603133433
         Max
 2.756058788

Number of Observations: 84
Number of Groups: 29
> shapiro.test(residuals(model_PBR1019_Temp))

        Shapiro-Wilk normality test

data:  residuals(model_PBR1019_Temp)
W = 0.99069, p-value = 0.8146

> model_PBR2025_Temp<-lme(PBR2025~Temp, random=~1|Patient, data = Fluid_ch
allenge_dataset_noNAs_noPCV_TS)
> summary(model_PBR2025_Temp)
Linear mixed-effects model fit by REML
  Data: Fluid_challenge_dataset_noNAs_noPCV_TS
       AIC      BIC    logLik
  125.8444 135.4713 -58.92221

Random effects:
```

```
 Formula: ~1 | Patient
         (Intercept)  Residual
StdDev: 1.290647e-05 0.4754809

Fixed effects:  PBR2025 ~ Temp
                Value Std.Error DF    t-value p-value
(Intercept) -4.594737  4.757414 54 -0.9658056  0.3384
Temp         0.200978  0.127656 54  1.5743731  0.1212
 Correlation:
     (Intr)
Temp -1

Standardized Within-Group Residuals:
       Min         Q1        Med         Q3        Max
-2.2882431 -0.5775912  0.1103111  0.6308346  2.1704011

Number of Observations: 84
Number of Groups: 29
> shapiro.test(residuals(model_PBR2025_Temp))

        Shapiro-Wilk normality test

data:  residuals(model_PBR2025_Temp)
W = 0.98227, p-value = 0.3015

> model_Segements_Temp<-lme(Segements~Temp, random=~1|Patient, data = Flui
d_challenge_dataset_noNAs_noPCV_TS)
> summary(model_Segements_Temp)
Linear mixed-effects model fit by REML
  Data: Fluid_challenge_dataset_noNAs_noPCV_TS
       AIC      BIC    logLik
  1233.554 1243.181 -612.7769

Random effects:
 Formula: ~1 | Patient
        (Intercept) Residual
StdDev:    215.5108 363.1573

Fixed effects:  Segements ~ Temp
                Value Std.Error DF   t-value p-value
(Intercept) 1819.4407  4917.906 54 0.3699625  0.7129
Temp           7.9011   131.959 54 0.0598754  0.9525
 Correlation:
     (Intr)
Temp -1

Standardized Within-Group Residuals:
       Min         Q1        Med         Q3        Max
-2.8027528 -0.4252488  0.0744401  0.6456585  1.9296363

Number of Observations: 84
Number of Groups: 29
> shapiro.test(residuals(model_Segements_Temp))

        Shapiro-Wilk normality test

data:  residuals(model_Segements_Temp)
W = 0.97536, p-value = 0.107

> qqnorm(residuals(model_Segements_Temp))
> qqline(residuals(model_Segements_Temp))
> model_VVD_Temp<-lme(VVD~Temp, random=~1|Patient, data = Fluid_challenge_
dataset_noNAs_noPCV_TS)
> summary(model_VVD_Temp)
Linear mixed-effects model fit by REML
  Data: Fluid_challenge_dataset_noNAs_noPCV_TS
       AIC      BIC    logLik
  924.5176 934.1445 -458.2588
```

```
Random effects:
 Formula: ~1 | Patient
        (Intercept) Residual
StdDev:    12.83678 60.73032

Fixed effects:  VVD ~ Temp
                Value Std.Error DF    t-value p-value
(Intercept) 24.250492  642.0086 54 0.03777285  0.9700
Temp         3.410746   17.2270 54 0.19798876  0.8438
 Correlation:
     (Intr)
Temp -1

Standardized Within-Group Residuals:
       Min         Q1        Med         Q3        Max
-1.5061562 -0.5912594 -0.3058755  0.4049043  3.1750368

Number of Observations: 84
Number of Groups: 29
> shapiro.test(residuals(model_VVD_Temp))

        Shapiro-Wilk normality test

data:  residuals(model_VVD_Temp)
W = 0.90506, p-value = 1.298e-05

> qqnorm(residuals(model_VVD_Temp))
> qqline(residuals(model_VVD_Temp))
> model_MedianP50_Temp<-lme(MedianP50~Temp, random=~1|Patient, data = Flui
d_challenge_dataset_noNAs_noPCV_TS)
> summary(model_MedianP50_Temp)
Linear mixed-effects model fit by REML
  Data: Fluid_challenge_dataset_noNAs_noPCV_TS
      AIC      BIC    logLik
  193.908 203.5348 -92.95398

Random effects:
 Formula: ~1 | Patient
        (Intercept)  Residual
StdDev:   0.5487693 0.5837331

Fixed effects:  MedianP50 ~ Temp
                Value Std.Error DF   t-value p-value
(Intercept) 35.32267  9.774425 54  3.613785  0.0007
Temp        -0.75849  0.262266 54 -2.892054  0.0055
 Correlation:
     (Intr)
Temp -1

Standardized Within-Group Residuals:
        Min          Q1         Med          Q3
-2.25405665 -0.52586492 -0.05899283  0.39335709
        Max
 2.13243657

Number of Observations: 84
Number of Groups: 29
> shapiro.test(residuals(model_MedianP50_Temp))

        Shapiro-Wilk normality test

data:  residuals(model_MedianP50_Temp)
W = 0.96424, p-value = 0.01966


> summary(model_MedianP50_Temp_TG)
Linear mixed-effects model fit by REML
  Data: Fluid_challenge_dataset_noNAs_noPCV_TS
       AIC     BIC    logLik
```

```
  197.2029 240.996 -78.60143

Random effects:
 Formula: ~1 | Patient
        (Intercept) Residual
StdDev:   0.4514925 0.564906

Fixed effects:  MedianP50 ~ Temp * Group * Time
                     Value Std.Error DF    t-value
(Intercept)        69.76401  29.25975 40  2.3842995
Temp               -1.68112   0.78484 40 -2.1419842
GroupB            -35.13521  33.72539 26 -1.0418031
GroupC             -7.00272  39.38864 26 -0.1777852
TimeE               6.12514  35.41310 40  0.1729624
TimeF              -9.99655  38.35154 40 -0.2606558
Temp:GroupB         0.93559   0.90283 40  1.0362892
Temp:GroupC         0.18764   1.05653 40  0.1776037
Temp:TimeE         -0.17054   0.95134 40 -0.1792615
Temp:TimeF          0.26028   1.03237 40  0.2521167
GroupB:TimeE      -28.15576  40.26172 40 -0.6993183
GroupC:TimeE      -84.23189  47.66864 40 -1.7670294
GroupB:TimeF      -32.56895  43.29316 40 -0.7522887
GroupC:TimeF      -20.86744  48.74869 40 -0.4280615
Temp:GroupB:TimeE   0.75933   1.07985 40  0.7031771
Temp:GroupC:TimeE   2.28571   1.28079 40  1.7846171
Temp:GroupB:TimeF   0.87582   1.16378 40  0.7525651
Temp:GroupC:TimeF   0.58239   1.31141 40  0.4440987
                   p-value
(Intercept)         0.0219
Temp                0.0383
GroupB              0.3071
GroupC              0.8603
TimeE               0.8636
TimeF               0.7957
Temp:GroupB         0.3063
Temp:GroupC         0.8599
Temp:TimeE          0.8586
Temp:TimeF          0.8022
GroupB:TimeE        0.4884
GroupC:TimeE        0.0849
GroupB:TimeF        0.4563
GroupC:TimeF        0.6709
Temp:GroupB:TimeE   0.4860
Temp:GroupC:TimeE   0.0819
Temp:GroupB:TimeF   0.4561
Temp:GroupC:TimeF   0.6594
 Correlation:
                   (Intr) Temp   GroupB GroupC TimeE
Temp               -1.000
GroupB             -0.868  0.868
GroupC             -0.743  0.743  0.644
TimeE              -0.500  0.500  0.434  0.372
TimeF              -0.437  0.437  0.379  0.324  0.430
Temp:GroupB         0.869 -0.869 -1.000 -0.646 -0.435
Temp:GroupC         0.743 -0.743 -0.644 -1.000 -0.372
Temp:TimeE          0.499 -0.499 -0.433 -0.370 -1.000
Temp:TimeF          0.433 -0.433 -0.376 -0.322 -0.429
GroupB:TimeE        0.440 -0.440 -0.507 -0.327 -0.880
GroupC:TimeE        0.372 -0.372 -0.322 -0.521 -0.743
GroupB:TimeF        0.387 -0.387 -0.447 -0.287 -0.381
GroupC:TimeF        0.343 -0.343 -0.298 -0.544 -0.338
Temp:GroupB:TimeE -0.439  0.439  0.505  0.326  0.881
Temp:GroupC:TimeE -0.370  0.370  0.321  0.519  0.743
Temp:GroupB:TimeF -0.384  0.384  0.443  0.285  0.380
Temp:GroupC:TimeF -0.341  0.341  0.296  0.541  0.338
                   TimeF  Tmp:GB Tmp:GC Tmp:TE Tmp:TF
Temp
GroupB
GroupC
```

```
TimeE
TimeF
Temp:GroupB        -0.379
Temp:GroupC        -0.324  0.646
Temp:TimeE         -0.430  0.434  0.371
Temp:TimeF         -1.000  0.377  0.322  0.428
GroupB:TimeE       -0.378  0.507  0.327  0.880  0.377
GroupC:TimeE       -0.320  0.323  0.521  0.743  0.319
GroupB:TimeF       -0.886  0.447  0.287  0.381  0.886
GroupC:TimeF       -0.787  0.299  0.544  0.338  0.787
Temp:GroupB:TimeE   0.378 -0.505 -0.326 -0.881 -0.377
Temp:GroupC:TimeE   0.319 -0.322 -0.519 -0.743 -0.318
Temp:GroupB:TimeF   0.887 -0.443 -0.286 -0.380 -0.887
Temp:GroupC:TimeF   0.787 -0.296 -0.541 -0.337 -0.787
                   GrB:TE GrC:TE GrB:TF GrC:TF T:GB:TE
Temp
GroupB
GroupC
TimeE
TimeF
Temp:GroupB
Temp:GroupC
Temp:TimeE
Temp:TimeF
GroupB:TimeE
GroupC:TimeE        0.653
GroupB:TimeF        0.437  0.283
GroupC:TimeF        0.298  0.455  0.697
Temp:GroupB:TimeE -1.000 -0.654 -0.436 -0.298
Temp:GroupC:TimeE -0.653 -1.000 -0.283 -0.455  0.654
Temp:GroupB:TimeF -0.435 -0.283 -1.000 -0.698  0.434
Temp:GroupC:TimeF -0.297 -0.454 -0.697 -1.000  0.297
                   T:GC:TE T:GB:TF
Temp
GroupB
GroupC
TimeE
TimeF
Temp:GroupB
Temp:GroupC
Temp:TimeE
Temp:TimeF
GroupB:TimeE
GroupC:TimeE
GroupB:TimeF
GroupC:TimeF
Temp:GroupB:TimeE
Temp:GroupC:TimeE
Temp:GroupB:TimeF   0.282
Temp:GroupC:TimeF   0.453   0.698

Standardized Within-Group Residuals:
        Min          Q1         Med          Q3
-2.98307791 -0.46071448 -0.01412714  0.49005020
        Max
 1.86554764

Number of Observations: 84
Number of Groups: 29
> shapiro.test(residuals(model_MedianP50_Temp_TG))

        Shapiro-Wilk normality test

data:  residuals(model_MedianP50_Temp_TG)
W = 0.97044, p-value = 0.05025
```

Annex V: Chapter IV Anaesthetic variable summary statistics

	Baseline			Intermediate (10 min)			Post fluid challenge (20 min)		
Variable	**Median**	**1st Quartile**	**3rd Quartile**	**Median**	**1st Quartile**	**3rd Quartile**	**Median**	**1st Quartile**	**3rd Quartile**
Lactated Ringer's group									
HR (bpm)	110.00	104.00	115.00	108.13	107.63	116.21	111.50	106.00	113.00
SpO_2 (%)	95.00	95.00	95.00	93.45	92.63	94.38	95.00	95.00	95.00
SAP (mmHg)	117.00	113.50	131.00	110.63	102.69	117.94	104.00	101.00	108.00
DAP (mmHg)	57.00	47.00	58.00	48.63	43.51	57.56	54.00	47.50	59.00
MAP (mmHg)	77.00	74.50	83.33	71.63	65.44	77.38	69.50	66.00	76.00
RR (brpm)	18.67	16.00	20.00	19.25	15.25	19.63	20.00	16.00	20.00
T (°C)	37.30	37.20	37.40	37.10	36.95	37.25	37.00	36.90	37.30
Hydroxyethyl Starch group									
HR (bpm)	130.00	111.88	140.75	127.70	113.81	136.49	130.00	109.69	134.67
SpO_2 (%)	95.25	95.00	95.88	94.90	94.00	95.50	95.42	95.08	96.63
SAP (mmHg)	113.75	111.25	119.38	114.13	105.50	118.63	114.00	106.46	117.69
DAP (mmHg)	58.25	54.63	65.13	57.50	49.84	62.13	57.75	52.13	61.38
MAP (mmHg)	76.00	73.00	84.38	76.75	69.31	80.56	75.50	71.50	79.81
RR (brpm)	19.00	18.00	20.00	18.70	18.00	19.15	20.00	19.08	20.00
T (°C)	37.53	37.40	37.85	37.43	37.13	37.59	37.23	37.05	37.42
Control group									
HR (bpm)	120.50	111.00	134.88	115.50	110.03	127.25	120.00	110.88	125.75
SpO_2 (%)	95.00	94.63	95.00	95.25	93.70	96.00	96.17	94.63	98.50
SAP (mmHg)	118.00	113.75	123.25	117.25	105.25	119.03	116.25	108.38	130.50
DAP (mmHg)	62.75	58.00	65.58	58.00	51.50	63.78	51.25	44.33	60.63
MAP (mmHg)	80.58	77.13	82.38	79.50	71.13	83.00	73.25	66.63	81.25
RR (brpm)	19.00	14.50	21.50	18.50	17.10	19.10	19.50	16.50	20.00
T (°C)	37.30	37.03	37.44	37.28	37.01	37.43	37.03	36.95	37.19

DAP – diastolic arterial pressure (in mmHg); HR – heart rate (beats per minute); MAP – mean arterial pressure (in mmHg); RR – respiratory rate (breaths per minute); SAP – systolic arterial pressure (in

mmHg) ; SpO_2 – arterial oxygen saturation using pulse oximetry (percentage); T – temperature (in degrees Celsius);

Statistical analysis for anaesthetic variables

There were no significant differences in monitoring variables (HR, SAP, DAP, MAP, Temperature, RR and SpO_2) at baseline. Systolic arterial pressure decreased significantly over time in the CRYS group (p = 0.003) compared to the control group. Diastolic arterial pressure decreased significantly over time independent of group allocation ($p < 0.001$) and was significantly lower over time in the CRYS group ($p = 0.009$) and HES group ($p = 0.017$) compared to the control group. Mean arterial pressure decreased significantly over time independent of group allocation ($p < 0.001$). Temperature decreased significantly at the end of intervention independent of group allocation ($p < 0.001$). Mean arterial pressure and temperature had no significant effects on GlycoCheck® parameters.

Annex VI: Chapter V Unformatted statistical report

Effects of transient intravascular volume overload on endothelial glycocalyx thickness in healthy anaesthetized cats

Age and Weight summary stats

Age - normality

```
> ggplot(data, aes(x = age)) +
+   geom_histogram(binwidth = 5, fill = "blue", color = "black", alpha = 0.7) +
+   labs(title = "Histogram of Age", x = "Age", y = "Frequency") +
+   theme_minimal()
> ggplot(data, aes(x = age)) +
+   geom_histogram(binwidth = 0.1, fill = "blue", color = "black", alpha = 0.7) +
+   labs(title = "Histogram of Age", x = "Age", y = "Frequency") +
+   theme_minimal()
> shapiro_test <- shapiro.test(data$age)
> print(shapiro_test)

        Shapiro-Wilk normality test

data:  data$age
W = 0.83659, p-value = 0.003204
```

Weight – normality

```
> ggplot(data, aes(x = Weight_1)) +
+   geom_histogram(binwidth = 0.5, fill = "blue", color = "black", alpha = 0.7) +
+   labs(title = "Histogram of Weight", x = "Weight", y = "Frequency") +
+   theme_minimal()
>
> shapiro_test <- shapiro.test(data$Weight_1)
> print(shapiro_test)

        Shapiro-Wilk normality test
```

```
data:  data$Weight_1
W = 0.95599, p-value = 0.4672
```

Age summary

```
> summary_stats <- data.frame(
+   Mean = mean(data$age, na.rm = TRUE),
+   Median = median(data$age, na.rm = TRUE),
+   Min = min(data$age, na.rm = TRUE),
+   Max = max(data$age, na.rm = TRUE),
+   SD = sd(data$age, na.rm = TRUE),
+   IQR = IQR(data$age, na.rm = TRUE),
+   N = sum(!is.na(data$age)) # Number of non-missing observations
+ )
>
> # Print the summary statistics
> print(summary_stats)
     Mean   Median     Min     Max     SD     IQR  N
1 4.050411 3.210959 2.438356 5.967123 1.213369 1.678767 20
```

Weight – summary

```
> summary_stats <- data.frame(
+   Mean = mean(data$Weight_1, na.rm = TRUE),
+   Median = median(data$Weight_1, na.rm = TRUE),
+   Min = min(data$Weight_1, na.rm = TRUE),
+   Max = max(data$Weight_1, na.rm = TRUE),
+   SD = sd(data$Weight_1, na.rm = TRUE),
+   IQR = IQR(data$Weight_1, na.rm = TRUE),
+   N = sum(!is.na(data$Weight_1)) # Number of non-missing observations
+ )
>
```

```
> # Print the summary statistics
> print(summary_stats)
   Mean Median   Min   Max      SD    IQR  N
1 3.77335  3.636 2.721 5.407 0.7551202 0.95775 20
```

Normality - PCV

```
> ggplot(data, aes(x = .data[[var_to_check]])) +
+   geom_histogram(binwidth = 1, fill = "skyblue", color = "black") +  # B
in width can be adjusted as needed
+   stat_function(fun = function(x) {
+     dnorm(x, mean = mean(data[[var_to_check]], na.rm = TRUE),
+           sd = sd(data[[var_to_check]], na.rm = TRUE)) *
+       length(data[[var_to_check]]) * 1  # Adjust for frequency
+   }, color = "red", size = 1) +
+   labs(title = paste("Histogram with Normal Curve for PCV", var_to_check
),
+        x = var_to_check, y = "Frequency")
> shapiro_test <- shapiro.test(data[['PCV']])
>
> # Print the result
> print(shapiro_test)
```

Shapiro-Wilk normality test

data: data[["PCV"]]

W = 0.97698, p-value = 0.00896

Look for outliers

```
> data$z_scores <- (data[['PCV']] - mean(data[['PCV']], na.rm = TRUE)) / s
d(data[['PCV']], na.rm = TRUE)
>
> # Identify potential outliers
> outliers <- data %>% filter(abs(z_scores) > 3)
> print(outliers)
# A tibble: 1 × 10
  number cat_name group group1  week timepoint1 timepoint   PCV    TS z_sc
ores
   <dbl> <chr>    <dbl> <chr>  <dbl>      <dbl> <chr>     <dbl> <dbl>    <
dbl>
1      4 Hazel        1 Fluids     2          4 T4           18    52    -
3.28
> Q1 <- quantile(data[['PCV']], 0.25, na.rm = TRUE)
> Q3 <- quantile(data[['PCV']], 0.75, na.rm = TRUE)
> IQR <- Q3 - Q1
> lower_bound <- Q1 - 1.5 * IQR
> upper_bound <- Q3 + 1.5 * IQR
>
> outlier_index <- which(data[['PCV']] < lower_bound | data[['PCV']] > upp
er_bound)
> print(outlier_index)
[1] 32
```

Hazel W2 timepoint 4 – outlier, row 32

Normality without the outlier

```
> filtered_data <- data[-32, ]
> shapiro_test_filtered <- shapiro.test(filtered_data[['PCV']])
> print(shapiro_test_filtered)

        Shapiro-Wilk normality test

data:  filtered_data[["PCV"]]
W = 0.97674, p-value = 0.008706
```

Normality - Total solids

```
> #Normality with histograms for TS
> var_to_check<-"TS"
> data<-VO_PCV_TS
>
> #Frequency
> ggplot(data, aes(x = .data[[var_to_check]])) +
+   geom_histogram(binwidth = 1, fill = "skyblue", color = "black") +  # B
in width can be adjusted as needed
+   stat_function(fun = function(x) {
+     dnorm(x, mean = mean(data[[var_to_check]], na.rm = TRUE),
+           sd = sd(data[[var_to_check]], na.rm = TRUE)) *
+       length(data[[var_to_check]]) * 1  # Adjust for frequency
+   }, color = "red", size = 1) +
+   labs(title = paste("Histogram with Normal Curve for TS", var_to_check)
,
+        x = var_to_check, y = "Frequency")
>
> shapiro_test <- shapiro.test(data[['TS']])
> print(shapiro_test)

        Shapiro-Wilk normality test

data:  data[["TS"]]
W = 0.94618, p-value = 8.584e-06
```

```
#Exclude outlier by with quinitles
> Q1 <- quantile(data[['TS']], 0.25, na.rm = TRUE)
> Q3 <- quantile(data[['TS']], 0.75, na.rm = TRUE)
> IQR <- Q3 - Q1
> lower_bound <- Q1 - 1.5 * IQR
> upper_bound <- Q3 + 1.5 * IQR
>
> #Find which row is the outlier
> outlier_index <- which(data[['TS']] < lower_bound | data[['TS']] > upper_bound)
> print(outlier_index)
 [1]   6  17  30  32  34  54 102 114 134 142 146 158
> #Exclude outlier by row
> outlier_rows <- c(6, 17, 30, 32, 34, 54, 102, 114, 134, 142, 146, 158)
>
> # Filter out these rows
> filtered_data <- data[-outlier_rows, ]
>
> # Verify the filtered dataset
> dim(filtered_data)  # Check the dimensions
[1] 148   9
> head(filtered_data)  # Preview the first few rows
# A tibble: 6 × 9
  number cat_name group group1   week timepoint1 timepoint   PCV    TS
   <dbl> <chr>    <dbl> <chr>   <dbl>      <dbl> <chr>     <dbl> <dbl>
1      1 Hermione     2 Control     1          1 T0           34    74
2      1 Hermione     2 Control     1          2 T1           32    68
3      1 Hermione     2 Control     1          3 T2           34    70
4      1 Hermione     2 Control     1          4 T4           35    70
```

```
5       1 Hermione      1 Fluids        2           1 T0            30     70
6       1 Hermione      1 Fluids        2           3 T2            30     66
```

```
> # Shapiro-Wilk test on filtered data
> shapiro_test_filtered <- shapiro.test(filtered_data[['TS']])
> print(shapiro_test_filtered)

        Shapiro-Wilk normality test

data:  filtered_data[["TS"]]
W = 0.97937, p-value = 0.02514

>
> ggplot(filtered_data, aes(x = .data[['TS']])) +
+   geom_histogram(binwidth = 1, fill = "skyblue", color = "black") +
+   stat_function(fun = function(x) {
+     dnorm(x, mean = mean(filtered_data[['TS']], na.rm = TRUE),
+           sd = sd(filtered_data[['TS']], na.rm = TRUE)) *
+       length(filtered_data[['TS']])
+   }, color = "red", size = 1) +
+   labs(title = "Histogram Without Outlier", x = "TS", y = "Frequency")
```

Interactions PCV Timepoint and Group

```
> # Ensure 'group' is a factor and set Group 2 as the reference level
> filtered_data$group <- relevel(as.factor(filtered_data$group), ref = "2")
>
> # Ensure 'timepoint' is also a factor
> filtered_data$timepoint <- as.factor(filtered_data$timepoint)
>
> # Fit the mixed-effects model with Group 2 as the control
> mixed_modelPCV <- lme(PCV ~ timepoint * group, random = ~1 | number, data = filtered_
>
> # Summarize the model
> summary(mixed_modelPCV)
Linear mixed-effects model fit by REML
  Data: filtered_data
       AIC      BIC    logLik
  719.6143 749.0307 -349.8071

Random effects:
 Formula: ~1 | number
        (Intercept) Residual
StdDev:    1.667592 2.450624

Fixed effects:  PCV ~ timepoint * group
                     Value Std.Error  DF  t-value p-value
(Intercept)        32.70000 0.6628131 121 49.33517  0.0000
timepointT1        -3.35000 0.7749555 121 -4.32283  0.0000
timepointT2         1.95000 0.7749555 121  2.51627  0.0132
timepointT4         2.20000 0.7749555 121  2.83887  0.0053
group1              0.32970 0.7861916 121  0.41937  0.6757
timepointT1:group1 -3.02414 1.2473941 121 -2.42437  0.0168
timepointT2:group1 -2.67970 1.1039263 121 -2.42743  0.0167
timepointT4:group1 -0.79530 1.1120347 121 -0.71517  0.4759
 Correlation:
                   (Intr) tmpnT1 tmpnT2 tmpnT4 group1 tmT1:1 tmT2:1
timepointT1        -0.585
timepointT2        -0.585  0.500
timepointT4        -0.585  0.500  0.500
group1             -0.576  0.493  0.493  0.493
timepointT1:group1  0.363 -0.621 -0.311 -0.311 -0.632
timepointT2:group1  0.410 -0.351 -0.702 -0.351 -0.712  0.450
timepointT4:group1  0.407 -0.348 -0.348 -0.697 -0.707  0.448  0.504

Standardized Within-Group Residuals:
```

```
        Min          Q1         Med          Q3         Max
-2.65031293 -0.58754322  0.02736642  0.66563264  2.08573876

Number of Observations: 148
Number of Groups: 20
> # Extract residuals from the model
> residuals_model <- resid(mixed_modelPCV)
>
> # Plot a histogram of residuals
> hist(residuals_model, breaks = 20, main = "Histogram of Model Residuals",
+      xlab = "Residuals", col = "skyblue", border = "black")
>
> shapiro_test <- shapiro.test(residuals_model)
> print(shapiro_test)

        Shapiro-Wilk normality test

data:  residuals_model
W = 0.9922, p-value = 0.5975
```

Interactions TS group and timepoint

```
> outlier_rows <- c(6, 17, 30, 32, 34, 54, 102, 114, 134, 142, 146, 158)
>
> # Filter out these rows
> filtered_data <- data[-outlier_rows, ]
> # Ensure 'timepoint' is also a factor
> filtered_data$timepoint <- as.factor(filtered_data$timepoint)
>
> # Fit the mixed-effects model with Group 2 as the control
> mixed_modelTS <- lme(TS ~ timepoint * group, random = ~1 | number, data
= filtered_data)
>
> # Summarize the model
> summary(mixed_modelTS)
Linear mixed-effects model fit by REML
  Data: filtered_data
       AIC      BIC    logLik
  802.6141 832.0305 -391.307

Random effects:
 Formula: ~1 | number
        (Intercept) Residual
StdDev:    2.783301 3.209345

Fixed effects:  TS ~ timepoint * group
                       Value Std.Error  DF  t-value p-value
(Intercept)         70.22611 0.9657726 121 72.71496  0.0000
timepointT1        -11.73912 1.2827437 121 -9.15157  0.0000
timepointT2         -2.62611 1.0297443 121 -2.55026  0.0120
timepointT4          0.18139 1.0448035 121  0.17361  0.8625
group2              -0.27611 1.0297443 121 -0.26814  0.7891
timepointT1:group2   9.53912 1.6356715 121  5.83193  0.0000
timepointT2:group2   5.22611 1.4458088 121  3.61466  0.0004
timepointT4:group2   0.66861 1.4565727 121  0.45903  0.6470
 Correlation:
                    (Intr) tmpnT1 tmpnT2 tmpnT4 group2 tmT1:2 tmT2:2
timepointT1         -0.443
timepointT2         -0.548  0.416
timepointT4         -0.541  0.413  0.507
group2              -0.548  0.416  0.514  0.507
timepointT1:group2   0.348 -0.784 -0.326 -0.324 -0.632
timepointT2:group2   0.391 -0.296 -0.712 -0.361 -0.712  0.450
timepointT4:group2   0.388 -0.296 -0.364 -0.717 -0.707  0.448  0.504

Standardized Within-Group Residuals:
```

```
        Min          Q1         Med          Q3         Max
-2.58499638 -0.50555661  0.03432521  0.52503178  2.65372362

Number of Observations: 148
Number of Groups: 20
>
> #Test normality of model
> # Extract residuals from the model
> residuals_model <- resid(mixed_modelTS)
>
> # Plot a histogram of residuals
> hist(residuals_model, breaks = 20, main = "Histogram of Model Residuals"
,
+      xlab = "Residuals", col = "skyblue", border = "black")
>
> shapiro_test <- shapiro.test(residuals_model)
> print(shapiro_test)

        Shapiro-Wilk normality test

data:  residuals_model
W = 0.98935, p-value = 0.323
```

Normality Glycocheck parameters

Density (VVD)

Shapiro

```
Call:
> shapiro_test <- shapiro.test(data[['density']])
>
> # Print the result
> print(shapiro_test)

Result:

     Shapiro-Wilk normality test

data:  data[["density"]]
W = 0.98877, p-value = 0.2468
```

Histogram

```
ggplot(data, aes(x = .data[[var_to_check]])) +
geom_histogram(binwidth = 1, fill = "skyblue", color = "black") +  # Bi
n width can be adjusted as needed
 stat_function(fun = function(x) {
dnorm(x, mean = mean(data[[var_to_check]], na.rm = TRUE),
sd = sd(data[[var_to_check]], na.rm = TRUE)) *
length(data[[var_to_check]]) * 1  # Adjust for frequency
 }, color = "red", linewidth = 1) +  # Updated from size to linewidth
labs(title = paste("Histogram with Normal Curve for Density", var_to_ch
eck),
 x = var_to_check, y = "Frequency")
```

rbcfilling (% RBC filling)

Shapiro

```
Call:
> shapiro_test <- shapiro.test(data[['rbcfilling']])
> print(shapiro_test)
```

```
Result:
     Shapiro-Wilk normality test
data:  data[["rbcfilling"]]
W = 0.97912, p-value = 0.01815
```

Histogram

```
Call:
> ggplot(data, aes(x = .data[[var_to_check]])) +
+   geom_histogram(binwidth = 0.05, fill = "skyblue", color = "black")
+  # Bin width can be adjusted as needed
+   stat_function(fun = function(x) {
+     dnorm(x, mean = mean(data[[var_to_check]], na.rm = TRUE),
+           sd = sd(data[[var_to_check]], na.rm = TRUE)) *
+       length(data[[var_to_check]]) * 0.05  # Adjust for frequency
+   }, color = "red", linewidth = 1) +  # Updated from size to linewidt
h
+   labs(title = paste("Histogram with Normal Curve for %RBC", var_to_c
heck),
+        x = var_to_check, y = "Frequency")
> ggplot(data, aes(x = .data[[var_to_check]])) +
+   geom_histogram(binwidth = 0.05, fill = "skyblue", color = "black")
+  # Bin width can be adjusted as needed
+   stat_function(fun = function(x) {
+     dnorm(x, mean = mean(data[[var_to_check]], na.rm = TRUE),
+           sd = sd(data[[var_to_check]], na.rm = TRUE)) *
+       length(data[[var_to_check]]) * 0.05  # Adjust for frequency
+   }, color = "red", linewidth = 0.5) +  # Updated from size to linewi
dth
+   labs(title = paste("Histogram with Normal Curve for %RBC", var_to_c
heck),
+        x = var_to_check, y = "Frequency")
>
```

prb525 (PBR 5 – 25 µm)

Shapiro

```
Call:
> var_to_check<-"prb525"
> data<-VO_combined_data
>
> #Frequency histogram
>
> #Size replaced with linewidth change bandwith and lenght to reflect v
ariable size
> ggplot(data, aes(x = .data[[var_to_check]])) +
+   geom_histogram(binwidth = 0.5, fill = "skyblue", color = "black") +
  # Bin width can be adjusted as needed
+   stat_function(fun = function(x) {
+     dnorm(x, mean = mean(data[[var_to_check]], na.rm = TRUE),
+           sd = sd(data[[var_to_check]], na.rm = TRUE)) *
+       length(data[[var_to_check]]) * 0.5  # Adjust for frequency
+   }, color = "red", linewidth = 1) +  # Updated from size to linewidt
h
+   labs(title = paste("Histogram with Normal Curve for BPR 5-25", var_
to_check),
+        x = var_to_check, y = "Frequency")
>
> #Normality Shapiro
> shapiro_test <- shapiro.test(data[['prb525']])
> # Print the result
> print(shapiro_test)

Result:
Shapiro-Wilk normality test
```

```
data:  data[["prb525"]]
W = 0.96521, p-value = 0.0005719
```

Histogram

```
Call:
> #Size replaced with linewidth change bandwith and lenght to reflect v
ariable size
> ggplot(data, aes(x = .data[[var_to_check]])) +
+   geom_histogram(binwidth = 0.05, fill = "skyblue", color = "black")
+  # Bin width can be adjusted as needed
+   stat_function(fun = function(x) {
+     dnorm(x, mean = mean(data[[var_to_check]], na.rm = TRUE),
+           sd = sd(data[[var_to_check]], na.rm = TRUE)) *
+       length(data[[var_to_check]]) * 0.05  # Adjust for frequency
+   }, color = "red", linewidth = 1) +  # Updated from size to linewidt
h
+   labs(title = paste("Histogram with Normal Curve for BPR 5-25", var_
to_check),
+        x = var_to_check, y = "Frequency")
```

Investigate for outliers

```
Call:
> Q1 <- quantile(data[['prb525']], 0.25, na.rm = TRUE)
> Q3 <- quantile(data[['prb525']], 0.75, na.rm = TRUE)
> IQR <- Q3 - Q1
> lower_bound <- Q1 - 1.5 * IQR
> upper_bound <- Q3 + 1.5 * IQR
>
> #Find which row is the outlier
> outlier_index <- which(data[['prb525']] < lower_bound | data[['prb525
']] > upper_bound)
> print(outlier_index)
[1]   9  47  72  82 111 127
> #Exclude outlier by row

Result:
[1]   9  47  72  82 111 127
```

Filter out outliers

```
> outlier_rows <- c(9, 47, 72, 82, 111, 127)

> # Filter out these rows
> filtered_data <- data[-outlier_rows, ]

Call:
> # Shapiro-Wilk test on filtered data
> shapiro_test_filtered <- shapiro.test(filtered_data[['prb525']])
> print(shapiro_test_filtered)

Result:

Shapiro-Wilk normality test

data:  filtered_data[["prb525"]]
W = 0.98437, p-value = 0.08761

> ggplot(filtered_data, aes(x = .data[['prb525']])) +
+   geom_histogram(binwidth = 0.05, fill = "skyblue", color = "black")
+
+   stat_function(fun = function(x) {
+     dnorm(x, mean = mean(filtered_data[['prb525']], na.rm = TRUE),
+           sd = sd(filtered_data[['prb525']], na.rm = TRUE)) *
```

```
+       length(filtered_data[['prb525']])*0.05
+   }, color = "red", size = 1) +
+   labs(title = "Histogram Without Outlier", x = "PBR 5-25", y = "Freq
uency")
>
```

prb59 (PBR 5 – 9 µm)

Note: Same call as before.

Shapiro

Shapiro-Wilk normality test

data: data[["prb59"]]

W = 0.96694, p-value = 0.0008544

Histogram (saved in Ivayla stats) – few outliers, some repeated from PBR 5 – 25, consider checking and excluding)

Outliers found in rows: 25 36 54 58 111 112 127

Shapiro-Wilk normality test without outliers

data: filtered_data[["prb59"]]

W = 0.99499, p-value = 0.8919

Histogram – distribution appears normal

prb1019 (PBR 10 – 19 µm)

Shapiro

Shapiro-Wilk normality test

data: data[["prb1019"]]

W = 0.97084, p-value = 0.002176

Outliers: [1]   9 47 82 127

Shapiro-Wilk normality test without outliers

data: filtered_data[["prb1019"]]

W = 0.98727, p-value = 0.1798

prb2025 (PBR 20 – 25 µm)

Shapiro-Wilk normality test

data: data[["prb2025"]]

W = 0.98165, p-value = 0.036

Outliers: [1]   2   9 18 47 80 155

Shapiro-Wilk normality test

data: filtered_data[["prb2025"]]

W = 0.98071, p-value = 0.03342

medianp50 (Median P50)

Shapiro-Wilk normality test

data: data[["medianp50"]]

W = 0.98109, p-value = 0.03093

Outliers: [1] 128 137

Shapiro-Wilk normality test – outliers removed

data: filtered_data[["medianp50"]]

W = 0.98506, p-value = 0.09579

Count_525 (Number of vascular segments between 5 – 25 µm)

Shapiro-Wilk normality test

data: data[["Count_525"]]

W = 0.97228, p-value = 0.003101

Outliers: Rows 7 21 106 109 134

Shapiro-Wilk normality test without outliers

data: filtered_data[["Count_525"]]

W = 0.98407, p-value = 0.07895

Count_59 (Number of vascular segments between 5 – 9 µm)

Shapiro-Wilk normality test

data: data[["Count_59"]]

W = 0.9092, p-value = 2.784e-08

Outliers: rows 7 23 36 62 83 89 94 106 109 134

Shapiro-Wilk normality test

data: filtered_data[["Count_59"]]

W = 0.98022, p-value = 0.03325

Note: Abnormally distributed

Count_1019 (Number of vascular segments between 10 - 19 µm)

Shapiro-Wilk normality test

data: data[["Count_1019"]]

W = 0.97237, p-value = 0.003173

Outliers: 21 62 129

Shapiro-Wilk normality test

data: filtered_data[["Count_1019"]]

W = 0.96813, p-value = 0.001293

Note: Abnormally distributed, removing outliers might have pulled the mean in the other direction

Count_2025 (Number of vascular segments between 20 - 25 µm)

Shapiro-Wilk normality test

data: data[["Count_2025"]]

W = 0.96158, p-value = 0.0002523

Outliers: 128 137

Shapiro-Wilk normality test

data: filtered_data[["Count_2025"]]

W = 0.97053, p-value = 0.002195

Note: Abnormally distributed

Density of vascular segments per mm^2

DensityInSquareMM_525

Shapiro-Wilk normality test

data: data[["DensityInSquareMM_525"]]

W = 0.98883, p-value = 0.2508

DensityInSquareMM_59

Shapiro-Wilk normality test

data: data[["DensityInSquareMM_59"]]

W = 0.98824, p-value = 0.2151

DensityInSquareMM_1019

Shapiro-Wilk normality test

data: data[["DensityInSquareMM_1019"]]

W = 0.98801, p-value = 0.2026

DensityInSquareMM_2025

Shapiro-Wilk normality test

data: data[["DensityInSquareMM_2025"]]

W = 0.94386, p-value = 7.124e-06

Outliers: 128 137

Shapiro-Wilk normality test

data: filtered_data[["DensityInSquareMM_2025"]]

W = 0.95383, p-value = 5.486e-05

Note: Abnormally distributed, possibly related to smaller sample size

Anaesthetic variables

Heart rate

Shapiro-Wilk normality test

data: data[["HR"]]

W = 0.98504, p-value = 0.09309

SAP

Shapiro-Wilk normality test

data: data[["SAP"]]

W = 0.95835, p-value = 0.0001254

Outliers: 4 17 30 44

Shapiro-Wilk normality test

data: filtered_data[["SAP"]]

W = 0.99189, p-value = 0.5422

DAP

Shapiro-Wilk normality test

data: data[["DAP"]]

W = 0.85609, p-value = 4.64e-11

Outliers: 17 32 44 74 131

Shapiro-Wilk normality test

data: filtered_data[["DAP"]]

W = 0.97783, p-value = 0.01532

MAP

Shapiro-Wilk normality test

data: data[["MAP"]]

W = 0.88068, p-value = 7.128e-10

Outliers: 4 17 32 44 74 131

Shapiro-Wilk normality test

data: filtered_data[["MAP"]]

W = 0.99083, p-value = 0.4414

Temperature

Remove NA first:

Call:

cleaned_data[[var_to_check]] <- as.numeric(as.character(cleaned_data[[var_to_check]]))

4 NA removed by coercion

Shapiro-Wilk normality test

data: cleaned_data[[var_to_check]]

W = 0.97362, p-value = 0.005088

Outliers: 11 34 41 51 52 73

Shapiro-Wilk normality test

data: filtered_data[["Temp"]]

W = 0.98145, p-value = 0.04054

Note: Summary stats without outliers for all variables exported in excel tables

Glycocheck parameters models

Time and Group interactions

1. Outliers included

```
> #Glycocheck models with outliers included
> library(nlme)
Warning message:
package ‘nlme’ was built under R version 4.3.2
> library(readxl)
Warning message:
package ‘readxl’ was built under R version 4.3.3
>
> # Read an Excel file
> # No outlier exclusion is performed in this script
>
> # --- Relevel Factors ---
> # Ensure 'Group' and 'Timepoint' are factors, and relevel 'Group' to set
 reference as "2"
> VO_combined_data$Group <- relevel(as.factor(VO_combined_data$Group), ref
 = "2")
> VO_combined_data$Timepoint <- as.factor(VO_combined_data$Timepoint)
>
```

Density - VVD

```
> # --- Density Model ---
> # Fit the Mixed-Effects Model
> mixed_model_density <- lme(density ~ Timepoint * Group, random = ~1 | ID
1, data = VO_combined_data)
>
> # Summarize the model
> summary(mixed_model_density)
Linear mixed-effects model fit by REML
  Data: VO_combined_data
       AIC      BIC    logLik
  1832.401 1862.373 -906.2005

Random effects:
 Formula: ~1 | ID1
        (Intercept) Residual
StdDev:    15.63678   100.76

Fixed effects:  density ~ Timepoint * Group
                     Value Std.Error  DF   t-value p-value
(Intercept)       466.9333  22.80032 129 20.479241  0.0000
```

```
Timepoint2        -18.1167  31.86312 129 -0.568578  0.5706
Timepoint3        -24.9000  31.86312 129 -0.781468  0.4360
Timepoint4         -4.2469  32.28818 129 -0.131531  0.8956
Group1            -13.9750  31.86312 129 -0.438595  0.6617
Timepoint2:Group1 -28.8583  45.06126 129 -0.640424  0.5230
Timepoint3:Group1   1.8452  45.36295 129  0.040676  0.9676
Timepoint4:Group1  -3.8867  45.99444 129 -0.084503  0.9328
 Correlation:
                  (Intr) Tmpnt2 Tmpnt3 Tmpnt4 Group1 Tm2:G1 Tm3:G1
Timepoint2        -0.699
Timepoint3        -0.699  0.500
Timepoint4        -0.690  0.493  0.493
Group1            -0.699  0.500  0.500  0.493
Timepoint2:Group1  0.494 -0.707 -0.354 -0.349 -0.707
Timepoint3:Group1  0.491 -0.351 -0.702 -0.347 -0.702  0.497
Timepoint4:Group1  0.484 -0.346 -0.346 -0.702 -0.693  0.490  0.487

Standardized Within-Group Residuals:
        Min          Q1         Med          Q3         Max
-2.99293378 -0.56827922 -0.01485611  0.67390426  2.40367389

Number of Observations: 156
Number of Groups: 20
>
> # Test Normality of Residuals
> residuals_density <- resid(mixed_model_density)
> hist(residuals_density, breaks = 20, main = "Histogram of Model Residual
s - Density",
+      xlab = "Residuals", col = "skyblue", border = "black")
> print(shapiro.test(residuals_density))

        Shapiro-Wilk normality test

data:  residuals_density
W = 0.98843, p-value = 0.2258
```

% RBC filling

```
> # --- RBC Filling Model ---
> mixed_model_rbcfilling <- lme(rbcfilling ~ Timepoint * Group, random = ~
1 | ID1, data = VO_combined_data)
> summary(mixed_model_rbcfilling)
Linear mixed-effects model fit by REML
  Data: VO_combined_data
        AIC       BIC   logLik
  -396.0863 -366.1141 208.0431

Random effects:
 Formula: ~1 | ID1
         (Intercept)   Residual
StdDev: 2.445572e-06 0.05475434

Fixed effects:  rbcfilling ~ Timepoint * Group
                       Value  Std.Error  DF  t-value p-value
(Intercept)        0.6254083 0.01224344 129 51.08108  0.0000
Timepoint2        -0.0287083 0.01731484 129 -1.65802  0.0997
Timepoint3        -0.0496417 0.01731484 129 -2.86700  0.0048
Timepoint4        -0.0100750 0.01754119 129 -0.57436  0.5667
Group1            -0.0251000 0.01731484 129 -1.44962  0.1496
Timepoint2:Group1  0.0152000 0.02448689 129  0.62074  0.5359
Timepoint3:Group1  0.0343684 0.02464746 129  1.39440  0.1656
Timepoint4:Group1  0.0304333 0.02498305 129  1.21816  0.2254
 Correlation:
                  (Intr) Tmpnt2 Tmpnt3 Tmpnt4 Group1 Tm2:G1 Tm3:G1
Timepoint2        -0.707
Timepoint3        -0.707  0.500
Timepoint4        -0.698  0.494  0.494
Group1            -0.707  0.500  0.500  0.494
Timepoint2:Group1  0.500 -0.707 -0.354 -0.349 -0.707
```

```
Timepoint3:Group1  0.497 -0.351 -0.703 -0.347 -0.703  0.497
Timepoint4:Group1  0.490 -0.347 -0.347 -0.702 -0.693  0.490  0.487

Standardized Within-Group Residuals:
        Min          Q1         Med          Q3         Max
-2.37488163 -0.68852984 -0.03629849  0.49448131  3.01163316

Number of Observations: 156
Number of Groups: 20
>
> residuals_rbcfilling <- resid(mixed_model_rbcfilling)
> hist(residuals_rbcfilling, breaks = 20, main = "Histogram of Model Resid
uals - RBC Filling",
+      xlab = "Residuals", col = "skyblue", border = "black")
> print(shapiro.test(residuals_rbcfilling))

        Shapiro-Wilk normality test

data:  residuals_rbcfilling
W = 0.97786, p-value = 0.01302
```

Median P50

```
> # --- Median P50 Model ---
> mixed_model_medianp50 <- lme(medianp50 ~ Timepoint * Group, random = ~1
| ID1, data = VO_combined_data)
> summary(mixed_model_medianp50)
Linear mixed-effects model fit by REML
  Data: VO_combined_data
       AIC      BIC    logLik
  536.0327 566.0048 -258.0164

Random effects:
 Formula: ~1 | ID1
        (Intercept) Residual
StdDev:    0.609075 1.188552

Fixed effects:  medianp50 ~ Timepoint * Group
                     Value Std.Error  DF   t-value p-value
(Intercept)       8.686000 0.2986326 129 29.085910  0.0000
Timepoint2        0.220500 0.3758532 129  0.586665  0.5585
Timepoint3        0.045833 0.3758532 129  0.121945  0.9031
Timepoint4       -0.416029 0.3812183 129 -1.091314  0.2772
Group1            0.420917 0.3758532 129  1.119897  0.2648
Timepoint2:Group1 -0.381417 0.5315366 129 -0.717574  0.4743
Timepoint3:Group1 -0.619370 0.5353764 129 -1.156887  0.2495
Timepoint4:Group1 -0.220011 0.5434062 129 -0.404874  0.6862
 Correlation:
                  (Intr) Tmpnt2 Tmpnt3 Tmpnt4 Group1 Tm2:G1 Tm3:G1
Timepoint2        -0.629
Timepoint3        -0.629  0.500
Timepoint4        -0.620  0.493  0.493
Group1            -0.629  0.500  0.500  0.493
Timepoint2:Group1  0.445 -0.707 -0.354 -0.349 -0.707
Timepoint3:Group1  0.442 -0.351 -0.702 -0.346 -0.702  0.496
Timepoint4:Group1  0.435 -0.346 -0.346 -0.702 -0.692  0.489  0.487

Standardized Within-Group Residuals:
       Min         Q1        Med         Q3        Max
-2.1315915 -0.5513739  0.1227832  0.4588826  2.9834159

Number of Observations: 156
Number of Groups: 20
>
> residuals_medianp50 <- resid(mixed_model_medianp50)
> hist(residuals_medianp50, breaks = 20, main = "Histogram of Model Residu
als - Median P50",
+      xlab = "Residuals", col = "skyblue", border = "black")
> print(shapiro.test(residuals_medianp50))
```

```
        Shapiro-Wilk normality test

data:  residuals_medianp50
W = 0.98446, p-value = 0.0775
```

PBR 5-25

```
> # --- PBR 5-25 Model ---
> mixed_model_prb525 <- lme(prb525 ~ Timepoint * Group, random = ~1 | ID1,
 data = VO_combined_data)
> summary(mixed_model_prb525)
Linear mixed-effects model fit by REML
  Data: VO_combined_data
        AIC       BIC   logLik
  -40.27585 -10.30372 30.13792

Random effects:
 Formula: ~1 | ID1
        (Intercept)  Residual
StdDev:   0.0234169 0.1807351

Fixed effects:  prb525 ~ Timepoint * Group
                      Value  Std.Error  DF  t-value p-value
(Intercept)        2.4842500 0.04075140 129 60.96109  0.0000
Timepoint2         0.0686667 0.05715346 129  1.20144  0.2318
Timepoint3         0.1504167 0.05715346 129  2.63180  0.0095
Timepoint4        -0.0073353 0.05791175 129 -0.12666  0.8994
Group1             0.0950000 0.05715346 129  1.66219  0.0989
Timepoint2:Group1 -0.0300833 0.08082720 129 -0.37219  0.7104
Timepoint3:Group1 -0.0920411 0.08136528 129 -1.13121  0.2601
Timepoint4:Group1 -0.1171447 0.08249122 129 -1.42009  0.1580
 Correlation:
                  (Intr) Tmpnt2 Tmpnt3 Tmpnt4 Group1 Tm2:G1 Tm3:G1
Timepoint2        -0.701
Timepoint3        -0.701  0.500
Timepoint4        -0.692  0.493  0.493
Group1            -0.701  0.500  0.500  0.493
Timepoint2:Group1  0.496 -0.707 -0.354 -0.349 -0.707
Timepoint3:Group1  0.493 -0.351 -0.702 -0.347 -0.702  0.497
Timepoint4:Group1  0.486 -0.346 -0.346 -0.702 -0.693  0.490  0.487

Standardized Within-Group Residuals:
        Min          Q1         Med          Q3         Max
-3.57752391 -0.47902690  0.05507735  0.57512708  2.91549369

Number of Observations: 156
Number of Groups: 20
>
> residuals_prb525 <- resid(mixed_model_prb525)
> hist(residuals_prb525, breaks = 20, main = "Histogram of Model Residuals
 - PBR 5-25",
+      xlab = "Residuals", col = "skyblue", border = "black")
> print(shapiro.test(residuals_prb525))

        Shapiro-Wilk normality test

data:  residuals_prb525
W = 0.96762, p-value = 0.001002
```

PBR 5-9

```
>
> # --- PBR 5-9 Model ---
> mixed_model_prb59 <- lme(prb59 ~ Timepoint * Group, random = ~1 | ID1, d
ata = VO_combined_data)
```

```
> summary(mixed_model_prb59)
Linear mixed-effects model fit by REML
  Data: VO_combined_data
        AIC       BIC   logLik
  -171.4534 -141.4813 95.72671

Random effects:
 Formula: ~1 | ID1
        (Intercept)  Residual
StdDev:   0.0189048 0.1155377

Fixed effects:  prb59 ~ Timepoint * Group
                       Value  Std.Error  DF  t-value p-value
(Intercept)        1.3361667 0.02617858 129 51.04046  0.0000
Timepoint2         0.0463333 0.03653624 129  1.26815  0.2070
Timepoint3         0.0886667 0.03653624 129  2.42681  0.0166
Timepoint4         0.0211819 0.03702456 129  0.57210  0.5682
Group1             0.0682500 0.03653624 129  1.86801  0.0640
Timepoint2:Group1 -0.0702500 0.05167004 129 -1.35959  0.1763
Timepoint3:Group1 -0.1156205 0.05201666 129 -2.22276  0.0280
Timepoint4:Group1 -0.1377854 0.05274228 129 -2.61243  0.0101
 Correlation:
                  (Intr) Tmpnt2 Tmpnt3 Tmpnt4 Group1 Tm2:G1 Tm3:G1
Timepoint2        -0.698
Timepoint3        -0.698  0.500
Timepoint4        -0.689  0.493  0.493
Group1            -0.698  0.500  0.500  0.493
Timepoint2:Group1  0.493 -0.707 -0.354 -0.349 -0.707
Timepoint3:Group1  0.490 -0.351 -0.702 -0.347 -0.702  0.497
Timepoint4:Group1  0.483 -0.346 -0.346 -0.702 -0.693  0.490  0.487

Standardized Within-Group Residuals:
        Min          Q1         Med          Q3         Max
-3.04050806 -0.51066263  0.05730926  0.55800425  3.12389782

Number of Observations: 156
Number of Groups: 20
>
> residuals_prb59 <- resid(mixed_model_prb59)
> hist(residuals_prb59, breaks = 20, main = "Histogram of Model Residuals
- PBR 5-9",
+      xlab = "Residuals", col = "skyblue", border = "black")
> print(shapiro.test(residuals_prb59))

        Shapiro-Wilk normality test

data:  residuals_prb59
W = 0.9743, p-value = 0.005159
```

PBR 10-19

```
>
> # --- PBR 10-19 Model ---
> mixed_model_prb1019 <- lme(prb1019 ~ Timepoint * Group, random = ~1 | ID
1, data = VO_combined_data)
> summary(mixed_model_prb1019)
Linear mixed-effects model fit by REML
  Data: VO_combined_data
        AIC      BIC   logLik
  -4.972156 24.99997 12.48608

Random effects:
 Formula: ~1 | ID1
        (Intercept)  Residual
StdDev: 0.004590146 0.2051904

Fixed effects:  prb1019 ~ Timepoint * Group
                       Value  Std.Error  DF  t-value p-value
(Intercept)        2.8258333 0.04589345 129 61.57378  0.0000
```

```
Timepoint2          0.0968333 0.06488691 129  1.49234  0.1381
Timepoint3          0.1750000 0.06488691 129  2.69700  0.0079
Timepoint4          0.0001329 0.06573556 129  0.00202  0.9984
Group1              0.1080000 0.06488691 129  1.66443  0.0985
Timepoint2:Group1 -0.0384167 0.09176394 129 -0.41865  0.6762
Timepoint3:Group1 -0.1083331 0.09236598 129 -1.17287  0.2430
Timepoint4:Group1 -0.1408503 0.09362430 129 -1.50442  0.1349
 Correlation:
                  (Intr) Tmpnt2 Tmpnt3 Tmpnt4 Group1 Tm2:G1 Tm3:G1
Timepoint2        -0.707
Timepoint3        -0.707  0.500
Timepoint4        -0.698  0.494  0.494
Group1            -0.707  0.500  0.500  0.494
Timepoint2:Group1  0.500 -0.707 -0.354 -0.349 -0.707
Timepoint3:Group1  0.497 -0.351 -0.702 -0.347 -0.702  0.497
Timepoint4:Group1  0.490 -0.347 -0.347 -0.702 -0.693  0.490  0.487

Standardized Within-Group Residuals:
        Min          Q1         Med          Q3         Max
-3.21927296 -0.56918640  0.06396134  0.61467095  2.61126699

Number of Observations: 156
Number of Groups: 20
>
> residuals_prb1019 <- resid(mixed_model_prb1019)
> hist(residuals_prb1019, breaks = 20, main = "Histogram of Model Residual
s - PBR 10-19",
+      xlab = "Residuals", col = "skyblue", border = "black")
> print(shapiro.test(residuals_prb1019))

        Shapiro-Wilk normality test

data:  residuals_prb1019
W = 0.97861, p-value = 0.01586
```

PBR 20-25

```
>
> # --- PBR 20-25 Model ---
> mixed_model_prb2025 <- lme(prb2025 ~ Timepoint * Group, random = ~1 | ID
1, data = VO_combined_data)
> summary(mixed_model_prb2025)
Linear mixed-effects model fit by REML
  Data: VO_combined_data
       AIC      BIC    logLik
  159.4672 189.4393 -69.7336

Random effects:
 Formula: ~1 | ID1
        (Intercept)  Residual
StdDev:  0.06590715 0.3522188

Fixed effects:  prb2025 ~ Timepoint * Group
                      Value  Std.Error  DF  t-value p-value
(Intercept)        2.9173333 0.08012548 129 36.40956  0.0000
Timepoint2         0.0651667 0.11138138 129  0.58508  0.5595
Timepoint3         0.2028333 0.11138138 129  1.82107  0.0709
Timepoint4         0.0077944 0.11287809 129  0.06905  0.9451
Group1             0.0663333 0.11138138 129  0.59555  0.5525
Timepoint2:Group1 -0.0401667 0.15751705 129 -0.25500  0.7991
Timepoint3:Group1 -0.0224101 0.15857975 129 -0.14132  0.8878
Timepoint4:Group1 -0.0157326 0.16080504 129 -0.09784  0.9222
 Correlation:
                  (Intr) Tmpnt2 Tmpnt3 Tmpnt4 Group1 Tm2:G1 Tm3:G1
Timepoint2        -0.695
Timepoint3        -0.695  0.500
Timepoint4        -0.686  0.493  0.493
Group1            -0.695  0.500  0.500  0.493
```

```
Timepoint2:Group1  0.491 -0.707 -0.354 -0.349 -0.707
Timepoint3:Group1  0.488 -0.351 -0.702 -0.347 -0.702  0.497
Timepoint4:Group1  0.481 -0.346 -0.346 -0.702 -0.693  0.490  0.487

Standardized Within-Group Residuals:
        Min          Q1         Med          Q3         Max
-2.69017494 -0.52257745  0.09269972  0.60262678  2.70291389

Number of Observations: 156
Number of Groups: 20
>
> residuals_prb2025 <- resid(mixed_model_prb2025)
> hist(residuals_prb2025, breaks = 20, main = "Histogram of Model Residual
s - PBR 20-25",
+      xlab = "Residuals", col = "skyblue", border = "black")
> print(shapiro.test(residuals_prb2025))

        Shapiro-Wilk normality test

data:  residuals_prb2025
W = 0.9846, p-value = 0.08047
```

2. Outliers excluded

Density – VVD

```
> #density
> # --- Exclude Outliers ---
> # Define the rows to exclude
> outlier_rows <- c(47, 56)
>
> # Remove the outlier rows from the dataset
> cleaned_data <- VO_combined_data[-outlier_rows, ]
>
> # --- Relevel Factors ---
> # Relevel 'Group' to set reference as "2"
> cleaned_data$Group <- relevel(as.factor(cleaned_data$Group), ref = "2")
>
> # Ensure 'Timepoint' is also a factor
> cleaned_data$Timepoint <- as.factor(cleaned_data$Timepoint)
>
> # --- Fit the Mixed-Effects Model ---
> # Fit the model with the cleaned dataset
> mixed_model <- lme(density ~ Timepoint * Group, random = ~1 | ID1, data
= cleaned_data)
>
> # Summarize the model
> summary(mixed_model)
Linear mixed-effects model fit by REML
  Data: cleaned_data
      AIC      BIC    logLik
  1793.93 1823.766 -886.9651

Random effects:
 Formula: ~1 | ID1
        (Intercept) Residual
StdDev:    23.57783 94.61211

Fixed effects:  density ~ Timepoint * Group
                     Value Std.Error  DF   t-value p-value
(Intercept)       483.7332  22.35945 127 21.634397  0.0000
Timepoint2        -34.9166  30.32692 127 -1.151339  0.2518
Timepoint3        -41.6999  30.32692 127 -1.375013  0.1715
Timepoint4        -21.5553  30.73125 127 -0.701414  0.4843
Group1            -30.7749  30.32692 127 -1.014772  0.3121
Timepoint2:Group1   0.1226  42.88745 127  0.002859  0.9977
```

```
Timepoint3:Group1  18.9708  42.88792 127  0.442335  0.6590
Timepoint4:Group1  13.5137  43.49121 127  0.310721  0.7565
 Correlation:
                  (Intr) Tmpnt2 Tmpnt3 Tmpnt4 Group1 Tm2:G1 Tm3:G1
Timepoint2        -0.696
Timepoint3        -0.696  0.513
Timepoint4        -0.687  0.507  0.507
Group1            -0.696  0.513  0.513  0.507
Timepoint2:Group1  0.492 -0.707 -0.363 -0.358 -0.707
Timepoint3:Group1  0.492 -0.363 -0.707 -0.358 -0.707  0.500
Timepoint4:Group1  0.485 -0.358 -0.358 -0.707 -0.697  0.493  0.494

Standardized Within-Group Residuals:
        Min          Q1         Med          Q3         Max
-2.62362164 -0.56845325  0.03629202  0.65403600  2.36773561

Number of Observations: 154
Number of Groups: 20
>
> # --- Test Normality of Residuals ---
> # Extract residuals from the model
> residuals_model <- resid(mixed_model)
>
> # Plot a histogram of residuals
> hist(residuals_model, breaks = 20, main = "Histogram of Model Residuals"
,
+      xlab = "Residuals", col = "skyblue", border = "black")
>
> # Perform the Shapiro-Wilk normality test
> shapiro_test <- shapiro.test(residuals_model)
> print(shapiro_test)

        Shapiro-Wilk normality test

data:  residuals_model
W = 0.99352, p-value = 0.7218
```

% RBC filling

```
> #RBC filing

>

> # --- Exclude Outliers ---

> # Define the rows to exclude

> outlier_rows <- c(9, 23, 36, 54, 113, 127)

>

> # Remove the outlier rows from the dataset

> cleaned_data <- VO_combined_data[-outlier_rows, ]

>

> # --- Relevel Factors ---

> # Relevel 'Group' to set reference as "2"

> cleaned_data$Group <- relevel(as.factor(cleaned_data$Group), ref = "2")

>

> # Ensure 'Timepoint' is also a factor

> cleaned_data$Timepoint <- as.factor(cleaned_data$Timepoint)

>
```

```
> # --- Fit the Mixed-Effects Model ---
> # Fit the model with the cleaned dataset
> mixed_model <- lme(rbcfilling ~ Timepoint * Group, random = ~1 | ID1,
data = cleaned_data)
>
> # Summarize the model
> summary(mixed_model)
Linear mixed-effects model fit by REML
  Data: cleaned_data
       AIC       BIC   logLik
  -422.734 -393.1757 221.367

Random effects:
 Formula: ~1 | ID1
        (Intercept)   Residual
StdDev:  0.00743106 0.04632137

Fixed effects:  rbcfilling ~ Timepoint * Group
                       Value  Std.Error  DF  t-value p-value
(Intercept)        0.6112066 0.01105579 123 55.28383  0.0000
Timepoint2        -0.0145066 0.01505832 123 -0.96336  0.3373
Timepoint3        -0.0443816 0.01524963 123 -2.91034  0.0043
Timepoint4         0.0040721 0.01524963 123  0.26703  0.7899
Group1            -0.0196197 0.01524963 123 -1.28657  0.2007
Timepoint2:Group1  0.0097197 0.02114517 123  0.45967  0.6466
Timepoint3:Group1  0.0451480 0.02157286 123  2.09282  0.0384
Timepoint4:Group1  0.0173114 0.02173865 123  0.79634  0.4274
 Correlation:
                  (Intr) Tmpnt2 Tmpnt3 Tmpnt4 Group1 Tm2:G1 Tm3:G1
Timepoint2        -0.718
Timepoint3        -0.709  0.520
Timepoint4        -0.709  0.520  0.514
Group1            -0.709  0.520  0.514  0.514
Timepoint2:Group1  0.511 -0.712 -0.371 -0.371 -0.721
Timepoint3:Group1  0.502 -0.368 -0.707 -0.364 -0.707  0.510
Timepoint4:Group1  0.498 -0.365 -0.361 -0.702 -0.702  0.506  0.497

Standardized Within-Group Residuals:
```

```
        Min          Q1         Med          Q3         Max
-2.20237621 -0.68930964 -0.02002747  0.60310662  2.52502933


Number of Observations: 150

Number of Groups: 20

>

> # --- Test Normality of Residuals ---

> # Extract residuals from the model

> residuals_model <- resid(mixed_model)

>

> # Plot a histogram of residuals

> hist(residuals_model, breaks = 20, main = "Histogram of Model Residuals
RBC filling",

+      xlab = "Residuals", col = "skyblue", border = "black")

>

> # Perform the Shapiro-Wilk normality test

> shapiro_test <- shapiro.test(residuals_model)

> print(shapiro_test)


      Shapiro-Wilk normality test


data:  residuals_model

W = 0.99218, p-value = 0.5843
```

Median P50

```
> #Median P50
> # --- Exclude Outliers ---
> # Define the rows to exclude
> outlier_rows <- c(128, 137)
>
> # Remove the outlier rows from the dataset
> cleaned_data <- VO_combined_data[-outlier_rows, ]
>
> # --- Relevel Factors ---
> # Relevel 'Group' to set reference as "2"
> cleaned_data$Group <- relevel(as.factor(cleaned_data$Group), ref = "2")
>
> # Ensure 'Timepoint' is also a factor
> cleaned_data$Timepoint <- as.factor(cleaned_data$Timepoint)
>
> # --- Fit the Mixed-Effects Model ---
> # Fit the model with the cleaned dataset
> mixed_model <- lme(medianp50 ~ Timepoint * Group, random = ~1 | ID1, dat
a = cleaned_data)
>
> # Summarize the model
> summary(mixed_model)
```

```
Linear mixed-effects model fit by REML
  Data: cleaned_data
       AIC      BIC    logLik
  512.4334 542.2695 -246.2167

Random effects:
 Formula: ~1 | ID1
        (Intercept) Residual
StdDev:   0.5489017 1.126412

Fixed effects:  medianp50 ~ Timepoint * Group
                     Value Std.Error  DF   t-value p-value
(Intercept)       8.686000 0.2801873 127 31.000695  0.0000
Timepoint2        0.012855 0.3613616 127  0.035574  0.9717
Timepoint3        0.045833 0.3562029 127  0.128672  0.8978
Timepoint4       -0.415156 0.3612724 127 -1.149149  0.2527
Group1            0.245390 0.3612724 127  0.679239  0.4982
Timepoint2:Group1 0.001754 0.5109389 127  0.003434  0.9973
Timepoint3:Group1 -0.464860 0.5110199 127 -0.909671  0.3647
Timepoint4:Group1 -0.066179 0.5185591 127 -0.127621  0.8987
 Correlation:
                  (Intr) Tmpnt2 Tmpnt3 Tmpnt4 Group1 Tm2:G1 Tm3:G1
Timepoint2        -0.627
Timepoint3        -0.636  0.493
Timepoint4        -0.627  0.486  0.493
Group1            -0.627  0.486  0.493  0.486
Timepoint2:Group1  0.443 -0.707 -0.349 -0.343 -0.707
Timepoint3:Group1  0.443 -0.341 -0.697 -0.344 -0.707  0.498
Timepoint4:Group1  0.437 -0.336 -0.343 -0.697 -0.697  0.491  0.494

Standardized Within-Group Residuals:
       Min         Q1        Med         Q3        Max
-2.2925009 -0.5807530  0.1936139  0.5692274  2.2519531

Number of Observations: 154
Number of Groups: 20
>
> # --- Test Normality of Residuals ---
> # Extract residuals from the model
> residuals_model <- resid(mixed_model)
>
> # Plot a histogram of residuals
> hist(residuals_model, breaks = 20, main = "Histogram of Model Residuals
Median P50",
+      xlab = "Residuals", col = "skyblue", border = "black")
>
> # Perform the Shapiro-Wilk normality test
> shapiro_test <- shapiro.test(residuals_model)
> print(shapiro_test)

        Shapiro-Wilk normality test

data:  residuals_model
W = 0.98471, p-value = 0.08704
```

PBR 5 – 25

```
> #PBR 5-25
> # --- Exclude Outliers ---
> # Define the rows to exclude
> outlier_rows <- c(9, 47, 72, 82, 111, 127)
>
> # Remove the outlier rows from the dataset
> cleaned_data <- VO_combined_data[-outlier_rows, ]
>
> # --- Relevel Factors ---
> # Relevel 'Group' to set reference as "2"
```

```
> cleaned_data$Group <- relevel(as.factor(cleaned_data$Group), ref = "2")
>
> # Ensure 'Timepoint' is also a factor
> cleaned_data$Timepoint <- as.factor(cleaned_data$Timepoint)
>
> # --- Fit the Mixed-Effects Model ---
> # Fit the model with the cleaned dataset
> mixed_model <- lme(prb525 ~ Timepoint * Group, random = ~1 | ID1, data =
 cleaned_data)
>
> # Summarize the model
> summary(mixed_model)
Linear mixed-effects model fit by REML
  Data: cleaned_data
        AIC       BIC   logLik
  -92.08223 -62.52396 56.04111

Random effects:
 Formula: ~1 | ID1
        (Intercept)  Residual
StdDev:  0.04429173 0.1449313

Fixed effects:  prb525 ~ Timepoint * Group
                       Value  Std.Error  DF  t-value p-value
(Intercept)        2.5343619 0.03566565 123 71.05890  0.0000
Timepoint2         0.0450551 0.04778467 123  0.94288  0.3476
Timepoint3         0.1003047 0.04716148 123  2.12684  0.0354
Timepoint4        -0.0298586 0.04846786 123 -0.61605  0.5390
Group1             0.0529769 0.04846786 123  1.09303  0.2765
Timepoint2:Group1 -0.0145606 0.06714234 123 -0.21686  0.8287
Timepoint3:Group1 -0.0507174 0.06720350 123 -0.75468  0.4519
Timepoint4:Group1 -0.1036491 0.06860505 123 -1.51081  0.1334
 Correlation:
                  (Intr) Tmpnt2 Tmpnt3 Tmpnt4 Group1 Tm2:G1 Tm3:G1
Timepoint2        -0.689
Timepoint3        -0.698  0.521
Timepoint4        -0.680  0.507  0.514
Group1            -0.680  0.507  0.514  0.500
Timepoint2:Group1  0.491 -0.712 -0.371 -0.361 -0.722
Timepoint3:Group1  0.492 -0.367 -0.703 -0.362 -0.722  0.522
Timepoint4:Group1  0.482 -0.360 -0.364 -0.708 -0.708  0.511  0.512

Standardized Within-Group Residuals:
        Min          Q1         Med          Q3         Max
-2.69356837 -0.62498159  0.02852801  0.60741887  2.10199092

Number of Observations: 150
Number of Groups: 20
>
> # --- Test Normality of Residuals ---
> # Extract residuals from the model
> residuals_model <- resid(mixed_model)
>
> # Plot a histogram of residuals
> hist(residuals_model, breaks = 20, main = "Histogram of Model Residuals
PBR 5-25",
+      xlab = "Residuals", col = "skyblue", border = "black")
>
> # Perform the Shapiro-Wilk normality test
> shapiro_test <- shapiro.test(residuals_model)
> print(shapiro_test)

        Shapiro-Wilk normality test

data:  residuals_model
W = 0.99091, p-value = 0.4496
```

PBR 5-9

```
> #PBR 5-9
> # --- Exclude Outliers ---
> # Define the rows to exclude
> outlier_rows <- c(25, 26, 58, 111, 112, 127)
>
> # Remove the outlier rows from the dataset
> cleaned_data <- VO_combined_data[-outlier_rows, ]
>
> # --- Relevel Factors ---
> # Relevel 'Group' to set reference as "2"
> cleaned_data$Group <- relevel(as.factor(cleaned_data$Group), ref = "2")
>
> # Ensure 'Timepoint' is also a factor
> cleaned_data$Timepoint <- as.factor(cleaned_data$Timepoint)
>
> # --- Fit the Mixed-Effects Model ---
> # Fit the model with the cleaned dataset
> mixed_model <- lme(prb59 ~ Timepoint * Group, random = ~1 | ID1, data =
cleaned_data)
>
> # Summarize the model
> summary(mixed_model)
Linear mixed-effects model fit by REML
  Data: cleaned_data
        AIC       BIC   logLik
  -204.4868 -174.9285 112.2434

Random effects:
 Formula: ~1 | ID1
        (Intercept)   Residual
StdDev:  0.01968149 0.09935057

Fixed effects:  prb59 ~ Timepoint * Group
                     Value  Std.Error  DF  t-value p-value
(Intercept)        1.3389694 0.02386479 123 56.10648  0.0000
Timepoint2         0.0388067 0.03269269 123  1.18701  0.2375
Timepoint3         0.0858640 0.03230614 123  2.65782  0.0089
Timepoint4         0.0186063 0.03272089 123  0.56864  0.5706
Group1             0.0464825 0.03272138 123  1.42055  0.1580
Timepoint2:Group1 -0.0278418 0.04591095 123 -0.60643  0.5453
Timepoint3:Group1 -0.0934016 0.04567677 123 -2.04484  0.0430
Timepoint4:Group1 -0.0980645 0.04667672 123 -2.10093  0.0377
 Correlation:
                  (Intr) Tmpnt2 Tmpnt3 Tmpnt4 Group1 Tm2:G1 Tm3:G1
Timepoint2        -0.704
Timepoint3        -0.714  0.520
Timepoint4        -0.705  0.514  0.521
Group1            -0.705  0.514  0.521  0.514
Timepoint2:Group1  0.501 -0.712 -0.370 -0.366 -0.711
Timepoint3:Group1  0.506 -0.368 -0.708 -0.369 -0.717  0.510
Timepoint4:Group1  0.496 -0.361 -0.366 -0.702 -0.702  0.499  0.504

Standardized Within-Group Residuals:
        Min          Q1         Med          Q3         Max
-3.63568850 -0.55419040  0.09411043  0.67114210  2.85268746

Number of Observations: 150
Number of Groups: 20
>
> # --- Test Normality of Residuals ---
> # Extract residuals from the model
> residuals_model <- resid(mixed_model)
>
> # Plot a histogram of residuals
> hist(residuals_model, breaks = 20, main = "Histogram of Model Residuals
PBR 5-9",
+      xlab = "Residuals", col = "skyblue", border = "black")
>
> # Perform the Shapiro-Wilk normality test
```

```
> shapiro_test <- shapiro.test(residuals_model)
> print(shapiro_test)

        Shapiro-Wilk normality test

data:  residuals_model
W = 0.98722, p-value = 0.184
```

PBR 10-19

```
> #PBR 10-19
> # --- Exclude Outliers ---
> # Define the rows to exclude
> outlier_rows <- c(9, 47, 82, 127)
>
> # Remove the outlier rows from the dataset
> cleaned_data <- VO_combined_data[-outlier_rows, ]
>
> # --- Relevel Factors ---
> # Relevel 'Group' to set reference as "2"
> cleaned_data$Group <- relevel(as.factor(cleaned_data$Group), ref = "2")
>
> # Ensure 'Timepoint' is also a factor
> cleaned_data$Timepoint <- as.factor(cleaned_data$Timepoint)
>
> # --- Fit the Mixed-Effects Model ---
> # Fit the model with the cleaned dataset
> mixed_model <- lme(prb525 ~ Timepoint * Group, random = ~1 | ID1, data =
 cleaned_data)
>
> # Summarize the model
> summary(mixed_model)
Linear mixed-effects model fit by REML
  Data: cleaned_data
       AIC       BIC   logLik
  -74.227 -44.52887 47.1135

Random effects:
 Formula: ~1 | ID1
        (Intercept)  Residual
StdDev:  0.03193331 0.1579199

Fixed effects:  prb525 ~ Timepoint * Group
                       Value  Std.Error  DF  t-value p-value
(Intercept)        2.5353681 0.03796076 125 66.78918  0.0000
Timepoint2         0.0175485 0.05135141 125  0.34173  0.7331
Timepoint3         0.0992985 0.05135141 125  1.93371  0.0554
Timepoint4        -0.0313859 0.05273486 125 -0.59516  0.5528
Group1             0.0789034 0.05201130 125  1.51704  0.1318
Timepoint2:Group1 -0.0139867 0.07210441 125 -0.19398  0.8465
Timepoint3:Group1 -0.0760279 0.07260580 125 -1.04713  0.2971
Timepoint4:Group1 -0.1283429 0.07410394 125 -1.73193  0.0858
 Correlation:
                  (Intr) Tmpnt2 Tmpnt3 Tmpnt4 Group1 Tm2:G1 Tm3:G1
Timepoint2        -0.713
Timepoint3        -0.713  0.527
Timepoint4        -0.695  0.513  0.513
Group1            -0.704  0.521  0.521  0.507
Timepoint2:Group1  0.508 -0.712 -0.375 -0.366 -0.721
Timepoint3:Group1  0.505 -0.373 -0.708 -0.364 -0.717  0.517
Timepoint4:Group1  0.495 -0.366 -0.366 -0.712 -0.703  0.507  0.504

Standardized Within-Group Residuals:
        Min          Q1         Med          Q3         Max
-2.93093660 -0.57748996  0.07355337  0.57202212  3.06513513

Number of Observations: 152
Number of Groups: 20
>
```

```
> # --- Test Normality of Residuals ---
> # Extract residuals from the model
> residuals_model <- resid(mixed_model)
>
> # Plot a histogram of residuals
> hist(residuals_model, breaks = 20, main = "Histogram of Model Residuals
PBR 10-19",
+      xlab = "Residuals", col = "skyblue", border = "black")
>
> # Perform the Shapiro-Wilk normality test
> shapiro_test <- shapiro.test(residuals_model)
> print(shapiro_test)

        Shapiro-Wilk normality test

data:  residuals_model
W = 0.99207, p-value = 0.5617
```

PBR 20-25

```
> #PBR 20-25
> # --- Exclude Outliers ---
> # Define the rows to exclude
> outlier_rows <- c(2, 9, 18, 47, 80, 155)
>
> # Remove the outlier rows from the dataset
> cleaned_data <- VO_combined_data[-outlier_rows, ]
>
> # --- Relevel Factors ---
> # Relevel 'Group' to set reference as "2"
> cleaned_data$Group <- relevel(as.factor(cleaned_data$Group), ref = "2")
>
> # Ensure 'Timepoint' is also a factor
> cleaned_data$Timepoint <- as.factor(cleaned_data$Timepoint)
>
> # --- Fit the Mixed-Effects Model ---
> # Fit the model with the cleaned dataset
> mixed_model <- lme(prb2025 ~ Timepoint * Group, random = ~1 | ID1, data
= cleaned_data)
>
> # Summarize the model
> summary(mixed_model)
Linear mixed-effects model fit by REML
  Data: cleaned_data
      AIC      BIC    logLik
  119.681 149.2392 -49.84049

Random effects:
 Formula: ~1 | ID1
        (Intercept)  Residual
StdDev:  0.06244765 0.3109527

Fixed effects:  prb2025 ~ Timepoint * Group
                       Value  Std.Error  DF  t-value p-value
(Intercept)        2.9580091 0.07274631 123 40.66198  0.0000
Timepoint2         0.0147643 0.10240863 123  0.14417  0.8856
Timepoint3         0.1621576 0.09965750 123  1.62715  0.1063
Timepoint4        -0.0329484 0.10096998 123 -0.32632  0.7447
Group1             0.0770296 0.10096998 123  0.76290  0.4470
Timepoint2:Group1  0.0090123 0.14381399 123  0.06267  0.9501
Timepoint3:Group1 -0.0713652 0.14289312 123 -0.49943  0.6184
Timepoint4:Group1 -0.0269702 0.14381499 123 -0.18753  0.8516
 Correlation:
                  (Intr) Tmpnt2 Tmpnt3 Tmpnt4 Group1 Tm2:G1 Tm3:G1
Timepoint2        -0.684
Timepoint3        -0.703  0.500
Timepoint4        -0.694  0.493  0.507
```

```
Group1            -0.694  0.493  0.507  0.500
Timepoint2:Group1  0.487 -0.712 -0.356 -0.351 -0.702
Timepoint3:Group1  0.490 -0.348 -0.697 -0.353 -0.707  0.496
Timepoint4:Group1  0.487 -0.346 -0.356 -0.702 -0.702  0.493  0.497

Standardized Within-Group Residuals:
       Min         Q1        Med         Q3        Max
-2.4892418 -0.5591579  0.1000045  0.5902624  2.2719072

Number of Observations: 150
Number of Groups: 20
>
> # --- Test Normality of Residuals ---
> # Extract residuals from the model
> residuals_model <- resid(mixed_model)
>
> # Plot a histogram of residuals
> hist(residuals_model, breaks = 20, main = "Histogram of Model Residuals
PBR 20-25",
+      xlab = "Residuals", col = "skyblue", border = "black")
>
> # Perform the Shapiro-Wilk normality test
> shapiro_test <- shapiro.test(residuals_model)
> print(shapiro_test)

        Shapiro-Wilk normality test

data:  residuals_model
W = 0.98657, p-value = 0.1557
```

Conclusion ➔ The model with outliers excluded has a better fit.

Counts of vascular segments per size analysis

```
> #Counts
> # Plot histograms for each variable
> par(mfrow = c(1, 3))  # Arrange plots in one row
> hist(VO_combined_data$Count_59, main = "Histogram of Count_59", xlab = "
Count_59")
> hist(VO_combined_data$Count_1019, main = "Histogram of Count_1019", xlab
 = "Count_1019")
> hist(VO_combined_data$Count_2025, main = "Histogram of Count_2025", xlab
 = "Count_2025")
> hist(VO_combined_data$Count_2025, main = "Histogram of Count_525", xlab
= "Count_525")
>
> #Q-Q plots
> qqnorm(VO_combined_data$Count_59); qqline(VO_combined_data$Count_59)
> qqnorm(VO_combined_data$Count_1019); qqline(VO_combined_data$Count_1019)
> qqnorm(VO_combined_data$Count_2025); qqline(VO_combined_data$Count_2025)
> qqnorm(VO_combined_data$Count_525); qqline(VO_combined_data$Count_525)
> # Perform Friedman test (requires wide format)
> friedman_results <- friedman.test(as.matrix(VO_combined_data[, c("Count_
59", "Count_1019", "Count_2025")]))
>
> # Display results
> print(friedman_results)

        Friedman rank sum test

data:  as.matrix(VO_combined_data[, c("Count_59", "Count_1019", "Count_202
5")])
Friedman chi-squared = 263.54, df = 2, p-value < 2.2e-16

> # Combine data into a long format for pairwise comparison
```

```
> long_counts <- data.frame(
+   Counts = c(VO_combined_data$Count_59, VO_combined_data$Count_1019, VO_
combined_data$Count_2025),
+   Group = rep(c("Count_59", "Count_1019", "Count_2025"), each = nrow(VO_
combined_data))
+ )
>
> # Perform pairwise Wilcoxon signed-rank test
> pairwise_results <- pairwise.wilcox.test(
+   x = long_counts$Counts,
+   g = long_counts$Group,
+   paired = TRUE,
+   p.adjust.method = "bonferroni"  # Adjust for multiple comparisons
+ )
>
> # Print the results
> print(pairwise_results)

        Pairwise comparisons using Wilcoxon signed rank test with continuit
y correction

data:  long_counts$Counts and long_counts$Group

           Count_1019 Count_2025
Count_2025 <2e-16     -
Count_59   <2e-16     <2e-16

> # Pie Chart
> # Summarize total counts for each variable
> pie_data <- data.frame(
+   Variable = c("Count_59", "Count_1019", "Count_2025"),
+   Total = colSums(VO_combined_data[, c("Count_59", "Count_1019", "Count_
2025")])
+ )
> ggplot(pie_data, aes(x = "", y = Total, fill = Variable)) +
+   geom_bar(stat = "identity", width = 1) +  # Create a bar chart
+   coord_polar(theta = "y") +  # Convert to pie chart
+   scale_fill_brewer(palette = "Set3") +  # Use a color palette
+   theme_void() +  # Remove axes for a clean pie chart
+   labs(
+     title = "Proportion of Counts",
+     fill = "Variable"
+   ) +
+   theme(
+     plot.title = element_text(hjust = 0.5, size = 14)
+   )
> ggplot(pie_data, aes(x = "", y = Total, fill = Variable)) +
+   geom_bar(stat = "identity", width = 1) +  # Create a bar chart
+   coord_polar(theta = "y") +  # Convert to pie chart
+   scale_fill_manual(
+     values = c("Count_59" = "navy", "Count_1019" = "red", "Count_2025" =
 "yellow")
+   ) +  # Assign custom colors
+   theme_void() +  # Remove axes for a clean pie chart
+   labs(
+     title = "Proportion of Counts",
+     fill = "Variable"
+   ) +
+   theme(
+     plot.title = element_text(hjust = 0.5, size = 14)
+   )
```

Summary Statistics for Counts

```
> #Summary stats for counts
> # Select the specific variables
> count_variables <- VO_combined_data[, c("Count_59", "Count_1019", "Count
_2025", "Count_525")]
>
```

```
> # Generate summary statistics
> summary_stats <- data.frame(
+   Variable = colnames(count_variables),
+   Mean = colMeans(count_variables, na.rm = TRUE),
+   Median = apply(count_variables, 2, median, na.rm = TRUE),
+   SD = apply(count_variables, 2, sd, na.rm = TRUE),
+   Min = apply(count_variables, 2, min, na.rm = TRUE),
+   Max = apply(count_variables, 2, max, na.rm = TRUE)
+ )
>
> # Display summary stats
> print(summary_stats)
             Variable       Mean    Median        SD      Min       Max
Count_59     Count_59  910.31923  849.3333 348.63776 233.3333 2179.0000
Count_1019 Count_1019  566.91357  587.0000 147.22510 147.6667  934.6667
Count_2025 Count_2025   42.81645   42.5000  24.77764   3.0000  131.0000
Count_525   Count_525 1520.04925 1469.6667 301.59355 750.0000 2636.6667
> # Select the specific variables
> count_variables <- VO_combined_data[, c("Count_59", "Count_1019", "Count
_2025", "Count_525")]
>
> # Generate summary statistics
> summary_stats <- data.frame(
+   Variable = colnames(count_variables),
+   Mean = colMeans(count_variables, na.rm = TRUE),
+   Median = apply(count_variables, 2, median, na.rm = TRUE),
+   SD = apply(count_variables, 2, sd, na.rm = TRUE),
+   Min = apply(count_variables, 2, min, na.rm = TRUE),
+   Max = apply(count_variables, 2, max, na.rm = TRUE),
+   IQR = apply(count_variables, 2, IQR, na.rm = TRUE)  # Calculate IQR fo
r each column
+ )
>
> # Display summary stats
> print(summary_stats)
             Variable       Mean    Median        SD      Min       Max
    IQR
Count_59     Count_59  910.31923  849.3333 348.63776 233.3333 2179.0000 34
8.75000
Count_1019 Count_1019  566.91357  587.0000 147.22510 147.6667  934.6667 17
2.83333
Count_2025 Count_2025   42.81645   42.5000  24.77764   3.0000  131.0000  3
3.83333
Count_525   Count_525 1520.04925 1469.6667 301.59355 750.0000 2636.6667 35
6.50000
> library(writexl)
Warning message:
package ‘writexl’ was built under R version 4.3.3
>
> # Write the summary statistics to an Excel file
> write_xlsx(summary_stats, "summary_statistics_counts.xlsx")
```

Density per Square MM Counts

```
> #Density per Square MM counts
> # Histograms for each variable
> par(mfrow = c(2, 2))  # Arrange plots in a 2x2 grid
> hist(VO_combined_data$DensityInSquareMM_59, main = "Histogram of Density
InSquareMM_59", xlab = "DensityInSquareMM_59")
> hist(VO_combined_data$DensityInSquareMM_1019, main = "Histogram of Densi
tyInSquareMM_1019", xlab = "DensityInSquareMM_1019")
> hist(VO_combined_data$DensityInSquareMM_2025, main = "Histogram of Densi
tyInSquareMM_2025", xlab = "DensityInSquareMM_2025")
> hist(VO_combined_data$DensityInSquareMM_525, main = "Histogram of Densit
yInSquareMM_525", xlab = "DensityInSquareMM_525")
>
> # Q-Q plots for normality
> qqnorm(VO_combined_data$DensityInSquareMM_59); qqline(VO_combined_data$D
ensityInSquareMM_59)
```

```
> qqnorm(VO_combined_data$DensityInSquareMM_1019); qqline(VO_combined_data
$DensityInSquareMM_1019)
> qqnorm(VO_combined_data$DensityInSquareMM_2025); qqline(VO_combined_data
$DensityInSquareMM_2025)
> qqnorm(VO_combined_data$DensityInSquareMM_525); qqline(VO_combined_data$
DensityInSquareMM_525)
>
> # Perform Friedman test (requires wide format)
> friedman_results <- friedman.test(as.matrix(VO_combined_data[, c("Densit
yInSquareMM_59", "DensityInSquareMM_1019", "DensityInSquareMM_2025")]))
>
> # Display results
> print(friedman_results)

        Friedman rank sum test

data:  as.matrix(VO_combined_data[, c("DensityInSquareMM_59", "DensityInSq
uareMM_1019", "DensityInSquareMM_2025")])
Friedman chi-squared = 262.32, df = 2, p-value < 2.2e-16

>
> # Post-hoc analysis using Wilcoxon signed-rank test
> # Combine data into a long format for pairwise comparison
> long_densities <- data.frame(
+   Densities = c(VO_combined_data$DensityInSquareMM_59, VO_combined_data$
DensityInSquareMM_1019, VO_combined_data$DensityInSquareMM_2025),
+   Group = rep(c("DensityInSquareMM_59", "DensityInSquareMM_1019", "Densi
tyInSquareMM_2025"), each = nrow(VO_combined_data))
+ )
>
> # Perform pairwise Wilcoxon signed-rank test
> pairwise_results <- pairwise.wilcox.test(
+   x = long_densities$Densities,
+   g = long_densities$Group,
+   paired = TRUE,
+   p.adjust.method = "bonferroni"  # Adjust for multiple comparisons
+ )
>
> # Print the results
> print(pairwise_results)

        Pairwise comparisons using Wilcoxon signed rank test with continuit
y correction

data:  long_densities$Densities and long_densities$Group

                        DensityInSquareMM_1019 DensityInSquareMM_2025
DensityInSquareMM_2025 <2e-16                 -
DensityInSquareMM_59   <2e-16                 <2e-16

P value adjustment method: bonferroni

# Create the pie chart
ggplot(pie_data, aes(x = "", y = Total, fill = Variable)) +
  geom_bar(stat = "identity", width = 1) +  # Create a bar chart
  coord_polar(theta = "y") +  # Convert to pie chart
  scale_fill_manual(
    values = c(
      "DensityInSquareMM_59" = "navy",
      "DensityInSquareMM_1019" = "red",
      "DensityInSquareMM_2025" = "yellow"
    )
  ) +  # Assign custom colors
  theme_void() +  # Remove axes for a clean pie chart
  labs(
    title = "Proportion of Densities",
    fill = "Variable"
  ) +
  theme(
```

```
    plot.title = element_text(hjust = 0.5, size = 14)
  )

> #Density in Square MM Summary Stats
> # Select the specific variables
> density_variables <- VO_combined_data[, c("DensityInSquareMM_59", "Densi
tyInSquareMM_1019", "DensityInSquareMM_2025", "DensityInSquareMM_525")]
>
> # Generate summary statistics
> summary_stats <- data.frame(
+   Variable = colnames(density_variables),
+   Mean = colMeans(density_variables, na.rm = TRUE),
+   Median = apply(density_variables, 2, median, na.rm = TRUE),
+   SD = apply(density_variables, 2, sd, na.rm = TRUE),
+   Min = apply(density_variables, 2, min, na.rm = TRUE),
+   Max = apply(density_variables, 2, max, na.rm = TRUE),
+   IQR = apply(density_variables, 2, IQR, na.rm = TRUE)  # Calculate IQR
for each column
+ )
>
> # Display summary stats
> print(summary_stats)
                                    Variable     Mean   Median        SD
        Min      Max       IQR
DensityInSquareMM_59     DensityInSquareMM_59 252.9094 244.8333 83.170562
 64.6666667 465.0000 107.75000
DensityInSquareMM_1019 DensityInSquareMM_1019 167.4147 168.5000 59.096288
 38.3333333 316.3333  83.79167
DensityInSquareMM_2025 DensityInSquareMM_2025  13.1515  12.5000  8.774309
  0.6666667  45.0000  12.75000
DensityInSquareMM_525   DensityInSquareMM_525 433.4756 429.8333 98.070538
164.3333333 657.6667 123.16667
> library(writexl)
>
> # Write the summary statistics to an Excel file
> write_xlsx(summary_stats, "summary_statistics_DensityInSqMM.xlsx")
```

Effects of PCV on Glycocheck parameters

```
> #density
> # --- Exclude Outliers ---
> # Define the rows to exclude
> outlier_density<-c(47,56)
>
> # Create a copy of the dataset for cleaning
> cleaned_data <- VO_combined_data
>
> # Remove outliers from Density
> cleaned_data$density[outlier_density] <- NA
>
> # Remove rows with NA values only in the variables used for the model
> final_data <- na.omit(cleaned_data[, c("PCV", "density", "Group", "Timep
oint", "ID1")])
>
> # --- Relevel Factors ---
> # Relevel 'Group' to set reference as "2"
> final_data$Group <- relevel(as.factor(final_data$Group), ref = "2")
>
> # Ensure 'Timepoint' is also a factor
> final_data$Timepoint <- as.factor(final_data$Timepoint)
>
> # --- Fit the Mixed-Effects Model ---
> # Fit the model with the cleaned dataset
> mixed_model <- lme(density ~ PCV, random = ~1 | ID1, data = final_data)
>
> # Summarize the model
> summary(mixed_model)
Linear mixed-effects model fit by REML
```

```
  Data: final_data
       AIC      BIC    logLik
  1835.689 1847.785 -913.8446

Random effects:
 Formula: ~1 | ID1
        (Intercept) Residual
StdDev:    14.96297 93.65748

Fixed effects:  density ~ PCV
                Value Std.Error  DF  t-value p-value
(Intercept) 284.68235  60.31984 133 4.719547  0.0000
PCV           5.08395   1.86187 133 2.730561  0.0072
 Correlation:
    (Intr)
PCV -0.991

Standardized Within-Group Residuals:
        Min          Q1         Med          Q3         Max
-2.75943523 -0.57442444  0.03573541  0.61957456  2.52604940

Number of Observations: 154
Number of Groups: 20
>
> # --- Test Normality of Residuals ---
> # Extract residuals from the model
> residuals_model <- resid(mixed_model)
>
> # Plot a histogram of residuals
> hist(residuals_model, breaks = 20, main = "Histogram of Model Residuals:
 Density PCV-TS",
+      xlab = "Residuals", col = "skyblue", border = "black")
>
> # Perform the Shapiro-Wilk normality test
> shapiro_test <- shapiro.test(residuals_model)
> print(shapiro_test)

        Shapiro-Wilk normality test

data:  residuals_model
W = 0.99199, p-value = 0.5434

> #RBC filling
> # --- Exclude Outliers ---
> # Define the rows to exclude
> outlier_rbcfilling<-c(9, 23, 36, 54, 113, 127)
>
> # Create a copy of the dataset for cleaning
> cleaned_data <- VO_combined_data
>
> # Remove outliers from Density
> cleaned_data$rbcfilling[outlier_rbcfilling] <- NA
>
> # Remove rows with NA values only in the variables used for the model
> final_data <- na.omit(cleaned_data[, c("PCV", "TS", "rbcfilling", "Group
", "Timepoint", "ID1")])
>
> # --- Relevel Factors ---
> # Relevel 'Group' to set reference as "2"
> final_data$Group <- relevel(as.factor(final_data$Group), ref = "2")
>
> # Ensure 'Timepoint' is also a factor
> final_data$Timepoint <- as.factor(final_data$Timepoint)
>
> # --- Fit the Mixed-Effects Model ---
> # Fit the model with the cleaned dataset
> mixed_model <- lme(rbcfilling ~ PCV, random = ~1 | ID1, data = final_dat
a)
>
```

```
> # Summarize the model
> summary(mixed_model)
Linear mixed-effects model fit by REML
  Data: final_data
        AIC       BIC   logLik
  -462.2844 -450.2956 235.1422

Random effects:
 Formula: ~1 | ID1
         (Intercept)   Residual
StdDev: 1.691375e-06 0.04730474

Fixed effects:  rbcfilling ~ PCV
                Value   Std.Error  DF   t-value p-value
(Intercept) 0.5178336 0.030237607 129 17.125482  0.0000
PCV         0.0024600 0.000939533 129  2.618279  0.0099
 Correlation:
    (Intr)
PCV -0.992

Standardized Within-Group Residuals:
        Min          Q1         Med          Q3         Max
-2.33970163 -0.61609189 -0.05346351  0.59485495  2.56565338

Number of Observations: 150
Number of Groups: 20
>
> # --- Test Normality of Residuals ---
> # Extract residuals from the model
> residuals_model <- resid(mixed_model)
>
> # Plot a histogram of residuals
> hist(residuals_model, breaks = 20, main = "Histogram of Model Residuals:
 RBC filling % PCV-TS",
+      xlab = "Residuals", col = "skyblue", border = "black")
>
> # Perform the Shapiro-Wilk normality test
> shapiro_test <- shapiro.test(residuals_model)
> print(shapiro_test)

        Shapiro-Wilk normality test

data:  residuals_model
W = 0.99025, p-value = 0.387

> #Median P50
> # --- Exclude Outliers ---
> # Define the rows to exclude
> outlier_medianp50<-c(128, 137)
>
> # Create a copy of the dataset for cleaning
> cleaned_data <- VO_combined_data
>
> # Remove outliers from Density
> cleaned_data$medianp50[outlier_medianp50] <- NA
>
> # Remove rows with NA values only in the variables used for the model
> final_data <- na.omit(cleaned_data[, c("PCV", "medianp50", "Group", "Tim
epoint", "ID1")])
>
> # --- Relevel Factors ---
> # Relevel 'Group' to set reference as "2"
> final_data$Group <- relevel(as.factor(final_data$Group), ref = "2")
>
> # Ensure 'Timepoint' is also a factor
> final_data$Timepoint <- as.factor(final_data$Timepoint)
>
> # --- Fit the Mixed-Effects Model ---
> # Fit the model with the cleaned dataset
```

```
> mixed_model <- lme(medianp50 ~ PCV, random = ~1 | ID1, data = final_data
)
>
> # Summarize the model
> summary(mixed_model)
Linear mixed-effects model fit by REML
  Data: final_data
       AIC      BIC    logLik
  506.0814 518.1769 -249.0407

Random effects:
 Formula: ~1 | ID1
        (Intercept) Residual
StdDev:   0.5607927 1.116367

Fixed effects:  medianp50 ~ PCV
                Value Std.Error  DF   t-value p-value
(Intercept)  9.617640 0.7561998 133 12.718385  0.0000
PCV         -0.029896 0.0230726 133 -1.295753  0.1973
 Correlation:
    (Intr)
PCV -0.979

Standardized Within-Group Residuals:
        Min          Q1         Med          Q3         Max
-2.17696100 -0.55051356  0.08406295  0.63918361  2.20570755

Number of Observations: 154
Number of Groups: 20
>
> # --- Test Normality of Residuals ---
> # Extract residuals from the model
> residuals_model <- resid(mixed_model)
>
> # Plot a histogram of residuals
> hist(residuals_model, breaks = 20, main = "Histogram of Model Residuals:
 Median P50 PCV-TS",
+      xlab = "Residuals", col = "skyblue", border = "black")
>
> # Perform the Shapiro-Wilk normality test
> shapiro_test <- shapiro.test(residuals_model)
> print(shapiro_test)

        Shapiro-Wilk normality test

data:  residuals_model
W = 0.98682, p-value = 0.1533

> #PBR 5-25
> # --- Exclude Outliers ---
> # Define the rows to exclude
> outlier_prb525<-c(9, 47, 72, 82, 111, 127)
>
> # Create a copy of the dataset for cleaning
> cleaned_data <- VO_combined_data
>
>
> # Remove outliers from Density
> cleaned_data$prb525[outlier_prb525] <- NA
>
> # Remove rows with NA values only in the variables used for the model
> final_data <- na.omit(cleaned_data[, c("PCV", "prb525", "Group", "Timepo
int", "ID1")])
>
> # --- Relevel Factors ---
> # Relevel 'Group' to set reference as "2"
> final_data$Group <- relevel(as.factor(final_data$Group), ref = "2")
>
> # Ensure 'Timepoint' is also a factor
```

```
> final_data$Timepoint <- as.factor(final_data$Timepoint)
>
> # --- Fit the Mixed-Effects Model ---
> # Fit the model with the cleaned dataset
> mixed_model <- lme(prb525 ~ PCV, random = ~1 | ID1, data = final_data)
>
> # Summarize the model
> summary(mixed_model)
Linear mixed-effects model fit by REML
  Data: final_data
        AIC       BIC   logLik
  -108.5918 -96.60297 58.29591

Random effects:
 Formula: ~1 | ID1
        (Intercept)  Residual
StdDev:  0.03559089 0.1529167

Fixed effects:  prb525 ~ PCV
                 Value  Std.Error  DF   t-value p-value
(Intercept)  2.8387788 0.10145659 129 27.980231  0.0000
PCV         -0.0083853 0.00313983 129 -2.670623  0.0085
 Correlation:
    (Intr)
PCV -0.989

Standardized Within-Group Residuals:
        Min          Q1         Med          Q3         Max
-2.47025704 -0.66968045  0.04727174  0.75739397  2.03144461

Number of Observations: 150
Number of Groups: 20
>
> # --- Test Normality of Residuals ---
> # Extract residuals from the model
> residuals_model <- resid(mixed_model)
>
> # Plot a histogram of residuals
> hist(residuals_model, breaks = 20, main = "Histogram of Model Residuals:
 PBR 5-25 PCV-TS",
+      xlab = "Residuals", col = "skyblue", border = "black")
>
> # Perform the Shapiro-Wilk normality test
> shapiro_test <- shapiro.test(residuals_model)
> print(shapiro_test)

        Shapiro-Wilk normality test

data:  residuals_model
W = 0.98106, p-value = 0.03665

> #PBR 5-9
> # --- Exclude Outliers ---
> # Define the rows to exclude
> outlier_prb59<-c(25, 26, 58, 111, 112, 127)
>
> # Create a copy of the dataset for cleaning
> cleaned_data <- VO_combined_data
>
> # Remove outliers from Density
> cleaned_data$prb59[outlier_prb59] <- NA
>
> # Remove rows with NA values only in the variables used for the model
> final_data <- na.omit(cleaned_data[, c("PCV", "prb59", "Group", "Timepoi
nt", "ID1")])
>
> # --- Relevel Factors ---
> # Relevel 'Group' to set reference as "2"
> final_data$Group <- relevel(as.factor(final_data$Group), ref = "2")
```

```
>
> # Ensure 'Timepoint' is also a factor
> final_data$Timepoint <- as.factor(final_data$Timepoint)
>
> # --- Fit the Mixed-Effects Model ---
> # Fit the model with the cleaned dataset
> mixed_model <- lme(prb59 ~ PCV, random = ~1 | ID1, data = final_data)
>
> # Summarize the model
> summary(mixed_model)
Linear mixed-effects model fit by REML
  Data: final_data
        AIC       BIC   logLik
  -229.1422 -217.1533 118.5711

Random effects:
 Formula: ~1 | ID1
        (Intercept)  Residual
StdDev:  0.01806038 0.1026155

Fixed effects:  prb59 ~ PCV
                 Value  Std.Error  DF   t-value p-value
(Intercept)  1.4673706 0.06701185 129 21.897180  0.0000
PCV         -0.0029768 0.00207290 129 -1.436046  0.1534
 Correlation:
    (Intr)
PCV -0.99

Standardized Within-Group Residuals:
       Min         Q1        Med         Q3        Max
-4.0893661 -0.5591047  0.0427982  0.6362355  2.4628011

Number of Observations: 150
Number of Groups: 20
>
> # --- Test Normality of Residuals ---
> # Extract residuals from the model
> residuals_model <- resid(mixed_model)
>
> # Plot a histogram of residuals
> hist(residuals_model, breaks = 20, main = "Histogram of Model Residuals:
 PBR 5-9 PCV-TS",
+      xlab = "Residuals", col = "skyblue", border = "black")
>
> # Perform the Shapiro-Wilk normality test
> shapiro_test <- shapiro.test(residuals_model)
> print(shapiro_test)

        Shapiro-Wilk normality test

data:  residuals_model
W = 0.98244, p-value = 0.05264

> #PBR 1019
> # --- Exclude Outliers ---
> # Define the rows to exclude
> outlier_prb1019<-c(9, 47, 82, 127)
>
> # Create a copy of the dataset for cleaning
> cleaned_data <- VO_combined_data
>
> # Remove outliers from Density
> cleaned_data$prb1019[outlier_prb1019] <- NA
>
> # Remove rows with NA values only in the variables used for the model
> final_data <- na.omit(cleaned_data[, c("PCV", "prb1019", "Group", "Timep
oint", "ID1")])
>
> # --- Relevel Factors ---
```

```
> # Relevel 'Group' to set reference as "2"
> final_data$Group <- relevel(as.factor(final_data$Group), ref = "2")
>
> # Ensure 'Timepoint' is also a factor
> final_data$Timepoint <- as.factor(final_data$Timepoint)
>
> # --- Fit the Mixed-Effects Model ---
> # Fit the model with the cleaned dataset
> mixed_model <- lme(prb1019 ~ PCV, random = ~1 | ID1, data = final_data)
>
> # Summarize the model
> summary(mixed_model)
Linear mixed-effects model fit by REML
  Data: final_data
       AIC       BIC   logLik
  -52.6061 -40.56356 30.30305

Random effects:
 Formula: ~1 | ID1
        (Intercept)  Residual
StdDev: 7.76457e-06 0.1894136

Fixed effects:  prb1019 ~ PCV
                Value  Std.Error  DF   t-value p-value
(Intercept)  3.209868 0.12120957 131 26.481965  0.0000
PCV         -0.008770 0.00376732 131 -2.328005  0.0214
 Correlation:
    (Intr)
PCV -0.992

Standardized Within-Group Residuals:
        Min          Q1         Med          Q3         Max
-2.67813931 -0.69838488  0.08007956  0.72847536  2.90134026

Number of Observations: 152
Number of Groups: 20
>
> # --- Test Normality of Residuals ---
> # Extract residuals from the model
> residuals_model <- resid(mixed_model)
>
> # Plot a histogram of residuals
> hist(residuals_model, breaks = 20, main = "Histogram of Model Residuals:
 PBR10-19 PCV-TS",
+      xlab = "Residuals", col = "skyblue", border = "black")
>
> # Perform the Shapiro-Wilk normality test
> shapiro_test <- shapiro.test(residuals_model)
> print(shapiro_test)

        Shapiro-Wilk normality test

data:  residuals_model
W = 0.99394, p-value = 0.7784

> #PBR 20-25
> # --- Exclude Outliers ---
> # Define the rows to exclude
> outlier_prb2025<-c(2, 9, 18, 47, 80, 155)
>
> # Create a copy of the dataset for cleaning
> cleaned_data <- VO_combined_data
>
> # Remove outliers from Density
> cleaned_data$prb2025[outlier_prb2025] <- NA
>
> # Remove rows with NA values only in the variables used for the model
> final_data <- na.omit(cleaned_data[, c("PCV", "prb2025", "Group", "Timep
oint", "ID1")])
```

```
>
> # --- Relevel Factors ---
> # Relevel 'Group' to set reference as "2"
> final_data$Group <- relevel(as.factor(final_data$Group), ref = "2")
>
> # Ensure 'Timepoint' is also a factor
> final_data$Timepoint <- as.factor(final_data$Timepoint)
>
> # --- Fit the Mixed-Effects Model ---
> # Fit the model with the cleaned dataset
> mixed_model <- lme(prb2025 ~ PCV, random = ~1 | ID1, data = final_data)
>
> # Summarize the model
> summary(mixed_model)
Linear mixed-effects model fit by REML
  Data: final_data
       AIC      BIC    logLik
  98.91666 110.9055 -45.45833

Random effects:
 Formula: ~1 | ID1
        (Intercept)  Residual
StdDev:  0.05010101 0.3114367

Fixed effects:  prb2025 ~ PCV
                Value  Std.Error  DF   t-value p-value
(Intercept)  3.366142 0.20066259 129 16.775133  0.0000
PCV         -0.010732 0.00619819 129 -1.731402  0.0858
 Correlation:
    (Intr)
PCV -0.99

Standardized Within-Group Residuals:
       Min         Q1        Med         Q3        Max
-2.8200816 -0.6739980  0.1364904  0.6536226  2.0935518

Number of Observations: 150
Number of Groups: 20
>
> # --- Test Normality of Residuals ---
> # Extract residuals from the model
> residuals_model <- resid(mixed_model)
>
> # Plot a histogram of residuals
> hist(residuals_model, breaks = 20, main = "Histogram of Model Residuals:
 PBR 20-25 PCV-TS",
+      xlab = "Residuals", col = "skyblue", border = "black")
>
> # Perform the Shapiro-Wilk normality test
> shapiro_test <- shapiro.test(residuals_model)
> print(shapiro_test)

        Shapiro-Wilk normality test

data:  residuals_model
W = 0.98205, p-value = 0.04755
```

Correlation between PCV and GlycoCheck parameters

```
> correlation_test<-cor.test(VO_combined_data$density, VO_combined_data$PC
V)
> print(correlation_test)

        Pearson's product-moment correlation

data:  VO_combined_data$density and VO_combined_data$PCV
t = 2.9983, df = 154, p-value = 0.003166
alternative hypothesis: true correlation is not equal to 0
```

```
95 percent confidence interval:
 0.08069321 0.37804479
sample estimates:
      cor
0.2348559


> correlation_test<-cor.test(VO_combined_data$rbcfilling, VO_combined_data
$PCV)
> print(correlation_test)

        Pearson's product-moment correlation

data:  VO_combined_data$rbcfilling and VO_combined_data$PCV
t = 3.5815, df = 154, p-value = 0.0004575
alternative hypothesis: true correlation is not equal to 0
95 percent confidence interval:
 0.1256240 0.4162922
sample estimates:
      cor
0.2772909


> correlation_test<-cor.test(VO_combined_data$density, VO_combined_data$PC
V)
> print(correlation_test)

        Pearson's product-moment correlation

data:  VO_combined_data$density and VO_combined_data$PCV
t = 2.9983, df = 154, p-value = 0.003166
alternative hypothesis: true correlation is not equal to 0
95 percent confidence interval:
 0.08069321 0.37804479
sample estimates:
      cor
0.2348559

> correlation_test<-cor.test(VO_combined_data$medianp50, VO_combined_data$
PCV)
> print(correlation_test)

        Pearson's product-moment correlation

data:  VO_combined_data$medianp50 and VO_combined_data$PCV
t = -0.87717, df = 154, p-value = 0.3818
alternative hypothesis: true correlation is not equal to 0
95 percent confidence interval:
 -0.22515432  0.08760316
sample estimates:
        cor
-0.07050821


> correlation_test<-cor.test(VO_combined_data$prb525, VO_combined_data$PCV
)
> print(correlation_test)

        Pearson's product-moment correlation

data:  VO_combined_data$prb525 and VO_combined_data$PCV
t = -3.0425, df = 154, p-value = 0.002759
alternative hypothesis: true correlation is not equal to 0
95 percent confidence interval:
 -0.3810010 -0.0841234
sample estimates:
       cor
```

```
-0.2381164

> correlation_test<-cor.test(VO_combined_data$prb59, VO_combined_data$PCV)
> print(correlation_test)

        Pearson's product-moment correlation

data:  VO_combined_data$prb59 and VO_combined_data$PCV
t = -1.2773, df = 154, p-value = 0.2034
alternative hypothesis: true correlation is not equal to 0
95 percent confidence interval:
 -0.25541769  0.05564974
sample estimates:
       cor
-0.1023864

> correlation_test<-cor.test(VO_combined_data$prb1019, VO_combined_data$PC
V)
> print(correlation_test)

        Pearson's product-moment correlation

data:  VO_combined_data$prb1019 and VO_combined_data$PCV
t = -3.2746, df = 154, p-value = 0.001307
alternative hypothesis: true correlation is not equal to 0
95 percent confidence interval:
 -0.3963883 -0.1020923
sample estimates:
       cor
-0.2551399

> correlation_test<-cor.test(VO_combined_data$prb2025, VO_combined_data$PC
V)
> print(correlation_test)

        Pearson's product-moment correlation

data:  VO_combined_data$prb2025 and VO_combined_data$PCV
t = -1.8474, df = 154, p-value = 0.06661
alternative hypothesis: true correlation is not equal to 0
95 percent confidence interval:
 -0.29749971  0.01013276
sample estimates:
       cor
-0.1472424
```

Kendall Tau – PBR 20-25 not normally distributed (Spearman's Rank not appropriate because of repeated values)

```
> correlation_test <- cor.test(VO_combined_data$prb2025, VO_combined_data$PCV, method = "kendall")

> print(correlation_test)


        Kendall's rank correlation tau


data:  VO_combined_data$prb2025 and VO_combined_data$PCV

z = -1.9801, p-value = 0.04769

alternative hypothesis: true tau is not equal to 0
```

sample estimates:

tau

-0.1108105

Annex VII: Chapter VI Unformatted statistical report

Endothelial glycocalyx thickness in cats with naturally occurring trauma or non-traumatic illness – an exploratory study

Distribution of data and summary statistics

Distribution of data (normality)

```
> variables <- c("Total_ATT", "Short_ATT", "Age_years", "Weight", "LOH",
+                "APPLE_fast",
+                "IV_fluid_challenge", "IV_fluids_rate", "IV_fluids_durati
on", "IV_fluids_total")
>
> for (var in variables) {
+   # Perform Shapiro-Wilk test
+   shapiro_test <- shapiro.test(Glycoheck_clinical_study_dataset_for_stat
s[[var]])
+
+   # Print results
+   cat("Shapiro-Wilk test for variable", var, ":\n\n")
+   print(shapiro_test)
+   cat("\n\n")
+   ggplot(Glycoheck_clinical_study_dataset_for_stats, aes_string(x = var)
) +
+     geom_histogram(binwidth = 10, fill = "blue", color = "black", alpha
= 0.7) +
+     labs(title = paste("Histogram of", var), x = var, y = "Frequency") +
+     theme_minimal() +
+     theme(plot.title = element_text(hjust = 0.5))
+ }


Shapiro-Wilk test for variable Age_years :

        Shapiro-Wilk normality test

data:  Glycoheck_clinical_study_dataset_for_stats[[var]]
W = 0.81139, p-value = 0.001284



Shapiro-Wilk test for variable Weight :

        Shapiro-Wilk normality test

data:  Glycoheck_clinical_study_dataset_for_stats[[var]]
W = 0.92006, p-value = 0.1134



Shapiro-Wilk test for variable LOH :

        Shapiro-Wilk normality test

data:  Glycoheck_clinical_study_dataset_for_stats[[var]]
W = 0.92649, p-value = 0.1492



Shapiro-Wilk test for variable APPLE_fast :

        Shapiro-Wilk normality test

data:  Glycoheck_clinical_study_dataset_for_stats[[var]]
W = 0.95194, p-value = 0.426
```

For trauma subset only

```
> shapiro_test <- shapiro.test(Glycoheck_clinical_study_trauma_dataset_for
_stats$Total_ATT)
>
> print(shapiro_test)

        Shapiro-Wilk normality test

data:  Glycoheck_clinical_study_trauma_dataset_for_stats$Total_ATT
W = 0.88213, p-value = 0.1107

> shapiro_test <- shapiro.test(Glycoheck_clinical_study_trauma_dataset_for
_stats$Short_ATT)
>
> print(shapiro_test)

        Shapiro-Wilk normality test

data:  Glycoheck_clinical_study_trauma_dataset_for_stats$Short_ATT
W = 0.94729, p-value = 0.6095
```

IV fluid variables distribution (normality) subset of IV fluids variables > 0

```
> filtered_data <- Glycoheck_clinical_study_dataset_for_stats[
+   Glycoheck_clinical_study_dataset_for_stats$IV_fluid_challenge > 0 |
+     Glycoheck_clinical_study_dataset_for_stats$IV_fluids_rate > 0 |
+     Glycoheck_clinical_study_dataset_for_stats$IV_fluids_duration > 0 |
+     Glycoheck_clinical_study_dataset_for_stats$IV_fluids_total > 0, ]
>
> iv_fluid_vars <- c("IV_fluid_challenge", "IV_fluids_rate",
"IV_fluids_duration", "IV_fluids_total")
> for (var in iv_fluid_vars) {
+   shapiro_test <- shapiro.test(filtered_data[[var]])
+   cat("Shapiro-Wilk test for variable", var, ":\n\n")
+   print(shapiro_test)
+   cat("\n\n")
+ }
Shapiro-Wilk test for variable IV_fluid_challenge :

      Shapiro-Wilk normality test

data:  filtered_data[[var]]
W = 0.7106, p-value = 0.001184


Shapiro-Wilk test for variable IV_fluids_rate :

      Shapiro-Wilk normality test

data:  filtered_data[[var]]
W = 0.82212, p-value = 0.02689
```

```
Shapiro-Wilk test for variable IV_fluids_duration :

      Shapiro-Wilk normality test

data:  filtered_data[[var]]

W = 0.9226, p-value = 0.3792


Shapiro-Wilk test for variable IV_fluids_total :

      Shapiro-Wilk normality test

data:  filtered_data[[var]]

W = 0.7628, p-value = 0.005109


> ggplot(filtered_data, aes(x = IV_fluid_challenge)) +

+   geom_histogram(binwidth = 1, fill = "blue", color = "black", alpha =
0.7) +

+   labs(title = "Histogram of IV_fluid_challenge (Filtered)", x =
"IV_fluid_challenge", y = "Frequency") +

+   theme_minimal() +

+   theme(plot.title = element_text(hjust = 0.5))

Warning message:

Removed 1 row containing non-finite outside the scale range
(`stat_bin()`).

> ggplot(filtered_data, aes(x = IV_fluids_rate)) +

+   geom_histogram(binwidth = 10, fill = "green", color = "black", alpha =
0.7) +

+   labs(title = "Histogram of IV_fluids_rate (Filtered)", x =
"IV_fluids_rate", y = "Frequency") +

+   theme_minimal() +

+   theme(plot.title = element_text(hjust = 0.5))

Warning message:

Removed 1 row containing non-finite outside the scale range
(`stat_bin()`).

> ggplot(filtered_data, aes(x = IV_fluids_duration)) +

+   geom_histogram(binwidth = 10, fill = "red", color = "black", alpha =
0.7) +

+   labs(title = "Histogram of IV_fluids_duration (Filtered)", x =
"IV_fluids_duration", y = "Frequency") +

+   theme_minimal() +

+   theme(plot.title = element_text(hjust = 0.5))

Warning message:

Removed 1 row containing non-finite outside the scale range
(`stat_bin()`).

> ggplot(filtered_data, aes(x = IV_fluids_total)) +
```

```
+   geom_histogram(binwidth = 50, fill = "purple", color = "black", alpha
= 0.7) +
+   labs(title = "Histogram of IV_fluids_total (Filtered)", x =
"IV_fluids_total", y = "Frequency") +
+   theme_minimal() +
+   theme(plot.title = element_text(hjust = 0.5))
Warning message:
Removed 1 row containing non-finite outside the scale range
(`stat_bin()`).
```

IV fluid variables summary stats

```
> library(dplyr)
> library(openxlsx)
>
> iv_fluid_vars <- c("IV_fluid_challenge", "IV_fluids_rate",
"IV_fluids_duration", "IV_fluids_total")
> summary_stats <- data.frame()
>
> for (var in iv_fluid_vars) {
+   filtered_data <- Glycoheck_clinical_study_dataset_for_stats %>%
+     filter(.data[[var]] > 0)
+   stats <- filtered_data %>%
+     summarise(
+       Variable = var,
+       Mean = mean(.data[[var]], na.rm = TRUE),
+       SD = sd(.data[[var]], na.rm = TRUE),
+       Min = min(.data[[var]], na.rm = TRUE),
+       Max = max(.data[[var]], na.rm = TRUE),
+       Median = median(.data[[var]], na.rm = TRUE),
+       IQR = IQR(.data[[var]], na.rm = TRUE)
+     )
+   summary_stats <- bind_rows(summary_stats, stats)
+ }
> print(summary_stats)
            Variable   Mean         SD Min Max Median     IQR
1 IV_fluid_challenge  48.25  27.427176  13  80     50  16.750
2     IV_fluids_rate  11.65   7.378836   4  25      9   6.625
3 IV_fluids_duration  18.70  11.898179   2  40     17   7.000
4    IV_fluids_total 221.90 190.776454  50 620    126 218.25
```

```
> write.xlsx(summary_stats, file =
"Filtered_IV_Fluids_Summary_Statistics.xlsx", row.names = FALSE)
Warning message:
Please use 'rowNames' instead of 'row.names'
> cat("Summary statistics exported to
'Filtered_IV_Fluids_Summary_Statistics.xlsx'\n")
Summary statistics exported to
'Filtered_IV_Fluids_Summary_Statistics.xlsx'


# List of IV fluid-related variables
iv_fluid_vars <- c("IV_fluid_challenge", "IV_fluids_rate",
"IV_fluids_duration", "IV_fluids_total")
summary_stats <- data.frame()


for (var in iv_fluid_vars) {
  # Filter the data where the variable is greater than 0
  filtered_data <- Glycoheck_clinical_study_dataset_for_stats %>%
    filter(.data[[var]] > 0)


  stats <- filtered_data %>%
    summarise(
      Variable = var,
      Mean = mean(.data[[var]], na.rm = TRUE),
      SD = sd(.data[[var]], na.rm = TRUE),
      Min = min(.data[[var]], na.rm = TRUE),
      Max = max(.data[[var]], na.rm = TRUE),
      Median = median(.data[[var]], na.rm = TRUE),
      Q1 = quantile(.data[[var]], 0.25, na.rm = TRUE),
      Q3 = quantile(.data[[var]], 0.75, na.rm = TRUE)
    )
  summary_stats <- bind_rows(summary_stats, stats)
}
print(summary_stats)
write.xlsx(summary_stats, file =
"Filtered_IV_Fluids_Summary_Statistics.xlsx", row.names = FALSE)
cat("Summary statistics exported to
'Filtered_IV_Fluids_Summary_Statistics.xlsx'\n")
```

GlycoCheck Variables data distribution (normality)

```
> library(ggplot2)
```

```
>
> variables <- c("VVD", "RBC_filling", "PBR525", "PBR59", "PBR1019",
"PBR2025", "Median_P50")
>
> for (var in variables) {
+   shapiro_test <-
shapiro.test(Glycoheck_clinical_study_dataset_for_stats[[var]])
+   cat("Shapiro-Wilk test for variable", var, ":\n\n")
+   print(shapiro_test)
+   cat("\n\n")
+ }
Shapiro-Wilk test for variable VVD :

      Shapiro-Wilk normality test

data:  Glycoheck_clinical_study_dataset_for_stats[[var]]
W = 0.94935, p-value = 0.3852


Shapiro-Wilk test for variable RBC_filling :

      Shapiro-Wilk normality test

data:  Glycoheck_clinical_study_dataset_for_stats[[var]]
W = 0.97286, p-value = 0.8318


Shapiro-Wilk test for variable PBR525 :

      Shapiro-Wilk normality test

data:  Glycoheck_clinical_study_dataset_for_stats[[var]]
W = 0.93572, p-value = 0.2206


Shapiro-Wilk test for variable PBR59 :

      Shapiro-Wilk normality test

data:  Glycoheck_clinical_study_dataset_for_stats[[var]]
W = 0.91309, p-value = 0.08437


Shapiro-Wilk test for variable PBR1019 :

      Shapiro-Wilk normality test

data:  Glycoheck_clinical_study_dataset_for_stats[[var]]
W = 0.96107, p-value = 0.5936


Shapiro-Wilk test for variable PBR2025 :

      Shapiro-Wilk normality test
```

```
data:  Glycoheck_clinical_study_dataset_for_stats[[var]]
W = 0.96418, p-value = 0.657


Shapiro-Wilk test for variable Median_P50 :

      Shapiro-Wilk normality test
data:  Glycoheck_clinical_study_dataset_for_stats[[var]]
W = 0.94466, p-value = 0.3193
 ggplot(Glycoheck_clinical_study_dataset_for_stats, aes(x = VVD)) +
+   geom_histogram(binwidth = 0.1, fill = "blue", color = "black", alpha =
0.7) +
+   labs(title = "Histogram of VVD", x = "VVD", y = "Frequency") +
+   theme_minimal() +
+   theme(plot.title = element_text(hjust = 0.5))
Warning message:
Removed 1 row containing non-finite outside the scale range
(`stat_bin()`).
 ggplot(Glycoheck_clinical_study_dataset_for_stats, aes(x = RBC_filling))
+
+   geom_histogram(binwidth = 0.1, fill = "green", color = "black", alpha
= 0.7) +
+   labs(title = "Histogram of RBC_filling", x = "RBC_filling", y =
"Frequency") +
+   theme_minimal() +
+   theme(plot.title = element_text(hjust = 0.5))
Warning message:
Removed 1 row containing non-finite outside the scale range
(`stat_bin()`).


> ggplot(Glycoheck_clinical_study_dataset_for_stats, aes(x = PBR525)) +
+   geom_histogram(binwidth = 0.1, fill = "red", color = "black", alpha =
0.7) +
+   labs(title = "Histogram of PBR525", x = "PBR525", y = "Frequency") +
+   theme_minimal() +
+   theme(plot.title = element_text(hjust = 0.5))
Warning message:
Removed 1 row containing non-finite outside the scale range
(`stat_bin()`).
> ggplot(Glycoheck_clinical_study_dataset_for_stats, aes(x = PBR59)) +
+   geom_histogram(binwidth = 0.1, fill = "purple", color = "black", alpha
= 0.7) +
+   labs(title = "Histogram of PBR59", x = "PBR59", y = "Frequency") +
```

```
+   theme_minimal() +
+   theme(plot.title = element_text(hjust = 0.5))
Warning message:
Removed 1 row containing non-finite outside the scale range
(`stat_bin()`).


> ggplot(Glycoheck_clinical_study_dataset_for_stats, aes(x = PBR1019)) +
+   geom_histogram(binwidth = 0.1, fill = "orange", color = "black", alpha
= 0.7) +
+   labs(title = "Histogram of PBR1019", x = "PBR1019", y = "Frequency") +
+   theme_minimal() +
+   theme(plot.title = element_text(hjust = 0.5))
Warning message:
Removed 1 row containing non-finite outside the scale range
(`stat_bin()`).
 ggplot(Glycoheck_clinical_study_dataset_for_stats, aes(x = PBR2025)) +
+   geom_histogram(binwidth = 0.1, fill = "cyan", color = "black", alpha =
0.7) +
+   labs(title = "Histogram of PBR2025", x = "PBR2025", y = "Frequency") +
+   theme_minimal() +
+   theme(plot.title = element_text(hjust = 0.5))
Warning message:
Removed 1 row containing non-finite outside the scale range
(`stat_bin()`).
 ggplot(Glycoheck_clinical_study_dataset_for_stats, aes(x = Median_P50)) +
+   geom_histogram(binwidth = 0.1, fill = "pink", color = "black", alpha =
0.7) +
+   labs(title = "Histogram of Median_P50", x = "Median_P50", y =
"Frequency") +
+   theme_minimal() +
+   theme(plot.title = element_text(hjust = 0.5))
Warning message:
Removed 1 row containing non-finite outside the scale range
(`stat_bin()`).


GlycoCheck Descriptive Stats
(Results in Excel table)


summary_fun <- function(x) {
stats <- cbind(
mean = mean(x),
```

```
sd = sd(x),
median = median(x),
 min = min(x),
 max = max(x),
Q1 = quantile(x, probs = 0.25),
Q3 = quantile(x, probs = 0.75)
 )
return(stats)
}
var_to_analyse<-c("VVD", "RBC_filling", "PBR525", "PBR59", "PBR1019",
"PBR2025", "Median_P50")
descriptive_stats <- Glycoheck_clinical_study_dataset_for_stats %>%
summarize(across(all_of(var_to_analyse), summary_fun))

View(descriptive_stats)

library(tidyr)

tidy_descriptive_stats <- descriptive_stats %>%
pivot_longer(cols = everything(),
names_to = "Variable",
values_to = "Statistics")
var_to_analyse_patient<-c("Age_years", "Weight", "LOH",
"APPLE_fast",,"Total_ATT", "Short_ATT", "IV_fluid_challenge",
"IV_fluids_rate",
"IV_fluids_duration","IV_fluids_total")
descriptive_stats <- Glycoheck_clinical_study_dataset_for_stats %>%
summarize(across(all_of(var_to_analyse_patient), summary_fun))
View(descriptive_stats_patient)
tidy_descriptive_stats_patient <- descriptive_stats_patient %>%
pivot_longer(cols = everything(),
names_to = "Variable",
values_to = "Statistics")
View(tidy_descriptive_stats_patient)

#Descriptive per group#

data<-Glycocheck_data_clinical_average_tidy
```

```
summary_fun <- function(x) {
stats <- cbind(
mean = mean(x),
sd = sd(x),
median = median(x),
 min = min(x),
max = max(x),
Q1 = quantile(x, probs = 0.25),
Q3 = quantile(x, probs = 0.75)
 )
return(stats)
}
var_to_analyse<-c("VVD", "RBC_filling", "PBR525", "PBR59", "PBR1019",
"PBR2025", "Median_P50")



descriptive_stats <- Glycoheck_clinical_study_dataset_for_stats %>%
  +     group_by(Group) %>%
  +     summarize(across(all_of(vars_to_analyse), summary_fun))
View(descriptive_stats)



library(tidyr)

tidy_descriptive_stats <- descriptive_stats %>%
  pivot_longer(cols = -Group,
               names_to = "Variable",
               values_to = "Statistics")

print(tidy_descriptive_stats)

Confidence intervals Glycocheck parameters
> t.test(Glycoheck_clinical_study_dataset_for_stats$PBR525)
      One Sample t-test
data:  Glycoheck_clinical_study_dataset_for_stats$PBR525
t = 51.57, df = 18, p-value < 2.2e-16
alternative hypothesis: true mean is not equal to 0
95 percent confidence interval:
```

```
 2.496771 2.708843
sample estimates:
mean of x
 2.602807

> clinidata<-Glycoheck_clinical_study_dataset_for_stats
> t.test(clinidata$RBC_filling)
      One Sample t-test
data:  clinidata$RBC_filling
t = 32.239, df = 18, p-value < 2.2e-16
alternative hypothesis: true mean is not equal to 0
95 percent confidence interval:
 0.5476972 0.6240572
sample estimates:
mean of x
0.5858772

> t.test(clinidata$VVD)
      One Sample t-test
data:  clinidata$VVD
t = 14.989, df = 18, p-value = 1.305e-11
alternative hypothesis: true mean is not equal to 0
95 percent confidence interval:
 331.6850 439.8237
sample estimates:
mean of x
 385.7544

> t.test(clinidata$PBR59)
      One Sample t-test
data:  clinidata$PBR59
t = 40.108, df = 18, p-value < 2.2e-16
alternative hypothesis: true mean is not equal to 0
95 percent confidence interval:
 1.306218 1.450624
sample estimates:
mean of x
```

```
 1.378421

> t.test(clinidata$PBR1019)
      One Sample t-test
data:  clinidata$PBR1019
t = 59.179, df = 18, p-value < 2.2e-16
alternative hypothesis: true mean is not equal to 0
95 percent confidence interval:
 2.909571 3.123762
sample estimates:
mean of x
 3.016667

> t.test(clinidata$PBR2025)
      One Sample t-test
data:  clinidata$PBR2025
t = 35.01, df = 18, p-value < 2.2e-16
alternative hypothesis: true mean is not equal to 0
95 percent confidence interval:
 2.851802 3.215918
sample estimates:
mean of x
  3.03386

> t.test(clinidata$Median_P50)
      One Sample t-test
data:  clinidata$Median_P50
t = 31.986, df = 18, p-value < 2.2e-16
alternative hypothesis: true mean is not equal to 0
95 percent confidence interval:
 7.713032 8.797494
sample estimates:
mean of x
 8.255263

Vascular segments analysis
Normality
```

```
> for (variable in variables) {
+   shapiro_test <-
shapiro.test(Glycoheck_clinical_study_dataset_for_stats[[variable]])
+   cat("Shapiro-Wilk test for", variable, ":\n")
+   cat("Test Statistic =", shapiro_test$statistic, ", p-value =",
shapiro_test$p.value, "\n\n")
+   bin_size <- 20
+   hist(Glycoheck_clinical_study_dataset_for_stats[[variable]],
+        breaks = bin_size,
+        main = paste("Distribution of", variable),
+        xlab = variable,
+        ylab = "Frequency",
+        col = "lightblue",
+        border = "black")}
Shapiro-Wilk test for Count_59 :
Test Statistic = 0.957989 , p-value = 0.5334377


Shapiro-Wilk test for Count_1019 :
Test Statistic = 0.9212702 , p-value = 0.119458


Shapiro-Wilk test for Count_2025 :
Test Statistic = 0.9149542 , p-value = 0.09131407


Shapiro-Wilk test for Count_525 :
Test Statistic = 0.9860171 , p-value = 0.989094


> hist(Glycoheck_clinical_study_dataset_for_stats$Count_59,
+      breaks = 5, # Specify the number of breaks directly
+      main = "Distribution of Count_59",
+      xlab = "Count_59",
+      ylab = "Frequency",
+      col = "lightblue",
+      border = "black",
+      prob = TRUE) # Set to TRUE to show density instead of frequency
> lines(density(Glycoheck_clinical_study_dataset_for_stats$Count_59, na.rm
= TRUE),
+       col = "red", lwd = 2) # Add a density line
```

```
> hist(Glycoheck_clinical_study_dataset_for_stats$Count_1019,
+      breaks = 5, # Specify the number of breaks directly
+      main = "Distribution of Count_1019",
+      xlab = "Count_1019",
+      ylab = "Frequency",
+      col = "lightblue",
+      border = "black",
+      prob = TRUE) # Set to TRUE to show density instead of frequency
> lines(density(Glycoheck_clinical_study_dataset_for_stats$Count_1019,
na.rm = TRUE),
+       col = "red", lwd = 2) # Add a density line
> hist(Glycoheck_clinical_study_dataset_for_stats$Count_2025,
+      breaks = 5, # Specify the number of breaks directly
+      main = "Distribution of Count_2025",
+      xlab = "Count_2025",
+      ylab = "Frequency",
+      col = "lightblue",
+      border = "black",
+      prob = TRUE) # Set to TRUE to show density instead of frequency
> lines(density(Glycoheck_clinical_study_dataset_for_stats$Count_2025,
na.rm = TRUE),
+       col = "red", lwd = 2) # Add a density line
>  hist(Glycoheck_clinical_study_dataset_for_stats$Count_525,
+      breaks = 5, # Specify the number of breaks directly
+      main = "Distribution of Count_525",
+      xlab = "Count_525",
+      ylab = "Frequency",
+      col = "lightblue",
+      border = "black",
+      prob = TRUE) # Set to TRUE to show density instead of frequency
> lines(density(Glycoheck_clinical_study_dataset_for_stats$Count_525,
na.rm = TRUE),
+       col = "red", lwd = 2) # Add a density line


Vascular segment count summary statistics
>
> library(openxlsx)
Warning message:
```

```
package ‘openxlsx’ was built under R version 4.3.3

>

> summary_stats <- data.frame(

+   Variable = c("Count_59", "Count_1019", "Count_2025", "Count_525"),

+   Mean = c(mean(Glycoheck_clinical_study_dataset_for_stats$Count_59,
na.rm = TRUE),

+            mean(Glycoheck_clinical_study_dataset_for_stats$Count_1019,
na.rm = TRUE),

+            mean(Glycoheck_clinical_study_dataset_for_stats$Count_2025,
na.rm = TRUE),

+            mean(Glycoheck_clinical_study_dataset_for_stats$Count_525,
na.rm = TRUE)),

+   Median = c(median(Glycoheck_clinical_study_dataset_for_stats$Count_59,
na.rm = TRUE),

+
median(Glycoheck_clinical_study_dataset_for_stats$Count_1019, na.rm =
TRUE),

+
median(Glycoheck_clinical_study_dataset_for_stats$Count_2025, na.rm =
TRUE),

+
median(Glycoheck_clinical_study_dataset_for_stats$Count_525, na.rm =
TRUE)),

+   SD = c(sd(Glycoheck_clinical_study_dataset_for_stats$Count_59, na.rm =
TRUE),

+          sd(Glycoheck_clinical_study_dataset_for_stats$Count_1019, na.rm
= TRUE),

+          sd(Glycoheck_clinical_study_dataset_for_stats$Count_2025, na.rm
= TRUE),

+          sd(Glycoheck_clinical_study_dataset_for_stats$Count_525, na.rm
= TRUE)),

+   IQR = c(IQR(Glycoheck_clinical_study_dataset_for_stats$Count_59, na.rm
= TRUE),

+            IQR(Glycoheck_clinical_study_dataset_for_stats$Count_1019,
na.rm = TRUE),

+            IQR(Glycoheck_clinical_study_dataset_for_stats$Count_2025,
na.rm = TRUE),

+            IQR(Glycoheck_clinical_study_dataset_for_stats$Count_525,
na.rm = TRUE))

+ )

>

> write.xlsx(summary_stats, file = "Summary_Statistics.xlsx")

>

> print(summary_stats)

    Variable       Mean Median        SD   IQR
```

```
1   Count_59  994.42105    910 350.76224 515.0
2 Count_1019  505.05263    505 171.65096 285.5
3 Count_2025   29.94737     28  19.38348  21.0
4  Count_525 1529.42105   1513 356.04218 471.0
```

Comparison between segment groups and subgroups

```
> friedman_data <- data.frame(
+   Count_59 = Glycoheck_clinical_study_dataset_for_stats$Count_59,
+   Count_1019 = Glycoheck_clinical_study_dataset_for_stats$Count_1019,
+   Count_2025 = Glycoheck_clinical_study_dataset_for_stats$Count_2025,
+   Count_525 = Glycoheck_clinical_study_dataset_for_stats$Count_525
+ )
>
> friedman_data_long <- data.frame(
+   Value = c(
+     friedman_data$Count_59,
+     friedman_data$Count_1019,
+     friedman_data$Count_2025,
+     friedman_data$Count_525
+   ),
+   Group = factor(rep(c("Count_59", "Count_1019", "Count_2025",
"Count_525"),
+                      each = nrow(friedman_data))),
+   Subject = factor(rep(1:nrow(friedman_data), times = 4))
+ )
> friedman_result <- friedman.test(Value ~ Group | Subject, data =
friedman_data_long)
> print(friedman_result)


      Friedman rank sum test


data:  Value and Group and Subject
Friedman chi-squared = 54.853, df = 3, p-value = 7.382e-12


> pairwise_results <- pairwise.wilcox.test(friedman_data_long$Value,
friedman_data_long$Group,
+                                          paired = TRUE, p.adjust.method
= "bonferroni")
```

```
> print(pairwise_results)

      Pairwise comparisons using Wilcoxon signed rank exact test

data:  friedman_data_long$Value and friedman_data_long$Group

           Count_1019 Count_2025 Count_525
Count_2025 2.3e-05    -          -
Count_525  2.3e-05    2.3e-05    -
Count_59   0.00023    2.3e-05    2.3e-05

P value adjustment method: bonferroni

> hist(residuals_PBR2025,
+      main = "Histogram of Residuals with Density Line for PBR2025",
+      xlab = "Residuals",
+      ylab = "Frequency",
+      col = "lightblue",
+      border = "black",
+      prob = TRUE)
> lines(density(residuals_PBR2025, na.rm = TRUE), col = "red", lwd = 2)
```

Vascular segment distribution per diameter from 5 to 25 bar plot

```
library(ggplot2)
ggplot(data = CS_vascular_segment_counts, aes(x = Diameter, y =
N_segments)) +
  geom_bar(stat = "identity", fill = "navy", width = 0.6) +
  labs(
    title = "Vascular segment distribution",
    x = "Major vascular segments with diameters from 5 to 25 µm",
    y = "Vascular segment counts"
  ) +
  scale_x_continuous(
    breaks = 5:25,
```

```
    labels = 5:25
  ) +
  geom_vline(xintercept = c(9.5, 19.5), linetype = "dashed", color =
"grey40") +
  theme_minimal() +
  theme(
    panel.grid = element_blank(),                    # Remove all grid
lines
    axis.line = element_line(color = "black"),       # Add axis lines
    axis.text.x = element_text(size = 10),
    axis.text.y = element_text(size = 10),
    axis.title = element_text(size = 12, face = "bold"),
    plot.title = element_text(size = 14, face = "bold", hjust = 0.5)
  )
```

PCV data distribution (normality)

```
> data <- Glycoheck_clinical_study_dataset_for_stats
>
> shapiro_test <- shapiro.test(data$PCV)
> print(shapiro_test)

      Shapiro-Wilk normality test

data:  data$PCV
W = 0.95942, p-value = 0.5905
```

PCV summary stats

```
> summary_stats <- data %>%
+   summarise(
+     Mean = mean(PCV, na.rm = TRUE),
+     SD = sd(PCV, na.rm = TRUE),
+     Min = min(PCV, na.rm = TRUE),
+     Max = max(PCV, na.rm = TRUE),
+     Median = median(PCV, na.rm = TRUE),
+     Q1 = quantile(PCV, 0.25, na.rm = TRUE),
+     Q3 = quantile(PCV, 0.75, na.rm = TRUE)
```

```
+   )
>
> print(summary_stats)
# A tibble: 1 × 7
   Mean    SD   Min   Max Median    Q1    Q3
  <dbl> <dbl> <dbl> <dbl>  <dbl> <dbl> <dbl>
1  32.8  10.1    13    48     35    25    39
>
> ggplot(data, aes(x = PCV)) +
+   geom_histogram(aes(y = ..density..), binwidth = 2, fill = "blue",
color = "black", alpha = 0.7) +
+   geom_density(color = "red", size = 1) +
+   labs(title = "Distribution of PCV", x = "PCV", y = "Density") +
+   theme_minimal() +
+   theme(plot.title = element_text(hjust = 0.5))
Warning messages:
1: Removed 1 row containing non-finite outside the scale range
(`stat_bin()`).
2: Removed 1 row containing non-finite outside the scale range
(`stat_density()`).
```

GlycoCheck vs Clinical variables
Generalized linear models

VVD

```
> glm_VVD <- glm(VVD ~ Group + APPLE_fast + LOH,
+                data = Glycoheck_clinical_study_dataset_for_stats,
+                family = Gamma(link = "log"))
> summary(glm_VVD)

Call:
glm(formula = VVD ~ Group + APPLE_fast + LOH, family = Gamma(link =
"log"),
    data = Glycoheck_clinical_study_dataset_for_stats)

Coefficients:
            Estimate Std. Error t value Pr(>|t|)
(Intercept)  5.89568    0.28397  20.762 1.83e-12 ***
GroupT      -0.25724    0.13497  -1.906   0.0760 .
APPLE_fast   0.02089    0.01532   1.364   0.1928
LOH         -0.04092    0.02254  -1.815   0.0895 .
---
Signif. codes:  0 ‘***’ 0.001 ‘**’ 0.01 ‘*’ 0.05 ‘.’ 0.1 ‘ ’ 1

(Dispersion parameter for Gamma family taken to be 0.0757046)

    Null deviance: 1.6208  on 18  degrees of freedom
Residual deviance: 1.1832  on 15  degrees of freedom
AIC: 236.05

Number of Fisher Scoring iterations: 6
```

```
>
> residuals_VVD <- residuals(glm_VVD, type = "pearson")
>
> hist(residuals_VVD,
+      main = "Histogram of Residuals for VVD",
+      xlab = "Residuals",
+      ylab = "Frequency",
+      col = "lightblue",
+      border = "black",
+      prob = TRUE)
> curve(dnorm(x, mean = mean(residuals_VVD, na.rm = TRUE),
+             sd = sd(residuals_VVD, na.rm = TRUE)),
+       col = "blue", lwd = 2, add = TRUE)

#CI (Exp Est)
                Estimate       2.5 %
(Intercept) 363.4625984 203.6256500
GroupT        0.7731851   0.5896762
APPLE_fast    1.0211142   0.9876256
LOH           0.9599069   0.9168381
                 97.5 %
(Intercept) 656.149667
GroupT        1.008563
APPLE_fast    1.055806
LOH           1.004616
```

RBC_filling

```
> glm_RBC_filling <- glm(RBC_filling ~ Group + APPLE_fast + LOH,
+                        data =
Glycoheck_clinical_study_dataset_for_stats,
+                        family = Gamma(link = "log"))
> summary(glm_RBC_filling)

Call:
glm(formula = RBC_filling ~ Group + APPLE_fast + LOH, family = Gamma(link
= "log"),
    data = Glycoheck_clinical_study_dataset_for_stats)

Coefficients:
             Estimate Std. Error t value Pr(>|t|)
(Intercept) -0.523342   0.152263  -3.437  0.00367 **
GroupT      -0.019639   0.072373  -0.271  0.78981
APPLE_fast   0.001664   0.008216   0.203  0.84222
LOH         -0.007324   0.012086  -0.606  0.55358
---
Signif. codes:  0 ‘***’ 0.001 ‘**’ 0.01 ‘*’ 0.05 ‘.’ 0.1 ‘ ’ 1

(Dispersion parameter for Gamma family taken to be 0.02176571)

    Null deviance: 0.33552  on 18  degrees of freedom
Residual deviance: 0.32725  on 15  degrees of freedom
AIC: -33.846

Number of Fisher Scoring iterations: 5

>
> residuals_RBC_filling <- residuals(glm_RBC_filling, type = "pearson")
>
> hist(residuals_RBC_filling,
+      main = "Histogram of Residuals for RBC_filling",
+      xlab = "Residuals",
+      ylab = "Frequency",
+      col = "lightblue",
+      border = "black",
+      prob = TRUE)
> curve(dnorm(x, mean = mean(residuals_RBC_filling, na.rm = TRUE),
+             sd = sd(residuals_RBC_filling, na.rm = TRUE)),
```

```
+       col = "blue", lwd = 2, add = TRUE)
>
> exp(cbind(
+   Estimate = coef(glm_RBC_filling),
+   confint(glm_RBC_filling)
+ ))
Estimate     2.5 %    97.5 %
(Intercept) 0.5925372 0.4352328 0.8091344
GroupT      0.9805523 0.8508274 1.1285740
APPLE_fast  1.0016653 0.9849083 1.0187305
LOH         0.9927028 0.9692344 1.0166863
```

Median_P50

```
> glm_Median_P50 <- glm(Median_P50 ~ Group + APPLE_fast + LOH,
+                       data = Glycoheck_clinical_study_dataset_for_stats,
+                       family = Gamma(link = "log"))
> summary(glm_Median_P50)

Call:
glm(formula = Median_P50 ~ Group + APPLE_fast + LOH, family = Gamma(link =
"log"),
    data = Glycoheck_clinical_study_dataset_for_stats)

Coefficients:
             Estimate Std. Error t value Pr(>|t|)
(Intercept)  2.1377140  0.1528324  13.987 5.19e-10 ***
GroupT       0.0244554  0.0726436   0.337    0.741
APPLE_fast  -0.0025952  0.0082463  -0.315    0.757
LOH          0.0008008  0.0121310   0.066    0.948
---
Signif. codes:  0 ‘***’ 0.001 ‘**’ 0.01 ‘*’ 0.05 ‘.’ 0.1 ‘ ’ 1

(Dispersion parameter for Gamma family taken to be 0.02192885)

    Null deviance: 0.33378  on 18  degrees of freedom
Residual deviance: 0.32940  on 15  degrees of freedom
AIC: 66.81

Number of Fisher Scoring iterations: 4

>
> residuals_Median_P50 <- residuals(glm_Median_P50, type = "pearson")
>
> hist(residuals_Median_P50,
+      main = "Histogram of Residuals for Median_P50",
+      xlab = "Residuals",
+      ylab = "Frequency",
+      col = "lightblue",
+      border = "black",
+      prob = TRUE)
> curve(dnorm(x, mean = mean(residuals_Median_P50, na.rm = TRUE),
+             sd = sd(residuals_Median_P50, na.rm = TRUE)),
+       col = "blue", lwd = 2, add = TRUE)


> exp(cbind(
+   Estimate = coef(glm_Median_P50),
+   confint.default(glm_Median_P50)
+ ))
             Estimate     2.5 %    97.5 %
(Intercept) 8.4800301 6.2850129 11.441649
GroupT      1.0247569 0.8887641  1.181558
APPLE_fast  0.9974081 0.9814171  1.013660
LOH         1.0008011 0.9772864  1.024882
```

PBR525

```
> glm_PBR525 <- glm(PBR525 ~ Group + APPLE_fast + LOH,
+                   data = Glycoheck_clinical_study_dataset_for_stats,
+                   family = Gamma(link = "log"))
> summary(glm_PBR525)

Call:
glm(formula = PBR525 ~ Group + APPLE_fast + LOH, family = Gamma(link =
"log"),
    data = Glycoheck_clinical_study_dataset_for_stats)

Coefficients:
            Estimate Std. Error t value Pr(>|t|)
(Intercept) 0.897154   0.094021   9.542 9.22e-08 ***
GroupT      0.001523   0.044689   0.034    0.973
APPLE_fast  0.003157   0.005073   0.622    0.543
LOH         0.001185   0.007463   0.159    0.876
---
Signif. codes:  0 ‘***’ 0.001 ‘**’ 0.01 ‘*’ 0.05 ‘.’ 0.1 ‘ ’ 1

(Dispersion parameter for Gamma family taken to be 0.008299109)

    Null deviance: 0.12737  on 18  degrees of freedom
Residual deviance: 0.12346  on 15  degrees of freedom
AIC: 4.4733

Number of Fisher Scoring iterations: 3

>
> residuals_PBR525 <- residuals(glm_PBR525, type = "pearson")
>
> hist(residuals_PBR525,
+      main = "Histogram of Residuals for PBR525",
+      xlab = "Residuals",
+      ylab = "Frequency",
+      col = "lightblue",
+      border = "black",
+      prob = TRUE)
> curve(dnorm(x, mean = mean(residuals_PBR525, na.rm = TRUE),
+             sd = sd(residuals_PBR525, na.rm = TRUE)),
+       col = "blue", lwd = 2, add = TRUE)


> exp(cbind(
+   Estimate = coef(glm_PBR525),
+   confint.default(glm_PBR525)
+ ))
            Estimate     2.5 %   97.5 %
(Intercept) 2.452614 2.0398521 2.948898
GroupT      1.001524 0.9175332 1.093204
APPLE_fast  1.003162 0.9932370 1.013186
LOH         1.001186 0.9866482 1.015938
```

PBR59

```
> glm_PBR59 <- glm(PBR59 ~ Group + APPLE_fast + LOH,
+                  data = Glycoheck_clinical_study_dataset_for_stats,
+                  family = Gamma(link = "log"))
> summary(glm_PBR59)

Call:
glm(formula = PBR59 ~ Group + APPLE_fast + LOH, family = Gamma(link =
"log"),
    data = Glycoheck_clinical_study_dataset_for_stats)

Coefficients:
             Estimate Std. Error t value Pr(>|t|)
(Intercept)  0.3773970  0.1195573   3.157  0.00652 **
GroupT      -0.0645504  0.0568274  -1.136  0.27382
```

```
APPLE_fast  -0.0006166  0.0064509  -0.096  0.92512
LOH         -0.0023202  0.0094898  -0.244  0.81016
---
Signif. codes:  0 ‘***’ 0.001 ‘**’ 0.01 ‘*’ 0.05 ‘.’ 0.1 ‘ ’ 1

(Dispersion parameter for Gamma family taken to be 0.01341952)

    Null deviance: 0.23410  on 18  degrees of freedom
Residual deviance: 0.21647  on 15  degrees of freedom
AIC: -9.1025

Number of Fisher Scoring iterations: 4

>
> residuals_PBR59 <- residuals(glm_PBR59, type = "pearson")
>
> hist(residuals_PBR59,
+      main = "Histogram of Residuals for PBR59",
+      xlab = "Residuals",
+      ylab = "Frequency",
+      col = "lightblue",
+      border = "black",
+      prob = TRUE)
> curve(dnorm(x, mean = mean(residuals_PBR59, na.rm = TRUE),
+             sd = sd(residuals_PBR59, na.rm = TRUE)),
+       col = "blue", lwd = 2, add = TRUE)
>

> exp(cbind(
+   Estimate = coef(glm_PBR59),
+   confint.default(glm_PBR59)
+ ))
             Estimate     2.5 %   97.5 %
(Intercept) 1.4584832 1.1538094 1.843609
GroupT      0.9374889 0.8386766 1.047943
APPLE_fast  0.9993836 0.9868274 1.012100
LOH         0.9976825 0.9792974 1.016413
```

PBR1019

```
> glm_PBR1019 <- glm(PBR1019 ~ Group + APPLE_fast + LOH,
+                    data = Glycoheck_clinical_study_dataset_for_stats,
+                    family = Gamma(link = "log"))
> summary(glm_PBR1019)

Call:
glm(formula = PBR1019 ~ Group + APPLE_fast + LOH, family = Gamma(link =
"log"),
    data = Glycoheck_clinical_study_dataset_for_stats)

Coefficients:
             Estimate Std. Error t value Pr(>|t|)
(Intercept) 1.0702963  0.0821361  13.031 1.39e-09 ***
GroupT      0.0111420  0.0390405   0.285    0.779
APPLE_fast  0.0008394  0.0044318   0.189    0.852
LOH         0.0033455  0.0065195   0.513    0.615
---
Signif. codes:  0 ‘***’ 0.001 ‘**’ 0.01 ‘*’ 0.05 ‘.’ 0.1 ‘ ’ 1

(Dispersion parameter for Gamma family taken to be 0.00633363)

    Null deviance: 0.096152  on 18  degrees of freedom
Residual deviance: 0.093832  on 15  degrees of freedom
AIC: 4.894

Number of Fisher Scoring iterations: 4

>
```

```
> residuals_PBR1019 <- residuals(glm_PBR1019, type = "pearson")
>
> hist(residuals_PBR1019,
+      main = "Histogram of Residuals for PBR1019",
+      xlab = "Residuals",
+      ylab = "Frequency",
+      col = "lightblue",
+      border = "black",
+      prob = TRUE)
> curve(dnorm(x, mean = mean(residuals_PBR1019, na.rm = TRUE),
+             sd = sd(residuals_PBR1019, na.rm = TRUE)),
+       col = "blue", lwd = 2, add = TRUE)


> #Confidence intervals for clinical study
> Glycoheck_clinical_study_dataset_for_stats <- read_excel("~/Scientific
projects/Glycocalyx/Glycocheck 2023/Glycocalyx clinical study/Raw
data/Glycoheck_clinical_study_dataset_for_stats.xlsx")
Error in read_excel("~/Scientific projects/Glycocalyx/Glycocheck
2023/Glycocalyx clinical study/Raw
data/Glycoheck_clinical_study_dataset_for_stats.xlsx") :
  could not find function "read_excel"

> #Confidence intervals for clinical study
> library(readxl)

Warning message:
package ‘readxl’ was built under R version 4.3.3
> Glycoheck_clinical_study_dataset_for_stats <- read_excel("~/Scientific
projects/Glycocalyx/Glycocheck 2023/Glycocalyx clinical study/Raw
data/Glycoheck_clinical_study_dataset_for_stats.xlsx")
Error:  `path` does not exist: ‘~/Scientific projects/Glycocalyx/Glycocheck
2023/Glycocalyx clinical study/Raw
data/Glycoheck_clinical_study_dataset_for_stats.xlsx’

> Glycocheck_clinical_study_dataset_for_stats <- read_excel("~/Scientific
projects/Glycocalyx/Glycocheck 2023/Glycocalyx clinical study/Raw
data/Glycocheck_clinical_study_dataset_for_stats.xlsx")
> View(Glycoheck_clinical_study_dataset_for_stats)
Error in View : object 'Glycoheck_clinical_study_dataset_for_stats' not
found
> View(Glycocheck_clinical_study_dataset_for_stats)
> lm_VVD <- lm(VVD ~ Group + APPLE_fast + LOH,
+              +              data =
Glycocheck_clinical_study_dataset_for_stats)
Error: unexpected '=' in:
"lm_VVD <- lm(VVD ~ Group + APPLE_fast + LOH,
             +              data ="

> lm_VVD <- lm(VVD ~ Group + APPLE_fast + LOH,
+              +              data =
Glycocheck_clinical_study_dataset_for_stats)
Error: unexpected '=' in:
"lm_VVD <- lm(VVD ~ Group + APPLE_fast + LOH,
             +              data ="

> #VVD
> lm_VVD <- lm(VVD ~ Group + APPLE_fast + LOH, data =
Glycocheck_clinical_study_dataset_for_stats)
> summary(lm_VVD)

Call:
lm(formula = VVD ~ Group + APPLE_fast + LOH, data =
Glycocheck_clinical_study_dataset_for_stats)

Residuals:
     Min       1Q   Median       3Q
-146.731  -44.282   -3.931   56.662
     Max
```

```
 243.659

Coefficients:
            Estimate Std. Error t value
(Intercept)  394.969    107.891   3.661
GroupT       -99.710     51.282  -1.944
APPLE_fast     6.200      5.821   1.065
LOH          -14.692      8.564  -1.716
            Pr(>|t|)
(Intercept)  0.00232 **
GroupT       0.07085 .
APPLE_fast   0.30368
LOH          0.10682
---
Signif. codes:
  0 ‘***’ 0.001 ‘**’ 0.01 ‘*’ 0.05 ‘.’
  0.1 ‘ ’ 1

Residual standard error: 104.5 on 15 degrees of freedom
Multiple R-squared:  0.2763,  Adjusted R-squared:  0.1316
F-statistic: 1.909 on 3 and 15 DF,  p-value: 0.1715

> #CI
> confint(lm_VVD, level = 0.95)
                  2.5 %     97.5 %
(Intercept)  165.004906 624.932837
GroupT      -209.014965   9.595799
APPLE_fast    -6.207729  18.608359
LOH          -32.944797   3.561772
> confint(lm_RBC_filling, level = 0.95)
Error: object 'lm_RBC_filling' not found

> #RBC filling
> lm_RBC_filling <- lm(RBC_filling ~ Group + APPLE_fast + LOH,data =
Glycocheck_clinical_study_dataset_for_stats)
> confint(lm_RBC_filling, level = 0.95)
                   2.5 %     97.5 %
(Intercept)  0.405460694 0.78245346
GroupT      -0.101650469 0.07753995
APPLE_fast  -0.009267218 0.01107398
LOH         -0.019199727 0.01072390
> #Median P50
> lm_Median_P50 <- lm(Median_P50 ~ Group + APPLE_fast + LOH,data =
Glycocheck_clinical_study_dataset_for_stats)
> confint)lm_Median_P50, level = 0.95)
Error: unexpected ')' in "confint)"

> confint(lm_Median_P50, level = 0.95)
                 2.5 %     97.5 %
(Intercept)  5.7725125 11.1602534
GroupT      -1.0856792  1.4751963
APPLE_fast  -0.1655012  0.1252023
LOH         -0.2087599  0.2188896
> #PBR 5-25
> lm_PBR525 <- lm(PBR525 ~ Group + APPLE_fast + LOH,data =
Glycocheck_clinical_study_dataset_for_stats)
> confint(lm_PBR525, level = 0.95)
                   2.5 %     97.5 %
(Intercept)  1.92143596 2.96488547
GroupT      -0.24359911 0.25236836
APPLE_fast  -0.01974811 0.03655274
LOH         -0.03786167 0.04496166
>
> #PBR 5-9
> lm_PBR59 <- lm(PBR59 ~ Group + APPLE_fast + LOH,data =
Glycocheck_clinical_study_dataset_for_stats)
> confint(lm_PBR59, level = 0.95)
                   2.5 %     97.5 %
(Intercept)  1.11042729 1.80206865
```

```
GroupT      -0.25208916 0.07665853
APPLE_fast  -0.01962436 0.01769417
LOH         -0.03016762 0.02473109
> #PBR 10-19
> lm_PBR1019 <- lm(PBR1019 ~ Group + APPLE_fast + LOH,data =
Glycocheck_clinical_study_dataset_for_stats)
> confint(lm_PBR1019, level = 0.95)
                2.5 %     97.5 %
(Intercept)  2.38045050 3.43813428
GroupT      -0.21831270 0.28442054
APPLE_fast  -0.02570923 0.03135966
LOH         -0.03169079 0.05226238
> #PBR 20-25
> lm_PBR2025 <- lm(PBR2025 ~ Group + APPLE_fast + LOH,data =
Glycocheck_clinical_study_dataset_for_stats)
> confint(lm_PBR2025, level = 0.95)
                2.5 %     97.5 %
(Intercept)  1.67715987 3.40828332
GroupT      -0.34877128 0.47405812
APPLE_fast  -0.02080728 0.07259803
LOH         -0.06529215 0.07211498
> #CI for GLM
> glm_VVD <- glm(VVD ~ Group + APPLE_fast + LOH,data =
Glycocheck_clinical_study_dataset_for_stats,family = Gamma(link = "log"))
> exp(cbind(
+   Estimate = coef(glm_VVD),
+   confint(glm_VVD)
+ ))
Waiting for profiling to be done...                Estimate       2.5 %
(Intercept) 363.4625984 203.6256500
GroupT        0.7731851   0.5896762
APPLE_fast    1.0211142   0.9876256
LOH           0.9599069   0.9168381
                97.5 %
(Intercept) 656.149667
GroupT        1.008563
APPLE_fast    1.055806
LOH           1.004616
> #RBC filling
> glm_RBC_filling <- glm(RBC_filling ~ Group + APPLE_fast + LOH,data =
Glycoheck_clinical_study_dataset_for_stats,family = Gamma(link = "log"))
Error in eval(mf, parent.frame()) :
  object 'Glycoheck_clinical_study_dataset_for_stats' not found

> #RBC filling
> glm_RBC_filling <- glm(RBC_filling ~ Group + APPLE_fast + LOH,data =
Glycocheck_clinical_study_dataset_for_stats,family = Gamma(link = "log"))
> exp(cbind(
+   Estimate = coef(glm_RBC_filling),
+   confint(glm_RBC_filling)
+ ))
Waiting for profiling to be done...              Estimate     2.5 %    97.5
%
(Intercept) 0.5925372 0.4352328 0.8091344
GroupT      0.9805523 0.8508274 1.1285740
APPLE_fast  1.0016653 0.9849083 1.0187305
LOH         0.9927028 0.9692344 1.0166863
> glm_Median_P50 <- glm(
+   Median_P50 ~ Group + APPLE_fast + LOH,
+   data = Glycocheck_clinical_study_dataset_for_stats,
+   family = Gamma(link = "log")
+ )
>
> exp(cbind(
+   Estimate = coef(glm_Median_P50),
+   confint.default(glm_Median_P50)
+ ))
             Estimate     2.5 %    97.5 %
(Intercept) 8.4800301 6.2850129 11.441649
```

```
GroupT      1.0247569 0.8887641  1.181558
APPLE_fast  0.9974081 0.9814171  1.013660
LOH         1.0008011 0.9772864  1.024882
> # PBR525
> glm_PBR525 <- glm(
+   PBR525 ~ Group + APPLE_fast + LOH,
+   data = Glycocheck_clinical_study_dataset_for_stats,
+   family = Gamma(link = "log")
+ )
>
> exp(cbind(
+   Estimate = coef(glm_PBR525),
+   confint.default(glm_PBR525)
+ ))
            Estimate     2.5 %   97.5 %
(Intercept) 2.452614 2.0398521 2.948898
GroupT      1.001524 0.9175332 1.093204
APPLE_fast  1.003162 0.9932370 1.013186
LOH         1.001186 0.9866482 1.015938
> glm_PBR59 <- glm(
+   PBR59 ~ Group + APPLE_fast + LOH,
+   data = Glycocheck_clinical_study_dataset_for_stats,
+   family = Gamma(link = "log")
+ )
>
> exp(cbind(
+   Estimate = coef(glm_PBR59),
+   confint.default(glm_PBR59)
+ ))
             Estimate     2.5 %   97.5 %
(Intercept) 1.4584832 1.1538094 1.843609
GroupT      0.9374889 0.8386766 1.047943
APPLE_fast  0.9993836 0.9868274 1.012100
LOH         0.9976825 0.9792974 1.016413
> glm_PBR1019 <- glm(
+   PBR1019 ~ Group + APPLE_fast + LOH,
+   data = Glycocheck_clinical_study_dataset_for_stats,
+   family = Gamma(link = "log")
+ )
>
> exp(cbind(
+   Estimate = coef(glm_PBR1019),
+   confint.default(glm_PBR1019)
+ ))
            Estimate     2.5 %   97.5 %
(Intercept) 2.916243 2.4826152 3.425612
GroupT      1.011204 0.9367151 1.091617
APPLE_fast  1.000840 0.9921840 1.009571
LOH         1.003351 0.9906119 1.016254
```

PBR2025

```
> glm_PBR2025 <- glm(PBR2025 ~ Group + APPLE_fast + LOH,
+                    data = Glycoheck_clinical_study_dataset_for_stats,
+                    family = Gamma(link = "log"))
> summary(glm_PBR2025)

Call:
glm(formula = PBR2025 ~ Group + APPLE_fast + LOH, family = Gamma(link =
"log"),
    data = Glycoheck_clinical_study_dataset_for_stats)

Coefficients:
             Estimate Std. Error t value Pr(>|t|)
(Intercept) 0.9539468  0.1350891   7.062 3.86e-06 ***
GroupT      0.0189200  0.0642099   0.295    0.772
APPLE_fast  0.0082903  0.0072889   1.137    0.273
LOH         0.0007412  0.0107226   0.069    0.946
```

```
---
Signif. codes:  0 ‘***’ 0.001 ‘**’ 0.01 ‘*’ 0.05 ‘.’ 0.1 ‘ ’ 1

(Dispersion parameter for Gamma family taken to be 0.01713268)

    Null deviance: 0.28782  on 18  degrees of freedom
Residual deviance: 0.26206  on 15  degrees of freedom
AIC: 24.461

Number of Fisher Scoring iterations: 4

>
> residuals_PBR2025 <- residuals(glm_PBR2025, type = "pearson")
>
> hist(residuals_PBR2025,
+      main = "Histogram of Residuals for PBR2025",
+      xlab = "Residuals",
+      ylab = "Frequency",
+      col = "lightblue",
+      border = "black",
+      prob = TRUE)
> curve(dnorm(x, mean = mean(residuals_PBR2025, na.rm = TRUE),
+             sd = sd(residuals_PBR2025, na.rm = TRUE)),
+       col = "blue", lwd = 2, add = TRUE)

> exp(cbind(
+   Estimate = coef(glm_PBR2025),
+   confint.default(glm_PBR2025)
+ ))
            Estimate     2.5 %   97.5 %
(Intercept) 2.595935 1.9920755 3.382843
GroupT      1.019100 0.8985894 1.155773
APPLE_fast  1.008325 0.9940222 1.022833
LOH         1.000741 0.9799293 1.021996

>
```

GlycoCheck vs IV fluid variables

```
> subset_data <- subset(Glycoheck_clinical_study_dataset_for_stats,
IV_fluids_Y_N == "Y")
>
```

VVD

```
> glm_VVD <- glm(VVD ~ IV_fluids_rate + IV_fluids_duration +
IV_fluids_total,
+                data = subset_data,
+                family = Gamma(link = "log"))
> summary(glm_VVD)

Call:
glm(formula = VVD ~ IV_fluids_rate + IV_fluids_duration + IV_fluids_total,
    family = Gamma(link = "log"), data = subset_data)

Coefficients:
                   Estimate Std. Error t value Pr(>|t|)
(Intercept)         4.804478   0.432182  11.117 3.16e-05 ***
IV_fluids_rate      0.071514   0.027046   2.644   0.0383 *
IV_fluids_duration  0.051562   0.024356   2.117   0.0786 .
IV_fluids_total    -0.003184   0.001613  -1.974   0.0958 .
---
Signif. codes:  0 ‘***’ 0.001 ‘**’ 0.01 ‘*’ 0.05 ‘.’ 0.1 ‘ ’ 1

(Dispersion parameter for Gamma family taken to be 0.0955655)

    Null deviance: 1.28050  on 9  degrees of freedom
Residual deviance: 0.55961  on 6  degrees of freedom
AIC: 126.99
```

```
Number of Fisher Scoring iterations: 5

>
> residuals_VVD <- residuals(glm_VVD, type = "pearson")
>
> hist(residuals_VVD,
+      main = "Histogram of Residuals for VVD (Group Y)",
+      xlab = "Residuals",
+      ylab = "Frequency",
+      col = "lightblue",
+      border = "black",
+      prob = TRUE)
> curve(dnorm(x, mean = mean(residuals_VVD, na.rm = TRUE),
+             sd = sd(residuals_VVD, na.rm = TRUE)),
+       col = "blue", lwd = 2, add = TRUE)

                      Estimate      2.5 %
(Intercept)        122.0557430 52.3219452
IV_fluids_rate       1.0741327  1.0186765
IV_fluids_duration   1.0529142  1.0038331
IV_fluids_total      0.9968212  0.9936753
                        97.5 %
(Intercept)        284.7295593
IV_fluids_rate       1.1326079
IV_fluids_duration   1.1043951
IV_fluids_total      0.9999771




R version 4.3.1 (2023-06-16 ucrt) -- "Beagle Scouts"
Copyright (C) 2023 The R Foundation for Statistical Computing
Platform: x86_64-w64-mingw32/x64 (64-bit)

R is free software and comes with ABSOLUTELY NO WARRANTY.
You are welcome to redistribute it under certain conditions.
Type 'license()' or 'licence()' for distribution details.

  Natural language support but running in an English locale

R is a collaborative project with many contributors.
Type 'contributors()' for more information and
'citation()' on how to cite R or R packages in publications.

Type 'demo()' for some demos, 'help()' for on-line help, or
'help.start()' for an HTML browser interface to help.
Type 'q()' to quit R.

[Workspace loaded from ~/.RData]

> #Exponentiated estimates + CI for PCV
> Glycocheck_clinical_study_dataset_for_stats$PCV <-
as.numeric(as.character(Glycocheck_clinical_study_dataset_for_stats$PCV))
Error: object 'Glycocheck_clinical_study_dataset_for_stats' not found

> confint(glm_VVD)
Waiting for profiling to be done...                              2.5 %
(Intercept)         3.913403929
IV_fluids_rate      0.019292015
IV_fluids_duration  0.003048313
IV_fluids_total    -0.006367730
                          97.5 %
(Intercept)         5.694266e+00
IV_fluids_rate      1.260561e-01
IV_fluids_duration  1.030987e-01
IV_fluids_total    -4.779418e-05
```

RBC_filling

```
> glm_RBC_filling <- glm(RBC_filling ~ IV_fluids_rate + IV_fluids_duration
+ IV_fluids_total,
+                        data = subset_data,
+                        family = Gamma(link = "log"))
> summary(glm_RBC_filling)

Call:
glm(formula = RBC_filling ~ IV_fluids_rate + IV_fluids_duration +
    IV_fluids_total, family = Gamma(link = "log"), data = subset_data)

Coefficients:
                     Estimate Std. Error t value Pr(>|t|)
(Intercept)        -0.8171511  0.2320649  -3.521   0.0125 *
IV_fluids_rate      0.0221445  0.0145227   1.525   0.1781
IV_fluids_duration  0.0099166  0.0130780   0.758   0.4770
IV_fluids_total    -0.0007713  0.0008660  -0.891   0.4074
---
Signif. codes:  0 ‘***’ 0.001 ‘**’ 0.01 ‘*’ 0.05 ‘.’ 0.1 ‘ ’ 1

(Dispersion parameter for Gamma family taken to be 0.02755406)

    Null deviance: 0.23969  on 9  degrees of freedom
Residual deviance: 0.15058  on 6  degrees of freedom
AIC: -14.603

Number of Fisher Scoring iterations: 4

>
> residuals_RBC_filling <- residuals(glm_RBC_filling, type = "pearson")
>
> hist(residuals_RBC_filling,
+      main = "Histogram of Residuals for RBC_filling (Group Y)",
+      xlab = "Residuals",
+      ylab = "Frequency",
+      col = "lightblue",
+      border = "black",
+      prob = TRUE)
> curve(dnorm(x, mean = mean(residuals_RBC_filling, na.rm = TRUE),
+             sd = sd(residuals_RBC_filling, na.rm = TRUE)),
+       col = "blue", lwd = 2, add = TRUE)

> exp(cbind(
+   Estimate = coef(glm_RBC_filling),
+   confint.default(glm_RBC_filling)
+ ))
                     Estimate     2.5 %
(Intercept)        0.4416882 0.2802734
IV_fluids_rate     1.0223915 0.9937005
IV_fluids_duration 1.0099660 0.9844071
IV_fluids_total    0.9992290 0.9975344
                      97.5 %
(Intercept)        0.6960649
IV_fluids_rate     1.0519109
IV_fluids_duration 1.0361884
IV_fluids_total    1.0009264

>
```

Median_P50

```
> glm_Median_P50 <- glm(Median_P50 ~ IV_fluids_rate + IV_fluids_duration +
IV_fluids_total,
+                       data = subset_data,
+                       family = Gamma(link = "log"))
> summary(glm_Median_P50)

Call:
glm(formula = Median_P50 ~ IV_fluids_rate + IV_fluids_duration +
    IV_fluids_total, family = Gamma(link = "log"), data = subset_data)
```

```
Coefficients:
                   Estimate Std. Error t value Pr(>|t|)
(Intercept)         2.435107   0.113352  21.483 6.64e-07 ***
IV_fluids_rate     -0.019890   0.007094  -2.804   0.0310 *
IV_fluids_duration -0.020748   0.006388  -3.248   0.0175 *
IV_fluids_total     0.001226   0.000423   2.897   0.0274 *
---
Signif. codes:  0 ‘***’ 0.001 ‘**’ 0.01 ‘*’ 0.05 ‘.’ 0.1 ‘ ’ 1

(Dispersion parameter for Gamma family taken to be 0.006573887)

    Null deviance: 0.110072  on 9  degrees of freedom
Residual deviance: 0.040195  on 6  degrees of freedom
AIC: 24.926

Number of Fisher Scoring iterations: 3

>
> residuals_Median_P50 <- residuals(glm_Median_P50, type = "pearson")
>
> hist(residuals_Median_P50,
+      main = "Histogram of Residuals for Median_P50 (Group Y)",
+      xlab = "Residuals",
+      ylab = "Frequency",
+      col = "lightblue",
+      border = "black",
+      prob = TRUE)
> curve(dnorm(x, mean = mean(residuals_Median_P50, na.rm = TRUE),
+             sd = sd(residuals_Median_P50, na.rm = TRUE)),
+       col = "blue", lwd = 2, add = TRUE)
>

> exp(cbind(
+   Estimate = coef(glm_Median_P50),
+   confint.default(glm_Median_P50)
+ ))
                     Estimate     2.5 %
(Intercept)        11.4170398 9.1425734
IV_fluids_rate      0.9803061 0.9667711
IV_fluids_duration  0.9794659 0.9672794
IV_fluids_total     1.0012263 1.0003965
                       97.5 %
(Intercept)        14.2573421
IV_fluids_rate      0.9940306
IV_fluids_duration  0.9918060
IV_fluids_total     1.0020567

> confint(glm_Median_P50)
Waiting for profiling to be done...                                  2.5 %
(Intercept)         2.2129127406
IV_fluids_rate     -0.0338446531
IV_fluids_duration -0.0331266641
IV_fluids_total     0.0003955371
                          97.5 %
(Intercept)         2.657575617
IV_fluids_rate     -0.005777280
IV_fluids_duration -0.008204790
IV_fluids_total     0.002054768
```

PBR525

```
> glm_PBR525 <- glm(PBR525 ~ IV_fluids_rate + IV_fluids_duration +
IV_fluids_total,
+                   data = subset_data,
+                   family = Gamma(link = "log"))
> summary(glm_PBR525)

Call:
```

```
glm(formula = PBR525 ~ IV_fluids_rate + IV_fluids_duration +
    IV_fluids_total, family = Gamma(link = "log"), data = subset_data)

Coefficients:
                    Estimate Std. Error t value Pr(>|t|)
(Intercept)         1.0454014  0.1273782   8.207 0.000177 ***
IV_fluids_rate     -0.0089994  0.0079714  -1.129 0.302017
IV_fluids_duration -0.0031983  0.0071784  -0.446 0.671550
IV_fluids_total     0.0003238  0.0004753   0.681 0.521115
---
Signif. codes:  0 ‘***’ 0.001 ‘**’ 0.01 ‘*’ 0.05 ‘.’ 0.1 ‘ ’ 1

(Dispersion parameter for Gamma family taken to be 0.008301516)

    Null deviance: 0.066967  on 9  degrees of freedom
Residual deviance: 0.049954  on 6  degrees of freedom
AIC: 4.3969

Number of Fisher Scoring iterations: 4

>
> residuals_PBR525 <- residuals(glm_PBR525, type = "pearson")
>
> hist(residuals_PBR525,
+      main = "Histogram of Residuals for PBR525 (Group Y)",
+      xlab = "Residuals",
+      ylab = "Frequency",
+      col = "lightblue",
+      border = "black",
+      prob = TRUE)
> curve(dnorm(x, mean = mean(residuals_PBR525, na.rm = TRUE),
+             sd = sd(residuals_PBR525, na.rm = TRUE)),
+       col = "blue", lwd = 2, add = TRUE)
>

> exp(cbind(
+   Estimate = coef(glm_PBR525),
+   confint.default(glm_PBR525)
+ ))
                     Estimate     2.5 %
(Intercept)        2.8445401 2.2160906
IV_fluids_rate     0.9910409 0.9756777
IV_fluids_duration 0.9968068 0.9828806
IV_fluids_total    1.0003239 0.9993924
                      97.5 %
(Intercept)        3.651208
IV_fluids_rate     1.006646
IV_fluids_duration 1.010930
IV_fluids_total    1.001256
```

PBR59

```
> glm_PBR59 <- glm(PBR59 ~ IV_fluids_rate + IV_fluids_duration +
IV_fluids_total,
+                  data = subset_data,
+                  family = Gamma(link = "log"))
> summary(glm_PBR59)

Call:
glm(formula = PBR59 ~ IV_fluids_rate + IV_fluids_duration +
IV_fluids_total,
    family = Gamma(link = "log"), data = subset_data)

Coefficients:
                    Estimate Std. Error t value Pr(>|t|)
(Intercept)         2.891e-01  2.048e-01   1.411    0.208
IV_fluids_rate     -1.157e-03  1.282e-02  -0.090    0.931
IV_fluids_duration  2.343e-03  1.154e-02   0.203    0.846
IV_fluids_total    -1.367e-05  7.643e-04  -0.018    0.986
```

```
(Dispersion parameter for Gamma family taken to be 0.02146437)

    Null deviance: 0.15329  on 9  degrees of freedom
Residual deviance: 0.14564  on 6  degrees of freedom
AIC: 2.2926

Number of Fisher Scoring iterations: 4

>
> residuals_PBR59 <- residuals(glm_PBR59, type = "pearson")
>
> hist(residuals_PBR59,
+      main = "Histogram of Residuals for PBR59 (Group Y)",
+      xlab = "Residuals",
+      ylab = "Frequency",
+      col = "lightblue",
+      border = "black",
+      prob = TRUE)
> curve(dnorm(x, mean = mean(residuals_PBR59, na.rm = TRUE),
+             sd = sd(residuals_PBR59, na.rm = TRUE)),
+       col = "blue", lwd = 2, add = TRUE)

> exp(cbind(
+   Estimate = coef(glm_PBR59),
+   confint.default(glm_PBR59)
+ ))
                    Estimate     2.5 %
(Intercept)        1.3351887 0.8937134
IV_fluids_rate     0.9988436 0.9740629
IV_fluids_duration 1.0023456 0.9799239
IV_fluids_total    0.9999863 0.9984894
                      97.5 %
(Intercept)        1.994743
IV_fluids_rate     1.024255
IV_fluids_duration 1.025280
IV_fluids_total    1.001485
```

PBR1019

```
> glm_PBR1019 <- glm(PBR1019 ~ IV_fluids_rate + IV_fluids_duration +
IV_fluids_total,
+                    data = subset_data,
+                    family = Gamma(link = "log"))
> summary(glm_PBR1019)

Call:
glm(formula = PBR1019 ~ IV_fluids_rate + IV_fluids_duration +
    IV_fluids_total, family = Gamma(link = "log"), data = subset_data)

Coefficients:
                     Estimate Std. Error t value Pr(>|t|)
(Intercept)         1.180e+00  1.116e-01  10.581 4.19e-05 ***
IV_fluids_rate     -6.571e-03  6.981e-03  -0.941    0.383
IV_fluids_duration -4.092e-04  6.287e-03  -0.065    0.950
IV_fluids_total     4.764e-05  4.163e-04   0.114    0.913
---
Signif. codes:  0 ‘***’ 0.001 ‘**’ 0.01 ‘*’ 0.05 ‘.’ 0.1 ‘ ’ 1

(Dispersion parameter for Gamma family taken to be 0.00636716)

    Null deviance: 0.055371  on 9  degrees of freedom
Residual deviance: 0.038076  on 6  degrees of freedom
AIC: 4.7736

Number of Fisher Scoring iterations: 4

>
> residuals_PBR1019 <- residuals(glm_PBR1019, type = "pearson")
```

```
>
> hist(residuals_PBR1019,
+      main = "Histogram of Residuals for PBR1019 (Group Y)",
+      xlab = "Residuals",
+      ylab = "Frequency",
+      col = "lightblue",
+      border = "black",
+      prob = TRUE)
> curve(dnorm(x, mean = mean(residuals_PBR1019, na.rm = TRUE),
+             sd = sd(residuals_PBR1019, na.rm = TRUE)),
+       col = "blue", lwd = 2, add = TRUE)

# PBR1019
glm_PBR1019 <- glm(
  PBR1019 ~ IV_fluids_rate + IV_fluids_duration + IV_fluids_total,
  data = subset_data,
  family = Gamma(link = "log")
)

exp(cbind(
  Estimate = coef(glm_PBR1019),
  confint.default(glm_PBR1019)
))
```

PBR2025

```
> glm_PBR2025 <- glm(PBR2025 ~ IV_fluids_rate + IV_fluids_duration +
IV_fluids_total,
+                    data = subset_data,
+                    family = Gamma(link = "log"))
> summary(glm_PBR2025)

Call:
glm(formula = PBR2025 ~ IV_fluids_rate + IV_fluids_duration +
    IV_fluids_total, family = Gamma(link = "log"), data = subset_data)

Coefficients:
                    Estimate Std. Error t value Pr(>|t|)
(Intercept)         1.2541281  0.1888149   6.642 0.000562 ***
IV_fluids_rate     -0.0172953  0.0118161  -1.464 0.193607
IV_fluids_duration -0.0084374  0.0106406  -0.793 0.458011
IV_fluids_total     0.0009359  0.0007046   1.328 0.232373
---
Signif. codes:  0 ‘***’ 0.001 ‘**’ 0.01 ‘*’ 0.05 ‘.’ 0.1 ‘ ’ 1

(Dispersion parameter for Gamma family taken to be 0.01824061)

    Null deviance: 0.17771  on 9  degrees of freedom
Residual deviance: 0.10785  on 6  degrees of freedom
AIC: 15.044

Number of Fisher Scoring iterations: 4

>
> residuals_PBR2025 <- residuals(glm_PBR2025, type = "pearson")
>
> hist(residuals_PBR2025,
+      main = "Histogram of Residuals for PBR2025 (Group Y)",
+      xlab = "Residuals",
+      ylab = "Frequency",
+      col = "lightblue",
+      border = "black",
+      prob = TRUE)
> curve(dnorm(x, mean = mean(residuals_PBR2025, na.rm = TRUE),
+             sd = sd(residuals_PBR2025, na.rm = TRUE)),
+       col = "blue", lwd = 2, add = TRUE)

> exp(cbind(
+   Estimate = coef(glm_PBR2025),
```

```
+   confint.default(glm_PBR2025)
+ ))
                    Estimate     2.5 %
(Intercept)        3.5047813 2.4207024
IV_fluids_rate     0.9828534 0.9603530
IV_fluids_duration 0.9915981 0.9711322
IV_fluids_total    1.0009363 0.9995550
                      97.5 %
(Intercept)        5.074350
IV_fluids_rate     1.005881
IV_fluids_duration 1.012495
IV_fluids_total    1.002320
```

Trauma dataset effects of ATT

```
> subset_data_T <- subset(Glycoheck_clinical_study_dataset_for_stats,
Group == "T")

VVD
> glm_VVD <- glm(VVD ~ Total_ATT,
+                data = subset_data_T,
+                family = Gamma(link = "log"))
> summary(glm_VVD)

Call:
glm(formula = VVD ~ Total_ATT, family = Gamma(link = "log"),
    data = subset_data_T)

Coefficients:
            Estimate Std. Error t value Pr(>|t|)
(Intercept)  6.00058    0.22627  26.519 7.45e-10 ***
Total_ATT   -0.03111    0.05216  -0.597    0.566
---
Signif. codes:  0 ‘***’ 0.001 ‘**’ 0.01 ‘*’ 0.05 ‘.’ 0.1 ‘ ’ 1

(Dispersion parameter for Gamma family taken to be 0.0623289)

    Null deviance: 0.65028  on 10  degrees of freedom
Residual deviance: 0.62564  on  9  degrees of freedom
AIC: 134.37

Number of Fisher Scoring iterations: 5

>
> residuals_VVD <- residuals(glm_VVD, type = "pearson")
>
> hist(residuals_VVD,
+      main = "Histogram of Residuals for VVD (Group T)",
+      xlab = "Residuals",
+      ylab = "Frequency",
+      col = "lightblue",
+      border = "black",
+      prob = TRUE)
> curve(dnorm(x, mean = mean(residuals_VVD, na.rm = TRUE),
+             sd = sd(residuals_VVD, na.rm = TRUE)),
+       col = "blue", lwd = 2, add = TRUE)

> exp(cbind(
+   Estimate = coef(glm_VVD),
+   confint.default(glm_VVD)
+ ))
                Estimate       2.5 %
(Intercept) 403.6646461 259.0706237
Total_ATT     0.9693651   0.8751618
                97.5 %
(Intercept) 628.960336
Total_ATT     1.073708
```

```
>

RBC_filling
> glm_RBC_filling <- glm(RBC_filling ~ Total_ATT,
+                        data = subset_data_T,
+                        family = Gamma(link = "log"))
> summary(glm_RBC_filling)

Call:
glm(formula = RBC_filling ~ Total_ATT, family = Gamma(link = "log"),
    data = subset_data_T)

Coefficients:
            Estimate Std. Error t value Pr(>|t|)
(Intercept) -0.59168    0.12805  -4.621  0.00125 **
Total_ATT    0.01322    0.02952   0.448  0.66492
---
Signif. codes:  0 ‘***’ 0.001 ‘**’ 0.01 ‘*’ 0.05 ‘.’ 0.1 ‘ ’ 1

(Dispersion parameter for Gamma family taken to be 0.01996133)

    Null deviance: 0.17699  on 10  degrees of freedom
Residual deviance: 0.17322  on  9  degrees of freedom
AIC: -20.417

Number of Fisher Scoring iterations: 4

>
> residuals_RBC_filling <- residuals(glm_RBC_filling, type = "pearson")
>
> hist(residuals_RBC_filling,
+      main = "Histogram of Residuals for RBC_filling (Group T)",
+      xlab = "Residuals",
+      ylab = "Frequency",
+      col = "lightblue",
+      border = "black",
+      prob = TRUE)
> curve(dnorm(x, mean = mean(residuals_RBC_filling, na.rm = TRUE),
+             sd = sd(residuals_RBC_filling, na.rm = TRUE)),
+       col = "blue", lwd = 2, add = TRUE)
>

> exp(cbind(
+   Estimate = coef(glm_RBC_filling),
+   confint.default(glm_RBC_filling)
+ ))
            Estimate     2.5 %    97.5 %
(Intercept) 0.553398 0.4305674 0.7112691
Total_ATT   1.013304 0.9563434 1.0736577

 Median_P50
> glm_Median_P50 <- glm(Median_P50 ~ Total_ATT,
+                       data = subset_data_T,
+                       family = Gamma(link = "log"))
> summary(glm_Median_P50)

Call:
glm(formula = Median_P50 ~ Total_ATT, family = Gamma(link = "log"),
    data = subset_data_T)

Coefficients:
            Estimate Std. Error t value Pr(>|t|)
(Intercept)  2.27506    0.13229  17.197 3.42e-08 ***
Total_ATT   -0.03826    0.03050  -1.255    0.241
---
Signif. codes:  0 ‘***’ 0.001 ‘**’ 0.01 ‘*’ 0.05 ‘.’ 0.1 ‘ ’ 1

(Dispersion parameter for Gamma family taken to be 0.02130641)
```

```
    Null deviance: 0.23340  on 10  degrees of freedom
Residual deviance: 0.19776  on  9  degrees of freedom
AIC: 39.455

Number of Fisher Scoring iterations: 4

>
> residuals_Median_P50 <- residuals(glm_Median_P50, type = "pearson")
>
> hist(residuals_Median_P50,
+      main = "Histogram of Residuals for Median_P50 (Group T)",
+      xlab = "Residuals",
+      ylab = "Frequency",
+      col = "lightblue",
+      border = "black",
+      prob = TRUE)
> curve(dnorm(x, mean = mean(residuals_Median_P50, na.rm = TRUE),
+             sd = sd(residuals_Median_P50, na.rm = TRUE)),
+       col = "blue", lwd = 2, add = TRUE)
>

> exp(cbind(
+   Estimate = coef(glm_Median_P50),
+   confint.default(glm_Median_P50)
+ ))
             Estimate     2.5 %    97.5 %
(Intercept) 9.7284791 7.5064761 12.608220
Total_ATT   0.9624615 0.9066186  1.021744


PBR525
> glm_PBR525 <- glm(PBR525 ~ Total_ATT,
+                   data = subset_data_T,
+                   family = Gamma(link = "log"))
> summary(glm_PBR525)

Call:
glm(formula = PBR525 ~ Total_ATT, family = Gamma(link = "log"),
    data = subset_data_T)

Coefficients:
             Estimate Std. Error t value Pr(>|t|)
(Intercept)  0.993916   0.079714  12.468 5.55e-07 ***
Total_ATT   -0.009211   0.018376  -0.501    0.628
---
Signif. codes:  0 ‘***’ 0.001 ‘**’ 0.01 ‘*’ 0.05 ‘.’ 0.1 ‘ ’ 1

(Dispersion parameter for Gamma family taken to be 0.007735741)

    Null deviance: 0.072208  on 10  degrees of freedom
Residual deviance: 0.070175  on  9  degrees of freedom
AIC: 2.594

Number of Fisher Scoring iterations: 4

>
> residuals_PBR525 <- residuals(glm_PBR525, type = "pearson")
>
> hist(residuals_PBR525,
+      main = "Histogram of Residuals for PBR525 (Group T)",
+      xlab = "Residuals",
+      ylab = "Frequency",
+      col = "lightblue",
+      border = "black",
+      prob = TRUE)
> curve(dnorm(x, mean = mean(residuals_PBR525, na.rm = TRUE),
+             sd = sd(residuals_PBR525, na.rm = TRUE)),
+       col = "blue", lwd = 2, add = TRUE)
```

```
>

> exp(cbind(
+   Estimate = coef(glm_PBR525),
+   confint.default(glm_PBR525)
+ ))
             Estimate     2.5 %   97.5 %
(Intercept) 2.7017950 2.3109977 3.158677
Total_ATT   0.9908312 0.9557804 1.027167


PBR59
> glm_PBR59 <- glm(PBR59 ~ Total_ATT,
+                  data = subset_data_T,
+                  family = Gamma(link = "log"))
> summary(glm_PBR59)

Call:
glm(formula = PBR59 ~ Total_ATT, family = Gamma(link = "log"),
    data = subset_data_T)

Coefficients:
             Estimate Std. Error t value Pr(>|t|)
(Intercept)  0.310531   0.124237   2.500   0.0339 *
Total_ATT   -0.003707   0.028639  -0.129   0.8998
---
Signif. codes:  0 ‘***’ 0.001 ‘**’ 0.01 ‘*’ 0.05 ‘.’ 0.1 ‘ ’ 1

(Dispersion parameter for Gamma family taken to be 0.01879031)

    Null deviance: 0.18533  on 10  degrees of freedom
Residual deviance: 0.18499  on  9  degrees of freedom
AIC: -1.3786

Number of Fisher Scoring iterations: 4

>
> residuals_PBR59 <- residuals(glm_PBR59, type = "pearson")
>
> hist(residuals_PBR59,
+      main = "Histogram of Residuals for PBR59 (Group T)",
+      xlab = "Residuals",
+      ylab = "Frequency",
+      col = "lightblue",
+      border = "black",
+      prob = TRUE)
> curve(dnorm(x, mean = mean(residuals_PBR59, na.rm = TRUE),
+             sd = sd(residuals_PBR59, na.rm = TRUE)),
+       col = "blue", lwd = 2, add = TRUE)
>

> exp(cbind(
+   Estimate = coef(glm_PBR59),
+   confint.default(glm_PBR59)
+ ))
             Estimate     2.5 %   97.5 %
(Intercept) 1.3641495 1.0693282 1.740255
Total_ATT   0.9962994 0.9419156 1.053823


PBR1019
> glm_PBR1019 <- glm(PBR1019 ~ Total_ATT,
+                    data = subset_data_T,
+                    family = Gamma(link = "log"))
> summary(glm_PBR1019)

Call:
glm(formula = PBR1019 ~ Total_ATT, family = Gamma(link = "log"),
    data = subset_data_T)
```

```
Coefficients:
            Estimate Std. Error t value Pr(>|t|)
(Intercept)  1.12828    0.05791  19.483 1.14e-08 ***
Total_ATT   -0.00544    0.01335  -0.407    0.693
---
Signif. codes:  0 ‘***’ 0.001 ‘**’ 0.01 ‘*’ 0.05 ‘.’ 0.1 ‘ ’ 1

(Dispersion parameter for Gamma family taken to be 0.0040827)

    Null deviance: 0.037542  on 10  degrees of freedom
Residual deviance: 0.036842  on  9  degrees of freedom
AIC: -1.1705

Number of Fisher Scoring iterations: 4

>
> residuals_PBR1019 <- residuals(glm_PBR1019, type = "pearson")
>
> hist(residuals_PBR1019,
+      main = "Histogram of Residuals for PBR1019 (Group T)",
+      xlab = "Residuals",
+      ylab = "Frequency",
+      col = "lightblue",
+      border = "black",
+      prob = TRUE)
> curve(dnorm(x, mean = mean(residuals_PBR1019, na.rm = TRUE),
+             sd = sd(residuals_PBR1019, na.rm = TRUE)),
+       col = "blue", lwd = 2, add = TRUE)
>

> exp(cbind(
+   Estimate = coef(glm_PBR1019),
+   confint.default(glm_PBR1019)
+ ))
            Estimate     2.5 %   97.5 %
(Intercept) 3.090340 2.7587519 3.461784
Total_ATT   0.994575 0.9688896 1.020941


PBR2025
> glm_PBR2025 <- glm(PBR2025 ~ Total_ATT,
+                    data = subset_data_T,
+                    family = Gamma(link = "log"))
> summary(glm_PBR2025)

Call:
glm(formula = PBR2025 ~ Total_ATT, family = Gamma(link = "log"),
    data = subset_data_T)

Coefficients:
            Estimate Std. Error t value Pr(>|t|)
(Intercept)  1.18286    0.11615  10.184 3.07e-06 ***
Total_ATT   -0.01594    0.02677  -0.595    0.566
---
Signif. codes:  0 ‘***’ 0.001 ‘**’ 0.01 ‘*’ 0.05 ‘.’ 0.1 ‘ ’ 1

(Dispersion parameter for Gamma family taken to be 0.01642222)

    Null deviance: 0.15475  on 10  degrees of freedom
Residual deviance: 0.14862  on  9  degrees of freedom
AIC: 14.334

Number of Fisher Scoring iterations: 4

>
> residuals_PBR2025 <- residuals(glm_PBR2025, type = "pearson")
>
> hist(residuals_PBR2025,
```

```
+      main = "Histogram of Residuals for PBR2025 (Group T)",
+      xlab = "Residuals",
+      ylab = "Frequency",
+      col = "lightblue",
+      border = "black",
+      prob = TRUE)
> curve(dnorm(x, mean = mean(residuals_PBR2025, na.rm = TRUE),
+             sd = sd(residuals_PBR2025, na.rm = TRUE)),
+       col = "blue", lwd = 2, add = TRUE)

> exp(cbind(
+   Estimate = coef(glm_PBR2025),
+   confint.default(glm_PBR2025)
+ ))
             Estimate    2.5 %   97.5 %
(Intercept) 3.2636920 2.599239 4.098001
Total_ATT   0.9841843 0.933870 1.037209
```

Effects of PCV

```
> Glycoheck_clinical_study_dataset_for_stats$PCV <-
as.numeric(as.character(Glycoheck_clinical_study_dataset_for_stats$PCV))
Warning message:
NAs introduced by coercion
```

VVD

```
> glm_VVD <- glm(VVD ~ PCV,
+                data = Glycoheck_clinical_study_dataset_for_stats,
+                family = Gamma(link = "log"))
> summary(glm_VVD)

Call:
glm(formula = VVD ~ PCV, family = Gamma(link = "log"), data =
Glycoheck_clinical_study_dataset_for_stats)

Coefficients:
            Estimate Std. Error t value Pr(>|t|)
(Intercept) 5.451805   0.235677  23.133    1e-13 ***
PCV         0.015037   0.006879   2.186    0.044 *
---
Signif. codes:  0 ‘***’ 0.001 ‘**’ 0.01 ‘*’ 0.05 ‘.’ 0.1 ‘ ’ 1

(Dispersion parameter for Gamma family taken to be 0.08142635)

    Null deviance: 1.6208  on 17  degrees of freedom
Residual deviance: 1.2648  on 16  degrees of freedom
  (1 observation deleted due to missingness)
AIC: 222.27

Number of Fisher Scoring iterations: 4

>
> residuals_VVD <- residuals(glm_VVD, type = "pearson")
>
> hist(residuals_VVD,
+      main = "Histogram of Residuals for VVD",
+      xlab = "Residuals",
+      ylab = "Frequency",
+      col = "lightblue",
+      border = "black",
+      prob = TRUE)
> curve(dnorm(x, mean = mean(residuals_VVD, na.rm = TRUE),
+             sd = sd(residuals_VVD, na.rm = TRUE)),
+       col = "blue", lwd = 2, add = TRUE)

> exp(cbind(
+   Estimate = coef(glm_VVD),
```

```
+   confint.default(glm_VVD)
+ ))
              Estimate      2.5 %
(Intercept) 233.178637 146.919725
PCV           1.015151   1.001555
              97.5 %
(Intercept) 370.081532
PCV           1.028931

> confint(glm_VVD)
Waiting for profiling to be done...                      2.5 %     97.5 %
(Intercept) 4.9837266953 5.94099603
PCV         0.0009473079 0.02897528
```

RBC_filling

```
> glm_RBC_filling <- glm(RBC_filling ~ PCV,
+                        data =
Glycoheck_clinical_study_dataset_for_stats,
+                        family = Gamma(link = "log"))
> summary(glm_RBC_filling)

Call:
glm(formula = RBC_filling ~ PCV, family = Gamma(link = "log"),
    data = Glycoheck_clinical_study_dataset_for_stats)

Coefficients:
             Estimate Std. Error t value Pr(>|t|)
(Intercept) -0.675719   0.114263  -5.914 2.18e-05 ***
PCV          0.004197   0.003335   1.258    0.226
---
Signif. codes:  0 ‘***’ 0.001 ‘**’ 0.01 ‘*’ 0.05 ‘.’ 0.1 ‘ ’ 1

(Dispersion parameter for Gamma family taken to be 0.01913982)

    Null deviance: 0.33353  on 17  degrees of freedom
Residual deviance: 0.30408  on 16  degrees of freedom
  (1 observation deleted due to missingness)
AIC: -35.991

Number of Fisher Scoring iterations: 4

>
> residuals_RBC_filling <- residuals(glm_RBC_filling, type = "pearson")
>
> hist(residuals_RBC_filling,
+      main = "Histogram of Residuals for RBC_filling",
+      xlab = "Residuals",
+      ylab = "Frequency",
+      col = "lightblue",
+      border = "black",
+      prob = TRUE)
> curve(dnorm(x, mean = mean(residuals_RBC_filling, na.rm = TRUE),
+             sd = sd(residuals_RBC_filling, na.rm = TRUE)),
+       col = "blue", lwd = 2, add = TRUE)

> exp(cbind(
+   Estimate = coef(glm_RBC_filling),
+   confint.default(glm_RBC_filling)
+ ))
             Estimate     2.5 %    97.5 %
(Intercept) 0.5087902 0.4067039 0.6365011
PCV         1.0042060 0.9976628 1.0107922

>
```

Median_P50

```
> glm_Median_P50 <- glm(Median_P50 ~ PCV,
```

```
+                       data = Glycoheck_clinical_study_dataset_for_stats,
+                       family = Gamma(link = "log"))
> summary(glm_Median_P50)

Call:
glm(formula = Median_P50 ~ PCV, family = Gamma(link = "log"),
    data = Glycoheck_clinical_study_dataset_for_stats)

Coefficients:
             Estimate Std. Error t value Pr(>|t|)
(Intercept)  2.239665   0.113415   19.75 1.16e-12 ***
PCV         -0.004007   0.003311   -1.21    0.244
---
Signif. codes:  0 ‘***’ 0.001 ‘**’ 0.01 ‘*’ 0.05 ‘.’ 0.1 ‘ ’ 1

(Dispersion parameter for Gamma family taken to be 0.01885681)

    Null deviance: 0.33247  on 17  degrees of freedom
Residual deviance: 0.30543  on 16  degrees of freedom
  (1 observation deleted due to missingness)
AIC: 59.344

Number of Fisher Scoring iterations: 4

>
> residuals_Median_P50 <- residuals(glm_Median_P50, type = "pearson")
>
> hist(residuals_Median_P50,
+      main = "Histogram of Residuals for Median_P50",
+      xlab = "Residuals",
+      ylab = "Frequency",
+      col = "lightblue",
+      border = "black",
+      prob = TRUE)
> curve(dnorm(x, mean = mean(residuals_Median_P50, na.rm = TRUE),
+             sd = sd(residuals_Median_P50, na.rm = TRUE)),
+       col = "blue", lwd = 2, add = TRUE)

> exp(cbind(
+   Estimate = coef(glm_Median_P50),
+   confint.default(glm_Median_P50)
+ ))
             Estimate     2.5 %    97.5 %
(Intercept) 9.3901887 7.5185770 11.727704
PCV         0.9960014 0.9895596  1.002485

>
```

PBR525

```
> glm_PBR525 <- glm(PBR525 ~ PCV,
+                   data = Glycoheck_clinical_study_dataset_for_stats,
+                   family = Gamma(link = "log"))
> summary(glm_PBR525)

Call:
glm(formula = PBR525 ~ PCV, family = Gamma(link = "log"), data =
Glycoheck_clinical_study_dataset_for_stats)

Coefficients:
             Estimate Std. Error t value Pr(>|t|)
(Intercept)  0.987703   0.073182  13.497 3.68e-10 ***
PCV         -0.000882   0.002136  -0.413    0.685
---
Signif. codes:  0 ‘***’ 0.001 ‘**’ 0.01 ‘*’ 0.05 ‘.’ 0.1 ‘ ’ 1

(Dispersion parameter for Gamma family taken to be 0.007851244)

    Null deviance: 0.12568  on 17  degrees of freedom
Residual deviance: 0.12433  on 16  degrees of freedom
```

```
  (1 observation deleted due to missingness)
AIC: 1.9399

Number of Fisher Scoring iterations: 3

>
> residuals_PBR525 <- residuals(glm_PBR525, type = "pearson")
>
> hist(residuals_PBR525,
+      main = "Histogram of Residuals for PBR525",
+      xlab = "Residuals",
+      ylab = "Frequency",
+      col = "lightblue",
+      border = "black",
+      prob = TRUE)
> curve(dnorm(x, mean = mean(residuals_PBR525, na.rm = TRUE),
+             sd = sd(residuals_PBR525, na.rm = TRUE)),
+       col = "blue", lwd = 2, add = TRUE)
>

> exp(cbind(
+   Estimate = coef(glm_PBR525),
+   confint.default(glm_PBR525)
+ ))
             Estimate    2.5 %   97.5 %
(Intercept) 2.6850608 2.326278 3.099179
PCV         0.9991184 0.994944 1.003310
```

PBR59

```
> glm_PBR59 <- glm(PBR59 ~ PCV,
+                  data = Glycoheck_clinical_study_dataset_for_stats,
+                  family = Gamma(link = "log"))
> summary(glm_PBR59)

Call:
glm(formula = PBR59 ~ PCV, family = Gamma(link = "log"), data =
Glycoheck_clinical_study_dataset_for_stats)

Coefficients:
             Estimate Std. Error t value Pr(>|t|)
(Intercept)  3.219e-01  9.519e-02   3.382  0.00381 **
PCV         -7.221e-05  2.779e-03  -0.026  0.97959
---
Signif. codes:  0 ‘***’ 0.001 ‘**’ 0.01 ‘*’ 0.05 ‘.’ 0.1 ‘ ’ 1

(Dispersion parameter for Gamma family taken to be 0.01328458)

    Null deviance: 0.23343  on 17  degrees of freedom
Residual deviance: 0.23342  on 16  degrees of freedom
  (1 observation deleted due to missingness)
AIC: -9.8248

Number of Fisher Scoring iterations: 4

>
> residuals_PBR59 <- residuals(glm_PBR59, type = "pearson")
>
> hist(residuals_PBR59,
+      main = "Histogram of Residuals for PBR59",
+      xlab = "Residuals",
+      ylab = "Frequency",
+      col = "lightblue",
+      border = "black",
+      prob = TRUE)
> curve(dnorm(x, mean = mean(residuals_PBR59, na.rm = TRUE),
+             sd = sd(residuals_PBR59, na.rm = TRUE)),
+       col = "blue", lwd = 2, add = TRUE)
```

```
> exp(cbind(
+   Estimate = coef(glm_PBR59),
+   confint.default(glm_PBR59)
+ ))
             Estimate     2.5 %   97.5 %
(Intercept) 1.3797484 1.1449085 1.662758
PCV         0.9999278 0.9944968 1.005388

>
```

PBR1019

```
> glm_PBR1019 <- glm(PBR1019 ~ PCV,
+                    data = Glycoheck_clinical_study_dataset_for_stats,
+                    family = Gamma(link = "log"))
> summary(glm_PBR1019)

Call:
glm(formula = PBR1019 ~ PCV, family = Gamma(link = "log"), data =
Glycoheck_clinical_study_dataset_for_stats)

Coefficients:
              Estimate Std. Error t value Pr(>|t|)
(Intercept)  1.1154077  0.0643281  17.339 8.54e-12 ***
PCV         -0.0003093  0.0018778  -0.165    0.871
---
Signif. codes:  0 ‘***’ 0.001 ‘**’ 0.01 ‘*’ 0.05 ‘.’ 0.1 ‘ ’ 1

(Dispersion parameter for Gamma family taken to be 0.006066403)

    Null deviance: 0.095729  on 17  degrees of freedom
Residual deviance: 0.095562  on 16  degrees of freedom
  (1 observation deleted due to missingness)
AIC: 2.5009

Number of Fisher Scoring iterations: 4

>
> residuals_PBR1019 <- residuals(glm_PBR1019, type = "pearson")
>
> hist(residuals_PBR1019,
+      main = "Histogram of Residuals for PBR1019",
+      xlab = "Residuals",
+      ylab = "Frequency",
+      col = "lightblue",
+      border = "black",
+      prob = TRUE)
> curve(dnorm(x, mean = mean(residuals_PBR1019, na.rm = TRUE),
+             sd = sd(residuals_PBR1019, na.rm = TRUE)),
+       col = "blue", lwd = 2, add = TRUE)
>
> exp(cbind(
+   Estimate = coef(glm_PBR1019),
+   confint.default(glm_PBR1019)
+ ))
             Estimate     2.5 %   97.5 %
(Intercept) 3.0508116 2.6894239 3.460760
PCV         0.9996907 0.9960183 1.003377
```

PBR2025

```
> glm_PBR2025 <- glm(PBR2025 ~ PCV,
+                    data = Glycoheck_clinical_study_dataset_for_stats,
+                    family = Gamma(link = "log"))
> summary(glm_PBR2025)

Call:
glm(formula = PBR2025 ~ PCV, family = Gamma(link = "log"), data =
Glycoheck_clinical_study_dataset_for_stats)
```

```
Coefficients:
             Estimate Std. Error t value Pr(>|t|)
(Intercept)  1.196738   0.103576  11.554 3.55e-09 ***
PCV         -0.002453   0.003023  -0.811    0.429
---
Signif. codes:  0 ‘***’ 0.001 ‘**’ 0.01 ‘*’ 0.05 ‘.’ 0.1 ‘ ’ 1

(Dispersion parameter for Gamma family taken to be 0.0157271)

    Null deviance: 0.27138  on 17  degrees of freedom
Residual deviance: 0.26104  on 16  degrees of freedom
  (1 observation deleted due to missingness)
AIC: 20.845

Number of Fisher Scoring iterations: 4

>
> residuals_PBR2025 <- residuals(glm_PBR2025, type = "pearson")
>
> hist(residuals_PBR2025,
+      main = "Histogram of Residuals for PBR2025",
+      xlab = "Residuals",
+      ylab = "Frequency",
+      col = "lightblue",
+      border = "black",
+      prob = TRUE)
> curve(dnorm(x, mean = mean(residuals_PBR2025, na.rm = TRUE),
+             sd = sd(residuals_PBR2025, na.rm = TRUE)),
+       col = "blue", lwd = 2, add = TRUE)

> exp(cbind(
+   Estimate = coef(glm_PBR2025),
+   confint.default(glm_PBR2025)
+ ))
             Estimate    2.5 %   97.5 %
(Intercept) 3.3093045 2.701299 4.054159
PCV         0.9975497 0.991656 1.003479
```

GlycoCheck vs clinical variables – linear models

```
> Glycoheck_clinical_study_dataset_for_stats <- read_excel("~/Scientific p
rojects/Glycocalyx/Glycocheck 2023/Glycocalyx clinical study/Raw data/Glyc
oheck_clinical_study_dataset_for_stats.xlsx")
> View(Glycoheck_clinical_study_dataset_for_stats)
```

VVD

```
> lm_VVD <- lm(VVD ~ Group + APPLE_fast + LOH,
+              data = Glycoheck_clinical_study_dataset_for_stats)
> summary(lm_VVD)

Call:
lm(formula = VVD ~ Group + APPLE_fast + LOH, data = Glycoheck_clinical_stu
dy_dataset_for_stats)

Residuals:
     Min       1Q   Median       3Q      Max
-146.731  -44.282   -3.931   56.662  243.659

Coefficients:
            Estimate Std. Error t value Pr(>|t|)
(Intercept)  394.969    107.891   3.661  0.00232 **
GroupT       -99.710     51.282  -1.944  0.07085 .
APPLE_fast     6.200      5.821   1.065  0.30368
LOH          -14.692      8.564  -1.716  0.10682
---
Signif. codes:  0 ‘***’ 0.001 ‘**’ 0.01 ‘*’ 0.05 ‘.’ 0.1 ‘ ’ 1
```

```
Residual standard error: 104.5 on 15 degrees of freedom
Multiple R-squared:  0.2763,   Adjusted R-squared:  0.1316
F-statistic: 1.909 on 3 and 15 DF,  p-value: 0.1715


> residuals_VVD <- residuals(lm_VVD)
> shapiro.test(residuals_VVD)

        Shapiro-Wilk normality test

data:  residuals_VVD
W = 0.92867, p-value = 0.1637

>
> hist(residuals_VVD,
+      main = "Histogram of Residuals for VVD",
+      xlab = "Residuals",
+      ylab = "Frequency",
+      col = "lightblue",
+      border = "black",
+      prob = TRUE)
> curve(dnorm(x, mean = mean(residuals_VVD, na.rm = TRUE),
+             sd = sd(residuals_VVD, na.rm = TRUE)),
+       col = "blue", lwd = 2, add = TRUE)

> #CI
> confint(lm_VVD, level = 0.95)
                2.5 %     97.5 %
(Intercept)  165.004906 624.932837
GroupT      -209.014965   9.595799
APPLE_fast    -6.207729  18.608359
LOH          -32.944797   3.561772


RBC filling
> lm_RBC_filling <- lm(RBC_filling ~ Group + APPLE_fast + LOH,
+                      data = Glycoheck_clinical_study_dataset_for_stats)
> summary(lm_RBC_filling)

Call:
lm(formula = RBC_filling ~ Group + APPLE_fast + LOH, data = Glycoheck_clin
ical_study_dataset_for_stats)

Residuals:
      Min        1Q    Median        3Q       Max
-0.142852 -0.056215  0.001938  0.045186  0.146359

Coefficients:
             Estimate Std. Error t value Pr(>|t|)
(Intercept)  0.5939571  0.0884358   6.716 6.91e-06 ***
GroupT      -0.0120553  0.0420349  -0.287    0.778
APPLE_fast   0.0009034  0.0047717   0.189    0.852
LOH         -0.0042379  0.0070195  -0.604    0.555
---
Signif. codes:  0 ‘***’ 0.001 ‘**’ 0.01 ‘*’ 0.05 ‘.’ 0.1 ‘ ’ 1

Residual standard error: 0.08569 on 15 degrees of freedom
Multiple R-squared:  0.02489,  Adjusted R-squared:  -0.1701
F-statistic: 0.1276 on 3 and 15 DF,  p-value: 0.9422

> residuals_RBC_filling <- residuals(lm_RBC_filling)
> shapiro.test(residuals_RBC_filling)

        Shapiro-Wilk normality test

data:  residuals_RBC_filling
W = 0.96963, p-value = 0.769
```

```
>
> hist(residuals_RBC_filling,
+      main = "Histogram of Residuals for RBC_filling",
+      xlab = "Residuals",
+      ylab = "Frequency",
+      col = "lightblue",
+      border = "black",
+      prob = TRUE)
> curve(dnorm(x, mean = mean(residuals_RBC_filling, na.rm = TRUE),
+             sd = sd(residuals_RBC_filling, na.rm = TRUE)),
+       col = "blue", lwd = 2, add = TRUE)

> #CI
> confint(lm_RBC_filling, level = 0.95)
                   2.5 %     97.5 %
(Intercept)  0.405460694 0.78245346
GroupT      -0.101650469 0.07753995
APPLE_fast  -0.009267218 0.01107398
LOH         -0.019199727 0.01072390


Median P50
> lm_Median_P50 <- lm(Median_P50 ~ Group + APPLE_fast + LOH,
+               data = Glycoheck_clinical_study_dataset_for_stats)
> summary(lm_Median_P50)

Call:
lm(formula = Median_P50 ~ Group + APPLE_fast + LOH, data = Glycoheck_clini
cal_study_dataset_for_stats)

Residuals:
     Min       1Q   Median       3Q      Max
-1.75279 -0.80006  0.04269  0.32181  2.18400

Coefficients:
             Estimate Std. Error t value Pr(>|t|)
(Intercept)  8.466383   1.263868   6.699 7.12e-06 ***
GroupT       0.194759   0.600736   0.324    0.750
APPLE_fast  -0.020149   0.068194  -0.295    0.772
LOH          0.005065   0.100319   0.050    0.960
---
Signif. codes:  0 ‘***’ 0.001 ‘**’ 0.01 ‘*’ 0.05 ‘.’ 0.1 ‘ ’ 1

Residual standard error: 1.225 on 15 degrees of freedom
Multiple R-squared:  0.01258,  Adjusted R-squared:  -0.1849
F-statistic: 0.06368 on 3 and 15 DF,  p-value: 0.9782

> residuals_Median_P50 <- residuals(lm_Median_P50)
> shapiro.test(residuals_Median_P50)

        Shapiro-Wilk normality test

data:  residuals_Median_P50
W = 0.94892, p-value = 0.3787

>
> hist(residuals_Median_P50,
+      main = "Histogram of Residuals for Median_P50",
+      xlab = "Residuals",
+      ylab = "Frequency",
+      col = "lightblue",
+      border = "black",
+      prob = TRUE)
> curve(dnorm(x, mean = mean(residuals_Median_P50, na.rm = TRUE),
+             sd = sd(residuals_Median_P50, na.rm = TRUE)),
+       col = "blue", lwd = 2, add = TRUE)

> #CI
> confint(lm_Median_P50, level = 0.95)
```

```
                 2.5 %     97.5 %
(Intercept)  5.7725125 11.1602534
GroupT      -1.0856792  1.4751963
APPLE_fast  -0.1655012  0.1252023
LOH         -0.2087599  0.2188896


PBR525
> lm_PBR525 <- lm(PBR525 ~ Group + APPLE_fast + LOH,
+               data = Glycoheck_clinical_study_dataset_for_stats)
> summary(lm_PBR525)

Call:
lm(formula = PBR525 ~ Group + APPLE_fast + LOH, data = Glycoheck_clinical_
study_dataset_for_stats)

Residuals:
     Min       1Q   Median       3Q      Max
-0.32125 -0.14881 -0.07358  0.14838  0.41612

Coefficients:
            Estimate Std. Error t value Pr(>|t|)
(Intercept) 2.443161   0.244775   9.981 5.12e-08 ***
GroupT      0.004385   0.116345   0.038    0.970
APPLE_fast  0.008402   0.013207   0.636    0.534
LOH         0.003550   0.019429   0.183    0.857
---
Signif. codes:  0 ‘***’ 0.001 ‘**’ 0.01 ‘*’ 0.05 ‘.’ 0.1 ‘ ’ 1

Residual standard error: 0.2372 on 15 degrees of freedom
Multiple R-squared:  0.0315,   Adjusted R-squared:  -0.1622
F-statistic: 0.1626 on 3 and 15 DF,  p-value: 0.9198


> residuals_PBR525 <- residuals(lm_PBR525)
> shapiro.test(residuals_PBR525)

        Shapiro-Wilk normality test

data:  residuals_PBR525
W = 0.93523, p-value = 0.216

>
> hist(residuals_PBR525,
+      main = "Histogram of Residuals for PBR525",
+      xlab = "Residuals",
+      ylab = "Frequency",
+      col = "lightblue",
+      border = "black",
+      prob = TRUE)
> curve(dnorm(x, mean = mean(residuals_PBR525, na.rm = TRUE),
+             sd = sd(residuals_PBR525, na.rm = TRUE)),
+       col = "blue", lwd = 2, add = TRUE)


> #CI
> confint(lm_PBR525, level = 0.95)
                 2.5 %     97.5 %
(Intercept)  1.92143596 2.96488547
GroupT      -0.24359911 0.25236836
APPLE_fast  -0.01974811 0.03655274
LOH         -0.03786167 0.04496166


PBR 59
> lm_PBR59 <- lm(PBR59 ~ Group + APPLE_fast + LOH,
+               data = Glycoheck_clinical_study_dataset_for_stats)
> summary(lm_PBR59)
```

```
Call:
lm(formula = PBR59 ~ Group + APPLE_fast + LOH, data = Glycoheck_clinical_s
tudy_dataset_for_stats)

Residuals:
     Min       1Q   Median       3Q      Max
-0.36125 -0.05652  0.01796  0.10011  0.22059

Coefficients:
             Estimate Std. Error t value Pr(>|t|)
(Intercept)  1.4562480  0.1622467   8.976 2.03e-07 ***
GroupT      -0.0877153  0.0771183  -1.137    0.273
APPLE_fast  -0.0009651  0.0087543  -0.110    0.914
LOH         -0.0027183  0.0128783  -0.211    0.836
---
Signif. codes:  0 ‘***’ 0.001 ‘**’ 0.01 ‘*’ 0.05 ‘.’ 0.1 ‘ ’ 1

Residual standard error: 0.1572 on 15 degrees of freedom
Multiple R-squared:  0.08228,  Adjusted R-squared:  -0.1013
F-statistic: 0.4483 on 3 and 15 DF,  p-value: 0.7222


> residuals_PBR59 <- residuals(lm_PBR59)
> shapiro.test(residuals_PBR59)

        Shapiro-Wilk normality test

data:  residuals_PBR59
W = 0.95038, p-value = 0.4012

>
> hist(residuals_PBR59,
+      main = "Histogram of Residuals for PBR59",
+      xlab = "Residuals",
+      ylab = "Frequency",
+      col = "lightblue",
+      border = "black",
+      prob = TRUE)
> curve(dnorm(x, mean = mean(residuals_PBR59, na.rm = TRUE),
+             sd = sd(residuals_PBR59, na.rm = TRUE)),
+       col = "blue", lwd = 2, add = TRUE)

> #CI
> confint(lm_PBR59, level = 0.95)
                  2.5 %     97.5 %
(Intercept)  1.11042729 1.80206865
GroupT      -0.25208916 0.07665853
APPLE_fast  -0.01962436 0.01769417
LOH         -0.03016762 0.02473109



PBR1019
> lm_PBR1019 <- lm(PBR1019 ~ Group + APPLE_fast + LOH,
+              data = Glycoheck_clinical_study_dataset_for_stats)
> summary(lm_PBR1019)

Call:
lm(formula = PBR1019 ~ Group + APPLE_fast + LOH, data = Glycoheck_clinical
_study_dataset_for_stats)

Residuals:
     Min       1Q   Median       3Q      Max
-0.30367 -0.17069 -0.02806  0.12863  0.41671

Coefficients:
            Estimate Std. Error t value Pr(>|t|)
(Intercept) 2.909292   0.248114  11.726 5.93e-09 ***
GroupT      0.033054   0.117932   0.280    0.783
```

```
APPLE_fast  0.002825   0.013387   0.211    0.836
LOH         0.010286   0.019694   0.522    0.609
---
Signif. codes:  0 ‘***’ 0.001 ‘**’ 0.01 ‘*’ 0.05 ‘.’ 0.1 ‘ ’ 1

Residual standard error: 0.2404 on 15 degrees of freedom
Multiple R-squared:  0.0245,   Adjusted R-squared:  -0.1706
F-statistic: 0.1256 on 3 and 15 DF,  p-value: 0.9435


> residuals_PBR1019 <- residuals(lm_PBR1019)
> shapiro.test(residuals_PBR1019)

        Shapiro-Wilk normality test

data:  residuals_PBR1019
W = 0.94168, p-value = 0.2827

>
> hist(residuals_PBR1019,
+      main = "Histogram of Residuals for PBR1019",
+      xlab = "Residuals",
+      ylab = "Frequency",
+      col = "lightblue",
+      border = "black",
+      prob = TRUE)
> curve(dnorm(x, mean = mean(residuals_PBR1019, na.rm = TRUE),
+             sd = sd(residuals_PBR1019, na.rm = TRUE)),
+       col = "blue", lwd = 2, add = TRUE)


> #CI
> confint(lm_PBR1019, level = 0.95)
                  2.5 %     97.5 %
(Intercept)  2.38045050 3.43813428
GroupT      -0.21831270 0.28442054
APPLE_fast  -0.02570923 0.03135966
LOH         -0.03169079 0.05226238



PBR525
> lm_PBR2025 <- lm(PBR2025 ~ Group + APPLE_fast + LOH,
+                  data = Glycoheck_clinical_study_dataset_for_stats)
> summary(lm_PBR2025)

Call:
lm(formula = PBR2025 ~ Group + APPLE_fast + LOH, data = Glycoheck_clinical
_study_dataset_for_stats)

Residuals:
     Min       1Q   Median       3Q      Max
-0.61557 -0.35139  0.01117  0.29533  0.66117

Coefficients:
            Estimate Std. Error t value Pr(>|t|)
(Intercept) 2.542722   0.406091   6.261 1.52e-05 ***
GroupT      0.062643   0.193021   0.325    0.750
APPLE_fast  0.025895   0.021911   1.182    0.256
LOH         0.003411   0.032233   0.106    0.917
---
Signif. codes:  0 ‘***’ 0.001 ‘**’ 0.01 ‘*’ 0.05 ‘.’ 0.1 ‘ ’ 1

Residual standard error: 0.3935 on 15 degrees of freedom
Multiple R-squared:  0.09573,  Adjusted R-squared:  -0.08512
F-statistic: 0.5293 on 3 and 15 DF,  p-value: 0.6689

> residuals_PBR2025 <- residuals(lm_PBR2025)
> shapiro.test(residuals_PBR2025)
```

```
        Shapiro-Wilk normality test

data:  residuals_PBR2025
W = 0.95122, p-value = 0.4144

>
> hist(residuals_PBR2025,
+      main = "Histogram of Residuals for PBR2025",
+      xlab = "Residuals",
+      ylab = "Frequency",
+      col = "lightblue",
+      border = "black",
+      prob = TRUE)
> curve(dnorm(x, mean = mean(residuals_PBR2025, na.rm = TRUE),
+             sd = sd(residuals_PBR2025, na.rm = TRUE)),
+       col = "blue", lwd = 2, add = TRUE)

> #CI
> confint(lm_PBR2025, level = 0.95)
                   2.5 %     97.5 %
(Intercept)  1.67715987 3.40828332
GroupT      -0.34877128 0.47405812
APPLE_fast  -0.02080728 0.07259803
LOH         -0.06529215 0.07211498
```

GlycoCheck vs IV fluid variables - Linear models

```
> subset_data <- subset(Glycoheck_clinical_study_dataset_for_stats,
IV_fluids_Y_N == "Y")

VVD
> lm_VVD <- lm(VVD ~ IV_fluids_rate + IV_fluids_duration +
IV_fluids_total,
+              data = subset_data)
>
> summary(lm_VVD)

Call:
lm(formula = VVD ~ IV_fluids_rate + IV_fluids_duration + IV_fluids_total,
    data = subset_data)

Residuals:
    Min      1Q  Median      3Q     Max
-107.15  -59.05  -12.19   67.21  134.03

Coefficients:
                  Estimate Std. Error t value Pr(>|t|)
(Intercept)        -33.1305   145.9701  -0.227   0.8280
IV_fluids_rate      28.7590     9.1348   3.148   0.0199 *
IV_fluids_duration  19.3932     8.2261   2.358   0.0565 .
IV_fluids_total     -1.2974     0.5447  -2.382   0.0546 .
---
Signif. codes:  0 ‘***’ 0.001 ‘**’ 0.01 ‘*’ 0.05 ‘.’ 0.1 ‘ ’ 1

Residual standard error: 104.4 on 6 degrees of freedom
Multiple R-squared:  0.6303,  Adjusted R-squared:  0.4454
F-statistic: 3.409 on 3 and 6 DF,  p-value: 0.09389

> residuals_VVD <- residuals(lm_VVD)
>
> shapiro.test(residuals_VVD)

      Shapiro-Wilk normality test
```

```
data:  residuals_VVD
W = 0.92205, p-value = 0.3744


> hist(residuals_VVD,
+      main = "Histogram of Residuals for VVD (Group Y)",
+      xlab = "Residuals",
+      ylab = "Frequency",
+      col = "lightblue",
+      border = "black",
+      prob = TRUE)
>
> curve(dnorm(x, mean = mean(residuals_VVD, na.rm = TRUE),
+             sd = sd(residuals_VVD, na.rm = TRUE)),
+       col = "blue", lwd = 2, add = TRUE)


RBC filling
> lm_RBC_filling <- lm(RBC_filling ~ IV_fluids_rate + IV_fluids_duration +
IV_fluids_total,
+              data = subset_data)
> summary(lm_RBC_filling)

Call:
lm(formula = RBC_filling ~ IV_fluids_rate + IV_fluids_duration +
    IV_fluids_total, data = subset_data)

Residuals:
     Min       1Q   Median       3Q      Max
-0.08624 -0.04170 -0.01628  0.01068  0.17852

Coefficients:
                    Estimate Std. Error t value Pr(>|t|)
(Intercept)         0.4214946  0.1260183   3.345   0.0155 *
IV_fluids_rate      0.0133548  0.0078863   1.693   0.1413
IV_fluids_duration  0.0058195  0.0071017   0.819   0.4439
IV_fluids_total    -0.0004660  0.0004703  -0.991   0.3600
---
Signif. codes:  0 ‘***’ 0.001 ‘**’ 0.01 ‘*’ 0.05 ‘.’ 0.1 ‘ ’ 1

Residual standard error: 0.09014 on 6 degrees of freedom
Multiple R-squared:  0.3981,  Adjusted R-squared:  0.09721
F-statistic: 1.323 on 3 and 6 DF,  p-value: 0.3514

> residuals_RBC_filling <- residuals(lm_RBC_filling)
>
> shapiro.test(residuals_RBC_filling)

      Shapiro-Wilk normality test

data:  residuals_RBC_filling
W = 0.84966, p-value = 0.05755

> hist(residuals_RBC_filling,
+      main = "Histogram of Residuals for RBC_filling (Group Y)",
+      xlab = "Residuals",
+      ylab = "Frequency",
+      col = "lightblue",
+      border = "black",
+      prob = TRUE)
>
> curve(dnorm(x, mean = mean(residuals_RBC_filling, na.rm = TRUE),
+             sd = sd(residuals_RBC_filling, na.rm = TRUE)),
+       col = "blue", lwd = 2, add = TRUE)

Median P50
> lm_Median_P50 <- lm(Median_P50 ~ IV_fluids_rate + IV_fluids_duration +
IV_fluids_total,
```

```
+              data = subset_data)
> summary(lm_Median_P50)

Call:
lm(formula = Median_P50 ~ IV_fluids_rate + IV_fluids_duration +
    IV_fluids_total, data = subset_data)

Residuals:
     Min       1Q   Median       3Q      Max
-1.09432 -0.26607 -0.05857  0.29582  0.83716

Coefficients:
                    Estimate Std. Error t value Pr(>|t|)
(Intercept)        10.816740   0.945579  11.439 2.68e-05 ***
IV_fluids_rate     -0.155693   0.059175  -2.631   0.0390 *
IV_fluids_duration -0.163159   0.053288  -3.062   0.0222 *
IV_fluids_total     0.009643   0.003529   2.733   0.0341 *
---
Signif. codes:  0 ‘***’ 0.001 ‘**’ 0.01 ‘*’ 0.05 ‘.’ 0.1 ‘ ’ 1

Residual standard error: 0.6764 on 6 degrees of freedom
Multiple R-squared:  0.615,   Adjusted R-squared:  0.4225
F-statistic: 3.195 on 3 and 6 DF,  p-value: 0.1051

> residuals_Median_P50 <- residuals(lm_Median_P50)
> shapiro.test(residuals_Median_P50)

      Shapiro-Wilk normality test

data:  residuals_Median_P50
W = 0.9629, p-value = 0.8184

> hist(residuals_Median_P50,
+      main = "Histogram of Residuals for Median_P50 (Group Y)",
+      xlab = "Residuals",
+      ylab = "Frequency",
+      col = "lightblue",
+      border = "black",
+      prob = TRUE)

> curve(dnorm(x, mean = mean(residuals_Median_P50, na.rm = TRUE),
+             sd = sd(residuals_Median_P50, na.rm = TRUE)),
+       col = "blue", lwd = 2, add = TRUE)



PBR525
> lm_PBR525 <- lm(PBR525 ~ IV_fluids_rate + IV_fluids_duration +
IV_fluids_total,
+              data = subset_data)
> summary(lm_PBR525)

Call:
lm(formula = PBR525 ~ IV_fluids_rate + IV_fluids_duration +
IV_fluids_total,
    data = subset_data)

Residuals:
     Min       1Q   Median       3Q      Max
-0.35738 -0.08553 -0.02319  0.08879  0.36206

Coefficients:
                     Estimate Std. Error t value Pr(>|t|)
(Intercept)         2.8261315  0.3347259   8.443 0.000151 ***
IV_fluids_rate     -0.0225727  0.0209472  -1.078 0.322618
IV_fluids_duration -0.0081065  0.0188634  -0.430 0.682384
IV_fluids_total     0.0008251  0.0012491   0.661 0.533398
---
```

```
Signif. codes:  0 ‘***’ 0.001 ‘**’ 0.01 ‘*’ 0.05 ‘.’ 0.1 ‘ ’ 1

Residual standard error: 0.2394 on 6 degrees of freedom
Multiple R-squared:  0.2414,  Adjusted R-squared:  -0.1378
F-statistic: 0.6366 on 3 and 6 DF,  p-value: 0.6184

> residuals_PBR525 <- residuals(lm_PBR525)

> shapiro.test(residuals_PBR525)

      Shapiro-Wilk normality test

data:  residuals_PBR525
W = 0.98162, p-value = 0.9732

> hist(residuals_PBR525,
+      main = "Histogram of Residuals for PBR525 (Group Y)",
+      xlab = "Residuals",
+      ylab = "Frequency",
+      col = "lightblue",
+      border = "black",
+      prob = TRUE)

> curve(dnorm(x, mean = mean(residuals_PBR525, na.rm = TRUE),
+             sd = sd(residuals_PBR525, na.rm = TRUE)),
+       col = "blue", lwd = 2, add = TRUE)

PBR59
> lm_PBR59 <- lm(PBR59 ~ IV_fluids_rate + IV_fluids_duration +
IV_fluids_total,
+               data = subset_data)
> summary(lm_PBR59)

Call:
lm(formula = PBR59 ~ IV_fluids_rate + IV_fluids_duration +
IV_fluids_total,
    data = subset_data)

Residuals:
     Min       1Q   Median       3Q      Max
-0.38710 -0.04725  0.04770  0.07507  0.19355

Coefficients:
                   Estimate Std. Error t value Pr(>|t|)
(Intercept)         1.342e+00  2.814e-01   4.770   0.0031 **
IV_fluids_rate     -2.018e-03  1.761e-02  -0.115   0.9125
IV_fluids_duration  2.826e-03  1.586e-02   0.178   0.8644
IV_fluids_total     6.359e-06  1.050e-03   0.006   0.9954
---
Signif. codes:  0 ‘***’ 0.001 ‘**’ 0.01 ‘*’ 0.05 ‘.’ 0.1 ‘ ’ 1

Residual standard error: 0.2013 on 6 degrees of freedom
Multiple R-squared:  0.0558,  Adjusted R-squared:  -0.4163
F-statistic: 0.1182 on 3 and 6 DF,  p-value: 0.9461

> residuals_PBR59 <- residuals(lm_PBR59)
> shapiro.test(residuals_PBR59)

      Shapiro-Wilk normality test

data:  residuals_PBR59
W = 0.87729, p-value = 0.1214

> hist(residuals_PBR59,
+      main = "Histogram of Residuals for PBR59 (Group Y)",
+      xlab = "Residuals",
+      ylab = "Frequency",
+      col = "lightblue",
+      border = "black",
```

```
+      prob = TRUE)
> curve(dnorm(x, mean = mean(residuals_PBR59, na.rm = TRUE),
+             sd = sd(residuals_PBR59, na.rm = TRUE)),
+       col = "blue", lwd = 2, add = TRUE)
>


PBR1019
> lm_PBR1019 <- lm(PBR1019 ~ IV_fluids_rate + IV_fluids_duration +
IV_fluids_total,
+              data = subset_data)
>
> summary(lm_PBR1019)

Call:
lm(formula = PBR1019 ~ IV_fluids_rate + IV_fluids_duration +
    IV_fluids_total, data = subset_data)

Residuals:
     Min       1Q   Median       3Q      Max
-0.32821 -0.11378 -0.01295  0.12643  0.37616

Coefficients:
                    Estimate Std. Error t value Pr(>|t|)
(Intercept)         3.2412881  0.3441530   9.418 8.14e-05 ***
IV_fluids_rate     -0.0191422  0.0215372  -0.889    0.408
IV_fluids_duration -0.0010220  0.0193947  -0.053    0.960
IV_fluids_total     0.0001254  0.0012843   0.098    0.925
---
Signif. codes:  0 ‘***’ 0.001 ‘**’ 0.01 ‘*’ 0.05 ‘.’ 0.1 ‘ ’ 1

Residual standard error: 0.2462 on 6 degrees of freedom
Multiple R-squared:  0.2959,  Adjusted R-squared:  -0.05618
F-statistic: 0.8404 on 3 and 6 DF,  p-value: 0.5195

> residuals_PBR1019 <- residuals(lm_PBR1019)

> shapiro.test(residuals_PBR1019)

      Shapiro-Wilk normality test

data:  residuals_PBR1019
W = 0.97691, p-value = 0.9465

> hist(residuals_PBR1019,
+      main = "Histogram of Residuals for PBR1019 (Group Y)",
+      xlab = "Residuals",
+      ylab = "Frequency",
+      col = "lightblue",
+      border = "black",
+      prob = TRUE)

> curve(dnorm(x, mean = mean(residuals_PBR1019, na.rm = TRUE),
+             sd = sd(residuals_PBR1019, na.rm = TRUE)),
+       col = "blue", lwd = 2, add = TRUE)


PBR2025
> lm_PBR2025 <- lm(PBR2025 ~ IV_fluids_rate + IV_fluids_duration +
IV_fluids_total,
+              data = subset_data)
> summary(lm_PBR2025)

Call:
lm(formula = PBR2025 ~ IV_fluids_rate + IV_fluids_duration +
    IV_fluids_total, data = subset_data)

Residuals:
     Min       1Q   Median       3Q      Max
```

```
-0.48245 -0.13922 -0.04434  0.09291  0.56708

Coefficients:
                   Estimate Std. Error t value Pr(>|t|)
(Intercept)         3.428024   0.555200   6.174 0.000829 ***
IV_fluids_rate     -0.047650   0.034745  -1.371 0.219314
IV_fluids_duration -0.024080   0.031288  -0.770 0.470729
IV_fluids_total     0.002703   0.002072   1.304 0.239864
---
Signif. codes:  0 ‘***’ 0.001 ‘**’ 0.01 ‘*’ 0.05 ‘.’ 0.1 ‘ ’ 1

Residual standard error: 0.3971 on 6 degrees of freedom
Multiple R-squared:  0.3865,  Adjusted R-squared:  0.07976
F-statistic:  1.26 on 3 and 6 DF,  p-value: 0.369

> residuals_PBR2025 <- residuals(lm_PBR2025)
> shapiro.test(residuals_PBR2025)

      Shapiro-Wilk normality test

data:  residuals_PBR2025
W = 0.94971, p-value = 0.6651

> hist(residuals_PBR2025,
+      main = "Histogram of Residuals for PBR2025 (Group Y)",
+      xlab = "Residuals",
+      ylab = "Frequency",
+      col = "lightblue",
+      border = "black",
+      prob = TRUE)
> curve(dnorm(x, mean = mean(residuals_PBR2025, na.rm = TRUE),
+             sd = sd(residuals_PBR2025, na.rm = TRUE)),
+       col = "blue", lwd = 2, add = TRUE)
```

GlycoCheck vs ATT for trauma subset

```
> subset_data_T <- subset(Glycoheck_clinical_study_dataset_for_stats, Grou
p == "T")
>
```

VVD

```
> lm_VVD <- lm(VVD ~ Total_ATT, data = subset_data_T)
>
> summary(lm_VVD)

Call:
lm(formula = VVD ~ Total_ATT, data = subset_data_T)

Residuals:
    Min      1Q  Median      3Q     Max
-126.94  -72.61   18.06   62.73  106.75

Coefficients:
            Estimate Std. Error t value Pr(>|t|)
(Intercept)   406.38      79.92   5.085 0.000658 ***
Total_ATT     -12.36      18.42  -0.671 0.519122
---
Signif. codes:  0 ‘***’ 0.001 ‘**’ 0.01 ‘*’ 0.05 ‘.’ 0.1 ‘ ’ 1

Residual standard error: 88.18 on 9 degrees of freedom
Multiple R-squared:  0.04763,  Adjusted R-squared:  -0.05819
F-statistic: 0.4501 on 1 and 9 DF,  p-value: 0.5191

> residuals_VVD <- residuals(lm_VVD)
> shapiro.test(residuals_VVD)
```

```
        Shapiro-Wilk normality test

data:  residuals_VVD
W = 0.90014, p-value = 0.1856

> hist(residuals_VVD,
+      main = "Histogram of Residuals for VVD (Group T)",
+      xlab = "Residuals",
+      ylab = "Frequency",
+      col = "lightblue",
+      border = "black",
+      prob = TRUE)
>
> curve(dnorm(x, mean = mean(residuals_VVD, na.rm = TRUE),
+             sd = sd(residuals_VVD, na.rm = TRUE)),
+       col = "blue", lwd = 2, add = TRUE)

RBC filling
> lm_RBC_filling <- lm(RBC_filling ~ Total_ATT, data = subset_data_T)
> summary(lm_RBC_filling)

Call:
lm(formula = RBC_filling ~ Total_ATT, data = subset_data_T)

Residuals:
      Min        1Q    Median        3Q       Max
-0.090833 -0.063208 -0.000917  0.042417  0.143083

Coefficients:
            Estimate Std. Error t value Pr(>|t|)
(Intercept)  0.55458    0.07423   7.471 3.81e-05 ***
Total_ATT    0.00725    0.01711   0.424    0.682
---
Signif. codes:  0 ‘***’ 0.001 ‘**’ 0.01 ‘*’ 0.05 ‘.’ 0.1 ‘ ’ 1

Residual standard error: 0.0819 on 9 degrees of freedom
Multiple R-squared:  0.01956,  Adjusted R-squared:  -0.08938
F-statistic: 0.1795 on 1 and 9 DF,  p-value: 0.6817

> residuals_RBC_filling <- residuals(lm_RBC_filling)

> shapiro.test(residuals_RBC_filling)

        Shapiro-Wilk normality test

data:  residuals_RBC_filling
W = 0.9151, p-value = 0.2799

> hist(residuals_RBC_filling,
+      main = "Histogram of Residuals for RBC_filling (Group T)",
+      xlab = "Residuals",
+      ylab = "Frequency",
+      col = "lightblue",
+      border = "black",
+      prob = TRUE)
>
> curve(dnorm(x, mean = mean(residuals_RBC_filling, na.rm = TRUE),
+             sd = sd(residuals_RBC_filling, na.rm = TRUE)),
+       col = "blue", lwd = 2, add = TRUE)

Median P50
> lm_Median_P50 <- lm(Median_P50 ~ Total_ATT, data = subset_data_T)

> summary(lm_Median_P50)

Call:
lm(formula = Median_P50 ~ Total_ATT, data = subset_data_T)
```

```
Residuals:
     Min       1Q   Median       3Q      Max
-1.69676 -1.06894 -0.02676  1.03773  1.39991

Coefficients:
            Estimate Std. Error t value Pr(>|t|)
(Intercept)   9.7275     1.1144   8.729  1.1e-05 ***
Total_ATT    -0.3410     0.2569  -1.327    0.217
---
Signif. codes:  0 ‘***’ 0.001 ‘**’ 0.01 ‘*’ 0.05 ‘.’ 0.1 ‘ ’ 1

Residual standard error: 1.23 on 9 degrees of freedom
Multiple R-squared:  0.1637,   Adjusted R-squared:  0.07082
F-statistic: 1.762 on 1 and 9 DF,  p-value: 0.217

> residuals_Median_P50 <- residuals(lm_Median_P50)
> shapiro.test(residuals_Median_P50)

        Shapiro-Wilk normality test

data:  residuals_Median_P50
W = 0.89735, p-value = 0.1715

> hist(residuals_Median_P50,
+      main = "Histogram of Residuals for Median_P50 (Group T)",
+      xlab = "Residuals",
+      ylab = "Frequency",
+      col = "lightblue",
+      border = "black",
+      prob = TRUE)
>
> curve(dnorm(x, mean = mean(residuals_Median_P50, na.rm = TRUE),
+             sd = sd(residuals_Median_P50, na.rm = TRUE)),
+       col = "blue", lwd = 2, add = TRUE)
```

PBR525

```
> lm_PBR525 <- lm(PBR525 ~ Total_ATT, data = subset_data_T)
> summary(lm_PBR525)

Call:
lm(formula = PBR525 ~ Total_ATT, data = subset_data_T)

Residuals:
     Min       1Q   Median       3Q      Max
-0.32107 -0.17119 -0.05417  0.19060  0.30024

Coefficients:
            Estimate Std. Error t value Pr(>|t|)
(Intercept)  2.70488    0.20861  12.966 3.97e-07 ***
Total_ATT   -0.02512    0.04809  -0.522    0.614
---
Signif. codes:  0 ‘***’ 0.001 ‘**’ 0.01 ‘*’ 0.05 ‘.’ 0.1 ‘ ’ 1

Residual standard error: 0.2302 on 9 degrees of freedom
Multiple R-squared:  0.02942,  Adjusted R-squared:  -0.07842
F-statistic: 0.2728 on 1 and 9 DF,  p-value: 0.614

> residuals_PBR525 <- residuals(lm_PBR525)
> shapiro.test(residuals_PBR525)

        Shapiro-Wilk normality test

data:  residuals_PBR525
W = 0.92963, p-value = 0.4071

> hist(residuals_PBR525,
+      main = "Histogram of Residuals for PBR525 (Group T)",
+      xlab = "Residuals",
```

```
+      ylab = "Frequency",
+      col = "lightblue",
+      border = "black",
+      prob = TRUE)
>
> curve(dnorm(x, mean = mean(residuals_PBR525, na.rm = TRUE),
+             sd = sd(residuals_PBR525, na.rm = TRUE)),
+       col = "blue", lwd = 2, add = TRUE)

PBR59
> lm_PBR59 <- lm(PBR59 ~ Total_ATT, data = subset_data_T)
> summary(lm_PBR59)

Call:
lm(formula = PBR59 ~ Total_ATT, data = subset_data_T)

Residuals:
     Min       1Q   Median       3Q      Max
-0.36413 -0.06246  0.05841  0.10984  0.22587

Coefficients:
             Estimate Std. Error t value Pr(>|t|)
(Intercept)  1.365714   0.166987   8.179 1.85e-05 ***
Total_ATT   -0.005397   0.038494  -0.140    0.892
---
Signif. codes:  0 ‘***’ 0.001 ‘**’ 0.01 ‘*’ 0.05 ‘.’ 0.1 ‘ ’ 1

Residual standard error: 0.1842 on 9 degrees of freedom
Multiple R-squared:  0.002179, Adjusted R-squared:  -0.1087
F-statistic: 0.01966 on 1 and 9 DF,  p-value: 0.8916

> residuals_PBR59 <- residuals(lm_PBR59)
> shapiro.test(residuals_PBR59)

        Shapiro-Wilk normality test

data:  residuals_PBR59
W = 0.92885, p-value = 0.3993

> hist(residuals_PBR59,
+      main = "Histogram of Residuals for PBR59 (Group T)",
+      xlab = "Residuals",
+      ylab = "Frequency",
+      col = "lightblue",
+      border = "black",
+      prob = TRUE)
>
> curve(dnorm(x, mean = mean(residuals_PBR59, na.rm = TRUE),
+             sd = sd(residuals_PBR59, na.rm = TRUE)),
+       col = "blue", lwd = 2, add = TRUE)

PBR1019

> lm_PBR1019 <- lm(PBR1019 ~ Total_ATT, data = subset_data_T)
> summary(lm_PBR1019)

Call:
lm(formula = PBR1019 ~ Total_ATT, data = subset_data_T)

Residuals:
     Min       1Q   Median       3Q      Max
-0.25397 -0.14397 -0.03333  0.15302  0.27508

Coefficients:
            Estimate Std. Error t value Pr(>|t|)
(Intercept)  3.09190    0.17587  17.581 2.82e-08 ***
Total_ATT   -0.01698    0.04054  -0.419    0.685
---
Signif. codes:  0 ‘***’ 0.001 ‘**’ 0.01 ‘*’ 0.05 ‘.’ 0.1 ‘ ’ 1
```

```
Residual standard error: 0.194 on 9 degrees of freedom
Multiple R-squared:  0.01913,  Adjusted R-squared:  -0.08986
F-statistic: 0.1755 on 1 and 9 DF,  p-value: 0.6851

> residuals_PBR1019 <- residuals(lm_PBR1019)
> shapiro.test(residuals_PBR1019)

        Shapiro-Wilk normality test

data:  residuals_PBR1019
W = 0.92992, p-value = 0.41

> hist(residuals_PBR1019,
+      main = "Histogram of Residuals for PBR1019 (Group T)",
+      xlab = "Residuals",
+      ylab = "Frequency",
+      col = "lightblue",
+      border = "black",
+      prob = TRUE)
>
> curve(dnorm(x, mean = mean(residuals_PBR1019, na.rm = TRUE),
+             sd = sd(residuals_PBR1019, na.rm = TRUE)),
+       col = "blue", lwd = 2, add = TRUE)

PBR2025
> lm_PBR2025 <- lm(PBR2025 ~ Total_ATT, data = subset_data_T)
> summary(lm_PBR2025)

Call:
lm(formula = PBR2025 ~ Total_ATT, data = subset_data_T)

Residuals:
     Min       1Q   Median       3Q      Max
-0.49316 -0.29983 -0.05172  0.29801  0.52306

Coefficients:
            Estimate Std. Error t value Pr(>|t|)
(Intercept)  3.26893    0.35545   9.197 7.15e-06 ***
Total_ATT   -0.05144    0.08194  -0.628    0.546
---
Signif. codes:  0 ‘***’ 0.001 ‘**’ 0.01 ‘*’ 0.05 ‘.’ 0.1 ‘ ’ 1

Residual standard error: 0.3922 on 9 degrees of freedom
Multiple R-squared:  0.04196,  Adjusted R-squared:  -0.06449
F-statistic: 0.3941 on 1 and 9 DF,  p-value: 0.5457

> residuals_PBR2025 <- residuals(lm_PBR2025)
> shapiro.test(residuals_PBR2025)

        Shapiro-Wilk normality test

data:  residuals_PBR2025
W = 0.92721, p-value = 0.3833

> hist(residuals_PBR2025,
+      main = "Histogram of Residuals for PBR2025 (Group T)",
+      xlab = "Residuals",
+      ylab = "Frequency",
+      col = "lightblue",
+      border = "black",
+      prob = TRUE)
>
> curve(dnorm(x, mean = mean(residuals_PBR2025, na.rm = TRUE),
+             sd = sd(residuals_PBR2025, na.rm = TRUE)),
+       col = "blue", lwd = 2, add = TRUE)
```

GlycoCheck vs PCV
Linear models

```
> Glycoheck_clinical_study_dataset_for_stats$PCV <- as.numeric(as.characte
r(Glycoheck_clinical_study_dataset_for_stats$PCV))


VVD
> lm_VVD <- lm(VVD ~ PCV, data = Glycoheck_clinical_study_dataset_for_stat
s)
> summary(lm_VVD)

Call:
lm(formula = VVD ~ PCV, data = Glycoheck_clinical_study_dataset_for_stats)

Residuals:
    Min      1Q  Median      3Q     Max
-193.33  -42.25  -16.39   35.23  243.07

Coefficients:
            Estimate Std. Error t value Pr(>|t|)
(Intercept)  212.806     87.294   2.438   0.0268 *
PCV            5.270      2.548   2.068   0.0552 .
---
Signif. codes:  0 ‘***’ 0.001 ‘**’ 0.01 ‘*’ 0.05 ‘.’ 0.1 ‘ ’ 1

Residual standard error: 105.7 on 16 degrees of freedom
  (1 observation deleted due to missingness)
Multiple R-squared:  0.2109,   Adjusted R-squared:  0.1616
F-statistic: 4.277 on 1 and 16 DF,  p-value: 0.05519

> residuals_VVD <- residuals(lm_VVD)
> shapiro.test(residuals_VVD)

        Shapiro-Wilk normality test

data:  residuals_VVD
W = 0.91899, p-value = 0.1241

> hist(residuals_VVD,
+      main = "Histogram of Residuals for VVD",
+      xlab = "Residuals",
+      ylab = "Frequency",
+      col = "lightblue",
+      border = "black",
+      prob = TRUE)
>
> curve(dnorm(x, mean = mean(residuals_VVD, na.rm = TRUE),
+             sd = sd(residuals_VVD, na.rm = TRUE)),
+       col = "blue", lwd = 2, add = TRUE)

Median P50
> lm_Median_P50 <- lm(Median_P50 ~ PCV, data = Glycoheck_clinical_study_da
taset_for_stats)
> summary(lm_Median_P50)

Call:
lm(formula = Median_P50 ~ PCV, data = Glycoheck_clinical_study_dataset_for
_stats)

Residuals:
     Min       1Q   Median       3Q      Max
-2.05247 -0.71457 -0.02136  0.49014  2.19796

Coefficients:
            Estimate Std. Error t value Pr(>|t|)
(Intercept)  9.30191    0.94363   9.858 3.35e-08 ***
PCV         -0.03238    0.02754  -1.175    0.257
```

```
---
Signif. codes:  0 ‘***’ 0.001 ‘**’ 0.01 ‘*’ 0.05 ‘.’ 0.1 ‘ ’ 1

Residual standard error: 1.143 on 16 degrees of freedom
  (1 observation deleted due to missingness)
Multiple R-squared:  0.07948,  Adjusted R-squared:  0.02195
F-statistic: 1.382 on 1 and 16 DF,  p-value: 0.257

> residuals_Median_P50 <- residuals(lm_Median_P50)
> shapiro.test(residuals_Median_P50)

        Shapiro-Wilk normality test

data:  residuals_Median_P50
W = 0.99083, p-value = 0.9993

> hist(residuals_Median_P50,
+      main = "Histogram of Residuals for Median_P50",
+      xlab = "Residuals",
+      ylab = "Frequency",
+      col = "lightblue",
+      border = "black",
+      prob = TRUE)
>
> curve(dnorm(x, mean = mean(residuals_Median_P50, na.rm = TRUE),
+             sd = sd(residuals_Median_P50, na.rm = TRUE)),
+       col = "blue", lwd = 2, add = TRUE)

RBC filling
> lm_RBC_filling <- lm(RBC_filling ~ PCV, data = Glycoheck_clinical_study_
dataset_for_stats)
> summary(lm_RBC_filling)

Call:
lm(formula = RBC_filling ~ PCV, data = Glycoheck_clinical_study_dataset_fo
r_stats)

Residuals:
      Min        1Q    Median        3Q       Max
-0.108626 -0.064823  0.004637  0.048076  0.140154

Coefficients:
            Estimate Std. Error t value Pr(>|t|)
(Intercept) 0.506386   0.066112   7.659  9.7e-07 ***
PCV         0.002377   0.001930   1.232    0.236
---
Signif. codes:  0 ‘***’ 0.001 ‘**’ 0.01 ‘*’ 0.05 ‘.’ 0.1 ‘ ’ 1

Residual standard error: 0.08005 on 16 degrees of freedom
  (1 observation deleted due to missingness)
Multiple R-squared:  0.08663,  Adjusted R-squared:  0.02955
F-statistic: 1.518 on 1 and 16 DF,  p-value: 0.2358

> residuals_RBC_filling <- residuals(lm_RBC_filling)
> shapiro.test(residuals_RBC_filling)

        Shapiro-Wilk normality test

data:  residuals_RBC_filling
W = 0.9471, p-value = 0.3813

> hist(residuals_RBC_filling,
+      main = "Histogram of Residuals for RBC_filling",
+      xlab = "Residuals",
+      ylab = "Frequency",
+      col = "lightblue",
+      border = "black",
+      prob = TRUE)
>
```

```
> curve(dnorm(x, mean = mean(residuals_RBC_filling, na.rm = TRUE),
+             sd = sd(residuals_RBC_filling, na.rm = TRUE)),
+       col = "blue", lwd = 2, add = TRUE)

PBR525
> lm_PBR525 <- lm(PBR525 ~ PCV, data = Glycoheck_clinical_study_dataset_fo
r_stats)
> summary(lm_PBR525)

Call:
lm(formula = PBR525 ~ PCV, data = Glycoheck_clinical_study_dataset_for_sta
ts)

Residuals:
     Min       1Q   Median       3Q      Max
-0.29706 -0.17832 -0.04123  0.19283  0.40988

Coefficients:
             Estimate Std. Error t value Pr(>|t|)
(Intercept)  2.684429   0.190457  14.095 1.94e-10 ***
PCV         -0.002312   0.005559  -0.416    0.683
---
Signif. codes:  0 ‘***’ 0.001 ‘**’ 0.01 ‘*’ 0.05 ‘.’ 0.1 ‘ ’ 1

Residual standard error: 0.2306 on 16 degrees of freedom
  (1 observation deleted due to missingness)
Multiple R-squared:  0.01069,  Adjusted R-squared:  -0.05114
F-statistic: 0.1729 on 1 and 16 DF,  p-value: 0.683

> residuals_PBR525 <- residuals(lm_PBR525)
> shapiro.test(residuals_PBR525)

        Shapiro-Wilk normality test

data:  residuals_PBR525
W = 0.93772, p-value = 0.2648

> hist(residuals_PBR525,
+      main = "Histogram of Residuals for PBR525",
+      xlab = "Residuals",
+      ylab = "Frequency",
+      col = "lightblue",
+      border = "black",
+      prob = TRUE)
>
> curve(dnorm(x, mean = mean(residuals_PBR525, na.rm = TRUE),
+             sd = sd(residuals_PBR525, na.rm = TRUE)),
+       col = "blue", lwd = 2, add = TRUE)

PBR 59

> lm_PBR59 <- lm(PBR59 ~ PCV, data = Glycoheck_clinical_study_dataset_for_
stats)
> summary(lm_PBR59)

Call:
lm(formula = PBR59 ~ PCV, data = Glycoheck_clinical_study_dataset_for_stat
s)

Residuals:
     Min       1Q   Median       3Q      Max
-0.39528 -0.06559  0.03040  0.10942  0.19489

Coefficients:
              Estimate Std. Error t value Pr(>|t|)
(Intercept)  1.380e+00  1.310e-01  10.531 1.33e-08 ***
PCV         -9.913e-05  3.824e-03  -0.026     0.98
---
Signif. codes:  0 ‘***’ 0.001 ‘**’ 0.01 ‘*’ 0.05 ‘.’ 0.1 ‘ ’ 1
```

```
Residual standard error: 0.1586 on 16 degrees of freedom
  (1 observation deleted due to missingness)
Multiple R-squared:  4.199e-05,       Adjusted R-squared:  -0.06246
F-statistic: 0.0006719 on 1 and 16 DF,  p-value: 0.9796

> residuals_PBR59 <- residuals(lm_PBR59)
> shapiro.test(residuals_PBR59)

        Shapiro-Wilk normality test

data:  residuals_PBR59
W = 0.91774, p-value = 0.1179

> hist(residuals_PBR59,
+      main = "Histogram of Residuals for PBR59",
+      xlab = "Residuals",
+      ylab = "Frequency",
+      col = "lightblue",
+      border = "black",
+      prob = TRUE)
>
> curve(dnorm(x, mean = mean(residuals_PBR59, na.rm = TRUE),
+             sd = sd(residuals_PBR59, na.rm = TRUE)),
+       col = "blue", lwd = 2, add = TRUE)

PBR1019
> lm_PBR1019 <- lm(PBR1019 ~ PCV, data = Glycoheck_clinical_study_dataset_
for_stats)
> summary(lm_PBR1019)

Call:
lm(formula = PBR1019 ~ PCV, data = Glycoheck_clinical_study_dataset_for_st
ats)

Residuals:
     Min       1Q   Median       3Q      Max
-0.31556 -0.18877 -0.02508  0.14422  0.49109

Coefficients:
             Estimate Std. Error t value Pr(>|t|)
(Intercept)  3.0512335  0.1940603  15.723 3.76e-11 ***
PCV         -0.0009513  0.0056647  -0.168    0.869
---
Signif. codes:  0 ‘***’ 0.001 ‘**’ 0.01 ‘*’ 0.05 ‘.’ 0.1 ‘ ’ 1

Residual standard error: 0.235 on 16 degrees of freedom
  (1 observation deleted due to missingness)
Multiple R-squared:  0.001759, Adjusted R-squared:  -0.06063
F-statistic: 0.0282 on 1 and 16 DF,  p-value: 0.8687

> residuals_PBR1019 <- residuals(lm_PBR1019)
> shapiro.test(residuals_PBR1019)

        Shapiro-Wilk normality test

data:  residuals_PBR1019
W = 0.95868, p-value = 0.5764

> hist(residuals_PBR1019,
+      main = "Histogram of Residuals for PBR1019",
+      xlab = "Residuals",
+      ylab = "Frequency",
+      col = "lightblue",
+      border = "black",
+      prob = TRUE)
>
> curve(dnorm(x, mean = mean(residuals_PBR1019, na.rm = TRUE),
+             sd = sd(residuals_PBR1019, na.rm = TRUE)),
```

```
+       col = "blue", lwd = 2, add = TRUE)

PBR2025
> lm_PBR2025 <- lm(PBR2025 ~ PCV, data = Glycoheck_clinical_study_dataset_
for_stats)
> summary(lm_PBR2025)

Call:
lm(formula = PBR2025 ~ PCV, data = Glycoheck_clinical_study_dataset_for_st
ats)

Residuals:
     Min       1Q   Median       3Q      Max
-0.69709 -0.23743 -0.01242  0.26453  0.51974

Coefficients:
             Estimate Std. Error t value Pr(>|t|)
(Intercept)  3.299892   0.315311  10.466 1.45e-08 ***
PCV         -0.007487   0.009204  -0.813    0.428
---
Signif. codes:  0 ‘***’ 0.001 ‘**’ 0.01 ‘*’ 0.05 ‘.’ 0.1 ‘ ’ 1

Residual standard error: 0.3818 on 16 degrees of freedom
  (1 observation deleted due to missingness)
Multiple R-squared:  0.03971,  Adjusted R-squared:  -0.02031
F-statistic: 0.6617 on 1 and 16 DF,  p-value: 0.4279

> residuals_PBR2025 <- residuals(lm_PBR2025)
> shapiro.test(residuals_PBR2025)

        Shapiro-Wilk normality test

data:  residuals_PBR2025
W = 0.95595, p-value = 0.5257

> hist(residuals_PBR2025,
+      main = "Histogram of Residuals for PBR2025",
+      xlab = "Residuals",
+      ylab = "Frequency",
+      col = "lightblue",
+      border = "black",
+      prob = TRUE)
>
> curve(dnorm(x, mean = mean(residuals_PBR2025, na.rm = TRUE),
+             sd = sd(residuals_PBR2025, na.rm = TRUE)),
+       col = "blue", lwd = 2, add = TRUE)
```

Sample size calculations for PBR 5 – 25 based on linear models of selected clinical variables

PCV

```
> Glycoheck_clinical_study_dataset_for_stats$PCV <-
as.numeric(as.character(Glycoheck_clinical_study_dataset_for_stats$P
CV))
```

PBR525

```
> lm_PBR525 <- lm(PBR525 ~ PCV, data =
Glycoheck_clinical_study_dataset_for_stats)
> summary(lm_PBR525)

Call:
lm(formula = PBR525 ~ PCV, data =
Glycoheck_clinical_study_dataset_for_stats)
```

```
Residuals:
     Min       1Q   Median       3Q      Max
-0.29706 -0.17832 -0.04123  0.19283  0.40988

Coefficients:
             Estimate Std. Error t value Pr(>|t|)
(Intercept)  2.684429   0.190457  14.095 1.94e-10 ***
PCV         -0.002312   0.005559  -0.416    0.683
---
Signif. codes:  0 ‘***’ 0.001 ‘**’ 0.01 ‘*’ 0.05 ‘.’ 0.1 ‘ ’ 1

Residual standard error: 0.2306 on 16 degrees of freedom
  (1 observation deleted due to missingness)
Multiple R-squared:  0.01069,    Adjusted R-squared:  -0.05114
F-statistic: 0.1729 on 1 and 16 DF,  p-value: 0.683

> R2 <- 0.01069
> f2 <- R2 / (1 - R2)
> u <- 1
> pwr_result <- pwr.f2.test(u = u, f2 = f2, sig.level = 0.05, power
= 0.80)
> sample_size <- ceiling(pwr_result$v + u + 1)
> cat("Required total sample size:", sample_size, "\n")
Required total sample size: 729
```

LOH

```
> lm_PBR525 <- lm(PBR525 ~ LOH, data =
Glycoheck_clinical_study_dataset_for_stats)
> summary(lm_PBR525)

Call:
lm(formula = PBR525 ~ LOH, data =
Glycoheck_clinical_study_dataset_for_stats)

Residuals:
    Min      1Q  Median      3Q     Max
-0.3200 -0.1658 -0.0831  0.1874  0.3868

Coefficients:
            Estimate Std. Error t value Pr(>|t|)
(Intercept) 2.583104   0.085083  30.360 2.99e-16 ***
LOH         0.005059   0.017330   0.292    0.774
---
Signif. codes:  0 ‘***’ 0.001 ‘**’ 0.01 ‘*’ 0.05 ‘.’ 0.1 ‘ ’ 1

Residual standard error: 0.2258 on 17 degrees of freedom
Multiple R-squared:  0.004988,   Adjusted R-squared:  -0.05354
F-statistic: 0.08522 on 1 and 17 DF,  p-value: 0.7739

> R2 <- 0.005
> f2 <- R2 / (1 - R2)
> u <- 1
> pwr_result <- pwr.f2.test(u = u, f2 = f2, sig.level = 0.05, power
= 0.80)
> sample_size <- ceiling(pwr_result$v + u + 1)
> cat("Required total sample size:", sample_size, "\n")
Required total sample size: 1564
```

APPLE fast

```
> lm_PBR525 <- lm(PBR525 ~ APPLE_fast, data =
Glycoheck_clinical_study_dataset_for_stats)
> summary(lm_PBR525)

Call:
lm(formula = PBR525 ~ APPLE_fast, data =
Glycoheck_clinical_study_dataset_for_stats)

Residuals:
     Min       1Q   Median       3Q      Max
-0.31901 -0.14978 -0.08478  0.15207  0.41279

Coefficients:
            Estimate Std. Error t value Pr(>|t|)
(Intercept) 2.453009   0.215236  11.397 2.21e-09 ***
APPLE_fast  0.008784   0.012260   0.717    0.483
---
Signif. codes:  0 ‘***’ 0.001 ‘**’ 0.01 ‘*’ 0.05 ‘.’ 0.1 ‘ ’ 1

Residual standard error: 0.223 on 17 degrees of freedom
Multiple R-squared:  0.02931,    Adjusted R-squared:  -0.02778
F-statistic: 0.5134 on 1 and 17 DF,  p-value: 0.4834

> R2 <- 0.03
> f2 <- R2 / (1 - R2)
> u <- 1
> pwr_result <- pwr.f2.test(u = u, f2 = f2, sig.level = 0.05, power
= 0.80)
> sample_size <- ceiling(pwr_result$v + u + 1)
> cat("Required total sample size:", sample_size, "\n")
Required total sample size: 256
```

Total ATT

```
> subset_data_T <-
subset(Glycoheck_clinical_study_dataset_for_stats, Group == "T")
```

PBR 525

```
> lm_PBR525 <- lm(PBR525 ~ Total_ATT, data = subset_data_T)
> summary(lm_PBR525)

Call:
lm(formula = PBR525 ~ Total_ATT, data = subset_data_T)

Residuals:
     Min       1Q   Median       3Q      Max
-0.32107 -0.17119 -0.05417  0.19060  0.30024

Coefficients:
            Estimate Std. Error t value Pr(>|t|)
(Intercept)  2.70488    0.20861  12.966 3.97e-07 ***
Total_ATT   -0.02512    0.04809  -0.522    0.614
---
Signif. codes:  0 ‘***’ 0.001 ‘**’ 0.01 ‘*’ 0.05 ‘.’ 0.1 ‘ ’ 1

Residual standard error: 0.2302 on 9 degrees of freedom
Multiple R-squared:  0.02942,    Adjusted R-squared:  -0.07842
F-statistic: 0.2728 on 1 and 9 DF,  p-value: 0.614
```

```
> R2 <- 0.03
> f2 <- R2 / (1 - R2)
> u <- 1
> pwr_result <- pwr.f2.test(u = u, f2 = f2, sig.level = 0.05, power
= 0.80)
> sample_size <- ceiling(pwr_result$v + u + 1)
> cat("Required total sample size:", sample_size, "\n")
Required total sample size: 256
```

IV fluid rate

```
> lm_PBR525 <- lm(formula = PBR525 ~ IV_fluids_rate, data =
subset_data)
> summary(lm_PBR525)

Call:
lm(formula = PBR525 ~ IV_fluids_rate, data = subset_data)

Residuals:
     Min       1Q   Median       3Q      Max
-0.36071 -0.10711 -0.02337  0.14225  0.32144

Coefficients:
                Estimate Std. Error t value Pr(>|t|)
(Intercept)     2.733279   0.134526  20.318  3.6e-08 ***
IV_fluids_rate -0.011898   0.009898  -1.202    0.264
---
Signif. codes:  0 ‘***’ 0.001 ‘**’ 0.01 ‘*’ 0.05 ‘.’ 0.1 ‘ ’ 1

Residual standard error: 0.2191 on 8 degrees of freedom
Multiple R-squared:  0.153,Adjusted R-squared:  0.04711
F-statistic: 1.445 on 1 and 8 DF,  p-value: 0.2637

> R2 <- 0.153
> f2 <- R2 / (1 - R2)
> u <- 1
> pwr_result <- pwr.f2.test(u = u, f2 = f2, sig.level = 0.05, power
= 0.80)
> sample_size <- ceiling(pwr_result$v + u + 1)
> cat("Required total sample size:", sample_size, "\n")
Required total sample size: 46
```

Annex VIII: Chapter VI Supplementary table 2

Descriptive statistics and GlycoCheck™ parameters in 11 cats with trauma and eight cats with non-traumatic illness presented per group

Variable	Mean	SD	Median	Min	Max	Q1	Q3
Non-traumatic systemic illness group							
Age (years)	6.47	4.68	7.76	0.83	13.01	1.71	9.46
Weight (kg)	4.57	1.77	4.25	2.70	8.14	3.42	5.24
LOH	5.00	3.74	5.50	1.00	10.00	1.00	7.50
$APPLE_{fast}$	17.00	5.26	16.50	8.00	24.00	14.75	19.50
VVD	426.92	136.09	418.67	195.00	666.67	378.00	488.25
%RBC filling	0.59	0.09	0.60	0.43	0.73	0.56	0.62
PBR 5-25 µm	2.60	0.23	2.56	2.33	2.98	2.43	2.76
PBR 5-9 µm	1.43	0.10	1.42	1.31	1.57	1.36	1.48
PBR10-19 µm	3.01	0.28	2.98	2.70	3.50	2.79	3.14
PBR 20-25 µm	3.00	0.40	3.09	2.30	3.41	2.75	3.33
Median P50	8.15	0.95	8.28	6.55	9.76	7.87	8.45
Trauma group							
Age (years)	3.67	5.38	1.00	0.33	17.02	0.69	3.13
Weight (kg)	4.24	1.28	4.67	2.50	5.91	2.90	5.31
LOH	3.09	2.34	3.00	0.00	7.00	1.50	4.50
$APPLE_{fast}$	17.09	3.70	17.00	13.00	23.00	14.00	20.00
Total_ATT	4.09	1.51	4.00	1.00	6.00	4.00	5.00
Short_ATT	2.00	1.18	2.00	0.00	4.00	1.00	3.00
VVD	355.82	85.72	381.33	225.00	455.00	284.33	421.67
%RBC filling	0.58	0.08	0.58	0.47	0.73	0.52	0.63
PBR 5-25 µm	2.60	0.22	2.51	2.28	2.98	2.46	2.80
PBR 5-9 µm	1.34	0.17	1.41	0.98	1.57	1.28	1.45
PBR10-19 µm	3.02	0.19	2.96	2.77	3.35	2.88	3.16
PBR 20-25 µm	3.06	0.38	2.96	2.57	3.61	2.76	3.38
Median P50	8.33	1.28	8.34	6.62	10.59	7.47	9.08

APPLEfast: Acute Patient Physiological and Laboratory Evaluation (fast); ATT: Animal Trauma Triage Score; LOH: length of hospitalization; Median P50: Median red blood cell column width;

PBR: Perfused boundary region; %RBC filling: percentage red blood cell filling; VVD: Valid vessel density;

Annex IX: Statement of Contribution Forms

MASSEY UNIVERSITY
TE KUNENGA KI PŪREHUROA
UNIVERSITY OF NEW ZEALAND

GRADUATE RESEARCH SCHOOL

STATEMENT OF CONTRIBUTION DOCTORATE WITH PUBLICATIONS/MANUSCRIPTS

We, the student and the student's main supervisor, certify that all co-authors have consented to their work being included in the thesis and they have accepted the student's contribution as indicated below in the Statement of Originality.

Student name:	Ivayla Danielova Yozova
Name and title of main supervisor:	Prof. John S Munday, BVSc, DSc, PhD, Diplomate ACVP
In which chapter is the manuscript/published work?	Chapter II
What percentage of the manuscript/published work was contributed by the student?	100

Describe the contribution that the student has made to the manuscript/published work:

The author of this thesis led the establishment of the collaboration, secured funding, designed the project, and was responsible for data collection, interpretation, reporting, and manuscript preparation.

Please select one of the following three options:

- (●) The manuscript/published work is published or in press

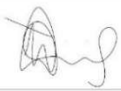
  Please provide the full reference of the research output:

  Yozova, I. D., Londono, L. A., Millar, K. K., Sano, H., Weidgraaf, K., Thomson, N. A., & Munday, J. S. (2021). Rapid Patient-Side Evaluation of Endothelial Glycocalyx Thickness in Healthy Sedated Cats Using GlycoCheck (R) Software. Front Vet Sci, 8, 727063. doi:10.3389/fvets.2021.727063

- ( ) The manuscript is currently under review for publication

  Please provide the name of the journal:

- ( ) It is intended that the manuscript will be published, but it has not yet been submitted to a journal

Student's signature:		Main supervisor's signature:	John Munday

This form should appear at the end of each thesis chapter/section/appendix submitted as a manuscript/ publication or collected as an appendix at the end of the thesis.

MASSEY UNIVERSITY
TE KUNENGA KI PŪREHUROA
UNIVERSITY OF NEW ZEALAND

GRADUATE RESEARCH SCHOOL

STATEMENT OF CONTRIBUTION
DOCTORATE WITH PUBLICATIONS/MANUSCRIPTS

We, the student and the student's main supervisor, certify that all co-authors have consented to their work being included in the thesis and they have accepted the student's contribution as indicated below in the Statement of Originality.

Student name:	Ivayla Danielova Yozova
Name and title of main supervisor:	Prof. John S Munday, BVSc, DSc, PhD, Diplomate ACVP
In which chapter is the manuscript/published work?	Chapter IV

Describe the contribution that the student and members of the supervisory team have made to the manuscript/published work:[1]

The author of this thesis led the establishment of the collaboration, secured funding, designed the project, and was responsible for data collection, interpretation, reporting and manuscript preparation.

Please select one of the following three options:

- (●) **The manuscript/published work is published or in press**

  Please provide the full reference of the research output:

  Yozova ID, Londoño LL, Sano H, Thomson N, Munday JS. Immediate effects of an intravenous fluid challenge on the endothelial glycocalyx in healthy anaesthetized cats. Vet J. 2025 Dec;314:106487. doi: 10.1016/j.tvjl.2025.106487.

- ( ) **The manuscript is currently under review for publication**

  Please provide the name of the journal:

- ( ) **It is intended that the manuscript will be published, but it has not yet been submitted to a journal**

Student's signature:	Ivayla Yozova	Main supervisor's signature:	John Munday Digitally signed by John Munday Date: 2026.06.15 14:05:23 +12'00'

This form should be placed at the beginning of each relevant thesis chapter.

[1] Refer to the Massey University Publishing and Authorship guidelines (OneMassey for staff, Stream for students) and/ or Contributor Roles Taxonomy (CRediT) guidelines for guidance.

MASSEY UNIVERSITY
TE KUNENGA KI PŪREHUROA
UNIVERSITY OF NEW ZEALAND

GRADUATE RESEARCH SCHOOL

STATEMENT OF CONTRIBUTION
DOCTORATE WITH PUBLICATIONS/MANUSCRIPTS

We, the student and the student's main supervisor, certify that all co-authors have consented to their work being included in the thesis and they have accepted the student's contribution as indicated below in the Statement of Originality.

Student name:	Ivayla Danielova Yozova
Name and title of main supervisor:	Prof John S Munday, BVSc, PhD, DSc, Diplomate ACVP
In which chapter is the manuscript/published work?	Chapter V

Describe the contribution that the student and members of the supervisory team have made to the manuscript/published work:[1]

The author of this thesis led the establishment of the collaboration, secured funding, designed the project, and was responsible for data collection, interpretation, reporting, and manuscript preparation.

Please select one of the following three options:

- (●) The manuscript/published work is published or in press

  Please provide the full reference of the research output:

  Yozova ID, Thomson N, Irie M, Owen R. Effects of transient intravascular volume overload on endothelial glycocalyx thickness in healthy anaesthetized cats. Front Vet Sci. 2026 (in press)

- ( ) The manuscript is currently under review for publication

  Please provide the name of the journal:

- ( ) It is intended that the manuscript will be published, but it has not yet been submitted to a journal

Student's signature:	Ivayla Yozova	Main supervisor's signature:	John Munday Digitally signed by John Munday Date: 2026.06.15 14:03:27 +12'00'

This form should be placed at the beginning of each relevant thesis chapter.

[1] Refer to the Massey University Publishing and Authorship guidelines (OneMassey for staff, Stream for students) and/ or Contributor Roles Taxonomy (CRediT) guidelines for guidance.

MASSEY UNIVERSITY
TE KUNENGA KI PŪREHUROA
UNIVERSITY OF NEW ZEALAND

GRADUATE RESEARCH SCHOOL

STATEMENT OF CONTRIBUTION
DOCTORATE WITH PUBLICATIONS/MANUSCRIPTS

We, the student and the student's main supervisor, certify that all co-authors have consented to their work being included in the thesis and they have accepted the student's contribution as indicated below in the Statement of Originality.

Student name:	Ivayla Danielova Yozova
Name and title of main supervisor:	Prof John Munday, BVSc, DSc, PhD, Diplomate ACVP
In which chapter is the manuscript/published work?	Chapter VI

Describe the contribution that the student and members of the supervisory team have made to the manuscript/published work:[1]

The author of this thesis has led the establishment of the collaboration, secured funding, designed the project, and was responsible for data collection, interpretation, reporting, and manuscript preparation.

Please select one of the following three options:

- (●) **The manuscript/published work is published or in press**

  Please provide the full reference of the research output:

  Yozova ID, Thomson N, Irie M, Owen R, Munday JS. Endothelial glycocalyx thickness in cats with naturally occurring trauma or non-traumatic illness: an exploratory study. Front Vet Sci. 2026 Feb 23;13:1751034. doi: 10.3389/fvets.2026.1751034.

- ( ) **The manuscript is currently under review for publication**

  Please provide the name of the journal:

- ( ) **It is intended that the manuscript will be published, but it has not yet been submitted to a journal**

Student's signature:	Ivayla Yozova	Main supervisor's signature:	John Munday Digitally signed by John Munday Date: 2026.06.15 14:04:46 +12'00'

This form should be placed at the beginning of each relevant thesis chapter.

[1] Refer to the Massey University Publishing and Authorship guidelines (OneMassey for staff, Stream for students) and/ or Contributor Roles Taxonomy (CRediT) guidelines for guidance.

References

1. (MHRA) MaHpRA. Press release: Class 2 drug alert (action within 48 hours): hydroxyethyl starch (HES) products – B Braun Melsungen AG and Fresenius Kabi Limited (EL (13)A/18). 2013 [Available from: http://www.mhra.gov.uk/home/groups/is-md/documents/drugalert/con287026.pdf.
2. Farrugia A. The Boldt affair: correcting a collective failure. Anesth Analg. 2012;115(1):207.
3. Editors-in-Chief statement regarding published clinical trials conducted without IRB approval by Joachim Boldt. Minerva Anestesiol. 2011;77(5):562-3.
4. Wise J. Boldt: the great pretender. BMJ. 2013;346:f1738.
5. Brunkhorst FM, Engel C, Bloos F, Meier-Hellmann A, Ragaller M, Weiler N, et al. Intensive insulin therapy and pentastarch resuscitation in severe sepsis. N Engl J Med. 2008;358(2):125-39.
6. Perner A, Haase N, Guttormsen AB, Tenhunen J, Klemenzson G, Aneman A, et al. Hydroxyethyl starch 130/0.42 versus Ringer's acetate in severe sepsis. N Engl J Med. 2012;367(2):124-34.
7. Myburgh JA, Finfer S, Bellomo R, Billot L, Cass A, Gattas D, et al. Hydroxyethyl starch or saline for fluid resuscitation in intensive care. N Engl J Med. 2012;367(20):1901-11.
8. Guidet B, Martinet O, Boulain T, Philippart F, Poussel JF, Maizel J, et al. Assessment of hemodynamic efficacy and safety of 6% hydroxyethylstarch 130/0.4 vs. 0.9% NaCl fluid replacement in patients with severe sepsis: the CRYSTMAS study. Crit Care. 2012;16(3):R94.
9. Zarychanski R, Abou-Setta AM, Turgeon AF, Houston BL, McIntyre L, Marshall JC, et al. Association of hydroxyethyl starch administration with mortality and acute kidney injury in critically ill patients requiring volume resuscitation: a systematic review and meta-analysis. JAMA. 2013;309(7):678-88.
10. Mutter TC, Ruth CA, Dart AB. Hydroxyethyl starch (HES) versus other fluid therapies: effects on kidney function. Cochrane Database Syst Rev. 2013;2013(7):CD007594.
11. (EMA) EMA. Hydroxyethyl starch solutions: CMDh introduces new measures to protect patients 2018 [Available from: https://www.ema.europa.eu/en/medicines/human/referrals/hydroxyethyl-starch-hes-containing-medicinal-products.
12. (EMA) EMA. Hydroxyethyl-starch solutions (HES) should no longer be used in patients with sepsis or burn injuries or in critically ill patients http://www.ema.europa.eu/ema/index.jsp?curl=pages/medicines/human/referrals/Hydroxyethyl_starch-containing_solutions/human_referral_prac_000012.jsp&mid=WC0b01ac05805c516f2013 [
13. (FDA) FaDA. Highlights of prescribing information for Voluven http://www.fda.gov/downloads/%E2%80%A6/UCM083138.pdf 2014 [
14. (FDA) FaDA. FDA Safety Communication: Boxed Warning on increased mortality and severe renal injury, and additional warning on risk of bleeding, for use of hydroxyethyl starch solutions in some settings http://www.fda.gov/biologicsbloodvaccines/safetyavailability/ucm358271.htm2013 [
15. Bion J, Bellomo R, Myburgh J, Perner A, Reinhart K, Finfer S. Hydroxyethyl starch: putting patient safety first. Intensive Care Med. 2014;40(2):256-9.
16. Bellomo R, Bion J, Finfer S, Myburgh J, Perner A, Reinhart K, et al. Open letter to the Executive Director of the European Medicines Agency concerning the licensing of hydroxyethyl starch solutions for fluid resuscitation. Br J Anaesth. 2014;112(3):595-600.
17. Chappell D, Jacob M. Twisting and ignoring facts on hydroxyethyl starch is not very helpful. Scand J Trauma Resusc Emerg Med. 2013;21:85.
18. Chappell D, Jacob M. Hydroxyethyl starch - the importance of being earnest. Scand J Trauma Resusc Emerg Med. 2013;21:61.
19. Chappell D, Jacob M. Protocols, physiology, and trials of hydroxyethyl starch. N Engl J Med. 2012;367(13):1266; author reply 7.
20. Doshi P. "Independent" reanalysis of landmark starch solutions trial was published by original authors. BMJ. 2017;358:j3552.
21. Doshi P. Update: New England Journal of Medicine publishes correction to 2012 CHEST trial of hydroxyethyl starch versus colloids. BMJ. 2016;352:i1571.

22. Doshi P. Data too important to share: do those who control the data control the message? BMJ. 2016;352:i1027.
23. Hjortrup PB, Haase N, Wetterslev J, Perner A. Gone fishing in a fluid trial. Crit Care Resusc. 2016;18(1):55-8.
24. Laake JH, Tonnessen TI, Chew MS, Lipcsey M, Hjelmqvist H, Wilkman E, et al. The SSAI fully supports the suspension of hydroxyethyl-starch solutions commissioned by the European Medicines Agency. Acta Anaesthesiol Scand. 2018;62(6):874-5.
25. Doshi P. EMA recommendation on hydroxyethyl starch solutions obscured controversy. BMJ. 2018;360:k1287.
26. Priebe HJ. Should hydroxyethyl starch be banned? Lancet. 2018;392(10142):117-8.
27. Vincent JL, Kellum JA, Shaw A, Mythen MG. Should hydroxyethyl starch solutions be totally banned? Crit Care. 2013;17(5):193.
28. Citizen P. Citizen Petition From Public Citizen: Immediately Require the Removal From the Market of HES IV Solutions (2017). Available online at: 2017 [Available from: https://www.regulations.gov/document?D=FDA-2017-P-0867-0001.
29. Yozova ID, Howard J, Sigrist NE, Adamik KN. Current Trends in Volume Replacement Therapy and the Use of Synthetic Colloids in Small Animals-An Internet-Based Survey (2016). Front Vet Sci. 2017;4:140.
30. Yozova ID, Howard J, Adamik KN. Retrospective evaluation of the effects of administration of tetrastarch (hydroxyethyl starch 130/0.4) on plasma creatinine concentration in dogs (2010-2013): 201 dogs. J Vet Emerg Crit Care (San Antonio). 2016;26(4):568-77.
31. Yozova ID, Howard J, Adamik KN. Effect of tetrastarch (hydroxyethyl starch 130/0.4) on plasma creatinine concentration in cats: a retrospective analysis (2010-2015). J Feline Med Surg. 2016.
32. Adamik KN, Yozova ID, Regenscheit N. Controversies in the use of hydroxyethyl starch solutions in small animal emergency and critical care. J Vet Emerg Crit Care (San Antonio). 2015;25(1):20-47.
33. Adamik KN, Yozova ID. Starch Wars-New Episodes of the Saga. Changes in Regulations on Hydroxyethyl Starch in the European Union. Front Vet Sci. 2018;5:336.
34. Adamik KN, Yozova ID. Colloids Yes or No? - a "Gretchen Question" Answered. Front Vet Sci. 2021;8:624049.
35. Jacob M, Chappell D, Becker BF. Regulation of blood flow and volume exchange across the microcirculation. Crit Care. 2016;20(1):319.
36. Guven G, Hilty MP, Ince C. Microcirculation: Physiology, Pathophysiology, and Clinical Application. Blood Purif. 2020;49(1-2):143-50.
37. Kirkpatrick CJ, Bittinger F, Klein CL, Hauptmann S, Klosterhalfen B. The role of the microcirculation in multiple organ dysfunction syndrome (MODS): a review and perspective. Virchows Arch. 1996;427(5):461-76.
38. Pries AR, Secomb TW, Gaehtgens P. The endothelial surface layer. Pflugers Arch. 2000;440(5):653-66.
39. Nieuwdorp M, Meuwese MC, Vink H, Hoekstra JB, Kastelein JJ, Stroes ES. The endothelial glycocalyx: a potential barrier between health and vascular disease. Current opinion in lipidology. 2005;16(5):507-11.
40. Fahraeus R, Lindqvist T. The viscosity of the blood in narrow capillary tubes. American Journal of Physiology-Legacy Content. 1931;96(3):562-8.
41. Danielli J. Capillary permeability and oedema in the perfused frog. The Journal of physiology. 1940;98(1):109-29.
42. Chambers R, Zweifach B. Intercellular cement and capillary permeability. Physiological reviews. 1947;27(3):436-63.
43. Bennett H. Morphological aspects of extracellular polysaccharides. Journal of Histochemistry and cytochemistry. 1963;11(1423).
44. Luft JH. Fine structures of capillary and endocapillary layer as revealed by ruthenium red. Fed Proc. 1966;25(6):1773-83.
45. Reitsma S, Slaaf DW, Vink H, van Zandvoort MA, oude Egbrink MG. The endothelial glycocalyx: composition, functions, and visualization. Pflugers Arch. 2007;454(3):345-59.

46. Gaudette S, Hughes D, Boller M. The endothelial glycocalyx: Structure and function in health and critical illness. J Vet Emerg Crit Care (San Antonio). 2020;30(2):117-34.
47. Gomez Toledo A, Golden GJ, Cummings RD, Malmstrom J, Esko JD. Endothelial Glycocalyx Turnover in Vascular Health and Disease: Rethinking Endothelial Dysfunction. Annu Rev Biochem. 2025.
48. Saunders S, Jalkanen M, O'Farrell S, Bernfield M. Molecular cloning of syndecan, an integral membrane proteoglycan. J Cell Biol. 1989;108(4):1547-56.
49. Leonova EI, Galzitskaya OV. Structure and functions of syndecans in vertebrates. Biochemistry (Mosc). 2013;78(10):1071-85.
50. Teng YH, Aquino RS, Park PW. Molecular functions of syndecan-1 in disease. Matrix Biol. 2012;31(1):3-16.
51. Alexopoulou AN, Multhaupt HA, Couchman JR. Syndecans in wound healing, inflammation and vascular biology. Int J Biochem Cell Biol. 2007;39(3):505-28.
52. Eriksson AS, Spillmann D. The mutual impact of syndecan-1 and its glycosaminoglycan chains--a multivariable puzzle. J Histochem Cytochem. 2012;60(12):936-42.
53. Rosenberg RD, Shworak NW, Liu J, Schwartz JJ, Zhang L. Heparan sulfate proteoglycans of the cardiovascular system. Specific structures emerge but how is synthesis regulated? J Clin Invest. 1997;99(9):2062-70.
54. Bernfield M, Kokenyesi R, Kato M, Hinkes MT, Spring J, Gallo RL, et al. Biology of the syndecans: a family of transmembrane heparan sulfate proteoglycans. Annu Rev Cell Biol. 1992;8:365-93.
55. Gopal S. Syndecans in Inflammation at a Glance. Front Immunol. 2020;11:227.
56. Gotte M. Syndecans in inflammation. FASEB J. 2003;17(6):575-91.
57. Uchimido R, Schmidt EP, Shapiro NI. The glycocalyx: a novel diagnostic and therapeutic target in sepsis. Crit Care. 2019;23(1):16.
58. Smart L, Hughes D. The Effects of Resuscitative Fluid Therapy on the Endothelial Surface Layer. Front Vet Sci. 2021;8:661660.
59. Thi MM, Tarbell JM, Weinbaum S, Spray DC. The role of the glycocalyx in reorganization of the actin cytoskeleton under fluid shear stress: a "bumper-car" model. Proc Natl Acad Sci U S A. 2004;101(47):16483-8.
60. Becker BF, Jacob M, Leipert S, Salmon AH, Chappell D. Degradation of the endothelial glycocalyx in clinical settings: searching for the sheddases. Br J Clin Pharmacol. 2015.
61. Simon Davis DA, Parish CR. Heparan sulfate: a ubiquitous glycosaminoglycan with multiple roles in immunity. Front Immunol. 2013;4:470.
62. Ihrcke NS, Wrenshall LE, Lindman BJ, Platt JL. Role of heparan sulfate in immune system-blood vessel interactions. Immunol Today. 1993;14(10):500-5.
63. Filmus J, Selleck SB. Glypicans: proteoglycans with a surprise. J Clin Invest. 2001;108(4):497-501.
64. Berg S, Engman A, Hesselvik JF, Laurent TC. Crystalloid infusion increases plasma hyaluronan. Crit Care Med. 1994;22(10):1563-7.
65. Mulivor AW, Lipowsky HH. Inflammation- and ischemia-induced shedding of venular glycocalyx. Am J Physiol Heart Circ Physiol. 2004;286(5):H1672-80.
66. Gao L, Lipowsky HH. Composition of the endothelial glycocalyx and its relation to its thickness and diffusion of small solutes. Microvasc Res. 2010;80(3):394-401.
67. Laurent TC, Fraser JR. Hyaluronan. FASEB J. 1992;6(7):2397-404.
68. Fraser JR, Laurent TC, Laurent UB. Hyaluronan: its nature, distribution, functions and turnover. J Intern Med. 1997;242(1):27-33.
69. Bevilacqua MP. Endothelial-leukocyte adhesion molecules. Annu Rev Immunol. 1993;11:767-804.
70. Golias C, Batistatou A, Bablekos G, Charalabopoulos A, Peschos D, Mitsopoulos P, et al. Physiology and pathophysiology of selectins, integrins, and IgSF cell adhesion molecules focusing on inflammation. A paradigm model on infectious endocarditis. Cell Commun Adhes. 2011;18(3):19-32.
71. Woodcock T, Woodcock TM. Revised Starling equation and the glycocalyx model of transvascular fluid exchange: an improved paradigm for prescribing intravenous fluid therapy. British journal of anaesthesia. 2012;108(3):384-94.

72. Jacob M, Paul O, Mehringer L, Chappell D, Rehm M, Welsch U, et al. Albumin augmentation improves condition of guinea pig hearts after 4 hr of cold ischemia. Transplantation. 2009;87(7):956-65.
73. Zeng Y, Adamson RH, Curry FR, Tarbell JM. Sphingosine-1-phosphate protects endothelial glycocalyx by inhibiting syndecan-1 shedding. Am J Physiol Heart Circ Physiol. 2014;306(3):H363-72.
74. Iba T, Levy JH, Aihara K, Kadota K, Tanaka H, Sato K, et al. Newly Developed Recombinant Antithrombin Protects the Endothelial Glycocalyx in an Endotoxin-Induced Rat Model of Sepsis. Int J Mol Sci. 2020;22(1).
75. Chappell D, Jacob M, Hofmann-Kiefer K, Rehm M, Welsch U, Conzen P, et al. Antithrombin reduces shedding of the endothelial glycocalyx following ischaemia/reperfusion. Cardiovasc Res. 2009;83(2):388-96.
76. Adachi T, Fukushima T, Usami Y, Hirano K. Binding of human xanthine oxidase to sulphated glycosaminoglycans on the endothelial-cell surface. Biochem J. 1993;289 (Pt 2)(Pt 2):523-7.
77. Dane MJ, van den Berg BM, Lee DH, Boels MG, Tiemeier GL, Avramut MC, et al. A microscopic view on the renal endothelial glycocalyx. Am J Physiol Renal Physiol. 2015;308(9):F956-66.
78. Chappell D, Jacob M, Paul O, Rehm M, Welsch U, Stoeckelhuber M, et al. The glycocalyx of the human umbilical vein endothelial cell: an impressive structure ex vivo but not in culture. Circ Res. 2009;104(11):1313-7.
79. Potter DR, Damiano ER. The hydrodynamically relevant endothelial cell glycocalyx observed in vivo is absent in vitro. Circ Res. 2008;102(7):770-6.
80. Jacob M, Bruegger D, Rehm M, Welsch U, Conzen P, Becker BF. Contrasting effects of colloid and crystalloid resuscitation fluids on cardiac vascular permeability. Anesthesiology. 2006;104(6):1223-31.
81. Chappell D, Hofmann-Kiefer K, Jacob M, Rehm M, Briegel J, Welsch U, et al. TNF-alpha induced shedding of the endothelial glycocalyx is prevented by hydrocortisone and antithrombin. Basic Res Cardiol. 2009;104(1):78-89.
82. van den Berg BM, Vink H, Spaan JA. The endothelial glycocalyx protects against myocardial edema. Circ Res. 2003;92(6):592-4.
83. Kataoka H, Ushiyama A, Kawakami H, Akimoto Y, Matsubara S, Iijima T. Fluorescent imaging of endothelial glycocalyx layer with wheat germ agglutinin using intravital microscopy. Microsc Res Tech. 2016;79(1):31-7.
84. Vink H, Constantinescu AA, Spaan JA. Oxidized lipoproteins degrade the endothelial surface layer : implications for platelet-endothelial cell adhesion. Circulation. 2000;101(13):1500-2.
85. Schmidt EP, Yang Y, Janssen WJ, Gandjeva A, Perez MJ, Barthel L, et al. The pulmonary endothelial glycocalyx regulates neutrophil adhesion and lung injury during experimental sepsis. Nat Med. 2012;18(8):1217-23.
86. Suzuki A, Tomita H, Okada H. Form follows function: The endothelial glycocalyx. Transl Res. 2022;247:158-67.
87. Megens RT, Reitsma S, Schiffers PH, Hilgers RH, De Mey JG, Slaaf DW, et al. Two-photon microscopy of vital murine elastic and muscular arteries. Combined structural and functional imaging with subcellular resolution. J Vasc Res. 2007;44(2):87-98.
88. Gavins FN. Intravital microscopy: new insights into cellular interactions. Curr Opin Pharmacol. 2012;12(5):601-7.
89. Corporate QS. Glycocheck 2017 [Available from: https://www.youtube.com/watch?v=w_xAaAJDwv4.
90. Lee DH, Dane MJ, van den Berg BM, Boels MG, van Teeffelen JW, de Mutsert R, et al. Deeper penetration of erythrocytes into the endothelial glycocalyx is associated with impaired microvascular perfusion. PLoS One. 2014;9(5):e96477.
91. Rovas A, Lukasz AH, Vink H, Urban M, Sackarnd J, Pavenstadt H, et al. Bedside analysis of the sublingual microvascular glycocalyx in the emergency room and intensive care unit - the GlycoNurse study. Scand J Trauma Resusc Emerg Med. 2018;26(1):16.

92. Astapenko D, Ticha A, Tomasova A, Hyspler R, Zadak Z, Lehmann C, et al. Evaluation of endothelial glycocalyx in healthy volunteers - An observational study. Clin Hemorheol Microcirc. 2020;75(3):257-65.
93. Ryan MA, Ford R, Ewer N, Hall KE, Guillaumin J, Edwards TH, et al. Sidestream dark field video microscopy demonstrates shelf-stable blood products preserve the endothelial glycocalyx in a canine hemorrhagic shock model. Am J Vet Res. 2024:1-7.
94. Cardillo JH, Tarbutton JD, Guillaumin J, Webb TL, Hall KE, Tucker CD, et al. Sidestream dark field imaging and biomarker evaluation reveal minimal significant changes to the microcirculation and glycocalyx in a canine hemorrhagic shock model. Am J Vet Res. 2023;84(12).
95. Londoño L, Bowen, CM, Buckley, GJ. EVALUATION OF THE ENDOTHELIAL GLYCOCALYX IN HEALTHY ANESTHETIZED DOGS USING RAPID, PATIENT-SIDE GLYCOCHECK ANALYSIS SOFTWARE. Journal of Veterinary Emergency and Critical Care. 2018;28(S1):S20.
96. Dostalova V, Astapenko D, Dostalova V, Jr., Kraus J, Cerny V, Ticha A, et al. The Effect of Fluid Loading and Hypertonic Saline Solution on Cortical Cerebral Microcirculation and Glycocalyx Integrity. J Neurosurg Anesthesiol. 2019;31(4):434-43.
97. Dostalova V, Schreiberova J, Dostalova V, Jr., Paral J, Kraus J, Ticha A, et al. Effects of Hypertonic Saline and Sodium Lactate on Cortical Cerebral Microcirculation and Brain Tissue Oxygenation. J Neurosurg Anesthesiol. 2018;30(2):163-70.
98. Dostal P, Schreiberova J, Dostalova V, Dostalova V, Jr., Tyll T, Paral J, et al. Effects of hypertonic saline and mannitol on cortical cerebral microcirculation in a rabbit craniotomy model. BMC Anesthesiol. 2015;15:88.
99. Astapenko D, Dostalova V, Dostalova V, Kraus J, Radochova V, Dostal P, et al. Effect of acute hypernatremia induced by hypertonic saline administration on endothelial glycocalyx in rabbits. Clin Hemorheol Microcirc. 2019;72(1):107-16.
100. Yozova ID, Londono LA, Millar KK, Sano H, Weidgraaf K, Thomson NA, et al. Rapid Patient-Side Evaluation of Endothelial Glycocalyx Thickness in Healthy Sedated Cats Using GlycoCheck(R) Software. Front Vet Sci. 2021;8:727063.
101. Haldenby KA, Chappell DC, Winlove CP, Parker KH, Firth JA. Focal and regional variations in the composition of the glycocalyx of large vessel endothelium. J Vasc Res. 1994;31(1):2-9.
102. Brouland JP, Gilbert MA, Bonneau M, Pignaud G, Bal Dit Solier C, Drouet L. Macro and microheterogeneity in normal endothelial cells: differential composition of luminal glycocalyx and functional implications. Endothelium. 1999;6(3):251-62.
103. Baldwin AL, Winlove CP. Effects of perfusate composition on binding of ruthenium red and gold colloid to glycocalyx of rabbit aortic endothelium. J Histochem Cytochem. 1984;32(3):259-66.
104. Kozar RA, Peng Z, Zhang R, Holcomb JB, Pati S, Park P, et al. Plasma restoration of endothelial glycocalyx in a rodent model of hemorrhagic shock. Anesth Analg. 2011;112(6):1289-95.
105. Ramani VC, Pruett PS, Thompson CA, DeLucas LD, Sanderson RD. Heparan sulfate chains of syndecan-1 regulate ectodomain shedding. J Biol Chem. 2012;287(13):9952-61.
106. Potter DR, Jiang J, Damiano ER. The recovery time course of the endothelial cell glycocalyx in vivo and its implications in vitro. Circ Res. 2009;104(11):1318-25.
107. Diab M, Nguyen F, Berthaud M, Maurel C, Gaschet J, Verger E, et al. Production and characterization of monoclonal antibodies specific for canine CD138 (syndecan-1) for nuclear medicine preclinical trials on spontaneous tumours. Vet Comp Oncol. 2017;15(3):932-51.
108. Jacob M, Bruegger D, Rehm M, Stoeckelhuber M, Welsch U, Conzen P, et al. The endothelial glycocalyx affords compatibility of Starling's principle and high cardiac interstitial albumin levels. Cardiovasc Res. 2007;73(3):575-86.
109. Nieuwdorp M, Meuwese MC, Mooij HL, Ince C, Broekhuizen LN, Kastelein JJ, et al. Measuring endothelial glycocalyx dimensions in humans: a potential novel tool to monitor vascular vulnerability. J Appl Physiol (1985). 2008;104(3):845-52.
110. Haeren RH, van de Ven SE, van Zandvoort MA, Vink H, van Overbeeke JJ, Hoogland G, et al. Assessment and Imaging of the Cerebrovascular Glycocalyx. Curr Neurovasc Res. 2016;13(3):249-60.
111. Anderle P, Niederer E, Rubas W, Hilgendorf C, Spahn-Langguth H, Wunderli-Allenspach H, et al. P-Glycoprotein (P-gp) mediated efflux in Caco-2 cell monolayers: the influence of culturing conditions and drug exposure on P-gp expression levels. J Pharm Sci. 1998;87(6):757-62.

112. Dull RO, Hahn RG. The glycocalyx as a permeability barrier: basic science and clinical evidence. Crit Care. 2022;26(1):273.
113. Hahn RG, Patel V, Dull RO. Human glycocalyx shedding: Systematic review and critical appraisal. Acta Anaesthesiol Scand. 2021;65(5):590-606.
114. Tsuruda T, Costello-Boerrigter LC, Burnett JC, Jr. Matrix metalloproteinases: pathways of induction by bioactive molecules. Heart Fail Rev. 2004;9(1):53-61.
115. Puchwein-Schwepcke A, Genzel-Boroviczény O, Nussbaum C. The Endothelial Glycocalyx: Physiology and Pathology in Neonates, Infants and Children. Front Cell Dev Biol. 2021;9:733557.
116. Chalkias A, Papagiannakis N, Mavrovounis G, Kolonia K, Mermiri M, Pantazopoulos I, et al. Sublingual microcirculatory alterations during the immediate and early postoperative period: A systematic review and meta-analysis. Clin Hemorheol Microcirc. 2022;80(3):253-65.
117. Cooper ES, Silverstein DC. Fluid Therapy and the Microcirculation in Health and Critical Illness. Front Vet Sci. 2021;8:625708.
118. Hahn RG, Dull RO, Zdolsek J. The Extended Starling principle needs clinical validation. Acta Anaesthesiol Scand. 2020;64(7):884-7.
119. Woodcock TE, Michel CC. Advances in the Starling Principle and Microvascular Fluid Exchange; Consequences and Implications for Fluid Therapy. Front Vet Sci. 2021;8:623671.
120. Oshima K, Haeger SM, Hippensteel JA, Herson PS, Schmidt EP. More than a biomarker: the systemic consequences of heparan sulfate fragments released during endothelial surface layer degradation (2017 Grover Conference Series). Pulm Circ. 2018;8(1):2045893217745786.
121. De Backer D, Orbegozo Cortes D, Donadello K, Vincent JL. Pathophysiology of microcirculatory dysfunction and the pathogenesis of septic shock. Virulence. 2014;5(1):73-9.
122. De Backer D. Is microcirculatory assessment ready for regular use in clinical practice? Curr Opin Crit Care. 2019;25(3):280-4.
123. Tuma M, Canestrini S, Alwahab Z, Marshall J. Trauma and Endothelial Glycocalyx: The Microcirculation Helmet? Shock. 2016;46(4):352-7.
124. Chappell D, Jacob M, Hofmann-Kiefer K, Conzen P, Rehm M. A rational approach to perioperative fluid management. Anesthesiology. 2008;109(4):723-40.
125. Tarbell JM, Cancel LM. The glycocalyx and its significance in human medicine. J Intern Med. 2016;280(1):97-113.
126. Martin L, Koczera P, Zechendorf E, Schuerholz T. The Endothelial Glycocalyx: New Diagnostic and Therapeutic Approaches in Sepsis. Biomed Res Int. 2016;2016:3758278.
127. Myburgh JA, Mythen MG. Resuscitation fluids. N Engl J Med. 2013;369(13):1243-51.
128. Chignalia AZ, Yetimakman F, Christiaans SC, Unal S, Bayrakci B, Wagener BM, et al. The glycocalyx and Trauma: A Review. Shock. 2015.
129. Becker BF, Chappell D, Bruegger D, Annecke T, Jacob M. Therapeutic strategies targeting the endothelial glycocalyx: acute deficits, but great potential. Cardiovasc Res. 2010;87(2):300-10.
130. Yiew XT, Bateman SW, Hahn RG, Bersenas AME. Evaluation of the Distribution and Elimination of Balanced Isotonic Crystalloid, 5% Hypertonic Saline, and 6% Tetrastarch 130/0.4 Using Volume Kinetic Modeling and Analysis in Healthy Conscious Cats. Front Vet Sci. 2020;7:587564.
131. Gelendi S, Yiew XT, Bateman S, Gerken K, Kuo KW, Ravis WR, et al. Mild hypothermia is associated with altered volume kinetic parameters of an intravenous crystalloid fluid bolus in healthy isoflurane-anesthetized cats. Am J Vet Res. 2024:1-10.
132. Levick JR, Michel CC. Microvascular fluid exchange and the revised Starling principle. Cardiovasc Res. 2010;87(2):198-210.
133. Henriksen JH. Ernest Henry Starling (1866-1927): the scientist and the man. J Med Biogr. 2005;13(1):22-30.
134. Finfer S, Myburgh J, Bellomo R. Intravenous fluid therapy in critically ill adults. Nat Rev Nephrol. 2018;14(9):541-57.
135. Singer M, Deutschman CS, Seymour CW, Shankar-Hari M, Annane D, Bauer M, et al. The Third International Consensus Definitions for Sepsis and Septic Shock (Sepsis-3). JAMA. 2016;315(8):801-10.
136. Raghunathan K, Shaw AD, Bagshaw SM. Fluids are drugs: type, dose and toxicity. Curr Opin Crit Care. 2013;19(4):290-8.

137. Malbrain M, Langer T, Annane D, Gattinoni L, Elbers P, Hahn RG, et al. Intravenous fluid therapy in the perioperative and critical care setting: Executive summary of the International Fluid Academy (IFA). Ann Intensive Care. 2020;10(1):64.
138. Pardo M, Spencer E, Odunayo A, Ramirez ML, Rudloff E, Shafford H, et al. 2024 AAHA Fluid Therapy Guidelines for Dogs and Cats. J Am Anim Hosp Assoc. 2024;60(4):131-63.
139. Johansson PI, Stensballe J, Ostrowski SR. Shock induced endotheliopathy (SHINE) in acute critical illness - a unifying pathophysiologic mechanism. Crit Care. 2017;21(1):25.
140. Parish CR. Heparan sulfate and inflammation. Nat Immunol. 2005;6(9):861-2.
141. Ostrowski SR, Johansson PI. Endothelial glycocalyx degradation induces endogenous heparinization in patients with severe injury and early traumatic coagulopathy. J Trauma Acute Care Surg. 2012;73(1):60-6.
142. Sukudom S, Smart L, Macdonald S. Association between intravenous fluid administration and endothelial glycocalyx shedding in humans: a systematic review. Intensive Care Med Exp. 2024;12(1):16.
143. Kuhn M. Endothelial actions of atrial and B-type natriuretic peptides. Br J Pharmacol. 2012;166(2):522-31.
144. Moro C, Berlan M. Cardiovascular and metabolic effects of natriuretic peptides. Fundam Clin Pharmacol. 2006;20(1):41-9.
145. Curry FR. Atrial natriuretic peptide: an essential physiological regulator of transvascular fluid, protein transport, and plasma volume. J Clin Invest. 2005;115(6):1458-61.
146. Rehm M, Bruegger D, Christ F, Conzen P, Thiel M, Jacob M, et al. Shedding of the endothelial glycocalyx in patients undergoing major vascular surgery with global and regional ischemia. Circulation. 2007;116(17):1896-906.
147. Svennevig K, Hoel T, Thiara A, Kolset S, Castelheim A, Mollnes T, et al. Syndecan-1 plasma levels during coronary artery bypass surgery with and without cardiopulmonary bypass. Perfusion. 2008;23(3):165-71.
148. Bruegger D, Schwartz L, Chappell D, Jacob M, Rehm M, Vogeser M, et al. Release of atrial natriuretic peptide precedes shedding of the endothelial glycocalyx equally in patients undergoing on- and off-pump coronary artery bypass surgery. Basic Res Cardiol. 2011;106(6):1111-21.
149. Belousoviene E, Pranskuniene Z, Vaitkaitiene E, Pilvinis V, Pranskunas A. Effect of high-dose intravenous ascorbic acid on microcirculation and endothelial glycocalyx during sepsis and septic shock: a double-blind, randomized, placebo-controlled study. BMC Anesthesiol. 2023;23(1):309.
150. Hasselgren E, Zdolsek M, Zdolsek JH, Bjorne H, Krizhanovskii C, Ntika S, et al. Long Intravascular Persistence of 20% Albumin in Postoperative Patients. Anesth Analg. 2019;129(5):1232-9.
151. Bruegger D, Brettner F, Rossberg I, Nussbaum C, Kowalski C, Januszewska K, et al. Acute degradation of the endothelial glycocalyx in infants undergoing cardiac surgical procedures. Ann Thorac Surg. 2015;99(3):926-31.
152. Hofmann-Kiefer KF, Knabl J, Martinoff N, Schiessl B, Conzen P, Rehm M, et al. Increased serum concentrations of circulating glycocalyx components in HELLP syndrome compared to healthy pregnancy: an observational study. Reprod Sci. 2013;20(3):318-25.
153. Vlahu CA, Lemkes BA, Struijk DG, Koopman MG, Krediet RT, Vink H. Damage of the endothelial glycocalyx in dialysis patients. J Am Soc Nephrol. 2012;23(11):1900-8.
154. Fernández-Sarmiento J, Lamprea S, Barrera S, Acevedo L, Duque C, Trujillo M, et al. The association between prolonged capillary refill time and microcirculation changes in children with sepsis. BMC Pediatr. 2024;24(1):68.
155. Fernández-Sarmiento J, Salazar-Peláez LM, Acevedo L, Niño-Serna LF, Flórez S, Alarcón-Forero L, et al. Endothelial and Glycocalyx Biomarkers in Children With Sepsis After One Bolus of Unbalanced or Balanced Crystalloids. Pediatr Crit Care Med. 2023;24(3):213-21.
156. Rovas A, Sackarnd J, Rossaint J, Kampmeier S, Pavenstädt H, Vink H, et al. Identification of novel sublingual parameters to analyze and diagnose microvascular dysfunction in sepsis: the NOSTRADAMUS study. Crit Care. 2021;25(1):112.
157. Belousoviene E, Kiudulaite I, Pilvinis V, Pranskunas A. Links between Endothelial Glycocalyx Changes and Microcirculatory Parameters in Septic Patients. Life (Basel). 2021;11(8).

158. Rovas A, Seidel LM, Vink H, Pohlkotter T, Pavenstadt H, Ertmer C, et al. Association of sublingual microcirculation parameters and endothelial glycocalyx dimensions in resuscitated sepsis. Crit Care. 2019;23(1):260.
159. Messmer AS, Zingg C, Muller M, Gerber JL, Schefold JC, Pfortmueller CA. Fluid Overload and Mortality in Adult Critical Care Patients-A Systematic Review and Meta-Analysis of Observational Studies. Crit Care Med. 2020;48(12):1862-70.
160. Ostroski CJ, Drobatz KJ, Reineke EL. Retrospective evaluation of and risk factor analysis for presumed fluid overload in cats with urethral obstruction: 11 cases (2002-2012). J Vet Emerg Crit Care (San Antonio). 2017;27(5):561-8.
161. Johansson PI, Ostrowski SR. Acute coagulopathy of trauma: balancing progressive catecholamine induced endothelial activation and damage by fluid phase anticoagulation. Med Hypotheses. 2010;75(6):564-7.
162. Damiani E, Carsetti A, Casarotta E, Domizi R, Scorcella C, Donati A, et al. Microcirculation-guided resuscitation in sepsis: the next frontier? Front Med (Lausanne). 2023;10:1212321.
163. Ait-Oufella H, Bourcier S, Lehoux S, Guidet B. Microcirculatory disorders during septic shock. Curr Opin Crit Care. 2015;21(4):271-5.
164. Komarova YA, Kruse K, Mehta D, Malik AB. Protein Interactions at Endothelial Junctions and Signaling Mechanisms Regulating Endothelial Permeability. Circ Res. 2017;120(1):179-206.
165. Inagawa R, Okada H, Takemura G, Suzuki K, Takada C, Yano H, et al. Ultrastructural Alteration of Pulmonary Capillary Endothelial Glycocalyx During Endotoxemia. Chest. 2018.
166. Rehm M, Zahler S, Lotsch M, Welsch U, Conzen P, Jacob M, et al. Endothelial glycocalyx as an additional barrier determining extravasation of 6% hydroxyethyl starch or 5% albumin solutions in the coronary vascular bed. Anesthesiology. 2004;100(5):1211-23.
167. Chappell D, Jacob M, Hofmann-Kiefer K, Bruegger D, Rehm M, Conzen P, et al. Hydrocortisone preserves the vascular barrier by protecting the endothelial glycocalyx. Anesthesiology. 2007;107(5):776-84.
168. Cerny V, Astapenko D, Burkovskiy I, Hyspler R, Ticha A, Trevors MA, et al. Glycocalyx in vivo measurement. Clin Hemorheol Microcirc. 2017;67(3-4):499-503.
169. Wright IM, Latter JL, Dyson RM, Levi CR, Clifton VL. Videomicroscopy as a tool for investigation of the microcirculation in the newborn. Physiol Rep. 2016;4(19).
170. Goodnight ME, Cooper ES, Butler AL. Assessment of microcirculatory perfusion in healthy anesthetized cats undergoing ovariohysterectomy using sidestream dark field microscopy. J Vet Emerg Crit Care (San Antonio). 2015;25(3):349-57.
171. Gommeren K, Allerton FJ, Morin E, Reynaud A, Peeters D, Silverstein DC. Evaluation of a rapid bedside scoring system for microcirculation videos acquired from dogs. J Vet Emerg Crit Care (San Antonio). 2014;24(5):554-61.
172. Silverstein DC, Cozzi EM, Hopkins AS, Keefe TJ. Microcirculatory effects of intravenous fluid administration in anesthetized dogs undergoing elective ovariohysterectomy. Am J Vet Res. 2014;75(9):809-17.
173. Silverstein DC, Pruett-Saratan A, 2nd, Drobatz KJ. Measurements of microvascular perfusion in healthy anesthetized dogs using orthogonal polarization spectral imaging. J Vet Emerg Crit Care (San Antonio). 2009;19(6):579-87.
174. Peruski AM, Cooper ES. Assessment of microcirculatory changes by use of sidestream dark field microscopy during hemorrhagic shock in dogs. Am J Vet Res. 2011;72(4):438-45.
175. Treu CM, Lupi O, Bottino DA, Bouskela E. Sidestream dark field imaging: the evolution of real-time visualization of cutaneous microcirculation and its potential application in dermatology. Arch Dermatol Res. 2011;303(2):69-78.
176. GlycoCheck. GlycoCheck Analysis, Measurement and Research Technology [Available from: https://glycocalyx.com/pages/glycocheck.
177. Ince C, Boerma EC, Cecconi M, De Backer D, Shapiro NI, Duranteau J, et al. Second consensus on the assessment of sublingual microcirculation in critically ill patients: results from a task force of the European Society of Intensive Care Medicine. Intensive Care Med. 2018;44(3):281-99.
178. Ikonomidis I, Voumvourakis A, Makavos G, Triantafyllidi H, Pavlidis G, Katogiannis K, et al. Association of impaired endothelial glycocalyx with arterial stiffness, coronary microcirculatory

dysfunction, and abnormal myocardial deformation in untreated hypertensives. J Clin Hypertens (Greenwich). 2018;20(4):672-9.
179. Martens RJ, Vink H, van Oostenbrugge RJ, Staals J. Sublingual microvascular glycocalyx dimensions in lacunar stroke patients. Cerebrovasc Dis. 2013;35(5):451-4.
180. Dane MJ, Khairoun M, Lee DH, van den Berg BM, Eskens BJ, Boels MG, et al. Association of kidney function with changes in the endothelial surface layer. Clin J Am Soc Nephrol. 2014;9(4):698-704.
181. Bol ME, Broddin BEK, Delhaas T, Sels JEM, van de Poll MCG. Variability of microcirculatory measurements in healthy volunteers. Sci Rep. 2022;12(1):19887.
182. Donati A, Damiani E, Domizi R, Romano R, Adrario E, Pelaia P, et al. Alteration of the sublingual microvascular glycocalyx in critically ill patients. Microvasc Res. 2013;90:86-9.
183. Puchwein-Schwepcke A, Artmann S, Rajwich L, Genzel-Boroviczény O, Nussbaum C. Effect of gestational age and postnatal age on the endothelial glycocalyx in neonates. Sci Rep. 2021;11(1):3133.
184. Valerio L, Peters RJ, Zwinderman AH, Pinto-Sietsma SJ. Reproducibility of sublingual microcirculation parameters obtained from sidestream darkfield imaging. PLoS One. 2019;14(3):e0213175.
185. Eickhoff MK, Winther SA, Hansen TW, Diaz LJ, Persson F, Rossing P, et al. Assessment of the sublingual microcirculation with the GlycoCheck system: Reproducibility and examination conditions. PLoS One. 2020;15(12):e0243737.
186. Bol ME, Beurskens DMH, Delnoij TSR, Roekaerts P, Reutelingsperger CPM, Delhaas T, et al. Variability of Microcirculatory Measurements in Critically Ill Patients. Shock. 2020;54(1):9-14.
187. Gu YM, Wang S, Zhang L, Liu YP, Thijs L, Petit T, et al. Characteristics and determinants of the sublingual microcirculation in populations of different ethnicity. Hypertension. 2015;65(5):993-1001.
188. Yuan L, Han J, van der Velden AIM, Vink H, de Mutsert R, Rosendaal FR, et al. Sex-specific association between microvascular health and coagulation parameters: the Netherlands Epidemiology of Obesity study. J Thromb Haemost. 2023;21(9):2585-95.
189. Haeren RH, Vink H, Staals J, van Zandvoort MA, Dings J, van Overbeeke JJ, et al. Protocol for intraoperative assessment of the human cerebrovascular glycocalyx. BMJ Open. 2017;7(1):e013954.
190. Haeren RHL, Rijkers K, Schijns O, Dings J, Hoogland G, van Zandvoort M, et al. In vivo assessment of the human cerebral microcirculation and its glycocalyx: A technical report. J Neurosci Methods. 2018;303:114-25.
191. Mullen KM, Regier PJ, Londoño LA, Millar K, Groover J. Evaluation of jejunal microvasculature of healthy anesthetized dogs with sidestream dark field video microscopy. Am J Vet Res. 2020;81(11):888-93.
192. Fuchs A, Groß S, Neumann T, Illerhaus A, Vink H, Klasen G, et al. Immediate effects of whole blood donation on the endothelial surface layer and glycocalyx shedding. Blood Transfus. 2021;19(3):190-6.
193. Gimblet CJ, Ernst JW, Bos KD, Stroud AK, Donato AJ, Jalal DI, et al. Effect of acute heparin administration on glycocalyx thickness and endothelial function in healthy younger adults. J Appl Physiol (1985). 2024;136(2):330-6.
194. Soubihe Neto N, de Almeida MCV, Couto HO, Miranda CH. Biomarkers of endothelial glycocalyx damage are associated with microvascular dysfunction in resuscitated septic shock patients. Microvasc Res. 2024;154:104683.
195. Fernandez-Sarmiento J, Hernandez-Sarmiento R, Salazar MP, Barrera S, Castilla V, Duque C. The association between hypoalbuminemia and microcirculation, endothelium, and glycocalyx disorders in children with sepsis. Microcirculation. 2023;30(8):e12829.
196. Lam PK, McBride A, Le DHT, Huynh TT, Vink H, Wills B, et al. Visual and Biochemical Evidence of Glycocalyx Disruption in Human Dengue Infection, and Association With Plasma Leakage Severity. Front Med (Lausanne). 2020;7:545813.
197. Liew H, Roberts MA, McMahon LP. Markers of the Endothelial Glycocalyx Are Improved following Kidney Transplantation. Kidney Blood Press Res. 2021;46(5):581-7.

198. Liew H, Roberts MA, Pope A, McMahon LP. Endothelial glycocalyx damage in kidney disease correlates with uraemic toxins and endothelial dysfunction. BMC Nephrol. 2021;22(1):21.
199. Regier M, Drost CC, Rauen M, Pavenstädt H, Rovas A, Kümpers P, et al. A Dietary Supplement Containing Fucoidan Preserves Endothelial Glycocalyx through ERK/MAPK Signaling and Protects against Damage Induced by CKD Serum. Int J Mol Sci. 2022;23(24).
200. Beurskens DM, Bol ME, Delhaas T, van de Poll MC, Reutelingsperger CP, Nicolaes GA, et al. Decreased endothelial glycocalyx thickness is an early predictor of mortality in sepsis. Anaesth Intensive Care. 2020;48(3):221-8.
201. Dekker NAM, Veerhoek D, van Leeuwen ALI, Vonk ABA, van den Brom CE, Boer C. Microvascular Alterations During Cardiac Surgery Using a Heparin or Phosphorylcholine-Coated Circuit. J Cardiothorac Vasc Anesth. 2020;34(4):912-9.
202. Dekker NAM, Veerhoek D, Koning NJ, van Leeuwen ALI, Elbers PWG, van den Brom CE, et al. Postoperative microcirculatory perfusion and endothelial glycocalyx shedding following cardiac surgery with cardiopulmonary bypass. Anaesthesia. 2019;74(5):609-18.
203. Nussbaum C, Haberer A, Tiefenthaller A, Januszewska K, Chappell D, Brettner F, et al. Perturbation of the microvascular glycocalyx and perfusion in infants after cardiopulmonary bypass. J Thorac Cardiovasc Surg. 2015;150(6):1474-81 e1.
204. Osiaevi I, Schulze A, Evers G, Harmening K, Vink H, Kümpers P, et al. Persistent capillary rarefication in long COVID syndrome. Angiogenesis. 2023;26(1):53-61.
205. Rovas A, Buscher K, Osiaevi I, Drost CC, Sackarnd J, Tepasse PR, et al. Microvascular and proteomic signatures overlap in COVID-19 and bacterial sepsis: the MICROCODE study. Angiogenesis. 2022;25(4):503-15.
206. Rovas A, Osiaevi I, Buscher K, Sackarnd J, Tepasse PR, Fobker M, et al. Microvascular dysfunction in COVID-19: the MYSTIC study. Angiogenesis. 2021;24(1):145-57.
207. Astapenko D, Pouska J, Benes J, Skulec R, Lehmann C, Vink H, et al. Neuraxial anesthesia is less harmful to the endothelial glycocalyx during elective joint surgery compared to general anesthesia. Clin Hemorheol Microcirc. 2019;72(1):11-21.
208. Brettner F, Heitzer M, Thiele F, Hulde N, Nussbaum C, Achatz S, et al. Non-invasive evaluation of macro- and microhemodynamic changes during induction of general anesthesia - A prospective observational single-blinded trial. Clin Hemorheol Microcirc. 2021;77(1):1-16.
209. Ikonomidis I, Pavlidis G, Tsoumani M, Kousathana F, Katogiannis K, Tsilivarakis D, et al. Endothelial Dysfunction Is Associated with Decreased Nitric Oxide Bioavailability in Dysglycaemic Subjects and First-Degree Relatives of Type 2 Diabetic Patients. J Clin Med. 2022;11(12).
210. Lambadiari V, Pavlidis G, Kousathana F, Maratou E, Georgiou D, Andreadou I, et al. Effects of Different Antidiabetic Medications on Endothelial Glycocalyx, Myocardial Function, and Vascular Function in Type 2 Diabetic Patients: One Year Follow-Up Study. J Clin Med. 2019;8(7).
211. Stougaard EB, Winther SA, Amadid H, Frimodt-Møller M, Persson F, Hansen TW, et al. Endothelial glycocalyx and cardio-renal risk factors in type 1 diabetes. PLoS One. 2021;16(7):e0254859.
212. Triantafyllidi H, Benas D, Vlachos S, Vlastos D, Pavlidis G, Schoinas A, et al. HDL cholesterol levels and endothelial glycocalyx integrity in treated hypertensive patients. J Clin Hypertens (Greenwich). 2018;20(11):1615-23.
213. Ikonomidis I, Pavlidis G, Lambadiari V, Rafouli-Stergiou P, Makavos G, Thymis J, et al. Endothelial glycocalyx and microvascular perfusion are associated with carotid intima-media thickness and impaired myocardial deformation in psoriatic disease. J Hum Hypertens. 2022;36(12):1113-20.
214. van der Velden AIM, van den Berg BM, de Mutsert R, van der Vlag J, Jukema JW, Rosendaal FR, et al. Microvascular differences in individuals with obesity at risk of developing cardiovascular disease. Obesity (Silver Spring). 2021;29(9):1439-44.
215. Weissgerber TL, Garcia-Valencia O, Milic NM, Codsi E, Cubro H, Nath MC, et al. Early Onset Preeclampsia Is Associated With Glycocalyx Degradation and Reduced Microvascular Perfusion. J Am Heart Assoc. 2019;8(4):e010647.
216. Diaz DM, Orton EC, de Rezende ML, Zersen K, Guillaumin J. Assessment of microcirculation variables and endothelial glycocalyx using sidestream dark field videomicroscopy in anesthetized dogs undergoing cardiopulmonary bypass. Front Vet Sci. 2023;10:1189738.

217. Wadowski PP, Kautzky-Willer A, Gremmel T, Koppensteiner R, Wolf P, Ertl S, et al. Sublingual microvasculature in diabetic patients. Microvasc Res. 2020;129:103971.
218. Obonyo NG, Fanning JP, Ng AS, Pimenta LP, Shekar K, Platts DG, et al. Effects of volume resuscitation on the microcirculation in animal models of lipopolysaccharide sepsis: a systematic review. Intensive Care Med Exp. 2016;4(1):38.
219. Rajan V, Varghese B, van Leeuwen TG, Steenbergen W. Review of methodological developments in laser Doppler flowmetry. Lasers Med Sci. 2009;24(2):269-83.
220. Sant S, Gouraud E, Boisson C, Nader E, Goparaju M, Cannas G, et al. Sublingual Microcirculation Specificity of Sickle Cell Patients: Morphology of the Microvascular Bed, Blood Rheology, and Local Hemodynamics. Int J Mol Sci. 2023;24(4).
221. Rawal G, Kumar R, Yadav S, Singh A. Anemia in Intensive Care: A Review of Current Concepts. J Crit Care Med (Targu Mures). 2016;2(3):109-14.
222. Damen T, Reinsfelt B, Redfors B, Nygren A. Pressure-dependent changes in haematocrit and plasma volume during anaesthesia, a randomised clinical trial. Acta Anaesthesiol Scand. 2016;60(5):560-8.
223. Cui N, Wang H, Long Y, Su L, Liu D. Dexamethasone Suppressed LPS-Induced Matrix Metalloproteinase and Its Effect on Endothelial Glycocalyx Shedding. Mediators Inflamm. 2015;2015:912726.
224. de Oliveira J, Miranda CH. Doxycycline protects against sepsis-induced endothelial glycocalyx shedding. Sci Rep. 2024;14(1):10477.
225. Lipowsky HH, Lescanic A. The effect of doxycycline on shedding of the glycocalyx due to reactive oxygen species. Microvasc Res. 2013;90:80-5.
226. Ramnath R, Foster RR, Qiu Y, Cope G, Butler MJ, Salmon AH, et al. Matrix metalloproteinase 9-mediated shedding of syndecan 4 in response to tumor necrosis factor alpha: a contributor to endothelial cell glycocalyx dysfunction. Faseb j. 2014;28(11):4686-99.
227. Manon-Jensen T, Multhaupt HA, Couchman JR. Mapping of matrix metalloproteinase cleavage sites on syndecan-1 and syndecan-4 ectodomains. FEBS J. 2013;280(10):2320-31.
228. Kinnunen P, Vuolteenaho O, Ruskoaho H. Mechanisms of atrial and brain natriuretic peptide release from rat ventricular myocardium: effect of stretching. Endocrinology. 1993;132(5):1961-70.
229. Mantymaa P, Vuolteenaho O, Marttila M, Ruskoaho H. Atrial stretch induces rapid increase in brain natriuretic peptide but not in atrial natriuretic peptide gene expression in vitro. Endocrinology. 1993;133(3):1470-3.
230. Vestweber D. VE-cadherin: the major endothelial adhesion molecule controlling cellular junctions and blood vessel formation. Arterioscler Thromb Vasc Biol. 2008;28(2):223-32.
231. Boffa MC, Karmochkine M. Thrombomodulin: an overview and potential implications in vascular disorders. Lupus. 1998;7 Suppl 2:S120-5.
232. Akwii RG, Sajib MS, Zahra FT, Mikelis CM. Role of Angiopoietin-2 in Vascular Physiology and Pathophysiology. Cells. 2019;8(5).
233. Behnoush AH, Khalaji A, Bahiraie P, Alehossein P, Shobeiri P, Peisepar M, et al. Endocan as a marker of endothelial dysfunction in hypertension: a systematic review and meta-analysis. Hypertens Res. 2023;46(10):2388-99.
234. Anand D, Ray S, Srivastava LM, Bhargava S. Evolution of serum hyaluronan and syndecan levels in prognosis of sepsis patients. Clin Biochem. 2016;49(10-11):768-76.
235. Braunstein M, Annecke T, Frey K, Kusmenkov T, Wornle M, Ney L, et al. Effect on Syndecan-1 and Hyaluronan Levels Depending on Multiple Organ Failure, Coagulopathy and Survival: An Observational Study in Major Trauma Patients. J Clin Med. 2024;13(22).
236. Johansson PI, Stensballe J, Rasmussen LS, Ostrowski SR. A high admission syndecan-1 level, a marker of endothelial glycocalyx degradation, is associated with inflammation, protein C depletion, fibrinolysis, and increased mortality in trauma patients. Ann Surg. 2011;254(2):194-200.
237. Rahbar E, Cardenas JC, Baimukanova G, Usadi B, Bruhn R, Pati S, et al. Endothelial glycocalyx shedding and vascular permeability in severely injured trauma patients. J Transl Med. 2015;13:117.
238. Nemme J, Krizhanovskii C, Ntika S, Sabelnikovs O, Vanags I, Hahn RG. Hypervolemia does not cause degradation of the endothelial glycocalyx layer during open hysterectomy performed under sevoflurane or propofol anesthesia. Acta Anaesthesiol Scand. 2020;64(4):538-45.

239. Bro-Jeppesen J, Johansson PI, Hassager C, Wanscher M, Ostrowski SR, Bjerre M, et al. Endothelial activation/injury and associations with severity of post-cardiac arrest syndrome and mortality after out-of-hospital cardiac arrest. Resuscitation. 2016;107:71-9.
240. Smart L, Macdonald SPJ, Bosio E, Fatovich D, Neil C, Arendts G. Bolus therapy with 3% hypertonic saline or 0.9% saline in emergency department patients with suspected sepsis: A pilot randomised controlled trial. J Crit Care. 2019;52:33-9.
241. Sallisalmi M, Tenhunen J, Yang R, Oksala N, Pettila V. Vascular adhesion protein-1 and syndecan-1 in septic shock. Acta Anaesthesiol Scand. 2012;56(3):316-22.
242. Ider M, Ceylan C, Naseri A, Ceylan O, Durgut MK, Ok M, et al. Evaluation of endothelial glycocalyx injury biomarkers in feline hemotropic mycoplasmosis. Sci Rep. 2024;14(1):12931.
243. Parlak K NA, Yalcin M, Akyol ET, Ok M, Arican M. Evaluation of trauma scoring and endothelial glyocalyx injury in cats with head trauma. Slovenian Veterinary Research. 2022;59(4):185-93.
244. Beiseigel M, Simon BT, Michalak C, Stickney MJ, Jeffery U. Effect of peri-operative crystalloid fluid rate on circulating hyaluronan in healthy dogs: A pilot study. Vet J. 2021;267:105578.
245. Berg S, Golster M, Lisander B. Albumin extravasation and tissue washout of hyaluronan after plasma volume expansion with crystalloid or hypooncotic colloid solutions. Acta Anaesthesiol Scand. 2002;46(2):166-72.
246. Aukland K, Reed RK. Interstitial-lymphatic mechanisms in the control of extracellular fluid volume. Physiol Rev. 1993;73(1):1-78.
247. Smart L, Boyd CJ, Claus MA, Bosio E, Hosgood G, Raisis A. Large-Volume Crystalloid Fluid Is Associated with Increased Hyaluronan Shedding and Inflammation in a Canine Hemorrhagic Shock Model. Inflammation. 2018.
248. Yini S, Heng Z, Xin A, Xiaochun M. Effect of unfractionated heparin on endothelial glycocalyx in a septic shock model. Acta Anaesthesiol Scand. 2015;59(2):160-9.
249. Hahn RG, Hasselgren E, Bjorne H, Zdolsek M, Zdolsek J. Biomarkers of endothelial injury in plasma are dependent on kidney function. Clin Hemorheol Microcirc. 2019;72(2):161-8.
250. Lockett MF. Effects of saline loading on the perfused cat kidney. J Physiol. 1966;187(3):489-500.
251. Sun Y YX, Beeler-Marfisi J, Kerr CL, Bateman S. Comparison of volume kinetics in awake, anesthetized spontaneously breathing, and anesthetized mechanically ventilated healthy female cats. In: Abstracts from the International Veterinary Emergency and Critical Care Symposium and the European Veterinary Emergency and Critical Care Annual Congress 2024. Journal of Veterinary Emergency and Critical Care. 2024;34(S2):S10-S1.
252. Groom AC, Rowlands S. The cardiac output and blood volume of the anaesthetized cat. Phys Med Biol. 1958;3(2):138-56.
253. John G. Gibson 2nd JLK, Michel Pijoan. THE BLOOD VOLUME OF NORMAL DOGS. American Journal of Physiology-Legacy Content. 1938;121(3):800-6.
254. Breznock EM, Strack D. Effects of the spleen, epinephrine, and splenectomy on determination of blood volume in cats. Am J Vet Res. 1982;43(11):2062-6.
255. Breznock EM, Strack D. Blood volume of nonsplenectomized and splenectomized cats before and after acute hemorrhage. Am J Vet Res. 1982;43(10):1811-4.
256. Tan AWK, Li RHL, Ueda Y, Stern JA, Hussain M, Haginoya S, et al. Platelet Priming and Activation in Naturally Occurring Thermal Burn Injuries and Wildfire Smoke Exposure Is Associated With Intracardiac Thrombosis and Spontaneous Echocardiographic Contrast in Feline Survivors. Frontiers in Veterinary Science. 2022;Volume 9 - 2022.
257. Rudloff E, Kirby R. Feline Circulatory Shock In: Little S, editor. August's Consultations in Feline Internal Medicine 7 St Lous, USA Elsevier 2016. p. 843-58.
258. Reineke EL, Rees C, Drobatz KJ. Association of blood lactate concentration with physical perfusion variables, blood pressure, and outcome for cats treated at an emergency service. J Am Vet Med Assoc. 2015;247(1):79-84.
259. Chalifoux NV, Hess RS, Silverstein DC. Effectiveness of intravenous fluid resuscitation in hypotensive cats: 82 cases (2012-2019). J Vet Emerg Crit Care (San Antonio). 2021;31(4):508-15.

260. Donati PA, Tunesi M, Araos J. Caudal vena cava measurements and fluid responsiveness in hospitalized cats with compromised hemodynamics and tissue hypoperfusion. J Vet Emerg Crit Care (San Antonio). 2023;33(1):29-37.
261. Silverstein DC, Kleiner J, Drobatz KJ. Effectiveness of intravenous fluid resuscitation in the emergency room for treatment of hypotension in dogs: 35 cases (2000-2010). J Vet Emerg Crit Care (San Antonio). 2012;22(6):666-73.
262. Donati PA, Guevara JM, Ardiles V, Guillemi EC, Londoño L, Dubin A. Caudal vena cava collapsibility index as a tool to predict fluid responsiveness in dogs. J Vet Emerg Crit Care (San Antonio). 2020;30(6):677-86.
263. Zweifach BW, Lipowsky HH. Quantitative studies of microcirculatory structure and function. III. Microvascular hemodynamics of cat mesentery and rabbit omentum. Circ Res. 1977;41(3):380-90.
264. Gore RW. Pressures in Cat Mesenteric Arterioles and Capillaries during Changes in Systemic Arterial Blood Pressure. Circulation Research. 1974;34:581–91.
265. Frasher WG, Jr., Wayland H. A repeating modular organization of the microcirculation of cat mesentery. Microvasc Res. 1972;4(1):62-76.
266. Clark ES, Granger DN. Effects of fenoldopam on feline intestinal microcirculation. The Journal of Pharmacology and Experimental Therapeutics. 1988;244(3):983-6.
267. Stock E, Daminet S, Paepe D, Buresova E, Vandermeulen E, Smets P, et al. Evaluation of Renal Perfusion in Hyperthyroid Cats before and after Radioiodine Treatment. J Vet Intern Med. 2017;31(6):1658-63.
268. Stock E, Vanderperren K, Bosmans T, Dobbeleir A, Duchateau L, Hesta M, et al. Evaluation of Feline Renal Perfusion with Contrast-Enhanced Ultrasonography and Scintigraphy. PLoS One. 2016;11(10):e0164488.
269. Liao PT, Tillson M, Clark-Price S, Kuo K, Gerken K. Microvascular reactivity in anesthetized cats: feasibility and proof of concept study. Am J Vet Res. 2025;86(1).
270. Friedrichs KR, Harr KE, Freeman KP, Szladovits B, Walton RM, Barnhart KF, et al. ASVCP reference interval guidelines: determination of de novo reference intervals in veterinary species and other related topics. Vet Clin Pathol. 2012;41(4):441-53.
271. Henrich M, Gruss M, Weigand MA. Sepsis-induced degradation of endothelial glycocalix. ScientificWorldJournal. 2010;10:917-23.
272. Valerio L, Peters RJ, Zwinderman AH, Pinto-Sietsma SJ. Sublingual endothelial glycocalyx and atherosclerosis. A cross-sectional study. PLoS One. 2019;14(3):e0213097.
273. Steppan J, Hofer S, Funke B, Brenner T, Henrich M, Martin E, et al. Sepsis and major abdominal surgery lead to flaking of the endothelial glycocalix. J Surg Res. 2011;165(1):136-41.
274. Chelazzi C, Villa G, Mancinelli P, De Gaudio AR, Adembri C. Glycocalyx and sepsis-induced alterations in vascular permeability. Crit Care. 2015;19:26.
275. Percie du Sert N, Hurst V, Ahluwalia A, Alam S, Avey MT, Baker M, et al. The ARRIVE guidelines 2.0: Updated guidelines for reporting animal research. PLoS Biol. 2020;18(7):e3000410.
276. Brands J, Hubel CA, Althouse A, Reis SE, Pacella JJ. Noninvasive sublingual microvascular imaging reveals sex-specific reduction in glycocalyx barrier properties in patients with coronary artery disease. Physiol Rep. 2020;8(2):e14351.
277. Hulde N, Rogenhofer N, Brettner F, Eckert NC, Gotzfried I, Nguyen T, et al. The CYCLOCALYX study: Ovulatory cycle affects circulating compartments of the endothelial glycocalyx in blood. Am J Reprod Immunol. 2018;79(1).
278. Ohtani O MT. Blood and Lymphatic Microvascular Organization of the Digestive Tract In: Motta P MT, Fujita H, editor. Scanning Electron Microscopy of Vascular Casts: Methods and Applications Kluwer Academic Publishers; 1992. p. 53-69.
279. Morrison JC, DeFrank MP, Van Buskirk EM. Comparative microvascular anatomy of mammalian ciliary processes. Invest Ophthalmol Vis Sci. 1987;28(8):1325-40.
280. Kieffer PJ, Williams JM, Shepard MK, Giguere S, Epstein KL. Comparison of the oral and rectal mucosal and colonic serosal microcirculations of healthy, anesthetized horses. Can J Vet Res. 2018;82(1):55-9.
281. Hamilton MN, Edelstein SJ. Cat hemoglobin. pH dependence of cooperativity and ligand binding. J Biol Chem. 1974;249(5):1323-9.

282. Herrmann K HS. Determination of P50 for feline hemoglobin. Journal of Veterinary Emergency and Critical Care 2005;15(1):26-31.
283. Grosenbaugh DAA, James O.; Muir, William W. Absorbance Spectra of Inter-Species Hemoglobins in the Visible and Near Infrared Regions. Journal of Veterinary Emergency and Critical Care. 1997;7(1):36-42.
284. Becker BF, Chappell D, Jacob M. Endothelial glycocalyx and coronary vascular permeability: the fringe benefit. Basic Res Cardiol. 2010;105(6):687-701.
285. Mehta D, Ravindran K, Kuebler WM. Novel regulators of endothelial barrier function. Am J Physiol Lung Cell Mol Physiol. 2014;307(12):L924-35.
286. Chappell D, Bruegger D, Potzel J, Jacob M, Brettner F, Vogeser M, et al. Hypervolemia increases release of atrial natriuretic peptide and shedding of the endothelial glycocalyx. Crit Care. 2014;18(5):538.
287. Gimblet CJ, Ernst JW, Bell B, Bos KD, Stroud AK, Wendt LH, et al. Effect of Glycocalyx-targeted Therapy on Vascular Function in Older Adults: A Randomized Controlled Trial. J Appl Physiol (1985). 2024.
288. Hobbs KJ, Johnson PJ, Wiedmeyer CE, Schultz L, Foote CA. Plasma syndecan-1 concentration as a biomarker for endothelial glycocalyx degradation in septic adult horses. Equine Vet J. 2023;55(3):456-62.
289. Andreasson U, Perret-Liaudet A, van Waalwijk van Doorn LJ, Blennow K, Chiasserini D, Engelborghs S, et al. A Practical Guide to Immunoassay Method Validation. Front Neurol. 2015;6:179.
290. Stiller J, Jasensky AK, Hennies M, Einspanier R, Kohn B. Validation of an enzyme-linked immunosorbent assay for measurement of feline haptoglobin. J Vet Diagn Invest. 2016;28(3):235-43.
291. Shaw KE, Bersenas AM, Bateman SW, Blois SL, Wood RD. Validation of a commercial human ELISA to measure hyaluronic acid concentration in feline plasma. J Vet Diagn Invest. 2022;34(1):86-9.
292. Konig ML, Lettry SC, Marti E, Mirkovitch J, Wyder M, Giger U, et al. Validation of a human angiopoietin-2 ELISA for measurement of angiopoietin-2 concentrations in canine plasma samples and supernatant of primary canine aortic endothelial cell cultures. Am J Vet Res. 2018;79(8):803-10.
293. Altschul SF, Gish W, Miller W, Myers EW, Lipman DJ. Basic local alignment search tool. J Mol Biol. 1990;215(3):403-10.
294. Soltis RD, Hasz D, Morris MJ, Wilson ID. The effect of heat inactivation of serum on aggregation of immunoglobulins. Immunology. 1979;36(1):37-45.
295. Gundry RL, White MY, Murray CI, Kane LA, Fu Q, Stanley BA, et al. Preparation of proteins and peptides for mass spectrometry analysis in a bottom-up proteomics workflow. Curr Protoc Mol Biol. 2009;Chapter 10:Unit10 25.
296. Eng JK, McCormack AL, Yates JR. An approach to correlate tandem mass spectral data of peptides with amino acid sequences in a protein database. J Am Soc Mass Spectrom. 1994;5(11):976-89.
297. Team RC. R: A Language and Environment for Statistical Computing. Vienna, Austria: R Foundation for Statistical Computing; 2023.
298. Lipman NS, Jackson LR, Trudel LJ, Weis-Garcia F. Monoclonal versus polyclonal antibodies: distinguishing characteristics, applications, and information resources. ILAR J. 2005;46(3):258-68.
299. Guo Y, Jia W, Yang J, Zhan X. Cancer glycomics offers potential biomarkers and therapeutic targets in the framework of 3P medicine. Front Endocrinol (Lausanne). 2022;13:970489.
300. Latta T. SALINE VENOUS INJECTION IN CASES OF MALIGNANT CHOLERA, PERFORMED WHILE IN THE VAPOUR-BATH. The Lancet. 1832;19(480):208-9.
301. McDermid RC, Raghunathan K, Romanovsky A, Shaw AD, Bagshaw SM. Controversies in fluid therapy: Type, dose and toxicity. World J Crit Care Med. 2014;3(1):24-33.
302. Monnet X, Marik PE, Teboul JL. Prediction of fluid responsiveness: an update. Ann Intensive Care. 2016;6(1):111.
303. Hopper K SD, Bateman S. Shock Syndromes. In: DiBartola S, editor. Fluid, Electrolyte, and Acid-Base Disorders in Small Animal Practice. 4th ed. 3251 Riverport Lane, St. Louis, Missouri 63043, USA: Elsevier Sounders; 2012. p. 557-83.
304. Davis H, Jensen T, Johnson A, Knowles P, Meyer R, Rucinsky R, et al. 2013 AAHA/AAFP fluid therapy guidelines for dogs and cats. J Am Anim Hosp Assoc. 2013;49(3):149-59.

305. Boysen SR, Gommeren K. Assessment of Volume Status and Fluid Responsiveness in Small Animals. Front Vet Sci. 2021;8:630643.
306. Payne JR, Brodbelt DC, Luis Fuentes V. Cardiomyopathy prevalence in 780 apparently healthy cats in rehoming centres (the CatScan study). J Vet Cardiol. 2015;17 Suppl 1:S244-57.
307. Malbrain ML, Marik PE, Witters I, Cordemans C, Kirkpatrick AW, Roberts DJ, et al. Fluid overload, de-resuscitation, and outcomes in critically ill or injured patients: a systematic review with suggestions for clinical practice. Anaesthesiol Intensive Ther. 2014;46(5):361-80.
308. Claure-Del Granado R, Mehta RL. Fluid overload in the ICU: evaluation and management. BMC Nephrol. 2016;17(1):109.
309. Pouska J, Tegl V, Astapenko D, Cerny V, Lehmann C, Benes J. Impact of Intravenous Fluid Challenge Infusion Time on Macrocirculation and Endothelial Glycocalyx in Surgical and Critically Ill Patients. Biomed Res Int. 2018;2018:8925345.
310. Fuller A, Hetem RS, Maloney SK, Mitchell D. Adaptation to heat and water shortage in large, arid-zone mammals. Physiology (Bethesda). 2014;29(3):159-67.
311. Withers PC, Cooper CE. Physiological regulation of evaporative water loss in endotherms: is the little red kaluta (Dasykaluta rosamondae) an exception or the rule? Proc Biol Sci. 2014;281(1784):20140149.
312. Byers CG. Crystalloids versus Colloids: Same Controversy, New Information. Vet Clin North Am Small Anim Pract. 2025.
313. Cazzolli D, Prittie J. The crystalloid-colloid debate: Consequences of resuscitation fluid selection in veterinary critical care. J Vet Emerg Crit Care (San Antonio). 2015;25(1):6-19.
314. Margraf A, Herter JM, Kuhne K, Stadtmann A, Ermert T, Wenk M, et al. 6% Hydroxyethyl starch (HES 130/0.4) diminishes glycocalyx degradation and decreases vascular permeability during systemic and pulmonary inflammation in mice. Crit Care. 2018;22(1):111.
315. Uzawa K, Ushiyama A, Mitsuda S, Ando T, Sawa M, Miyao H, et al. The protective effect of hydroxyethyl starch solution on the glycocalyx layer in an acute hemorrhage mouse model. J Anesth. 2020;34(1):36-46.
316. Ergin B, Guerci P, Uz Z, Westphal M, Ince Y, Hilty M, et al. Hemodilution causes glycocalyx shedding without affecting vascular endothelial barrier permeability in rats. J Clin Transl Res. 2020;5(5):243-52.
317. Ando T, Uzawa K, Yoshikawa T, Mitsuda S, Akimoto Y, Yorozu T, et al. The effect of tetrastarch on the endothelial glycocalyx layer in early hemorrhagic shock using fluorescence intravital microscopy: a mouse model. J Anesth. 2023;37(1):104-18.
318. Zhao H, Zhu Y, Zhang J, Wu Y, Xiang X, Zhang Z, et al. The Beneficial Effect of HES on Vascular Permeability and Its Relationship With Endothelial Glycocalyx and Intercellular Junction After Hemorrhagic Shock. Front Pharmacol. 2020;11:597.
319. Fulton B, Sorkin EM. Propofol. An overview of its pharmacology and a review of its clinical efficacy in intensive care sedation. Drugs. 1995;50(4):636-57.
320. Lee B, Shin HJ, Kweon KH, Kim NY. Effect of sevoflurane-remifentanil and propofol-remifentanil anesthesia on glycocalyx shedding during deep inferior epigastric perforator flap breast reconstruction: a prospective randomized, controlled trial. Anesth Pain Med (Seoul). 2023;18(2):148-58.
321. Lin MC, Chen CL, Yang TT, Choi PC, Hsing CH, Lin CF. Anesthetic propofol overdose causes endothelial cytotoxicity in vitro and endothelial barrier dysfunction in vivo. Toxicol Appl Pharmacol. 2012;265(2):253-62.
322. Lin MC, Lin CF, Li CF, Sun DP, Wang LY, Hsing CH. Anesthetic propofol overdose causes vascular hyperpermeability by reducing endothelial glycocalyx and ATP production. Int J Mol Sci. 2015;16(6):12092-107.
323. Van S, Lam V, Patel K, Humphries A, Siddiqi J. Propofol-Related Infusion Syndrome: A Bibliometric Analysis of the 100 Most-Cited Articles. Cureus. 2023;15(10):e46497.
324. Kotani Y, Pruna A, Landoni G. Mechanisms of Action of the Detrimental Effects of Propofol on Survival. J Cardiothorac Vasc Anesth. 2023;37(11):2176-80.
325. Fang FQ, Sun JH, Wu QL, Feng LY, Fan YX, Ye JX, et al. Protective effect of sevoflurane on vascular endothelial glycocalyx in patients undergoing heart valve surgery: A randomised controlled trial. Eur J Anaesthesiol. 2021;38(5):477-86.

326. Kim NY, Kim KJ, Lee KY, Shin HJ, Cho J, Nam DJ, et al. Effect of volatile and total intravenous anesthesia on syndecan-1 shedding after minimally invasive gastrectomy: a randomized trial. Sci Rep. 2021;11(1):1511.
327. Maldonado F, Morales D, Gutierrez R, Barahona M, Cerda O, Caceres M. Effect of sevoflurane and propofol on tourniquet-induced endothelial damage: a pilot randomized controlled trial for knee-ligament surgery. BMC Anesthesiol. 2020;20(1):121.
328. Pascoe PJ, Ilkiw JE, Frischmeyer KJ. The effect of the duration of propofol administration on recovery from anesthesia in cats. Vet Anaesth Analg. 2006;33(1):2-7.
329. Bley CR, Roos M, Price J, Ruess-Melzer K, Buchholz J, Poirier V, et al. Clinical assessment of repeated propofol-associated anesthesia in cats. J Am Vet Med Assoc. 2007;231(9):1347-53.
330. Andress JL, Day TK, Day D. The effects of consecutive day propofol anesthesia on feline red blood cells. Vet Surg. 1995;24(3):277-82.
331. Baetge CL, Smith LC, Azevedo CP. Clinical Heinz Body Anemia in a Cat After Repeat Propofol Administration Case Report. Front Vet Sci. 2020;7:591556.
332. Pries AR, Reglin B, Secomb TW. Structural adaptation of microvascular networks: functional roles of adaptive responses. Am J Physiol Heart Circ Physiol. 2001;281(3):H1015-25.
333. Yuan SY RR. Chapter 2, Structure and Function of Exchange Microvessels.Regulation of Endothelial Barrier Function. Regulation of Endothelial Barrier Function: San Rafael (CA): Morgan & Claypool Life Sciences;; 2010.
334. Bruegger D, Jacob M, Rehm M, Loetsch M, Welsch U, Conzen P, et al. Atrial natriuretic peptide induces shedding of endothelial glycocalyx in coronary vascular bed of guinea pig hearts. Am J Physiol Heart Circ Physiol. 2005;289(5):H1993-9.
335. Powell M, Mathru M, Brandon A, Patel R, Frolich M. Assessment of endothelial glycocalyx disruption in term parturients receiving a fluid bolus before spinal anesthesia: a prospective observational study. Int J Obstet Anesth. 2014;23(4):330-4.
336. Damen T, Kolsrud O, Dellgren G, Hesse C, Ricksten SE, Nygren A. Atrial natriuretic peptide does not degrade the endothelial glycocalyx: A secondary analysis of a randomized porcine model. Acta Anaesthesiol Scand. 2021;65(9):1305-12.
337. Li Y, Yi S, Zhu Y, Hahn RG. Volume kinetics of Ringer's lactate solution in acute inflammatory disease. Br J Anaesth. 2018;121(3):574-80.
338. Damen T, Saadati S, Forssell-Aronsson E, Hesse C, Bentzer P, Ricksten SE, et al. Effects of different mean arterial pressure targets on plasma volume, ANP and glycocalyx-A randomized trial. Acta Anaesthesiol Scand. 2021;65(2):220-7.
339. Paige CF, Abbott JA, Elvinger F, Pyle RL. Prevalence of cardiomyopathy in apparently healthy cats. J Am Vet Med Assoc. 2009;234(11):1398-403.
340. Yozova ID LL, Sano H, Thomson N, Munday J, Cave N. Assessment of the Endothelial Glycocalyx after a Fluid Bolus in Healthy Anesthetized Cats Using Rapid, Patient-Side Glycocheck Analysis Software. In: Abstracts from the International Veterinary Emergency and Critical Care Symposium, and the European Veterinary Emergency and Critical Care Annual Congress 2020. Journal of Veterinary Emergency and Critical Care. 2020;30(S1):S27.
341. Loughran KA, Rush JE, Rozanski EA, Oyama MA, Larouche-Lebel E, Kraus MS. The use of focused cardiac ultrasound to screen for occult heart disease in asymptomatic cats. J Vet Intern Med. 2019;33(5):1892-901.
342. Wickham H. ggplot2: Elegant Graphics for Data Analysis. New York: Springer-Verlag; 2016.
343. Wickham H, Vaughan D, Girlich M. tidyr: Tidy Messy Data. R package version 1.3.0 ed2023.
344. Wickham H, François R, Henry L, Müller K, Vaughan D. dplyr: A Grammar of Data Manipulation. R package version 1.1.4 ed2023.
345. Bates D, Mächler M, Bolker B, Walker S. Fitting Linear Mixed-Effects Models Using lme4. Journal of Statistical Software. 2015;67(1):1-48.
346. Weaver AJ, Jr., Venn EC, Ford R, Ewer N, Hildreth KE, Williams CE, et al. Comparing the effects of various fluid resuscitative strategies on Glycocalyx damage in a canine hemorrhage model. Vet J. 2024;307:106221.
347. Sano Y, Sakamoto A, Oi Y, Ogawa R. Anaesthesia and circulating blood volume. Eur J Anaesthesiol. 2005;22(4):258-62.

348. Short E, Chagas J, Kurihara M, Ishikawa Y, Chambers JP, Bridges J, et al. Effect of common sedation agents on feline splenic size determined via ultrasonography. N Z Vet J. 2023;71(5):244-50.
349. The human protein atlas 2000 [Available from: https://www.proteinatlas.org/.
350. Baldo CF, Garcia-Pereira FL, Nelson NC, Hauptman JG, Shih AC. Effects of anesthetic drugs on canine splenic volume determined via computed tomography. Am J Vet Res. 2012;73(11):1715-9.
351. Auger M, Fazio C, de Swarte M, Bussieres G, Schaefer D, Springer CM. Administration of certain sedative drugs is associated with variation in sonographic and radiographic splenic size in healthy cats. Vet Radiol Ultrasound. 2019;60(6):717-28.
352. Dhumeaux MP, Snead EC, Epp TY, Taylor SM, Carr AP, Dickinson RM, et al. Effects of a standardized anesthetic protocol on hematologic variables in healthy cats. J Feline Med Surg. 2012;14(10):701-5.
353. Casanova J, Simon C, Vara E, Sanchez G, Rancan L, Abubakra S, et al. Sevoflurane anesthetic preconditioning protects the lung endothelial glycocalyx from ischemia reperfusion injury in an experimental lung autotransplant model. J Anesth. 2016;30(5):755-62.
354. Mokken FC, Henny CP, Gelb AW, Biervliet JD, Hardeman MR, Kedaria M, et al. The effects of propofol compared to high-dose fentanyl anesthesia on rheologic parameters in coronary artery surgery. J Cardiothorac Vasc Anesth. 1993;7(1):10-6.
355. Reinhart WH, Felix C. Influence of propofol on erythrocyte morphology, blood viscosity and platelet function. Clin Hemorheol Microcirc. 2003;29(1):33-40.
356. Jalava S HT, Boysen SR, Yozova ID. Effects of hypovolemia and volume overload on ultrasonographically derived caudal vena cava parameters in healthy lightly sedated cats. In: Abstracts from the International Veterinary Emergency and Critical Care Symposium, the European Veterinary Emergency and Critical Care Annual Congress, and the ACVECC VetCOT Veterinary Trauma & Critical Care Conference 2022. Journal of Veterinary Emergency and Critical Care. 2022;32:S27-S8.
357. Khoo A, Waldner CL, Carr AP, Gaunt MC. Effect of three resuscitative fluid therapy strategies on NT-proBNP concentration in healthy dogs. J Vet Emerg Crit Care (San Antonio). 2019;29(2):143-8.
358. Hahn RG. Volume kinetics for infusion fluids. Anesthesiology. 2010;113(2):470-81.
359. den Os MM, van den Brom CE, van Leeuwen ALI, Dekker NAM. Microcirculatory perfusion disturbances following cardiopulmonary bypass: a systematic review. Crit Care. 2020;24(1):218.
360. Massey MJ, Hou PC, Filbin M, Wang H, Ngo L, Huang DT, et al. Microcirculatory perfusion disturbances in septic shock: results from the ProCESS trial. Crit Care. 2018;22(1):308.
361. Ostrowski SR, Haase N, Muller RB, Moller MH, Pott FC, Perner A, et al. Association between biomarkers of endothelial injury and hypocoagulability in patients with severe sepsis: a prospective study. Crit Care. 2015;19(1):191.
362. Jaffer U, Wade RG, Gourlay T. Cytokines in the systemic inflammatory response syndrome: a review. HSR Proc Intensive Care Cardiovasc Anesth. 2010;2(3):161-75.
363. Harper SJ, Tomson CR, Bates DO. Human uremic plasma increases microvascular permeability to water and proteins in vivo. Kidney Int. 2002;61(4):1416-22.
364. Mazzaferro E, Powell LL. Fluid Therapy for the Emergent Small Animal Patient: Crystalloids, Colloids, and Albumin Products. Vet Clin North Am Small Anim Pract. 2022;52(3):781-96.
365. Gomez DE, Kamr A, Gilsenan WF, Burns TA, Mudge MC, Hostnik LD, et al. Endothelial glycocalyx degradation in critically ill foals. J Vet Intern Med. 2024;38(5):2748-57.
366. Yozova ID MJ, Avendaño Veas FA, Irie M, Thomson N Effects of acute intravascular volume overload on endothelial glycocalyx thickness in healthy cats – preliminary results. In: Abstracts from the International Veterinary Emergency and Critical Care Symposium and the European Veterinary Emergency and Critical Care Annual Congress 2024. Journal of Veterinary Emergency and Critical Care. 2024;34(S2):S36.
367. Hayes G, Mathews K, Doig G, Kruth S, Boston S, Nykamp S, et al. The Feline Acute Patient Physiologic and Laboratory Evaluation (Feline APPLE) Score: a severity of illness stratification system for hospitalized cats. J Vet Intern Med. 2011;25(1):26-38.
368. Lapsley J, Hayes GM, Sumner JP. Performance evaluation and validation of the Animal Trauma Triage score and modified Glasgow Coma Scale in injured cats: A Veterinary Committee on Trauma registry study. J Vet Emerg Crit Care (San Antonio). 2019;29(5):478-83.

369. Houben K AF, Tan WKA, Yozova ID. Influence of estimated costs on euthanasia decision for cats presented with trauma to an emergency center in New Zealand: a retrospective analysis. In: Abstracts from the International Veterinary Emergency and Critical Care Symposium and the European Veterinary Emergency and Critical Care Annual Congress 2024. Journal of Veterinary Emergency and Critical Care. 2024;34(S2):S33-S4.
370. Hickey MC, Gray R, van Galen G, Ward MP. Distribution of mortality patterns in cats with naturally occurring trauma: A Veterinary Committee on Trauma registry study. Vet J. 2021;278:105765.
371. Nascimento DC, Costa Neto JM, Solca MS, Estrela-Lima A, Barbosa VF. Clinicoepidemiological profile and risk factors associated with mortality in traumatized cats admitted to a veterinary teaching hospital in Brazil. J Feline Med Surg. 2021:1098612X211028027.
372. Gates MC, Walker J, Zito S, Dale A. Cross-sectional survey of pet ownership, veterinary service utilisation, and pet-related expenditures in New Zealand. N Z Vet J. 2019;67(6):306-14.
373. Lue TW, Pantenburg DP, Crawford PM. Impact of the owner-pet and client-veterinarian bond on the care that pets receive. J Am Vet Med Assoc. 2008;232(4):531-40.
374. Sandoe P, Palmer C, Corr SA, Springer S, Lund TB. Do people really care less about their cats than about their dogs? A comparative study in three European countries. Front Vet Sci. 2023;10:1237547.
375. Groen BB, Hamer HM, Snijders T, van Kranenburg J, Frijns D, Vink H, et al. Skeletal muscle capillary density and microvascular function are compromised with aging and type 2 diabetes. J Appl Physiol (1985). 2014;116(8):998-1005.
376. Kruger-Genge A, Blocki A, Franke RP, Jung F. Vascular Endothelial Cell Biology: An Update. Int J Mol Sci. 2019;20(18).
377. Feldschuh J, Enson Y. Prediction of the normal blood volume. Relation of blood volume to body habitus. Circulation. 1977;56(4 Pt 1):605-12.
378. McMillan DE. The microcirculation in diabetes. Microcirc Endothelium Lymphatics. 1984;1(1):3-24.
379. Bagi Z, Feher A, Cassuto J. Microvascular responsiveness in obesity: implications for therapeutic intervention. Br J Pharmacol. 2012;165(3):544-60.
380. Oncken AK, Kirby R, Rudloff E. Hypothermia in Critically Ill Dogs and Cats. COMPENDIUM ON CONTINUING EDUCATION FOR THE PRACTISING VETERINARIAN-NORTH AMERICAN EDITION-. 2001;23(6):506-23.
381. R K, editor Feline Shock and Resuscitation. WSAVA; 2005: VIN.
382. Muir WW, Ueyama Y, Noel-Morgan J, Kilborne A, Page J. A Systematic Review of the Quality of IV Fluid Therapy in Veterinary Medicine. Front Vet Sci. 2017;4:127.
383. Hopper K, Rojas AG, Barter L. Fluid Therapy in Dogs and Cats: An Internet Based Survey. J Am Vet Med Assoc 2016;In press.
384. Harris BA, Hofmeister EH, Gicking JC. A survey of emergency and critical care veterinarians regarding IV fluid bolus therapy and monitoring practices in small animals. J Vet Emerg Crit Care (San Antonio). 2021;31(5):564-73.
385. White C. Global spending on health research still skewed towards wealthy nations. BMJ. 2004;329(7474):1064.
386. Pedersen NC. An update on feline infectious peritonitis: virology and immunopathogenesis. Vet J. 2014;201(2):123-32.
387. Kennedy MA. Feline Infectious Peritonitis: Update on Pathogenesis, Diagnostics, and Treatment. Vet Clin North Am Small Anim Pract. 2020;50(5):1001-11.
388. Wolfe LG, Griesemer RA. Feline infectious peritonitis: review of gross and histopathologic lesions. J Am Vet Med Assoc. 1971;158(6):Suppl 2:987+.
389. Evermann JF, Henry CJ, Marks SL. Feline infectious peritonitis. J Am Vet Med Assoc. 1995;206(8):1130-4.
390. Pedersen NC. An update on feline infectious peritonitis: diagnostics and therapeutics. Vet J. 2014;201(2):133-41.
391. Izes AM, Yu J, Norris JM, Govendir M. Current status on treatment options for feline infectious peritonitis and SARS-CoV-2 positive cats. Vet Q. 2020;40(1):322-30.

392. Delaplace M, Huet H, Gambino A, Le Poder S. Feline Coronavirus Antivirals: A Review. Pathogens. 2021;10(9).
393. Krentz D, Bergmann M, Felten S, Hartmann K. [Options for treatment of feline infectious peritonitis - previously and today]. Tierarztl Prax Ausg K Kleintiere Heimtiere. 2023;51(5):351-60.
394. Tasker S, Addie DD, Egberink H, Hofmann-Lehmann R, Hosie MJ, Truyen U, et al. Feline Infectious Peritonitis: European Advisory Board on Cat Diseases Guidelines. Viruses. 2023;15(9).
395. Thayer V, Gogolski S, Felten S, Hartmann K, Kennedy M, Olah GA. 2022 AAFP/EveryCat Feline Infectious Peritonitis Diagnosis Guidelines. J Feline Med Surg. 2022;24(9):905-33.
396. Paltrinieri S, Giordano A, Stranieri A, Lauzi S. Feline infectious peritonitis (FIP) and coronavirus disease 19 (COVID-19): Are they similar? Transbound Emerg Dis. 2021;68(4):1786-99.
397. Tseng YY, Liao GR, Lien A, Hsu WL. Current concepts in the development of therapeutics against human and animal coronavirus diseases by targeting NP. Comput Struct Biotechnol J. 2021;19:1072-80.
398. Shaw KE, Bersenas AM, Bateman SW, Blois SL, Guieu LS, Wood RD. Use of serum hyaluronic acid as a biomarker of endothelial glycocalyx degradation in dogs with septic peritonitis. Am J Vet Res. 2021;82(7):566-73.
399. Plickert HD, Bondzio A, Einspanier R, Tichy A, Brunnberg L. Hyaluronic acid concentrations in synovial fluid of dogs with different stages of osteoarthritis. Res Vet Sci. 2013;94(3):728-34.
400. Hiratzka JL, Licari LG, Peters LK. Incidence of hospital-acquired anemia in hospitalized dogs and cats. J Am Vet Med Assoc. 2018;252(5):560-4.
401. Lynch AM, Respess M, Boll AE, Bozych M, McMichael M, Fletcher DJ, et al. Hospital-acquired Anemia in Critically Ill Dogs and Cats: A Multi-Institutional Study. J Vet Intern Med. 2016;30(1):141-6.
402. De Backer D, Hollenberg S, Boerma C, Goedhart P, Buchele G, Ospina-Tascon G, et al. How to evaluate the microcirculation: report of a round table conference. Crit Care. 2007;11(5):R101.
403. Piagnerelli M, Ince C, Dubin A. Microcirculation. Crit Care Res Pract. 2012;2012:867176.